University of Southampton

The Effects of Acute and Chronic Applications of Kainic Acid to the Rodent Hippocampus

Alan Cook

Doctor of Philosophy

Faculty of Science

School of Biological Sciences

2003

UNIVERSITY OF SOUTHAMPTON

ABSTRACT

FACULTY OF SCIENCE
SCHOOL OF BIOLOGICAL SCIENCES

Doctor of Philosophy

THE EFFECTS OF ACUTE AND CHRONIC APPLICATIONS OF KAINIC ACID TO THE RODENT HIPPOCAMPUS

by Alan Cook

Kainic acid is an excitotoxin in mammalian brain. Here the mechanisms underlying the physiological versus the pathological effects of kainate (KA) were compared. The acute effects were studied on rat hippocampal slices, and the chronic effects in mouse organotypic hippocampal slice cultures (over the course of 7 days).

Two approaches were used: First, in acute hippocampal slices, receptor selective drugs were used to determine the receptor subtypes involved in the response to KA (15-30 minutes) using simultaneous recordings of evoked field potentials from the stratum pyramidale and s. radiatum of CA1. The role of CA3 in driving the response in CA1 was determined by repeating these experiments following excision of the CA3. Second in organotypic mouse hippocampal slice cultures the response to longer applications of KA (2 - 24 hours) was determined using evoked field potential recordings from the s. pyramidale of either CA1 or CA3.

Acute applications of KA reduced the EPSP slopes, initially increased and then reduced the population spike amplitudes (PSA) and decreased the paired-pulse inhibition. The underlying mechanisms for these effects could be either presynaptic, postsynaptic or a combination of both. For example, KA may decrease EPSP slope via GluR6 containing receptors on CA1 pyramidal cells, or by presynaptic inhibition at Schaffer collateral terminals via GluR5 containing receptors. Pharmacological evidence supports the latter, as the GluR5 selective agonist ATPA mimicked this effect of KA, and it was not blocked by the GluR6 antagonist NS102. A further possibility is that KA may activate GABAergic interneurones via GluR5 containing receptors and this could also result in a decreased EPSP slope. However, concomitant with the decreased EPSP slope KA also increased population spike amplitude (PSA) and decreased paired-pulse inhibition (PPI), arguing against the involvement of GABA. CA3 was not required for these effects of KA.

In the later phase of 15 minutes application of KA, ATPA and Fwill, the PSA was reduced. In the case of KA, the CA3 region was required for this to occur. The onset of this inhibition was delayed in the presence of the $GABA_B$ receptor antagonist SCH50911, which indicates the involvement of GABAergic interneurones in this effect of KA. It is likely that this response is mediated via GluR5 activation of interneurones.

PPI was reduced throughout the KA application period. ATPA initially increased PPI, consistent with a GluR5 mediated excitation of interneurones. Fwill differed significantly to KA again suggesting a KA receptor mediated phenomenon. No involvement was observed for $GABA_B$ receptors.

To study the consequences of long-term exposure of hippocampus to KA, experiments were performed on organotypic slices, which provided the opportunity to assess the electrophysiological status of the slice up to 7 days post exposure. Application of KA (1μM) for 2 hours to these slices decreased PSA as in the acute slice. Incubation of slices with 1μM KA for 24 hours was subtoxic. However, this treatment reduced PPI in both CA1 and CA3 and reduced excitability to exogenous stimuli in CA1from 4-7 days post treatment. Furthermore, this treatment decreased the toxic effects of KA as observed with both thionin and propidium iodide.

This study has highlighted some novel effects of KA. For example, although it has been used for a number of years as an excitotoxin, it is paradoxically capable of reducing the output of the CA1 at concentrations that are likely to be selective for KA rather than AMPA receptors.

Furthermore, at KA receptor selective concentrations it is capable of inducing neuroprotection in the CA3 following prolonged exposure, despite the apparent reduction in inhibitory function in both the CA1 and CA3. The mechanisms for this protection are as yet unclear and may provide a source of fruitful further investigation.

Table of Contents

Table of Figures

List of Tables

Abbreviations

AC	action current
ACSF	artificial cerebrospinal fluid
AMPA	DL-α-amino-3-hydroxy-5-methyl-4-isoxalone-propionic acid
ATP	adenosine triphosphate
ATPA	[(RS)-2-amino-3-(3-hydroxy-5-tert-butylisoxazol-4-yl)propanoic acid]
Bic	bicuculline methiodide
cDNA	complementary deoxyribonucleic acid
CNQX	6-cyano-7-nitroquinoxaline-2,3-dione
CNS	central nervous system
CPP	3-((R)-2-carboxypiperazin-4-yl)-propyl-1-phosphonic acid
DAB	diaminobenzidine
D-AP5	D(-)-2-amino-5-phosphonopentanoic acid
DAG	diacylglycerol
DIV	days *in vitro*
DNQX	6,7-Dinitroquinoxaline-2,3-dione
DMPX	3,7-dimethyl-1-(2-propynyl)xanthine
DMSO	dimethyl sulphoxide
DPCPX	8-cyclopentyl-1,3-dipropylxanthine
DRG	dorsal root ganglion cells
EAA	excitatory amino acid
EC_{50}	effective concentration for 50% response
EPSC	excitatory postsynaptic current
EPSP	excitatory postsynaptic potential
Fwill	(S)-(-)-αAmino-5-fluoro-3,4-dihydro-2,4-dioxo-1(2H)pyridinepropanoic acid
GABA	γ-amino butyric acid
GAD	glutamic acid decarboxylase
GBZ	6-Imino-3-(4-methoxyphenyl)-1 (6H)-pyridazinebutanoic acid
GYKI 53655	1-(4-aminophenyl)-3-methylcarbamyl-4-methyl-7,8-methylenedioxy-3,4 -dihydro-5H-2,3-benzodiazepine
H-7	1-(5-isoquinolinesulphonyl)-2-methylpiperazine dihydrochloride
HEK 293	human embryonic kidney cell line
HSP 72	heat shock protein 72
Hz	Hertz
ICV	intraventricular
IP_3	inositol trisphosphate
IPI	inter-pulse interval
I_{sAHP}	slow afterhyperpolarisation current
I-V	current – voltage plot
KA	kainic acid (([2S-(2 α, 3β, 4β)]-2-Carboxy-4-(1-methylethylenyl)-3-pyrrolidineacetic acid)

KBP	kainate binding protein
K_d	equilibrium dissociation constant
L-AP4	L-(+)-2-amino-4-phosphonobutyric acid
LTP	long-term potentiation
LY382884	((3S, 4aR, 6S, 8aR)-6-((carboxyphenyl)methyl)-1,2,3,4,4a,5,6,7,8,8a-decahydroisoquinoline-3-carboxylic acid
MCPG	(S)-αmethyl-4-carboxyphenylglycine
mGluR	metabotropic glutamate receptor
mIPSC	miniature inhibitory postsynaptic current
MK801	(5R,10S)-(+)-5-methyl-10,11-dihydro-5H-dibenzo[a,d] cyclohepten-5,10-imine
MnSOD	manganese super-oxide dismutase
MPPG	(RS)-αmethyl-4-phosphonophenylglycine
mRNA	messenger ribonucleic acid
MSOP	α–methylserine-O-phosphate
NBQX	2,3-(dioxo-6-nitro-1,2,3,4-tetrahydrobenzo[f]quinoxaline-7-) sulphonamide
NMDA	N-methyl-D-aspartic acid
NPY	neuropeptide Y
NS102	6,7,8,9-tetrahydro-5-nitro-1H-benz[g]indole-2,3-dione 3-oxime
O/A	oriens/ alveus
pA	pico Amps
PBS	phosphate buffered saline
PCR	polymerase chain reaction
PFA	paraformaldehyde
PI	propidium iodide
PKA	protein kinase A
PKC	protein kinase C
PLC	phospholipase C
PLD	phospholipase D
pO_2	partial pressure of oxygen
PSD-95	postsynaptic density 95
PTX	pertussis toxin
RNA	ribonucleic acid
ROS	reactive oxygen species
SAP90	synapse associated protein 90
SAP97	synapse associated protein 97
SCH50911	(2S)(+)5,5-dimethyl-2-morpholineacetic acid
S.E.M.	standard error of the mean
TBS	tris-buffered saline
trans-ACPD	trans-(1S,3R)-1-amino-1,3-cyclopentanedicarboxylic acid
TLE	temporal lobe epilepsy

Acknowledgements

I would like to thank Dr. John Chad, Dr. Lars Sundstrom and Prof. Howard Wheal for all their help and the opportunity to carry out this exciting piece of research.

I would especially like to thank Dr. Lindy Holden-Dye for all her help, encouragement and patience not to mention very generously allowing me time off work to write.

For their technical help and advice, I would like to thank Dr Nick Best, who helped me with the cultures and Maureen Gatherer, who helped with the immunohistochemistry.

I would also like to thank everyone who has made my time so far in Southampton so enjoyable – you'll know who you are.

Most importantly, I would like to thank my family, especially Mum and Dad. Cheers for everything, I'd never have come this far without you!

General Introduction

The existence of high affinity binding sites for kainate (KA) in mammalian brain has been known for a number of years. Since this discovery, six genes to date have been found which encode KA receptor subunits. These have been grouped by their homology, and pharmacology, into two groups, comprised of the high affinity KA1 and KA2 and the lower affinity GluR5 – GluR7. However, the delineation of their physiological roles has been confounded until recently by a lack of specific agonists and antagonists for KA receptor subunits, and by the fact that KA is an agonist at AMPA receptors, which are often co-expressed in the same neurones as KA receptors.

This study aims to address the physiological versus the pathological effects of KA on the function of a relatively simple neuronal net, namely the hippocampal slice preparation, at concentrations which are likely to be selective for KA receptors.

Chapter 1 of this report covers the general background to the field, with reference to the structure and functional properties of the non-NMDA type glutamate receptors. Attention has been focused especially on the KA receptors. The structure of the hippocampus is then described, followed by details of the distributions of the various KA receptor subunits within the hippocampus. The known physiological roles of these receptors are then discussed, followed by a brief discussion of further excitatory and inhibitory receptors found within the hippocampus. Chapter 2 describes the methods used.

In chapter 3, the question of how KA application affects evoked field responses in the CA1 will be addressed. The role of specific KA receptor subunits in these responses will be investigated using subunit selective drugs. Chapter 4 deals with the possible indirect activation of a number of excitatory and inhibitory receptor populations within the hippocampus, thus leading, or contributing, to the observed responses during KA application.

In the final results chapter, the effects of chronic applications of KA in organotypic hippocampal slice cultures are described with regard to both their effect on function and toxicity.

Chapter 6 presents a discussion of the results obtained during the course of this investigation and attempts to elucidate the mechanisms consistent with data by which KA exerts it's effects within the hippocampus.

Chapter 1

Introduction

1.1 Excitatory amino acids

Glutamate has been recognised as being an excitatory neurotransmitter within the nervous system for over 30 years, but it has only become possible to clarify the roles of the excitatory amino acid receptors with the development of specific agonists and antagonists for these receptors (Watkins & Evans, 1981).

1.1.1 Excitatory amino acid receptors

The amino acid glutamate is the principal excitatory neurotransmitter of the mammalian nervous system (Somer & Seeburg, 1992). The receptors for this neurotransmitter can be broadly divided into ionotropic receptors, in which an intrinsic ion channel is present, and metabotropic receptors, whose activation in turn cause the activation of a G-protein.

The ionotropic class of glutamate receptors can be further subdivided on the basis of their pharmacological specificity for various agonists. This provides us with three classes of ionotropic glutamate receptor, those activated by NMDA, those activated by AMPA and those activated by kainate (KA). A more extensive (but by no means exhaustive) outline of the pharmacology of AMPA, KA and NMDA receptors is presented in table 1.

AMPA receptors gain their name from the fact that they have a high affinity for the compound DL-α-amino-3-hydroxy-5-methyl-4-isoxalone-propionic acid (AMPA). They contain an intrinsic ion channel, which is largely permeable to sodium and potassium ions but may pass some calcium under certain conditions.

Receptor channels	AMPA receptors	Kainate receptors	NMDA channels
Most selective agonist	**(*S*)-(-)-5-Fluorowillardiine** **AMPA** **Quisqualate** **CI-HIBO** (GluR1 & GluR2) **(*S*)-CPW 399**	**KA** **Domoate** **ATPA** (GluR5) **SYM 2081**	**NMDA** **Ibotenic Acid** **Spermidine trihydrochloride** (Polyamine site)
Mixed agonists	**Glutamate** **Aspartate**	**Glutamate** **Aspartate**	**Glutamate** Aspartate
Competitive antagonists	CNQX **DNQX** **GYKI 53655**	**CNQX** **DNQX** **LY293558** (GluR5) **NS102** (GluR6)	**D-AP5** **CPP**
Channel Blockers	———	———	**MK801** **Remacemide hydrochloride**

Table 1.1 Example of some of the pharmacological agents with activity at the ionotropic class of glutamate receptors. (Modified from Hammond 1996)

1.1.2 Structure of non-NMDA receptors

Early work to elucidate the structure of non-NMDA receptors utilised three basic approaches. It was assumed at first that their structure shared some homology with nicotinic acetylcholine receptors, and so cross-hybridisation techniques, such as screening cDNA libraries at low stringency, or the polymerase chain reaction (PCR) primed with oligonucleotide sequences which recognise conserved regions of muscle or neuronal nicotinic receptors were used (Barnard & Henley, 1990). Unfortunately, this approach proved to be fruitless since the binding regions of non-NMDA receptors exhibit little homology to those of nicotinic receptors.

More successful approaches involved the use of techniques such as expression cloning to isolate cDNA cloning receptor subunits from rat brain (Keinanen *et al* 1990), which could then be expressed in a vector such as Xenopus oocytes and screened electrophysiologically. The other successful approach involved the sequencing of receptors isolated by affinity chromatography (Shimazaki *et al* 1992, Brose *et al* 1994).

The non-NMDA glutamate receptors are thought to comprise of a tetrameric structure (Mano and Teichberg 1998, Rosenmund *et al* 1998), the subunits of which are all approximately 900 amino acid residues in length. Initial hydrophobicity studies suggested the existence of four transmembrane domains which were designated MD1-MD4, although later evidence suggests that MD2 does not actually cross the membrane but is either located within the cytoplasm or folds into a β-sheet which is buried in the membrane.

The N- and C-terminal domains of these receptors undergo alternative splicing. For example, the GluR1-4 subunits of AMPA receptors occur as 'flip' and 'flop' variants, which exhibit differences in their kinetics and pharmacology (Sommer *et al* 1990). In addition to this, the functional properties of AMPA receptor subunits can be modulated by the process known as RNA editing (Sommer *et al* 1991). The importance of this process is perhaps best seen with reference to the GluR2 subunit, which has been shown to confer a degree of impermeability to Ca^{2+} to receptors containing this subunit. This contrasts with the properties of GluR1,-3 and -4, which are relatively permeable to Ca^{2+}. This difference has been identified as being due to a single residue (the so called Q/R site) on the MD2 domain, where RNA editing converts the CAG codon which codes for glutamine (Q) in GluR1,-3,-4 to the CGG codon which codes for arginine in GluR2 subunits. KA receptors also appear to undergo additional RNA editing of the MD1 domain of GluR6 subunits at two sites, the I/V and Y/C sites (Bettler and Mulle 1995).

Mutagenesis studies have been used to characterise the structure/function relationships of the non-NMDA receptor subunits. As previously mentioned, the site controlling Ca^{2+} permeability has been identified as the Q/R site on the MD2 domain. Furthermore, it is known that two lobes are present which are separated by the region containing MD1-3 which show considerable homology with the amino acid binding site of bacterial proteins. It is postulated that the agonist binding site of the subunits are to be found in this domain, a proposal which is further strengthened by the work of Uchino *et al.* in 1992 who found that mutations at arginine-481 of the GluR1 subunit significantly

affected agonist binding. This is the only charged amino acid residue in the region of the N-terminal domain proposed as the agonist binding site which is conserved throughout the family of ionotropic glutamate receptors.

A further characteristic of native non-NMDA receptors is their rapid desensitisation in the presence of glutamate. Desensitisation is the process whereby there is a loss of ion channel gating despite the continued receptor occupancy by an agonist (Mayer *et al.*, 1991). This characteristic of AMPA receptors was first demonstrated in acutely isolated or cultured hippocampal neurones and spinal cord neurones (Kiskin *et al.*, 1986, Mayer and Vyklicky, 1989, Trussell *et al.*, 1988). The rate of desensitisation of AMPA receptors differs according to whether the receptor is a 'flip' or 'flop' splice variant, the 'flip' variant desensitising to a lesser degree than the 'flop' (Sommer *et al.*, 1990; Partin *et al.*, 1993).

1.1.3 Kainate Receptors

The existence of KA receptors has been known for over a decade when Agrawal *et al.* (1986) demonstrated that dorsal root fibres could be depolarised by glutamate or KA, but not by AMPA or NMDA. Since then the elucidation of their physiological function has been seriously hampered by the similarity in the pharmacology and biophysics of KA and AMPA receptors, owing to the fact that KA receptors are very often coexpressed in the same cells as AMPA receptors. However since the advent of compounds such as the 2,3-benzodiazepines which have a selective AMPA antagonist action the physiological roles of KA receptors have begun to be elucidated. The most selective of these is GYKI 53655 (Wilding *et al.*, 1995), a drug which has become a valuable tool in unmasking the physiological and biophysical effects of KA receptor activation.

Kainate receptors are encoded by two gene families, giving rise to the GluR5-7 and KA1 and KA2 subunits. These show significant structural homology to the AMPA receptor GluR1-4. The Glur5-7 subunits may express to form homomeric non-selective cation channels (Bettler *et al* 1990, Egebjerg *et al.* 1991, Schiffer *et al.* 1997) or may be coexpressed with KA-1 or KA-2 subunits to form heteromeric channels (Cui and Mayer 1999).

In the following sections I will discuss the structure of each of these subunits and their properties when assembled as homomeric receptors. Following this I will discuss the functional significance of various heteromeric combinations of KA receptor subunits.

1.1.3.1 GluR5

The GluR5 subtype of KA receptor undergoes alternative splicing giving rise to two forms, which have been classified as GluR5-1 and GluR5-2 (Bettler *et al* 1990). Of these, GluR5-1 is the longer, containing 15 amino acid residues more than GluR5-2 in the N-terminal region.

Further splice variants of GluR2 also occur. Introduction of an exon into the mRNA coding for the C- terminal domain of GluR5-2b gives rise to GluR5-2c, whereas the introduction of a stop codon results in the shortened GluR5-2a.

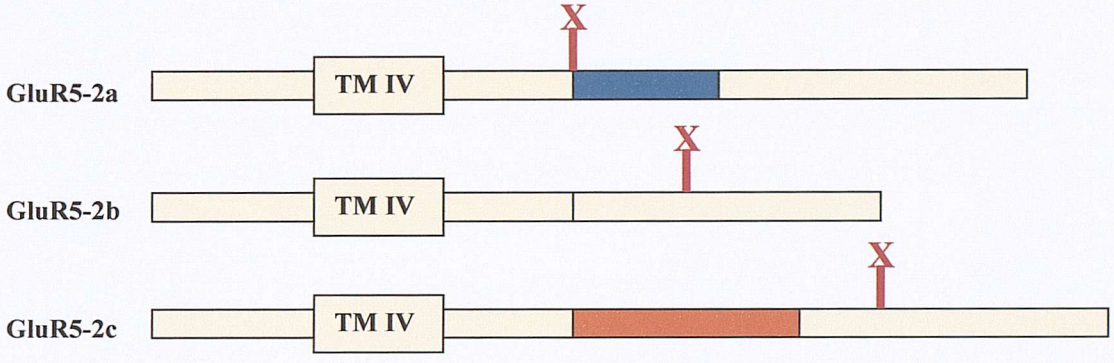

Figure 1.1 Diagram of the 3' end of the mRNA transcripts for the alternative splice variants of GluR5-2 coding for the C-terminal end of the receptor. The blue and orange boxes represent additional exons, whilst stop codons are represented by the red line and X, TM IV represents the coding region for the fourth transmembrane domain. (Adapted from Sommer *et al* 1992).

Further complexity is added to the array of GluR5 subtypes by the occurrence of RNA editing of the M2 domain of the receptor. This editing is similar to that seen in AMPA receptors, in which a glutamine (Q) residue at position 591 is substituted by an arginine (R) residue (Somer *et al* 1991). In the hippocampus it has been found that somewhere between 50-60% of the GluR5 subunits present in the adult are in the edited (GluR5(R)) form (Chittajalu *et al* 1999, Vissel *et al* 2001).

The editing of GluR5 does not affect KA binding, the K_d= 73.3 ± 19.2 nM irrespective of editing. With regard to channel properties of homomeric GluR5 receptors, it has been found (Sommer *et al* 1992) that the unedited version displays an inwardly rectifying I-V plot with a reversal potential close to 0mV when expressed in transfected HEK 293 cells. Co-expression of GluR5(R) with GluR5(Q) results in a linearisation of this I-V plot, which indicates the possibility of functional co-assembly of edited with unedited versions of this subunit.

In addition to this, homomeric GluR5(R) displays a lower single channel conductance (femtosiemens compared to picosiemens) than GluR5(Q) which is likely to

be as a result of the introduction of a ring of positively charged arginine residues into the channel pore. As would be expected, this also results in a reduced permeability to Ca^{2+}.

1.1.3.2 GluR6

Low-stringency hybridisation of a rat cerebellar cDNA library using the coding region from a GluR5 cDNA clone gave rise to the discovery of the GluR6 subunit (Egebjerg *et al* 1991). This subunit was found to be encoded for by a 4559 base pair cDNA which gave rise to a protein containing 884 amino acids, exhibiting 80% homology to the GluR5 subunit, but less than 40% homology to any of those for AMPA receptors.

Recordings from *Xenopus* oocytes in the presence of KA and glutamate showed GluR6 capable of assembling to form functional homomeric receptors which produced desensitising inward currents when held at –100mV. This desensitisation could be blocked by pre-treatment of oocytes with concanavalin A. The EC_{50} for KA in the presence of concanavalin A was found to be approximately 1μM, a value 35 fold lower than that for the GluR1 AMPA receptor subunit.

I-V plots revealed a reversal potential of 10 ±3mV, with a significant degree of outward rectification.

In a similar fashion to the GluR5 subunit, GluR6 may undergo Q/R editing of the M2 domain (Somer *et al* 1991) which changes the channel's properties in a manner reminiscent of GluR5. Thus the edited form of the subunit (GluR6(R)) displays a lower Ca^{2+} permeability (Egebjerg *et al* 1993). In addition to this, the GluR6(R) form, when expressed homomerically, displays a more linear I-V relationship than is seen with homomeric GluR6(Q).

The GluR6 subunit differs from GluR5 however, in that it may also undergo RNA editing in the TM I domain (Kohler *et al.* 1993) at two sites. Thus it is possible for the isoleucine (I) residue at position 536 to be edited in such a way as to be substituted for by a valine (V) residue and for the tyrosine residue at position 540 to be substituted for a cysteine.

The GluR6 subunit appears to interact with at least two components of the postsynaptic scaffolding protein complex, namely SAP-90/ PSD-95 and more weakly with SAP-97 (Garcia *et al* 1998, Mehta *et al* 2001). Binding of GluR6 to SAP-90 exhibits an absolute dependence on the presence of the last four C-terminal amino acids

1.1.3.3 GluR7

Until 1997 it was thought that the GluR7 subunit was incapable of forming functional homomeric channels (Bettler and Mulle 1995). However, Schiffer *et al* (1997) have shown that both GluR7a and GluR7b form functional receptor channels with a 10-fold higher EC_{50} for glutamate (5.9mM for GluR7a) than other AMPA or KA subunits. Homomeric channels comprising either splice variant also lack any significant affinity for the high affinity KA receptor ligand domoate.

The splice variants of GluR7 arise from the insertion of a 40 nucleotide cassette into the 3' end of the mRNA encoding for the TM IV domain. Thus the C-terminal end of GluR7b exhibits no significant homology for any of the other KA receptor subunits (Schiffer *et al* 1997).

In addition to being able to form functional homomeric channels, GluR7a was also shown to be able to co-assemble with the high affinity subunits KA-1 and KA-2 in HEK 293 cells to form functional receptors. Co-expression with either of these subunits did not significantly alter the channel properties of the receptor. The pharmacological profile was altered somewhat, in that high concentrations of AMPA (1mM) were able to activate the channel.

1.1.3.4 KA-1

The KA-1 subunit is composed of 956 amino acids with a relative molecular mass of 105 000 (Werner *et al.* 1991). The carboxy terminus bears a significant degree of homology to both the GluR1-4 subunits of AMPA receptors as well as to the KA binding proteins (KBP) of both the chick and frog. The N-terminal end however bears little similarity to either AMPA subunits or the KBPs.

When expressed in cultured cells, KA-1 shows a high affinity for the binding of KA (K_d= 4.7 ±0.7nM). The rank order of agonist potencies for various ligands was found to be KA> quisqualate > glutamate>> AMPA. To date there are no reports extant of the existence of a functional homomeric KA-1 receptor.

1.1.3.5 KA-2

Like the KA-1 subunit, KA-2 is unable to form a functional homomeric receptor assembly (Herb *et al* 1992). Encoded by the GRIK5 gene it is widely expressed throughout the CNS and binds KA with a K_d of approximately 15nM. GRIK5 has been

mapped to chromosome 1 in the rat (Szpirer *et al* 1994) and encodes a protein that exhibits approximately 68% amino-acid sequence homology to KA-1.

The C-terminal of the KA-2 subunit protein is able to bind with a K_d of 20nM to the SH3 and GK domains of SAP-90, possible *via* two proline rich domains within the C-terminus (Garcia *et al* 1998). This would tend to suggest that the clustering of KA-2 containing receptors may be mediated by the SAP-90/ PSD-95 complex of proteins.

1.1.4 Heteromeric KA receptor assemblies

All 5 KA receptor subunits appear to be capable of coassembly with each other. However, as will be discussed in the next section, the pattern of expression within the hippocampus suggests this promiscuous assembly does not necessarily occur. Furthermore, they do not appear to be able to form functional receptors with any of the AMPA receptor subunits (Partin *et al* 1993, Brose *et al* 1994).

Coassembly of the various KA receptor subunits changes the channel properties and pharmacological profile from those observed for homomeric assemblies. Thus, for example, expression of the KA-2 subunit with GluR5(Q) causes the receptor to desensitise more rapidly than homomeric GluR5(Q) receptors. In addition, the I-V plot becomes more linear (Herb *et al* 1992). Coexpression of KA-2 with GluR6 enables the channel to be activated by AMPA. This property is not observed in homomeric GluR6 receptors.

Expressing GluR5 with GluR6 in HEK 293 cells increases the sensitivity of the receptor to iodowillardine when compared to homomeric GluR5 (Cui and Mayer 1999). In addition to this, the peak response of homomeric GluR5(R) receptors increases from a few pico Amps (pA) to approximately 165pA when co-expressed with GluR6(Q). This response also shows strong outward rectification.

Changes in the rate of desensitisation also occur following the formation of GluR5/ GluR6 heteromers. Whilst both GluR5 and GluR6 exhibit rapid desensitisation and almost total when expressed homomerically, coexpression of, for example GluR5(Q) with GluR6(R) reduces the degree, if not the rate to onset of desensitisation.

The coexpression of GluR5(Q) with a mutagenised GluR7 to produce an edited Q/R site (Cui and Mayer 1999) results in the reduction of the biphasic rectification seen with heteromeric GluR5/GluR6 receptors. A change in rectification properties was also found to occur when the unedited (*i.e.* unmutagenised) version of GluR7 was co-expressed with GluR6(Q).

The ability of KA receptor subunits to coassemble in this seemingly promiscuous manner presumably increases the potential processing power of these assemblies significantly.

Having discussed the functional properties of both homomeric and heteromeric KA subunit assemblies, I will now describe the structure of the hippocampal formation in order to better understand the expression patterns observed for these subunits within the hippocampus (section 1.3).

1.2 The Hippocampus

The hippocampus is a part of the mesolimbic system located inferiorly to the temporal lobe. It can be divided into four simple cortical regions, namely the dentate gyrus; the hippocampus proper, which can be divided in the rodent into CA3, CA2 and CA1, and the subicular complex.

A photomicrograph of a transverse slice through the hippocampus may be seen in figure 1.2 below. The hilus, CA3 and CA1 regions are labelled, as are the various *strata* within the CA1 region.

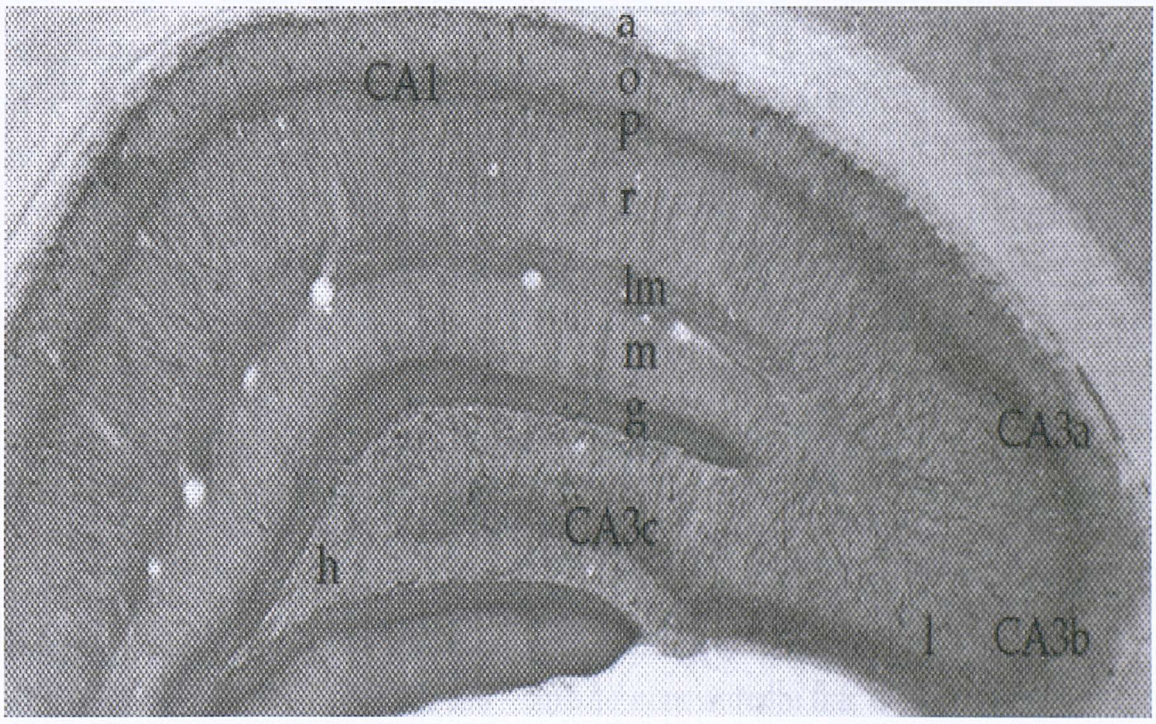

Figure 1.2: Photomicrograph of a hippocampal slice. Several strata are shown a: alveus; o: oriens; p: pyramidale; r: radiatum; lm: lacunosum moleculare; m: moleculare; g: granule cell layer; h: hilus. Areas CA3 c, b and a and CA1 are also shown.

One of the major cell types in the hippocampus is the pyramidal cell, the aggregation of which forms the stratum pyramidale of the hippocampus proper. They are oriented in such a way that their base faces the alveus. The basal dendrites of these cells comprise the stratum oriens, which is the layer of the hippocampus between the alveus and stratum pyramidale. Apical dendrites extend from the opposite pole of the pyramidal cells, forming the layers known as stratum radiatum, and the more distal stratum lacunosum-moleculare.

The basic circuit of the hippocampus originates in the entorhinal cortex, giving rise to the excitatory perforant pathway, which synapses onto the granule cells of the dentate gyrus. These cells give rise to mossy fibres, which ascend to the stratum radiatum of CA3, where they form *en passant* synapses with pyramidal cell dendrites. The pyramidal cells of CA3 give rise to the Schaffer collateral pathway, which provides the excitatory input to the pyramidal cells of CA1. In all these synapses, the excitatory amino acid glutamate is used as the neurotransmitter.

In addition to this excitatory pathway, there are a number of inhibitory interneurones, which are activated in both a feedforward and feedback manner by these excitatory neurones. In the stratum oriens may be found a species of interneurone known as the basket cells, which give off axons which form synapses mainly with the soma of the pyramidal cells, and to a lesser extent with the proximal dendrites. These cells are capable of inhibiting pyramidal cell activity via both feedforward and feedback mechanisms. A diagrammatic representation of this circuitry is shown below. Bordering the stratum oriens and the alveus can be found another type of interneurone known as an O/A interneurone. These are also involved in the feedforward and feedback inhibition of pyramidal cells (Knowles and Schwartzkroin 1981).

These cells, along with other interneurones such as bistratified cells, which synapse preferentially with dendritic shafts and spines (Halsay *et al.*, 1996) provide a means of self-regulation of neuronal excitability in the hippocampus via feed forward and feed back mechanisms. This inhibitory circuitry is outlined in figure 1.3 below.

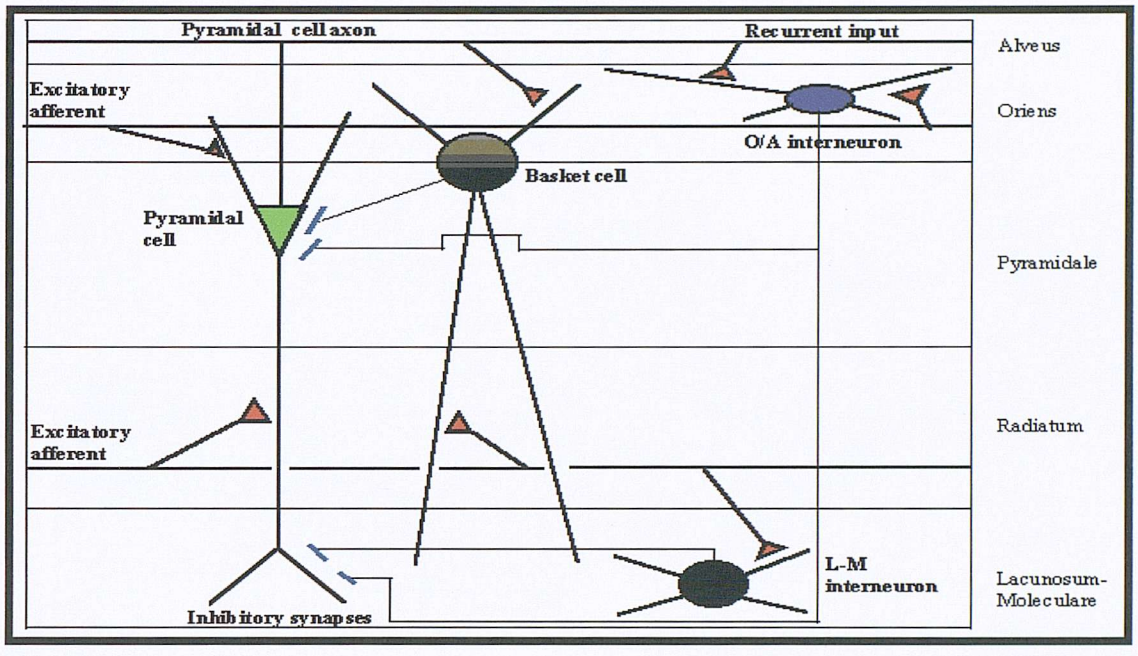

Figure 1.3: Diagram showing the layers of CA1region of the hippocampus, displaying the localisation of the pyramidal cells, inhibitory interneurones and their connections. Red triangles indicate excitatory synapses, and blue bars indicate inhibitory synapses. (From Schwartzkroin *et al.*, 1990).

1.2.1 Circuitry of the Hippocampus

The main circuit of the hippocampus is known as the tri-synaptic circuit (Andersen *et al.* 1966). The major excitatory input of the dentate gyrus arises in the entorhinal cortex and enters the dentate gyrus via the perforant pathway, where they synapse onto granule cells. These granule cells of the dentate gyrus give rise to mossy fibres that project to the CA3 region of the hippocampus, where they synapse onto the dendrites of the pyramidal cells in this region. These cells in turn give rise to axons, which form associational connections within CA3. In addition to these projections, the CA3 region gives rise to axon collaterals that form the major input to CA1. These are termed the Schaffer collaterals. This obviously is a gross oversimplification of the actual situation. For instance, the tri-synaptic path (figure 1.4) is not an open ended circuit, but instead there is a projection of axons from CA1 to the subiculum and also, to a lesser extent to the entorhinal cortex, thus closing the circuit. (Kohler 1986).

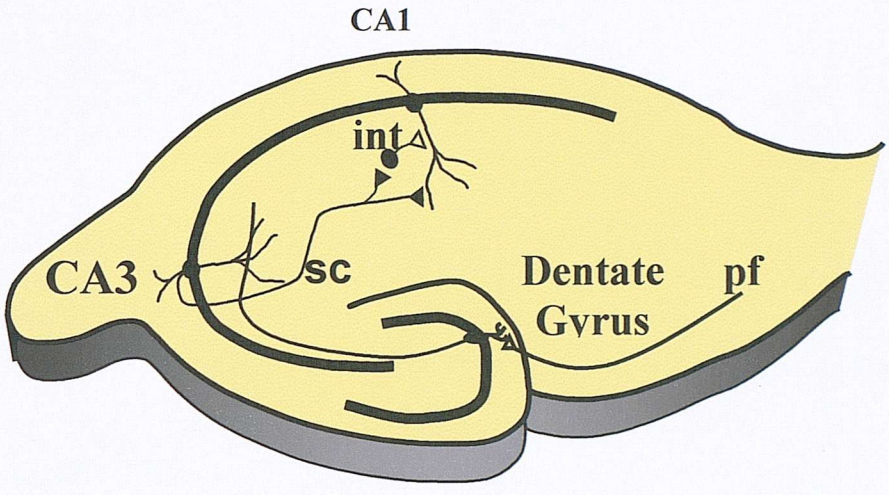

Figure 1.4 The tri-synaptic pathway. The diagram shows a cross section of the hippocampus, with pyramidal cells in the CA1, CA3 and the cells of the dentate gyrus: pf= perforant pathway; sc= Schaffer collateral pathway; int= interneurone.

In addition to this, the various regions of the hippocampus receive differentially weighted inputs from the preceding areas within the circuit (figure 1.5). This means that while the entorhinal cortex provides a heavy connection to the CA3 region of the hippocampus it also provides, to a lesser extent, a direct projection to CA1. Similarly, in addition to its major projection to CA1, the CA3 region provides a lesser projection to the subiculum, and so on around the circuit (Swanson *et al.*,1981).

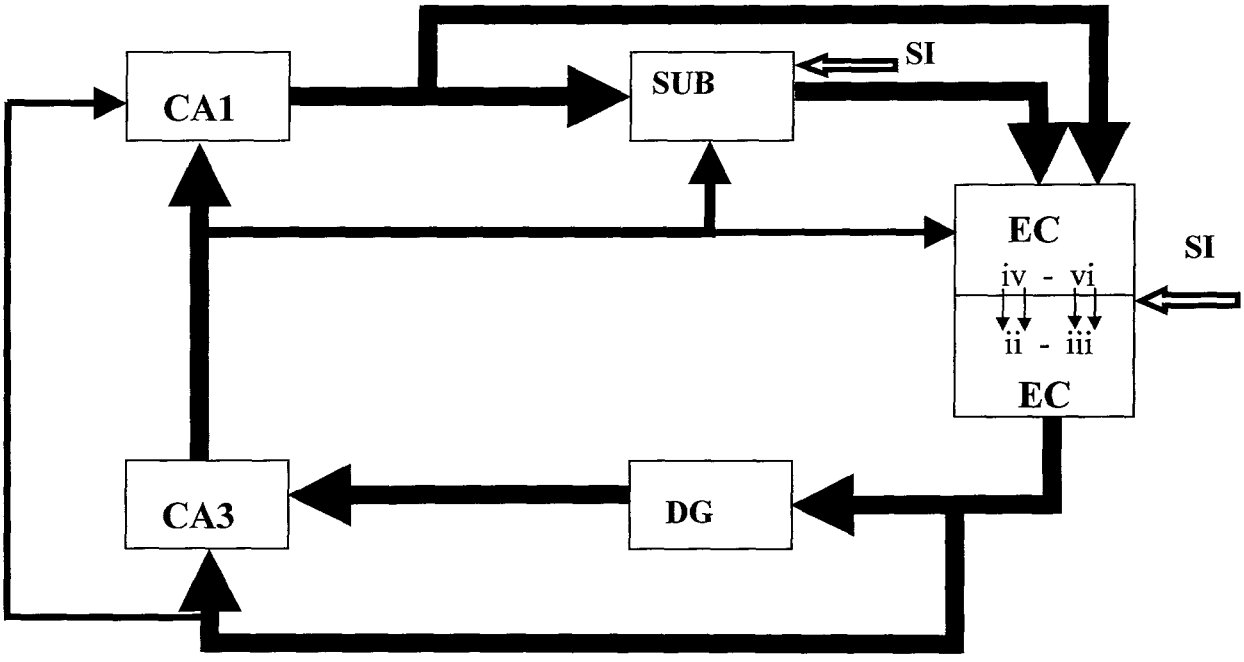

Figure 1.5 A diagrammatic representation of the differentially weighted projections found within the hippocampus. EC entorhinal cortex; DG dentate gyrus; SUB subiculum; SI sensory inputs. (Taken from Deadwyler *et al.*, 1988).

In the next section, the known distribution of the various KA receptor subunits within the hippocampus will be discussed.

1.3 Localisation of kainate receptors

Kainate receptors are known to be present throughout the both the central and peripheral nervous systems. Within the hippocampal formation, the subunit distribution of defined areas has been shown using *in situ* hybridisation and immunohistochemistry. Messenger RNA (mRNA) for the KA-1 and KA-2 subunits are by far the most abundant of the KA receptor transcripts found within the hippocampus (Wisden and Seeburg 1993), high levels of KA-1 mRNA being found in both the dentate gyrus and CA3 (Werner *et al* 1991), and KA-2 found abundantly throughout the CA1, CA3 and dentate. Interestingly, despite the current evidence for the role of GluR5 containing receptors in the modulation of synaptic activity in both the Schaffer collateral pathway and at the mossy fibre-CA3 synapse (Vignes *et al* 1998) and mediating somato-dendritic activation of CA1 interneurones (Cossart *et al* 1998), mRNA for GluR5 was barely detectable in the CA1 region and not detected in CA3 or the dentate gyrus (Wisden and Seeburg 1993).

Transcripts for the GluR6 subunit were detectable in the CA3 and CA1 and were moderately abundant in the dentate gyrus. A similar pattern was observed for GluR7 mRNA.

Using monoclonal antibodies raised to the KA-2 subunit and an antibody that recognised both GluR6 and to some extent GluR7 subunits, Petralia *et al* (1994) were able extend this information to elucidate the ultrastructural distribution of these KA receptor subunits. They found that the KA-2 subunit stained the CA3 pyramidal cell population more densely than those of CA1. The neuropil of the CA3 *stratum lucidum* was also densely stained with this antibody. In the dentate gyrus, the staining for KA-2 was most dense in the inner one third of the molecular layer and in hilar neurones. They also found a moderate staining pattern in non-pyramidal cells of the *stratum oriens* throughout CA3-CA1.

Staining with the GluR6/7 antibody was observed to occur again in the *stratum lucidum*, with CA3 pyramidal cells staining more densely than those in CA1, which correlates well with the findings of Egebjerg *et al.* (1991) for the levels of expression of mRNA for GluR6 in the hippocampus. Staining in these cells was found to be located on small dendritic spines. Similarly to the pattern seen for KA-2, the inner one third of the molecular layer exhibited the highest degree of staining for GluR6/7 in the dentate. The expression of GluR6/7 appeared to be more dense in hilar neurones than KA-2.

Double *in situ* hybridisation studies carried out by Paternain *et al* (2000) have shown a colocalisation of mRNA transcripts for both GluR5 and GluR6 in cells in both CA1 and CA3 which express mRNA for the GABA synthesising enzyme glutamic acid decarboxylase (GAD).

1.4 Physiological actions of KA receptors in the hippocampus

1.4.1 Postsynaptic actions of KA receptor activation

Using various pharmacological tools to dissect out the effects of KA receptor activation has shown them to exert two main effects within the hippocampus corresponding to either a presynaptic or postsynaptic locus of action. Postsynaptically, KA receptors have been shown to contribute to the EPSC evoked by glutamate release from mossy fibre synapses onto CA3 pyramidal cells (Vignes and Collingridge 1997 Nature). In addition to this, KA has also been shown to evoke an EPSP in interneurones within the

CA1 region (Frerking *et al.,* 1998; Cossart *et al.*, 1998), leading to an increase in interneuronal spiking *via* activation of KA receptors. Curiously, although functional KA receptors have been demonstrated on CA1 pyramidal cells (Bureau *et al.,* 1999), there would appear to be no resolvable KA receptor mediated EPSC in these cells.

Compared to the AMPA receptor mediated EPSC, the KA receptor mediated current is much smaller in peak amplitude and exhibits slower decay kinetics. This last property has led to the postulation of an extrasynaptic location for KA receptors at the mossy fibre-CA3 synapse. Credence was lent to this idea by the fact that repetitive stimulation of the mossy fibre pathway facilitated the KA mediated EPSC (Castillo *et al.*, 1997). However, since blocking uptake of glutamate does not appear to enhance the KA mediated EPSC (Castillo *et al.* 1997; Vignes *et al.* 1997) it is unlikely that KA receptors are located extrasynaptically on CA3 pyramidal cells. It is more likely that repetitive mossy fibre stimulation causes a use dependent facilitation of glutamate release from the mossy fibre terminals, thus enhancing the KA mediated EPSC.

Further evidence against the extrasynaptic location of KA receptors comes from studies performed in the thalamocortical slice preparation (Kidd and Isaac 2001). Taking advantage of the large size of the KA component of transmission at thalamocortical synapses in developing animals (postnatal days 3-9) they were able to show that neither increasing the amount of extrasynaptic glutamate by high frequency stimulation or blockade of glutamate transport nor increasing the rate of glutamate clearance from the synapse by increasing the experimental temperature had an effect on either the size or kinetics of the KA receptor mediated component at these synapses. Since these manipulations were without effect, they concluded that KA receptors at thalamocortical synapses were likely to be located within the synapse close to the site of glutamate release and did not sense glutamate diffusing from distant release sites (Kidd and Isaac 2001).

At present there are two principal hypotheses to explain the slow decay kinetics of KA receptors. Firstly it may simply be that heteromeric channels function differently to the more extensively studied homomeric channels, which exhibit fast decay kinetics. Alternatively it is possible that this feature may be due to the receptors being clustered by SAP90, a member of the PSD-95 (postsynaptic density 95) family of proteins. Garcia *et al.* (1998) have shown that SAP90 binds both GluR6 and KA2, causing the receptors to cluster. This leads to a reduction in steady state desensitisation although the mechanism for this negative regulation has not been elucidated. However, it would appear that a heteromeric assembly of GluR6/ KA-2 and SAP90 is more sensitive to this negative

regulation of desensitisation than a homomeric GluR6/SAP90 interaction alone (Garcia *et al* 1998). Kainate receptors have also been reported to be important for the induction of mossy fibre LTP (Borlotto *et al.,* 1999), although it is still unclear whether their role is obligatory or one of modulation.

More recently, Melyan *et al.* (2002) have demonstrated a metabotropically coupled KA receptor mediated regulation of the slow afterhyperpolarisation (I_{sAHP}) current found in CA1 pyramidal cells of 15-19 day old rats. The I_{sAHP} current occurs as a result of short bursts of activity within the pyramidal cell and is mediated by a Ca^{2+} dependent K^+ current (Lancaster and Adams 1986). Presumably therefore it's activation functions to limit the excitability of the pyramidal cell population.

Melyan *et al* (2002) found that application of nanomolar concentrations of KA of between 5 and 15 minutes in duration resulted in a long lasting inhibition of the I_{sAHP} current by approximately 35%. This inhibition persisted for up to an hour after the removal of KA from the recording chamber.

This inhibition was not reproduced by the application of the GluR5 agonist ATPA, but was blocked by both N-ethylmaleimide and calphostin C. These compounds block the action of pertussis toxin sensitive G proteins and protein kinase C (PKC) respectively. In addition, the application of 200nM KA was demonstrated to increase CA1 pyramidal cell excitability as measured by the spike frequency.

This suggests that a GluR6 containing KA receptor is present on rat CA1 pyramidal cells which is capable of increasing the excitability of these neurones *via* coupling to a pertussis toxin sensitive G-protein which activates PKC, leading to an inhibition of the I_{sAHP} current.

1.4.2 KA receptors and glutamate release

In addition to these postsynaptic actions of KA receptors, there is a growing body of evidence to support a presynaptic location for KA receptors. Presynaptic activation of KA receptors appears to exert a downregulatory effect on glutamate release from mossy fibre and Schaffer collateral terminals (Kamiya and Ozawa 2000, 1998) and also on the release of GABA from interneuronal terminals (Fisher and Alger, 1986; Frerking *et al.*, 1998).

Kamiya and Ozawa (1998, 2000) have shown that the reduction of glutamate release from Schaffer collateral terminals and more recently from mossy fibre terminals is due to a reduced Ca^{2+} influx into the terminal. In the case of the mossy fibre pathway it

would seem that this is at least in part due to an increase in mossy fibre excitability, which blocks action potential conduction and thus Ca^{2+} influx. A similar effect has been seen in primary afferent C-fibres (Agrawal & Evans 1986). Since there was no change in the size of the afferent volley recorded from the Schaffer collaterals this did not appear to be the mechanism for the downregulation of transmitter release in CA1. This is not to say that there are no "localised" depolarising effects of KA presynaptically on Schaffer collateral terminals. If presynaptic KA receptors were located in the vicinity of the presynaptic terminals this would be entirely possible without necessarily altering the afferent fibre volley.

It is also possible that KA induced depolarisation of the terminal causes Ca^{2+} to accumulate, thus leading to inactivation of the presynaptic Ca^{2+} channels. This would also lead to a reduction in transmitter release. However, resting levels of rhod-2 fluorescence did not increase in the Schaffer collateral terminals during 1μM KA application, so this would not appear to be the case (Kamiya & Ozawa 1998). Thus it would appear that more work is necessary in order to elucidate the exact mechanism of this KA-induced reduction in excitatory transmission.

More recently, the inhibitory nature of the KA receptor located on mossy fibres has been called into question in a study by Lauri *et al* (2001a). Using high frequency stimulation (25-100Hz) of the mossy fibre pathway in order to observe the effects of synaptically released glutamate at this receptor, they were able to show a concentration dependent reduction of the frequency dependent facilitation of mossy fibre transmission with the GluR5 antagonist LY382884. Thus it may be that under physiological conditions, the KA autoreceptor located on the mossy fibre pathway acts to facilitate the release of glutamate onto CA3 pyramidal cells in a frequency dependant manner. Furthermore, this autoreceptor has been demonstrated to play a role in the induction of NMDA independent LTP at the mossy fibre synapse (Lauri *et al* 2001b).

1.4.3 KA receptors and GABA release

It has been known for a number of years that KA is able to depress evoked GABAergic transmission (Fisher & Alger 1984). More recently this response has been shown to be mediated by KA receptors and is capable of being evoked both by the application of exogenous ligands (Frerking *et al.* 1998, Cossart *et al.* 1998) as well as endogenous glutamate (Min M-Y *et al*, 1999). However, the mechanism for this response is once again a matter of controversy. It is known that KA increases the frequency of

stimulus evoked synaptic failures at GABAergic terminals (Rodriguez-Moreno *et al.*, 1997). In addition to this Lerma's group also observed a reduction in miniature IPSC's during the application of KA in the presence of tetrodotoxin (TTX) (Rodriguez-Moreno *et al.* 1997, Rodriguez-Moreno & Lerma 1998). These two factors both indicate a presynaptic locus for the mode of action of KA.

Rodriguez-Moreno & Lerma (1998) then went on to show that the KA evoked reduction in GABAergic transmission could be prevented by the application of pertussis toxin (a blocker of the G-proteins G_i and G_o) and inhibitors of protein kinase C (PKC). As KA has not been demonstrated to be an agonist at metabotropic glutamate receptors, this result may well lend credence to the idea that some KA receptors may act *via* a G-protein (Cunha *et al.* 1999).

Thus one model (figure 1.6) to explain the downregulation of GABA release by KA receptor activation postulates a signalling cascade beginning with the activation of a G-protein linked presynaptic KA receptor which activates phospholipase C (PLC) which leads to PKC activation *via* diacylglycerol (DAG). PKC, *via* as yet unknown intermediaries downregulates GABA release probably by modulating presynaptic Ca^{2+} channel activity.

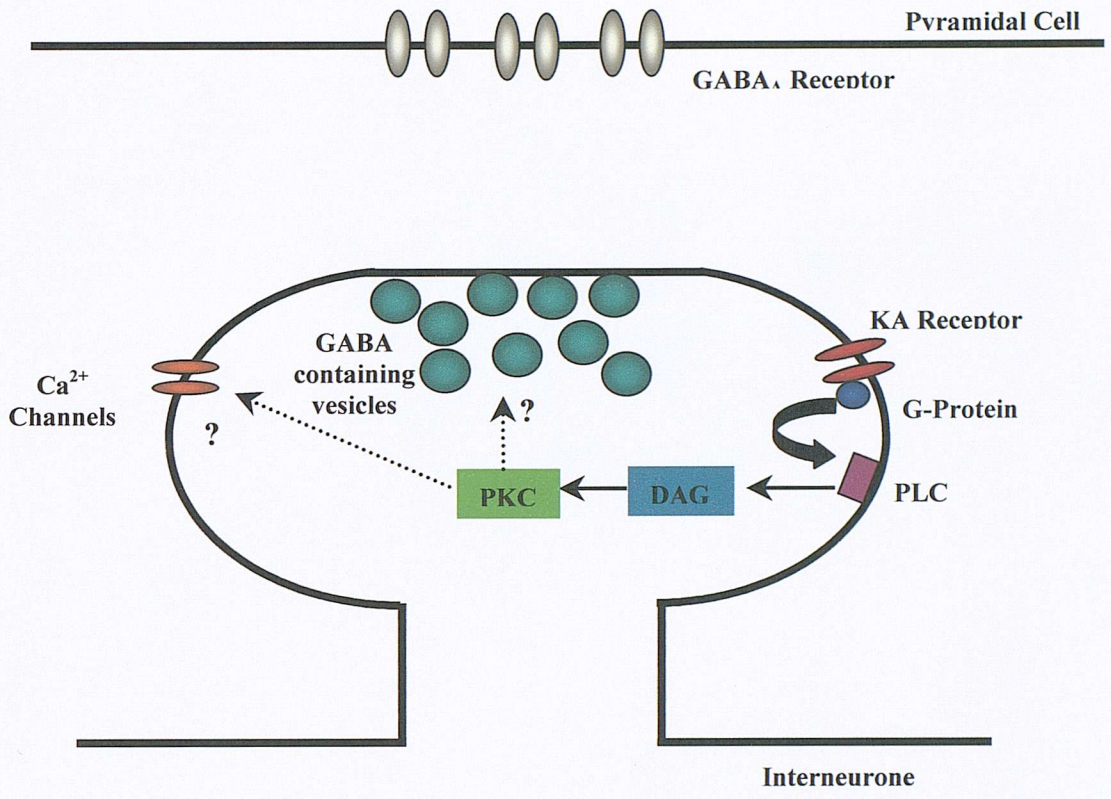

Figure 1.6 One of the two contending hypotheses as to how KA receptor activation results in the downregulation of GABA release from interneuronal terminals (Rodriguez-Moreno and Lerma 1998, Cunha *et al* 1999). Activation of G-protein coupled KA receptors located presynaptically on interneuronal terminals results in the activation of PLC. This in turn leads to the formation of DAG (as well as IP_3). The formation of DAG leads to activation of PKC, resulting in a reduction in GABA release by an as yet unknown mechanism. (Adapted from Frerking and Nicholl 2000)

The contending hypothesis (figure 1.7) to explain this phenomenon takes into consideration the fact that postsynaptic KA receptor activation on interneurones increases their activity. This increased interneuronal spiking may elevate the concentration of GABA diffusing from the synapse sufficiently to bring about the activation of $GABA_B$ receptors, which in turn may modulate presynaptic Ca^{2+} influx. Reduced Ca^{2+} influx then results in a reduction of GABA release from the terminal. In support of this hypothesis, Frerking *et al.* (1999) found that antagonising $GABA_B$ receptors reduced the inhibition of GABA release by approximately 50%.

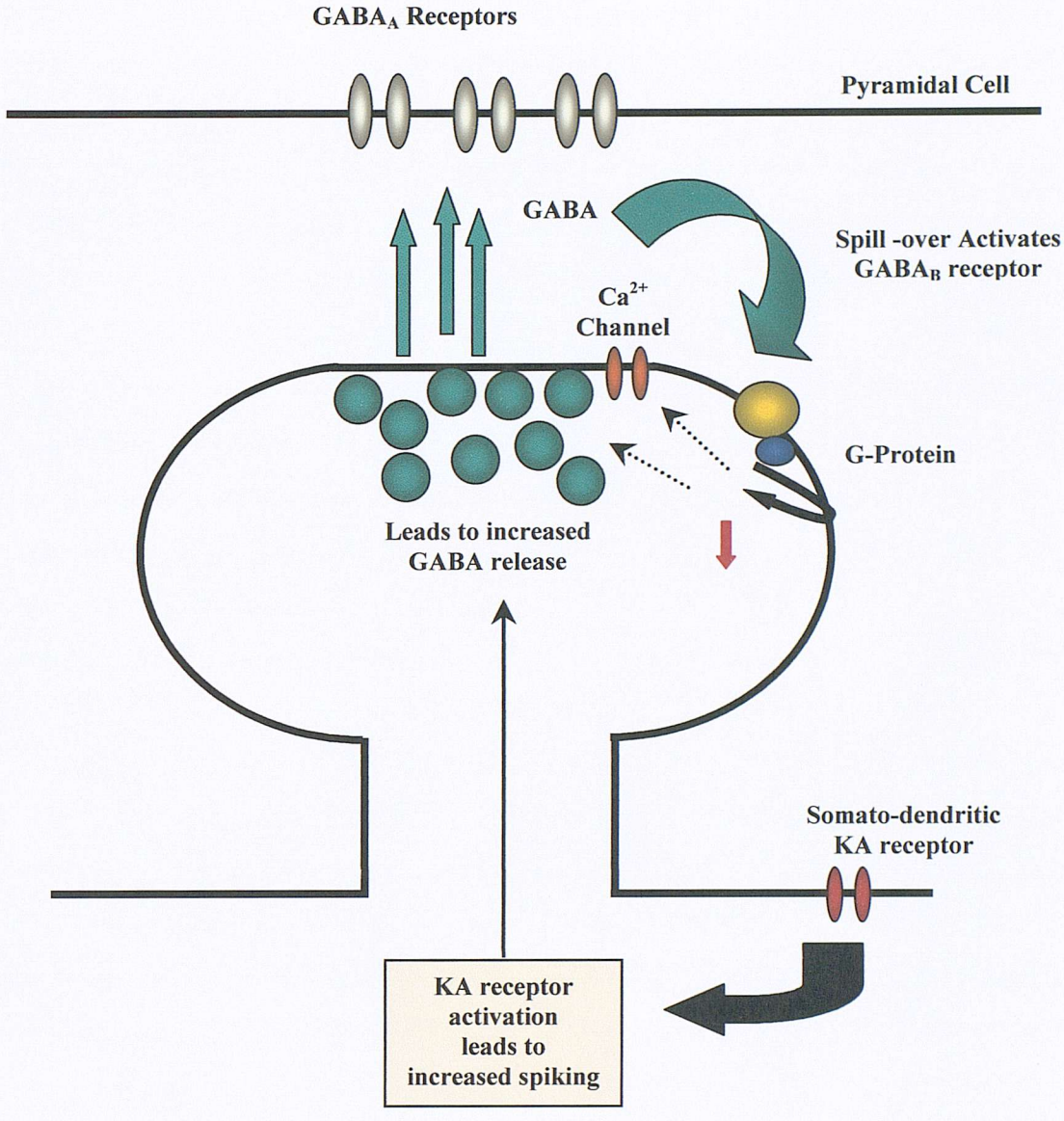

Figure 1.7 Alternative hypothesis as to how GABA release is reduced following KA receptor activation in interneurones (Frerking *et al.* 1998). Increased activation of interneurones *via* somato-dendritic KA receptor activation leads to an increase in GABA release from the terminal. Spillover of GABA from the synaptic cleft activates pre-synaptic $GABA_B$ receptors leading to a reduction in further GABA release.

From the preceding sections can see that KA receptors may play a modulatory role in both excitatory and inhibitory transmission in the hippocampus, as well as contributing to the postsynaptic depolarising response to glutamate release in CA3 and in GABAergic interneurones.

It would appear from recent evidence (Cossart *et al* 2001, Mulle *et al* 2001) that, in addition to reducing the release of GABA at inhibitory synapses with pyramidal cells, KA receptor activation on the presynaptic terminals of interneurones synapsing with other

interneurones is capable of facilitating GABA release. This may suggest further evidence supporting the $GABA_B$ model for KA receptor modulation of GABA release (figure 1.9).

Cossart *et al* (2001) found that the frequency of miniature IPSCs (mIPSC) recorded from interneurones increased in the presence of 250nM KA. The failure rate of evoked IPSCs (eIPSC) decreased at the same concentration of KA. Bath application of the GluR5 agonist ATPA did not result in a similar reduction in the number of failures, nor did AMPA or NMDA show any significant effect. A similar response could be elicited by delivering trains of stimuli to the Schaffer collateral pathway, implying that synaptically released glutamate was capable of increasing the inhibition of the interneuronal population in CA1. Furthermore, since the PKA/PKC inhibitor staurosporine did not block the increase in mIPSC frequency in the presence of KA, and PKC has been implicated in the signalling pathway of G-protein coupled KA receptors (Rodriguez-Moreno & Lerma 1998, Melyan 2002), they concluded that this effect was likely to be mediated by ionotropic rather than G-protein coupled KA receptors.

A similar facilitation of GABA release onto *stratum radiatum* interneurones was observed in both wild type and $GluR5^{-/-}$ mice by Mulle *et al* (2001) which was not present in $GluR6^{-/-}$ mice. This, coupled with Cossart *et al* (2001) observation that ATPA did not elicit the same response as KA would tend to suggest that this facilitatory effect is mediated *via* a GluR6 containing receptor without the involvement of the GluR5 subunit. It is not clear however as to whether this receptor is homomeric for GluR6 or is a heteromer containing one of the other KA receptor subunits.

It is possible however, that this facilitation of GABA release onto interneurones may occur as a result of KA receptor mediated interneuronal axon depolarisation thus leading to disinhibition of the network. This has recently been demonstrated to be the case in the guinea pig hippocampus by Semyanov and Kullmann (2001). Using whole cell patch clamp recordings from *stratum radiatum* interneurones under voltage clamp (in the presence of antagonists for AMPA, NMDA, $GABA_B$ and group III mGluRs) they were able to show that low concentrations of KA (between 250nM and 1μM) reduced the threshold for antidromically evoked action currents (ACs) following stimulation of the *stratum oriens* with a monopolar stimulating electrode. KA also increased the frequency of spontaneous ACs, a phenomenon which was independent of the holding potential at the soma. This further suggests an axonal location of the receptors responsible for this phenomenon.

Semyanov and Kullmann (2001) also demonstrated a physiological relevance for these receptors using a conditioning train of stimuli (5 pulses at 100Hz) to the Schaffer collateral pathway in order to raise the extracellular concentration of glutamate. Following this stimulation protocol, stimulation in *stratum oriens* resulted in an increase in the success rate for the evocation of an antidromic AC, indicating that an increase in extracellular glutamate was capable of increasing fibre excitability thus increasing the probability of successful antidromic ACs.

1.4.4 KA receptors and synaptic plasticity

KA receptors have been implicated in the induction of mossy fibre long-term potentiation (LTP), a form of LTP which has been shown to be independent of NMDA receptor activation (Nicoll and Malenka 1995). Bortolotto *et al* (1999) have shown that the GluR5 specific antagonist LY382884 blocks the induction of mossy fibre LTP, thus highlighting the importance of GluR5 containing receptors for the induction of this form of LTP. Mulle *et al* (1998) also found this phenomenon to be absent in GluR6$^{-/-}$ mice, which tends to imply that the receptor involved in this repsonse is a heteromer containing at least GluR5 and GluR6 subunits. However, Contractor *et al* (2001) observed no change in the induction of mossy fibre LTP in GluR5 knockout mice, but found a significant reduction in mossy fibre LTP in GluR6 knockouts. Thus the subunit composition of the receptors responsible for mossy fibre LTP remain controversial.

It would also appear that editing of the Q/R site of the GluR6 subunit is an important factor in the induction of NMDA receptor independent LTP at the medial perforant path-dentate granule cell synapse. Vissel *et al* (2001) generated mutant mice which were deficient in the Q/R editing site and compared them to wild type mice. This mutation reduced the occurrence of edited GluR6 transcripts by around 95%, allowing them to assess the functional importance of editing of GluR6 subunits in the adult mouse. As would be expected, reduction in the degree of Q/R editing of GluR6 subunits results in the increased permeability of GluR6 containing receptors to Ca^{2+}. It was found that it was possible to induce NMDA independent LTP at this synapse only in the mutant mice.

In addition to the possible physiological roles delineated above, KA has been used for a number of years as a potent neurotoxin. Therefore, the next section will expand on the theme of KA and pathology.

1.5 KA toxicity

The neurotoxic effects of KA have been known for a number of years (Schwob *et al* 1980, Heggli *et al* 1981, Lothman *et al* 1981), although the exact mechanisms by which KA causes cell death are unclear.

A number of mechanisms have been implicated in the neurotoxic actions of KA. For example, activation of NMDA receptors in populations of cells susceptible to excitation by KA (Berg *et al* 1993, Baran *et al* 1994) is thought to lead to an increase in oxygen-free radical production (Lafon-Cazal *et al* 1993) following an increased influx of Ca^{2+}. In support of this hypothesis, Bruce and Baudry (1995) have reported increased levels of lipid peroxidation and protein oxidation in the hippocampus of rats at 8 and 16 hours after the induction of KA seizures. In addition, they reported that KA administration increased the activity of two transcription factors (activator protein-1 and NFκB) which have previously been reported to be markers for cellular stress (Pinkus *et al* 1996, Schmitz *et al* 1995). Furthermore, KA toxicity is blocked by compounds such as EUK-134, which exhibit superoxide dismutase and catalase activity (Rong *et al* 1999).

Production of oxygen-free radicals can lead to DNA damage, giving rise to base mismatching. Indeed, hydroxyl and superoxide free radicals appear to selectively target guanine and thymidine (Belloni *et al* 1999). Intra-amygdala administration of KA has been demonstrated to result in DNA fragmentation (Henshall *et al*, 2000), although it is likely that this phenomenon is a consequence rather than a cause of a KA-induced cell death process.

DNA fragmentation is one of the features of cell death observed during apoptosis, as is induction of the p53 tumour suppressor gene (Sakhi *et al* 1997). The transcriptional activity of p53 has been shown to be upregulated following KA-induced excitotoxicity (Liu *et al* 1999). This may lead to increased expression of the *bax* gene, the product of which causes a release of cytochrome C from the mitochondrion into the cytoplasm (Gross *et al* 1999). When this binds to a complex of Apaf-1 and caspase-9, it causes a subsequent activation of the pro-apoptotic caspase-3 (Liu *et al* 2001). This cleaves aspartate residues in a number of essential proteins, leading to cell death (Liu *et al* 2001).

1.6 The KA lesion model of Temporal Lobe Epilepsy

Approximately 60% of people with pharmacologically intractable epilepsy suffer from temporal lobe complex partial seizures, a condition that is very often associated with

selective lesions of the various sub-fields of the hippocampus. This is also known as hippocampal sclerosis.

There are three basic stances that can be taken in relation to the importance of hippocampal sclerosis. It may be that hippocampal sclerosis is not involved in the causation of seizures, but occurs rather as a consequence of them. Alternatively it may be that the lesion occurs prior to the onset of seizures and is the direct cause of temporal lobe epilepsy. The third view takes the middle ground and postulates that hippocampal sclerosis is a progressive condition which develops in tandem with temporal lobe epilepsy as increasing numbers of selectively vulnerable neurones are lost (Frank 1993).

In order to investigate the specific role of hippocampal sclerosis it is possible to produce an artificial lesion using kainic acid. This may be administered either intra-ventricularly (Nadler *et al* 1978, Cornish and Wheal 1989, Best *et al* 1993)) or intra-peritoneally (Feank and Schwartzkroin 1984) *in vivo* or may be added to the medium bathing organotypic hippocampal cultures (Best *et al* 1996).

The patterns of damage and plasticity produced by kainic acid administration vary depending on the route of administration. When administered systemically, kainic acid produces variable bilateral damage of the subfields in the hippocampus. Typically there is cell loss from CA3, but there is often loss of pyramidal neurones from CA1. This may be the result of a direct excitotoxic action of KA on CA3 pyramidal cells, in turn inducing acute recurrent seizures throughout the limbic system, causing damage in CA1.

Similar to the pattern of pathology in hippocampal sclerosis, glutamic acid decarboxylase (GAD) containing interneurones are not affected by systemic KA injection, although somatostatin containing interneurones are also not affected, which is a point where the model diverges from the actual situation. Mossy cells of the dentate gyrus are also damaged, as can be seen by a dense band of terminal degeneration within the inner molecular layer of the dentate gyrus (Frank 1993).

A further similarity to temporal lobe epilepsy is the growth of a recurrent mossy fibre pathway from the dentate granule cells to the inner molecular layer.

Intraventricular (ICV) injection of kainic acid again causes a loss of CA3 pyramidal cells as well as a population of hilar neurones in the dentate gyrus (Nadler *et al* 1978, Nadler *et al* 1980, Shetty and Turner 1999). Again CA1 pyramidal cells are spared, however, due to synaptic reorganisation, the pyramidal cell population of the CA1 region becomes hyperexcitable. This phenomenon is linked to an increase in NMDA mediated excitation of CA1 pyramidal cells (Turner and Wheal 1991) coupled with a decrease in

inhibitory mechanisms (Williams *et al* 1993). Administration of KA *via* this route also appears to cause a permanent reduction in the number of interneurones expressing GAD-67 in all subfields of the hippocampus and dentate gyrus (Shetty and Turner 2001) although the number of interneurones revealed using the Nissl stain cresyl violet do not change significantly post-lesion. However, a reduction in GAD-67 expression presumably implies a reduction in the effectiveness of GABAergic transmission within the hippocampus, which would be expected to contribute to the hyperexcitable condition which occurs.

1.7 Other receptor types within the hippocampal formation

Since KA receptors are not found in isolation at the various synapses within the hippocampus, the following section will deal with those that have been investigated with respect to the actions of KA in subsequent chapters. The NMDA and metabotropic glutamate receptors will be described first followed by inhibitory GABA receptors and finally the neuromodulatory adenosine receptors.

1.7.1 The NMDA receptor

The NMDA receptor family is comprised of at least five subunits, namely NR1 and NR2A-D (Ozawa *et al.* 1998). These subunits vary in length from between 938-1482 amino acids. The NR1 subunit is expressed throughout the central nervous system (CNS). NR2A and B are found in high levels in the cortex and hippocampus in addition to other brain regions. The expression of NR2C and NR2D within the hippocampus appears to be mainly restricted to a specific subset of interneurones (Monyer *et al.* 1994)

One of the key features of NMDA receptors is that at hyperpolarised membrane potentials they exhibit a channel blockade by Mg^{2+} ions (Mayer *et al.* 1984, Nowak *et al.* 1984). Thus at a membrane potential of around –80mV their current flow is negligible, only reaching a maximal level at between –20 to –30 mV.

In addition to allowing the passage of Na^{+} and K^{+} ions, NMDA receptors display a high permeability to Ca^{2+} ions (MacDermott *et al* 1986, Mayer and Westbrook 1987). This permeability to calcium appears to be due to the presence of an asparagine residue in the M2 domain in the region which corresponds to the Q/R editing site of AMPA receptors (Burnashev *et al.* 1992). This site also appears to have a role in the degree of Mg^{2+} block, although the subunit composition of the receptor also appears to be an important factor. Thus NMDA receptors composed of an NR1 subunit and either NR2A or NR2B appear to

be more sensitive to Mg^{2+} blockade than those in which the NR2C or NR2D receptors are present (Monyer *et al.* 1992, 1994). It is also known that NMDA receptors exhibit an absolute requirement for glycine for channel opening to occur (Kleckner and Dingledine 1988).

NMDA receptors have been shown to play a role in the induction of both long-term potentiation (Neumann *et al* 1987, Bliss and Collingridge 1983) and long-term depression (Desmond *et al.* 1991, Mulkey and Malenka 1992). In addition to this, activation of NMDA receptors, and the resultant influx of Ca^{2+}, appears to be an important factor in the initiation of excitotoxic cell death (Peterson *et al.* 1989, Abele *et al* 1990).

1.7.2 Metabotropic glutamate receptors

In addition to the ionotropic class of glutamate receptors outlined above, there is a further class of glutamate receptors known as metabotropic glutamate receptors (mGluRs) which are linked to the activation of G-proteins.

These have been classified of the basis of their structural homology and signal transduction pathway into three groups, namely group I (consisting of mGluR1 and mGluR5), group II (consisting of mGluR2 and mGluR3) and group three (consisting of mGluR4, mGluR7 and mGluR8). Each subtype, in much the same way as other G-protein coupled receptors, possesses 7 transmembrane spanning domains consisting of between 854 and 1179 amino acids. All mGluRs tend to possess a large extracellular N-terminal and an intracellular C-terminal the length of which varies depending upon the subtype in question (Ozawa *et al.* 1998)

It has been suggested (Pin *et al* 1994) that the second intracellular loop, which is not well conserved between subtypes, confers a degree of specificity as to the type of G-protein to which the receptor couples. It may also be the case that the well conserved first and second intracellular loops play a role in G-protein activation.

As previously mentioned, mGluRs are categorised on the basis of their signal transduction pathway as well as their sequence homology. Thus we find that group I mGluRs positively couple to phospholipase C (PLC), leading to an increase in the production of inositol trisphosphate (IP_3), which causes a release of Ca^{2+} from intracellular stores (Gereau and Conn 1995, Bruno *et al* 1995).

Both group II (Wright and Schoepp 1996) and group III (Schoepp *et al* 1995) mGluRs are negatively coupled to adenylate cyclase, an effect which has been shown to

be pertussis toxin (PTX) sensitive. This suggests that a G-protein of either a G_i or G_o type is involved in this signalling pathway.

Within the hippocampus, mGluRs may be found both pre- and post-synaptically. Group I mGluRs have been localised to hippocampal pyramidal cells using immunohistochemistry (Luján *et al* 1996) where they modulate the activity of a number of K^+, Ca^{2+} and non-selective cation channels (Conn and Pin 1997) leading to an increase in neuronal excitability. In addition to this, presynaptic mGluRs are thought to downregulate transmitter release. For example group I and III mGluRs are found on the terminals of the Schaffer collateral pathway (Gereau and Conn 1995), whereas group II and III mGluRs are found located presynaptically on the terminals of both the mossy fibre pathway and the perforant path synapse with dentate gyrus granule cells (Shigemoto *et al.* 1997).

Group I mGluRs have also been shown to mediate a slow excitation of oriens-alveus interneurones in the CA1 (van Hooft *et al* 2000). In contrast to this Semyanov and Kullmann have found the group III agonist L-(+)-2-amino-4-phosphonobutyric acid (L-AP4) to reduce GABAergic signalling among interneurones in CA1. This effect could be mimicked by the administration of brief trains of stimuli to the Schaffer collaterals and was blocked by the group III antagonist α–methylserine-O-phosphate (MSOP). They concluded that this effect was likely due to activation of presynaptic group III mGluRs on interneuronal terminals.

1.7.3 The $GABA_A$ receptor

Inhibitory neurotransmission in the CNS is mainly mediated by gamma amino butyric acid (GABA). Fast inhibitory mechanisms act via the $GABA_A$ receptor, which comprises a family of 5 subunits encoded by up to 16 genes. These subunits, each of which possess four transmembrane domains, have been named α, β, γ, δ and ε (Sieghart 1995). Each of these subunits posses 4 transmembrane domains, and it is thought that they coassemble to form a pentameric structure similar to the nicotinic acetylcholine receptor (Nayeem *et al.* 1994).

Binding of two molecules of GABA to the receptor causes a rapid and transient increase in the permeability to chloride ions. This causes an increase in the Cl^- conductance of the neurone, which in turn tends to inhibit the firing of the cell.

In addition to a GABA binding site, the $GABA_A$ receptor possesses a number of distinct sites capable of binding various substances such as benzodiazepines and barbiturates. These are capable of allosterically modulating the activity of the ion channel.

1.7.4 The $GABA_B$ Receptor

The $GABA_B$ receptor is a 7-transmembrabe domain protein capable of coupling to a G-protein (Hill *et al.* 1984), the activation of which leads to the inhibition of adenylate cyclase (Wojcik *et al.* 1984). Postsynaptically this results in the opening of a K^+ channel, leading to the hyperpolarisation of the cell membrane (Dutar and Nicoll 1988). This event follows activation of a G_i protein. However, $GABA_B$ receptors are also located presynaptically both on glutamatergic and GABAergic terminals within the hippocampus (Nicholl *et al.* 1990, Thompson 1994), where their activation leads to a downregulation of transmitter release. This modulation of trasmitter release occurs as a result of both the inhibition of Ca^{2+} channel activity, probably *via* activation of a G_o protein (Costa *et al* 1998), and also *via* an increased K^+ conductance (Thompson and Gähwiller 1992).

To date, two $GABA_B$ receptor subunits have been identified, $GABA_B1$ (GB1) and $GABA_B2$ (GB2) (Kaupmann *et al* 1997, Jones *et al* 1998). These subunits share approximately 35% sequence identity and are related to the family 3 G-protein-coupled receptors, which includes both metabotropic glutamate receptors and calcium-sensing receptors (Galvez *et al 2001).* Two splice variants of the GB1 subunit have been demonstrated to exist and have been termed GB1a and GB1b (Kaupmann *et al* 1997). Of these, GB1b is the shorter (844 amino-acids), differing from the 960 amino-acid GB1a variant at the amino-terminal end. $GABA_B$ receptors have been shown to function as heterodimers composed of both GB1 and GB2 subunits (Jones *et al* 1998). Within this heterodimer, the GB1 subunit N-terminus is the site of ligand binding, whilst the GB2 subunit N-terminus translates that binding into receptor activation (Galvez *et al* 2001). Furthermore, it is the GB2 subunit that appears to be responsible for G-protein coupling, however the presence of the GB1 subunit increases the G-protein coupling efficacy (Galvez *et al* 2001).

1.7.5 Adenosine receptors

Adenosine plays a major neuromodulatory role within the CNS. Activation of A_1 receptors has been shown to be both anticonvulsant (Young and Dragunow 1994) and neuroprotective (Schubert *et al* 1997). In contrast to this, A_2 receptor activation (more

specifically A_{2A} activation) leads to a facilitation of synaptic activity, for example, in the CA3 region of the hippocampus (Goncalves *et al* 1997).

The inhibitory role of the A_1 receptor is mediated mainly by a presynaptic action, but also exhibits some activity within the postsynaptic cell (de Mendonca *et al* 2000). Presynaptically there is a reduction in Ca^{2+} influx, leading to a reduction of transmitter release whereas postsynaptically an increase in a K^+ conductance occurs resulting in hyperpolarisation of the postsynaptic neurone. However, this latter effect is more readily observed in neurones derived from embryonic animals rather than adults (Thompson *et al* 1993).

Adenosine A_1 receptors have been shown to couple to the G_i/ G_o class of G-protein (Cunha 2001) leading to a decrease in cAMP formation *via* inhibition of adenylate cyclase. However, it appears likely that the presynaptic regulation of transmitter release by A_1 receptors occurs *via* a direct connection between G-protein activation and the activity of mainly N-type Ca^{2+} channels (Wu and Saggau 1994).

The A_{2A} receptor has been shown to couple predominantly to the G_s class of G-protein (Olah 1997). Thus A_{2A} activation leads to an increase in activity of adenylate cyclase, leading to facilitation of the activity of P-type Ca^{2+} channels.

1.8 Aims

The general aim of this study is to investigate the mechanisms underlying the physiological versus the pathological effects of KA using acute and chronic applications of KA to the hippocampus.

More specifically these aims were to:

1. Determine how acute (15-30 minute) applications of KA affect evoked field potentials from the CA1 of rat hippocampal slices.
2. Evaluate the role of GluR5 and GluR6 containing receptors in these responses using subunit selective agonists and antagonists.
3. Compare the effects of KA (1μM) to those of an AMPA receptor specific agonist in order to assess the specificity of this concentration of KA for KA receptors.

4. Assess the role of the CA3 in driving responses in CA1 during KA application. This was achieved by repeating experiments in slices from which the CA3 and dentate gyrus had been excised.
5. Investigate the potential involvement of metabotropic glutamate receptors, $GABA_B$ receptors and adenosine receptors as indirect mediators of the responses observed with KA using receptor selective antagonists during co-application with KA.
6. Compare and contrast the evoked field population spike responses and paired-pulse inhibition from acute rat and mouse slices with mouse organotypic hippocampal slice cultures.
7. Determine the effects of longer duration (2 hour) KA applications on the evoked field population spike responses in the CA1 and CA3 of these cultures.
8. Evaluate the toxicity of chronic (24 hour) applications of 1μM KA to organotypic cultures, and if subtoxic, will it induce tolerance to subsequent applications of toxic concentrations of KA (Best *et al* 1996).
9. Investigate how chronic applications of 1μM KA affect physiological function in both the CA1 and CA3 of organotypic hippocampal slice cultures.

Chapter 2

Methods

The hippocampal slice preparation provides an ideal model by which to study the physiology and pharmacology of an intact network of neurones. The basic circuitry has been elucidated as outlined in the previous chapter, and comprises of a basic excitatory glutamatergic pathway. This has been termed the trisynaptic pathway. In addition, the output of this excitatory pathway is modulated by a number of GABAergic interneurones. These are activated in both a feed forward and feedback manner.

According to Andersen *et al* (1971) the circuitry of the hippocampus is organised into discrete lamellae. This enables an intact "functional unit" of the hippocampal network to be isolated by transverse section and maintained for a number of hours in a recording chamber as acute slices or subjected to organotypic culture and maintained in a viable state for several weeks.

2.1 Acute Slices

Electrophysiological experiments were performed on acute slices from 15-19 day old male Wistar rats. These slices were prepared in the following way:

Whole brains were dissected from 15-19 day old Wistar rats killed by terminal halothane anaesthesia and placed into ACSF (in mM: NaCl 117.8, $NaHCO_3$ 26.0, KCl 3.3, KH_2PO_4 1.3, $MgSO_4.7H_2O$ 1.0, $CaCl_2$ 2.5, glucose 21.0, pH 7.4) chilled to 4° C on ice and the hippocampi removed. These were placed in turn on a McIlwain tissue chopper and 400μM transverse slices taken and placed onto filter paper moistened with chilled ACSF. The slices were placed for at least 1 hour into a humidified recovery chamber and continuously gassed with 95% O_2/5% CO_2.

Following this recovery period, slices were placed into a submersion-type recording chamber and superfused with ACSF continuously bubbled with 95% O_2/5% CO_2 at a rate of approximately 5ml min^{-1}. A twisted nichrome bipolar stimulating electrode was placed into the dentate hilus or the Schaffer collaterals and field responses recorded from either the CA3 or CA1 region respectively. Recording electrodes were pulled from GC100-F10 glass micropipettes (4-10MΩ, 3M NaCl) on a Flaming Brown Micropipette puller (Sutter Instruments) and mounted onto an HS-2a headstage connected to an Axoclamp 2B amplifier. Half-maximal stimuli were administered to the Schaffer collateral pathway using a twisted bipolar NiCr stimulating electrode (0.1msec pulse width). Acute slices were stimulated using a constant current stimulator (Axon Instruments Isolator-11). Recording electrodes were placed either into *stratum pyramidale* to record field

population spikes, or into both *stratum pyramidale* and *stratum radiatum* to record population spikes and field EPSPs. Data was recorded on a computer running pClamp6 software (Axon Instruments) *via* a Digidata 1200 analog/digital interface. This data was sampled at 10kHz and filtered at 3kHz.

2.2 Electrophysiological Recordings: the rationale

By placing a glass electrode into the extracellular space within a hippocampal slice it is possible to measure the field potentials produced by the firing of a population of neurones by virtue of the fact that the extracellular fluid constitutes a conductive field around them. When at rest, neuronal membranes are uniformly polarised, and thus there is no net flow of current in the extracellular space. When the neurone becomes active however, this uniformity is lost, and the neuronal membrane may exist at a number of different potentials along its length. This in turn produces current flow from one part of a neurone to another through the extracellular space (Johnston & Wu, 1995).

It is possible, by placing a recording electrode into the *stratum pyramidale* of, for example, CA1 while at the same time stimulating the Schaffer collaterals, to measure what has been described as a population spike (Andersen *et al.* 1971). This has been defined as the summation of the individual action potentials of a population of synchronously discharging neighbouring pyramidal cell bodies. Similarly, placing an electrode into the *stratum radiatum* enables the field excitatory postsynaptic potential (EPSP) to be recorded upon stimulation of the Schaffer collateral pathway.

The shape of these recordings is determined by both the position of the electrode and the direction in which current is flowing through the population of neurones. For example, if we are recording events from an electrode placed in the *stratum radiatum* then, upon stimulation of the Schaffer collateral pathway, current will flow into the dendrites as a result of the activation of neurotransmitter-gated postsynaptic receptors. This forms a so-called current "sink". Thus, as current flows along the dendrites towards the somatic region (*ie.* towards a "source") it also flows away from the recording electrode. This gives rise to a negative going field EPSP recording. Similarly this event, recorded by an electrode in the *stratum pyramidale* region, gives rise to a positive going EPSP as current flows towards this electrode forming part of the extracellular circuit.

If the EPSP in the dendrites exceeds a certain threshold level then an action potential will occur in the somata. Thus recordings made at the "sink" for this event (*ie.* in the pyramidal cell layer) will exhibit the typical negative going population spike. This

population spike may be observed to contaminate the EPSP recorded in the dendrites as a positive going deflection, as in this case the dendrites are acting as a source.

Examples of the recordings obtained from the CA1 of an intact hippocampal slice are presented in figure 2.1 below.

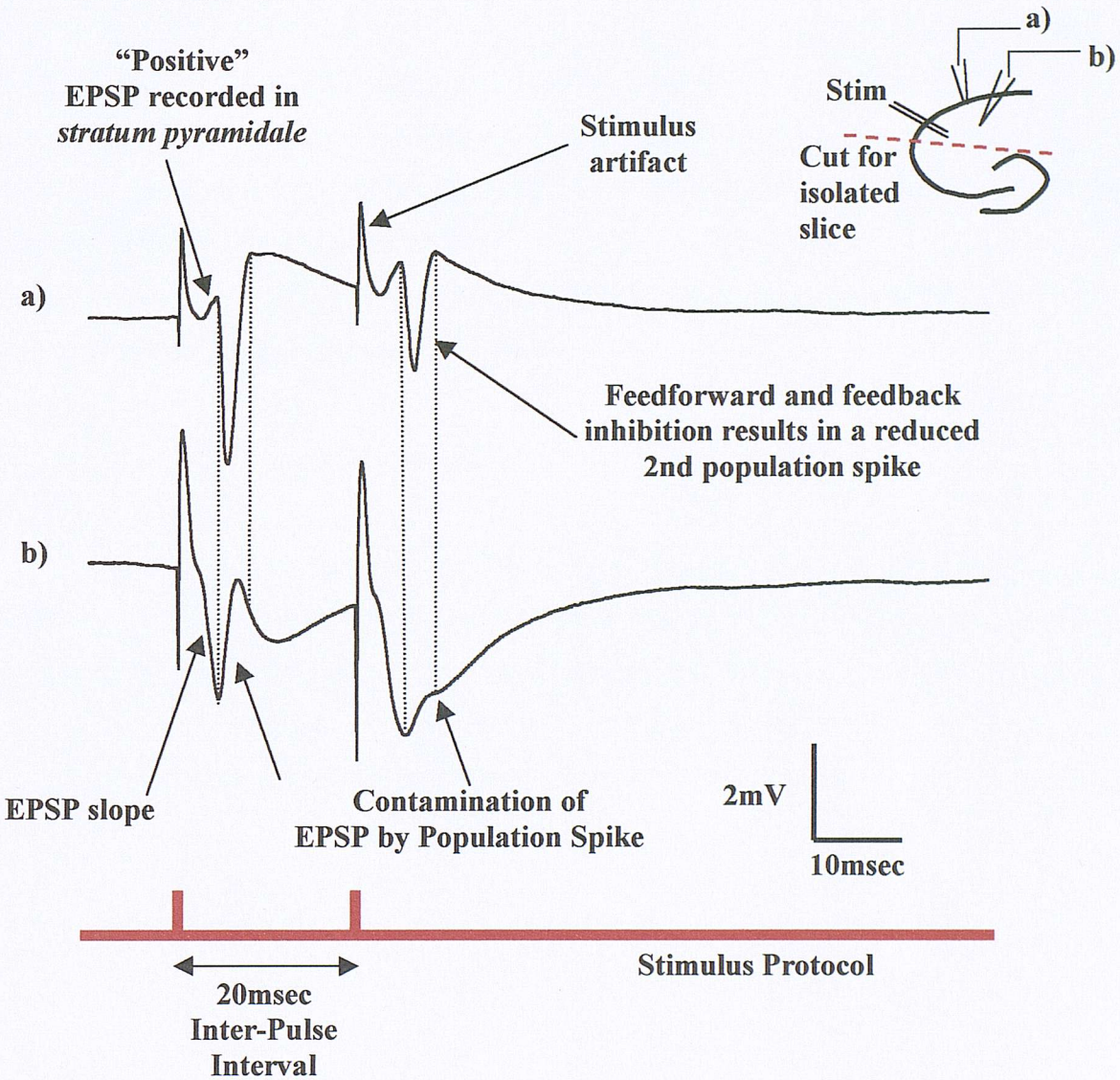

Figure 2.1 Placement of glass microelectrodes (see inset) into the a) *stratum pyramidale* and b) *stratum radiatum* of CA1 yield population spike and population EPSP recordings respectively upon the stimulation of the Schaffer collateral pathway. Current flowing with respect to the recording electrode and earth will produce a negative going trace at an electrode placed in the *stratum radiatum* and a positive going trace in an electrode placed in the *stratum pyramidale*. Hence the EPSP recorded from *stratum radiatum* appears as a negative deflection of the trace and in *stratum pyramidale* as a positive deflection. The same is true for the population spike recorded from the pyramidal cell layer and the positive going population spike contamination which occasionally occurs in the EPSP recording. Use of a paired-pulse stimulation protocol with a 20msec inter-pulse interval allows the observation of $GABA_A$ mediated feedforward and feedback inhibition resulting in a reduction of the second population spike amplitude.

2.3 Analysis of the EPSP slope

In the following chapters, EPSP data will be presented as a percentage slope value. Measurement of the slope of the EPSP rather than the amplitude or area is useful for a number of reasons. Firstly, since the field EPSP is often contaminated at higher stimulus intensities by the population spike, the peak of the EPSP is often curtailed. Therefore measurements of the peak response may be misleading. This is evidenced by the fact that the second EPSP often appears larger than the first as the feedforward and feedback inhibitory mechanisms reduce the amplitude of the second population spike and thus limit the contamination of the second EPSP.

In addition to this, slope measurements are useful as they can be directly related to the synaptic current (Johnston and Wu 1995).

Slope of field EPSP $\propto$ Peak synaptic current

It is possible to calculate the slope of the field EPSP from data derived by the Clampfit analysis package. Thus if we know the peak of the field EPSP and the time-to-peak, then the slope of the EPSP can be obtained using the equation:

Slope = (EPSP peak x 0.8) / 10-90% Rise Time

These data points are shown in figure 2.2 below.

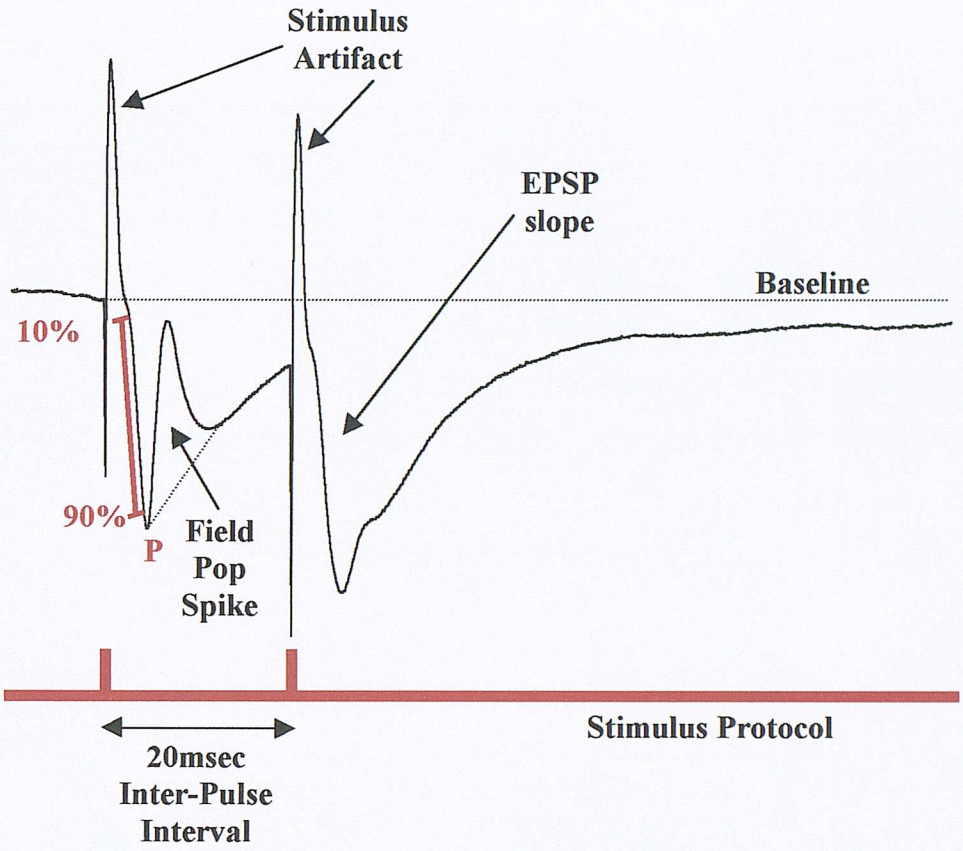

Figure 2.2 Analysis of the EPSP slope involves the calculation of the peak of the trough of the EPSP (denoted by the letter P in the example above) and the 10-90% rise time for the EPSP slope. These are obtained using the Clampfit data analysis program. The EPSP slope is calculated using the formula:

Slope = ((P * 0.8) / 10-90% Rise Time)

2.4 Analysis of the Population Spike amplitude

Analyses of the population spike amplitudes recorded at the electrode in *stratum pyramidale* were achieved using the Clampfit package from the pClamp 6 software (Axon Instruments). This enabled the determination of numerical values for the points on the positive going EPSP either side of the population spike proper, and also the bottom of the trough formed by the population spike itself. By assuming the amplitude of the population spike to correspond to the length of a line drawn from the bottom of this trough (point c in figure 2.3) to the mid-point of a line joining either side of the positive going EPSP (a-b in figure 2.3), it was possible to calculate the absolute amplitude in mV using the following formula:

$$\text{Amplitude} = ((a + b)/2) - c$$

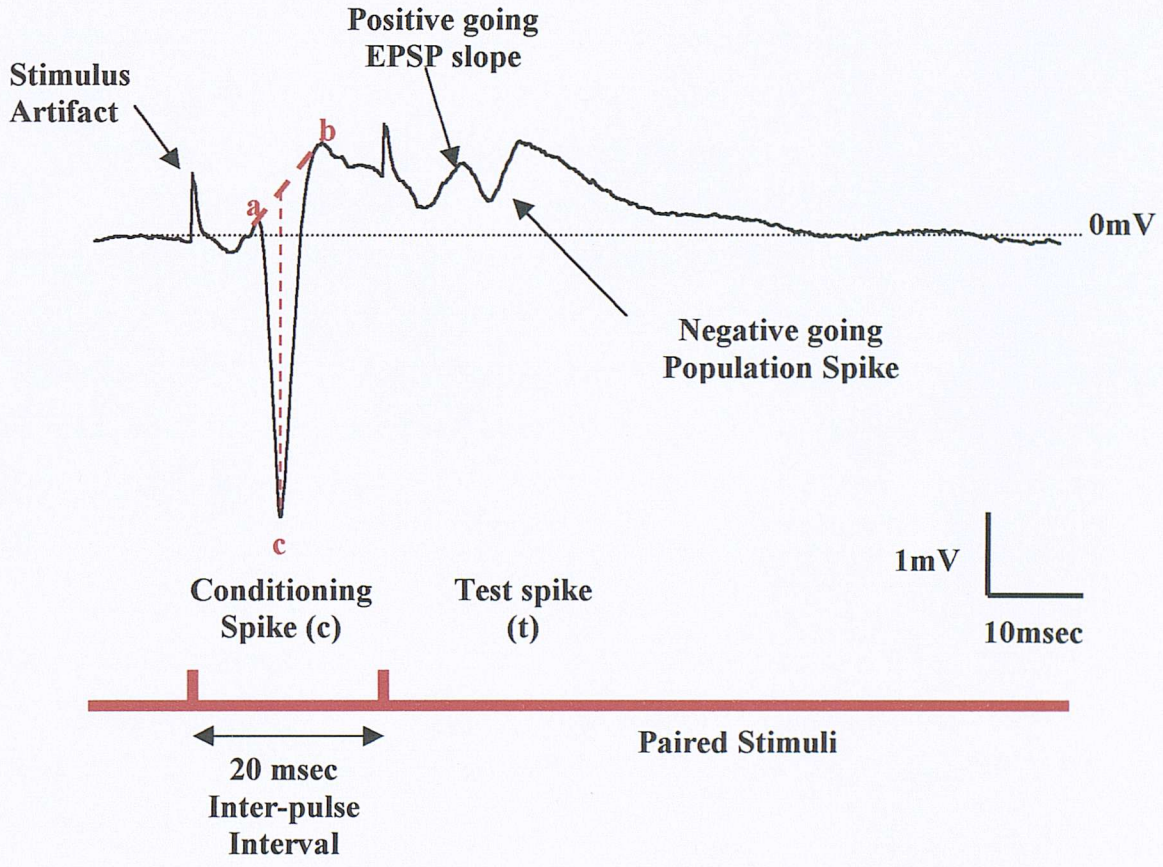

Figure 2.3 In order to calculate the amplitude of the population spikes elicited during the paired pulse protocol it was first necessary, using the Clampfit package from pClamp6, to ascertain numerical values for certain points within the population spike. These points have been superimposed on an example trace in red letters. Once a value had been obtained for the points denoted a, b and c then the amplitude of the population spike could be calculated using the formula ((a+b)/2)-c. This provides a value (in mV) corresponding to the length of a line drawn from the bottom of the negative going spike (c) to a point midway into the positive going EPSP (a to b). Using the amplitude data for the first and second spikes it was possible to calculate the percentage inhibition of the second population spike compared to the first using the formula % Inhibition= ((C-T)/C)*100, where C is the amplitude of the first population spike and T that of the second spike. This value provides an indication of the efficacy of the fast feedforward and feedback inhibitory mechanisms in action within the slice.

The percentage inhibition of the second (test) population spike was calculated relative to the first (conditioning) spike using the formula:

$$\textbf{\% Inhibition} = ((C - T)/ C)* 100$$

where C= conditioning and T= test population spike amplitudes.

This comparison allows the efficacy of the feedforward and feedback inhibitory mechanisms mediated by $GABA_A$ receptor activation to be assessed throughout the course of the experiment.

For the time-course experiments in chapter 3 a sub-maximal stimulus was selected and used throughout the course of the experiment. Stimuli were administered *via* a twisted nichrome bipolar stimulating electrode (custom-made 80/20 NiCr wire with a final resistance between 14-15M Ω) placed into the Schaffer collateral pathway in *stratum radiatum*. Paired stimuli 20 msec apart (0.1 msec pulse width every 30 seconds) were administered in order to assess the efficacy of $GABA_A$ mediated inhibition.

For the electrophysiological experiments in chapter 5 stimulus-response curves were constructed by administering steadily increasing stimuli (0.1 msec pulses). This stimulus-response curve provided a measure of the half-maximal stimulus, which was then used with a paired-pulse protocol (20 msec IPI) during the application of various drug treatments. Drugs were applied *via* the superfusing ACSF and were purchased from either Sigma Aldrich or Tocris-Cookson.

2.5 Organotypic Culture

Organotypic mouse hippocampal slice cultures were prepared according to a modified method of Stoppini *et al.* (1991) thus providing a long-term model of hippocampal circuitry.

Mice aged between 5-7 days old were killed by decapitation and their hippocampi dissected out into chilled medium containing 10% horse serum, 40% Hank's Balanced Salt Solution, 50% Eagle's Minimal Essential Medium, 30mM D-glucose and 1mM L-glutamine (Sigma Aldrich Ltd.). From these, 300μm slices were prepared on a McIlwain tissue chopper on Melinex Film. These slices were then transferred to a petri dish containing 5ml of chilled culture medium and separated using plastic paddle pasteur

pipettes (BDH). These slices were then removed individually from the medium using a pastette and placed onto Millicell-CM membranes (Millipore) in a six well dish. Each well contained 1ml of culture medium and each tray had been pre-incubated in a 5% CO_2 incubator at 37°C for at least 30 minutes prior to the dissection. Each well contained a maximum of four slices. Following this the trays were kept at 37°C in a 5% CO_2 environment for 7 days prior to the start of the experiment.

2.6 Electrophysiology

Electrophysiological measurements in organotypic cultures during kainate (1μM) application were carried out between 9-12 days *in vitro* (DIV). The culture membrane was placed into a break and cut tool (BDH) and excised from the plastic ring to which it is attached using a scalpel blade. This tool is a rubber disk that holds the membrane steady while it is being cut. The culture membrane was then transferred to a modified slice recording chamber at room temperature and superfused with standard artificial cerebrospinal fluid (ACSF) with the composition (in mM): NaCl 117.8, $NaHCO_3$ 26.0, KCl 3.3, KH_2PO_4 1.3, $MgSO_4$ 1.0, $CaCl_2$ 2.5, glucose 21.0. This ACSF was continually bubbled with 95% O_2/5% CO_2. The membrane was kept submerged in the recording chamber with a metal ring, which encircled the cut edge of the membrane (figure 2.4).

Extracellular field potentials were recorded from stratum pyramidale of CA1 and CA3, following stimulation of the Schaffer collateral pathway and perforant pathway respectively, in a similar manner to acute slice recordings. Recordings were made using glass micropipettes (4-10 MΩ, 3M NaCl). Graded stimuli were applied from 0 mV until maximal population spike amplitude was reached to produce stimulus-response curves. These provided a half-maximal stimulus value that could then be used during a paired pulse protocol with stimuli 20 msec apart, thus providing information about the inhibitory systems within the hippocampus.

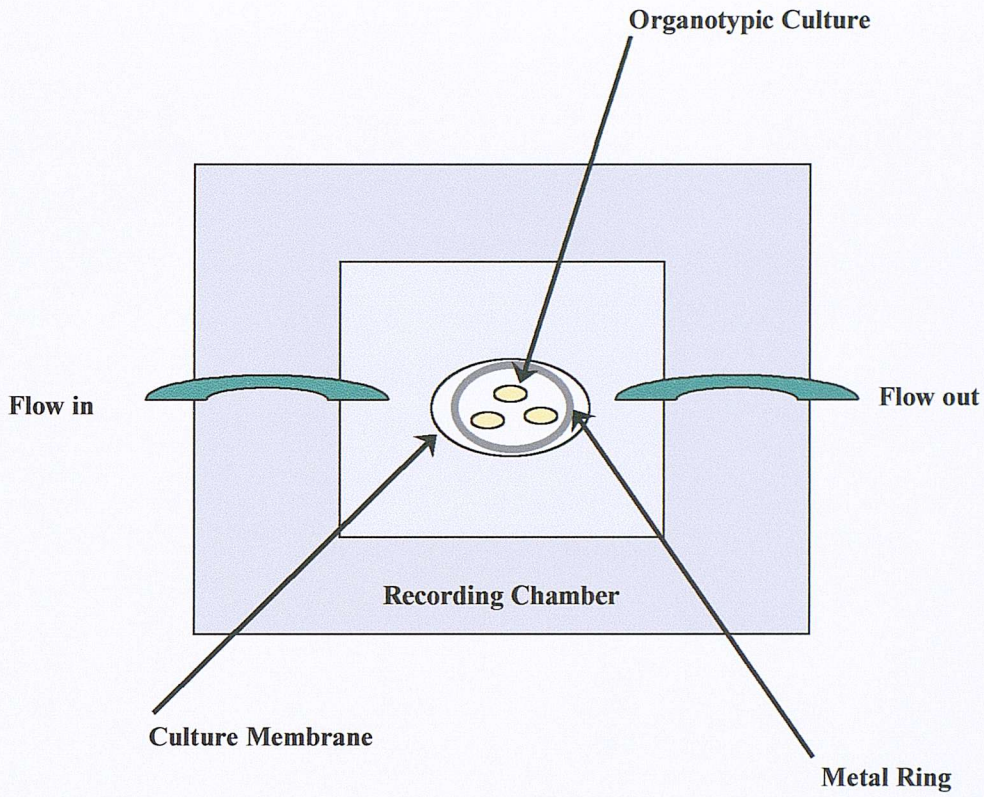

Figure 2.4 Diagrammatic representation of the placement of the metal ring around the culture membrane in order to keep slices submerged during the recording procedure. Electrodes were placed in much the same manner as in acute slices.

2.7 Kainic Acid Treatment

Previous work by Best *et al.* (1996) had demonstrated that an increase in the tolerance to kainic acid induced toxicity occurred in rat organotypic hippocampal slices which had been previously incubated for 24 hours with a subtoxic dose of KA. Propidium iodide staining was used as an indicator of culture viability. At 7 DIV cultures were incubated with 1μM kainic acid (KA) in medium, a concentration previously found to be subtoxic in rats (Best *et al.* 1996). After 24 hours the medium was removed and replaced with fresh medium. Following this, at 11 DIV, slices were incubated with 5μM KA for a further 24 hours (figure 2.5). At 15 DIV slices were stained with the fluorescent exclusion dye, propidium iodide (PI), which is a marker for dead cells (Darzynkiewicz *et al.* 1992), and visualised on a fluorescence microscope using a rhodamine filter set.

In experiments to assess function following preconditioning, electrophysiological recordings were made between 9-12 DIV from the *stratum pyramidale* of either CA1 or CA3 following stimulation of the Schaffer collateral pathway or dentate hilus respectively.

In experiments to assess KA induced toxicity histologically, cultures were fixed in 4% paraformaldehyde and subsequently stained with the Nissl stain thionin. The extent of damage to the cell layers in the cultures was compared to untreated controls and controls treated with 1μM and 5μM kainate at 15 DIV.

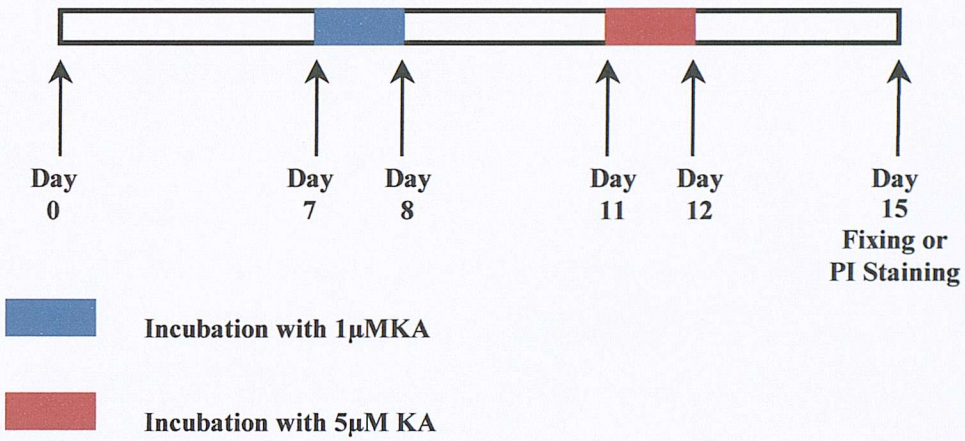

Figure 2.5 Time-line showing the protocol for a KA preconditioning experiment carried out in organotypic culture. Hippocampal slices from 5-7 day old MF1 mice were plated out onto Millipore CM membranes at day 0. Between day 0 and 7 the medium was changed at an interval of 3-4 days. On day 7 the medium was replaced with medium containing 1μM KA for 24 hours. This was changed for fresh, drug free medium on day 8. On day 11 the medium was again replaced this time for medium containing 5μM KA for 24 hours. This was again replaced on day 12 for drug free medium. On day 15, slices were either fixed with 4% paraformaldehyde and stained with thionin, or unfixed cultures were stained with propidium iodide to assess cell viability. (Modified from Best *et al* 1996)

2.8 Thionin Staining

Culture medium was removed from each well using a pipette and replaced with enough 4% paraformaldehyde (PFA) to cover the slices and left overnight in a refridgerator (for PFA composition see section 2.11 below). The next day they were removed from the membrane using a paintbrush and transferred to glass slides. These were placed into an aqueous solution of 0.1% thionin for 10 minutes and then washed with tap water. At this point they appeared jet black in colour. Several drops of differentiator solution were then applied in order to remove the stain from non-Nissl substance. This differentiator solution was made by mixing 90ml of 95% ethanol with 10ml chloroform and 3 drops of acetic acid. No further processing of the slides was carried out.

2.9 Propidium Iodide Staining

Unfixed cultures were stained with propidium iodide at 15 DIV in the following manner. Six μl ml^{-1} of 10mg ml^{-1} propidium iodide (PI) solution (100nM) (Sigma Aldrich) were introduced into the culture medium of each well to be studied and replaced into the incubator. Cultures were incubated with PI for at least 30 minutes prior to fluorescence microscopy. The severity of damage was assessed following KA treatment in a qualitative manner and the percentage of slices exhibiting severe damage to the CA3 region calculated per treatment group.

2.10 Glutamic Acid Decarboxylase Staining

GAD 67 is the constitutive synthetic enzyme that synthesises GABA within interneurones. Antibodies raised to GAD therefore provide a useful method for the localisation of GABA-ergic interneurones. Using Chemicon International's AB108 (rabbit anti-GAD polyclonal antibody) ABC detection kit, organotypic cultures were stained for GAD following pretreatment with 1μM KA, 5μM KA and 1+ 5μM KA after fixation with 4% paraformaldehyde (PFA) at 15 DIV. These were compared to age matched control cultures.

The protocol for the immunohistochemistry was as follows:

1) Cultures were removed from their membranes using a fine paintbrush and washed 3 times for 10 minutes in tris-buffered saline (TBS)

2) They were then incubated for 60 minutes in TBS with 5% horse serum to block non-specific binding of the primary antibody

3) Following this they were incubated for 2 hours at room temperature with the primary antibody (1: 3000 dilution) in TBS with 1% horse serum followed by 16 hours at 4^{o} C

4) Slices were then washed a further 3 times, again for 10 minutes each wash, in TBS

5) Incubation with the biotinylated secondary antibody (diluted 1:500 in TBS with 1% serum)

6) This was followed by a further 3 x 10 minute washes in TBS

7) Visualisation of the antibody using an ABC Elite kit (1:200 Vector Labs) in TBS. This involves the incubation of avidin (a globulin found in egg white with a high affinity for biotin) with biotinylated peroxidase in order to allow them to complex. This complex is then incubated with the slices, allowing any free biotin binding sites on the avidin-biotinylated peroxidase complex to bind to the biotinylated secondary antibody.

8) 2 x 10 minute washes in TBS

9) 1 x 10 minute wash in phosphate buffer (no saline)

10) Diaminobenzidine (DAB) reaction. DAB is a substrate for hydrogen peroxidase and is added to the system with hydrogen peroxide, which acts as a catalyst. DAB is hydrolysed to form a brown reaction product, which can then be visualised, using light microscopy.

11) 2 x 10 minute washes in phosphate buffered saline (PBS)

12) 1 x 10 minute wash in phosphate buffer (no saline)

Slices were then counterstained with propidium iodide and mounted onto slides using the aqueous mountant Crystal/Mount (Biomedia) with cover slips for light microscopy. The number of GAD stained cells were counted for the following regions: dentate gyrus and hilus, CA3 and CA1. The cell counts for the dentate gyrus and hilus were taken as a single value.

2.11 Paraformaldehyde (PFA) Preparation

10 ml of PBS was added to 4g of paraformaldehyde powder and heated to 70°C. To this was added 2 drops of 5M NaOH until the mixture goes clear. A further 90 ml of PBS was then added and the solution adjusted to pH 7.2-7.4 with NaOH.

2.12 Phosphate Buffered Saline (PBS - 0.01M)

0.26 g sodium phosphate ($Na_2HPO_4.12H_2O$), 2.90g potassium phosphate (KH_2PO_4) and 8.75g sodium chloride (NaCl) were added to 1l distilled water and mixed. The pH was adjusted to 7.4 when necessary.

2.13 Tris Buffered Saline (TBS – 0.05M)

To 900ml distilled water were added 6.06g tris (hydroxymethyl)- aminomethane ($NH_2.C(CH_2OH)_3$), 38.4ml hydrochloric acid (HCl - 1M) and 8.75g sodium chloride (NaCl). The solution was made up to 1l and the pH adjusted where necessary to pH 7.6.

Drug	*Supplier*	*Salt*	*Supplier*	*Stain/ Fix/ Antibody*	*Supplier*
KA	Sigma	**NaCl**	Sigma	**Thionin**	Sigma
Fwill	Sigma RBI	**$NaHCO_3$**	Sigma	**GAD-67 Ab/ ABC Detection Kit**	Chemicon
ATPA	Tocris	**KCl**	Sigma	**PFA**	Sigma
NS102	Sigma RBI	**KH_2PO_4**	Sigma	**EtOH**	Sigma
MCPG	Tocris	**$MgSO_4$**	Sigma	**Chloroform**	Sigma
MPPG	Tocris	**$CaCl_2$**	Sigma	**Acetic Acid**	Sigma
H-7	Tocris	**D-glucose**	Sigma	**NaOH**	Sigma
SCH50911	Tocris	**Hanks Balanced Salt Solution**	Sigma	**PBS**	Sigma
DMPX	Sigma RBI	**Eagle's Minimum Essential Salt Solution**	Sigma	**Propidium Iodide**	Sigma
DPCPX	Sigma RBI	**Na_2HPO_4**	Sigma		
D-AP5	Tocris	**$NH_2.C(CH_2OH)_3$**	Sigma		
MK801	Tocris	**L-glutamine**	Sigma		
Bicuculline methiodide	Sigma RBI				

Table 2.1 Sources for the drugs, salts and stains used during the course of the experiments detailed above.
Chemicon = CHEMICON Europe, Ltd., Eagle Close, Chandlers Ford, Hampshire SO53 4NF, UK
Sigma = Sigma-Aldrich Company Ltd., Fancy Road, Poole, Dorset, BH12 4QH, UK
Tocris = Tocris Cookson Ltd., Northpoint, Fourth Way, Avonmouth, Bristol, BS11 8TA, UK.

Chapter 3

Pharmacology of the Kainate Response in the CA1 Of Acute Slices

Ionotropic Glutamate Receptors

3.1 Introduction

Much work has been carried out in recent years on the physiology and pharmacology of the effects of KA receptor activation within the hippocampus, resulting in several postulated roles for them.

These effects include the modulation of both inhibitory and excitatory transmission, as well as a role in NMDA independent forms of LTP of the mossy fibre pathway. Paternain *et al* (2000) have shown using *in situ* hybridisation that mRNA for the GluR5 subunit is expressed predominantly in hippocampal interneurones with a much lower amount of mRNA for GluR6 being colocalised in a significant proportion of these cells (Paternain *et al.* 2000, Bureau *et al.* 1999). Activation of GluR5 containing receptors located in the somato-dendritic compartment of these interneurones has been observed to increase interneuronal spiking and thus lead to an increase in the frequency of spontaneous IPSCs recorded from CA1 pyramidal cells (Cossart *et al.* 1998, Frerking *et al.* 1998, 1999). In contrast to this, activation of KA receptors presumed to be located on the presynaptic terminals of interneurones also leads to a reduction in the evoked IPSCs recorded from CA1 pyramidal cells (Rodriguez-Moreno and Lerma 1998; Frerking *et al* 1999). In support of this, KA has been demonstrated to reduce GABA release from hippocampal synaptosomes (Cunha *et al.* 2000). This involves a metabotropic component linked to the activation of protein kinase C (PKC). It is also possible that $GABA_B$ receptors have a role to play in this presynaptic response (Frerking *et al* 1999). This effect has been shown by Min *et al.* (1999) to be induced by synaptically released glutamate during brief bursts of activity in the Schaffer collaterals, indicating that spillover of glutamate from excitatory synapses is capable of reducing the effects of GABAergic inhibition. More recently it has been shown that activation of KA receptors on the presynaptic terminals of interneurones which synapse onto other interneurones is able to enhance the release of GABA from these sites (Mulle *et al.* 2000, Cossart *et al.* 2001). This again would be expected to reduce the release of GABA onto pyramidal cells. Since this action has been observed in $GluR5^{-/-}$ mice but not those deficient in GluR6 it has been proposed that these receptors may be homomeric for the GluR6 subunit (Mulle *et al.* 2000).

In addition to these numerous effects on the inhibitory network of CA1, KA receptor activation is also capable of depressing excitatory transmission in both CA3 and CA1 (Chittajalu *et al* 1996; Vignes *et al* 1998; Kamiya and Ozawa 1998, 2000). This

response is likely to occur *via* the activation of presynaptic KA receptors on the mossy fibre and Schaffer collateral terminals. It is possible that this receptor subtype contains or is comprised of the GluR5 subunit since ATPA effectively reduces evoked EPSCs in both CA3 and CA1 at a concentration at which it acts specifically at GluR5 containing receptors (Vignes *et al* 1998). It is interesting to note however that Contractor *et al* (2000) found the application of KA reduced EPSCs in CA3 pyramidal cells of wild-type and GluR5$^{-/-}$ but not GluR6$^{-/-}$ mice. This discrepancy may possibly reflect differences in the subunit composition of these receptors in rats and mice, or alternatively differences in the pharmacology of ATPA in heteromeric KA receptors of varying subunit composition. This last comment is made since Contractor and co-workers found no effect on the EPSC in wild type mice with ATPA, and Paternain *et al* (2000) have found ATPA capable of activating heteromeric receptors containing GluR5/GluR6 and GluR6/KA2 subunits.

Kamiya and Ozawa (1998) have found that this effect in CA1 occurred as a result of a decrease in presynaptic Ca^{2+} influx into the Schaffer collateral terminals possibly *via* localised depolarisation in the region of the terminal preventing the action potential induced membrane depolarisation which precedes transmitter release. The mechanism of action in CA3 appears to be somewhat different. KA receptor activation on mossy fibre axons increases fibre excitability, probably by causing them to depolarise, leading to an inhibition of presynaptic Ca^{2+} influx. This in turn has the effect of reducing glutamate release and hence the amplitude of the EPSC recorded from CA3 pyramidal cells (Kamiya and Ozawa 2000).

In addition to this, it would also appear that activation of postsynaptic KA receptors on pyramidal cells of both CA3 (Robinson and Deadwyler 1981, Castillo *et al* 1997) and CA1 (Bureau *et al.* 1999) is capable of eliciting an inward depolarising current. It is known that both of these cell types express the GluR6 subunit (Egebjerg *et al* 1991, Wisden and Seeburg 1993), with the level of expression in CA3 being much higher than in CA1 (Bureau *et al.* 1999).

One further possible consequence of GluR6 receptor activation on the pyramidal cells of CA1 is the inhibition of the slow afterhyperpolarisation (I_{sAHP}) (Melyan *et al.* 2002) which has been shown to be reduced following KA lesion (Ashwood *et al.* 1986). This has been found to be a non-desensitising inhibition that can be blocked by the PKC inhibitor calphostin C. This leads to an increase in the excitability of CA1 pyramidal cells.

Furthermore, Bortolotto *et al.* (1999) have reported that the induction of mossy fibre long term potentiation (LTP), which is independent of NMDA receptors is blocked

in the presence of the antagonist LY382884 at concentrations at which it shows great selectivity for the GluR5 subunit compared to GluR2.

3.1.2 Developmental status of the rat hippocampus between p15-19

During the first few weeks after birth, the nervous system of the rat undergoes several developmentally regulated changes. This is true of the hippocampus as much as any brain region. It is therefore important, in view of the fact that these experiments use hippocampal slices obtained from juvenile rats between postnatal day 15 (P15) and P19, that we have some overview of the "developmental status" of the hippocampus at this time. In other words, what receptors are present, and how does this compare to an adult rat's hippocampus?

With regards to the circuitry of the hippocampal formation, it has been shown that the Schaffer collateral/ commissural pathway is present at birth (P0) (Diabira *et al* 1999). This pathway was functional, since stimulation of this pathway was able to evoke a field EPSP that was mediated by AMPA receptors.

The AMPA receptor population within the hippocampus varies during the postnatal period as does the agonist sensitivity of the receptors (Siefert *et al* 2000). For example *in situ* hybridisation studies (Pellegrini-Giampietro *et al.* 1991) have shown that expression of the GluR1 mRNA rises to a peak of 195% of adult levels in the hippocampus by P14, falling to 100% (adult) by around P60. In contrast, the presence of the GluR2 subunit is relatively constant throughout postnatal development, reaching adult levels by about P14. The expression of transcripts for the GluR3 subunit are well below adult levels at P4, reach adult levels at P14 but then transiently overshoot to approximately 130% by P21.

The KA receptor subunits GluR6, GluR7, KA1 and KA2 can all be detected in neural tube tissue as early as E10 (Scherer and Gallo 1998). GluR6 expression appears to be totally in the unedited state at this time. By E18 approximately 30% of GluR6 transcripts are in the edited form (Bernard *et al* 1999). Indeed, the extent of editing of the GluR5 and GluR6 subunits appears to be developmentally regulated (Bernard and Khrestchatisky 1994). Levels of edited GluR5 are stable in the hippocampus between P14 and P21 with approximately 40% of the Glur5 population exhibiting Q/R editing in TMII. This is just below that observed in adult, where the level of editing is approximately 50% (Bernard *et al* 1999). The editing of GluR6 mRNA reaches a peak between P10-P14, by which point 90% of the GluR6 mRNA in the hippocampus is in the edited form. At this

point, the levels of editing of hippocampal GluR6 are practically those of adult rats, in which 88% of GluR6 is in the edited form (Bernard *et al.* 1999).

Transcripts for KA1 appear during the embryonic development of the hippocampus and remain localised to the CA3 and dentate gyrus (Bahn *et al* 1994). KA2 has been detected as early as E12 and remains at constant levels through to adulthood (Bahn *et al.* 1994).

NMDA receptors also undergo postnatal developmental changes. For example, at birth NMDA receptors display little or no sensitivity to Mg^{2+} blockade (Bowe and Nadler 1990). As the animal matures this sensitivity becomes more evident. Other studies however have suggested that the sensitivity of NMDA receptors to Mg^{2+} does not change during postnatal development (Strecker *et al.* 1994) but that it is only after P4 that depolarisation is able to relieve the Mg^{2+} blockade of the receptor channel (Kirson *et al.* 1999). This switch found to correlate with a downregulation of the expression of the NR2D subunit in CA1 pyramidal cells. In contrast, the proportion of cells expressing the NR2A and NR2B subunits remained relatively constant throughout the first five weeks of life, although it would appear that the NR2B subunit's contribution to the activity of the NMDA receptor population on CA1 pyramidal cells increased after P7. This was inferred from a decrease in sensitivity to the NR2B specific antagonist ifenprodil (Kirson *et al.* 1999).

The ability of the group I mGluR agonist trans-ACPD and the group III agonist L-AP4 to reduce excitatory transmission *via* the Schaffer collaterals appears to be maximal within the first month after birth (Baskys and Malenka 1991). It would appear that the group I mGluRs are capable of coupling to the activation of phospholipase D (PLD) between P3 and P15 (Klein *et al.* 1997). This ability peaks around P8 and declines thereafter, therefore this effector system is not likely to be significantly involved in the mGluR pathway in the age of animals used for this study.

Both isoforms of glutamic acid decarboxylase (GAD) namely GAD 67 and GAD 65 have been detected as early on in hippocampal development as E17- E18 (Dupuy and Houser 1996), however the cells expressing these GABA producing enzymes do not display an adult localisation until around P5 (Seress *et al* 1989). During the first week after birth, GABA is capable of causing a depolarisation of the CA3 (Ben-Ari *et al.* 1989) and CA1 (Janigro and Schwartzkroin 1989) pyramidal cell populations. This is no longer

the case after about P10 in the CA1 (Mueller *et al.* 1984) and P12 in the CA3 region (Ben-Ari *et al.* 1989).

This switch from a depolarising response to GABA to the hyperpolarising response observed in juvenile and adult rats appears to coincide with the induction of the expression of the KCC2 K^+/ Cl^- cotransporter (Lu *et al* 1999, Rivera *et al* 1999) and a downregulation of the expression of the BSC2 isoform of Na^+/ K^+/ 2 Cl^- cotransporter (Plotkin *et al* 1997). Therefore, by P15, GABA has assumed its adult role of an inhibitory neurotransmitter.

Western blots from whole rat brain homogenates for the two known splice variants of the $GABA_B$ receptor show that the expression of GB-1a is about 200% that observed in the adult at P0. This begins to decline from P5 to approximately adult levels by P21. Expression of GB-1b is low at P0, being approximately 50% that of the adult rat. By P10 this value has overshot adult levels to approximately 150% and declines thereafter. From about P10 onwards the relative amounts of these two splice variants has assumed a more adult pattern, there being a greater amount of GB-1b than GB-1a (Fritschy *et al* 1999). In the hippocampus immunoreactivity for the GB-1a isoform was observed within the CA1 pyramidal cell layer and the dentate gyrus. GB-1b staining was confined to the *stratum lacunosum* of CA1 and throughout the CA3 (Fritschy *et al* 1999).

It would appear that the depressant effects of exogenously applied adenosine on the field EPSP evoked within CA1 does not differ throughout the course of postnatal development (Psarropoulou *et al* 1990). This effect is due to a decrease in glutamate release from the Schaffer collateral terminals (Tancredi *et al* 1998). It would appear that the levels of the adenosine A_1 receptor expression do rise in the CA2/ CA3a region of the rat hippocampus between P7 and P28, at which time adult levels are achieved (Ochiishi *et al* 1999). It is also possible that the levels of endogenous adenosine within the hippocampus are lower in immature rats since the effects of both caffeine and the adenosine uptake blocker nitrobenzylthioinosine were reduced compared to adult animals (Psarropoulou *et al* 1990).

	Schaffer collateral pathway	GluR1	GluR2	GluR3	GluR5 Editing	GluR6 Editing	KA1	KA2
Level at p15 vs adult	Adult	Higher	Adult	Adult	Lower	Adult	Adult	Adult
	NR2A	**NR2B**	**NR2D**	**GABA**	**GB1a**	**GB1b**	**Aden.**	**A1**
Level at p15 vs adult	Constant 1st 5 weeks	Constant 1st 5 weeks	Decrease after p4	Hyperpol p10 (CA1) p12 (CA3)	Higher	Higher	Lower	Lower

Table 3.1 A comparison of the levels of expression between p15-19 and adult of a number of developmentally regulated receptor subunits and neurotransmitters/ neuromodulators in rat hippocampus. Adult denotes adult levels of expression, higher denotes increased and lower reduced levels of expression between p15-19 compared to adult rat hippocampus.

Figure 3.1 On the following two pages. Circuitry in the CA1 (a and b) and CA3 (c and d) regions of the hippocampal formation and the main receptor subunits' location. Pyr: pyramidal cell; In: interneurone. Excitatory synapses are represented by red triangles, inhibitory by blue triangles. See appended key for receptor identifications.

a)

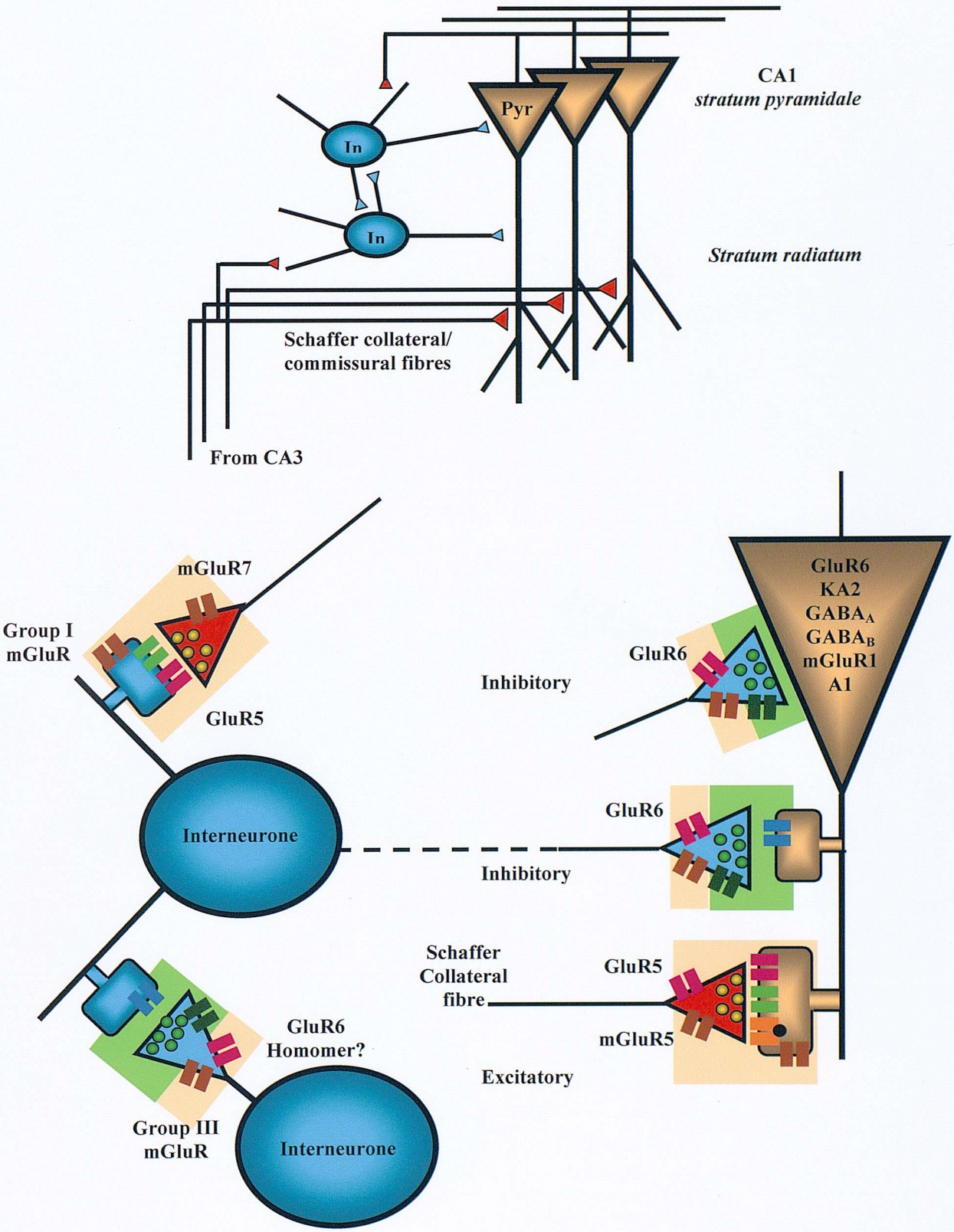
CA1
stratum pyramidale
Pyr
In
In
Stratum radiatum
Schaffer collateral/
commissural fibres
From CA3
mGluR7
Group I
mGluR
GluR5
Interneurone
GluR6
KA2
GABA$_A$
GABA$_B$
mGluR1
A1
GluR6
Inhibitory
GluR6
Inhibitory
Schaffer
Collateral
fibre
GluR5
mGluR5
Excitatory
GluR6
Homomer?
Group III
mGluR
Interneurone

b)

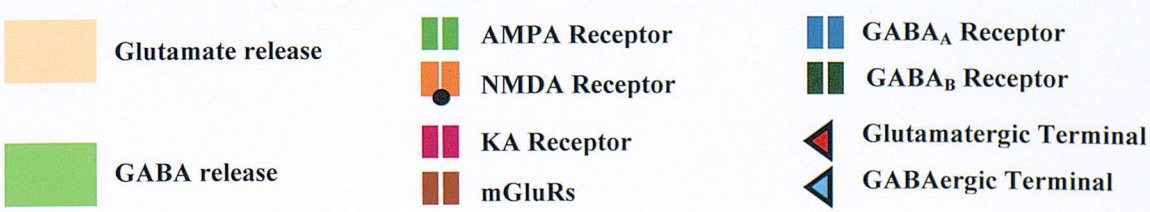
Glutamate release
GABA release
AMPA Receptor
NMDA Receptor
KA Receptor
mGluRs
GABA$_A$ Receptor
GABA$_B$ Receptor
Glutamatergic Terminal
GABAergic Terminal

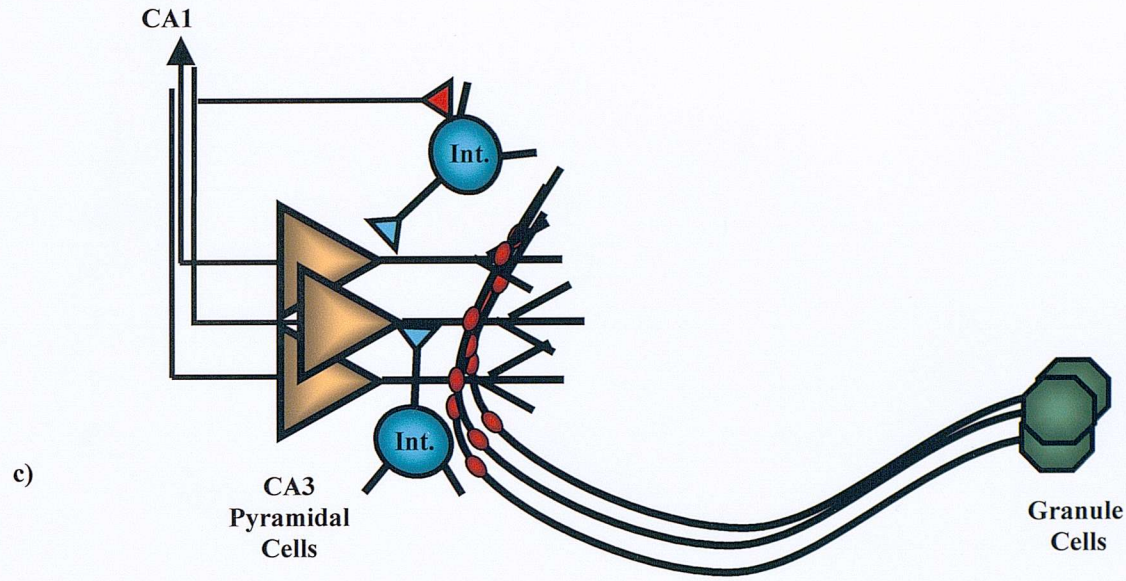
CA1
Int.
Int.
CA3
Pyramidal
Cells
Granule
Cells
Mossy Fibre
Pathway

c)

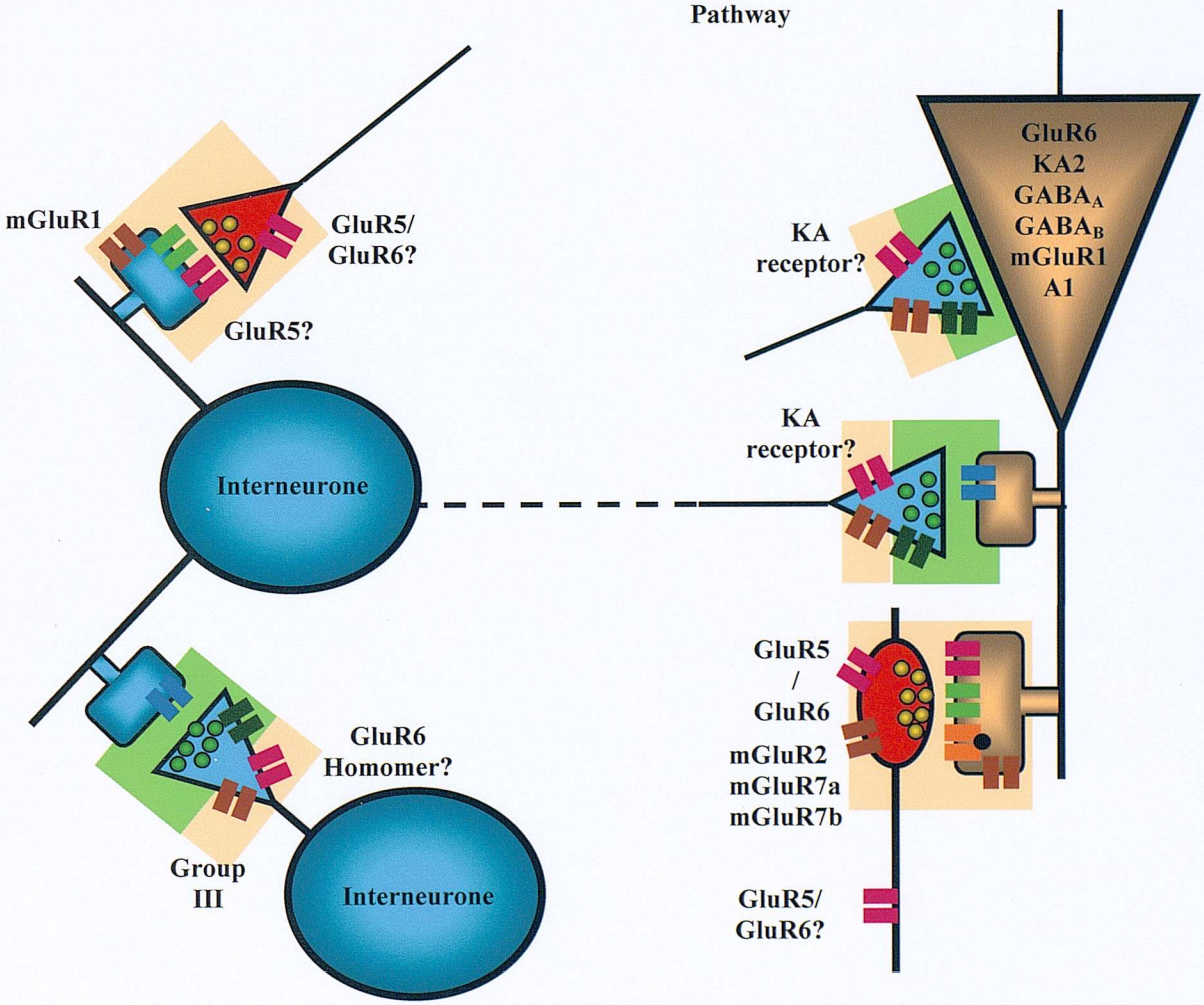
mGluR1
GluR5/
GluR6?
GluR5?
Interneurone
GluR6
KA2
GABA$_A$
GABA$_B$
mGluR1
A1
KA
receptor?
KA
receptor?
GluR5
/
GluR6
mGluR2
mGluR7a
mGluR7b
GluR5/
GluR6?
GluR6
Homomer?
Group
III
Interneurone

d)

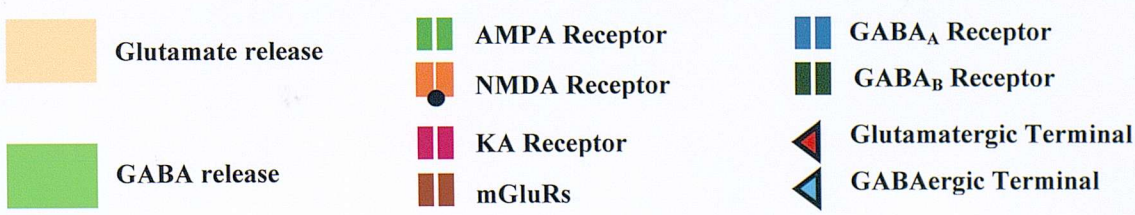
Glutamate release
GABA release
AMPA Receptor
NMDA Receptor
KA Receptor
mGluRs
GABA$_A$ Receptor
GABA$_B$ Receptor
Glutamatergic Terminal
GABAergic Terminal

3.2 Objectives

Many of the findings discussed above have utilised techniques such as whole cell patch clamp or intracellular recordings from single cells, often pharmacologically isolated using AMPA and NMDA antagonists. The data presented in this chapter has been obtained using evoked field potential recordings of population spikes from the *stratum pyramidale* and field EPSPs from the *stratum radiatum* of CA1. This has the advantage of enabling one to observe the net effects that are being elicited by KA in terms of both the inhibitory and excitatory networks within the hippocampus as a whole and in the CA1 as an isolated unit.

Thus it is hoped that the data in this chapter will help to supplement the already extant data regarding the effects of KA with regard to several points:

1. The effect of KA on excitatory transmission from the Schaffer collaterals using the slope of the first field EPSP recorded from the *stratum radiatum* of the CA1.
2. The direct effect of KA on the pyramidal cell population in CA1. Measurements of the first population spike amplitude will provide this information. It should be borne in mind that the EPSP slope and population spike amplitude are directly related under control conditions. If the EPSP slope increases then the population spike amplitude also increases. Therefore, it is expected that any divergence from this relationship should aid in the differentiation between the pre- and post-synaptic effects of drug treatment. However, it is also possible that an increase in the first and second population spike amplitudes could occur as a result of a reduction in feedforward and feedback inhibition.
3. The effect of KA on the evoked inhibition. This will be studied by using paired stimuli 20msec apart in order to observe the effects of both feedforward and feedback inhibition on the second population spike. Calculation of the paired-pulse inhibition will provide an index of the efficacy of the inhibitory mechanisms throughout the course of the experiment.
4. The effect of the CA3 region on the responses observed in the CA1. This will be studied by comparing the responses of intact hippocampal slices to those from slices in which CA1 has been isolated by transection of the Schaffer collateral/ commissural pathway.

3.3 Methods

3.3.1 Hippocampal slice preparation

Experiments were performed on acute slices taken from 15-19 day old Wistar rats. These slices were prepared in the following way:

Whole brains were dissected from rats killed by terminal halothane anaesthesia and placed into ACSF (in mM: NaCl 117.8, $NaHCO_3$ 26.0, KCl 3.3, KH_2PO_4 1.3, $MgSO_4$ 1.0, $CaCl_2$ 2.5, glucose 21.0) chilled to 4° C on ice and the hippocampi removed. These were placed in turn on a McIlwain tissue chopper and 400μM transverse slices taken and transferred to a petri dish containing a piece of filter paper moistened with chilled ACSF. These were allowed to recover for at least 1 hour in a humidified chamber and continuously gassed with 95% O_2/5% CO_2.

3.3.2 Electrophysiology

Following this recovery period, slices were placed into a recording chamber and superfused with ACSF continuously bubbled with 95% O_2/5% CO_2. A twisted nichrome bipolar stimulating electrode was placed into the Schaffer collateral pathway and field responses recorded from CA1. Recording electrodes (pulled from GC100-F10 glass micropipettes, 4-10MΩ, 3M NaCl) were placed into both *stratum pyramidale* and *stratum radiatum* to record population spikes and field EPSPs respectively. Responses were sampled at 10kHz and filtered at 3kHz. Paired, half-maximal stimuli 20msec apart were administered, allowing for the assessment of feedforward and feedback $GABA_A$ mediated inhibitory circuitry by comparing the amplitude of the second population spike with that of the first. By using the formula ((C-T)/C)*100, where C= first (conditioning) spike amplitude and T= second (test) spike amplitude, it was thus possible to calculate the percentage inhibition of the second spike compared to the first.

Application of KA ([2S-(2 α, 3β, 4β)]-2-Carboxy-4-(1-methylethylenyl)-3-pyrrolidineacetic acid) to intact hippocampal slices is known to cause a depolarisation of CA3 pyramidal cells (Castillo *et al.* 1997) which may result in epileptiform activity (Ben-Ari 2000). This activity is presumably capable of spreading to the CA1 region *via* the Schaffer collateral pathway. Therefore, in order to compare the effects of drugs in CA1 in the absence of a downstream effect from CA3, a number of experiments were carried out in isolated CA1 preparations. To achieve this, the CA3 and the dentate gyrus were

dissected from the slice in the petri-dish using a fresh scalpel blade. Slices were then transferred as usual to the recording chamber using an artist's 00 paint brush.

3.3.3 Drug application

Drugs were applied in the superfusing ACSF. For all experiments other than the KA dose response curve, a concentration of 1μM KA was chosen as a concentration which results in a sequential enhancement and reduction in the field population spike amplitude in addition to a reduction in the field EPSP slope. This increase followed by a decrease in the field population spike was presumed to represent the activity of KA at both interneuronal terminals and dendrites coupled with it's presynaptic action at Schaffer collateral terminals. KA has been reported to activate KA receptors preferentially to AMPA receptors at a concentration of 1μM (Kamiya and Ozawa 1998, 2000; Mulle *et al.* 2000) and this concentration is around the EC_{50} value for several homomeric KA receptor types (Table 3.2 and Chittajalu *et al.* 1999). AMPA receptor activation by KA is unlikely until a concentration of >3μM is reached (Mulle *et al.* 2000), the EC_{50} being in the region of 64-240μM (Table 3.2 and Chittajalu *et al.* 1999).

Further evidence that a concentration of 1μM KA is likely to specifically activate KA rather than AMPA receptors is presented in table 3.2 below. The potency of KA at various homomeric and heteromeric AMPA or KA receptors has been outlined, using the EC_{50} for KA induced receptor activation as a measure of potency. Where possible the K_d for KA binding has also been presented, although where stated the IC_{50} values for the displacement of AMPA binding by KA have been substituted.

Subunit	GluR1	GluR2	GluR3	GluR4	GluR5	GluR5Q	GluR5R/ KA1	GluR5R/ KA2
KA EC_{50} (μM)	35_e	–	37.6_o 45.5_l[4,7]	100_s[4, 14]	–	27_n[2,4]	4.2_n[2,4]	6.6_n[2,4]
K_d (nM)		$9\mu M_r$[13]			73_k			

Subunit	GluR6	GluR6 R	GluR6 R/ KA1	GluR6 R/ KA2	GluR7	KA1	KA2	Native KA	Native AMPA
KA EC_{50} (μM)	1_c[1,2] 3.4_b[3] 1.2_h[2] 299_h	2.7_n[2,4] 0.47_f	1.7_n[2,4]	0.45_n[2,4] 1.62_f[4]	mM range$_i$[8]	HNF	HNF	0.81_g 23_q[3]	226_j[9] 320_j[10,12] 180_j[11]
K_d (nM)	12.9_m[6] 95_a				77_a[5]	5_p	15_d		

Table 3.2 The relative potency (EC_{50}) or affinity (K_d) of kainic acid for either AMPA or KA receptors. Receptors are either homomeric or heteromeric for the named subunits or combination. The values for native KA or AMPA receptors were obtained from hippocampal neurones. The three potency values for native AMPA receptors were obtained during the same study at various developmental stages of animals as outlined in the key. HNF indicates a non-functional homomer. Superscripted numbers refer to the following conditions or expression systems: 1. Xenopus oocytes; 2. In the presence of concancvalin A; 3. Cultured hippocampal neurones; 4. HEK 293 cells; 5. HeLa cells; 6. BHK570 cells; 7. Human homologue; 8. Threshold approx. 1mM; 9. Postnatal day 5; 10. Postnatal day 18; 11. Postnatal day 40; 12.Threshold between 5–10μM; 13) IC_{50} value against ^{3}[H] AMPA binding; 14. Measured by ^{45}[Ca] influx. Subscripts refer to the references for the quoted values: a) Bettler *et al* 1992; b) Bleakman *et al.* 1999; c) Egebjerg *et al.* 1991; d) Herb *et al.* 1992; e) Hollmann *et al.* 1989; f) Howe 1996; g) Malva *et al.* 1995; h) Paternain *et al.* 1998; i) Schiffer *et al.* 1997; j) Siefert *et al.* 2000; k) Sommer *et al.* 1992; l) Stern-Bach *et al.* 1994; m) Tygessen *et al.* 1994; n) Valenzuela and Cordoso 1999; o) Watase *et al.* 1997; p) Werner *et al.* 1991; q) Wilding and Heutner 1997; r) Keinanen *et al.* 1990; s) Cushing *et al.* 1999.

Of greatest note are the values presented for native hippocampal AMPA and KA receptor activation by KA. From this it is clear that the EC_{50} values for KA at KA receptors are at least 10 times lower than for AMPA receptors.

3.3.4 Data Acquisition and Analysis

Data was acquired using an Axoclamp 2B amplifier connected to a computer running pClamp 6 software *via* a Digidata 1200 interface.

Population spike amplitudes and EPSP slopes were calculated as a percentage of the average control response for the first population spike and EPSP respectively, thus allowing data from a number of experiments to be pooled more easily. The figures quoted for the responses to various drug treatments have been obtained by calculating the mean and standard error of the mean (S.E.M) for the last three responses in each application period unless otherwise stated using Sigma Plot version 4. Since the response to KA appeared to be biphasic, the mean (±S.E.M.) for the three recordings between 1.5 to 3 minutes into the drug application period have been calculated in addition to the last three

responses of the drug application period for each experiment. Statistical significance was calculated using Student's paired t-test, $p < 0.05$ being deemed significant and $p < 0.01$ highly significant. In order to compare the responses obtained for the various drug application protocols, data at each of the stated time-points were normalised to either the final three responses of the pre-drug control period (in the case of agonist experiments) or those obtained at the end of the antagonist application. This allowed a comparison of the relative shifts in the parameters to be studied in response to drug application. Statistical comparisons of these normalised data were made using Student's unpaired t-test.

Figure 3.2 shows the positioning of the stimulating electrode and both extracellular electrodes in the hippocampal slice during the following series of experiments. The bipolar stimulating electrode was positioned in the *stratum radiatum* such that it would stimulate the Schaffer collateral pathway. Extracellular recording electrodes filled with 3M NaCl were placed into the *stratum radiatum* to record field EPSPs and the *stratum pyramidale* to record field population spikes. The red dotted lines represent the dissection of the CA3 and dentate gyrus resulting in an isolated CA1 preparation.

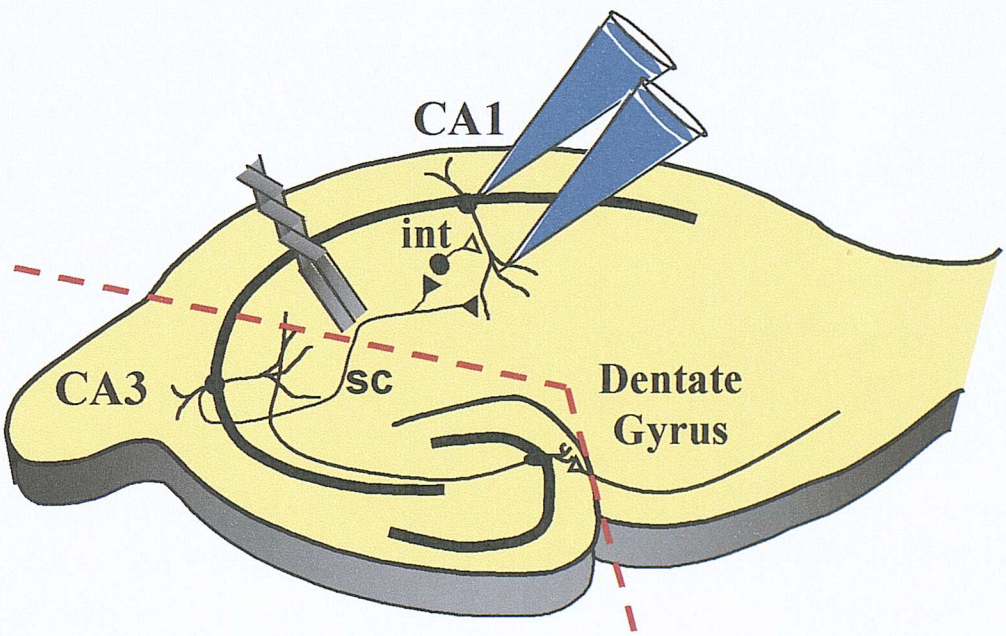

Figure 3.2 Diagrammatic representation of the positioning of the bipolar stimulating electrode in the Schaffer collateral pathway and extracellular recording electrodes in *stratum radiatum and pyramidale* recording field EPSPs and population spikes respectively. Electrode positions are identical in the isolated CA1 preparation. Sc= Schaffer collateral pathway, int= interneurone. Dotted red line represents lines of cut to produce the isolated CA1 preparation.

3.4 Results

In order to investigate the effects of a series of agonists and antagonists for ionotropic glutamate receptors on the EPSP slope, population spike amplitudes and paired-pulse inhibition recorded from the CA1 region of the hippocampus during the application of KA, the following series of experiments were carried out. The responses in whole slices were compared to those in hippocampal slices from which the CA3 and dentate gyrus had been excised in order to separate the down stream effects of KA in the CA3 from CA1 specific responses.

3.4.1.1 Threshold concentration for the action of KA in intact slice CA1

A series of cumulative concentration-response experiments were carried out in order to ascertain the threshold concentration of KA required to elicit a change in the field response of the CA1 in intact slices (figures 3.3-3.6). An example of the raw data obtained during the course of these experiments is presented in figure 3.3.

Cumulative concentration-response data for the first and second EPSP slopes recorded from the CA1 region of intact slices is presented in figure 3.4. Application of 250nM KA resulted in a significant reduction ($p<0.01$ Student's paired t-test) in the slope of the second EPSP (figure 3.4). This was augmented by further additions of KA up to a concentration of 1μM KA. The first EPSP slope also began to decrease at 250nM KA, but was not significantly affected until the concentration of KA in the recording chamber reached 500nM.

Figure 3.5 shows the first and second population spike amplitudes recorded from *stratum pyramidale* during the same experiments presented in figure 3.4. Application of 250nM KA also resulted in a significant increase ($p<0.01$) in the amplitude of both the first and second population spike amplitudes (figure 3.5). Further increases in the KA concentration resulted in a significant reduction in population spike amplitude below control values.

This apparent separation between the threshold sensitivity of the first EPSP and the first population spike to the actions of KA suggests that KA may be acting at more than one site with slightly differing affinities. This is supported by the uncoupling of the reduction in EPSP slope from the increase in population spike amplitude.

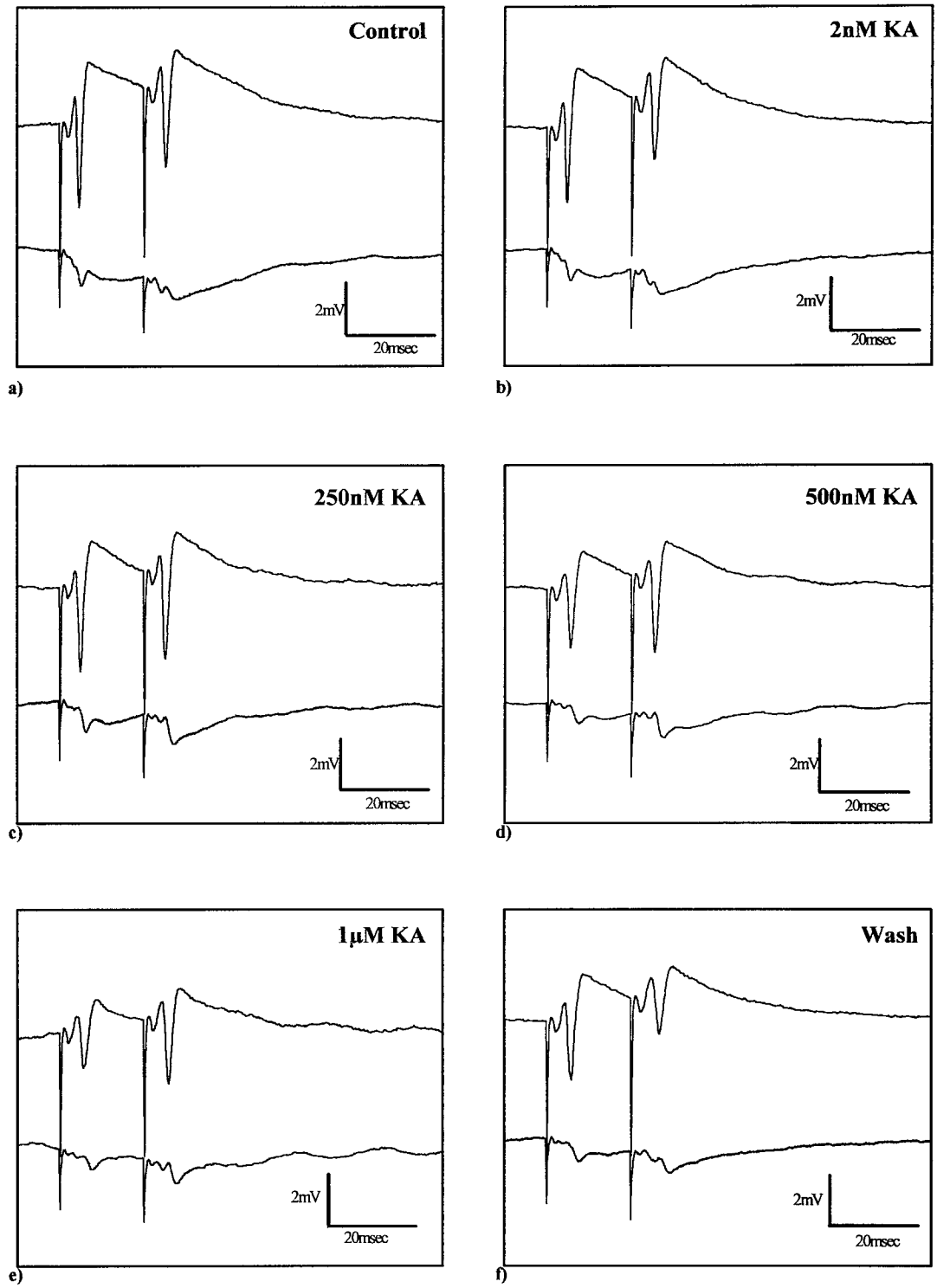

Figure 3.3 Example traces taken during a cumulative KA dose-response time course experiment carried out in the CA1 region of an intact slice using a 20msec paired-pulse protocol. Each figure shows the average of three population spikes and EPSPs recorded for a given stimulus at the end of each application period. a) Control; b) 2nM KA; c) 250nM KA; d) 500nM KA; e) 1μM KA; f) wash.

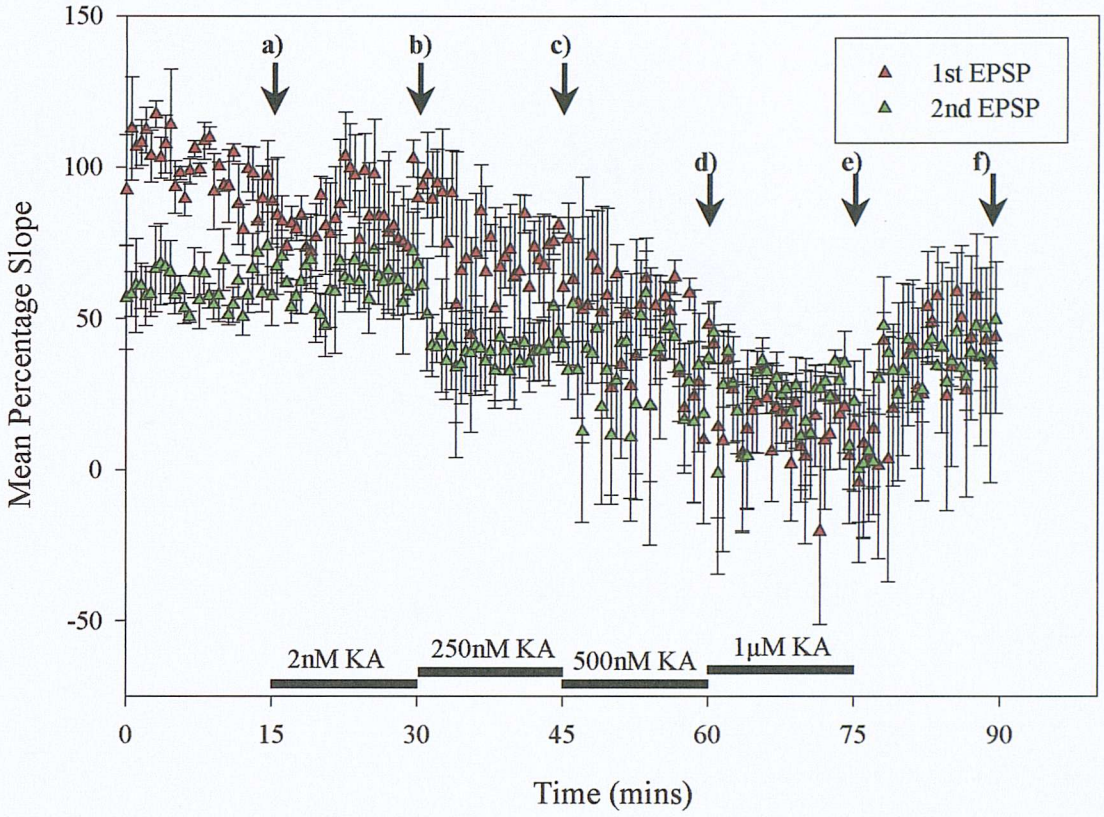

Figure 3.4 Time-course data for the effect of cumulatively increasing concentrations of KA in the intact CA1 on the mean percentage slope of the first and second EPSPs. The second EPSP is reduced in slope within the first three minutes of increasing the concentration of KA in the recording chamber to 250nM (62% (±7.0) to 42% (±6.4), $p<0.01$). The second EPSP continues to decrease reaching 29% (±11.5) ($p<0.05$) by the end of 500nM KA. The first EPSP does not show a significant change in slope until the end of 15 minutes at 500nM KA, when it is reduced from 54% (±16.5) to 21% (±14.8), $p<0.01$). Both EPSP slopes continue to fall during 1µM KA application, but neither are significantly different to the values for the end of 500nM (n=3). Arrows and letters represent the time-points for which example traces are shown and quoted numbers were calculated.

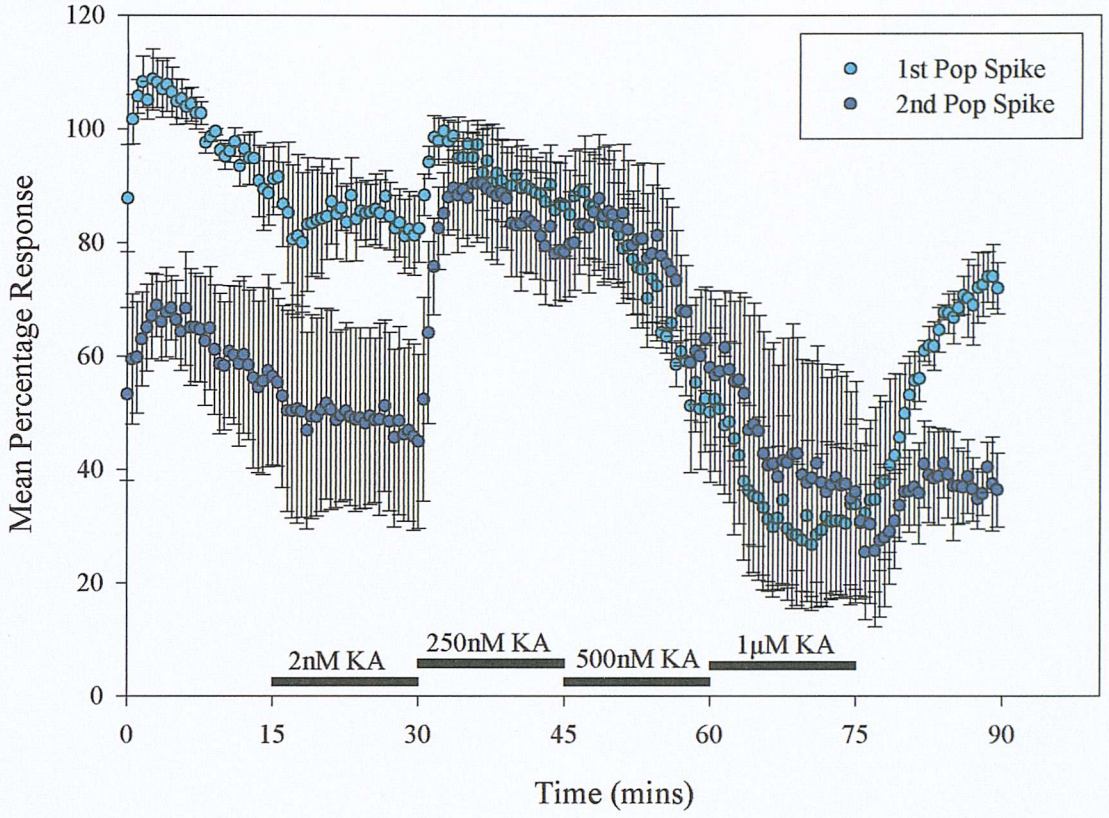

Figure 3.5 Time-course data for the effect of cumulatively increasing concentrations of KA on the mean percentage population spike amplitude recorded from the CA1 region of intact hippocampal slices (n=3). Application of 250nM KA causes a marked increase in the amplitude of both the first and second population spike from 82% (±3.4) to 99% (±1.78) ($p<0.01$) and 46% (±8.0) to 81% (±4.1) ($p<0.01$) respectively. The first spike decreases significantly during the 15 minute application period to 88% (±3.9) ($p<0.01$). The decrease in the second population spike during this time is not statistically significant (80% (±4.6)). The responses seen within the first three minutes of 500nM KA application do not differ significantly from the end of the 250nM KA period (89% (±4.2) and 83% (±4.7) respectively. However, by the end of this period both the first and second population spike have begun to decrease in amplitude and continue to do so throughout the application of 1μM KA (32% (±6.9) and 37% (±9.7) respectively ($p<0.01$).

Data for the mean percentage inhibition throughout the course of the cumulative KA concentration-response experiment in intact slices is presented in figure 3.6. Application of 250nM KA results in a significant reduction ($p<0.01$) in the mean percentage inhibition. This is further reduced by subsequent increases in the concentration of KA in the recording chamber.

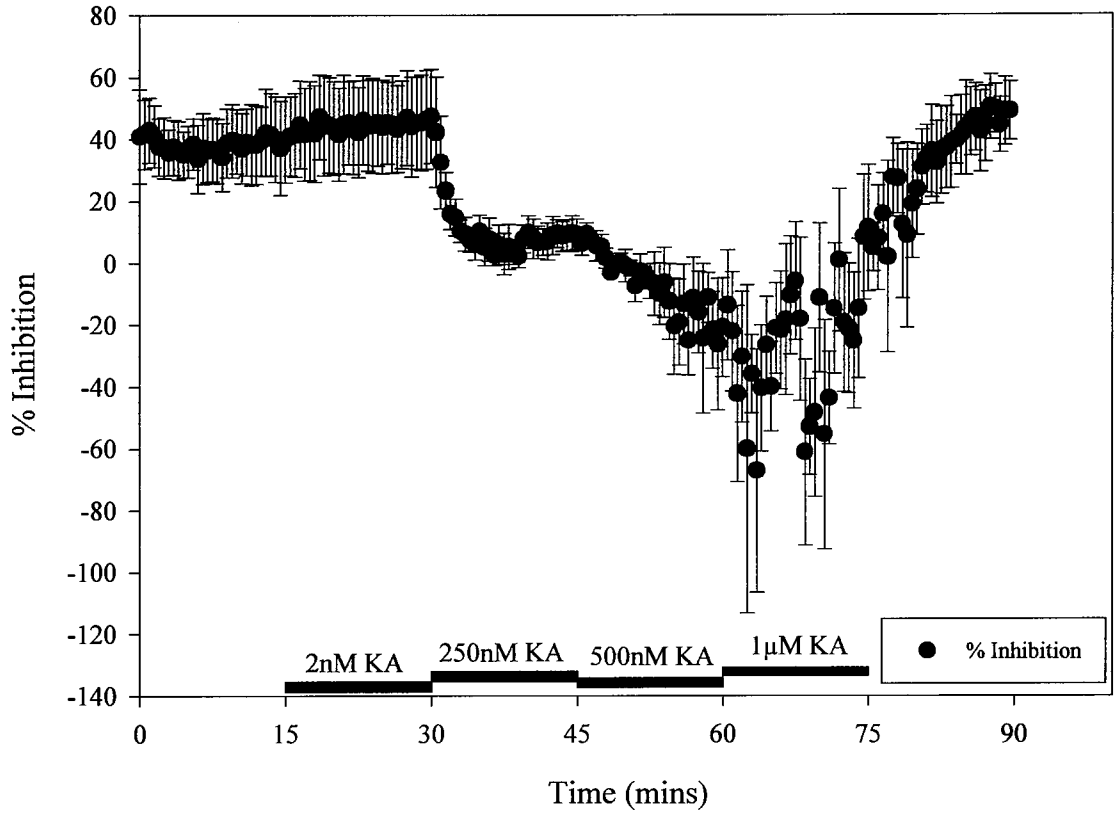

Figure 3.6 Shows the effects of cumulative increases of KA concentration on the mean percentage inhibition (± S.E.M.) of the second population spike with respect to the first recorded using a paired pulse protocol with a 20msec interpulse interval from the CA1 region of intact hippocampal slices (n=3). Introduction of 2nM KA to the recording chamber produces a small but significant increase in the mean percentage inhibition from 40% (±7.1) to 46% (±7.7) ($p<0.01$). As the concentration of KA rises to 250nM the percentage inhibition falls rapidly, reaching 9% (±2.6) after 15 minutes ($p<0.01$). During the superfusion with 500nM the inhibition is further reduced, resulting in a facilitation of the second spike (-20% (±7.8), $p<0.01$) which is further exacerbated in the presence of 1μM KA (-44% (±18.9).

3.4.1.2 KA threshold: the role of CA3

The role of the CA3 region in the observed threshold concentration for the action of KA in the CA1 was investigated in slices from which the CA3 and dentate gyrus had been removed (figures 3.7- 3.10). Example traces obtained during the course of these experiments are presented in figure 3.7. Data for the first and second EPSP slopes are presented in figure 3.8 and the population spike amplitude data in figure 3.9.

Increasing the concentration of KA in the recording chamber from 2nM to 250nM KA resulted in a significant reduction in the slope of both the first ($p<0.01$) and second EPSP ($p<0.05$) slopes (figure 3.8). Thus it would appear that the EPSP exhibits sensitivity to KA at a threshold of 250nM irrespective of the presence of CA3 (figure 3.4).

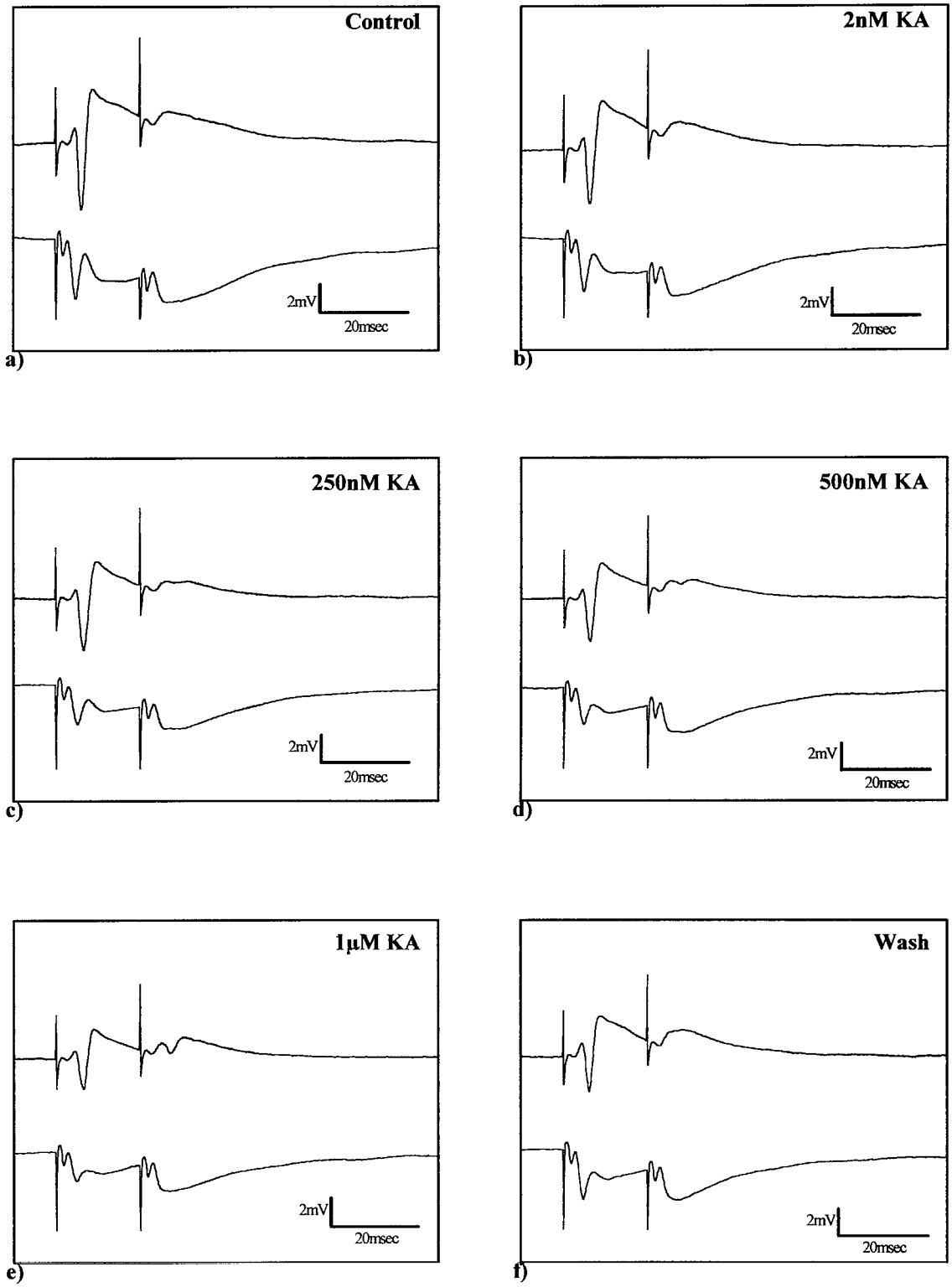

Figure 3.7 Example traces of recordings made from *stratum pyramidale* and *stratum radiatum* of an isolated CA1 preparation during the time course of a cumulative KA dose-response experiment. Each figure represents the average of three traces taken at the end of each application period. a) Control; b) 2nM KA; c) 250nM KA; d) 500nM KA; e) 1μM KA; f) wash.

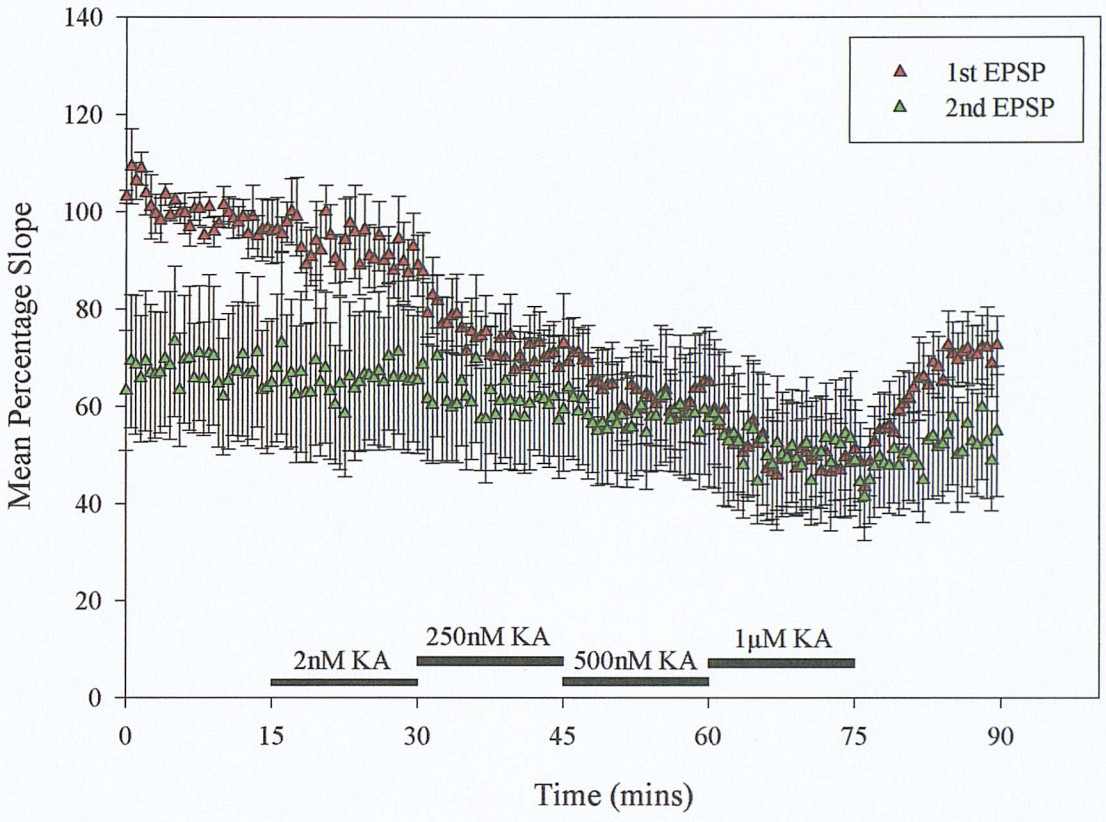

Figure 3.8 Time-course data for the mean percentage EPSP slope taken from cumulative dose-responses to KA in isolated CA1 preparations. There is no significant difference in the slope of either the first or second EPSP recorded during the control period and either the beginning or end of 2nM KA. Within the first three minutes of the concentration of KA in the recording chamber reaching 250nM the mean first EPSP slope decreases from 90% (±4.0) to 80% (±3.5) ($p<0.01$). By the end of 15 minutes 250nM KA the second EPSP slope is also significantly reduced from 66% (±7.6) to 60% (±6.6) ($p<0.05$). This downward trend continues as the concentration of KA increases although it is only at a concentration of 1μM that any further significant change occurs (55% (±5.7) within the first three minutes of 1μM KA for the first EPSP ($p<0.01$) and 54% (±7.4) for the second ($p<0.01$).

The second population spike amplitude increased significantly at a concentration of 250nM KA (figure 3.9) although not to such an extent as observed in the intact slice preparation (figure 3.5). However, this suggests a direct action of KA on the interneurone population of CA1. Since the amplitude of the first population spike appears to be decreasing from the control period onwards it is difficult to determine whether the first population spike amplitude is also sensitive to KA in the absence of CA3 from this data set.

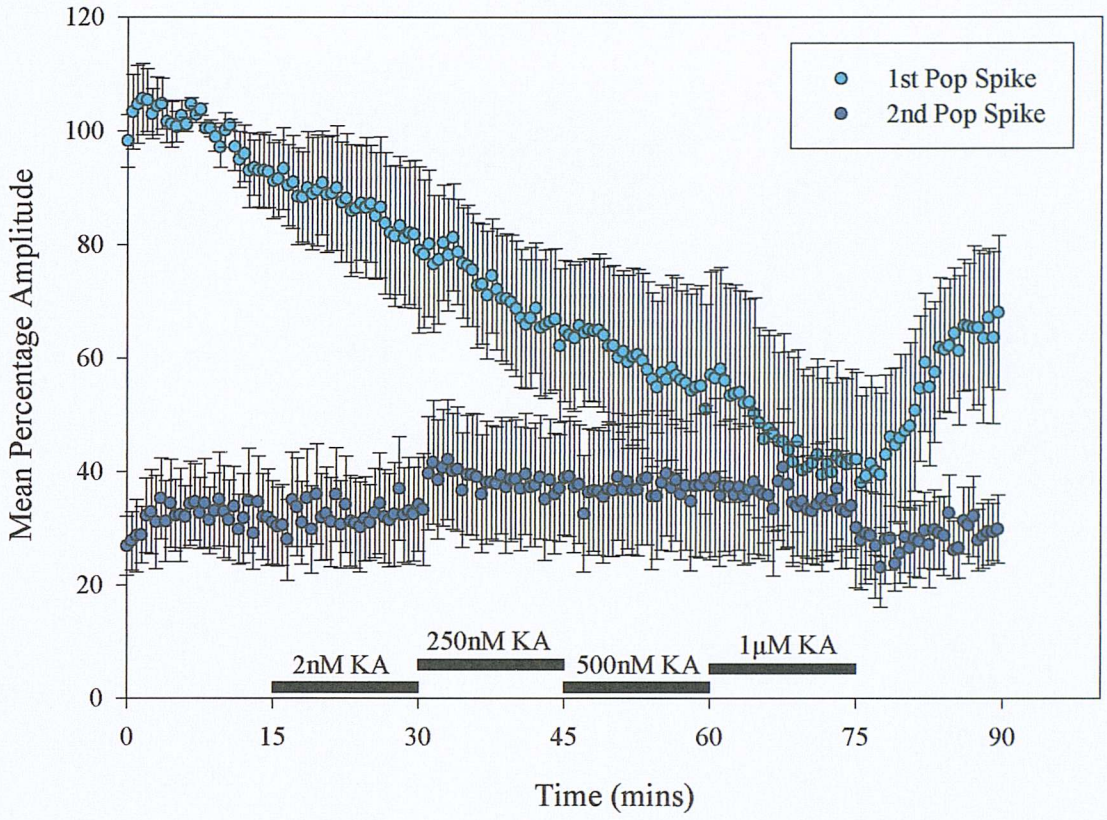

Figure 3.9 Percentage mean population spike amplitude data for the effect of cumulatively increasing concentrations of KA in isolated CA1 preparations (n=5). The first population spike amplitude decreases steadily from 93% (±3.5) to 42% (±8.2) by the end of 15 minutes superfusion with 1μM KA ($p<0.01$). The second population spike amplitude increases significantly within the first three minutes of the concentration of KA reaching 250nM from 33% (±4.7) at the end of the application of 2nM KA to 40% (±5.7) ($p<0.01$). It does not significantly change from this value until the end of the experiment.

The falling amplitude of the first population spike during the control period also makes the interpretation of the paired-pulse inhibition data for the isolated slice preparation (figure 3.10) problematical. However, as would be expected with a falling first population spike amplitude and a relatively stable second population spike amplitude, the percentage inhibition calculated from these data continues to decrease throughout the experiment.

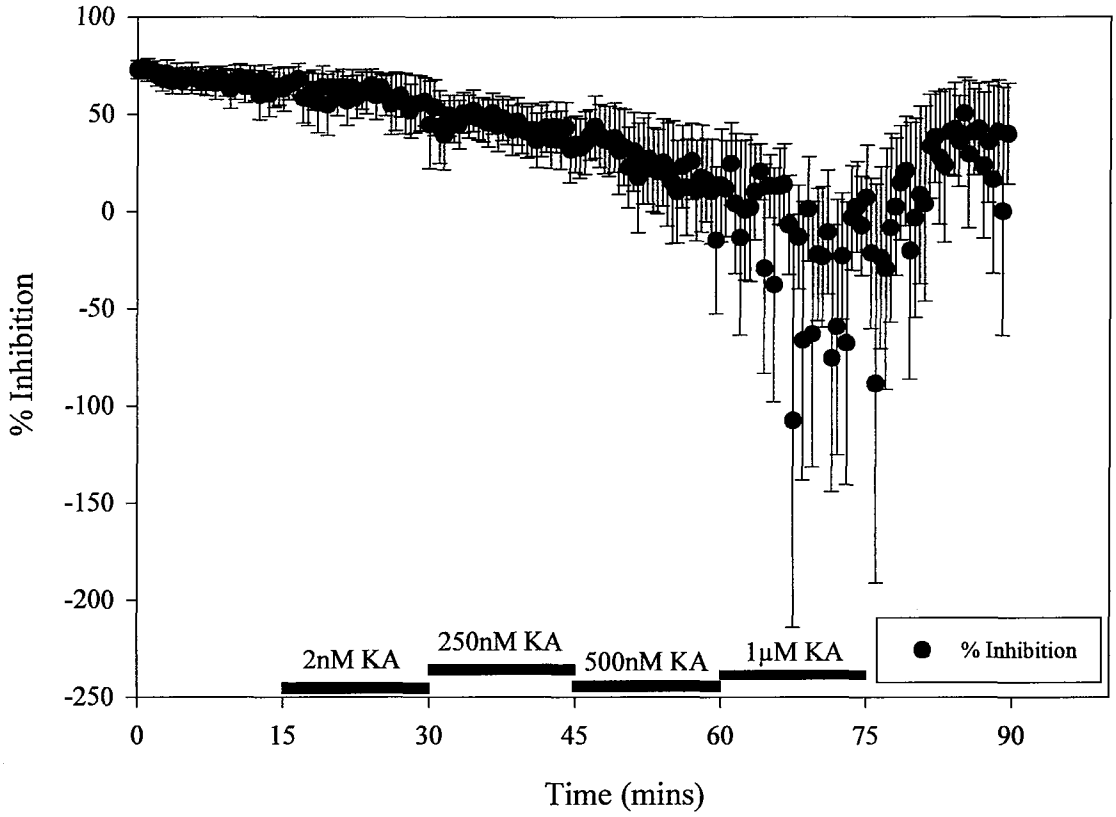

Figure 3.10 Time-course for the effect of cumulative increases in KA concentration on the percentage inhibition of the second population spike with respect to the first recorded from isolated CA1 preparations (mean % inhibition ± S.E.M., n=5). At a concentration of 2nM there is a small, but significant decrease in the mean percentage inhibition from 63% (±5.6) to 56% (±7.4) ($p<0.05$). This trend continues as the concentration of KA rises until facilitation of the second population spike occurs at a concentration of 1μM KA (-3% (±13.5), $p<0.01$)).

3.4.2.1 1μM KA time-course: the intact slice preparation

Single applications of 1μM KA were carried out in order to investigate whether the data obtained from the cumulative concentration-response experiments (figures 3.4-3.6 and 3.8-3.10) were a true representation of the action of KA at this concentration or represented the effects of receptor desensitisation. Furthermore, a concentration of 1μM KA was chosen since it is at or below the EC_{50} for KA at native KA receptors in various brain regions and well below the EC_{50} values for the activation of native AMPA receptors by KA (table 3.2). Thus it was anticipated that at 1μM, KA application would exhibit phenomena commensurate with the selective activation of KA receptors over AMPA receptors. Indeed such a case has previously been put forward by both Kamiya and Ozawa (1998) and Mulle *et al.* (2001).

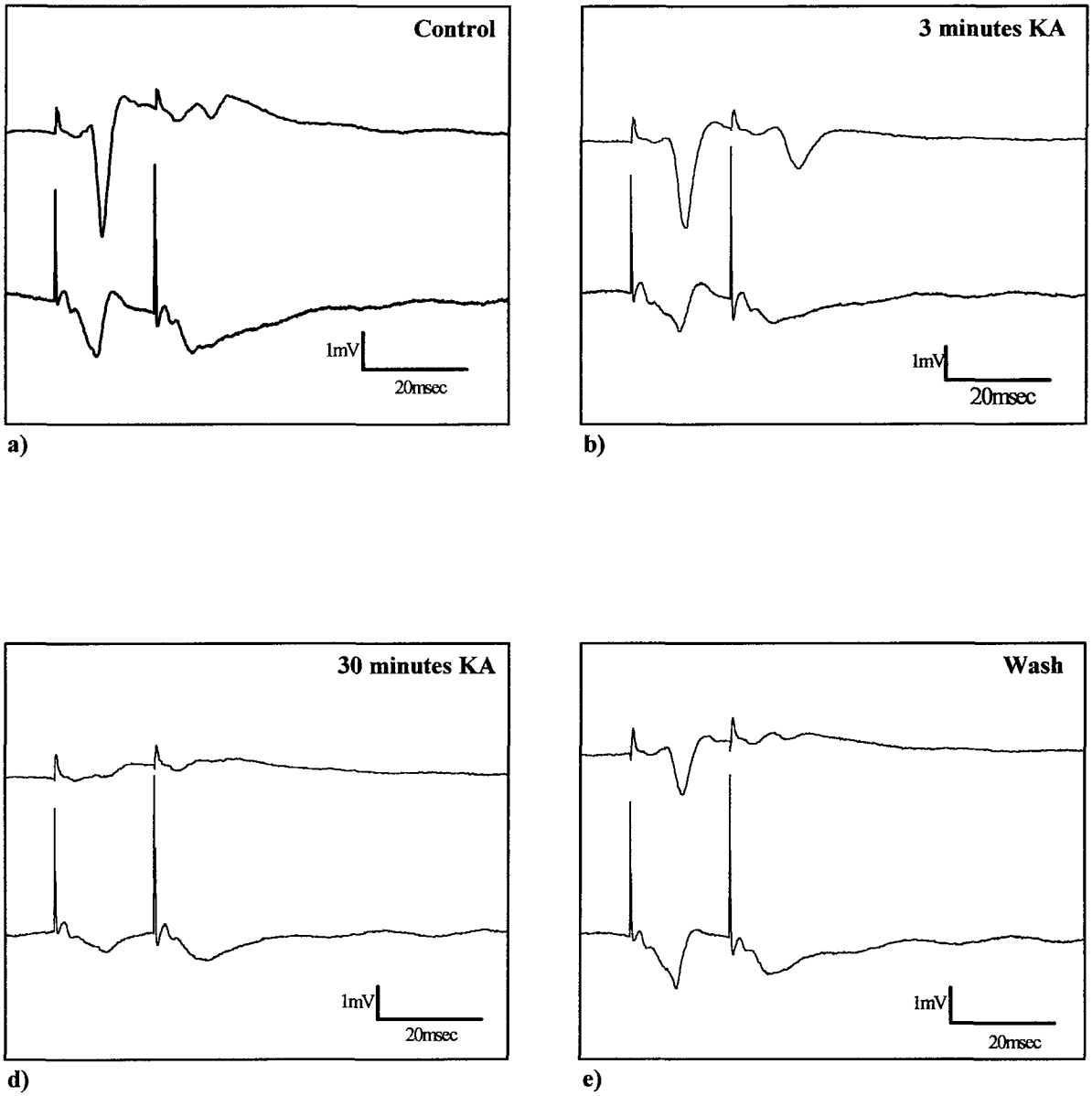

Figure 3.11 Example traces for the effect of 1μM KA on the population spike amplitude and EPSP slope recorded from the CA1 region of an intact hippocampal slice. Each trace represents the average of three responses. a) Control, b) onset of the KA effect, c) end of the KA application period, d) following 30 minutes ACSF wash.

Application of 1μM KA in the intact slice preparation resulted in a number of effects (figures 3.11-3.13). Within the first three minutes of application, the first and second EPSP slopes began to decrease (figure 3.12). At this same time, there was a marked, transient increase in the amplitude of both the first and second population spikes. Since this occurs at a time when the EPSP slope had begun to decrease, it would suggest that KA is acting at more than one site in this preparation.

Following this, both first and second population spikes reduced in amplitude to well below control values (figure 3.12). Thus at this concentration, KA exhibits a biphasic response with regards to population spike amplitude, which was not observed during the cumulative concentration response experiments (figure 3.5). This reduction persists for at least 30 minutes following wash of KA.

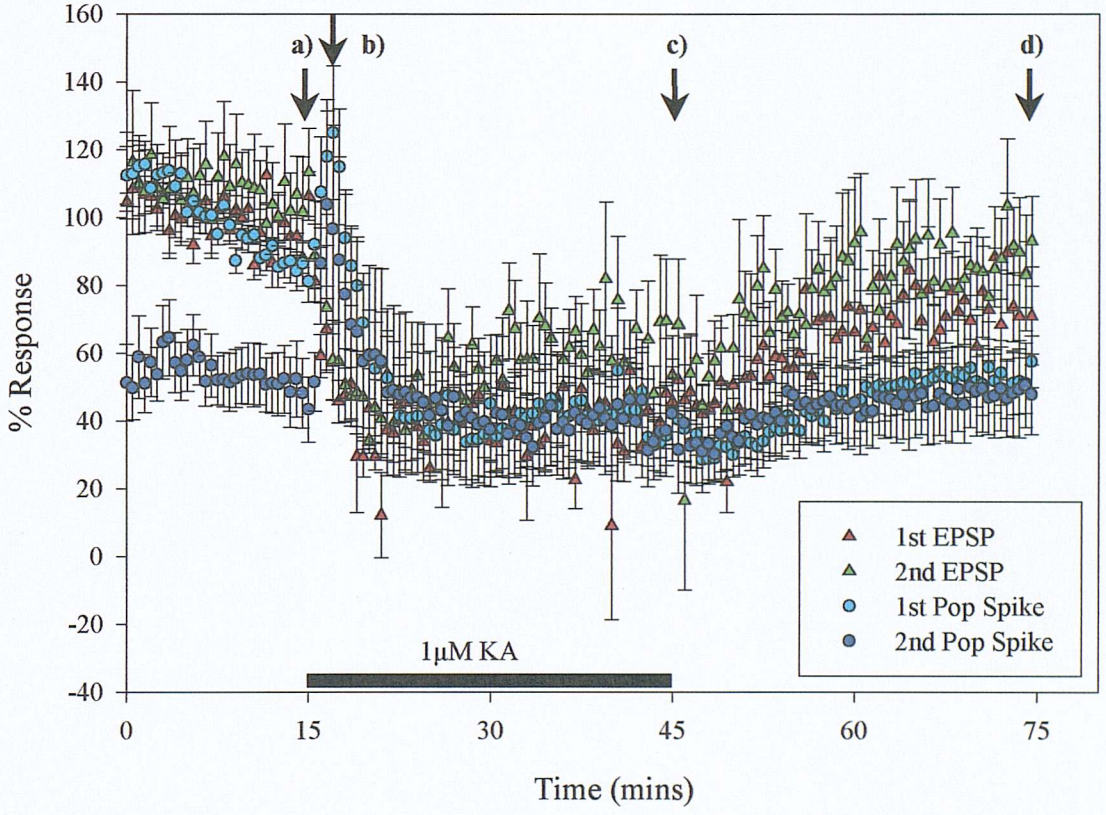

Figure 3.12 Time-course for the effects of application of 1μM KA in the CA1 region of intact hippocampal slices (n=5). It is interesting to note that there is an initial increase in the amplitude of both the first and second population spikes recorded using a paired-pulse protocol with a 20 msec interpulse interval from 86% (± 3.4) to 119% (±9.7) ($p=0.01$) for the first spike and from 50% (±5.7) to 96% (±16.0) ($p<0.05$) for the second. This implies a rapid and transient reduction in both evoked and tonic inhibition. This is coupled with a decrease in the slope of the EPSP recorded from *stratum radiatum* from 92% (±3.0) to 41% (±6.4) ($p<0.01$) for the first EPSP, 103% (±7.1) to 62% (±9.0) ($p<0.01$) for the second by the end of the KA application period. It can also be seen that, while the EPSP slope begins to return to control values following 30 minutes wash, the population spike amplitude remains depressed compared to control. Arrows and letters correspond to the example traces in the previous figure. Quoted numbers were calculated at these time-points.

Calculation of the mean percentage inhibition from this data (figure 3.13) reveals a rapid marked reduction in the paired-pulse inhibition following the application of 1μM KA that persists throughout the KA application period.

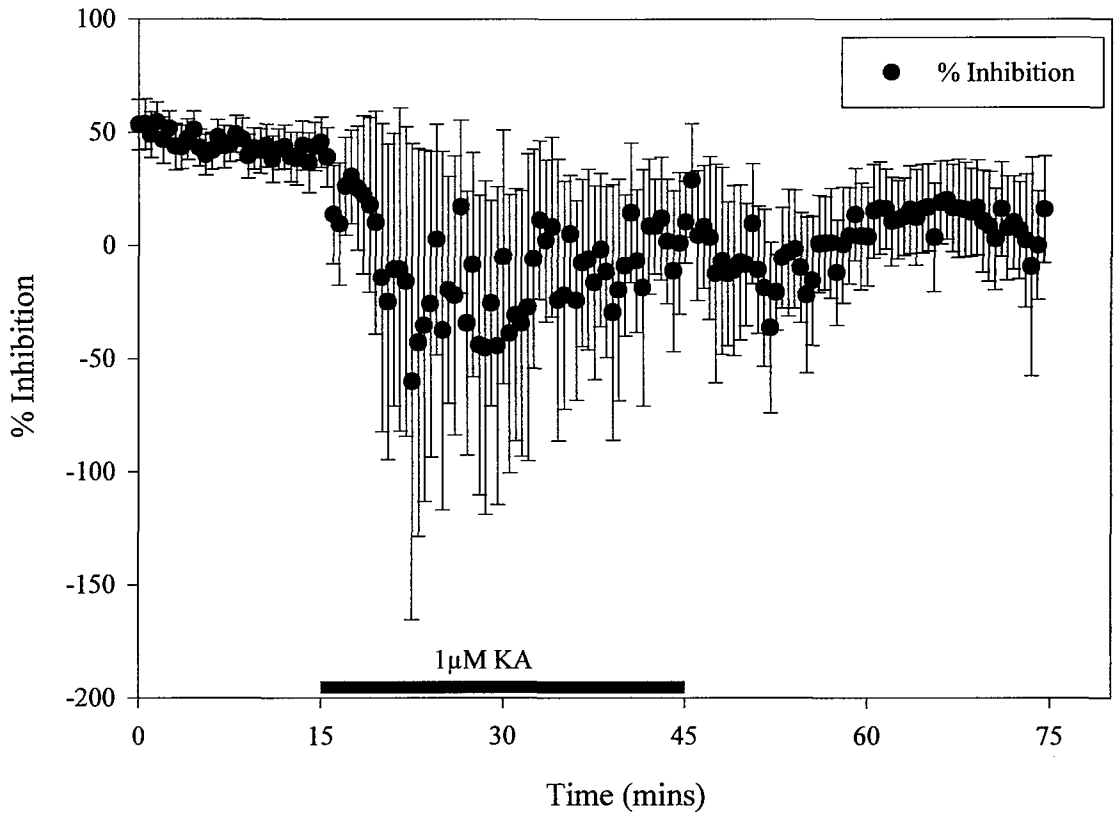

Figure 3.13 The effect of 1μM KA application on the mean percentage inhibition (± S.E.M.) of the second population spike with respect to the first spike recorded from the CA1 region of intact hippocampal slices during a paired-pulse protocol using a 20msec inter-pulse interval (n=5). The effect of KA appears highly variable, but the net result appears to be a reduction in the percentage inhibition from 42% (±6.3) to -3% (±17.0) ($p<0.05$ Student's paired t-test) by the end of the KA application period.

3.4.2.3 The response to 1μM KA: the role of CA3

The effect of KA application in CA1 was studied in the absence of CA3 in order to gain an understanding of how the CA3 may be affecting the response to KA in the CA1 region (figures 3.14- 3.16).

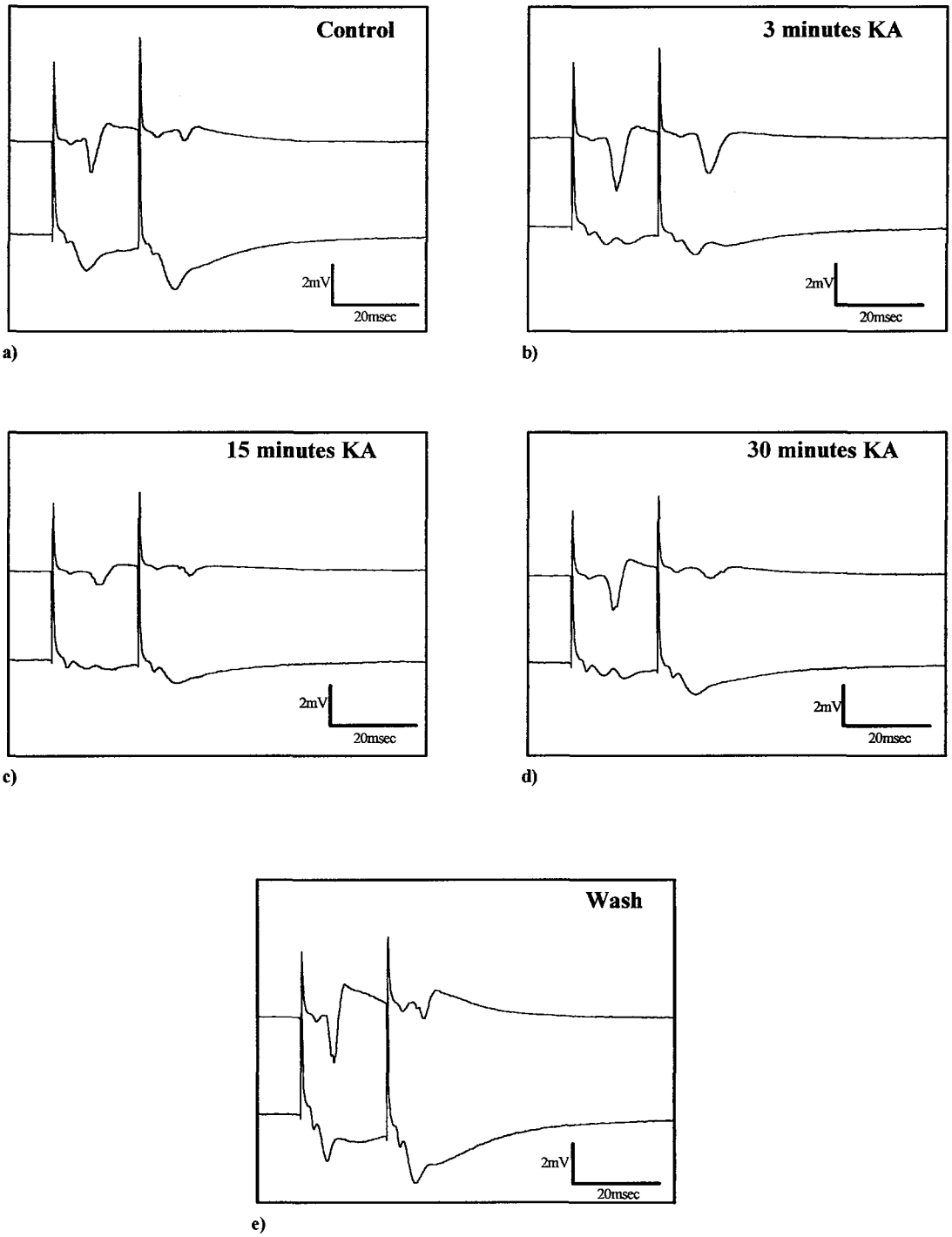

Figure 3.14 Example traces taken from a time-course experiment to observe the effects of 1μM KA on the population spike amplitude and EPSP slope in an isolated CA1 preparation. Each trace represents the average of three responses recorded at the following time points: a) the end of 15 minutes control period, b) within the first three minutes of KA application, c) 15 minutes into the KA application period, d) after 30 minutes of KA superfusion, e) the end of 30 minutes ACSF wash.

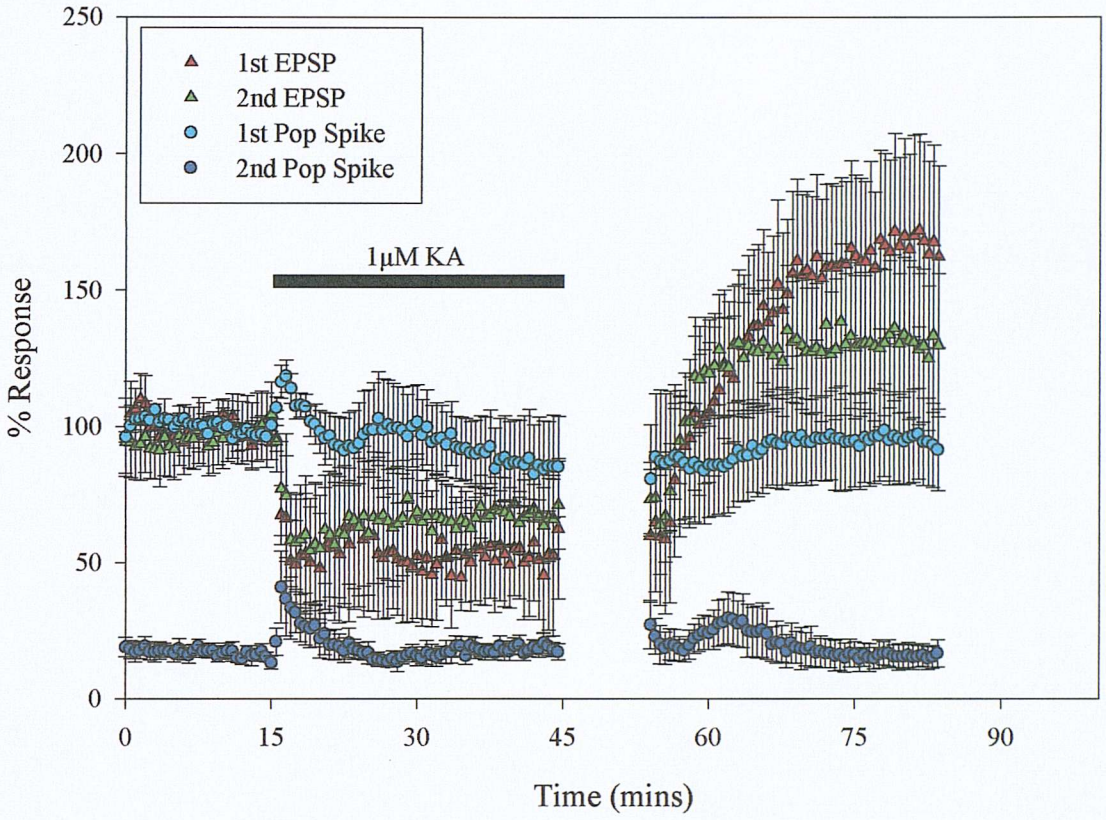

Figure 3.15 Time-course data for the effect of 1μM KA application on the population spike amplitude and EPSP slope (mean percentage ±S.E.M.) recorded from *stratum pyramidale* and *stratum radiatum* respectively in isolated CA1 preparations (n=5). As in the intact preparation, the amplitude of both the first and second population spikes increases within the first three minutes of drug application (97% (±1.3) to 113% (±3.2) ($p<0.01$) and 16% (±1.3) to 34% (±6.0) ($p<0.01$) for the first and second spikes respectively. This is coupled with a simultaneous decrease in the EPSP slope (from 100% (±2.11) to 55% (±10.0) ($p<0.01$) and 100% (±7.0) to 63% (±10.5) ($p<0.01$) for the first and second EPSPs respectively. In the absence of CA3 the population spikes recover to control values whilst the EPSPs appear to undergo potentiation, although this may be due to the steadily increasing stimulation which occurred during the stimulus-response curve carried out during the break in the time-course.

As previously observed in the intact slice (figure 3.12), application of 1μM KA to isolated CA1 preparations resulted in a rapid reduction in the EPSP slope (figure 3.15) which remained depressed throughout the KA application period. This was coupled with an increase in the amplitude of both the first and second population spikes within the first three minutes of application. However, in contrast to the intact slice preparation (figure 3.12), following this transient increase the population spike amplitudes did not decrease significantly below initial control values (figure 3.15).

This suggests that both the reduction in EPSP slope and the transient increase in population spike amplitudes occur independently of the presence of the CA3 region.

However, the subsequent reduction in the population spike amplitude observed in the intact slice (figure 3.12) may occur as a result of the action of KA on the CA3 pyramidal cell population.

The mean percentage inhibition calculated from these data (figure 3.16) also differ from that observed in the intact slice preparation (figure 3.13). During the first three minutes of KA application, there is a transient decrease in the paired-pulse inhibition corresponding to the observed increase in both the first and second population spike amplitudes.

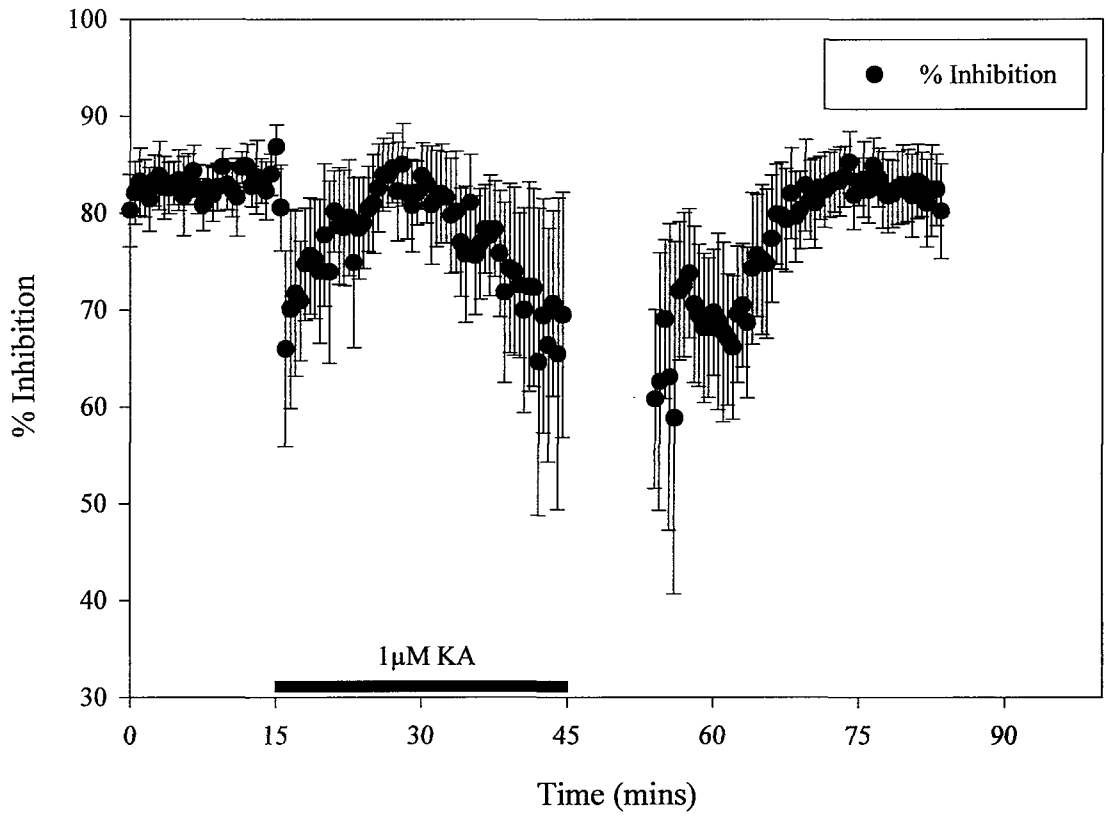

Figure 3.16 Time-course for the effects of 1μM KA application on the percentage inhibition (mean ± S.E.M.) of the second population spike recorded using a paired-pulse protocol with a 20msec inter-pulse interval in isolated CA1 preparations (n=5). This protocol allows the assessment of $GABA_A$ mediated inhibition within the preparation throughout the course of the experiment. It can be seen that the percentage inhibition decreases with the onset of KA (1μM) application from 83% (±1.4) to 71% (±4.5) ($p<0.01$). By the end of the KA application period there is no significant difference in the percentage inhibition to control ($p=0.08$). The percentage inhibition also appears to be far less variable in the absence of CA3.

3.4.2.3 The effect of 1μM KA in the CA3

In order to gain a better understanding of how the CA3 may be modulating the responses observed in the CA1 during KA application, 1μM KA was applied to an acute slice taken from a 15 day old Wistar rat whilst recording from both the *stratum radiatum* and *stratum pyramidale* of the CA3 (figures 3.17 - 3.18).

Intact slices were prepared as described in section 3.3.1, and half-maximal stimuli administered to the hilar region. Recordings were made *via* extracellular electrodes placed into the *stratum pyramidale* and *stratum radiatum* of the CA3 region.

KA application resulted in a rapid and marked reduction of both the first and second population spike amplitudes and also both the first and second EPSP slopes (figure 3.18). This would tend to suggest that 1μM KA results in a strong depolarising block of the CA3 region, resulting in a cessation of field activity.

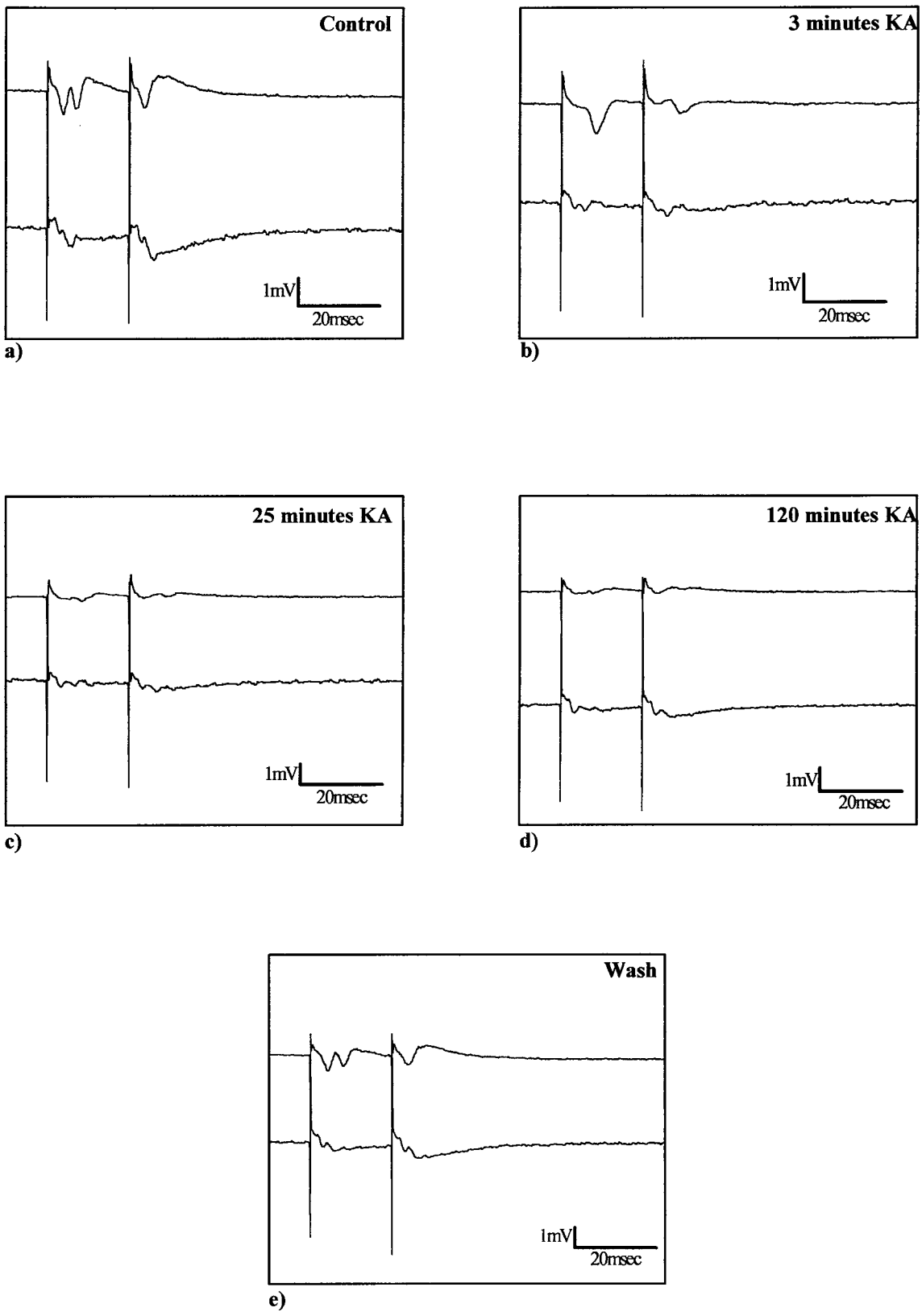

Figure 3.17 Example traces showing the effect of 1μM KA on the field population spike and EPSP recorded from the CA3 region of a hippocampal slice taken from a 15 day old Wistar rat. Each trace represents the average of three responses taken at the following time points: a) at the end of 15 minutes control stimulation, b) within three minutes of the start of KA administration, c) after 25 minutes KA application, d) at the end of 120 minutes KA application, e) the end of 60 minutes ACSF wash.

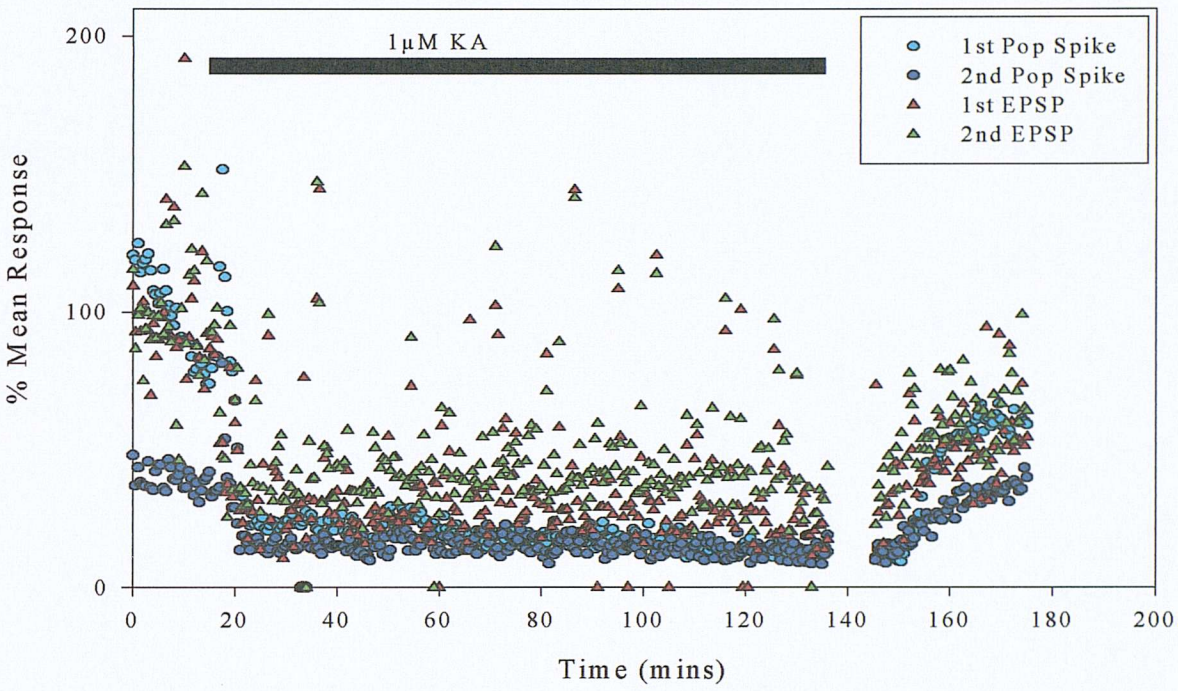

Figure 3.18 Time course for the application of 1µM KA in CA3 of acute slices. Recordings were taken from *stratum radiatum* and *stratum pyramidale* of a hippocampal slice taken from a 15 day old Wistar rat following stimulation of the hilus. Light blue and dark blue circles represent first and second population spike amplitudes and red and green triangles represent first and second EPSPs respectively. (n=1)

3.4.3.1 The response to ATPA in intact slice preparations

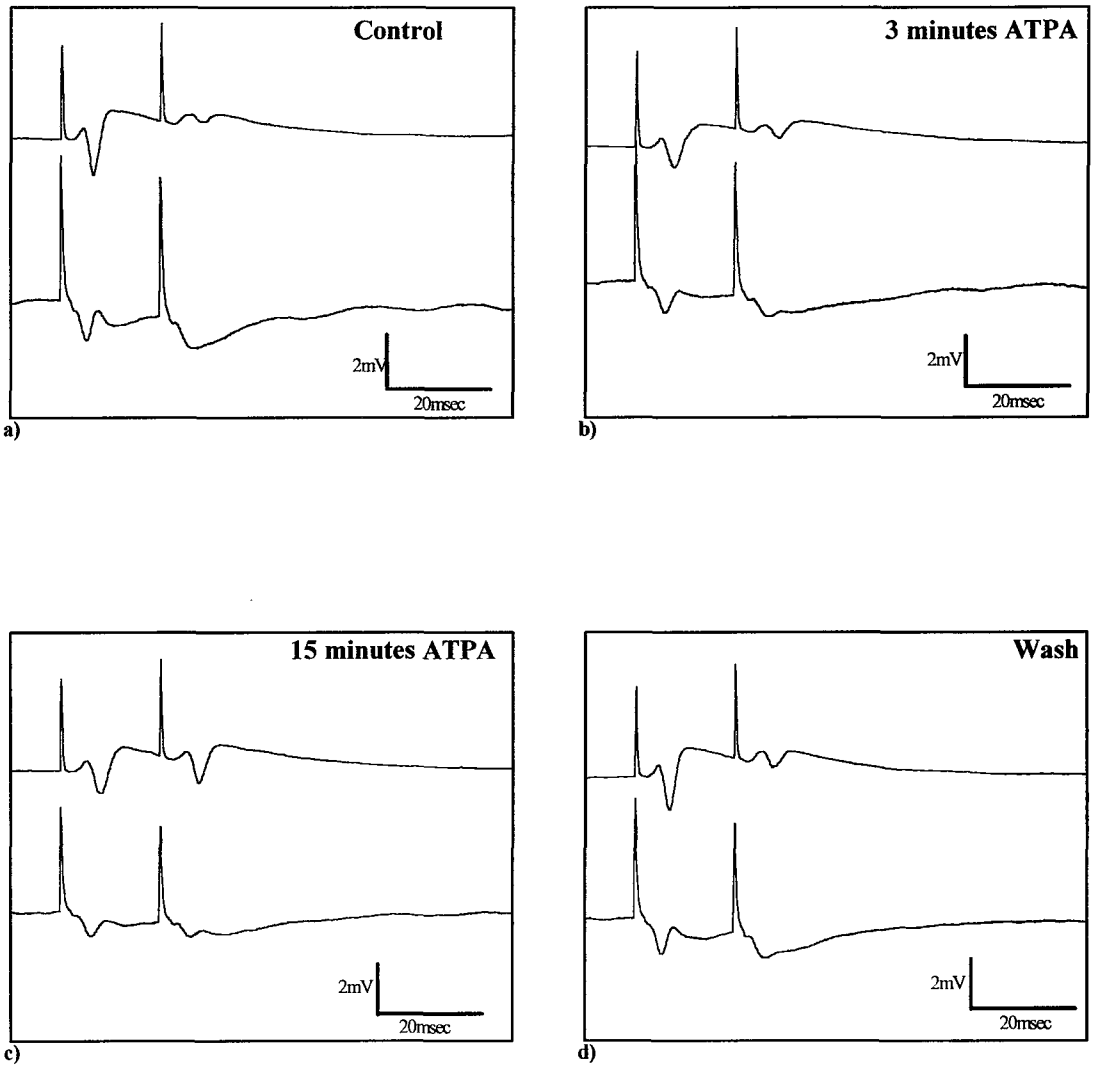

Figure 3.19 Example traces recorded from the CA1 of an intact slice a) prior to application of 1μM ATPA, b) within the first three minutes of the addition of ATPA, c) after 15 minutes in the presence of 1μM ATPA and d) at the end of a 30 minute wash. Each trace represents the average of 3 recordings.

In order to attempt to elucidate the role of the GluR5 subunit in the native KA receptors responsible for the effects observed during the application of 1μM KA, intact slices were superfused with 1μM ATPA ((RS)-2-Amino-3-(3-hydroxy-5-tbutylisoxazol-4-yl)propanoic acid) and evoked field responses recorded from the *stratum pyramidale and radiatum* of CA1 (figure 3.19). Thus, any similarities between the field response to 1μM ATPA (figure 3.20) and 1μM KA (figure 3.12) would tend to suggest that the response occurs as a result of the activation of GluR5 containing receptors.

Application of 1μM ATPA to the superfusing ACSF resulted in a marked reduction in the EPSP slopes (figure 3.20). However, in contrast to the observed effects of 1μM KA in the CA1 of intact preparations (figure 3.12), ATPA application did not result in a transient increase in population spike amplitude (figure 3.20). In fact, ATPA application resulted in a marked reduction in the first population spike amplitude and a significant increase in the amplitude of the second population spike ($p<0.01$).

Since ATPA is selective for receptors containing the GluR5 subunit at a concentration of 1μM (Vignes *et al.* 1998) these data suggest agreement with reports of the ability of GluR5 activation to reduce the EPSP slope recorded from the CA1 region (Kamiya and Ozawa 1998, Vignes *et al* 1998). They also suggest that KA is probably causing a similar effect in the CA1 *via* GluR5 activation.

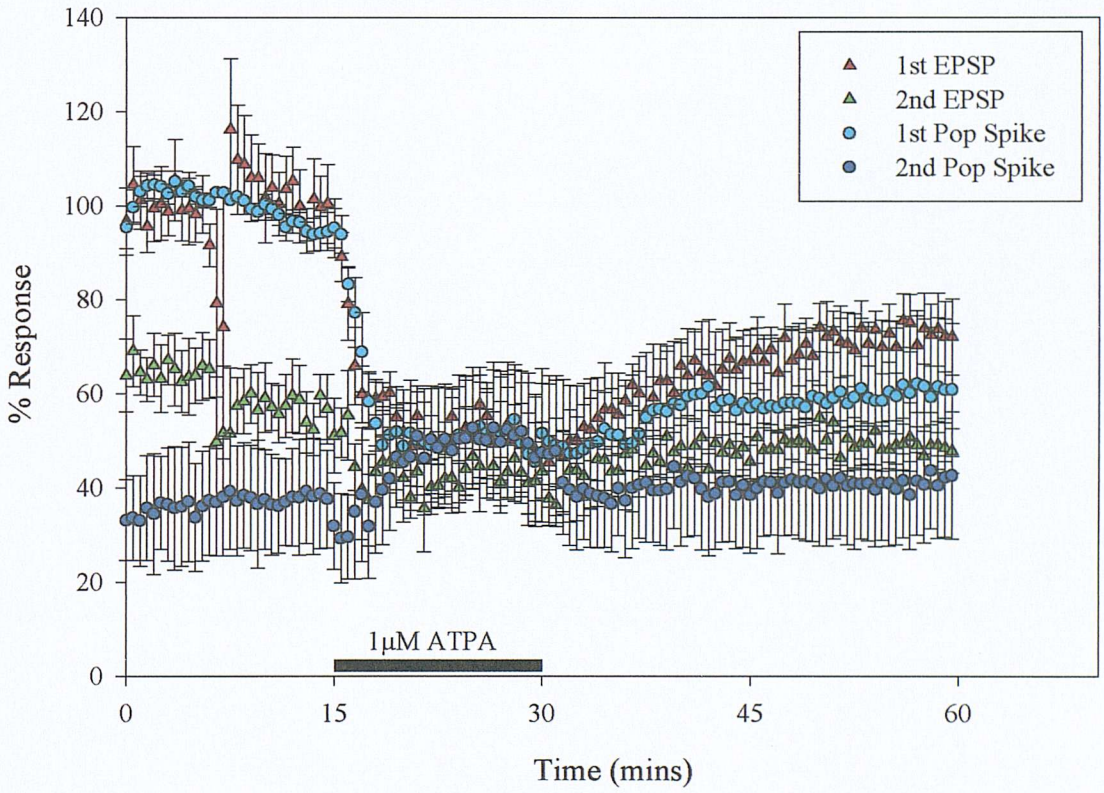

Figure 3.20 Time-course for the application of 1μM ATPA to intact hippocampal slices. The graph shows the effect of ATPA on the mean percentage population spike amplitudes and EPSP slopes (± S.E.M.) recorded from *stratum pyramidale* and *stratum radiatum* respectively. ATPA causes a reduction of both the EPSPs and first population spike amplitudes from 100% (±4.2) to 62% (±3.7) ($p<0.01$) for the first EPSP, 56% (±3.3) to 40% (±4.8) ($p<0.01$) for the second EPSP and 94% (±2.0) to 68% (±4.4) ($p<0.01$) for the first population spike within the first three minutes of drug application. This occurs without the initial increases in both the first and second population spike amplitudes seen during the application of 1μM KA. In addition to this the second population spike amplitude is seen to increase during the application period from 38% (±6.1) to 49% (±7.4) by the end of the ATPA application ($p<0.01$). It is interesting to note however that there is a small but significant decrease in the amplitude of the second population spike as ATPA is washed into the recording chamber (30% (± 4.9), $p<0.01$ n=5).

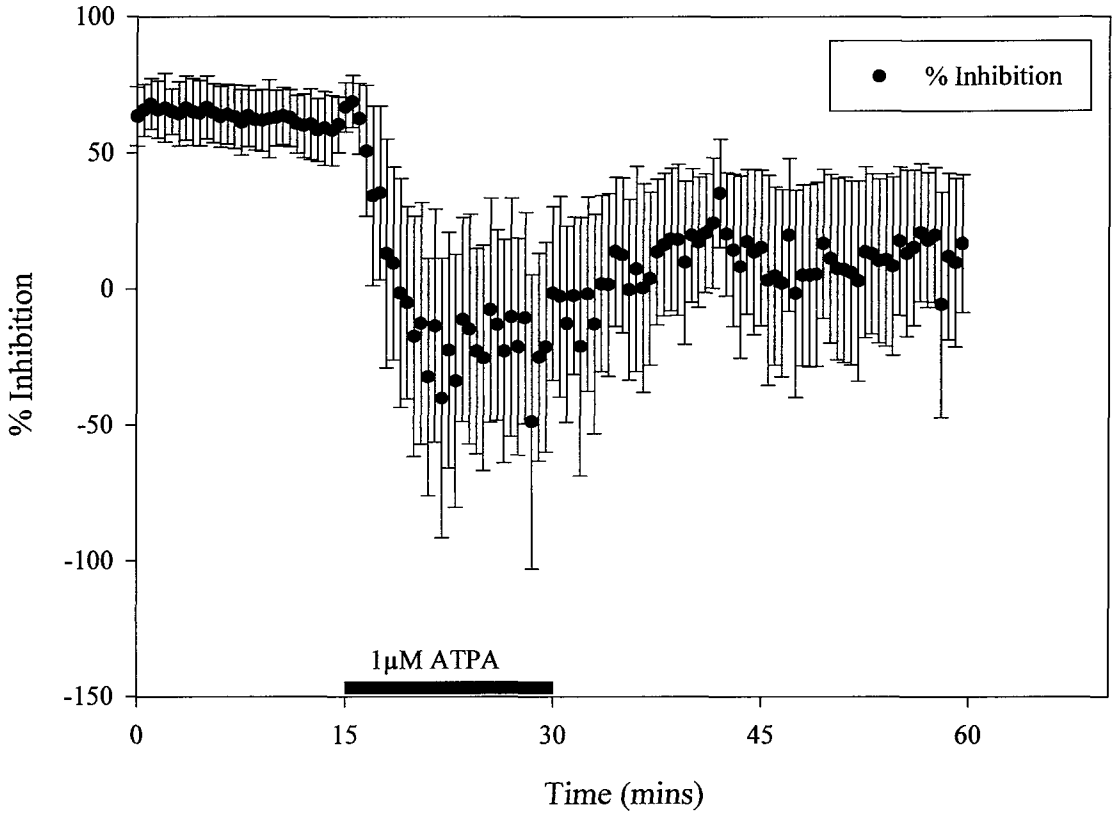

Figure 3.21 Shows the time course for changes in the percentage inhibition of the second population spike with respect to the first (mean percentage inhibition ± S.E.M.) following the application of 1μM ATPA in the CA1 region of intact hippocampal slices (n=5). ATPA application causes a reduction in the paired-pulse inhibition to the extent that the second population spike becomes potentiated with respect to the first from 59% (±6.6) to -32% (±23.9) by the end of 15 minutes ATPA application ($p<0.01$). However, during the introduction of ATPA to the recording chamber the percentage inhibition transiently increases to 66% (±5.7). This increase is seen to reach significance ($p<0.05$, Student's paired t-test).

The percentage inhibition calculated during the application of 1μM ATPA in intact hippocampal slices (figure 3.21) (n=5) transiently increases as ATPA washes into the recording chamber ($p<0.05$). This again is in contrast to the response seen with KA (figure 3.13) and provides indirect evidence agreeing with Cossart *et al.* (1998) that activation of dendritic GluR5 receptors on interneurones increases interneuronal spiking and thus leads, at least initially, to an increase in GABA release. Since Mulle *et al.* (2000) have shown that domoate is able to increase the spontaneous IPSC frequency in CA1 pyramidal cells of $GluR5^{-/-}$ mice it is likely that these dendritic receptors are actually heteromeric receptors probably also containing the GluR6 subunit. Recent evidence from studies in guinea pig hippocampus (Semyanov *et al* 2001) suggests that these receptors may be located on interneuronal axons. However, there is no evidence to date that this is also true

in the rat hippocampus. By the end of the application period, the percentage inhibition decreased to well below control values.

3.4.3.2 The response to ATPA in isolated slice preparations: the role of CA3

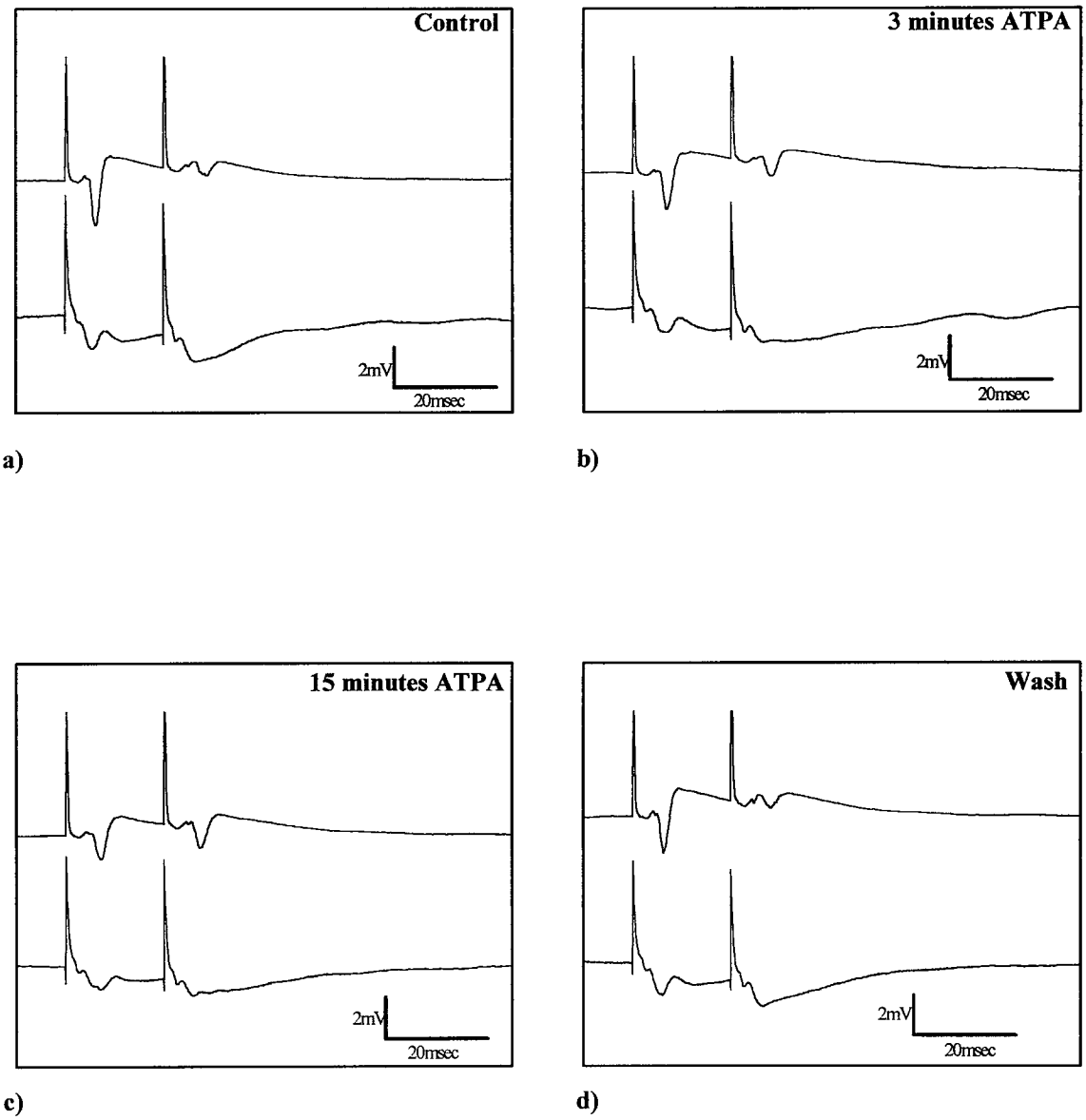

Figure 3.22 Example traces recorded from an isolated CA1 preparation during a time-course experiment to observe the effects of 1μM ATPA on the population spike amplitude and EPSP slopes elicited using a 20msec paired-pulse protocol with a submaximal stimulus. Each figure represents the average of three traces taken a) at the end of a 15 minute control period, b) within 3 minutes of ATPA application, c) at the end of 15 minutes ATPA application and d) following 30 minutes wash.

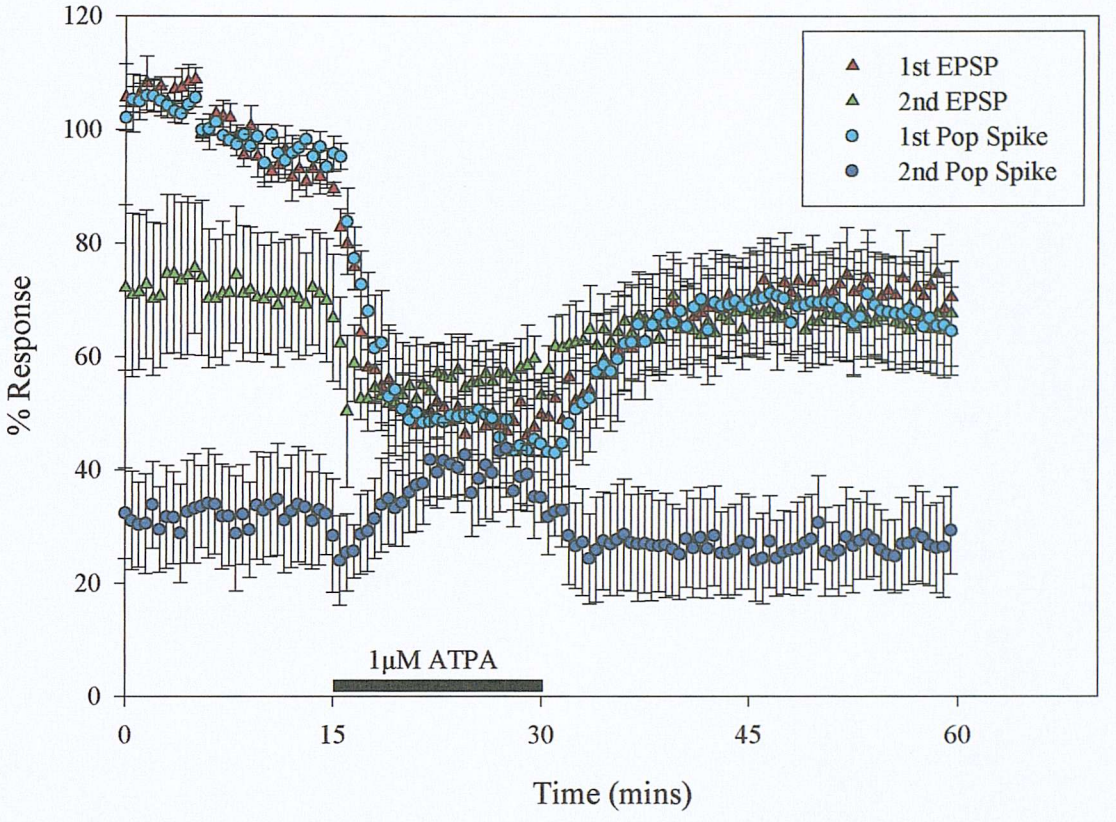

Figure 3.23 Time-course for the effects of 1μM ATPA on the population spike amplitude and EPSP slope (mean percentage response ± S.E.M.) recorded from isolated CA1 preparations (n=5). In the absence of CA3, 1μM ATPA still causes a reduction in the first population spike and both EPSPs (from 95% (±1.5) to 73% (±3.4) for the first population spike, 93% (±1.7) to 66% (±3.4) and 71% (±5.6) to 55% (±3.0) for the first and second EPSPs respectively, $p<0.01$) within the first three minutes of drug application. As in the intact slice, the second population spike is first seen to transiently decrease in amplitude from 32% (±4.6) to 26% (±4.5) during the first one and a half minutes. (n=5)

The response to application of ATPA in the absence of the CA3 region (figure 3.23) shows great similarity to the intact preparation (figure 3.20). Once again there is no apparent potentiation of the first or second population spikes as is seen with 1μM KA (figure 3.15). In fact the amplitude of the first population spike decreases from 95% (±1.5) to 73% (±3.4) ($p<0.01$). The second population spike appears to transiently decrease in size also, but this does not reach significance. As in the intact slice preparation (figure 3.20), the EPSP slopes decrease significantly within the first three minutes of drug application ($p<0.01$). An example of the raw-data obtained during the course of this experiment is presented in figure 3.22.

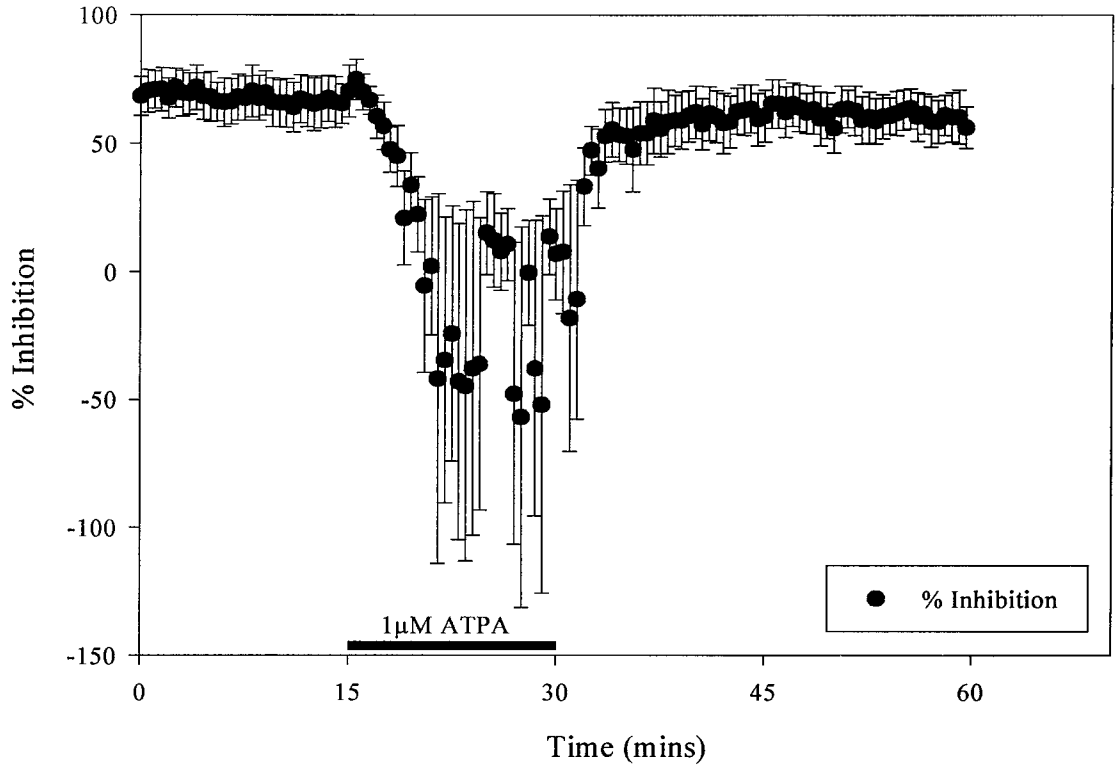

Figure 3.24 Shows the effect of 1μM ATPA application on the percentage inhibition of the second population spike recorded from isolated CA1 preparations using a paired-pulse protocol with a 20msec interpulse interval (mean percentage inhibition (± S.E.M.), n=5). Coinciding with the decrease in second population spike amplitude which occurs with the onset of ATPA's effects, the percentage inhibition undergoes a small but significant increase during the first minute and a half of the drug application period (from 67% (±4.8) to 72% (±4.5), $p<0.05$). Following this ATPA application causes a marked reduction in the percentage inhibition, leading to facilitation of the second population spike (-25% (±30.2) at the end of 15 minutes application, $p<0.01$).

During the first 1.5 minutes of ATPA application in the isolated CA1 preparation (figure 3.24) there is a small, but significant transient increase in the mean percentage inhibition ($p<0.05$). However, by the end of the application period, the inhibition has decreased significantly below control values ($p<0.01$). It is of note that the effects of ATPA appear to wash out more thoroughly in the isolated slice (figure 3.24) than the intact slice (figure 3.19) preparation.

3.4.4.1 Kainate receptor antagonism: Intact slice preparation

NS102 acts as a competitive antagonist (Johansen *et al* 1993) at both the GluR5 (Wilding and Heuttner 1996) and GluR6 subtype of KA receptor (Verdoorn *et al.* 1994). However it would appear that it acts most potently as an antagonist at the largely homomeric GluR6 subtype of KA receptors expressed on embryonic hippocampal neurones (Lerma *et al* 1993). The following figure (3.25) shows example traces taken from a time-course experiment to investigate the effects of 10μM NS102 (6,7,8,9-Tetrahydro-5-nitro-1H-benz[g]indole-2,3-dione 3-oxime) on the KA response in an intact hippocampal slice.

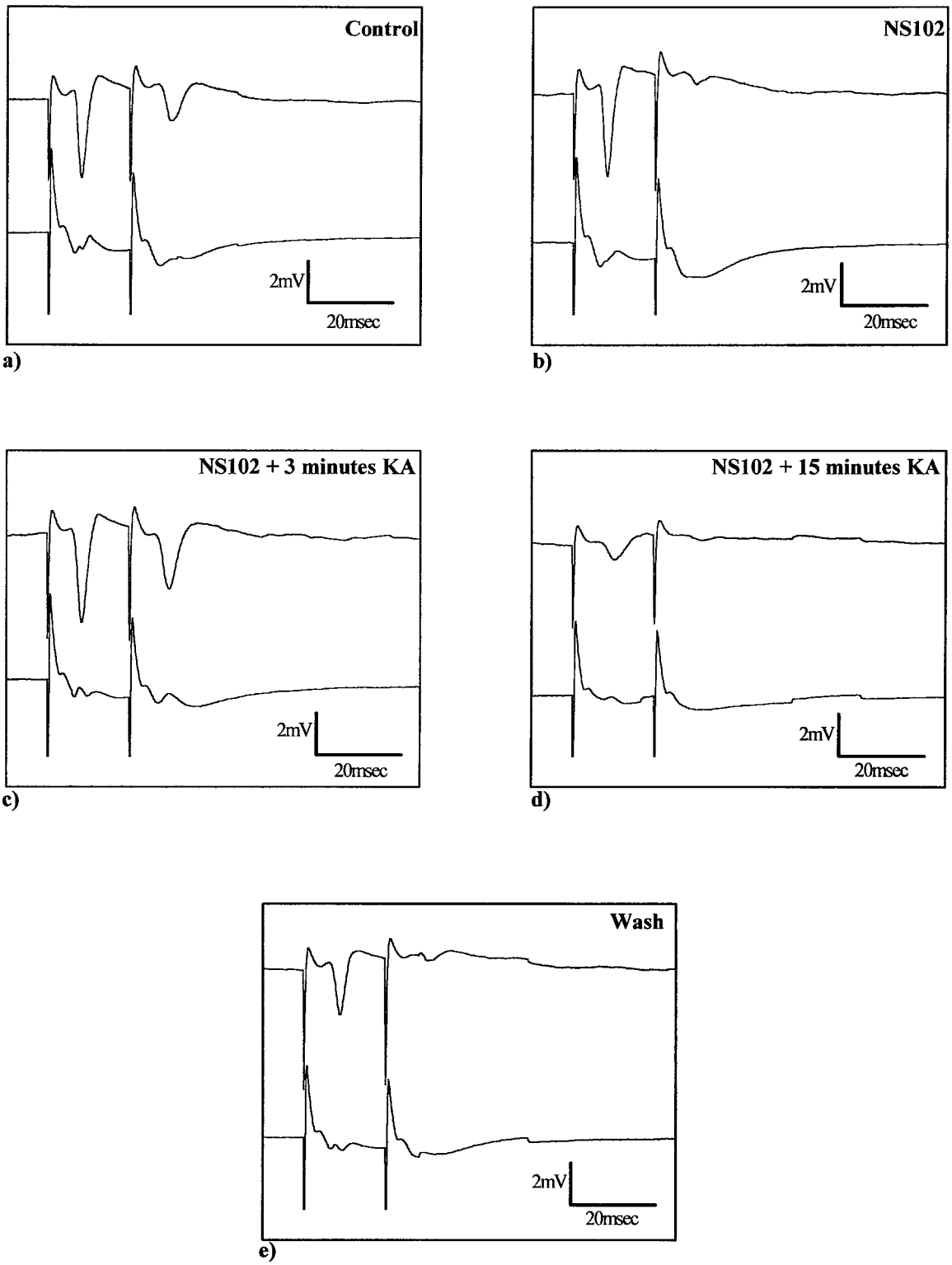

Figure 3.25 Example traces taken from a time-course experiment examining the effect of 10μM NS102 on the response to 1μM KA recorded from the CA1 region of intact hippocampal slices. Each trace represents the average of three recordings made from *stratum radiatum* for EPSPs and *stratum pyramidale* for population spikes. These recordings were made at the following time points: a) at the end of a 15 minute control stimulation period, b) at the end of 15 minutes NS102 application, c) within the first three minutes of 1μM KA addition, d) at the end of 15 minutes KA co-application and e) at the end of 30 minutes ACSF wash.

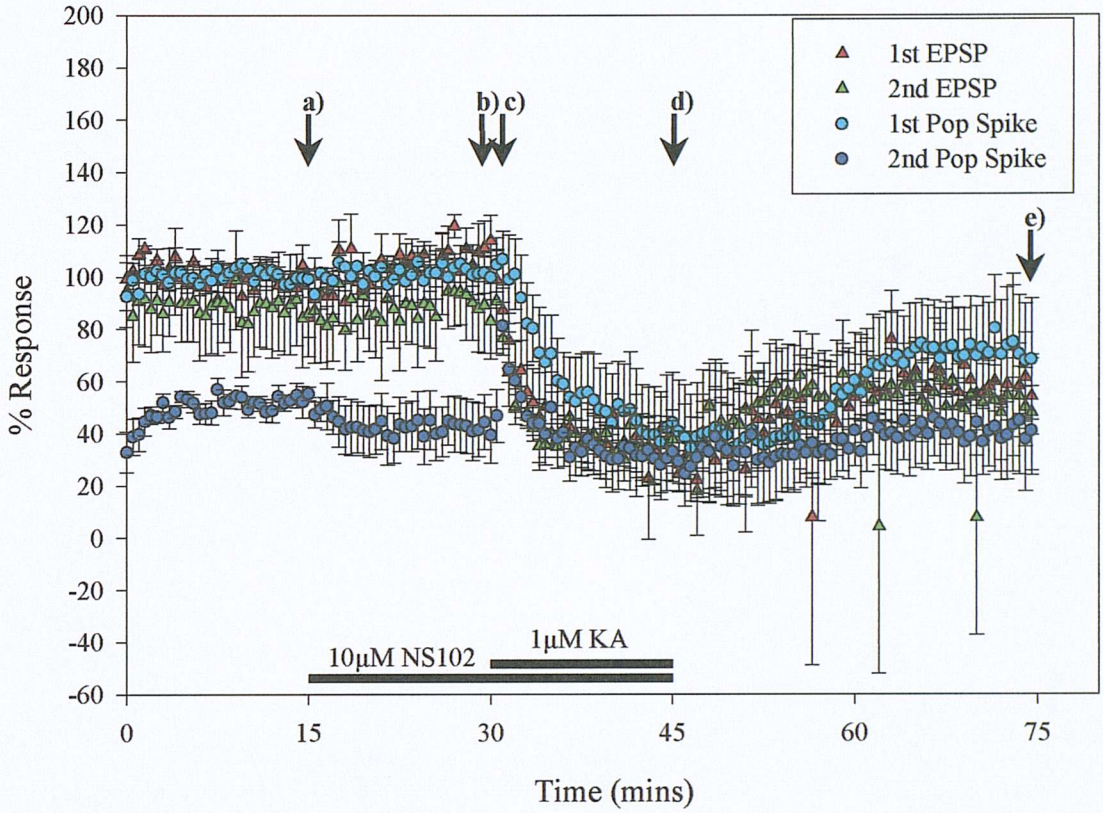

Figure 3.26 Time-course for the effect of 10μM NS102 application on the mean percentage response (± S.E.M.) to 1μM KA recorded from the *stratum pyramidale* and *stratum radiatum* of the CA1 region of intact hippocampal slices (n=4). The graph shows the mean first and second population spike amplitudes and EPSP slopes recorded using a 20 msec paired-pulse protocol as a percentage of the mean baseline response for the first population spike and first EPSP respectively. During the application of NS102 there is no significant change in the slope of either of the two EPSPs or the amplitude of the first population spike. The second population spike however undergoes a small but significant decrease from 53% (±2.4) to 42% (±5.6) ($p<0.05$). With the onset of the effects of 1μM KA the second population spike increases significantly from the NS102 values to 60% (±4.9) ($p<0.05$). At the same time, both EPSP slopes begin to decrease from 108% (±5.2) to 67% (±7.8) for the first EPSP and 89% (±8.6) to 56% (±3.1) ($p<0.01$). In the presence of 10μM NS102, the first population spike does not undergo a transient increase in amplitude following addition of 1μKA. Arrows and letters correspond to the time-points at which example traces were taken and quoted numbers calculated. All experiments involving the use of antagonists were sampled at the same times unless otherwise stated.

Application of NS102 to intact slices (figure 3.26) causes a small but significant decrease in the amplitude of the second population spike ($p<0.05$), n=5). Introduction of KA to the recording chamber results in a significant increase in the amplitude of the second spike ($p<0.05$), although the amplitude of the first spike does not change significantly. This is in contrast to the response observed for KA alone (figure 3.12). In addition to this, the percentage slopes of both the first and second EPSPs decrease

significantly from control ($p<0.01$). The graph of the percentage inhibition of the second population spike calculated with respect to the first is shown below in figure 3.27.

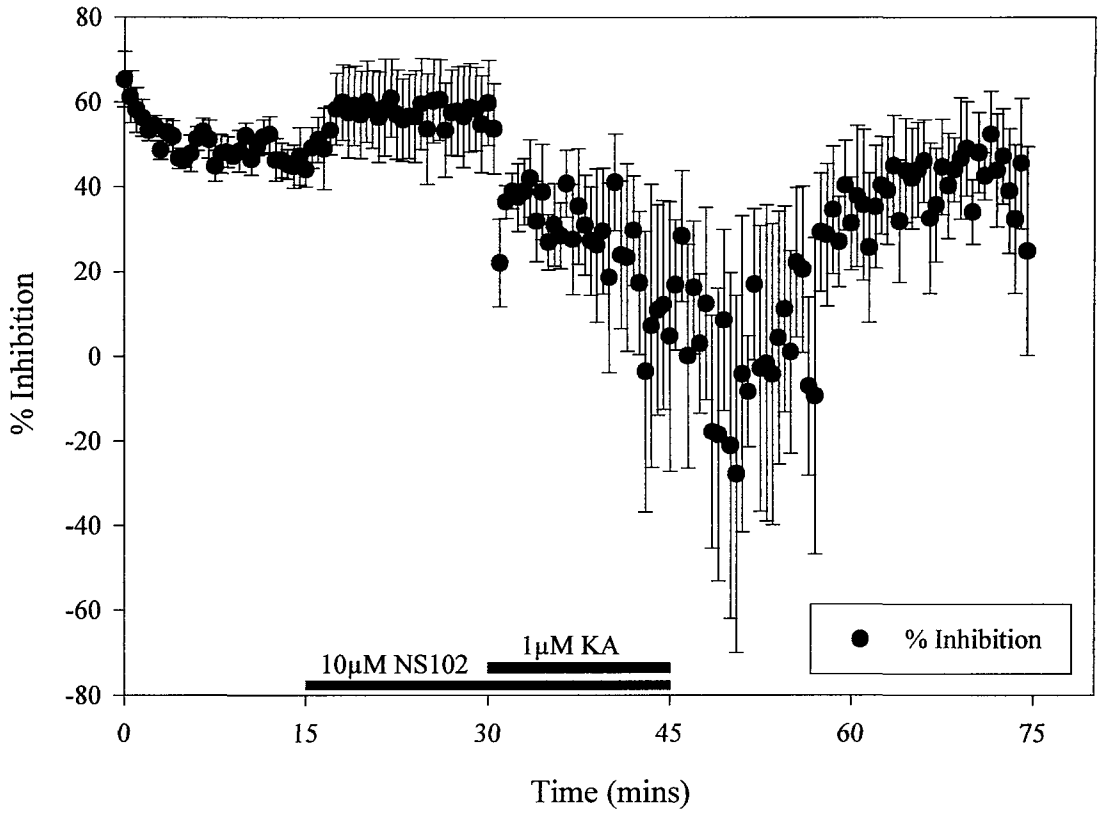

Figure 3.27 Change in the mean percentage inhibition (± S.E.M.) of the second population spike with respect to the first recorded from the CA1 region of intact hippocampal slices (n=4). NS102 causes a small but significant ($p<0.01$) increase in the paired pulse inhibition from 46% (±2.8) to 57% (±5.5). NS102 does not block the marked reduction in inhibition following addition of 1μM KA.

In the presence of 10μM NS102 the percentage inhibition increases from 46% (±2.8) to 57% (±5.5) ($p<0.01$). However NS102 does not appear to prevent the reduction in percentage inhibition by the end of 15 minutes KA application when compared to the action of KA alone (figure 3.13).

3.4.4.2 Kainate receptor antagonism: The role of CA3

The raw data traces for the effect of NS102 on the KA response in the isolated CA1 preparation can be seen in figure 3.28 below.

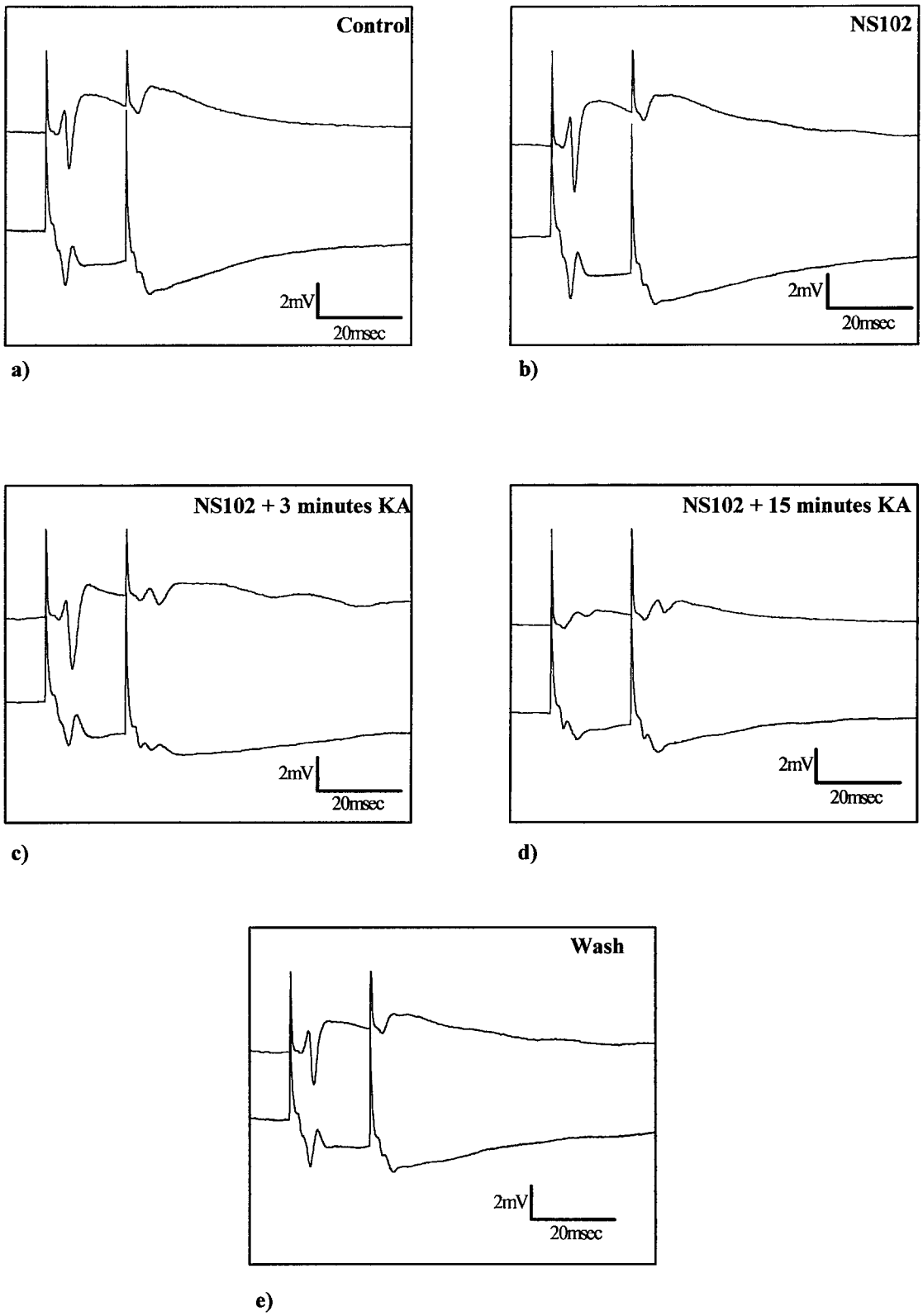

Figure 3.28 Example traces showing the effects of co-application of 10μM NS102 and 1μM KA on the population spike amplitude and EPSP slope recorded from isolated CA1 preparations. Each trace represents the average of three responses recorded at the following time points: a) the end of 15 minutes control stimulation, b) the end of 15 minutes 10μM NS102 application, c) within the first three minutes of the addition of 1μM KA, d) at the end of 15 minutes KA co-application, e) at the end of 30 minutes ACSF wash.

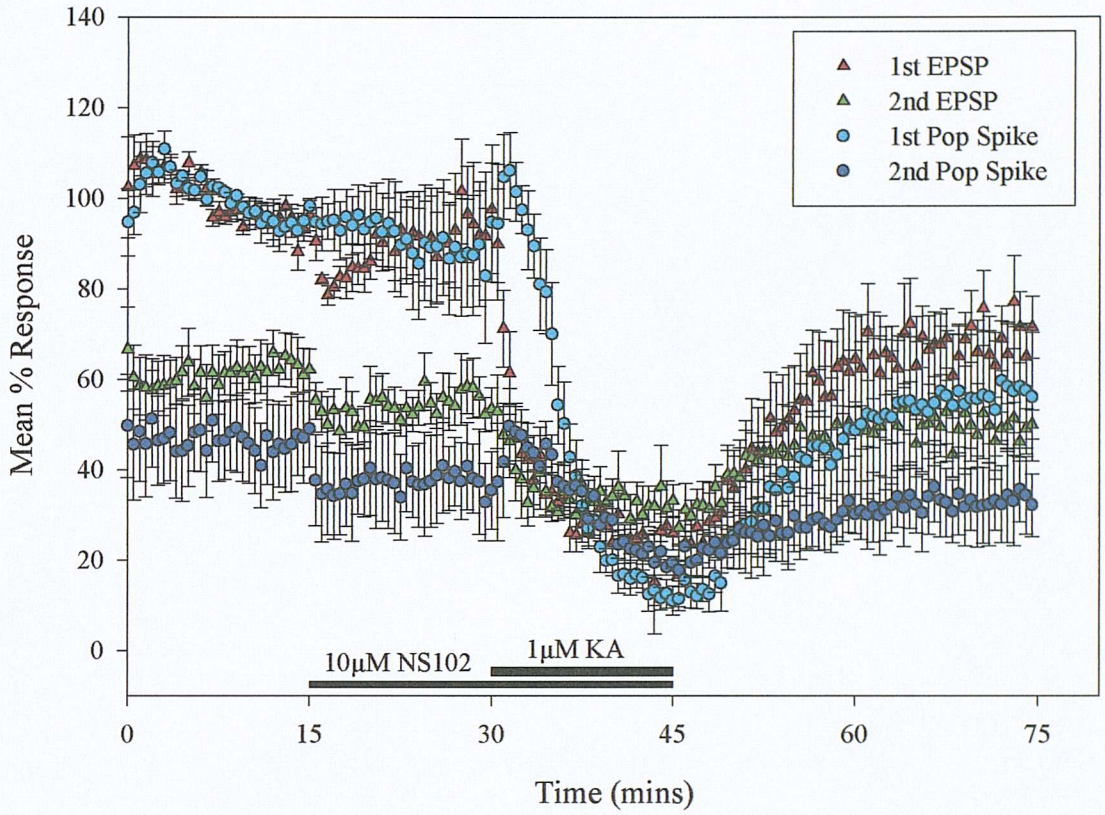

Figure 3.29 Time-course showing the effects of 10μM NS102 and 1μM KA on the mean percentage amplitude of the population spike and EPSP slope (± S.E.M.) recorded from isolated CA1 preparations (n=4). Application of 10μM NS102 causes a decrease in the slope of both the first and second EPSPs from 92% (±2.0) to 81% (±1.3) and 63% (±3.1) to 51% (±2.8) respectively ($p<0.01$). The second population spike is also reduced from 47% (±5.2) to 35% (±5.0). There is a further marked decrease in the EPSP slopes upon the addition of KA (23% ±4.1 for the first and 33% ±3.5 for the second EPSP). Both first and second population spike amplitudes undergo a transient but significant increase as KA is washed into the recording chamber from 87% (±7.4) to 102% (±3.7) and 36% (±5.0) to 49% (±3.6) respectively ($p<0.01$). This is followed by a marked decrease in the amplitudes for both spikes, down to 13% (±1.6) for the first and 20% (±1.4) for the second population spikes.

During the application of NS102 to isolated CA1 preparations (figure 3.29) the first and second EPSP slopes are both significantly reduced ($p<0.01$, n=4). In addition to this the second population spike amplitude is also reduced ($p<0.01$). The first population spike amplitude, however, is not significantly affected by NS102. Coapplication of 1μM KA causes a transient, siginificant increase in the amplitudes of both the first and second population spikes ($p<0.01$). Following this, both population spike amplitudes decrease below control values ($p<0.01$). This reduction does not occur in the presence of KA alone

(figure 3.15). The first and second EPSP slopes decrease with the onset of KA, remain reduced throughout the KA application period ($p<0.01$).

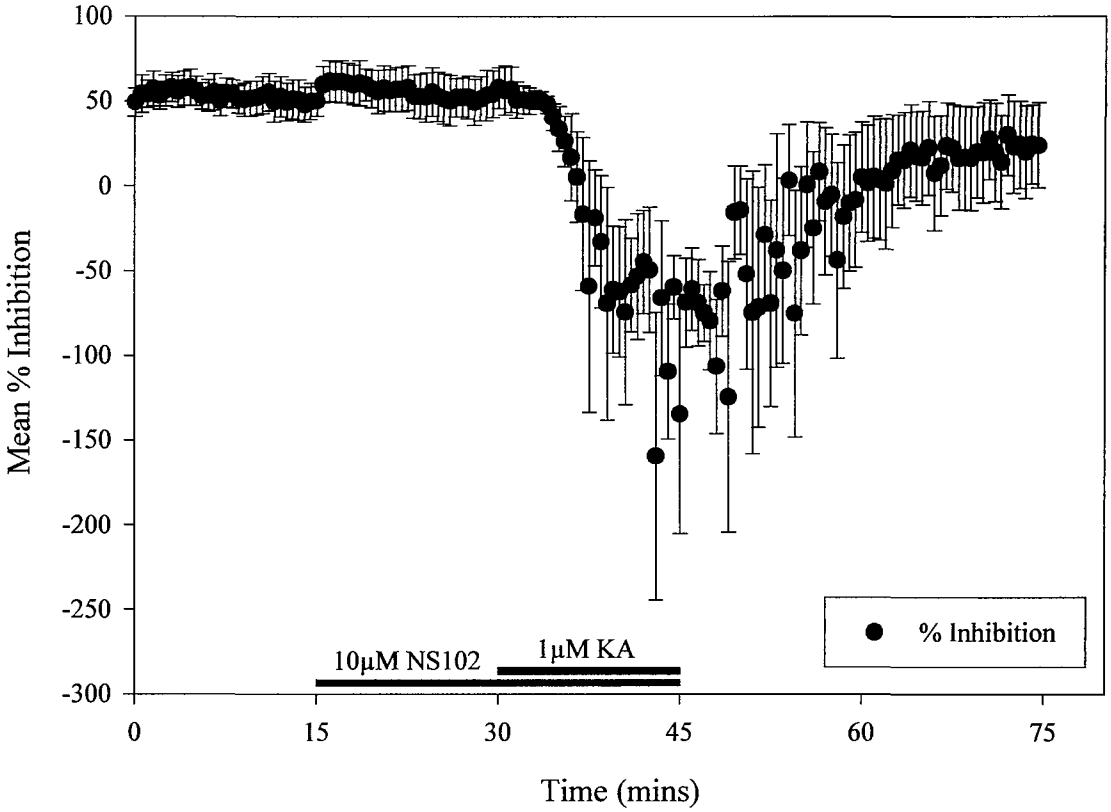

Figure 3.30 Time-course for the effect of 10μM NS102 and 1μM KA on the mean percentage inhibition (± S.E.M.) recorded from isolated CA1 preparations (n=4). NS102 causes an increase in the percentage inhibition from 50% (±5.8) to 61% (±6.2) ($p<0.01$) within the first three minutes of application. This is reduced to -79% (±20.3) by the end of 15 minutes KA application ($p<0.01$)

In the isolated CA1 preparation (figure 3.30), 10μM NS102 causes an increase in the percentage inhibition when administered alone ($p<0.01$). Addition of 1μM KA again causes a reduction in the inhibition leading to paired pulse facilitation (-79% (±20.3), $p<0.01$).

Mulle *et al* (2000) have shown, at least in mice, that the presynaptic terminals of interneurones in *stratum radiatum* of the CA1 which synapse onto other interneurones possess a homomeric KA receptor comprising of the GluR6 subunit. These receptors have been shown (Cossart *et al.* 2001) to facilitate the release of GABA onto other interneurones and thus inhibit their function. It is therefore possible to explain this increase in the percentage inhibition with NS102 in terms of the disinhibition of inhibitory

interneurones allowing them to release more GABA. This leads to a depression of the amplitude of the second population spike and thus an increase in the percentage inhibition.

3.4.5.1 AMPA receptor activation in the intact slice CA1

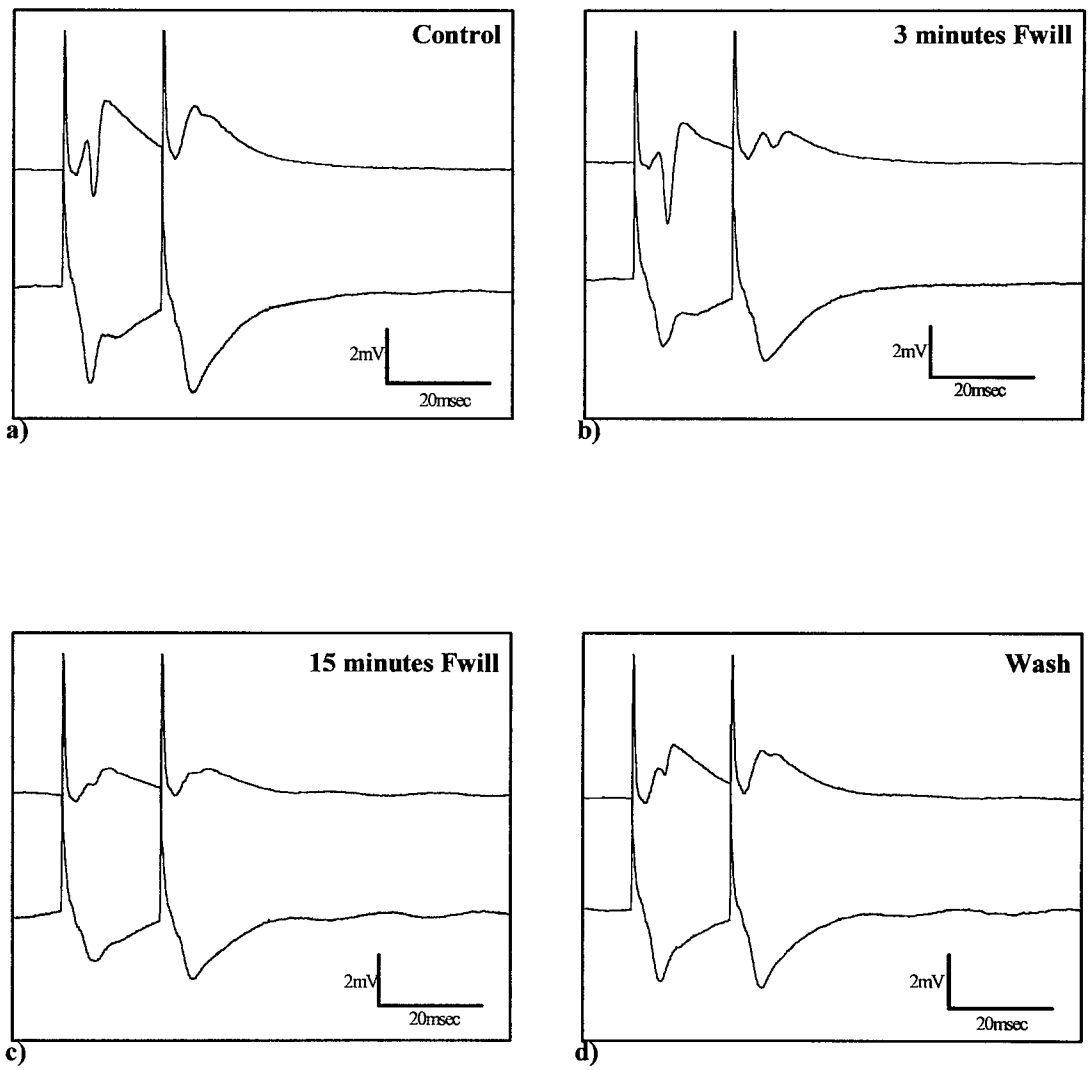

Figure 3.31 Example traces recorded from the CA1 region of an intact slice showing the effects of the application of 300nM fluorowillardine on the population spike amplitude and the EPSP slope. Each trace is the average of three responses taken at a) the end of the control period, b) within the first 3 minutes of fluorowillardine application, c) at the end of 15 minutes fluorowillardine application and d) at the end of thirty minutes ACSF wash.

In order to allow a comparison between the responses in CA1 evoked by KA (figure 3.12) and those that result from the activation of AMPA receptors, slices were perfused with the AMPA specific agonist (S)-5-fluorowillardine ((S)-(-)-αAmino-5-fluoro-3,4-dihydro-2,4-dioxo-1(2H)pyridinepropanoic acid) (300nM). This bypassed the need to block AMPA receptors during the perfusion of KA, a strategy which in all likelihood would have made the production of a field response impossible under these ionic conditions.

Figure 3.31 above shows examples of the responses recorded from the CA1 region of an intact slice during the application of 300nM fluorowillardine, a potent agonist of AMPA receptors (Wong *et al.* 1994).

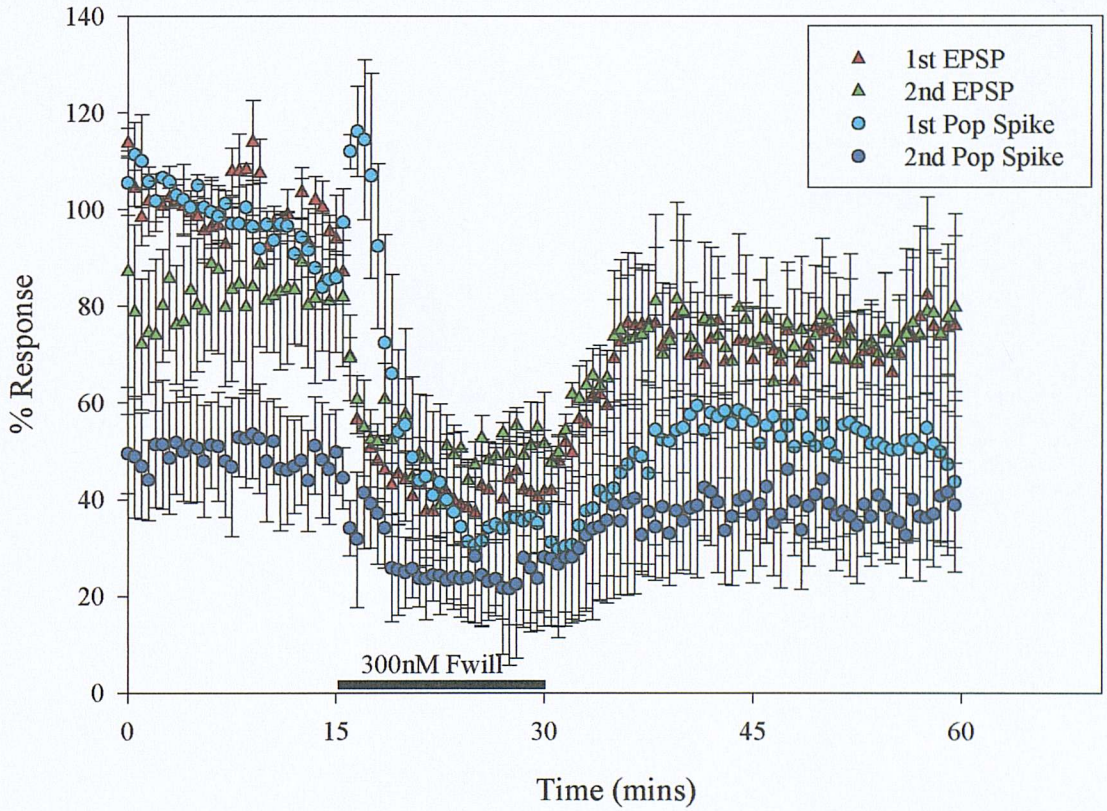

Figure 3.32 Time-course for the effect of the application of 300nM fluorowillardine on the mean population spike amplitude and EPSP slope (± S.E.M.) recorded from the CA1 region of intact slices (n=3). Superfusion with fluorowillardine causes a reduction in both the first and second EPSP slopes (99% (±2.6) to 41% (± 5.7) and 83% (±8.1) to 52% (±2.0) respectively, $p<0.01$) and the amplitude of both the first and second population spikes (86% (±2.3) to 36% (±10.2) and 49% (±5.6) to 26% (±6.2) respectively, $p<0.01$). However there is an initial increase in the first population spike within the first three minutes of fluorowillardine application (113% (±8.3), $p<0.05$).

Application of 300nM fluorowillardine to intact slices (figure 3.32) caused an initial increase in the first population spike amplitude ($p<0.05$). However, there is no corresponding increase observed in the second population spike, such as is found to occur during the application of KA (figure 3.12). This would be consistent with an activation of AMPA receptors on both pyramidal cells and interneurones within CA1 increasing the response to submaximal stimuli of both cell types, thus leading to an increased first population spike amplitude and an increased inhibition of the second. As the effects of fluorowillardine continue, both first and second population spikes are significantly reduced in amplitude ($p<0.01$). The first and second EPSP slopes rapidly decrease in the presence of 300nM fluorowillardine ($p<0.01$). This may be due to a partial depolarisation block of CA1 pyramidal cells, resulting in a decrease in the size of the population spike and EPSP that it is possible to evoke.

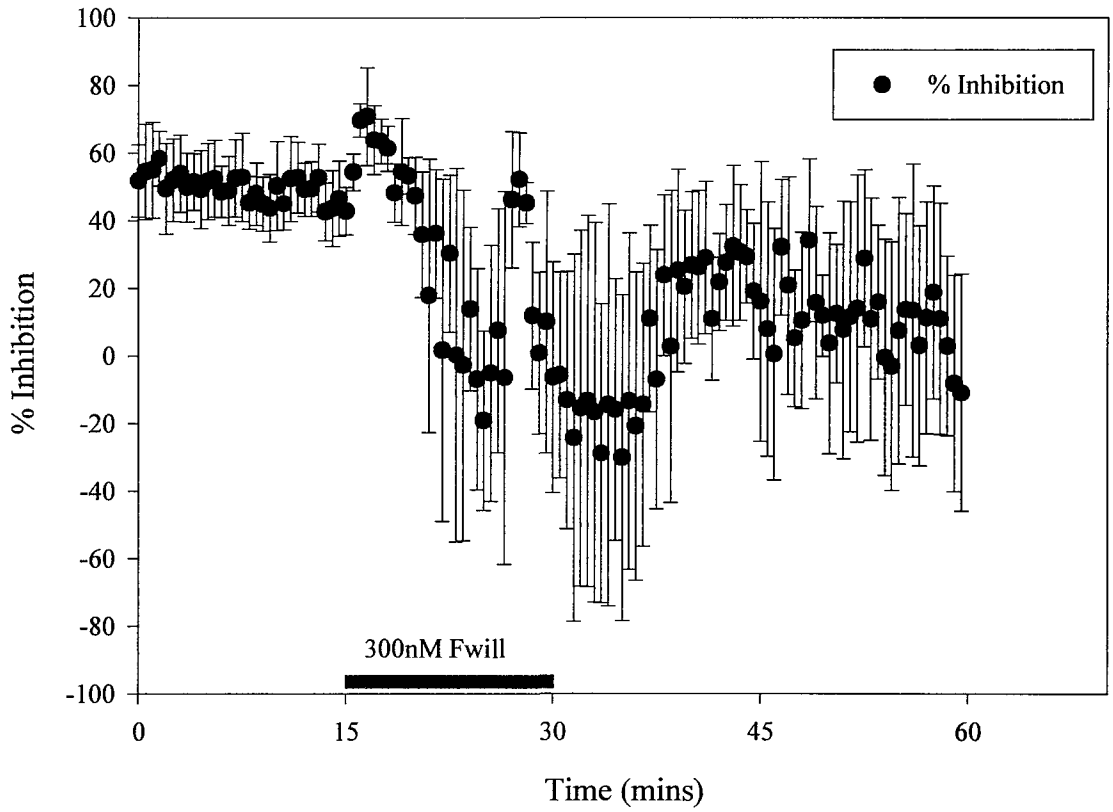

Figure 3.33 Time-course graph for the effect of 300nM fluorowillardine on the percentage inhibition measured from the CA1 region of intact hippocampal slices (mean percentage inhibition ± S.E.M., n=3). Fluorowillardine causes an initial increase in the paired-pulse inhibition from 44% (±5.2) to 66% (±5.6) ($p<0.01$) which correlates with the potentiation of the first population spike. This is followed by a reduction in the percentage inhibition (8% (±14.7), $p<0.01$) as the depolarising block increases.

Addition of 300nM fluorowillardine to the superfusing ACSF (figure 3.33) causes an initial increase in the percentage inhibition ($p<0.01$), which is to be expected considering the potentiation of the first population spike with no corresponding increase in the second spike. This does not occur during the application of 1μM KA to intact slices (figure 3.13). As the application period continues the percentage inhibition decreases significantly ($p<0.01$).

3.4.5.2 AMPA receptor activation in isolated CA1 preparations- a role for CA3?

Figure 3.34 presents examples of the raw data traces of the population spikes and EPSPs obtained during the application of 300nM fluorowillardine in an isolated CA1 preparation.

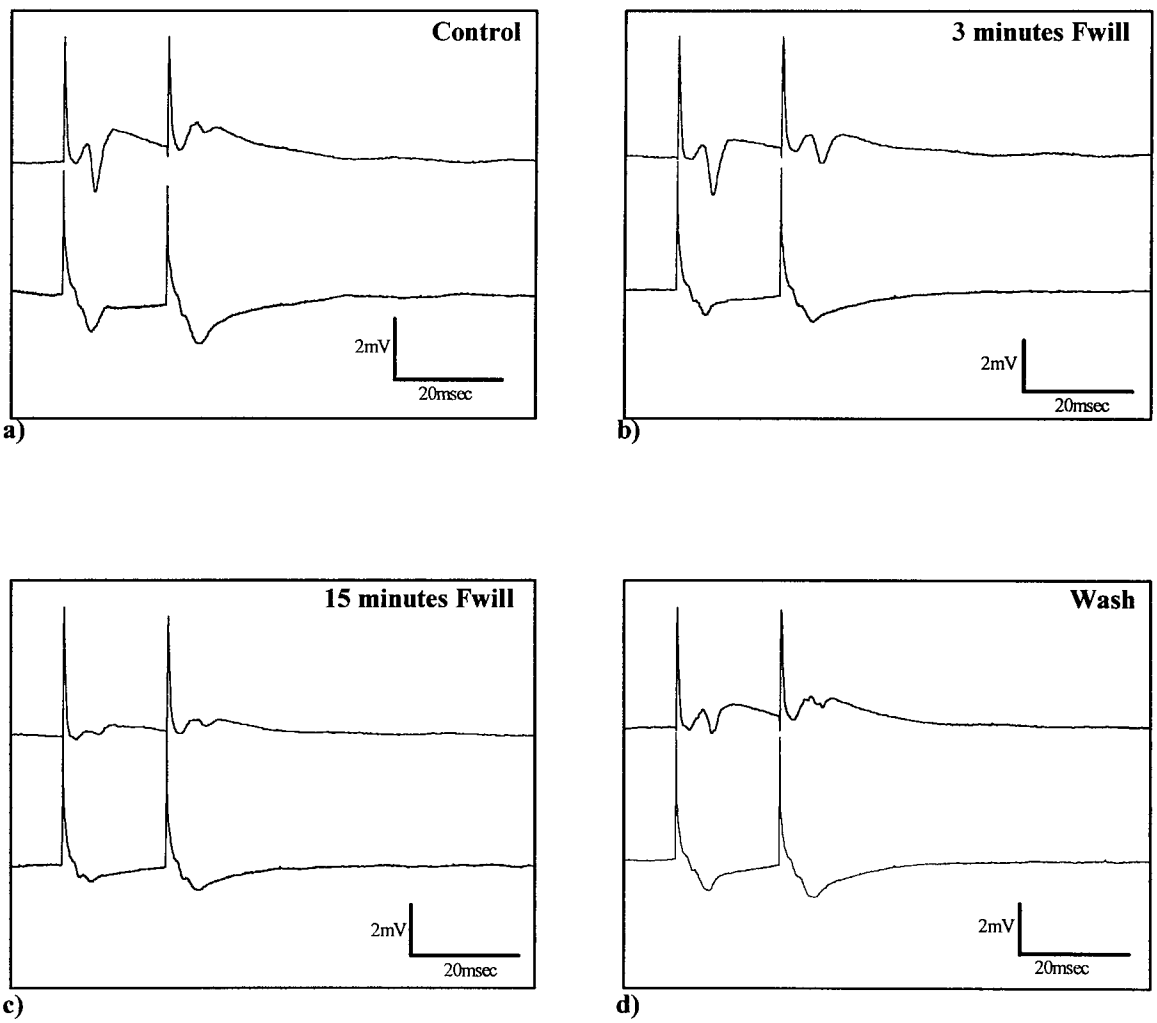

Figure 3.34 Example traces recorded from an isolated CA1 preparation. Each trace represents the average of three traces taken at a) the end of the baseline period, b) within the first three minutes of 300nM fluorowillardine application, c) the end of the 15 minute fluorowillardine application and d) at the end of 30 minutes ACSF wash.

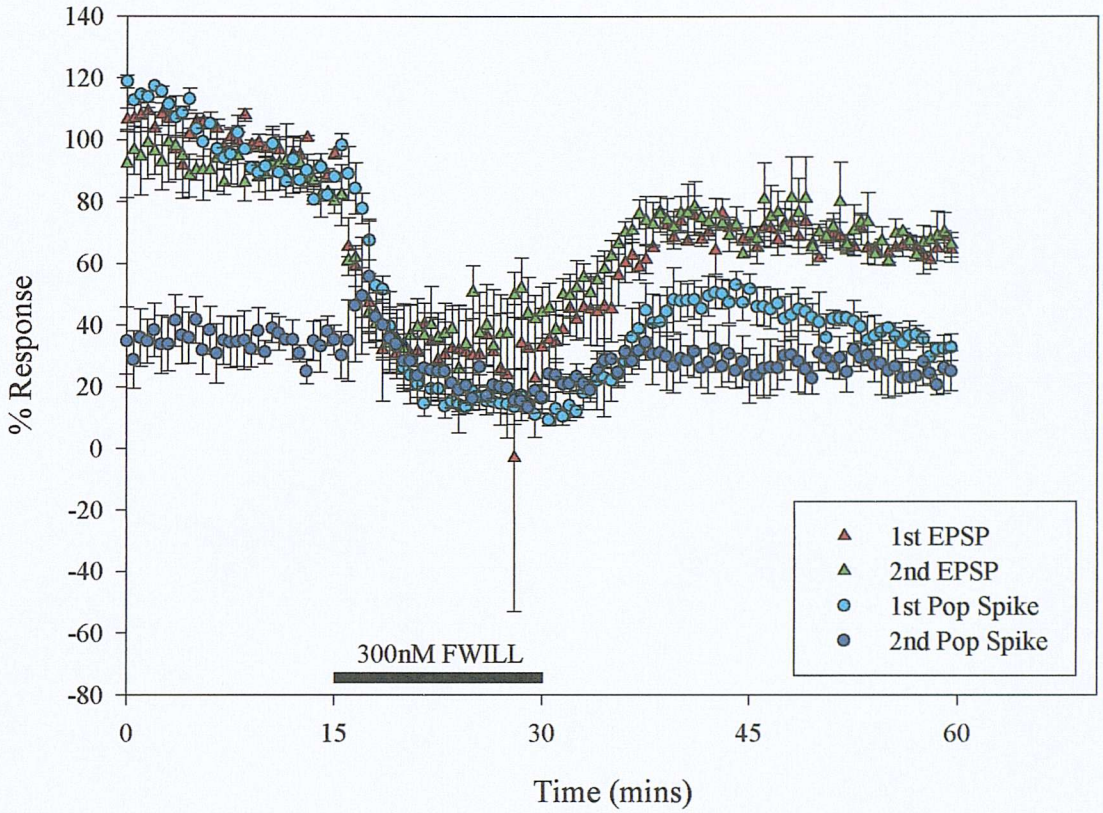

Figure 3.35 Time-course for the effect of 300nM fluorowillardine application on the population spike amplitude and EPSP slope recorded from *stratum pyramidale* and *stratum radiatum* of isolated hippocampal slices (mean percentage response ± S.E.M., n=3). As in the intact slice, fluorowillardine application causes a reduction in the amplitude of both population spikes (85% (±2.2) to 14% (±2.7) for the first spike, $p<0.01$ and 35% (±3.4) to 16 (±1.6), $p<0.01$ for the second) and EPSPs (89% (±1.6) to 30 (±7.6) $p<0.01$ for the first and 84 (±2.9) to 46% (±5.2) $p<0.01$ for the second). However, in contrast to the response seen in intact slices, there is an initial increase in the second population spike amplitude (51% (±9.4) $p<0.05$) as well as that of the first (92% (±3.2), $p<0.01$).

In the absence of CA3, 300nM fluorowillardine (figure 3.35) once again causes the amplitude of the first population spike to rise in the CA1 within the first three minutes of application ($p<0.01$, n=3). The second population spike amplitude also increases, although this just fails to achieve significance. As in the intact preparation (figure 3.32) the amplitude of both population spikes decrease significantly below control as the drug application period progresses ($p<0.01$). This would suggest a difference in the sites of

action between KA and fluorowillardine since this decrease does not occur to any significant extent in the isolated CA1 preparation with KA (figure 3.15). Once again the first and second EPSP slopes are significantly reduced during the application of fluorowillardine ($p<0.01$).

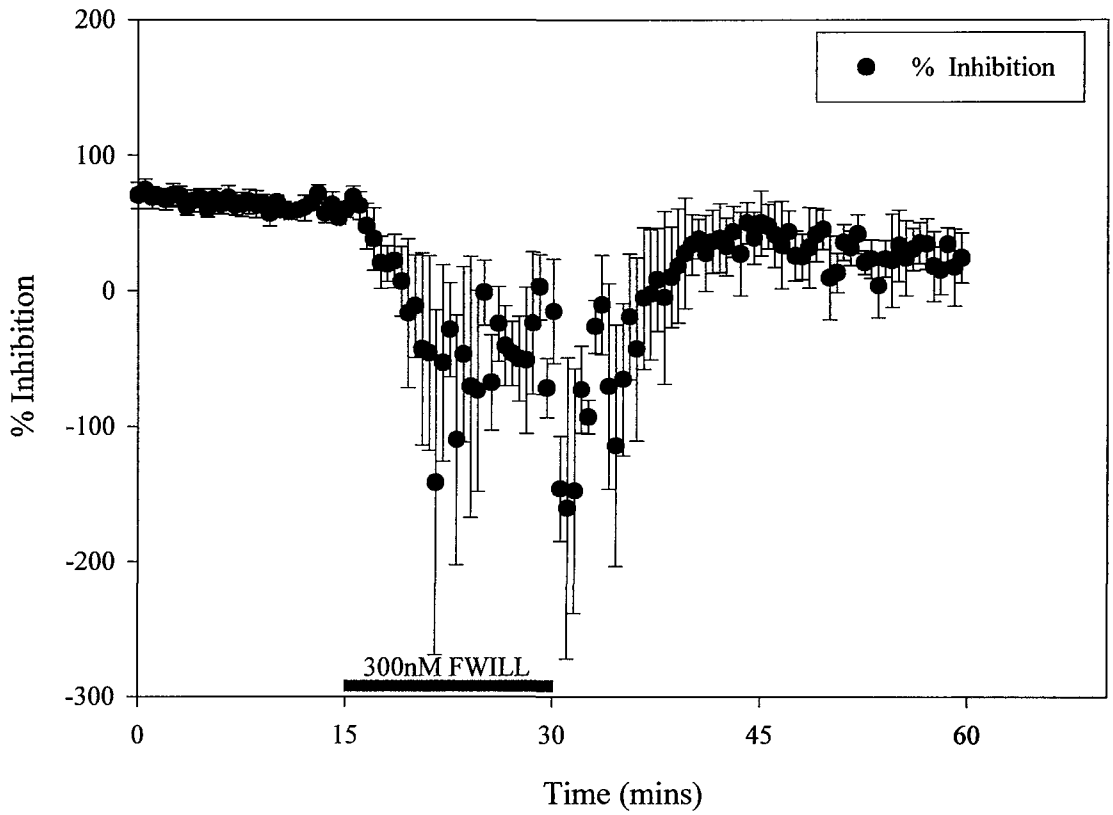

Figure 3.36 Time-course for the changes in the percentage inhibition recorded from isolated CA1 preparations following application of 300nM fluorowillardine (mean percentage inhibition ± S.E.M., n=3). Following an initial small, but significant, increase in the percentage inhibition as fluorowillardine is washed in (58% (±3.9) to 64% (±4.4), $p<0.05$), addition of the drug causes a progressive reduction in the percentage inhibition, resulting in paired pulse facilitation (-31% (±20.9), $p<0.01$).

The percentage inhibition data during the application of 300nM fluorowillardine in isolated CA1 preparations is presented in figure 3.36 above. As in the intact slice (figure 3.33), fluorowillardine causes a small increase in the percentage inhibition during the first three minutes of application ($p<0.05$, n=3). In the continued presence of the drug this decreases to -31% (±20.9) ($p<0.01$) implying a facilitation of the second spike with respect to the first.

3.4.7 Drugs acting at ionotropic glutamate receptors: Comparison of results

The following graphs compare the results obtained so far for the effect of various agonists of ionotropic glutamate receptors with those obtained for 1μM KA in both the intact slice and isolated CA1 preparation. In each graph the three responses spanning one and a half minutes of stimulation at each stated time point for each experiment within a group have been normalised to either the last three responses during the control period in the case of experiments using a single agonist. In the case of co-application of antagonists with KA, the last three responses in the presence of the antagonist prior to the addition of KA have been used.

Each graph will compare the normalised responses obtained for a single parameter during the various drug application protocols in either the intact or isolated CA1 preparation in order to highlight differences in the responses observed. These are namely the first EPSP slope (figures3.37-3.38), the second EPSP slope (figures 3.39-3.40), first population spike amplitude (figures 3.41-3.42), second population spike amplitude (figures 3.43-3.44) or the mean percentage inhibition (figures 3.45-3.46).

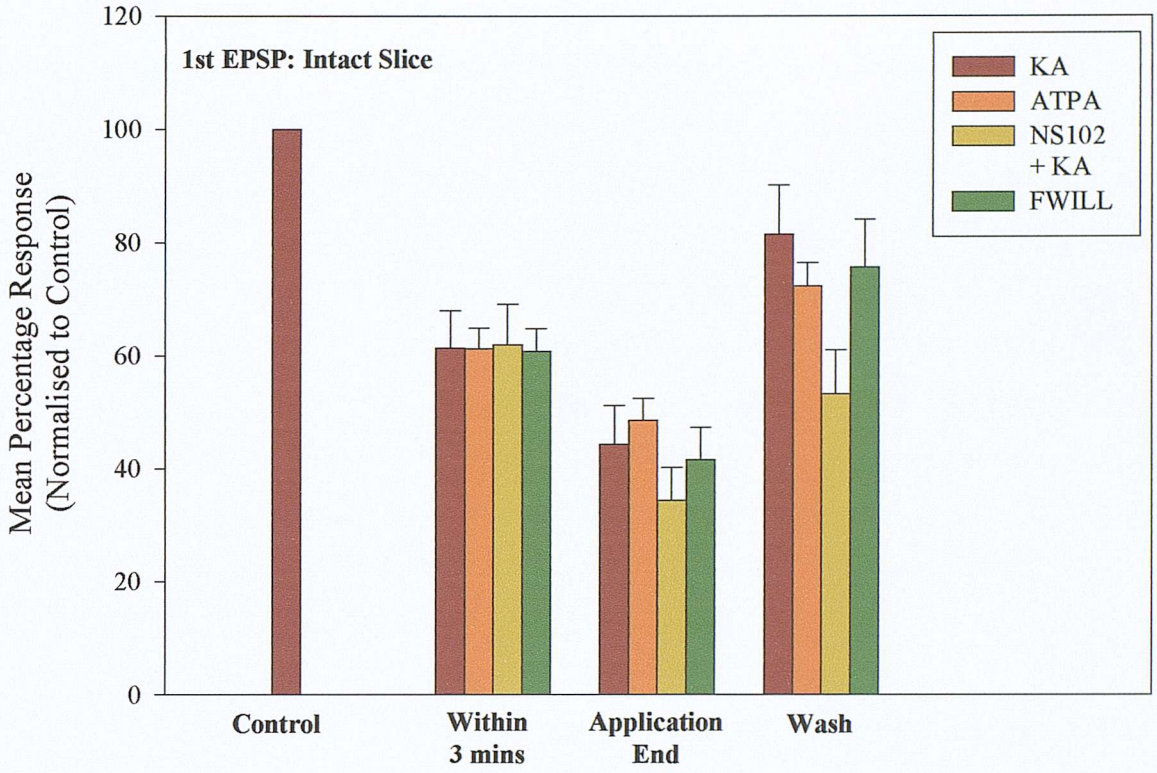

Figure 3.37 KA, ATPA and FWILL decrease the 1st EPSP slope recorded from the *stratum radiatum* of intact slice CA1. This is not blocked by NS102.

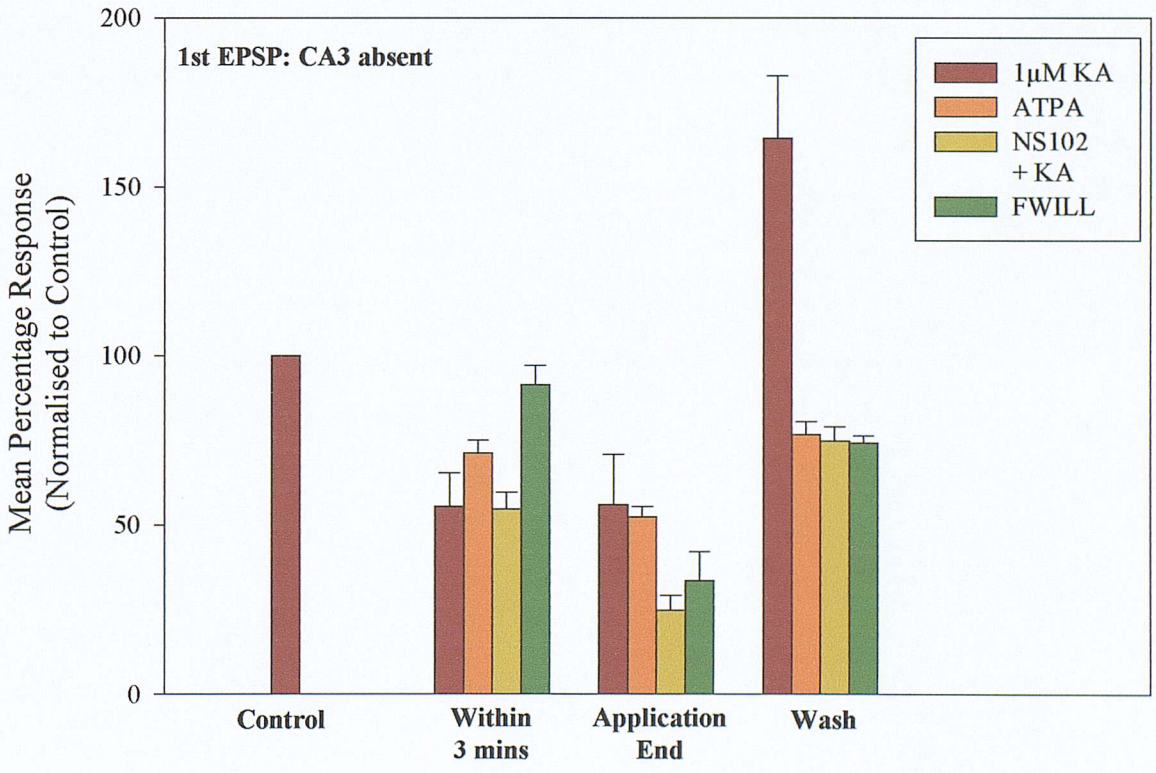

Figure 3.38 The reduction in the first EPSP slope is still observed in the absence of the CA3. FWILL has a slower onset of action. The presence of NS102 reduced the EPSP slope significantly from KA alone by the end of the application period.

Figure 3.37 (on the previous page) compares the slope of the first EPSP in the intact slice prior to the application of any drugs (control) and during the application of 1μM KA, 1μM ATPA, 300nM flurowillardine and the co-application of 10μM NS102 with 1μM KA. In each case, the mean percentage slope values for each time point have been normalised to the values recorded during the final 1.5 minutes of the control period. For the co-application of NS102 and KA, responses were normalised to the last 1.5 minutes of NS102 application prior to the addition of KA. In this way, it is possible to directly compare the responses obtained during different treatment protocols. All other comparisons have been obtained *via* the same method. In the intact slice preparation there is no significant difference observed between the response to KA alone and any other treatment protocol with regards to the slope of the first EPSP until the end of the wash phase. At this point the slope is significantly lower in the NS102 co-application group (53%, ±7.8 compared to 82%, ±8.7, $p<0.05$).

In the isolated CA1 preparation (figure 3.38) it is clear that there is a significant difference between the time-course for the effect of KA and that for fluorowillardine. Whilst KA reduced the first EPSP slope to 56% (±10.0) of control within the first three minutes, fluorowillardine fails to produce any substantial reduction during this time (91%, ± 5.8, $p<0.05$). There is, however, no significant difference at this time between KA and ATPA (71%, ±8.0) or KA in the presence of NS102 (55%, ±5.1). By the end of the application period there is no significant difference between the effects of KA (56%, ±14.9) and either ATPA (52%, ±3.0) or fluorowillardine (34%, ±8.6). However, in the presence of NS102, the slope of the first EPSP is further reduced to 25% (±4.4). This just fails to reach significance ($p= 0.08$).

Comparing the slope of the second EPSPs during the same drug protocols in intact slices (figure 3.39 on the following page) we can see that once again the only significant difference which was observed occurred as a result of coapplication of KA with 10μM NS102. This is again also true for the isolated CA1 preparation (figure 3.40). In both cases, the slope at the end of the KA application period and the wash is significantly lower than that for KA only ($p<0.05$). In intact slices the normalised percentage slope at the end of the KA period following NS102 superfusion is 38% (±4.1) compared to 60% (±8.7) for KA. By the end of the wash this has changed to 57% (±10.6) for NS102 compared to 86% (±7.0) for KA. In isolated slices these normalised percentage values are 59% (±6.4) compared to 68% (±8.4). By the end of the wash this has increased to 87% (±3.9) compared to 130% (±14.5) for KA alone.

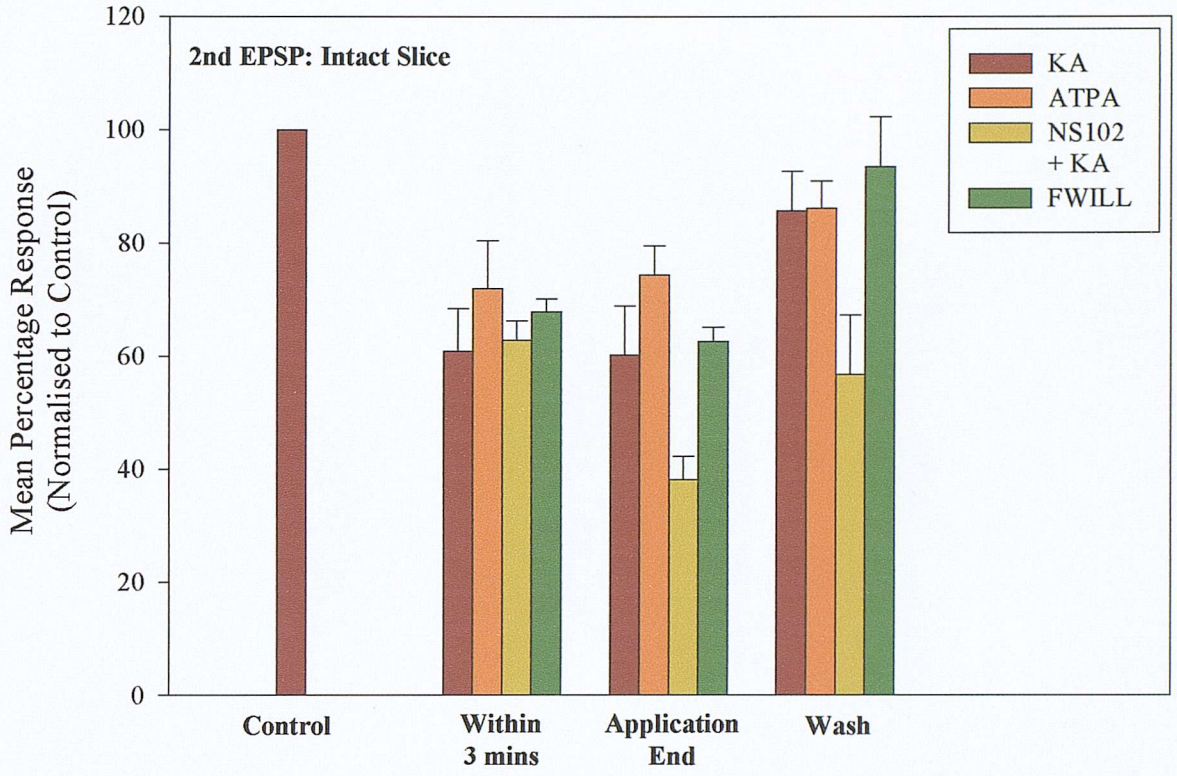

Figure 3.39 1μM KA, 1μM ATPA and 300nM flurowillardine similarly reduce the slope of the second EPSP recorded from the CA1 region of intact hippocampal slices. This is not blocked by NS102, which potentiates the effect of KA by the end of the application period.

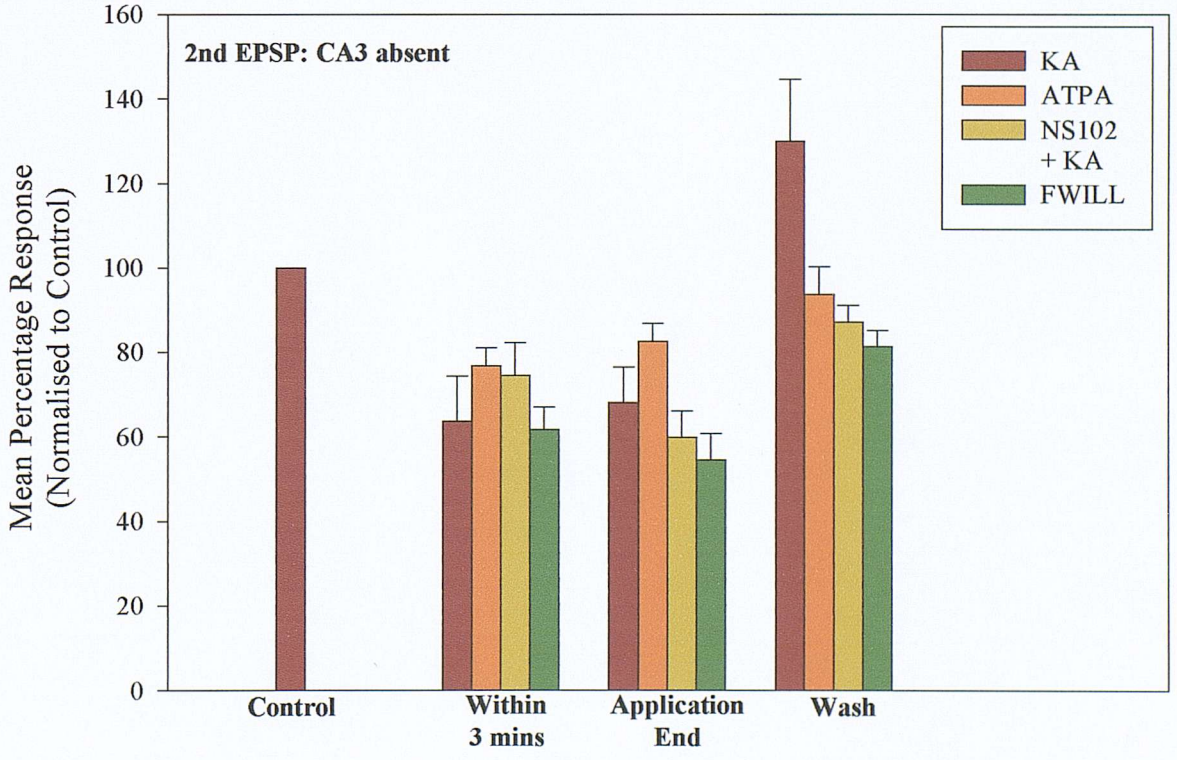

Figure 3.40 Application of 1μM KA, 1μM ATPA, or 300nM fluorowillardine reduced mean percentage slope of the second EPSP recorded from isolated CA1 preparations.

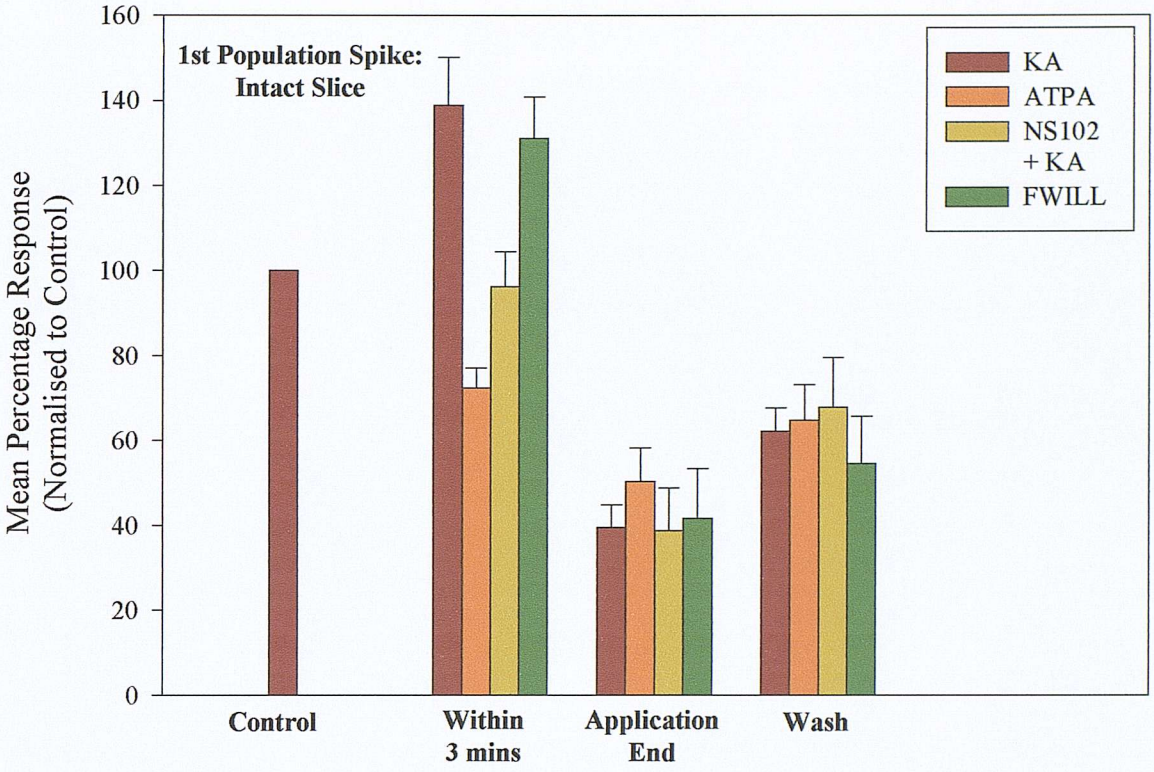

Figure 3.41 The application of 1μM KA, and 300nM fluorowillardine transiently increased the mean percentage first population spike amplitude recorded from the *stratum pyramidale* of the CA1 region of intact hippocampal slices. NS102 blocked this initial response to 1μM KA. ATPA reduced the first population spike amplitude during this time.

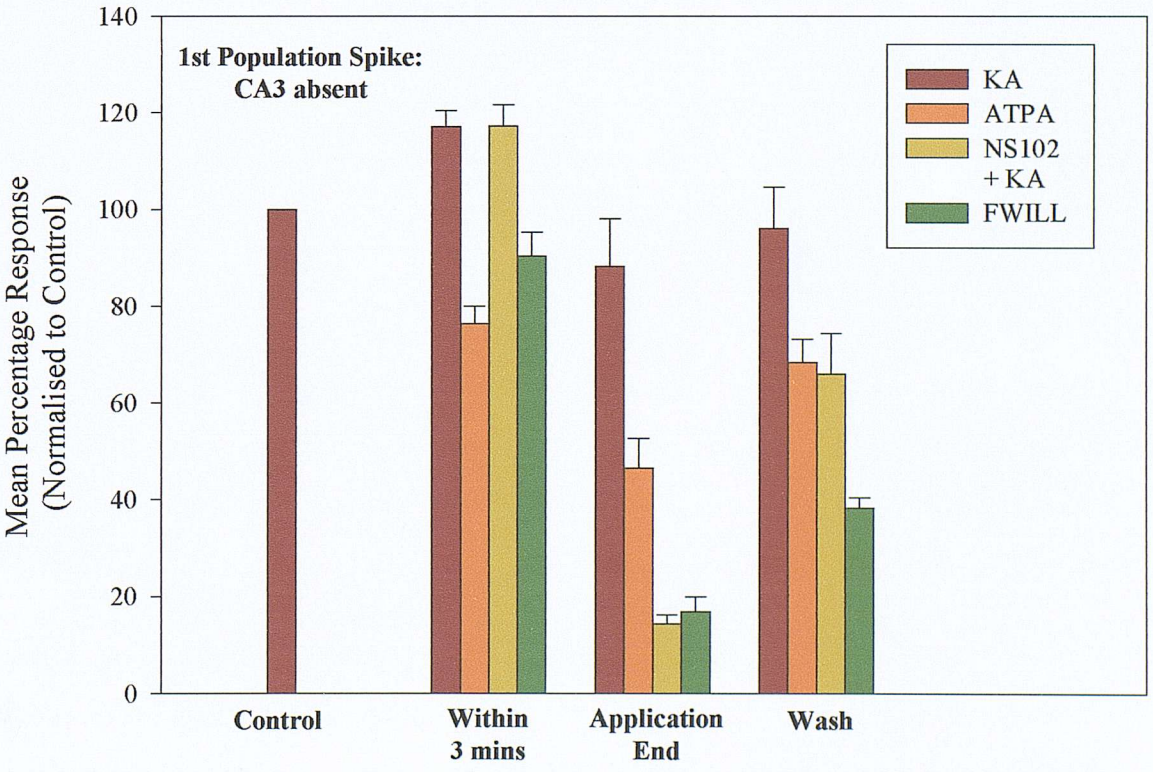

Figure 3.42 KA initially increased the mean percentage first population spike ampliutde in the isolated CA1 preparation. This was not blocked by NS102. Neither ATPA nor fluorowillardine resulted in a similar initial increase. By the end of the drug application period, all treatments differed significantly from KA alone.

The application of KA and flurowillardine resulted in a marked potentiation of the first population spike in the intact slice preparation (figure 3.41), within the first three minutes of applying the drug (139%, ±11.3 and 131%, ±9.7) respectively. In contrast to this, application of ATPA, or KA in the presence of NS102, resulted in a reduction of the first population spike amplitude within this time frame (72%, ±4.7 and 96%, ±8.2 respectively, $p<0.01$). This however is the only significant difference between the drug effects.

In isolated CA1 preparations (figure 3.42) the effects of these drugs differ in the responses observed. Within the first three minutes of drug application, both ATPA and fluorowillardine differ significantly from KA alone (76%, ±3.6 and 90%, ±4.9 respectively compared to 117%, ±3.3 for KA alone, $p<0.01$). By the end of this period all three drug protocols exhibit responses which are markedly reduced compared to that for KA (ATPA: 47%, ±6.2, NS102 and KA: 14%, ±1.9 and fluorwillardine: 17%, ±3.1 compared to 88%, ±9.9 for KA, $p<0.01$). These values remain reduced with respect to that for KA alone until the end of the wash period. The values for ATPA and flurowillardine remain highly significantly different from that for KA (68%, ±4.8 and 38%, ±2.2 respectively compared to 96%, ±8.6; $p<0.01$) whilst KA in the presence of NS102 is only significantly different form KA (66%, ±8.4; $p<0.05$).

The normalised response of the second population spike recorded from intact slices in the presence of this series of drugs is presented in figure 3.43 on the following page. In the presence of both ATPA and fluorowillardine the second population spike is markedly reduced compared to KA alone within the first three minutes of application. Whilst KA produces a strong potentiation of the second spike (193%, ±32.2), ATPA reduces the normalised response to 79% (±12.9) ($p<0.01$) and flurowillardine to 77% (±12.5) ($p<0.01$). By the end of this period the normalised amplitude of the second population spike falls in all groups to a comparable amount except for slices treated with ATPA, which becomes potentiated with respect to KA (129%, ±19.4 compared to 72%, ±13.5; $p<0.05$).

Within the first three minutes of drug application in isolated CA1 preparations (figure 3.44), only the response of the second population spike in the presence of ATPA differs significantly to that observed with 1μM KA (81%, ±14.0 compared to 209%, ±37.2 for KA, $p<0.01$). By the end of the drug application period the response to ATPA is no longer significantly different to that of KA. However, the second population spike in the

presence of both NS102 and fluorowillardine are significantly reduced when compared to the KA response at this time (55%, ±4.0 and 44%, ±4.5 compared to 112%, ±10.3; $p<0.01$).

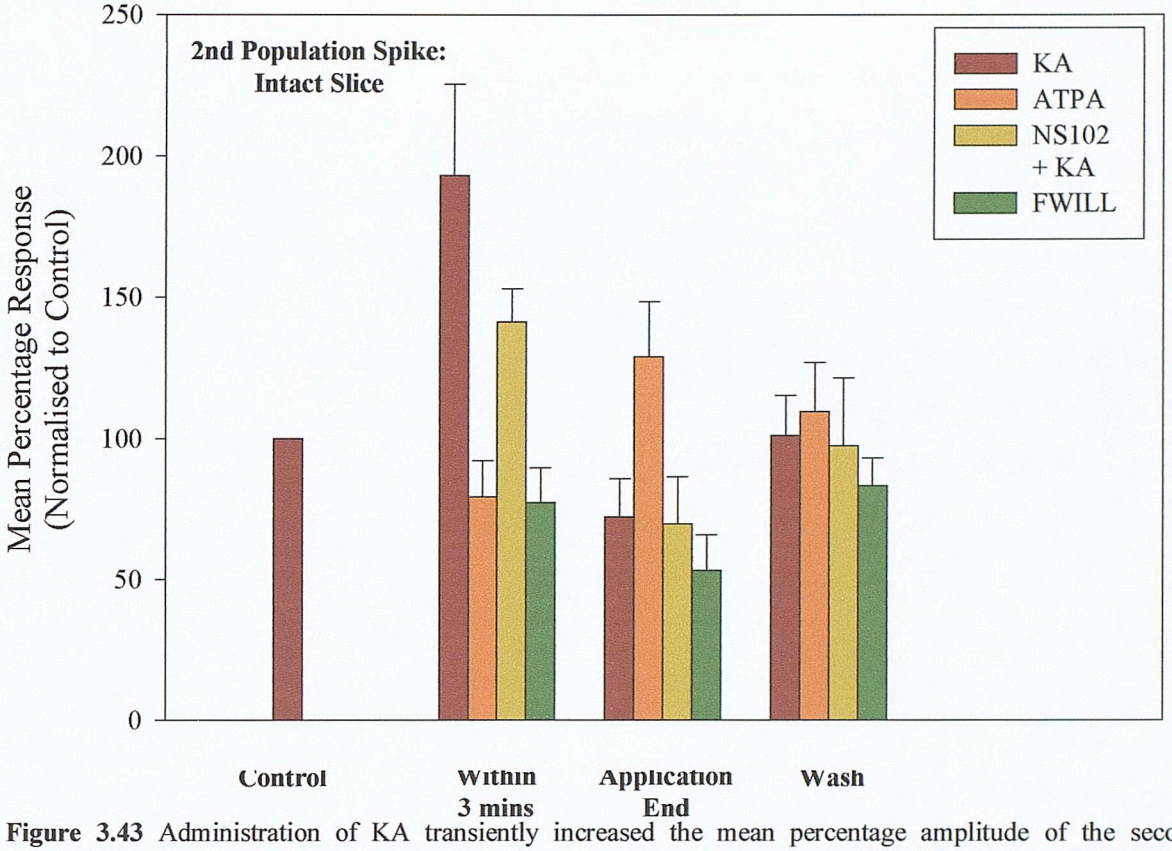

Figure 3.43 Administration of KA transiently increased the mean percentage amplitude of the second population spike recorded from the *stratum pyramidale* of the CA1 region of intact hippocampal slices. This was reduced, but not blocked by NS102. Neither ATPA nor fluorowillardine resulted in a similar increase.

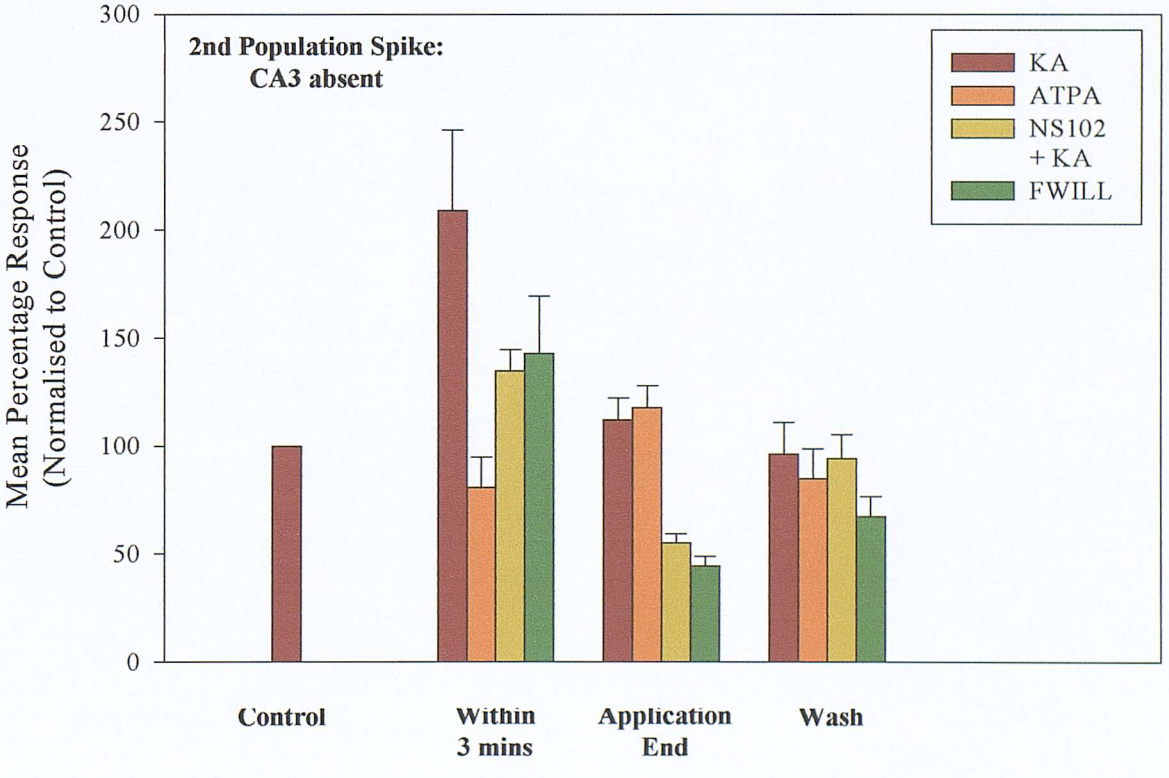

Figure 3.44 Only the effect of ATPA application on the second population spike amplitude differed significantly from KA during the first 3 minutes of application to isolated CA1 preparations. By the end of the drug application period, NS102 significantly potentiated the effects of KA. FWILL treated slices also displayed a significant reduction in the amplitude of the second population spike compared to KA at this time.

Comparison of the effects these drugs have on the normalised percentage inhibition shows us that in the intact slice CA1 (figure 3.45 on the following page) fluorwillardine application differs significantly to KA within the first three minutes of application. While KA causes a marked reduction in the normalised percentage inhibition initially (53%, ±30.6), flurowillardine application results in an increased inhibition (149%, ±12.6; $p<0.05$). This difference occurs due to the fact that, although both drugs produce an increase in the first population spike during the initial phase of the application, only KA results in an increase in the second population spike amplitude at the same time. ATPA application also differs from the KA response during the first three minutes the mean normalised percentage inhibition being 112% (±9.7). However this just fails to reach significance ($p=0.08$ Student's unpaired t-test). Throughout the rest of the drug application periods and wash there is no significant difference between the inhibition calculated for any of these drugs.

In the isolated CA1 preparation (figure 3.46), there is a marked difference between the response to KA and the other drug treatments. Within the first three minutes of application, the normalised percentage inhibition recorded in the presence of ATPA increased to 108% (±6.8) compared to 85% (±5.5) for KA ($p<0.05$). The action of KA in the presence of the GluR6 antagonist NS102 does not differ significantly from that of KA alone. However, the response to the AMPA receptor agonist fluorowillardine exhibits a significant increase (110%, ±7.6) in the percentage inhibition when compared to KA at this time point ($p<0.05$).

By the end of the drug application period, only the slices treated with 1μM KA alone exhibit any appreciable degree of inhibition (71%, ±11.1). In slices superfused with ATPA, the normalised percentage inhibition decreased to –38% (±45.5) ($p<0.05$) indicating a significant potentiation of the second population spike compared to the first. The presence of NS102 also exacerbates the effect of KA on the inhibitory mechanisms within the isolated CA1 preparation by the end of the application period, the normalised inhibition falling to –148% (±38.2) ($p<0.01$). The response to fluorowillardine at this time-point also exhibits a marked reduction in inhibitory function (-53%, ±36.0) compared to that of KA alone ($p<0.01$).

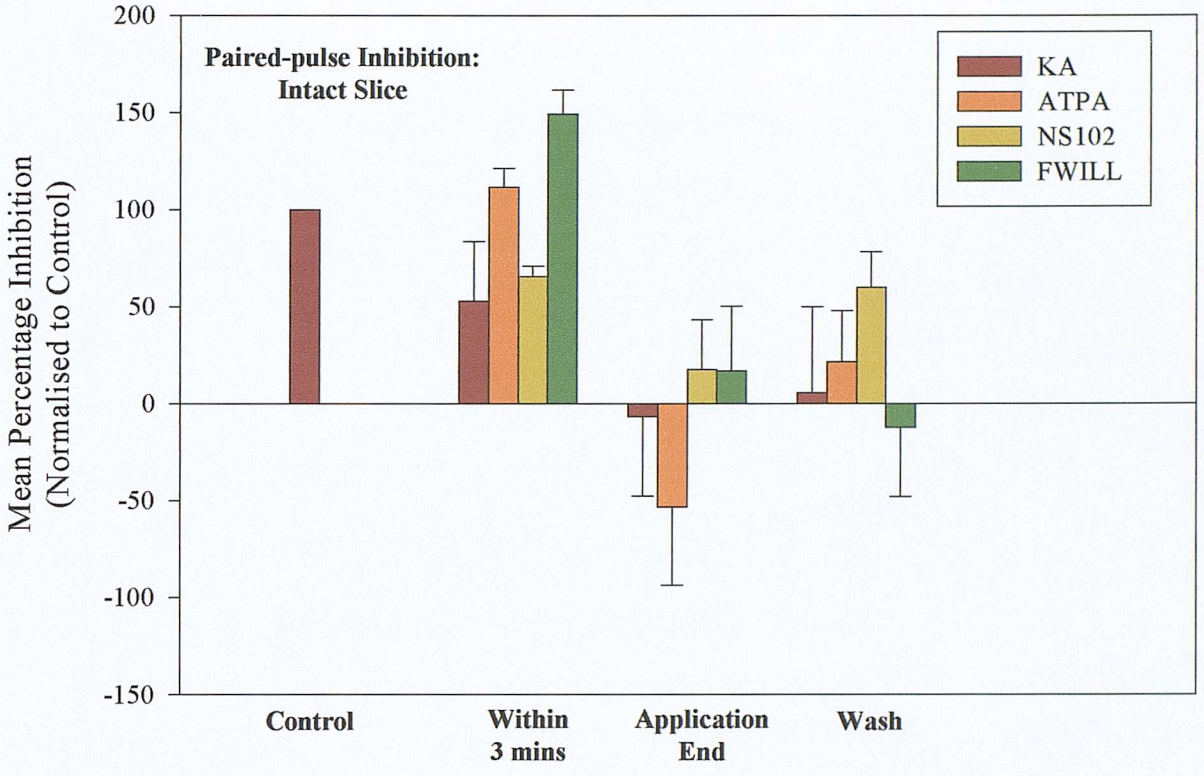

Figure 3.45 KA reduces paired-pulse inhibition in the intact slice CA1. In contrast, FWILL and ATPA initially increase the mean percentage inhibition. The effect of ATPA just fails to reach significance. Inhibition is reduced by the end of the drug application period. NS102 does not block the effect of KA.

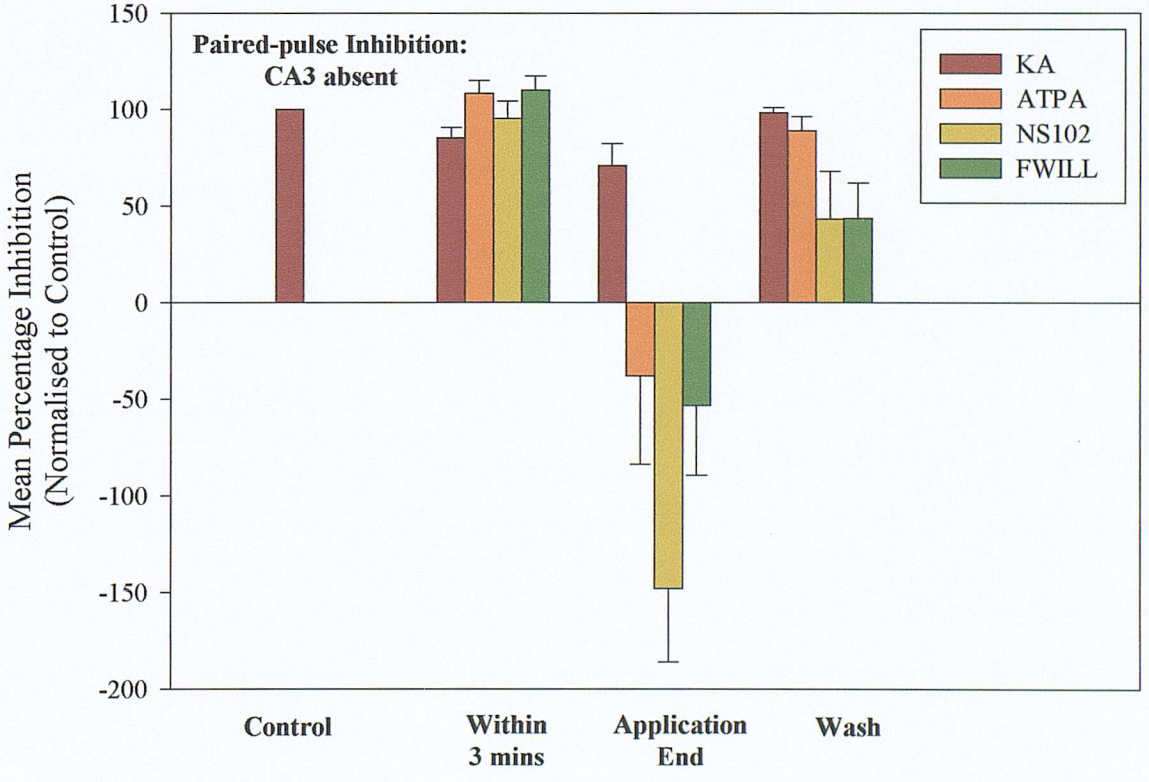

Figure 3.46 During the initial 3 minutes of drug application in the isolated CA1 preparation, ATPA and FWILL differ significantly from KA alone in their effects on paired-pulse inhibition. By the end of the application, the presence of NS102 has greatly potentiated the response to KA.

3.5 Discussion

3.5.1 The Effect of KA on field recordings in the CA1: An overview

In both the intact (figure 3.12) and isolated CA1 (figure 3.15) hippocampal slice preparations, introduction of KA results in a rapid, significant reduction in the first and second EPSP slopes and a transient increase in the first and second population spike amplitudes. This is followed by a prolonged reduction in population spike amplitude in the intact slice preparation and a return of the population spike to control values in the isolated CA1 preparation. During the course of KA application, the percentage inhibition of the second population spike with respect to the first remains depressed in the intact slice preparation (figure 3.13). In the isolated CA1 preparation, it is transiently reduced during both the beginning and end of the KA application period (figure 3.16).

This increase in population spike amplitude recorded from CA1 is greater in the intact slice (figure 3.41) than the isolated slice (figure 3.42), indicating a role for CA3 in this response. Since this increased population spike amplitude occurs in the intact slice at concentrations of KA as low as 250nM (figure 3.5 also see table 3.2), it is highly likely that this is due to activation of KA receptors rather than AMPA receptors. It is possible therefore that excitation of the CA3 pyramidal cell population by KA (Castillo *et al.* 1997) leads to increased glutamate release from the Schaffer collateral pathway and hence increased AMPA receptor activation in CA1. This would be expected to lead to an increased excitation of the CA1 pyramidal cell population and presumably also the interneuronal population in both a feedforward and feedback manner. However, since this response also occurs in slices from which the dentate gyrus and CA3 have been removed, CA3 excitation alone is unlikely to be solely responsible.

Thus it may be that KA is exerting a direct excitatory effect upon the CA1 pyramidal cell population itself. This could occur in a number of possible ways. Firstly, activation of GluR6 (Mulle *et al* 2000, Beureau *et al.* 1999) containing KA receptors present on the pyramidal cells of CA1 may result in a depolarising current in these neurones, leading to an increase in the amplitude of the evoked response.

However, Melyan *et al* (2002) were unable to elicit an inward current in CA1 pyramidal cells with nanomolar concentrations of KA in animals of the same age and strain as used in this study. Therefore this direct effect of KA on CA1 pyramidal cell excitability may occur as a result of a KA receptor mediated inhibition of a slow afterhypolarisation current (I_{sAHP}) which has been shown to be reduced in KA lesioned

animals (Ashwood *et al.* 1986) rendering these cells more excitable. Melyan *et al.* (2002) have shown, using whole-cell patch clamp recordings from CA1 pyramidal cells, that application of between 100-200nM KA is capable of reducing the I_{sAHP} by some 34%. This effect of KA was observed to persist in the presence of tetrodotoxin (TTX), implying a postsynaptic locus of action. This response also continued in the presence of the AMPA specific antagonist GYKI 54266 but not the non-selective AMPA/KA antagonist CNQX. Evidence in support of this will be presented in the next chapter.

A further possibility is that feedforward inhibition has been reduced by the application of KA leading to an increase in the amplitude of the first population spike. Since this does not occur in the presence of ATPA it is unlikely that GluR5 is involved in this response. However, there is much evidence (Frerking *et al* 1998.) for a GluR6 mediated reduction in GABA release from interneurone terminals that could support this possibility.

A reduction in EPSP slope at the same time as an increase in population spike could be interpreted in a number of different ways.

Firstly, it is possible that KA partially depolarises the CA1 pyramidal cell population directly. This would be expected to lead to a decrease in the postsynaptic current as the cells are now nearer their equilibrium potential. In turn this would result in a decrease in the slope of the field EPSP measured from *stratum radiatum*. However, ATPA application (figures 3.20, 3.23) reduces the field EPSP slope without increasing the population spike amplitude, which may argue against this mechanism for the reduction in the field EPSP by KA.

An alternative explanation for this reduction in EPSP slope involves activation of interneurones by KA. It is known that activation of GluR5 containing receptors on interneurones will lead to an increase in interneruonal spiking (Cossart *et al*) and hence to an increase in GABA release from these neurones. This in turn may lead to increased activation of postsynaptic $GABA_A$ receptors and hence an increase in postsynaptic Cl^- influx. This would have the effect of shunting glutamatergic excitation in the dendrites of CA1 pyramidal cells, and thus leading to a reduction in the measured field EPSP slope. However, were this the case then it would be expected that the increase in synaptic concentration of GABA would lead to an inhibition of both the first and second population spike amplitudes, whilst this is clearly not the case during the initial phase of the KA

response (figures 3.12 and 3.15). This suggests that this is not the mechanism by which KA reduces EPSP slope.

Given the current data for the known actions of KA in the CA1, another explanation is just as likely. It is known that KA receptor activation on CA3 pyramidal neurones produces a slow depolarising current (Castillo *et al.* 1997) probably *via* activation of GluR6 containing receptors (Mulle *et al.* 1998). This excitatory current may be sufficient to cause a partial depolarising block of CA3 pyramidal cells (figure 3.18) and thus lead to a reduction of glutamate release from the Schaffer collateral terminals. This would be expected to reduce the slope of the EPSP recorded from the *stratum radiatum* in CA1. However, for this to be the explanation, the presence of CA3 would be an absolute requirement for the reduction in EPSP slope to occur. This is not the case, since the EPSP slope is reduced with KA in the isolated CA1 preparation (figure 3.15).

The more likely explanation is that activation of presynaptic KA receptors on the Schaffer collateral terminals themselves causes a localised depolarisation which renders incoming action potentials less effective with regard to initiating the Ca^{2+} influx necessary for transmitter release (Vignes *et al* 1998, Kamiya and Ozawa 1998). It is unlikely that this occurs as a result of inactivation of voltage gated Ca^{2+} channels however, since Kamiya and Ozawa (1998) did not observe a change in the resting levels of rhod-2 fluorescence in the Schaffer collateral terminals in the presence of 1μM KA. However, a localised depolarisation at the terminal would be expected to elevate the membrane potential nearer to the equilibrium potential for Na^{+}. This would be expected to reduce the amplitude of incoming action potentials, thus reducing the activation of presynaptic voltage-gated Ca^{+} channels and hence reducing the amount of transmitter released. A further possibility is that these two possible mechanisms are acting in tandem to produce the observed effect. Since this phenomenon occurs irrespective of the presence of CA3 it is likely that this response is mediated mainly *via* an effect at the presynaptic terminal rather than *via* a depolarising block of CA3 pyramidal cells.

Furthermore, it is interesting to note that the second population spike increases at the same time as the first during KA application. Since a depolarisation of the CA1 pyramidal cell population either *via* CA3 excitation or directly in the CA1 by KA would be expected, at least transiently, to increase the excitatory drive to both the feedforward and feedback interneurone populations of CA1. Thus an increase in paired-pulse inhibition would be expected to occur. This suggests an inhibitory action of KA on the interneuronal population in CA1.

A schematic for the sites of action of the compounds investigated in this chapter is presented in figure 3.47 below.

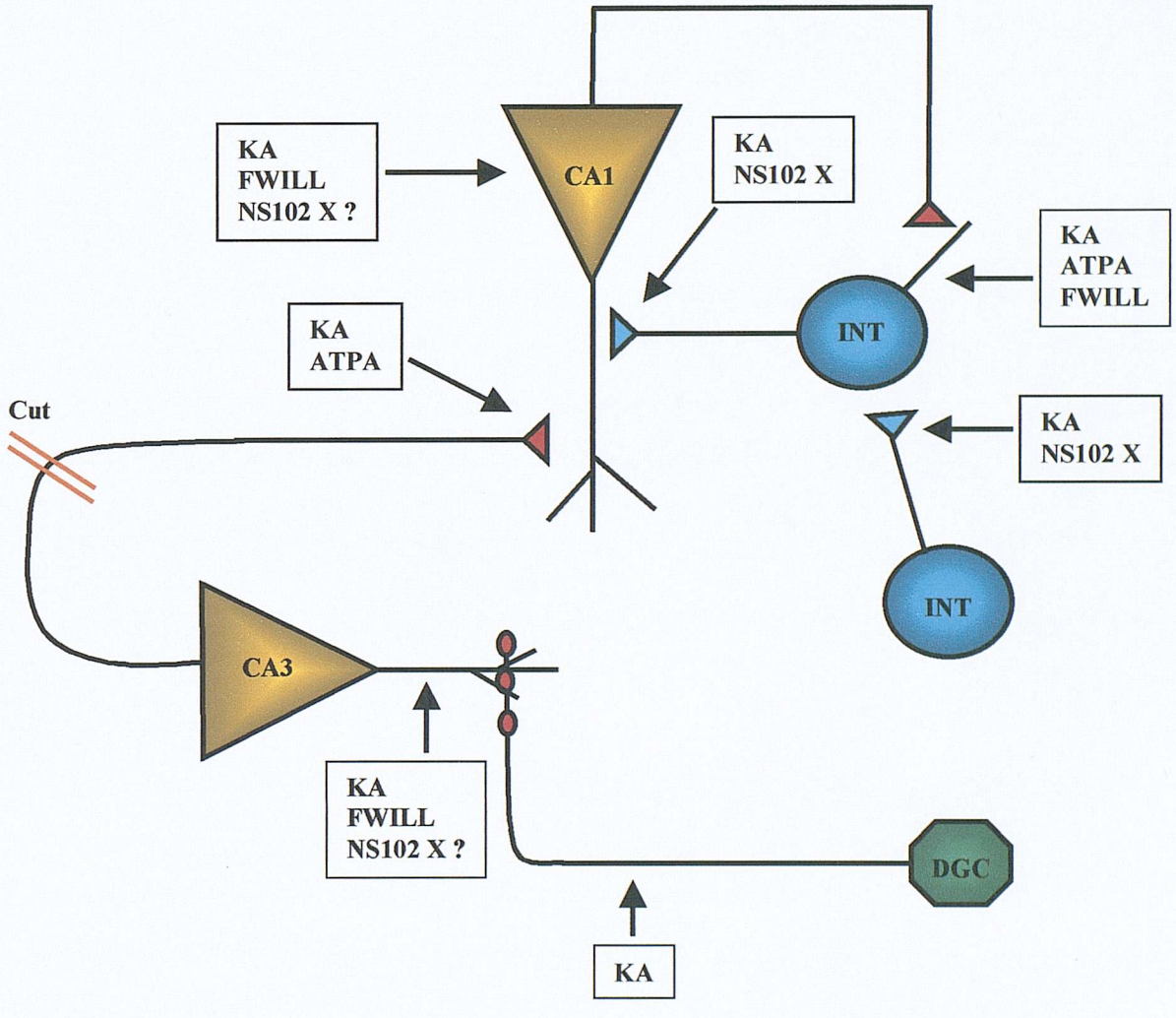

Figure 3.47 Presumed sites of action within the hippocampal tri-synaptic pathway for KA, ATPA, NS102 and FWILL. DGC, dentate granule cell; INT, interneurone; red triangles/ circles, glutamatergic synapse; blue triangles, GABAergic synapse; X= antagonism

The effects of KA on each of these parameters will be discussed in more detail in the following sections with reference to the data presented in this chapter for ATPA, NS102 and fluorowillardine.

3.5.2 Effect of KA on the EPSP slope in CA1

The cumulative dose response data indicates that the EPSP slopes in the intact slice (figure 3.4) and isolated CA1 (figure 3.8) preparations exhibit slight differences in their sensitivity to KA. Although there is a significant decrease in the first EPSP slope in the isolated CA1 (figure 3.8) at a concentration of 250nM KA, a similar response is not seen in the intact slice until the end of 15 minutes superfusion with 500nM KA (figure 3.4). This may reflect excitation of CA3 pyramidal cells at a concentration of 250nM KA enabling the presynaptic actions of KA to be overcome. Interestingly, the second EPSP shows sensitivity to 250nM KA in both preparations. This may indicate an incomplete repolarisation of the terminals following the first stimulus, enabling lower doses of KA to produce a significant effect.

3.5.2.2 Single application of 1μM KA

Comparing the responses seen in the intact hippocampal slice (figure 3.12) with those of the isolated CA1 preparation (figure 3.15) we can see that the mean first EPSP slope is inhibited by 56% from control in the intact slice in the presence of 1μM KA. It is reduced by 45% in the isolated CA1. Thus it would appear that whilst the presence of CA3 may contribute to the reduction in the EPSP slope recorded from the *stratum radiatum* of CA1, it does not play a major part in the response.

As mentioned previously, there are four possible mechanisms that may account for the decrease in the EPSP slope recorded from the CA1 of intact hippocampal slices during the application of KA.

1. Firstly, it is known that KA receptor activation on CA3 pyramidal neurones produces a slow depolarising current (Castillo *et al.* 1997) probably *via* activation of GluR6 containing receptors (Mulle *et al.* 1998). This excitatory current may be sufficient to cause a depolarising block of CA3 pyramidal cells and indeed, the data presented in figure 3.18 is indicative that this is the case, since the population spike amplitudes and EPSP slopes are markedly reduced throughout the application of KA. This could conceivably lead in turn to a reduction of glutamate release from the Schaffer collateral terminals. However, Kamiya and Ozawa (1998) did not observe a change in the afferent fibre volley in the Schaffer collaterals following 1μM KA application. Since it is likely that depolarisation block of CA3 pyramidal cells would lead to an inactivation of axonal Na^+ channels, this may not be the mechanism involved. Furthermore, this fact tends to discount an effect of KA on afferent fibre excitability

such as has been reported for the actions of KA on the mossy fibre pathway (Kamiya and Ozawa 2000) and interneuronal axons (Semyanov *et al* 2001).

2. Secondly, depolarising block of CA1 pyramidal cells following increased glutamate release from the Schaffer collaterals or direct activation of these neurones by KA may result in a reduction in EPSP slope.
3. The third possibility is that activation of interneurones in CA1 by KA (Cossart *et al* 1998) may lead to an increase in the extracellular concentration of GABA, in turn leading to increased activation of $GABA_A$ receptors on CA1 pyramidal cells. The increased Cl^- influx that would be expected to occur as a result of this could conceivably shunt excitation in the dendrites, leading to a reduction in the slope of the EPSP. However, since the population spike amplitudes increase at the same time as the EPSP slopes begin to decrease then it is unlikely that this is the case.
4. A further possibility is that activation of presynaptic KA receptors on the Schaffer collateral terminals themselves causes a localised depolarisation which renders incoming action potentials less effective with regard to initiating the Ca^{2+} influx necessary for transmitter release (Kamiya and Ozawa 1998). It is unlikely that this occurs as a result of inactivation of voltage gated Ca^{2+} channels however, since Kamiya and Ozawa (1998) did not observe a change in the resting levels of rhod-2 fluorescence in the Schaffer collateral terminals in the presence of 1μM KA.

A further possibility is that these mechanisms are acting in tandem to produce the observed effect. Since this phenomenon occurs irrespective of the presence of CA3 it is likely that this response is mediated mainly *via* an effect at the presynaptic terminal or directly at CA1 pyramidal cells rather than *via* a depolarising block of CA3 pyramidal cells.

Unfortunately, from this data alone it is not possible to define whether the observed response is the result of a presynaptic or postsynaptic site of action. It is reasonable to infer from the published data (Vignes *et al* 1998, Kamiya and Ozawa 1998) that this response has a presynaptic origin. Further evidence for this is presented in the next section on the action of the GluR5 agonist ATPA.

3.5.2.3 Comparison of KA to ATPA

The response to the GluR5 agonist ATPA (Vignes *et al.* 1998) in both preparations (figures 3.20 and 3.23) shows some differences to that for KA (figures 3.12 and 3.15). It is likely, given the potency and affinity data presented in table 3.2 that a concentration of 1μM KA is activating KA receptors in a non-specific manner irrespective of their constituent subunits. In the CA1, pyramidal cells are known to express GluR6 subunits (Bureau *et al.* 1999), whilst the expression of GluR5 has been localised to the somato-dendritic compartment of interneurones and functionally to the terminals of excitatory afferent fibres (Vignes *et al* 1998). In addition to this, the major KA receptor subunit of the CA3 pyramidal cell population has also been demonstrated to be GluR6 (Bureau *et al.* 1999).

Thus it should be possible to separate the functional effects of KA receptor activation within the hippocampus by the use of subunit specific agonists and antagonists.

In much the same way as with KA, the EPSP slopes are markedly reduced following the introduction of 1μM ATPA to the recording chamber in both preparations (figures 3.37 –3.40). However, the population spike amplitude does not increase in either intact slices or isolated CA1 preparations with 1μM ATPA (3.41 – 3.44) and is in fact reduced compared to control. This suggests at least two points.

1. Since the EPSP slope decreases without a concomitant rise in population spike amplitude following ATPA application, this response is very likely to be due to an action of the drug at a presynaptic locus of action rather than a direct depolarisation of the CA1 pyramidal cell population. This further suggests that KA is modulating the EPSP slope *via* a presynaptic action.
2. Although (S)-ATPA has been reported to also weakly activate GluR6/KA2 containing heteromeric receptors (Stensbol *et al* 1999) it appears to be relatively selective for the GluR5 subunit at a concentration of 1μM (Vignes *et al* 1998). Therefore, it is very probable that the receptor mediating this phenomenon contains the GluR5 subunit.

This is in agreement with the data of Vignes *et al.* (1998) who found ATPA to depress the field EPSP recorded from CA1 in a concentration dependent manner, without affecting the size of the afferent volley, thus pointing to a presynaptic action at the Schaffer collateral terminals. This was also found to be the case for the field EPSP recorded in CA3.

The similarity of the response of the EPSP to that observed for KA (figures 3.37, 3.38) tend to suggest that KA is also causing a decrease in the EPSP slope by an action at the presynaptic terminals of the Schaffer collaterals.

3.5.2.4 NS102 antagonism

The low affinity KA receptor antagonist NS102 has been demonstrated to show selectivity for blocking receptors containing the GluR6 subunit over those comprising AMPA receptor subunits (Lerma *et al* 1993, Verdoorn *et al.* 1994). In addition to this, Wilding and Heuttner (1996) have shown NS102, to a lesser extent, to antagonise GluR5 containing receptors in dorsal root ganglion (DRG) cells preferentially to AMPA receptors.

Coapplication of NS102 does not significantly inhibit the action of KA on the EPSP slope (figures 3.37 – 3.40). In fact in the isolated CA1 preparation (figure 3.38) there is a further significant reduction in the first EPSP slope by the end of the KA application period compared to KA alone. However, this may be due to the antagonism of postsynaptic GluR6 containing receptors on the CA1 pyramidal cells preventing the inhibition of the I_{sAHP} current by KA (Melyan *et al.* 2002).

In the isolated CA1 preparation (figure 3.29), it would appear that NS102 has significantly enhanced the effect of 1μM KA on the first EPSP slope by the end of 15 minutes KA application, but does not significantly affect the second EPSP throughout this time. Thus it may be that antagonism of GluR6 containing receptors by NS102 may accentuate the effect of KA at receptors comprised of GluR5 subunits, for example at the GluR5 containing KA receptor proposed to be localised presynaptically on the Schaffer collateral terminals (Vignes *et al* 1998, Kamiya and Ozawa 1998).

NS102 did not significantly affect the reduction in EPSP slope induced by 1μM KA in either intact slices (figure 3.26) or isolated CA1 preparations (figure 3.29). However NS102 is only a weak antagonist. Kamiya and Ozawa (1998) only observed a partial blockade of the KA induced depression of the field EPSP, and Verdoorn *et al.* (1994) only found a 50% reduction in the glutamate response of recombinant GluR6 receptors. Thus, the poor solubility of NS102 in physiological solutions (Verdoorn *et al.* 1994) and the weak antagonistic effects of this drug do not render it a useful pharmacological tool for the dissection of KA receptor mediated effects.

3.5.2.5 Comparison with AMPA receptor activation

The potent AMPA receptor agonist, (S)-5-fluorowillardine (300nM) (Patneau *et al.* 1992, Wong *et al.* 1994) reduced the EPSP slopes in intact slices (figure 3.32) in a manner which was not significantly different to that observed with 1μM KA. In contrast to the initial response to KA however, the first population spike increased (figure 3.41) and then decreased whilst the second population spike decreased below control values (figure 3.43) indicating differences in the mechanisms of the two compounds.

However, in the isolated CA1 preparation (figure 3.38), fluorowillardine produces a significantly smaller reduction in the first EPSP slope than KA alone ($p<0.05$) within the first three minutes of application. At the same time, the amplitude of the first population spike begins to decrease below control (figure 3.42) whilst the second population spike is increased (figure 3.44). This increase is significantly less than that for KA. However, by the end of the drug application period there is no significant difference to the first EPSP in the presence of KA (figure 3.38)

It would be expected that fluorowillardine would activate AMPA receptors on both CA3 and CA1 pyramidal cells. Such an action could quite conceivably lead to a depolarising block in the CA1 by both an increased glutamate release from the Schaffer collateral pathway following the excitation of CA3 neurones combined with a direct activation of the CA1 pyramidal cell population.

Unfortunately, it would appear that the combination of field recordings and the pharmacological tools used here do not provide enough information by which to categorically differentiate the receptor populations being activated by both KA and fluorowillardine. However, published data for the affinity and potency of KA for native KA and AMPA receptors (table 3.2) coupled with the high specificity of fluorowillardine for AMPA receptors over KA receptors would suggest that their sites of action are in fact different.

3.5.3 Effect of KA on the first Population Spike Amplitude

3.5.3.1 Response to Kainic Acid

In both the intact slice (figure 3.12) and the isolated CA1 preparation (figure 3.15) application of 1μM KA caused a marked transient increase in the first population spike amplitude within the first three minutes. From the previous section it is clear that this phenomenon occurs at a time during which the EPSP slope has already begun to decrease.

Since the field EPSP slope bears a direct relationship to the evoked synaptic current and hence to the amount of glutamate released from the Schaffer collateral terminals, this would tend to suggest that the observed increase is not a consequence of an increase in glutamate from the Schaffer collaterals following the stimulation of CA3 pyramidal cells by KA. In support of this, the normalised data shows (figures 3.41 and 3.42) that this increase in amplitude from control is only marginally greater in the intact slice CA1 (139% (±11.3)) when compared to the response of the isolated CA1 preparation (117% (±3.3)). It is therefore probable that KA is either directly causing an excitation of the CA1 pyramidal cell population, indirectly increasing the pyramidal cell output (as measured by population spike amplitude) *via* a reduction in the efficacy of GABAergic inhibitory mechanisms, or a combination of both of these.

By the end of the KA application period, the population spike amplitude is significantly reduced from control in the intact slice, but not the isolated CA1 preparation. This may be due to the somato-dendritic KA receptor activation of interneurones (Cossart *et al* 1998; Frerking *et al* 1998, 1999). This would be expected to lead to an increase in GABA release and thus to a reduction in the output from the CA1 pyramidal cell population.

3.5.3.2 The initial response to ATPA

Application of the GluR5 agonist ATPA did not result in a similar response in either the intact slice (figure 3.20) or the isolated CA1 preparation (figure 3.26). In fact addition of ATPA to the superfusing ACSF resulted in a reduction in the amplitude of the first population spike in both preparations within the first three minutes of application. It is likely that this response occurs as a result of a decrease in the EPSP slope without any concomitant direct excitation of the postsynaptic cell.

However, it is also possible that activation of GluR5 containing KA receptors on the somato-dendritic compartment of GABAergic interneurones within the CA1 results in an increase in the tonic release of GABA from these cells (Cossart *et al.* 1998; Frerking *et al.* 1998, 1999). Such an event, coupled with a reduction in the EPSP slope, would be expected to limit the amplitude of the population spike that it is possible to elicit from the CA1 for any given stimulus.

Once again, by the end of the ATPA application period, the amplitude of the population spike decreases further, which may be due to prolonged activation of the interneuronal population leading to further tonic GABA release.

3.5.3.3 KA receptor antagonism with NS102

Co-administration of the GluR6 antagonist NS102 (10μM) with 1μM KA resulted in a significant blockade of the initial response to KA ($p<0.01$) in the intact slice (figure 3.26) but, interestingly, not in the isolated CA1 preparation (figure 3.29).

Melyan *et al* (2002) have proposed a mechanism whereby activation of a GluR6 containing post-synaptic receptor on CA1 pyramidal cells leads to an inhibition in the slow after-hyperpolarisation (I_{sAHP}) recorded from these cells. This leads to an increased CA1 pyramidal cell excitability. Previous data shows that the initial increase in the population spike amplitude in response to KA alone does not differ greatly in the presence (figure 3.12) or absence (figure 3.15) of the CA3 region. We can also infer from the affinity data presented in table 3.2 that the activation of AMPA receptors is unlikely with a concentration of 1μM KA. Thus, it would appear that this difference in the blockade of the initial rise in population spike amplitude in the presence of NS102 may arise as a result of its poor antagonist ability or solubility in physiological solutions (Johansen *et al* 1993, Verdoorn *et al.* 1994). Thus it may be the case that a sufficient tissue concentration was achieved in the intact slice preparations but not during experiments on the isolated CA1 preparations to prevent a KA induced inhibition of the I_{sAHP} and therefore the expected increase in the population spike amplitude.

3.5.3.4 AMPA receptor activation

It is interesting to note that the response to the AMPA receptor specific agonist fluorowillardine (figure 3.32) strongly resembles the response to KA (figure 3.12) in the intact slice CA1 with regard to both the EPSP slope and the first population spike amplitude. Within the first three minutes of fluorowillardine application in the intact slice the amplitude of the first population spike is observed to increase.

However, although this is the case in the intact slice, the pattern of response observed in the isolated CA1 preparation to fluorowillardine (figure 3.35) is significantly different from that recorded in the presence of KA (figure 3.15). In this case the EPSP slope remains at or near to control values during the first three minutes and the amplitude of the first population spike does not increase significantly during this time. By the end of the respective drug application periods this difference has become more pronounced. In the presence of 1μM KA, a concentration likely to be KA receptor selective (Kamiya and

Ozawa 1998, 2000; Mulle *et al.* 2000 and see table 3.2) the population spike amplitudes in the isolated CA1 preparation are not significantly different from control (figure 3.15). In the presence of 300nM fluorowillardine (figure 3.35) they are markedly reduced.

3.5.4 Effect of KA on paired-pulse inhibition

3.5.4.2 1μM KA

Within the first three minutes of KA application, the amplitudes of both the first and second population spikes increase rapidly. This occurs in both the intact slice (figure 3.12) and the isolated CA1 preparation (figure 3.15). As mentioned in the previous section, the increase in the amplitude of the first population spike, at a time when the EPSP slope has already begun to decrease, is likely to be due to a direct effect of KA acting at a GluR6 containing receptor. Activation of this receptor leads *via* a PKC dependent mechanism to a reduction in the slow after-hyperpolarising potential in the CA1 pyramidal cell population and thus to an increase in cell excitability (Melyan *et al* 2002). This in turn results in an increase in the population spike amplitude for any given stimulus.

However, it is also possible to explain the increase in first population spike amplitude by a reduction in the efficacy of feedforward inhibition in CA1, *via* a similar mechanism to that discussed below for the reduced function of the feedback inhibitory circuitry.

To explain the increase in the second population spike following a second stimulus separated from the first by a 20 msec interval, we need to take into account the effects of the feedforward and feedback inhibitory circuitry which is present in the hippocampus. Under drug-free control conditions, the amplitude of the second population spike is reduced with regard to the first at this stimulus interval. This is due to the activation, in both a feedforward and feedback manner, of GABAergic interneurones throughout the CA1 region. This leads to a release of GABA, which activates both $GABA_A$ and $GABA_B$ receptors leading to a hyperpolarisation of the pyramidal cell population. At an inter-pulse interval of 20 msec, the effect of fast $GABA_A$, but not $GABA_B$ receptor mediated inhibition is visible (Stanford *et al* 1995)

It would be expected that, under conditions where the excitability of the pyramidal cell population, and hence the pyramidal cell output itself is increased, that the feedback excitatory drive to the interneurones would also be increased. This would be expected to further decrease the amplitude of the second population spike and hence increase the

percentage inhibition. However, this is clearly not the case. In fact the amplitude of the second population spike actually increases. This suggests that application of 1μM KA is in fact decreasing the efficacy of the inhibitory circuit in some way.

3.5.4.3 ATPA and inhibition

Application of the GluR5 agonist ATPA to the intact slice preparation resulted in an increase in the normalised percentage inhibition within the first three minutes, a period during which KA causes a reduction (figure 3.45). This just failed to reach significance ($p=0.08$, Student's unpaired t-test), although this may be due largely to the large standard error for the inhibition data for KA alone. This correlated with a decrease in the mean amplitude of the second population spike (figure 3.20) while the first population spike amplitude did not change during this time. This would tend to suggest that the interneuronal population may be releasing more GABA on the second stimulus than during the control period. Such an eventuality could be possible if the interneurones were preferentially excited by ATPA without a corresponding excitation of the pyramidal cell population. In support of this argument is the fact that the EPSP slopes are reduced during this time, implying a reduced excitatory drive to both the CA1 pyramidal cell and interneuronal population. Since the EPSP slopes are reduced at this time, indicating a reduced glutamatergic drive to both the pyramidal cell and interneuronal populations, this would appear to be the most likely explanation for this phenomenon.

This is in agreement with the data published by Cossart *et al* (1998), who saw an increase in the frequency of sIPSCs recorded from CA1 pyramidal cells in the presence of 1μM ATPA. As time progresses the amplitude of the second population spike increases somewhat possibly pointing to a use dependent shut down of GABA release from these interneurones following continued activation. This response is the same irrespective of the presence of CA3.

By the end of the KA application period, the presence of ATPA has significantly exacerbated the reduction in inhibition in the isolated CA1 preparation (figure 3.46) when compared to KA alone ($p<0.01$).

3.5.4.4 KA receptor antagonism

When introduced into the recording chamber, 10μM NS102 produced a small but significant increase in the paired-pulse inhibition in both intact slices (figure 3.26) and

isolated CA1 preparations (figure 3.29). This correlated in both preparations with a significant decrease in the amplitude of the second population spike, a response which points to an increase in evoked inhibition rather than the tonic release of GABA from interneurones. There is evidence for the existence of KA receptors located presynaptically on GABAergic afferent terminals which synapse with other interneurones (Mulle *et al*, 2000, Cossart *et al* 2001). Their activation leads to an increase in the release of GABA onto interneurones and presumably to a downregulation of evoked inhibition seen within the CA1. These receptors appear to be homomeric receptors containing the GluR6 subunit or at least do not contain the GluR5 subunit, since this particular phenotype is ablated in GluR6$^{-/-}$, but not in GluR5$^{-/-}$ mice (Mulle *et al* 2000). Therefore it is possible that NS102 in these preparations is causing a disinhibition of interneurones within the CA1 by antagonising these GluR6 containing receptors and thus leading to an increase in the evoked inhibition.

The mean normalised percentage inhibition is marginally less reduced in both the intact slice and isolated CA1 preparation by KA in the presence of NS102 within the first three minutes of KA application (figure 3.45 and 3.46). However, in both cases this difference fails to reach significance.

3.5.4.5 The effect of Fluorwillardine

Application of the AMPA receptor agonist fluorowillardine produced a significant increase in the normalised mean percentage inhibition in the intact slice preparation within the first three minutes (figure 3.45). This was significantly different ($p<0.05$) to the effect of 1μM KA at the same time point, during which the inhibition was observed to decrease from control. This increase in the inhibition was due to a potentiation of the first population spike amplitude during the onset of fluorowillardine's effect that was not accompanied by a similar increase in the second population spike amplitude (figure 3.32). This may reflect an increased excitation of the interneuronal population during the second stimulus as a result of an additive effect between synaptically released glutamate following Schaffer collateral stimulation and fluorowillardine. By the end of the application period there was no significant difference between the normalised inhibition in the presence of KA or fluorowillardine.

The profile of the initial response to fluorowillardine in the isolated CA1 preparation (figure 3.35) differed from that observed in the intact slice (figure 3.32). While

the normalised percentage inhibition also increased in the isolated slice (figure 3.46), it did not rise as dramatically. The data (figures 3.31 and 3.34) shows that while the first population spike increased in both preparations, the second population spike amplitude only increased in the isolated CA1. This may indicate that the excitatory drive to the interneurones is stronger in the presence of the CA3, possibly due to activation of AMPA receptors on the CA3 pyramidal cells contributing further to the release of glutamate from the Schaffer collaterals. Therefore in the isolated CA1, addition of fluorowillardine to the superfusing ACSF excites the pyramidal cell population sufficiently to overcome the effects of feedforward and feedback inhibition.

3.5.4 Summary

3.5.4.1 EPSP downregulation by KA

Application of 1μM KA to both isolated CA1 preparations and intact hippocampal slices results in a reduction of the slopes of both the first and second EPSP, an event that is independent of the presence of an intact CA3- CA1 connection. Since the population spike amplitude increases at this time, it is suggestive of a pre-synaptic effect of KA on the Schaffer collateral terminals.

Since this reduction in the EPSP slope occurs at submicromolar concentrations as well as at a concentration of 1μM KA, it is very likely that this is due to the activation of KA receptors rather than AMPA receptors. As the population spike amplitudes are increasing at this time, it is unlikely that GABAergic transmission is increased at this time, leading to increased shunting of excitation by GABA.

Application of the GluR5 specific agonist ATPA mimics the effects of KA on the EPSP without increasing the population spike amplitude. This points to the involvement of more than one site of action in the response to KA. Furthermore, it tends to suggest that the reduction of the EPSP slope by KA is mediated by a GluR5 containing KA receptor.

The KA antagonist NS102 does not appear to significantly reduce the effects of KA application, which may point to a lack of involvement of the GluR6 subunit in this response. However, this may also be due to NS102's poor solubility in physiological solutions preventing a sufficient concentration to be achieved in the tissue to effectively compete with 1μM KA at the receptor. It would therefore be potentially more informative to repeat this experiment using lower concentrations of KA.

3.5.4.2 KA induced potentiation of the population spike

Addition of KA to the recording chamber results in a potentiation of the first population spike in both the intact slice and the isolated CA1 preparations. This occurs at a time when the EPSP slope has already begun to decrease. This response occurs in the intact slice at a concentration of 250nM, but not in the isolated slice. However, this latter data may be unreliable since the first population spike amplitude appears to be following a downward trend that began during the control period throughout the course of the experiment. Once again, sensitivity to nanomolar concentrations of KA would tend to suggest that this is a KA receptor mediated event.

With a single administration of 1μM KA, the potentiation of the first population spike amplitude occurs in both the presence and absence of the CA3 region. Interestingly, the potentiation is greater in the presence of a functional contact between CA3 and CA1. However, an increase in the population spike amplitude occurring at a time when the EPSP slopes are decreasing in both preparations would tend to suggest a postsynaptic effect for KA.

It may be the case, however that the increase in first population spike amplitude occurs as a result of a KA induced reduction in feedforward inhibition presumably *via* activation of GluR6 containing receptors located on the presynaptic terminals of interneurones to reduce GABA release.

Alternatively both pre- and post-synaptic mechanisms may be acting in tandem to produce the observed response.

The application of ATPA (1μM) does not result in a similar potentiation, suggesting a lack of involvement for the GluR5 subunit in this response. It is blocked by NS102 in the intact slice CA1 but not in the isolated slice. This discrepancy may again occur as a result of the poor solubility of NS102 resulting in inconsistent concentrations of the antagonist in the tissues. However, this may point to the involvement of a GluR6 containing receptor. This again would be more consistent with a postsynaptic site in CA1 for the action of KA on the initial population spike amplitude.

This initial effect of KA is mimicked by AMPA receptor activation in the intact slice but not the isolated CA1 preparation. This may again point to differences in the outcome following AMPA receptor and KA receptor activation. Since the application of fluorowillardine only results in a significant potentiation of the first population spike in the presence of a viable connection between CA3 and CA1 it is possible that this potentiation occurs as a result of an excitation of CA3 pyramidal cells which leads to an

increased release of glutamate from the Schaffer collaterals. In addition, the action of this glutamate on the CA1 pyramidal cell population may be enhanced in the presence of fluorowillardine.

3.5.4.2.1 The effect of prolonged KA application

By the end of 15 minutes KA application the amplitude of the first (and second) population spikes are reduced in the intact, but not the isolated slice preparation. This suggests a need for a functional connection between CA3 and CA1 for this reduction to occur. Since the reduction in the EPSP slope is comparable in both preparations, it is possible that this effect is brought about by an activation of one of the lesser excitatory pathways into the CA1 from either the dentate gyrus or the entorrhinal cortex.

However, the elevated population spike amplitude observed in the isolated CA1 preparation is also of interest. Since this reduction does not occur in the isolated CA1 preparation, it would tend to argue against the production of a depolarising block of the CA1 pyramidal cell population by KA. However, it is possible that, since the EPSP slope is reduced at this time, that it represents a direct excitation of the CA1 pyramidal cell population by KA such as has been reported by Melyan *et al* (2002).

Since this response is not reproduced in the isolated CA1 preparation by the GluR5 agonist ATPA it is unlikely that a receptor containing this subunit is involved. Furthermore, since the population spike amplitude in the isolated CA1 in the presence of the GluR6 antagonist NS102 and KA is also reduced after the initial 3 minutes of KA application it would appear likely that the GluR6 subunit is involved.

Application of the AMPA receptor agonist fluorowillardine also resulted in a reduced population spike amplitude in the isolated CA1 preparation, suggesting that AMPA receptors are not involved in this response.

3.5.4.3 KA and the modulation of inhibitory function

Application of concentrations of KA as low as 250nM are capable of reducing the paired-pulse inhibition in both intact and isolated CA1 preparations indicating that this response is very likely to be mediated by a KA receptor rather than an AMPA receptor. This reduction in the paired-pulse inhibition occurs as a result of a greater potentiation of the second population spike amplitude than the first, thus changing the ratio between them.

It occurs in both intact and isolated CA1 preparations, although the response is markedly greater in intact slices.

It would appear that the receptor responsible for this reduction in inhibition is not comprised of GluR5 subunits, since application of 1μM ATPA actually increases the paired-pulse inhibition within the first three minutes. This could be explained by activation of a GluR5 containing receptor located on the soma or dendrites of interneurones in CA1 leading to an increased release of GABA and hence an increase in the percentage inhibition. Indeed ATPA has been reported to cause an increase in interneuronal spiking (Cossart *et al* 1998; Frerking *et al.* 1998, 1999) which would presumably lead to the increased inhibition observed here.

Blockade of GluR6 containing receptors with NS102 resulted in a small increase in the percentage inhibition in both preparations. This may correspond to the antagonism of a homomeric GluR6 receptor found to facilitate the release of GABA onto other interneurones (Cossart *et al* 2001; Mulle *et al.* 2001). This would be expected to result in a disinhibition of the interneurone network, leading to greater inhibitory function. However, although NS102 did not significantly antagonise the effects of KA on the inhibition, this may reflect it's poor solubility preventing effective competition with 1μM KA for receptor binding sites. It may have been more instructive therefore to look at the effects of NS102 on a lower concentration of KA.

It would again appear unlikely that the responses observed here are a result of KA activating AMPA receptors on interneurones since the effects of fluorwillardine differed from those of KA. Application of fluorowillardine resulted in an initial increase in the inhibition calculated from CA1 population spike data which occurred as a result of a potentiation of the first population spike amplitude without a corresponding increase in the second. This suggests that the presence of an AMPA agonist is exciting both the pyramidal cell and interneuronal population leading to an increased effect of feedforward and feedback inhibition, whereas KA appears to increase the output from the pyramidal cell population, reducing the paired-pulse inhibition at the same time.

Chapter 4

Pharmacology of the acute kainate response in CA1

The role of non-ionotropic glutamate receptors

4.1 Introduction

In the previous chapter, the application of KA at concentrations as low as 250nM was shown to result in a number of effects in CA1. These included a reduction in the slope of the EPSP recorded from *stratum radiatum*, a transient increase in the population spike amplitude followed by a more prolonged decrease, which was dependent on the presence of the CA3 region, and a decrease in the percentage inhibition.

In the following chapter, these effects will be studied with a view to determining whether there are any indirect components to this response. In other words, does the application of 1μM KA result in the release of either neurotransmitters, such as glutamate or GABA, or neuromodulators, such as adenosine, which may either produce or contribute to the responses observed in the previous chapter.

Since KA receptor activation of CA3 pyramidal cells results in their excitation (Robinson and Deadwyler 1981, Castillo *et al* 1997) it is conceivable that this could lead initially to more fibres being recruited into the response per submaximal stimulus, and hence to an increase in the release of glutamate from the Schaffer collateral fibres. This in turn may then activate presynaptic metabotropic glutamate receptors (mGluRs) leading to the observed reduction in EPSP slope.

Group I mGluRs are found both pre- and post-synaptically within the CA1 (Luján *et al.* 1996) (see also figure 4.1). Postsynaptically, on CA1 pyramidal cells, they modulate the activity of a number of K^+, Ca^{2+} and non-selective cation channels (Conn and Pinn 1997) leading to an increase in excitability. Thus their activation could conceivably lead to the observed increase in the population spike amplitude during the initial phase of the KA response as the increased excitability of the pyramidal cell population would be expected to lead to an increased probability to generate action potentials. Furthermore excitation of CA1 pyramidal cells following mGluR activation by increased glutamate release from the Schaffer collateral pathway in response to KA receptor mediated excitation of the CA3 could account for the observed reduction in EPSP slope during the application of KA.

In addition to a postsynaptic locus for mGluRs they have also been demonstrated to be present on both the Schaffer collateral and mossy fibre pathway terminals, where they downregulate neurotransmitter release. Thus group I and III mGluRs are found on the Schaffer collateral terminals (Gereau and Conn 1995), whereas group II and III mGluRs are located on the mossy fibre pathway terminals (Shigemoto *et al.* 1997). Thus it is possible that glutamate spillover from the Schaffer collateral pathway following CA3

excitation by KA may inhibit the presynaptic release of glutamate and thus reduce the EPSP slope.

Activation of group I mGluRs on oriens-alveus interneurones has been demonstrated to result in a slow depolarisation of these neurones (van Hooft *et al* 2000). Therefore, it is possible that synaptically released glutamate may contribute to interneuronal excitation in addition to GluR5 mediated excitation by KA (Cossart *et al* 1998, Frerking 1998).

In a similar way, it is known that activation of postsynaptic GluR5 containing receptors on interneurones leads to an increase in the number of excitatory potentials recorded from these cells (Cossart *et al.* 1998, Frerking *et al.* 1998). If this leads to an increased release of GABA from these neurones, then it may be that some of the downregulatory responses previously described may occur as a result of, for example, $GABA_B$ receptor activation.

$GABA_B$ receptors have been demonstrated to be present on both glutamatergic and GABAergic terminals within the hippocampus (Nicholl *et al* 1990, Thompson 1994). They couple to what is thought to be G_o (Costa *et al.* 1998) leading to an inhibition of Ca^{2+} channel activity and hence a reduction in transmitter release. They are also capable of presynaptically increasing K^+ channel activity (Thompson and Gähwiller 1992), also leading to an inhibition of transmitter release.

Indeed, Frerking *et al* (1998, 1999) have reported that approximately 50% of the presynaptic downregulation of GABA release from interneuronal terminals may occur as a result of $GABA_B$ receptor activation. However, other groups have reported that $GABA_B$ receptor activation is not involved in this response (Min M-Y *et al* 1999).

Thus it is possible that GluR5 mediated activation of interneurones by KA may lead to an increase in the extracellular concentration of GABA. This could lead to a reduction in both excitatory and inhibitory transmission, leading to a reduction in the EPSP slope and an increase in the population spike amplitudes.

Postsynaptically, activation of $GABA_B$ receptors on CA1 pyramidal cells leads to the activation of a K^+ conductance (Dutar and Nicoll 1988), decreasing excitability. Thus, it is possible that the reduction in the population spike amplitudes observed in the later phase of the KA response may occur as a result of interneurone excitation by KA, increasing the extracellular concentration of KA.

It is therefore of interest to investigate the possible involvement of this receptor type in the response to KA.

Furthermore, it is known that KA application can lead to an increase in the release of adenosine during kainate induced seizure activity in the dorsal hippocampus (Berman *et al* 2000, Carswell *et al* 1997). Thus it may be that adenosine receptor activation plays a role in the action of 1μM KA in these preparations.

In the hippocampus, adenosine A_1 receptors have been shown to be located presynaptically, where they inhibit transmitter release *via* either a G_i or G_o protein (Cunha 2001). These appear to directly inhibit mainly N-type Ca^{2+} channels, leading to a decrease in the release of neurotransmitter (Wu and Saggau 1994). Therefore it is possible that KA induced release of adenosine may result in both a reduction of glutamate, leading to a reduced EPSP slope, and a decrease in the release of GABA, leading to an increase in population spike amplitude.

Alternatively, presynaptic A_{2A} receptor activation may result, *via* activation of a G_s protein (Olah 1997), in the facilitation of P-type Ca^{2+} channels, leading to an increase in neurotransmitter release, for example in the CA3 (Goncalves *et al* 1997). Were this the case, it is possible that this could result in an increase in Schaffer collateral glutamate release, which would be consistent with an increased population spike amplitude and could also account for a reduced EPSP slope.

In order to investigate these possibilities, slices were perfused with antagonists for group I/II and group II/III mGluRs, $GABA_B$ receptors and both adenosine A_1 and A_2 receptors for 15 minutes prior to the application of 1μM KA. Once again, in order to investigate any potential role for the excitation of CA3 pyramidal cells by KA, experiments were performed in both intact slices and in isolated CA1 preparations, from which the CA3 and dentate gyrus had been excised.

4.1.2 Receptor expression at 15-19 days in the rat hippocampus

The developmental expression of the various receptor populations in the rat hippocampus has been dealt with in detail in the previous chapter. However, in order to aid in the interpretation of the data to follow, this information will be reiterated briefly with regard to the modulatory systems investigated.

The ability of both group I and group III mGluR agonists to inhibit glutamate release from the Schaffer collateral pathway peaks during the first postnatal month (Baskys and Malenka 1991). The group I mGluR agonist ACPD depresses EPSP slope in CA1 in young adult rat slices (postnatal day (P) 28-35) to a greater extent than is observed in slices from P15-21 rats (Dumas and Foster, 1997).

Within the hippocampus, mGluRs may be found both pre- and post-synaptically. Group I mGluRs have been localised to hippocampal pyramidal cells using immunohistochemistry (Luján et al 1996) where they modulate the activity of a number of K^+, Ca^{2+} and non-selective cation channels (Conn and Pin 1997) leading to an increase in neuronal excitability. In addition to this, presynaptic mGluRs are thought to downregulate transmitter release. For example group I and III mGluRs are found on the terminals of the Schaffer collateral pathway (Gereau and Conn 1995), whereas group II and III are found located presynaptically on the terminals of both the mossy fibre pathway and the perforant path synapse with dentate gyrus granule cells (Shigemoto et al. 1997).

Immunohistochemistry for mGluR1α has demonstrated it to be present between P4-P8 on pyramidal cells in both CA1 and CA3. From P35 onwards however, staining for this mGluR subtype is found to be most intense in fibres and cell bodies within the alveus and in the superficial layers of the *stratum oriens* (Defagot *et al* 2002). In situ hybridisation studies (Minakami *et al*, 1995) have shown that the levels of mRNA for the mGluR5a splice variant predominates throughout the hippocampus until P7. By P14, levels of the alternatively spliced mGluR5b mRNA dominate.

Immunoreactivity for mGluR2/3 was observed in the hippocampus from week 2 onwards (Defagot *et al* 2002). Staining was onserved on fibres within the *stratum lacunosum moleculare* of both CA1 and CA3. Staining for mGluR4a increased in intensity in pyramidal cells of the CA1 and CA3 between P12 and P35. It was also observed in the dentate gyrus. Between P35 and P60 the intensity of staining appeared to remain consistent (Defagot *et al* 2002).

Expression of the mGluR7 subtype of metabotropic glutamate receptor aslo appears to be developmentally regulated (Bradley *et al*, 1998). Using antibodies raised against a peptide sequence in the C-terminal domain of mGluR7a, they found that the distribution pattern of this receptor is similar to that of adults. It was found to be abundant in the middle third of the molecular layer of the dentate gyrus, in *strata radiatum* and *lacunosum moleculare* of CA1 and CA3, but sparse in the *stratum pyramidale* and granule cell layers (Bradley *et al* 1998). Levels of expression were highest by P14, but declined thereafter.

Group I mGluRs have also been shown to mediate a slow excitation of oriens-alveus interneurones in the CA1 (van Hooft et al 2000). In contrast to this Semyanov and Kullmann have found the group III agonist L-(+)-2-amino-4-phosphonobutyric acid (L-

AP4) to reduce GABAergic signalling among interneurones in CA1. This effect could be mimicked by the administration of brief trains of stimuli to the Schaffer collaterals and was blocked by the group III antagonist α–methylserine-O-phosphate (MSOP). They concluded that this effect was likely due to activation of presynaptic group III mGluRs on interneuronal terminals.

By around P5 the expression pattern of the GABA synthesising enzymes GAD-65 and GAD-67 in the hippocampus resemble that of adult rats (Seress *et al* 1989). Furthermore, the switch from a depolarising GABA response to the adult inhibitory effect has already occurred in both the CA1 (Mueller *et al* 1984) and the CA3 (Ben Ari *et al* 1989) by P15.

The levels of expression of the $GABA_B$ receptor subtypes are nearing those of an adult rat between P15 – P19. Of these, the GB-1a subtype appears to be localised to the *stratum pyramidale* and of CA1 and the dentate gyrus. In contrast to this, the GB-1b subtype appears to be expressing in the *stratum lacunosum* of the CA1 and throughout the CA3 (Fritschy *et al* 1999).

It is possible that the levels of endogenous adenosine are lower in P15 – P19 rats compared to adults since the effects of both caffeine and the adenosine uptake blocker nitrobenzylthioinosine are reduced in immature rats (Psarropolou *et al* 1990). In addition to this, the levels of adenosine A_1 receptor expression do not reach adult levels until around P28 (Ochiishi *et al* 1999).

The sites of receptor expression within the circuitry of the CA1 and CA3 are presented in figure 4.1 on the following pages.

Figure 4.1 Assumed circuitry and receptor expression patterns in the CA1 (page 128) and CA3 (page 129)

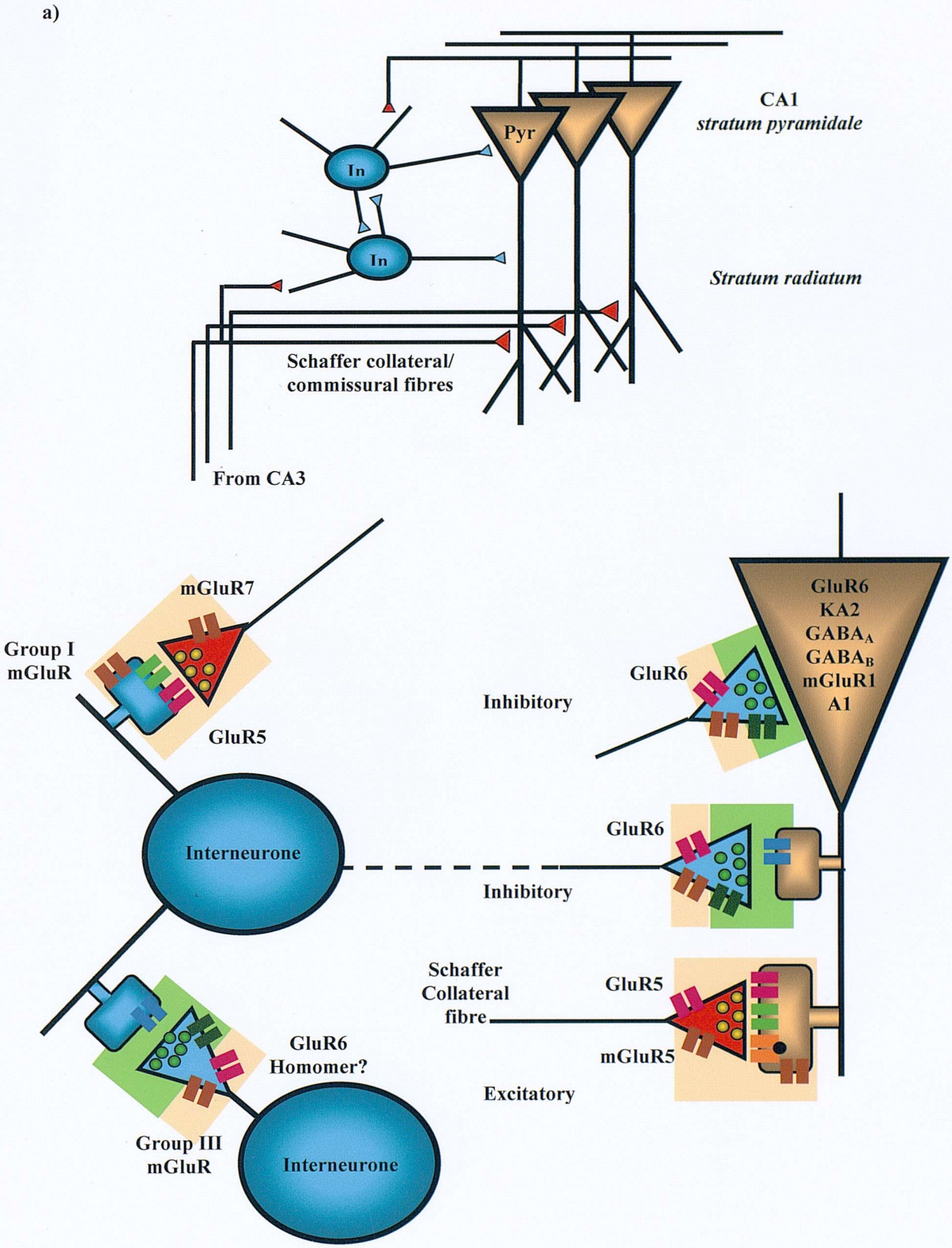
a)
CA1
stratum pyramidale
Pyr
In
In
Stratum radiatum
Schaffer collateral/
commissural fibres
From CA3
mGluR7
Group I
mGluR
GluR5
Interneurone
GluR6
KA2
GABA$_A$
GABA$_B$
mGluR1
A1
GluR6
Inhibitory
GluR6
Inhibitory
Schaffer
Collateral
fibre
GluR5
mGluR5
Excitatory
GluR6
Homomer?
Group III
mGluR
Interneurone
b)
Glutamate release
GABA release
AMPA Receptor
NMDA Receptor
KA Receptor
mGluRs
GABA$_A$ Receptor
GABA$_B$ Receptor
Glutamatergic Terminal
GABAergic Terminal

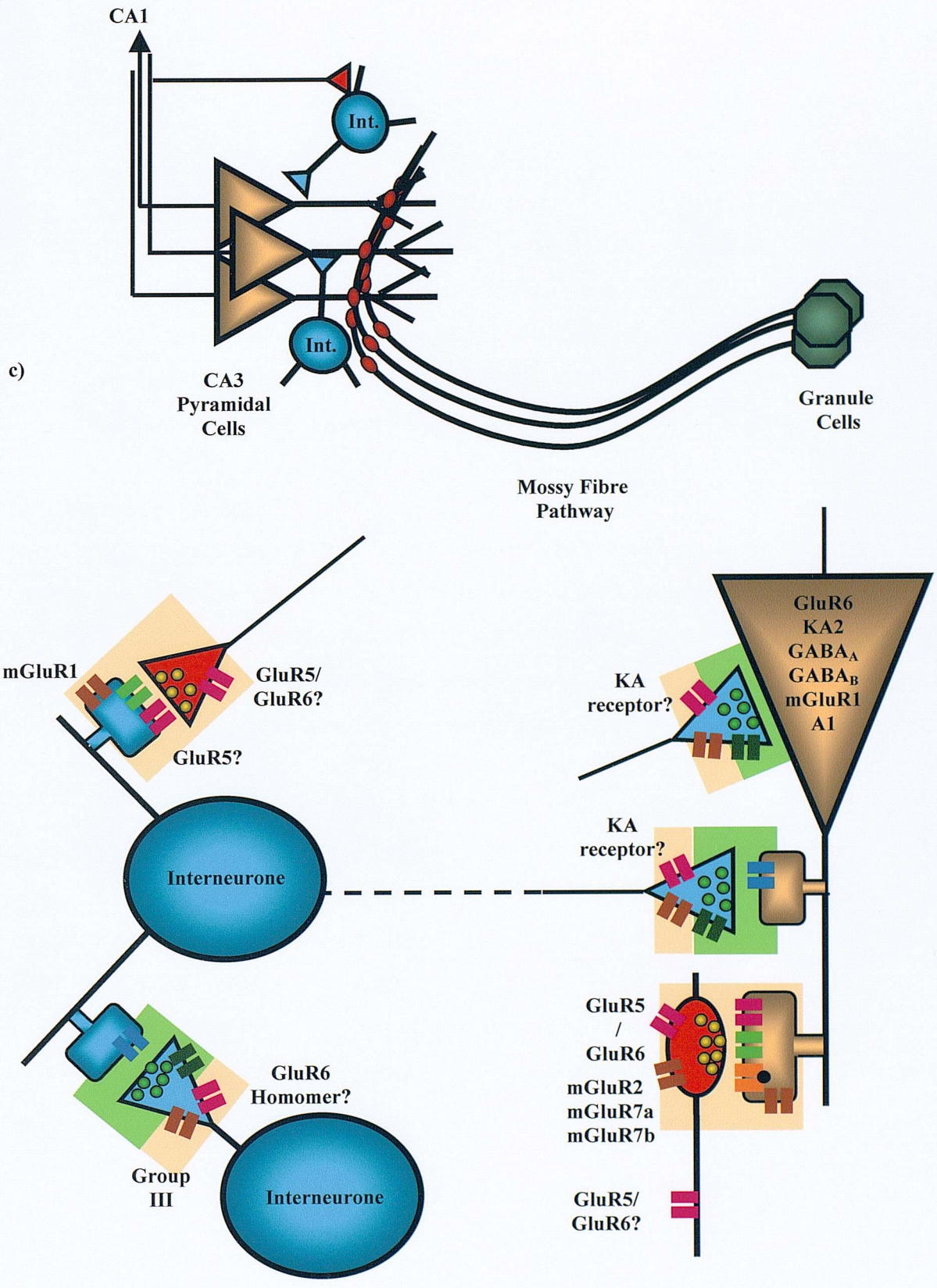
CA1
Int.
Int.
c)
CA3
Pyramidal
Cells
Granule
Cells
Mossy Fibre
Pathway
mGluR1
GluR5/
GluR6?
GluR5?
Interneurone
GluR6
KA2
GABA$_A$
GABA$_B$
mGluR1
A1
KA
receptor?
KA
receptor?
GluR5
/
GluR6
mGluR2
mGluR7a
mGluR7b
GluR5/
GluR6?
GluR6
Homomer?
Group
III
Interneurone
d)
Glutamate release
GABA release
AMPA Receptor
NMDA Receptor
KA Receptor
mGluRs
GABA$_A$ Receptor
GABA$_B$ Receptor
Glutamatergic Terminal
GABAergic Terminal

4.2 Methods

4.2.1 Hippocampal slice preparation

The experimental procedure has been described in detail previously in Chapter 3. Briefly, experiments were performed on acute slices taken from 15-19 day old Wistar rats. Hippocampi were dissected from rats killed by terminal halothane anaesthesia and then placed into ACSF (in mM: NaCl 117.8, $NaHCO_3$ 26.0, KCl 3.3, KH_2PO_4 1.3, $MgSO_4.7H_2O$ 1.0, $CaCl_2$ 2.5, glucose 21.0) chilled to 4^o C on ice. Transverse slices (400μM) were cut on a McIlwain tissue chopper and transferred to a petri dish containing a piece of filter paper moistened with chilled ACSF. These were allowed to recover for at least 1 hour in a humidified chamber continuously gassed with 95% O_2/5% CO_2.

4.2.2 Electrophysiology

Slices were placed into a recording chamber and superfused with ACSF continuously bubbled with 95% O_2/5% CO_2. Stimuli were administered *via* a nichrome bipolar stimulating electrode placed into the Schaffer collateral pathway and field responses recorded simultaneously from both *stratum pyramidale* and *stratum radiatum* of the CA1. Recordings were made at room temperature, and were sampled at 10Hz and filtered at 3Hz.

Feedforward and feedback $GABA_A$ mediated inhibition was assessed from population spike data following the administration of paired submaximal stimuli with an interpulse interval of 20msec. Percentage inhibition of the second population spike was calculated using the formula ((C-T)/C)*100, where C= first (conditioning) spike amplitude and T= second (test) spike amplitude.

Isolated CA1 preparations were produced by the removal of the dentate gyrus and CA3 from the slice prior to its introduction to the recording chamber.

4.2.3 Drugs

Drugs were applied *via* the superfusing ACSF. All antagonists were applied for 15 minutes prior to as well as during the addition of 1μM KA.

4.2.4 Analysis and Statistics

EPSP slopes and population spike amplitudes were calculated as previously described. Statistical significance was assessed using Student's unpaired t-test, $p<0.05$ being deemed significant and $p<0.01$ highly significant.

4.3 Results

4.3.1.1 1μM KA time-course: the intact slice preparation

Single applications of 1μM KA were carried out in intact slices (figures 4.2- 4.4). This data is repeated from chapter 3 (figures 3.11-3.13) for ease of comparison with subsequent data in this chapter. A concentration of 1μM KA was chosen, as previously stated, since it is at or below the EC_{50} for KA at native KA receptors in various brain regions and well below the EC_{50} values for the activation of native AMPA receptors by KA.

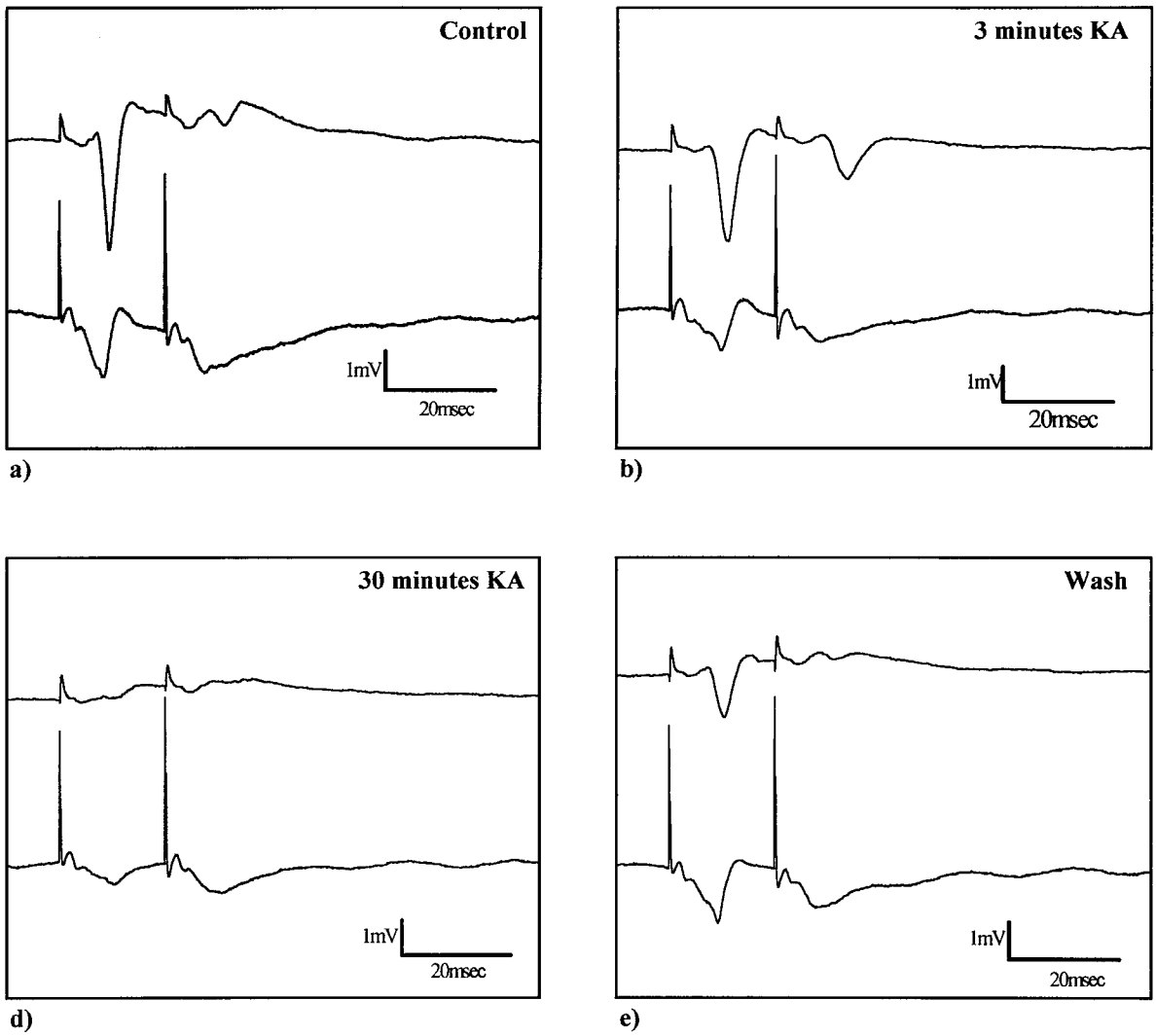

Figure 4.2 Example traces for the effect of 1μM KA on the population spike amplitude and EPSP slope recorded from the CA1 region of an intact hippocampal slice. This figure is presented in chapter 3 as figure 3.11. Each trace represents the average of three responses. a) Control, b) onset of the KA effect, c) end of the KA application period, d) following 30 minutes ACSF wash.

Application of 1μM KA in the intact slice preparation resulted in a number of effects (figures 4.2 - 4.4). Within the first three minutes of application, the first and second EPSP slopes began to decrease (figure 4.3). At this same time, there was a marked, transient increase in the amplitude of both the first and second population spikes. Since this occurs at a time when the EPSP slope had begun to decrease, it would suggest that KA is acting at more than one site in this preparation.

Following this, both first and second population spikes reduced in amplitude to well below control values (figure 4.3). Thus at this concentration, KA exhibits a biphasic response with regards to population spike amplitude. This reduction persists for at least 30 minutes following wash of KA.

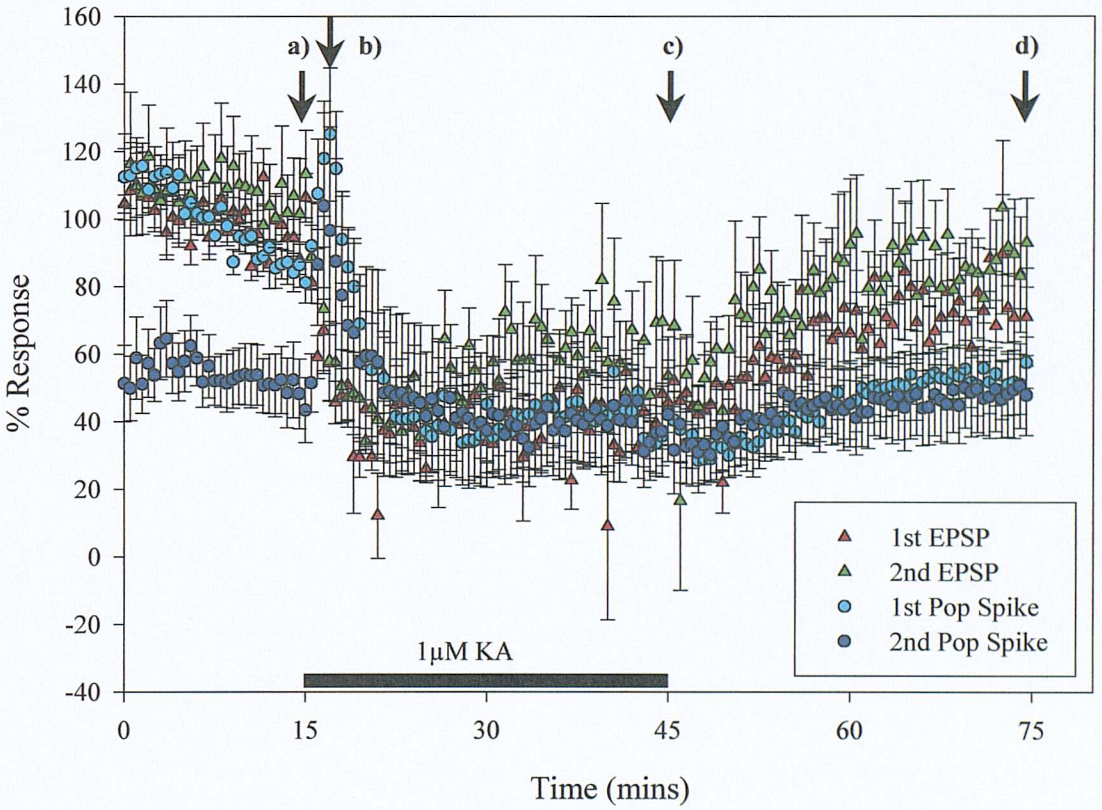

Figure 4.3 Time-course for the effects of application of 1μM KA in the CA1 region of intact hippocampal slices (n=5). Reproduced from figure 3.12 for ease of comparison. It is interesting to note that there is an initial increase in the amplitude of both the first and second population spikes recorded using a paired-pulse protocol with a 20 msec interpulse interval from 86% (± 3.4) to 119% (±9.7) ($p=0.01$) for the first spike and from 50% (±5.7) to 96% (±16.0) ($p<0.05$) for the second. This implies a rapid and transient reduction in both evoked and tonic inhibition. This is coupled with a decrease in the slope of the EPSP recorded from *stratum radiatum* from 92% (±3.0) to 41% (±6.4) ($p<0.01$) for the first EPSP, 103% (±7.1) to 62% (±9.0) ($p<0.01$) for the second by the end of the KA application period. It can also be seen that, while the EPSP slope begins to return to control values following 30 minutes wash, the population spike amplitude remains depressed compared to control. Arrows and letters correspond to the example traces in the previous figure. Quoted numbers were calculated at these time-points.

Calculation of the mean percentage inhibition from this data (figure 4.4) reveals a rapid marked reduction in the paired-pulse inhibition following the application of 1μM KA that persists throughout the KA application period.

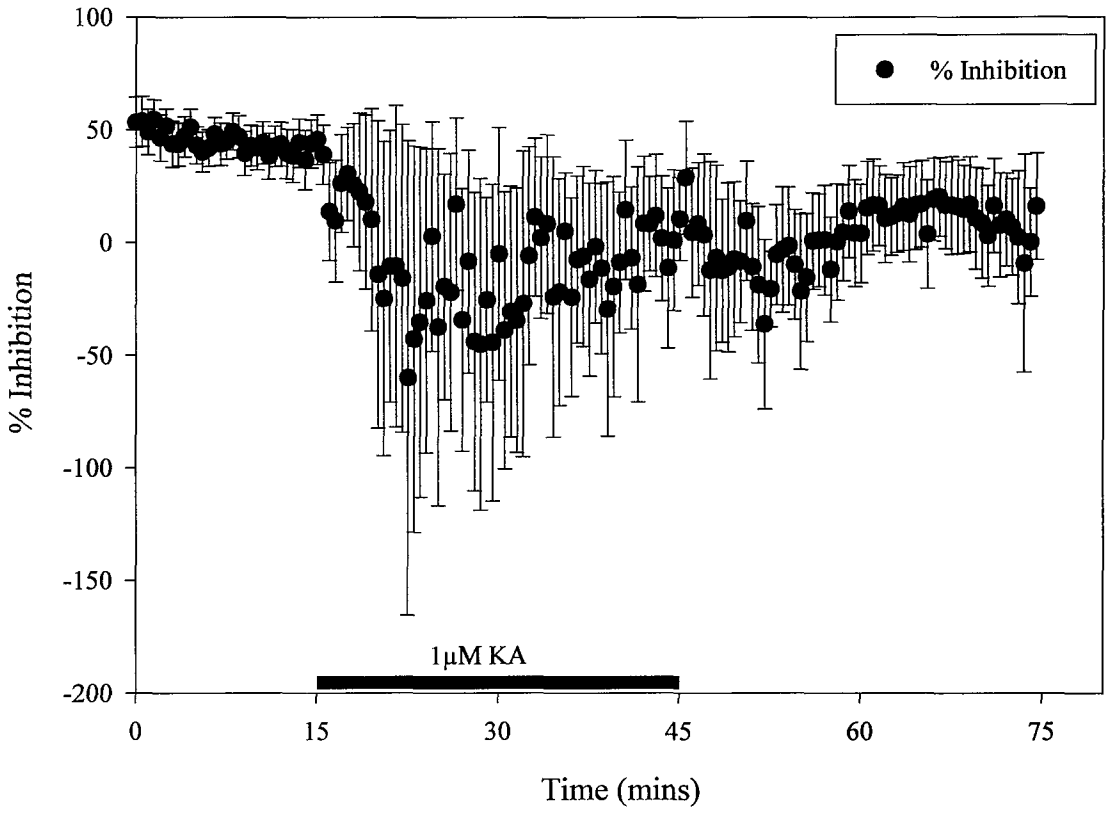

Figure 4.4 The effect of 1μM KA application on the mean percentage inhibition (± S.E.M.) of the second population spike with respect to the first spike recorded from the CA1 region of intact hippocampal slices during a paired-pulse protocol using a 20msec inter-pulse interval (n=5). Reproduced from figure 3.13. The effect of KA appears highly variable, but the net result appears to be a reduction in the percentage inhibition from 42% (±6.3) to -3% (±17.0) ($p<0.05$ Student's paired t-test) by the end of the KA application period.

4.3.1.2 The response to 1μM KA: the role of CA3

The effect of KA application in CA1 was studied in the absence of CA3 in order to gain an understanding of how the CA3 may be affecting the response to KA in the CA1 region (figures 4.5 – 4.7). Again these data are reproduced from figures 3.14 – 3.16 for ease of comparison with the data presented in this chapter.

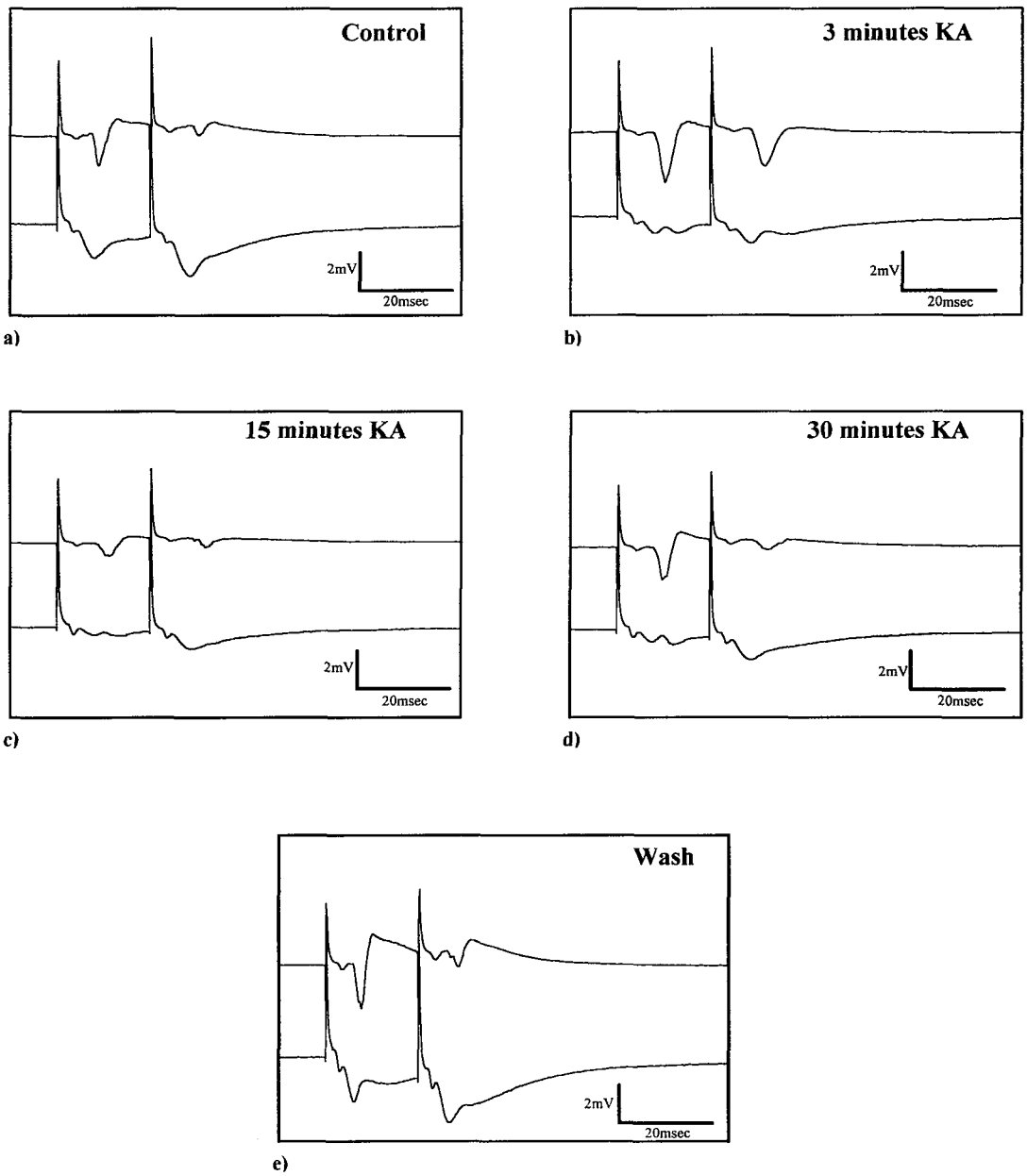

Figure 4.5 Example traces taken from a time-course experiment to observe the effects of 1μM KA on the population spike amplitude and EPSP slope in an isolated CA1 preparation. Reproduced from figure 3.14. Each trace represents the average of three responses recorded at the following time points: a) the end of 15 minutes control period, b) within the first three minutes of KA application, c) 15 minutes into the KA application period, d) after 30 minutes of KA superfusion, e) the end of 30 minutes ACSF wash.

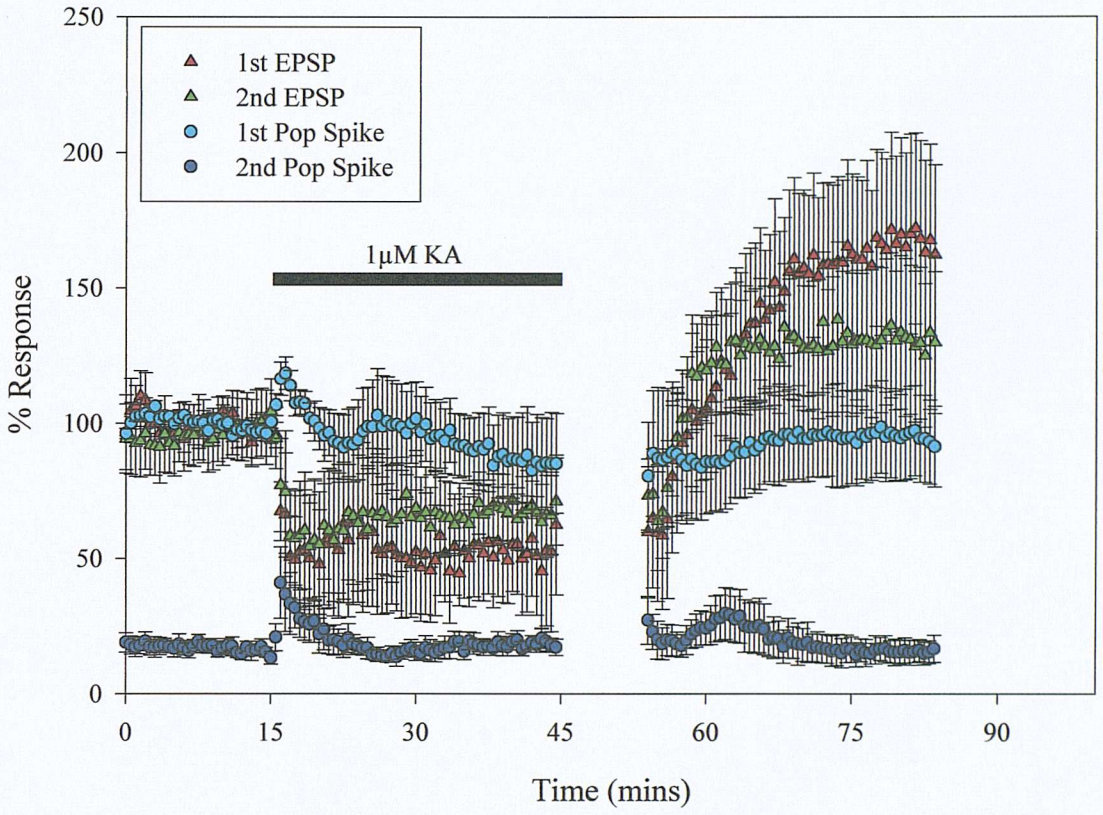

Figure 4.6 Time-course data for the effect of 1μM KA application on the population spike amplitude and EPSP slope (mean percentage ±S.E.M.) recorded from *stratum pyramidale* and *stratum radiatum* respectively in isolated CA1 preparations (n=5). Reproduced here from figure 3.15 for ease of comparison. As in the intact preparation, the amplitude of both the first and second population spikes increases within the first three minutes of drug application (97% (±1.3) to 113% (±3.2) ($p<0.01$) and 16% (±1.3) to 34% (±6.0) ($p<0.01$) for the first and second spikes respectively. This is coupled with a simultaneous decrease in the EPSP slope (from 100% (±2.1) to 55% (±10.0) ($p<0.01$) and 100% (±7.0) to 63% (±10.5) ($p<0.01$) for the first and second EPSPs respectively. In the absence of CA3 the population spikes recover to control values whilst the EPSPs appear to undergo potentiation, although this may be due to the steadily increasing stimulation which occurred during the stimulus-response curve carried out during the break in the time-course.

As previously observed in the intact slice (figure 4.3), application of 1μM KA to isolated CA1 preparations resulted in a rapid reduction in the EPSP slope (figure 4.6) which remained depressed throughout the KA application period. This was coupled with an increase in the amplitude of both the first and second population spikes within the first three minutes of application. However, in contrast to the intact slice preparation (figure 4.3), following this transient increase the population spike amplitudes did not decrease significantly below initial control values (figure 4.6).

This suggests that both the reduction in EPSP slope and the transient increase in population spike amplitudes occur independently of the presence of the CA3 region. However, the subsequent reduction in the population spike amplitude observed in the intact slice (figure 4.3) may occur as a result of the action of KA on the CA3 pyramidal cell population.

The mean percentage inhibition calculated from these data (figure 4.7) also differ from that observed in the intact slice preparation (figure 4.4). During the first three minutes of KA application, there is a transient decrease in the paired-pulse inhibition corresponding to the observed increase in both the first and second population spike amplitudes.

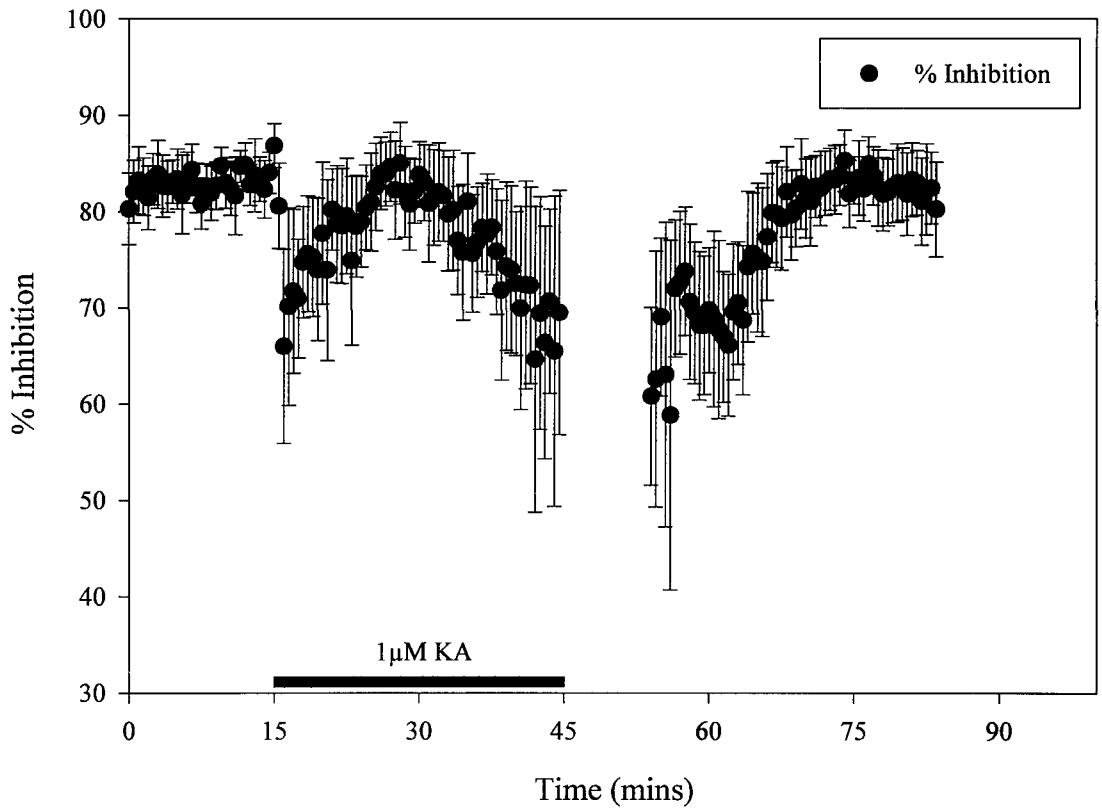

Figure 4.7 Time-course for the effects of 1μM KA application on the percentage inhibition (mean ± S.E.M.) of the second population spike recorded using a paired-pulse protocol with a 20msec inter-pulse interval in isolated CA1 preparations (n=5). This data was first presented as figure 3.16 and is reproduced here for ease of comparison. This protocol allows the assessment of $GABA_A$ mediated inhibition within the preparation throughout the course of the experiment. It can be seen that the percentage inhibition decreases with the onset of KA (1μM) application from 83% (±1.4) to 71% (±4.5) ($p<0.01$). By the end of the KA application period there is no significant difference in the percentage inhibition to control ($p=0.08$). The percentage inhibition also appears to be far less variable in the absence of CA3.

4.3.2.1 Group I/II mGluRs and the KA response: Intact slices

The data presented from figure 4.8 onwards represents the start of the new data in this chapter.

Metabotropic glutamate receptors are known to modulate both excitatory and inhibitory synaptic neurotransmission in CA1 *via* a presynaptic mechanism (Gereau and Conn 1995). One possible scenario for an involvement of mGluRs could occur as a result of the activation of CA3 pyramidal cells by KA, resulting in an increased release of glutamate from the Schaffer collaterals. This could lead to the activation of presynaptic mGluRs on the Schaffer collateral terminals and thus to a reduction in the amount of glutamate released by subsequent stimuli. To test this hypothesis, the non-selective Group I/II metabotropic glutamate antagonist (S)-MCPG ((S)-αMethyl-4-carboxyphenylglycine) (Jane *et al.* 1993, Collingridge and Watkins 1994) and the Group II/III antagonist MPPG ((RS)-αMethyl-4-phosphonophenylglycine) (Jane *et al.* 1995) were co-applied with 1μM KA.

Figure 4.8 shows examples of the recordings made from an intact hippocampal slice during the application of 250μM MCPG and 1μM KA.

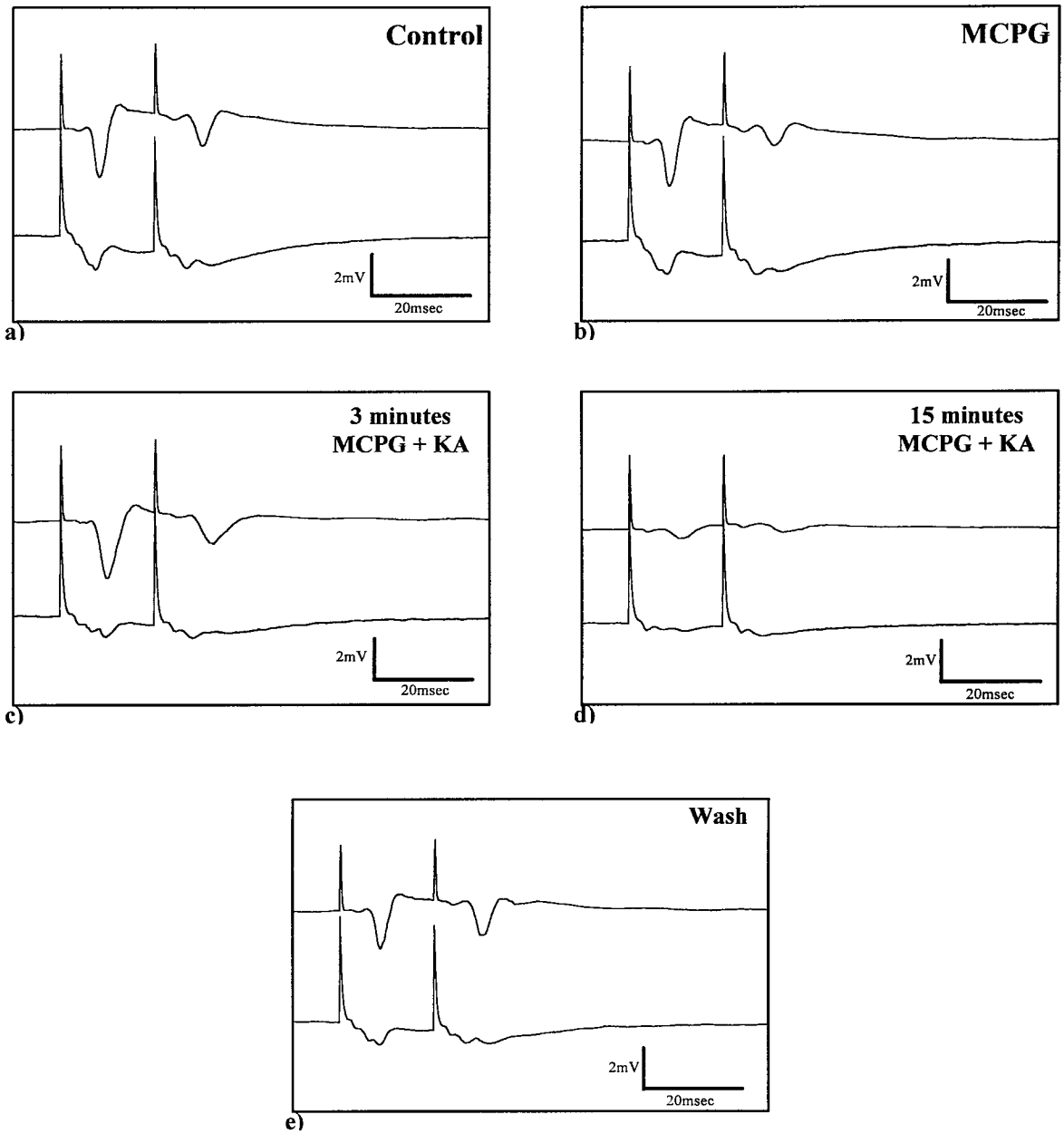

Figure 4.8 Example traces taken from a time-course experiment to observe the effects of co-application of 250μM MCPG and 1μM KA in the CA1 region of an intact hippocampal slice preparation. Each box represents the average of three traces recorded at the following time points: a) at the end of 15 minutes control stimulation, b) at the end of 15 minutes MCPG (250μM) application, c) within the first three minutes of KA (1μM) co-application, d) at the end of 15 minutes KA co-application, e) at the end of 30 minutes ACSF wash.

Application of 250μM MCPG causes a reduction of both the first and second population spikes ($p<0.01$) (figure 4.9). It has, however, no significant effect on the slope of the EPSPs. Addition of 1μM KA to the superfusing ACSF causes a typical KA response, there being a transient increase in the amplitude of both first and second population spikes coupled with a reduction in the EPSP slopes.

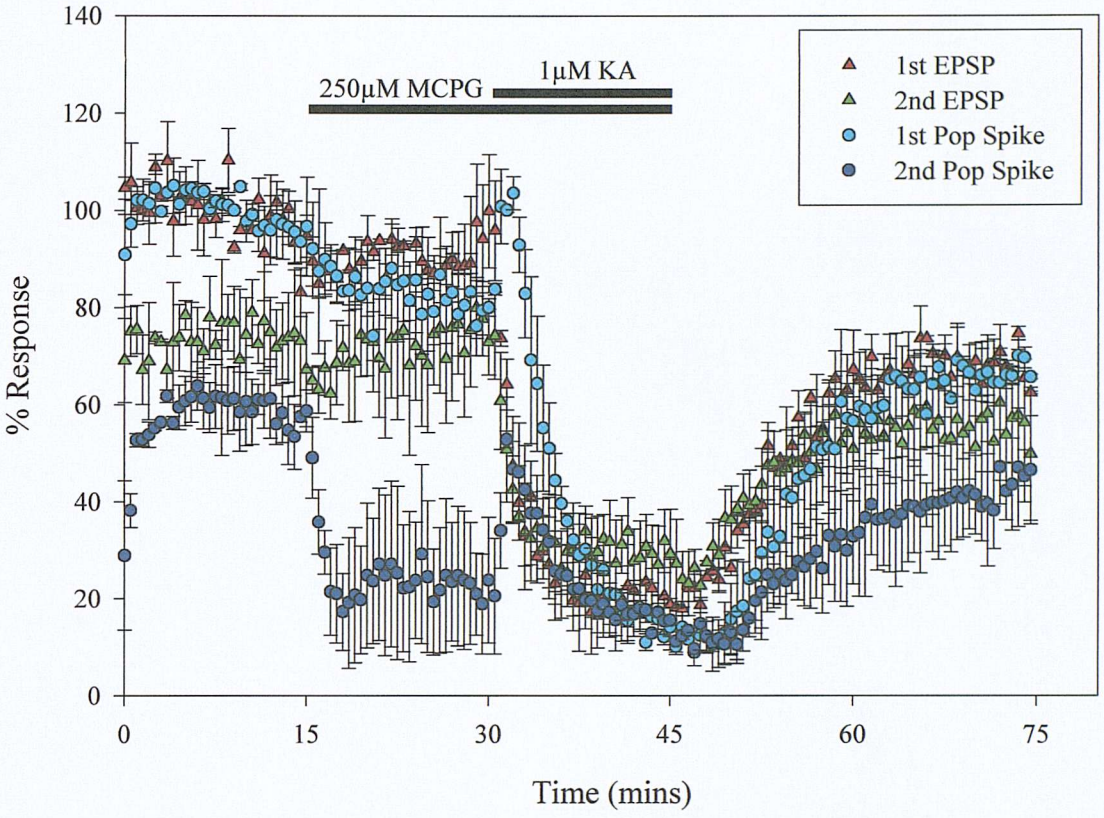

Figure 4.9 Time-course for the effect of 250μM MCPG on the response to 1μM KA recorded from the CA1 region of intact hippocampal slices (n=2). The graph shows the mean percentage population spike amplitudes and EPSP slopes (± S.E.M.) recorded throughout the experiment. MCPG alone causes a decrease in both the first and second population spike amplitudes from 95% (±2.3) to 80% (±3.2) ($p<0.05$) and 55% (±2.6) to 21% (±4.8) ($p<0.01$) respectively. The slopes of the first and second EPSPs do not change significantly. Upon addition of 1μM KA there is a marked transient increase in the amplitudes of both the first (99% (±2.6), $p<0.01$) and second (49% (±4.1), $p<0.05$) population spikes. This is followed by a large reduction (15% (±1.0) and 15% (±1.4) respectively, $p<0.01$), which follows the reduction seen in the EPSPs from 94% (±5.8) to 20% (±2.3) for the first EPSP and 78% (±4.0) to 29% (±3.2) for the second ($p<0.01$).

MCPG produces an increase in the percentage inhibition (figure 4.10) ($p<0.01$). This may be due to a disinhibition of interneurones. Upon the addition of KA this inhibition is markedly reduced ($p<0.01$).

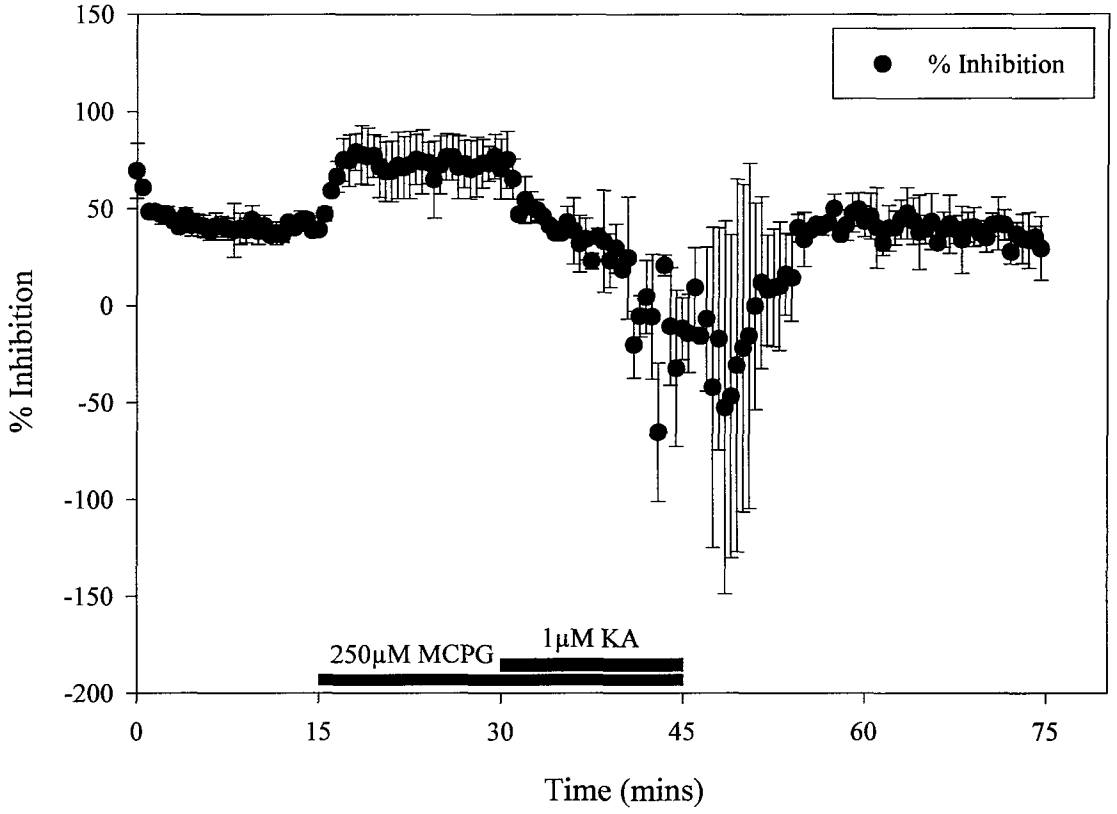

Figure 4.10 Time-course graph showing the effects of 250μM MCPG and 1μM KA on the paired-pulse inhibition recorded from the CA1 region of intact hippocampal slices (n=2). The graph shows the mean percentage inhibition (± S.E.M.) of the second population spike calculated with respect to the first. It can be seen that 250μM MCPG causes an increase in the percentage inhibition from 42% (±2.0) to 75% (±5.0) ($p<0.01$) which correlates with the large reduction in the second population spike seen in figure 4.9. Following the addition of 1μM KA there is a large reduction in the paired-pulse inhibition to -8% (±16.3) ($p<0.01$) which recovers following 30 minutes ACSF wash.

4.3.2.2 Group I/II mGluRs and the KA response in the isolated CA1: the role of CA3

In order to investigate the role of CA3 in the response to KA in the presence of 250μM MCPG experiments were repeated in slices from which the CA3 and dentate gyrus had been excised. Examples of the traces obtained during the course of these experiments are presented in figure 4.11.

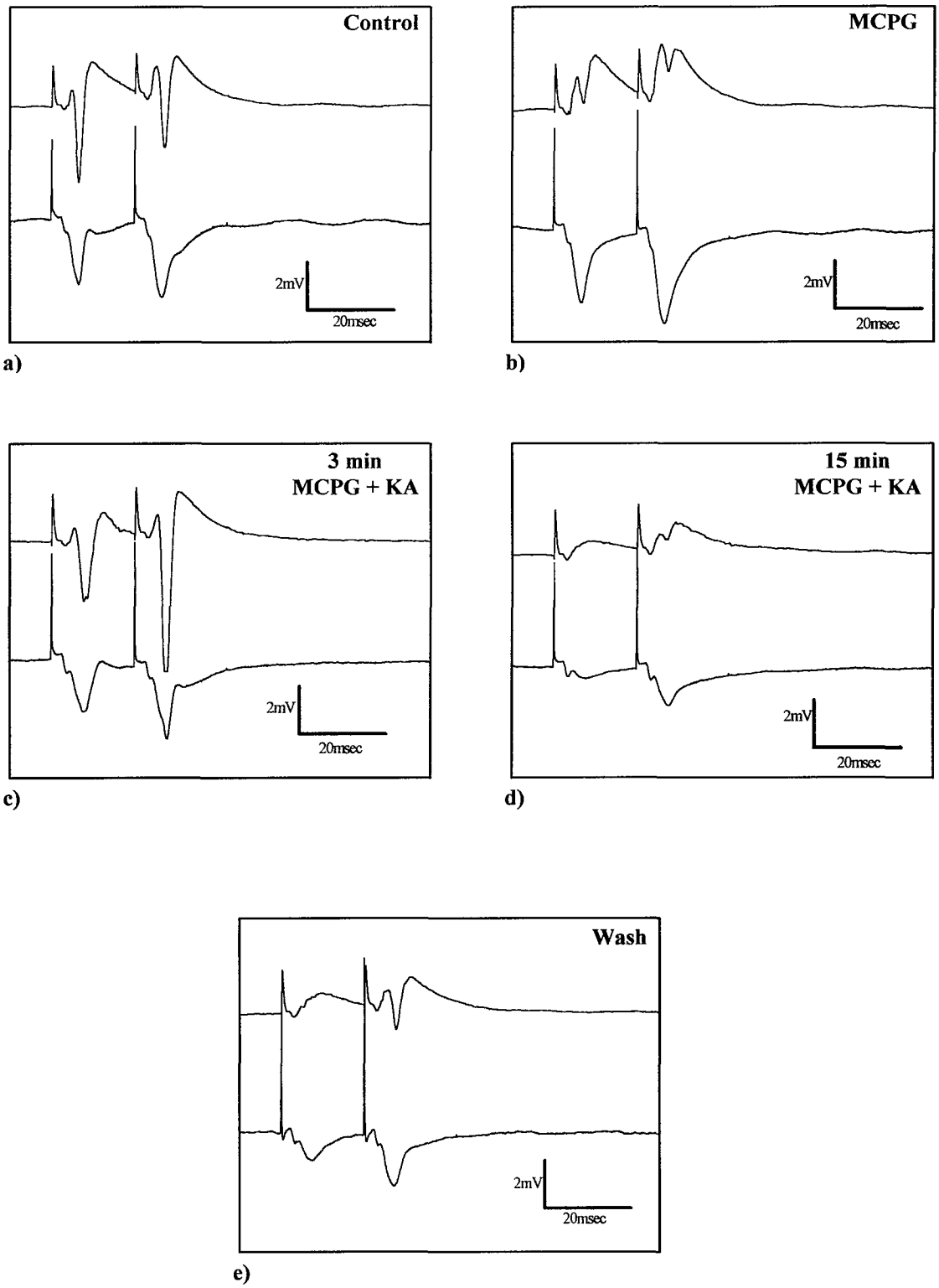

Figure 4.11 Examples of traces recorded from an isolated CA1 preparation during the application of 250μM MCPG and 1μm KA. Each box shows the average of three traces recorded at the following time points: a) at the end of 15 minutes control stimulation, b) at the end of 15 minutes of MCPG (250μM) application, c) within the first three minutes of 1μM KA co-application, d) at the end of this 15 minute period, e) at the end of 30 minutes ACSF wash.

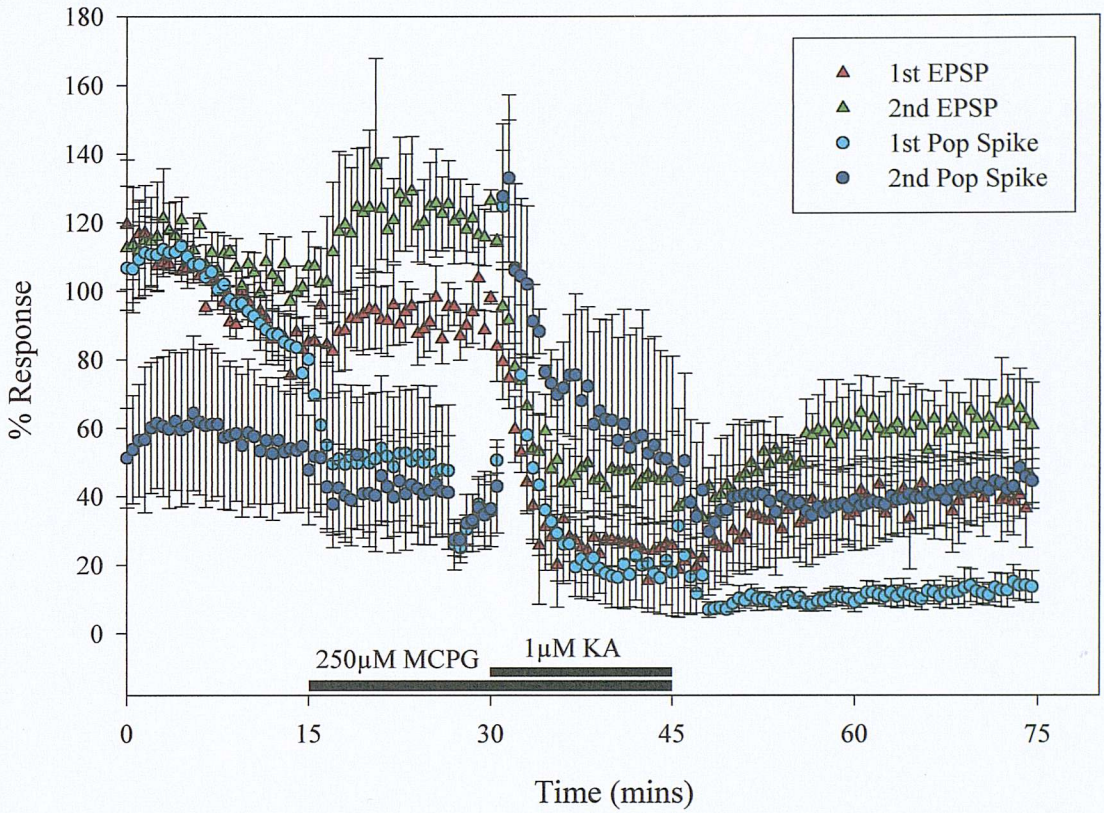

Figure 4.12 Graph showing the effect of 250µM MCPG and 1µM KA application on the mean percentage population spike amplitude and EPSP slope (± S.E.M.) recorded from the *stratum pyramidale* and *stratum radiatum* of isolated CA1 preparations (n=3). In contrast to the intact slice, MCPG application causes a marked reduction in the population spike amplitudes from 81% (±5.3) to 35% (±4.8) ($p<0.01$) for the first and 54% (±9.1) to 35% (±4.2) ($p<0.05$) for the second. There is also an increase in the percentage EPSP slopes from 82% (±3.9) to 95% (±4.6) ($p<0.05$) for the first EPSP and from 99% (±2.5) to 118% (±4.6) ($p<0.01$) for the second. Upon addition of 1µM KA there is once more a transient increase in the amplitude of both population spikes to 121% (±9.5) ($p<0.01$) for the first spike and 114 (±13.0) ($p<0.01$) for the second. This is again followed by a marked reduction in both EPSP slopes (25% (±3.7), $p<0.01$and 45% (±5.3), $p<0.01$) and population spike amplitudes (18% (±5.9) and 52% (±15.6)) although neither value for the population spikes are statistically different from those for MCPG.

When added to isolated CA1 preparations (n=3), MCPG again reduces the amplitude of both the first and second population ($p<0.05$) (figure 4.12). However, in contrast to the intact hippocampal slice there is also a significant increase in the slope of both the first ($p<0.05$) and second EPSPs ($p<0.01$). Application of 1µM KA causes both the first and second population spike amplitudes to increase transiently ($p<0.01$). This is accompanied by a significant decrease in the slope of both EPSPs ($p<0.01$). By the end of

the KA application period the population spike amplitudes have returned to values which were not significantly different to those for MCPG.

MCPG alone significantly reduces the percentage inhibition (figure 4.13, $p<0.01$). This decreases further by the end of the KA application ($p<0.01$).

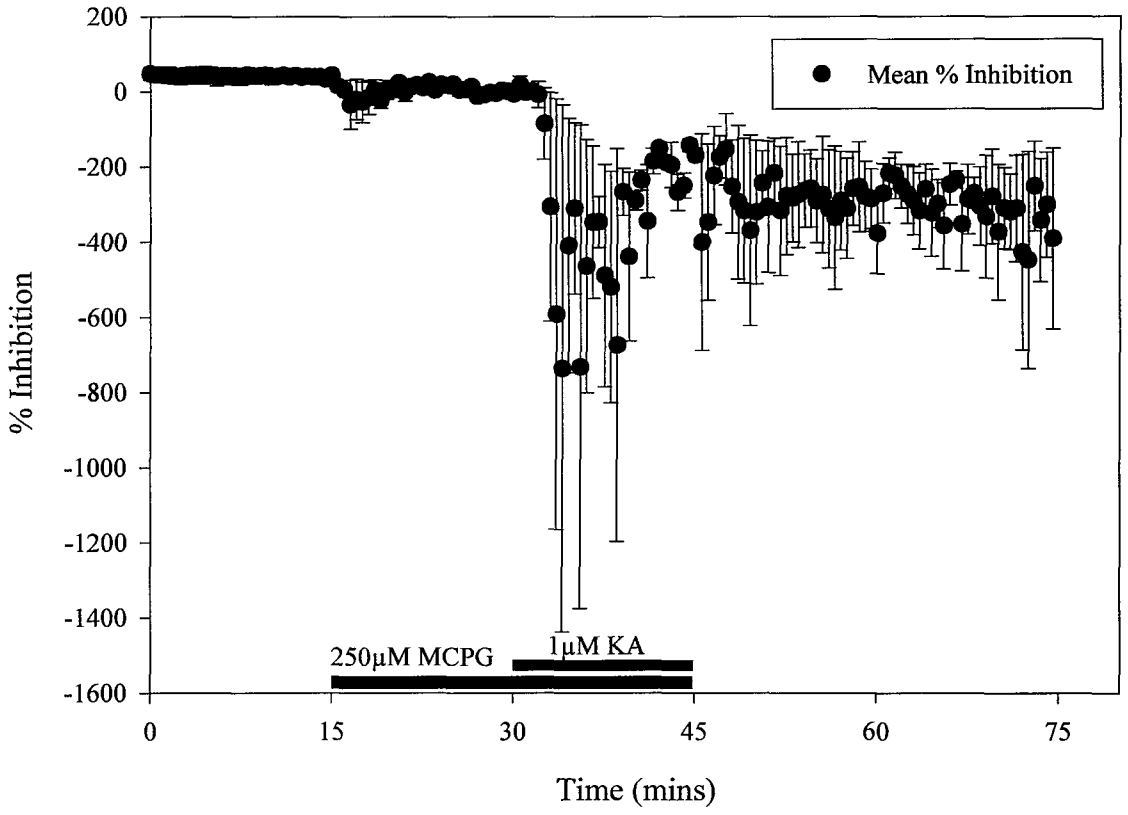

Figure 4.13 Time-course for the mean percentage inhibition (± S.E.M.) calculated during the application of 250μM MCPG and 1μM KA to isolated CA1 preparations. MCPG causes a reduction in the paired-pulse inhibition from 37% (±8.3) to -0.10% (±3.7) ($p<0.01$) which is exacerbated by the addition of 1μM KA for 15 minutes to -220% (±26.3) ($p<0.01$). This effect did not wash out after 30 minutes.

4.3.3.1 Group II/III mGluR antagonism and the KA response: Intact slices

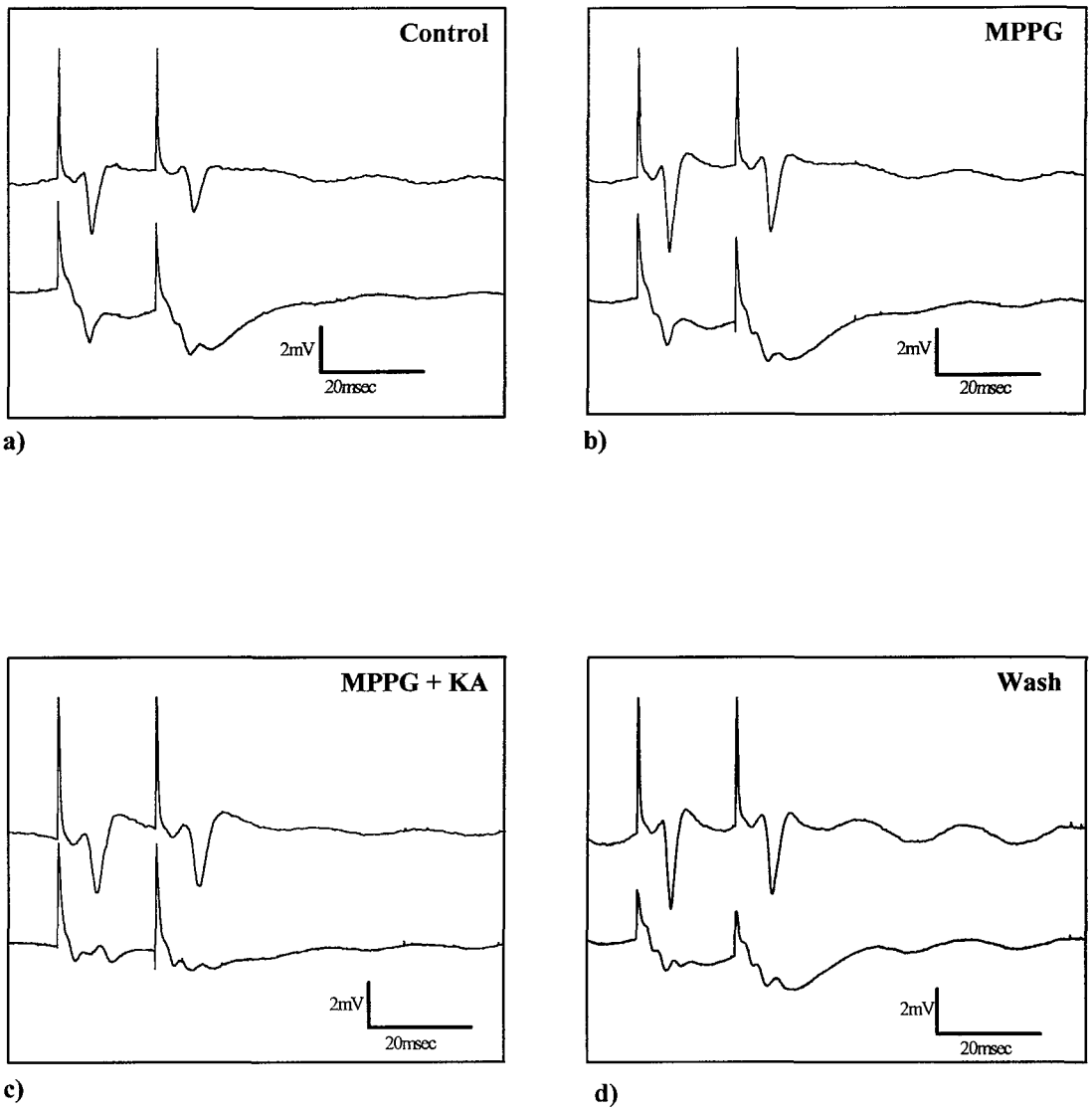

Figure 4.14 Example traces for the effects of MPPG (500μM) on the response to 1μM KA in intact slice CA1. a) control, b) 500μM MPPG, c) MPPG + 1μM KA, d) 30 minute wash. All examples taken from the end of their respective application periods.

In order to asses the involvement of group II/III metabotropic receptors in the response to 1μM KA intact slices were treated with 500μM MCPG for 15 minutes before the addition of 1μM KA. Examples of the recordings obtained during these treatments can be seen in figure 4.14 above.

Application of 500μM MPPG to intact slices (figure 4.15) results in a significant increase in the slope of both the first and second EPSPs ($p<0.01$ and $p<0.05$ respectively). At the same time the population spike amplitudes are significantly increased ($p<0.01$ and $p<0.05$ for the first and second spikes respectively).

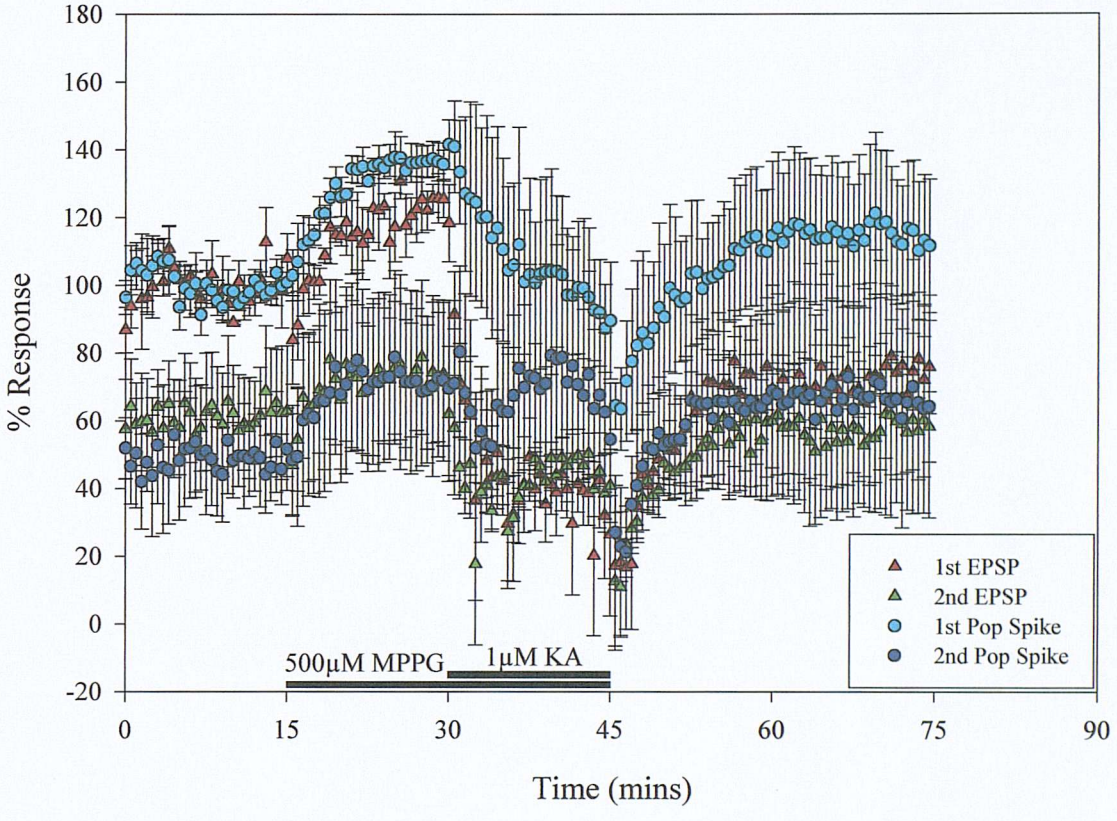

Figure 4.15 Time-course for the application of 500μM MPPG and 1μM KA in intact hippocampal slices (n=3). The graph shows the percentage mean population spike amplitudes and EPSP slopes recorded from the CA1 region using a paired-pulse protocol. It can be seen that addition of 500μM MPPG causes a potentiation of both the first (98% (±3.6) to 126% (±2.9), $p<0.01$) and second (63% (±9.2) to 74% (±10.2), $p<0,05$) EPSPs, which is mirrored by a corresponding increase in the population spike amplitudes from 101% (±1.7) to 136% (±2.5) ($p<0.01$) for the first population spike and 49% (±6.1) to 72% ±(12.3) ($p<0.05$) for the second. Introduction of 1μM KA to the superfusing solution causes a reduction in the first (32% (±10.1), $p<0.01$) and second (41% (±4.4), $p<0.01$) EPSP slopes which is again followed by the first population spike (91% (±7.3), $p<0.01$) (n=3).

Addition of 1μM KA to the superfusing ACSF causes a significant decrease in the first population spike amplitude ($p<0.01$) and both the first and second EPSP slopes ($p<0.01$) by the end of the application period. The second population spike was not significantly affected.

There is no significant change in the inhibition (figure 4.16) following the application of MPPG, nor during the first three minutes of KA application. By the end of this period however, the inhibition is significantly impaired ($p<0.01$).

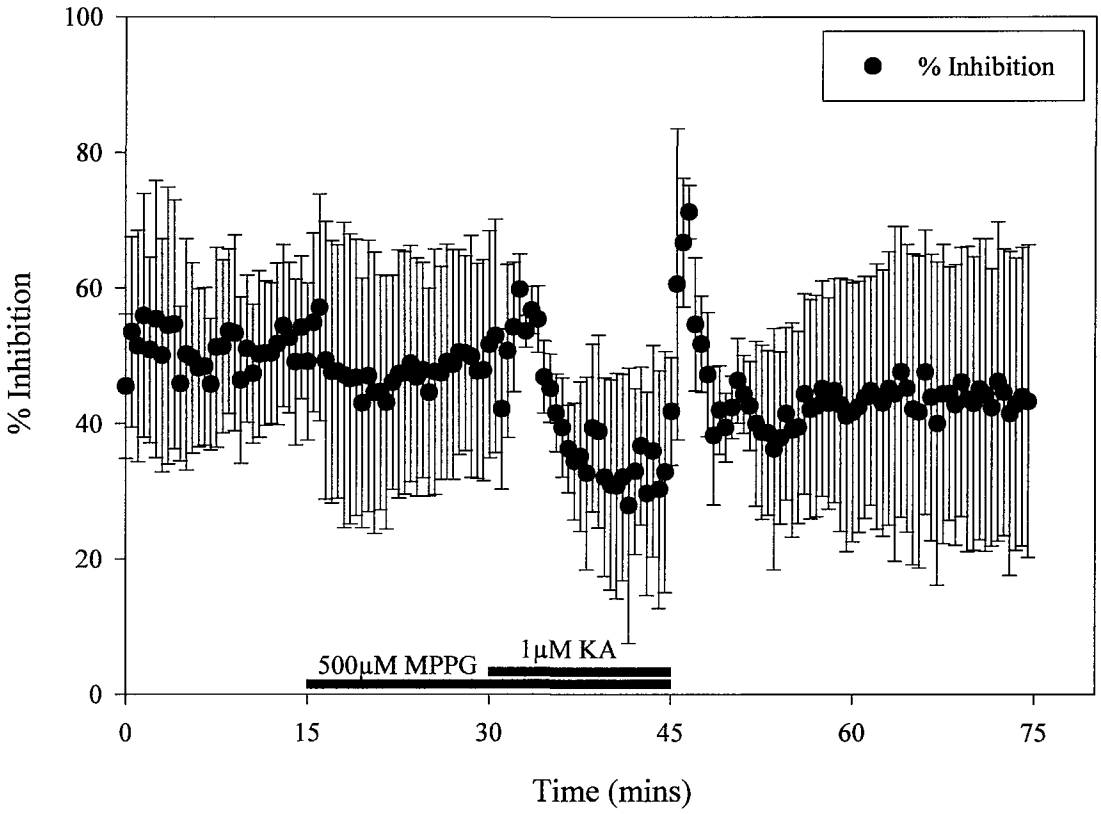

Figure 4.16 Time-course for the effects of MPPG and KA on the percentage inhibition (± S.E.M.) calculated for recordings made of the first and second population spikes elicited from the CA1 region of intact hippocampal slices using a paired-pulse protocol. MPPG does not significantly change the mean percentage inhibition, but by the end of 15 minutes co-application with 1μM KA the inhibition has dropped from 49% (±8.4) to 33% (±8.6) ($p<0.01$, n=3)

4.3.3.2 Group II/III mGluR antagonism and the KA response: The role of CA3

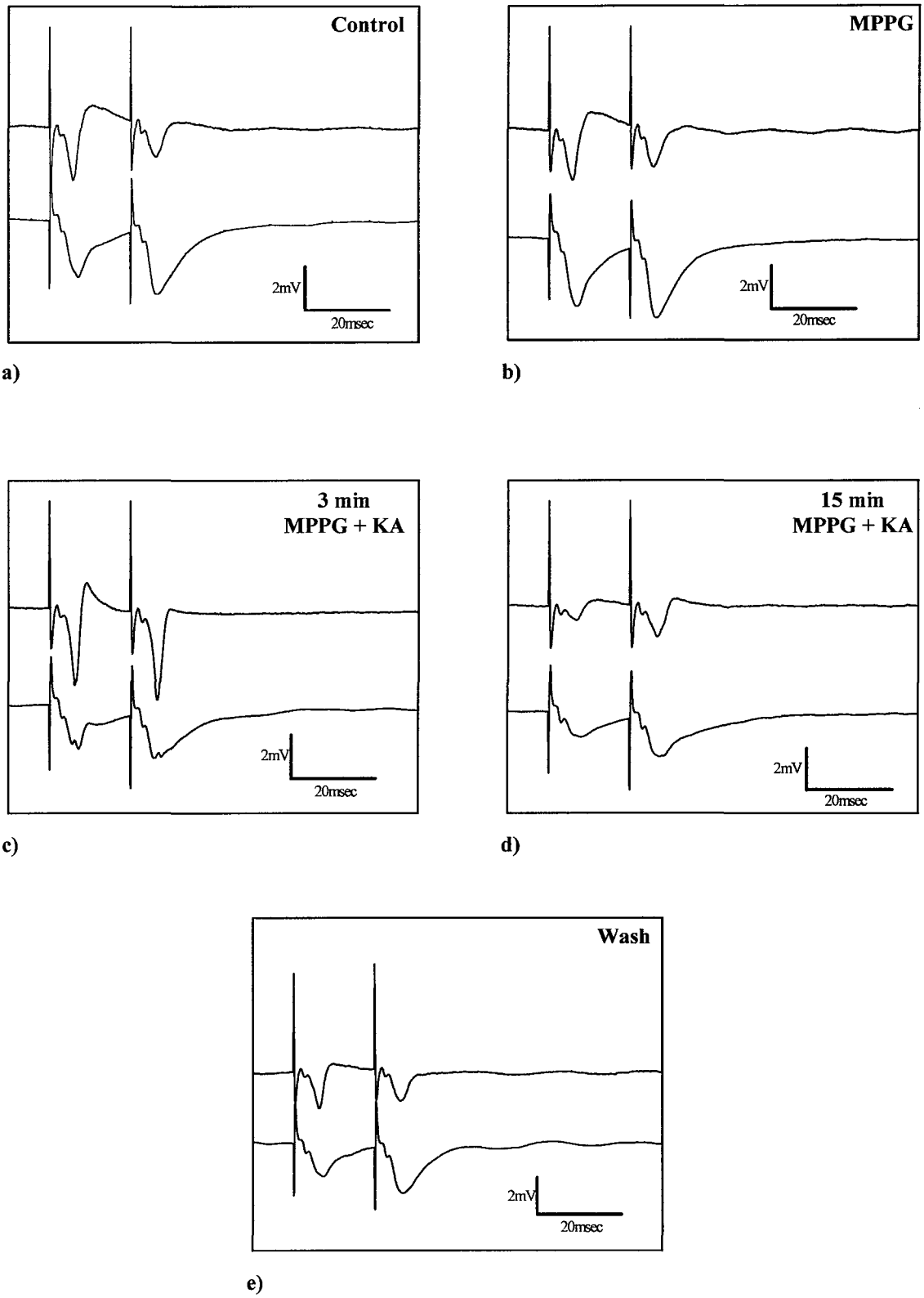

Figure 4.17 Example traces for the effects of 500μM MPPG and 1μM KA on the population spike amplitude and EPSP slopes recorded from an isolated CA1 preparation. a) Control, b) 500μM MPPG, c) onset of KA effect, d) end of KA application period, e) wash.

MPPG causes a marked increase in the slope of both the first ($p<0.05$)) and second ($p<0.01$)) EPSPs (figure 4.17). There is no significant corresponding increase in the amplitude of either population spike. Examples of the traces obtained during the course of this experiment can be seen in figure 4.16.

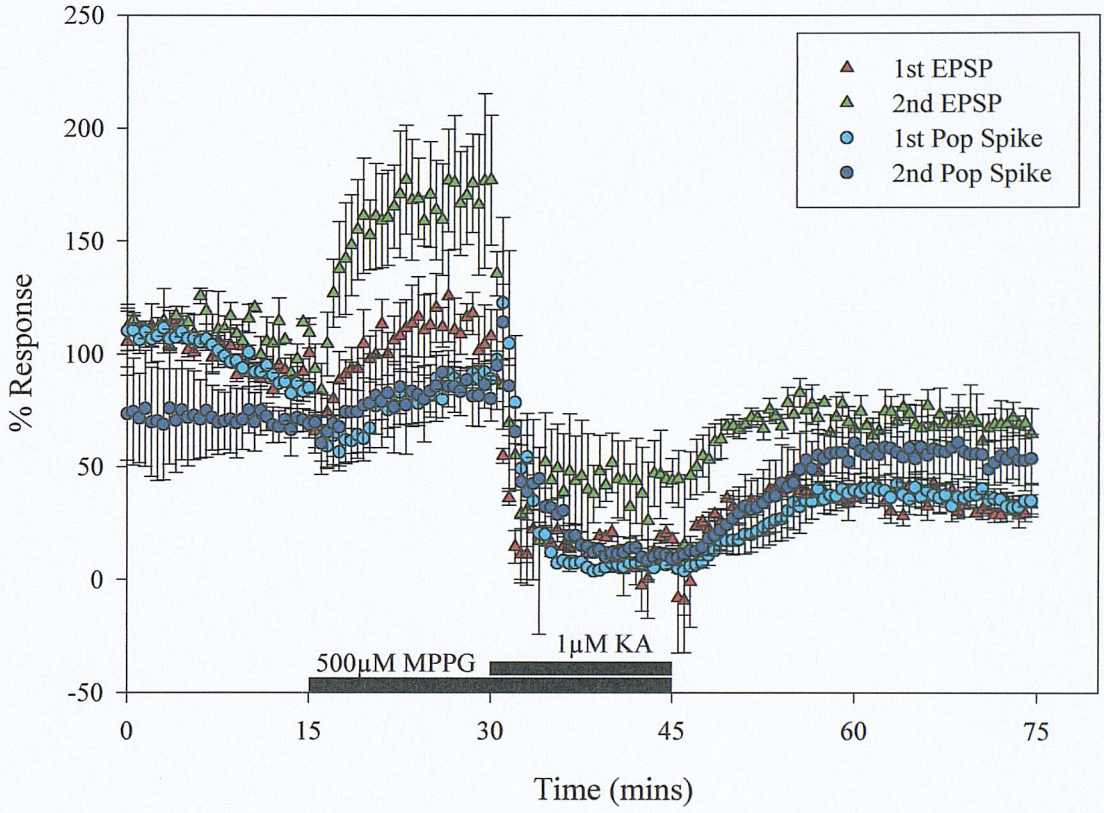

Figure 4.18 Time-course for the effects of co-application of 500μM MPPG and 1μM KA in isolated CA1 hippocampal preparations. The graph shows the mean percentage population spike amplitude and EPSP slope (± S.E.M.) recorded from *stratum pyramidale* and *stratum radiatum* respectively. Application of 500μM MPPG does not significantly alter the amplitude of either the first or second population spikes, but does cause a marked potentiation of both the first and second EPSP slopes from 82% (±5.8) to 108% (±7.7) ($p<0.05$) and 101% (±4.5) to 173%1 (±15.8) ($p<0.01$) respectively. There appears to be a transient rise in the amplitude of the first (91% (±3.6) to 103% (±13.9)) and second population spikes (83% (±6.3) to 96% (±7.7)) upon the addition of 1μM KA, but these do not reach significance. By the end of 15 minutes KA application both first and second population spikes are reduced to 7% (±1.2, $p<0.01$) and 11% (±1.4, $p<0.01$) respectively. The first and second EPSP slopes reduce over the same period to 17% (±1.9, $p<0.01$) and 46% (±7.2, $p<0.01$, $n=3$).

Addition of 1μM KA to the superfusing ACSF does not result in a significant initial increase in the population spike amplitude. However, by the end of 15 minutes there is a reduction in the amplitude of the first and second population spikes ($p<0.01$). The first and second EPSP slopes are similarly affected ($p<0.01$).

MPPG does not significantly change the degree of inhibition recorded from isolated CA1 preparations (figure 4.19) (n=3). Co- application of 1μM KA significantly reduces the inhibition by the end of the application period ($p<0.05$).

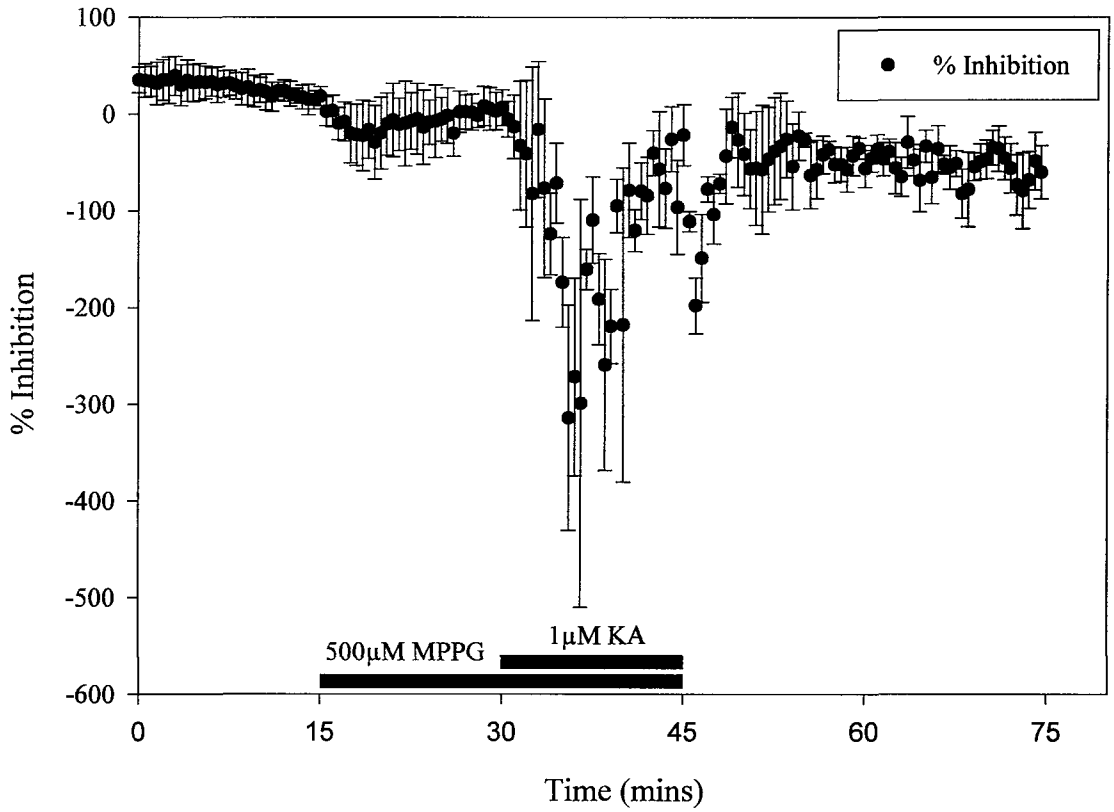

Figure 4.19 Time-course for the effect of 500μM MPPG and 1μM KA on the mean percentage inhibition (± S.E.M.) calculated from population spike data recorded from isolated CA1 preparations elicited using a paired-pulse protocol with a 20msec inter-pulse interval. It can be seen that MPPG causes a reduction in the percentage inhibition from 16% (±6.4) to 6% (±10.3) although this change is not significant. Addition of 1μM KA for 15 minutes markedly exacerbates this condition (-67% (±23.3), $p<0.05$ n=3).

4.3.4.1 Inhibition of PKC and the KA response: Intact slices

In 1998, Rodriguez-Moreno and Lerma found that the modulation of GABA release from synaptosomes by KA receptors involved a pertussis toxin (PTX) sensitive mechanism which could also be blocked by the protein kinase C (PKC) inhibitor calphostin C and by the inhibition of phospholipase C (PLC). This reduction of GABA release could also be blocked by raising the intracellular Ca^{2+} concentration, but did not significantly change following the blockade of protein kinase A (PKA).

The following series of experiments, which involved the co-application of 1μM KA with the PKC inhibitor H-7 (1-(5-Isoquinolinesulphonyl)-2-methylpiperazine dihydrochloride), were performed in order to investigate whether a similar mechanism could be involved in the reduction of glutamate release from the Schaffer collateral terminals. It was also hoped that these experiments might provide further experimental evidence for the mechanism of the modulation of GABA release from paired-pulse inhibition data. Unfortunately, as we shall see, the effects of H-7 alone were such as to induce epileptiform bursting within the CA1 region of both the intact and isolated hippocampal slices. Thus obtaining meaningful data for this parameter was rendered unlikely.

Moreover, it has been recently demonstrated (Melyan *et al* 2002) that a slow afterhyperpolarisation current in the CA1 pyramidal cells of 15-19 day old Wistar rats, mediated by a Ca^{2+} dependent K^+ channel, is inhibited by nanomolar concentrations of KA, leading to an increase in pyramidal cell excitability. This inhibition appears to be mediated by a non-GluR5 containing receptor and is blocked by inhibitors of PKC and pertussis toxin sensitive G-proteins, indicating the likelyhood of a metabotropically coupled KA receptor. It is possible therefore, that the observed initial increase in population spike amplitude that occurs with KA could result from an inhibition of the I_{sAHP} current in CA1 pyramidal cells. Were this the case then co-application of KA with H-7 could provide further evidence for this.

Figure 4.20 shows examples of the traces obtained during the co-application of 50μM H-7 and 1μM KA in an intact hippocampal slice. As previously mentioned it can be seen in 4.20 (b) that H-7 has produced epileptiform bursting, characterised by an increased number of population spikes prior to the second stimulus. Although the amplitude of the epileptiform spikes reduces during the application of 1μM KA, these spikes are still detectable, and thus any calculation of percentage inhibition is rendered meaningless.

However data on the release of glutamate may still be obtained by comparison of the EPSP slope before, during and after drug application.

Application of 50μM H-7 to intact slices (figure 4.21) causes a significant increase in the slope of the first EPSP ($p<0.01$) whereas the second EPSP slope is reduced ($p<0.01$). Upon the addition of 1μM KA the first EPSP slope undergoes a marked reduction ($p< 0.01$). The second EPSP also undergoes a small, but significant reduction to ($p<0.05$) by the end of the application period.

In order to gain an idea of the excitability of the pyramidal cell population, and hence to deduce whether KA application is increasing this excitability, the number of population spikes in the epileptiform burst have been counted in the presence of H-7 alone and in co-application with KA (figure 4.22).

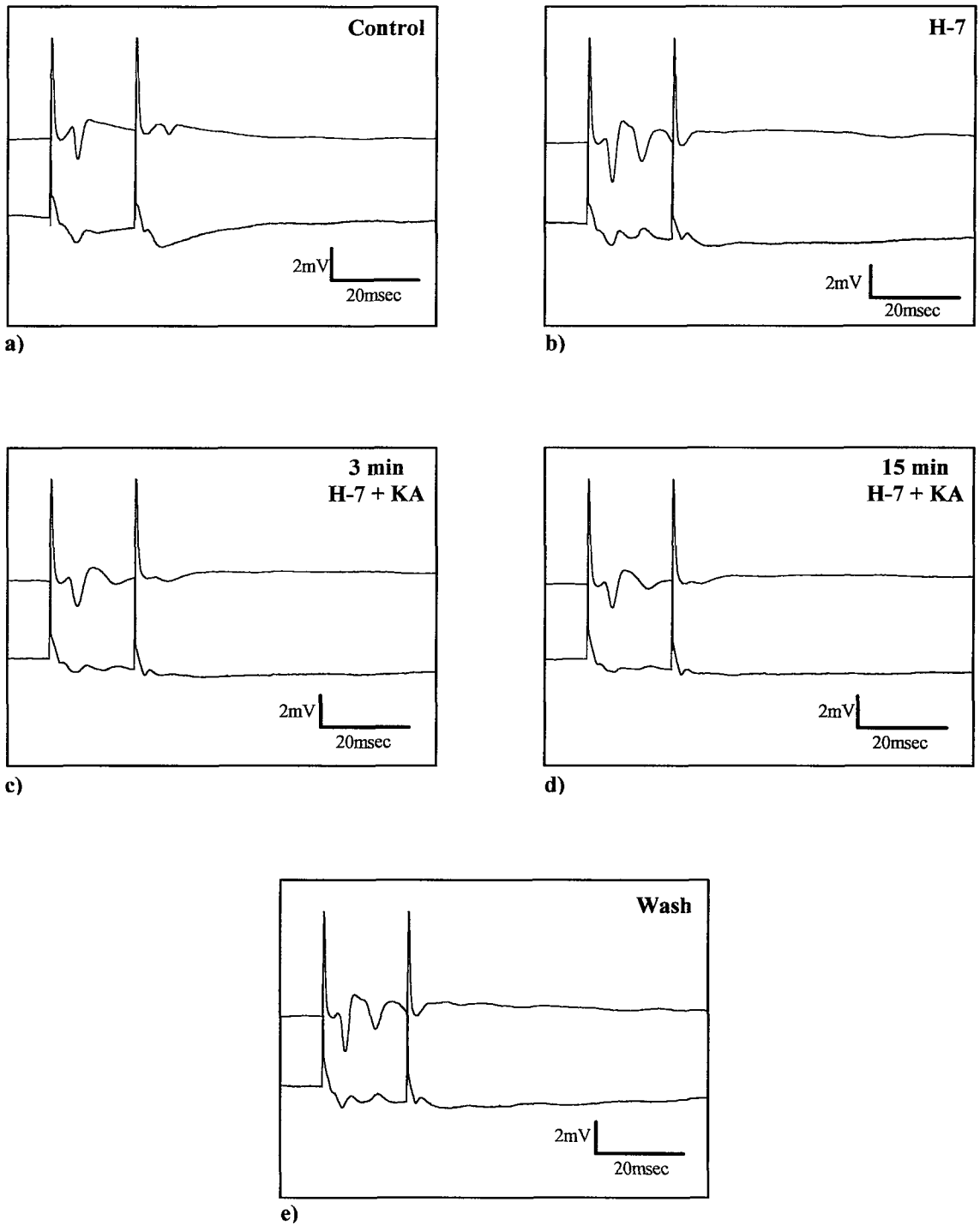

Figure 4.20 Example traces showing the effects of co-application of 50μM H-7 and 1μM KA in the CA1 of an intact slice. Each trace shows the average of three recordings taken 30 seconds apart at the following time points: a) at the end of 15 minutes control stimulation, b) at the end of 15 minutes H-7 application, c) within three minutes of the addition of 1μM KA, d) at the end of 15 minutes KA application and e) at the end of 30 minutes ACSF wash

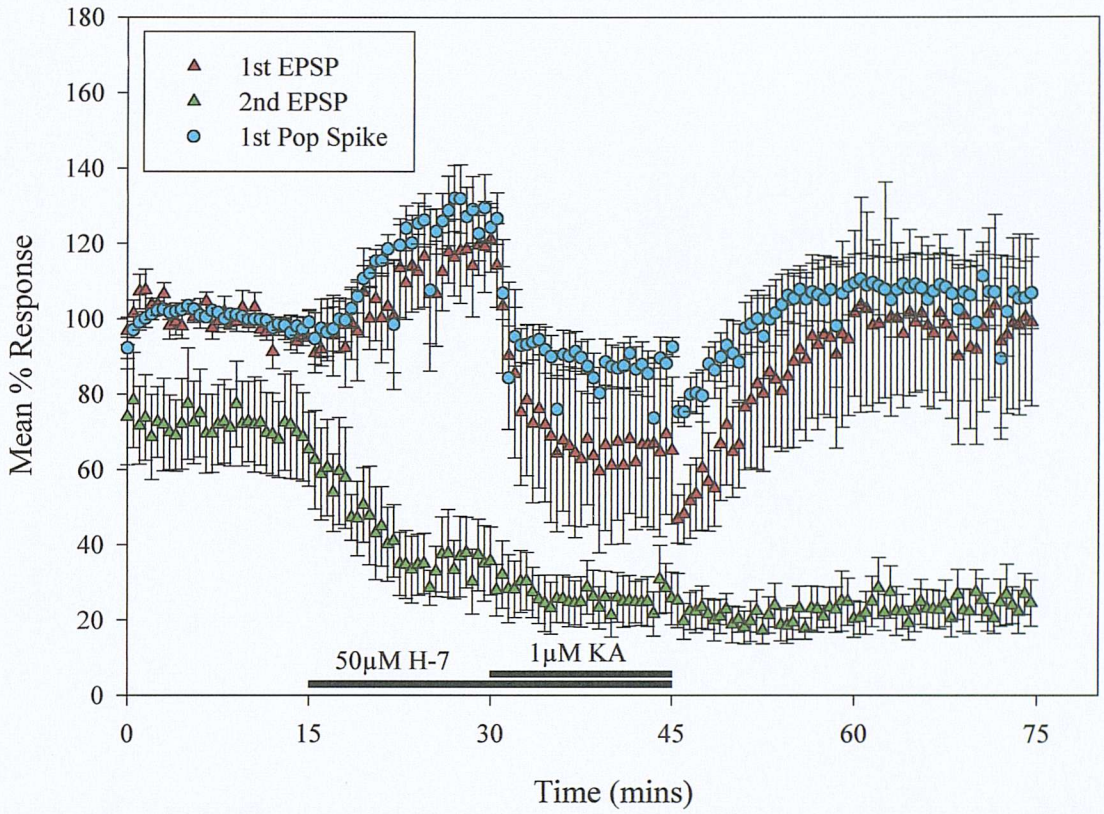

Figure 4.21 1μM KA causes a large reduction (118% (±6.2) to 67% (±11.9), $p< 0.01$) of the mean first EPSP slope (± S.E.M) in the presence of 50μM H-7 in the CA1 region of intact hippocampal slices (n=5). The first EPSP is increased in the presence of H-7 (96% (±1.7) to 118% (±6.2), $p<0.01$) and the second EPSP is reduced (70% (±7.0) to 34% (±5.1), $p<0.01$) but still undergoes a further small, but significant decrease upon addition of 1μM KA (27% (±4.0), $p<0.05$). The mean percentage amplitude of the first population spike closely follows the pattern of response observed for the first EPSP slope. Application of 50μM H-7 causes an increase in the first population spike amplitude from 98% (±1.7) to 126% (±4.4) ($p<0.01$). Upon addition of 1μM KA, this falls to 96% (±5.9) ($p<0.01$, n=5).

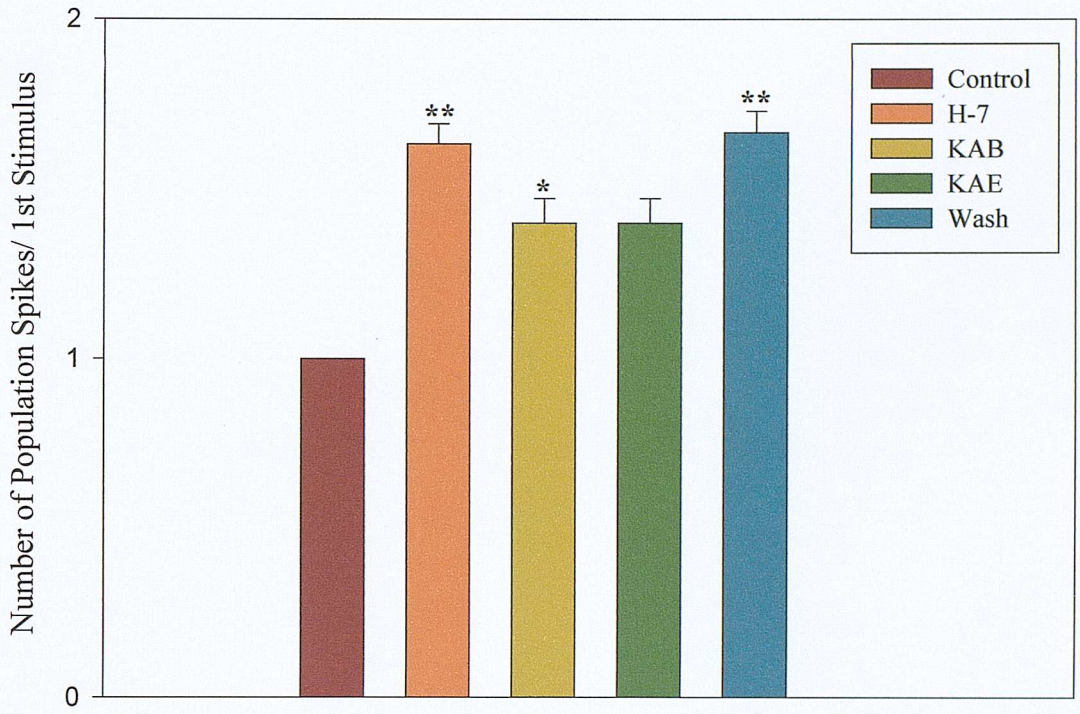

Figure 4.22 Mean number of population spikes per trace before during and after the application of 20μM H-7and 1μM KA in the intact slice CA1. Application of the PKC inhibitor causes an epileptiform burst, which persists with marginally less severity during the addition of 1μM KA. The effects of H-7 do not wash out after 30 minutes ACSF wash. Key: KAB, within the first three minutes of KA co-application, KAE, at the end of 15 minutes KA application. Statistical significance was calculated with respect to the immediately preceding time period. *= $p<0.05$ **= $p<0.01$, Student's paired t-test.

4.3.4.2 Inhibition of PKC and the KA response: Isolated CA1

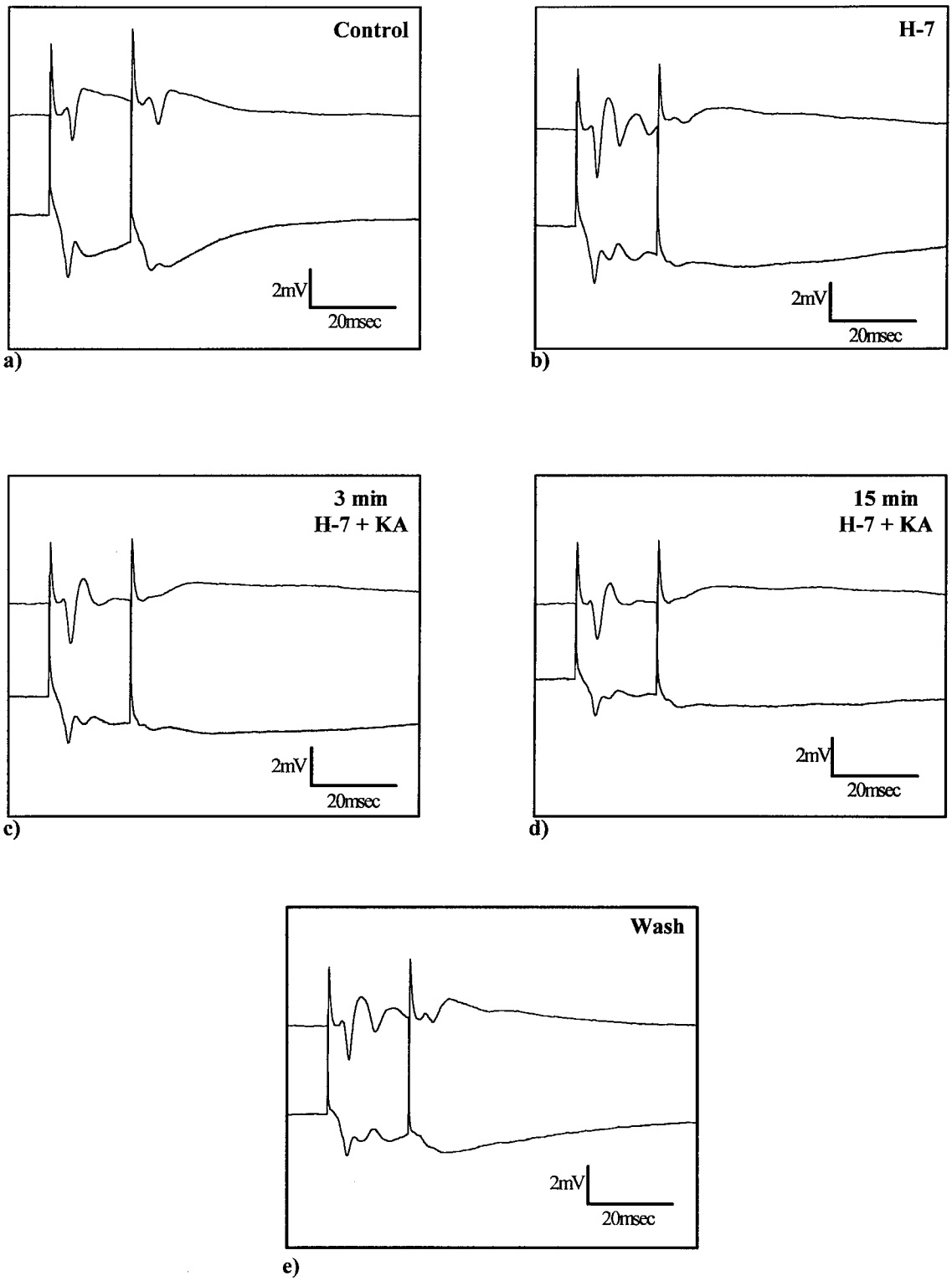

Figure 4.23 Example traces showing the effect of 50μM H-7 and 1μM KA co-application of the population spike amplitudes and EPSP slopes recorded from isolated CA1 preparations using a 20msec paired-pulse protocol. Each trace is derived from the average of three responses recorded at the following time points: a) the end of 15 minutes control stimulation, b) the end of 15 minutes H-7 application, c) within the first three minutes of the addition of 1μM KA, d) at the end of 15 minutes KA application, e) at the end of 30 minutes ACSF wash.

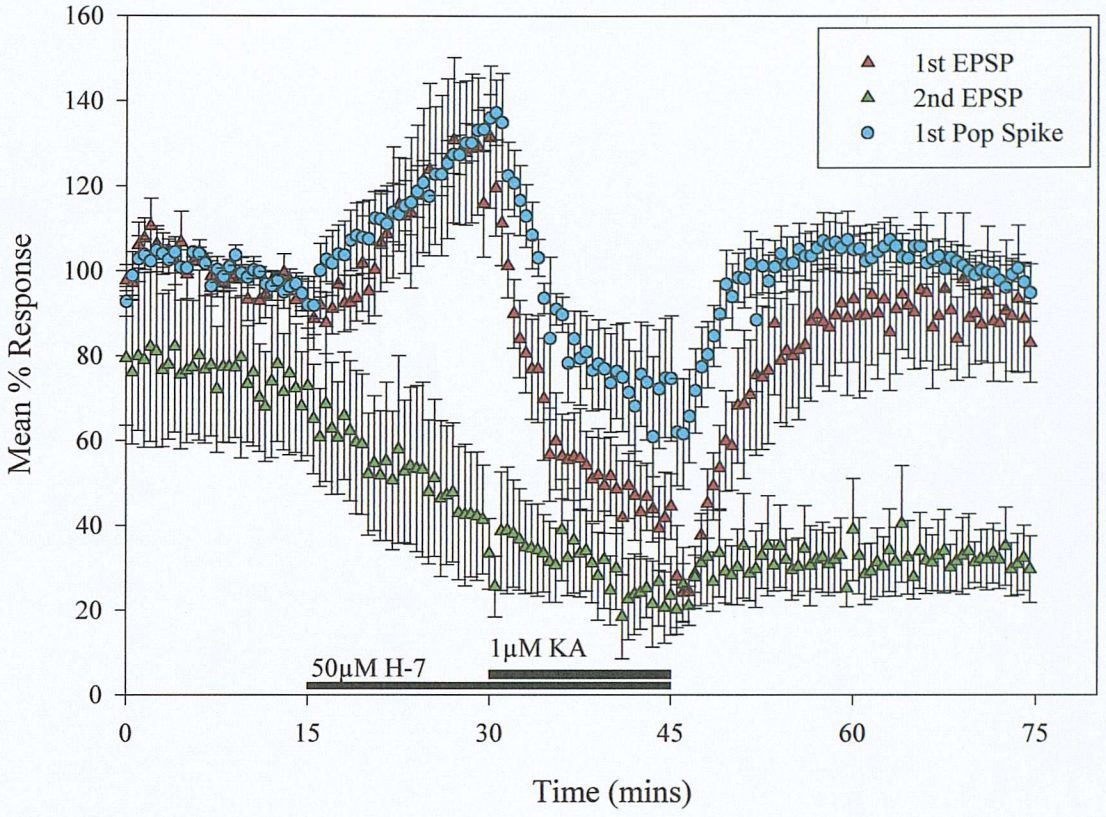

Figure 4.24 In the presence of 50µM H-7 1µM KA reduces the first EPSP slope from 125% (± 8.5) to 42% (± 5.1) ($p<0.01$). The second EPSP slope is also decreased from 42% (± 7.6) to 23% (± 5.2) ($p<0.05$). Application of H-7 alone causes an increase in the slope of the first EPSP from 95% (± 1.8) to 125% (± 8.5) ($p<0.01$), while the second EPSP decreases from 72% (± 8.6) to 42% (± 7.6) ($p<0.01$). The mean percentage amplitude of the first population spike again closely mirrors the changes observed for the first EPSP slope. Thus application of 50µM H-7 caused an increase in the amplitude from 96% (±1.6) to 131% (±2.5) ($p<0.01$). This had decreased to 69% (±8.5) by the end of 15 minutes co-application of 1µM KA. Figures quoted represent mean percentage response (± S.E.M), p values derived from Student's Paired t-test, n=5.

From the raw data for the effect of 50μM H-7 and 1μM KA in the isolated CA1 preparation (figure 4.23), it is again clear that the introduction of H-7 to the recording chamber produces an epileptiform burst. Therefore time-course data has only been presented for the slope of both EPSPs and the amplitude of the first population spike (figure 4.24). The pattern of response seen in the isolated slice is very similar to that of the intact slice. Upon the addition of H-7 the first EPSP slope increases significantly ($p<0.01$) whilst the second EPSP slope is significantly decreased below control ($p<0.01$). The first population spike amplitude increases with the first EPSP ($p<0.01$). With the addition of 1μM KA, the first ($p<0.01$) and second ($p<0.05$) EPSP slopes decreases significantly. Only the first EPSP appears to recover within 30 minutes after the removal of both drugs and, as can be seen in figure 4.23 (e), the population spike still exhibits an epileptiform burst.

Figure 4.25 shows the number of population spikes per stimulus for control, 50μM H-7, 1μM KA and control.

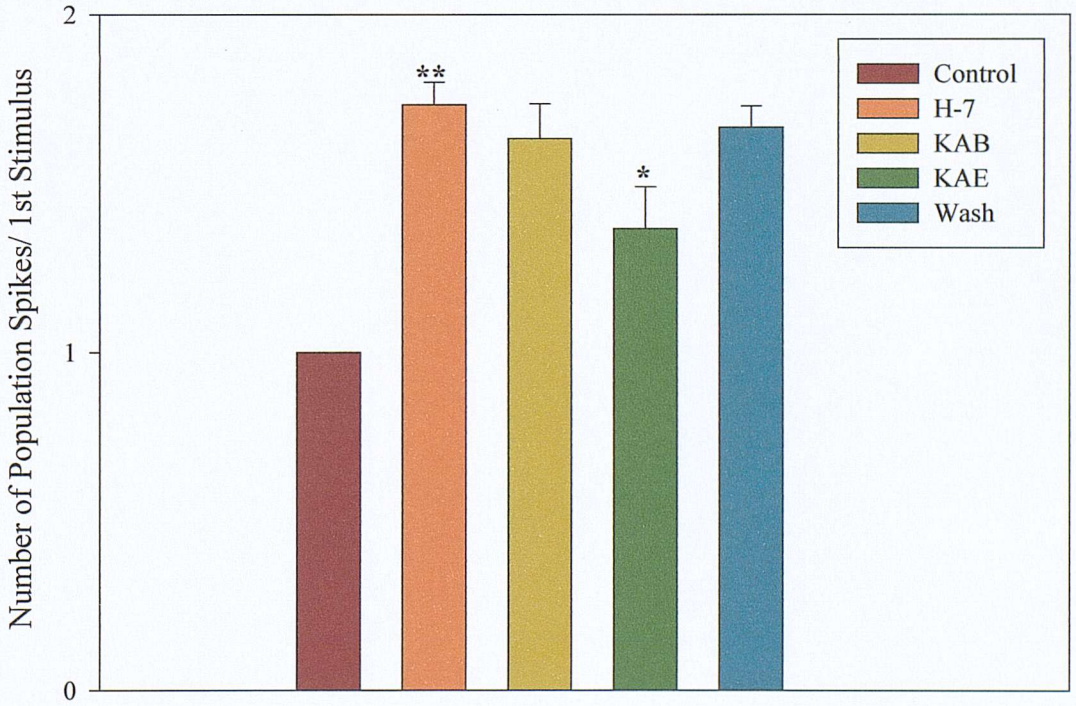

Figure 4.25 Mean number of population spikes per trace during control stimulation, the application of 20μM H-7, within the first three minutes of 1μM KA addition (KAB), at the end of 15 minutes 1μM KA (KAE) and at the end of 30 minutes wash recorded from. AS in the intact slice H-7 produces an epileptiform burst, which persists in the presence of 1μM KA. Again the effect of H-7 does not wash out after 30 minutes. Statistical significance was assessed to the immediately preceding time period *= $p<0.05$ **=$p<0.01$ Student's paired t-test.

4.3.5.1 $GABA_B$ receptor blockade and the KA response: Intact slice

One of the mechanisms by which it has been postulated that KA may bring about a reduction in GABAergic inhibition is by activation of post-synaptic KA receptors on the dendrites of interneurones leading to an increase in GABA release from their terminals. GABA spill over from the synaptic cleft then leads to the activation of $GABA_B$ autoreceptors on the terminals of these interneurones and thus to a reduction in GABA release (Frerking *et al.* 1999, Frerking and Nicholl 2000).

In order to test this hypothesis, a number of experiments were carried out in the presence of the $GABA_B$ antagonist SCH50911 ((2S)(+)5,5-Dimethyl-2-morpholineacetic acid) (Ong *et al.* 1998). Figure 4.26 shows examples of the recordings made from the CA1 of an intact hippocampal slice during the co-application of 20μM SCH50911 and 1μM KA.

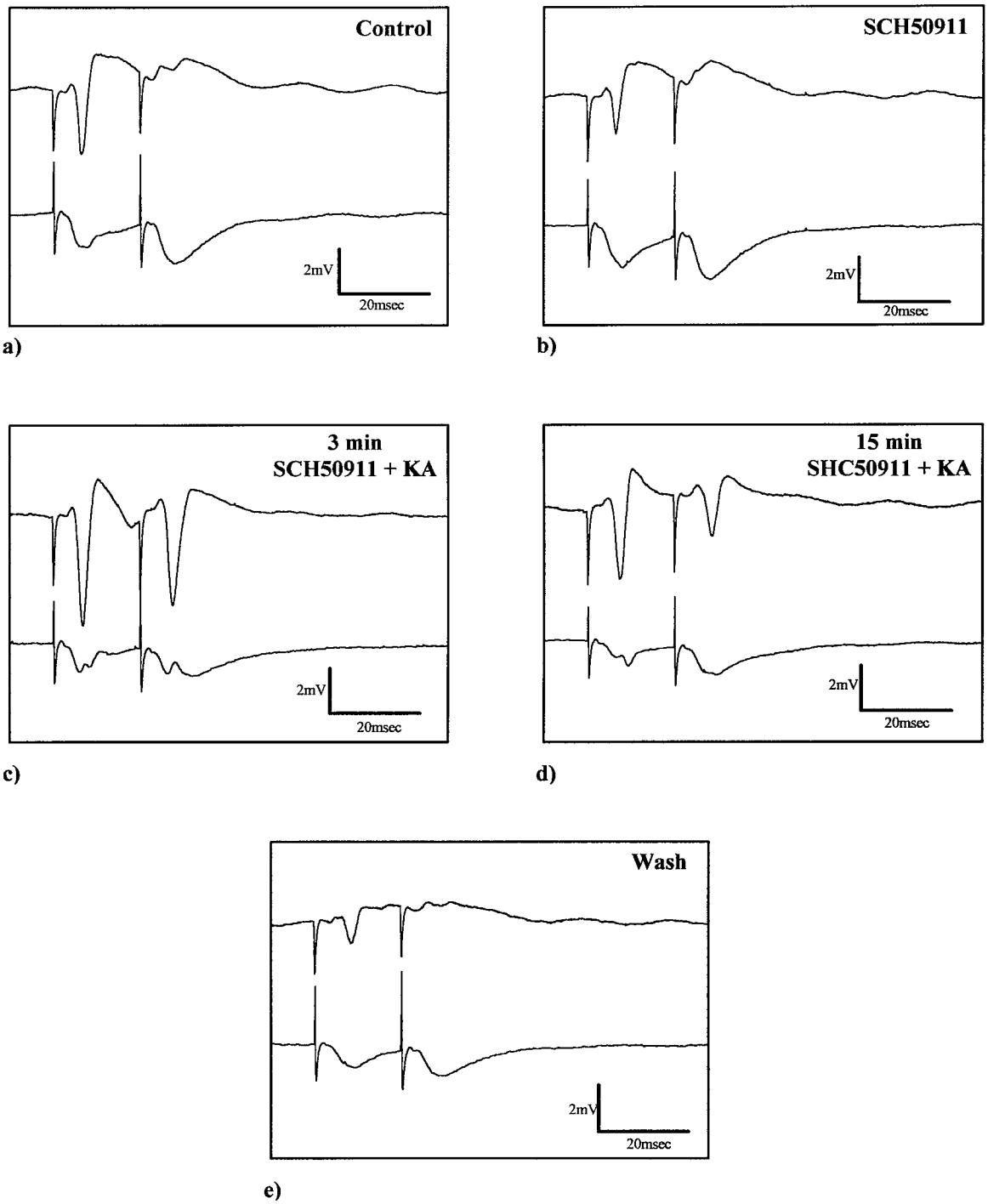

Figure 4.26 Example traces of recordings taken from *stratum pyramidale* and *stratum radiatum* of CA1 in an intact hippocampal slice during the application of 20μM SCH50911 and 1μM KA. a) Control, b) 20μM SCH50911, c) within the first three minutes of the coapplication of SCH50911 and 1μM KA, d) at the end of the coapplication period, e) following 30 minutes wash. Each example represents the average of 3 traces.

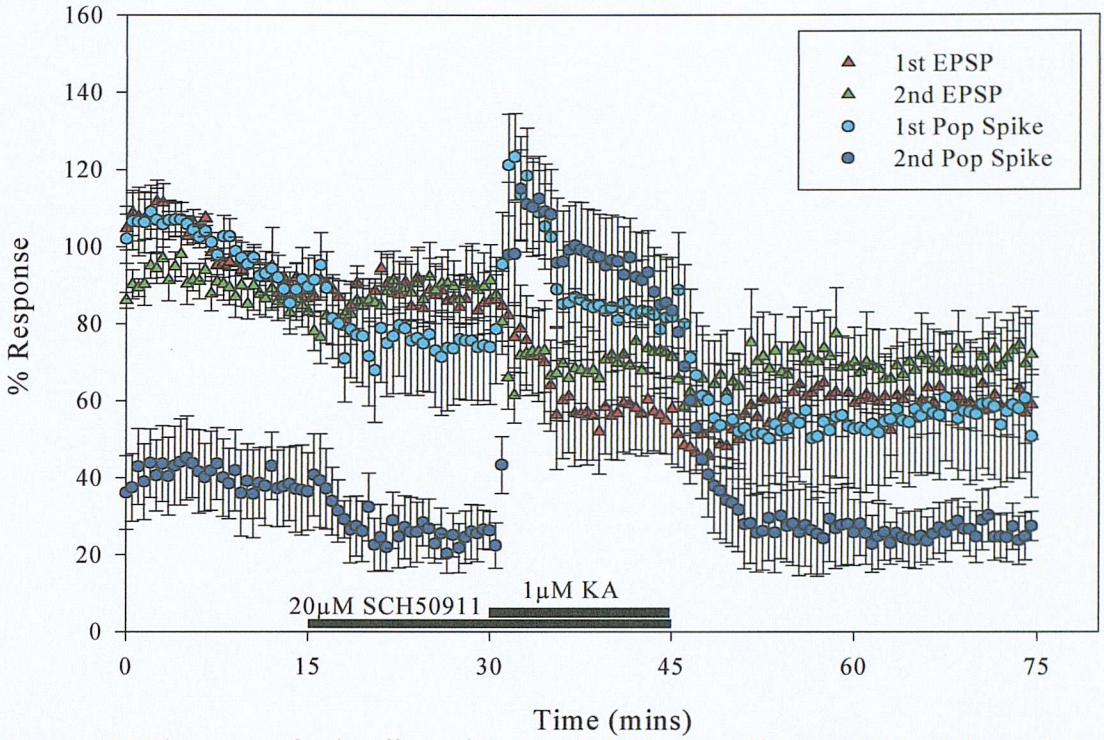

Figure 4.27 Time-course for the effects of 20μM SCH50911 co-application with 1μM KA on the mean percentage population spike amplitude and EPSP slope (± S.E.M., n=5) recorded from the CA1 region of intact hippocampal slices. Application of SHC 50911 does not significantly alter the EPSP slope, but causes a reduction in the amplitude of the first (89% (±4.2) to 75% (±8.0), $p<0.01$) and second population spikes (37% (±5.8) to 26% (±3.5), $p<0.05$). However, the presence of SCH 50911 does not appear to alter the response to 1μM KA, in as much as the first population spike is transiently increased (119% (±6.5), $p<0.01$) and the first and second EPSP slopes are reduced (86% (±4.3) to 56% (±5.1), $p<0.01$ and 90% (±4.7) to 73% (±5.8), $p<0.01$) respectively. The response of the second population spike is somewhat altered in that the increased amplitude following the addition of KA (104% (±8.5), $p<0.01$) is sustained until the end of the application period (86% (±6.4)).

Application of SCH50911 to intact slices (figure 4.27) significantly reduces the amplitude of both the first ($p<0.01$) and second ($p<0.05$) population spikes. There is no corresponding change in the slope of either EPSP.

The presence of 20μM SCH50911 does not prevent the increase in the amplitude of the first and second population spike that occurs during the initial phase of the KA response. However, it is interesting to note that the second population spike remains elevated if somewhat diminished in amplitude until the end of the application period. Both the first and second EPSP slopes decrease significantly in the presence of 1μM KA ($p<0.01$).

The paired-pulse inhibition recorded from the CA1 of intact slices is not significantly altered by the application of SCH50911 (figure 4.28). This is to be expected, since the fast feedforward and feedback inhibition observed using a 20msec inter-pulse interval in the CA1 is mediated by $GABA_A$ receptors (Stanford *et al.* 1994). There is a

marked, rapid reduction in this inhibition upon the addition of 1μM KA which persists until the end of the 15 minute application period ($p<0.01$).

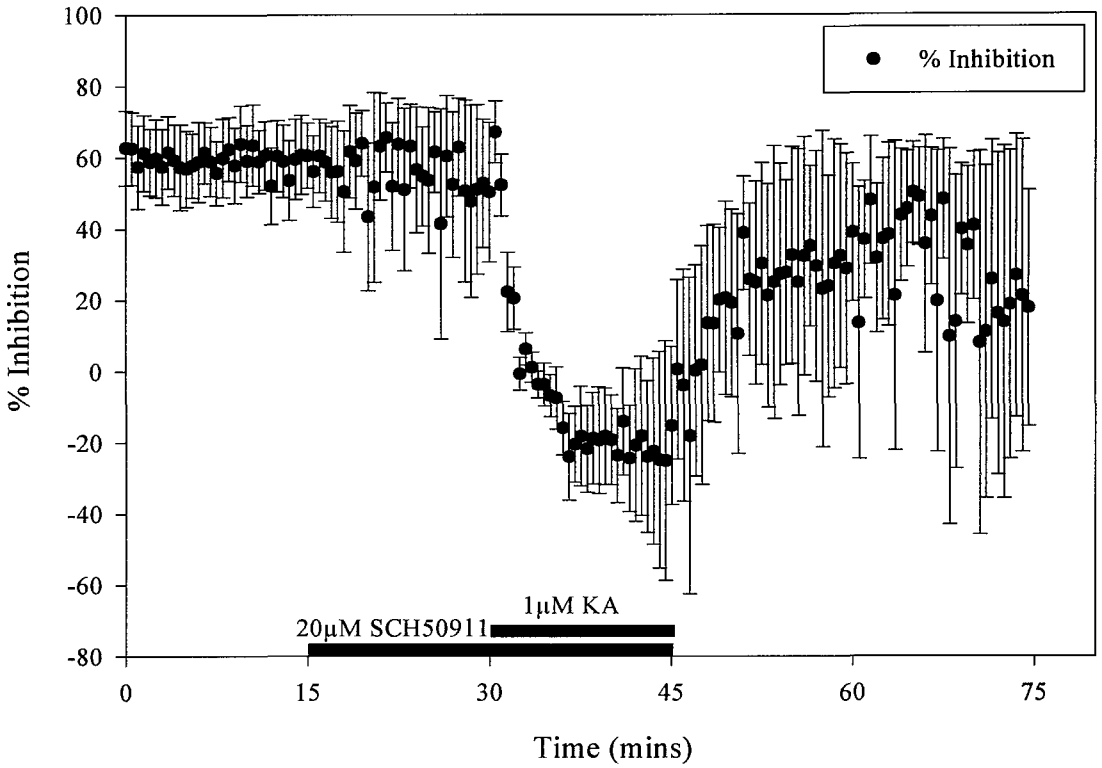

Figure 4.28 Time-course showing the changes in the percentage inhibition (± S.E.M.) of the second population spike with respect to the first recorded from the CA1 region of intact hippocampal slices (n=5). Application of SCH50911 does not significantly alter the percentage inhibition. On addition of 1μM KA the percentage inhibition is reduced from 51% (±12.4) to -24% (±16.2) by the end of the application period ($p<0.01$).

4.3.5.2 $GABA_B$ receptor blockade and the KA response: Isolated CA1 responses

The role of CA3 in the response to KA in the presence of SCH50911 was investigated in the isolated CA1 preparation. Figure 4.29 on the next page shows an example of the traces obtained from dual recordings from the *stratum pyramidale* and *stratum radiatum* of an isolated CA1 preparation during the application of 20μM SCH50911 and 1μM KA.

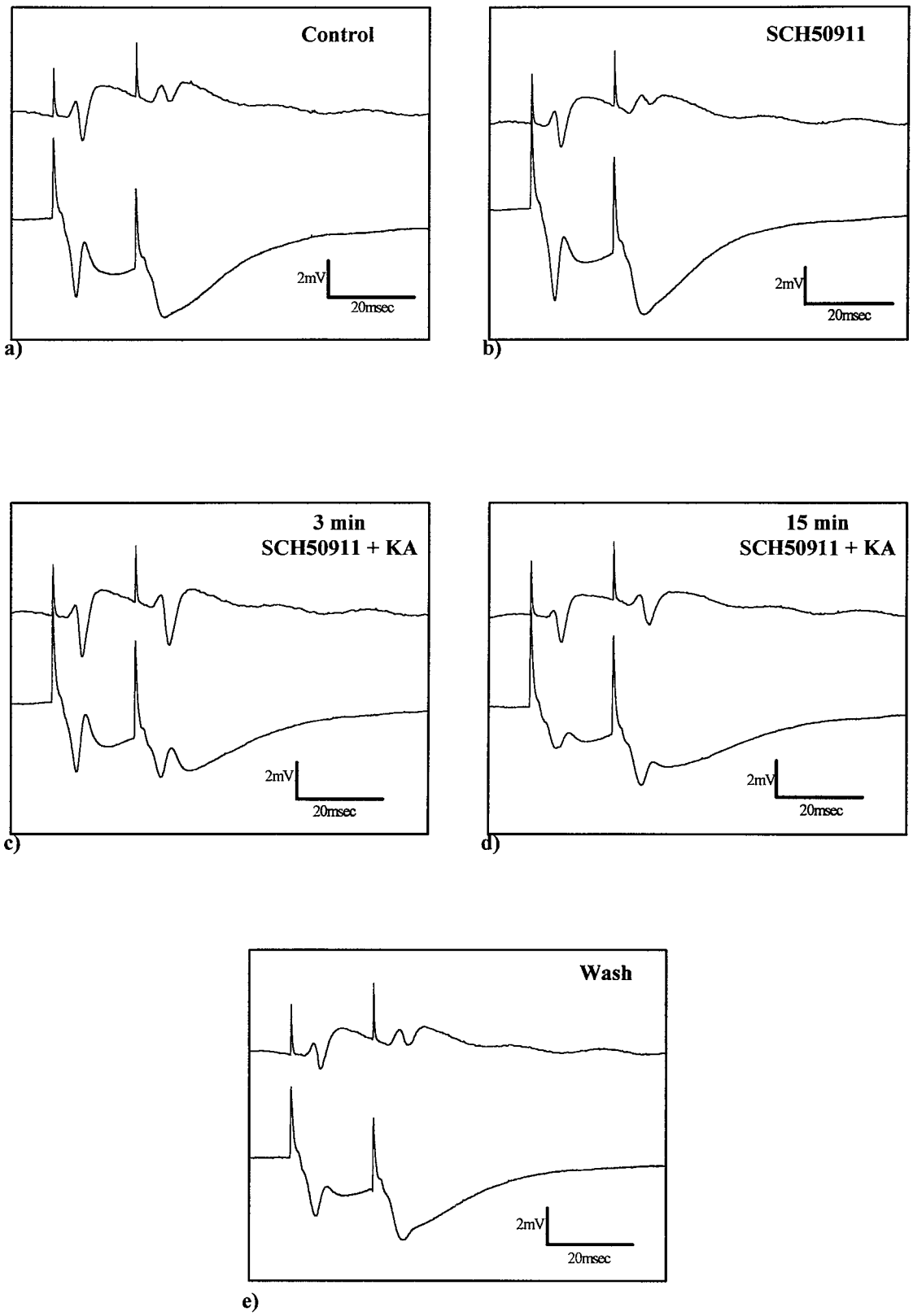

Figure 4.29 Example traces taken from a time-course carried out in an isolated CA1 preparation to observe the effects of coapplication of 20μM SCH50911 and 1μM KA. Each trace represents the average of three recordings from *stratum pyramidale* and *stratum radiatum*. a) Control, b) 20μM SCH50911, c) within the first three minutes of KA application, d) at the end of 15 minutes KA application, e) wash.

The EPSP slopes remain unaffected by the application of SCH50911 in the isolated CA1 preparation (figure 4.30). However, both the first and second population spikes are significantly reduced from control ($p<0.01$). As in the intact slice, SCH50911 fails to prevent the increase in the first and second population spike amplitudes that occur as a result of the addition of 1μM KA to the superfusing ACSF. Following this, the amplitudes of both population spikes decrease significantly ($p<0.01$) by the end of 15 minutes KA application. This value for the second population spike is not significantly different from the value for SCH50911 alone, which tends to suggest that an excitatory drive from CA3 is necessary for the continued elevation of the second population spike throughout the KA application.

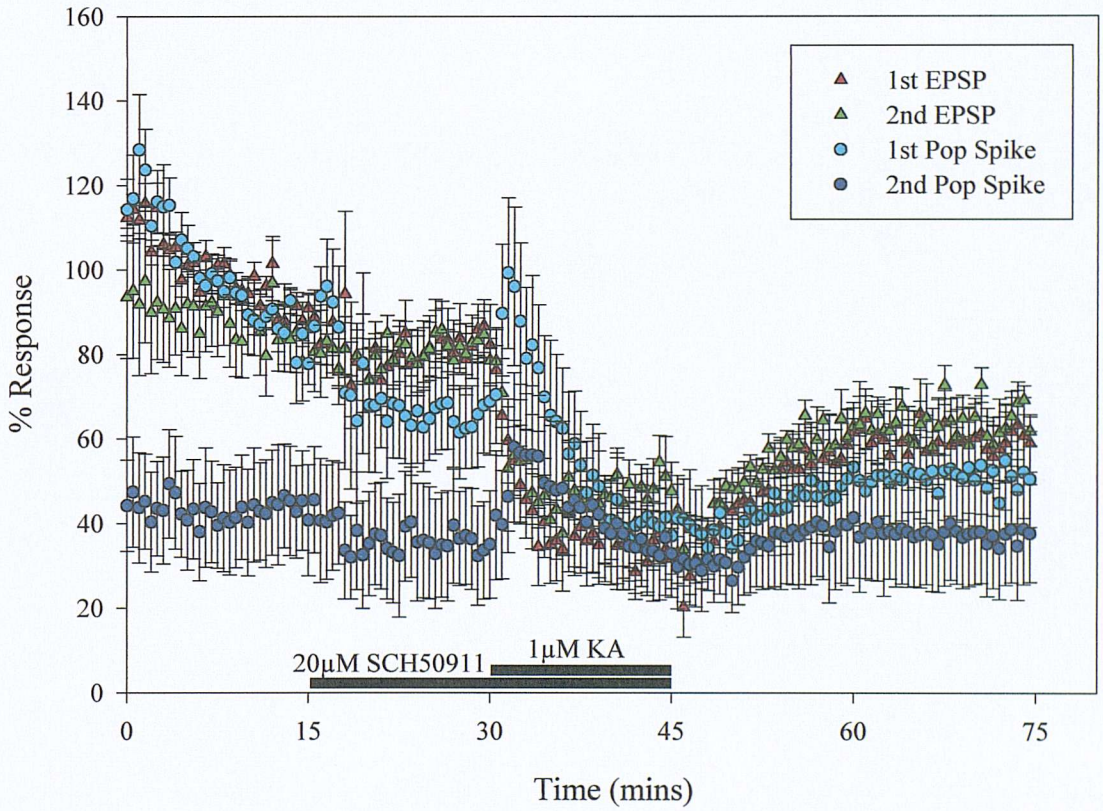

Figure 4.30 Time course for the effects of 20μM SCH 50911 co-application with 1μM KA in isolated CA1 preparations (n=5). The graph shows the mean percentage population spike amplitudes and EPSP slopes (± S.E.M.) recorded from *stratum pyramidale* and *stratum radiatum* respectively using a paired-pulse protocol with a 20msec inter-pulse interval. KA causes an increase in both the first (66% (±6.0) to 94% (±9.9), $p<0.01$) and second population spike amplitudes (34% (±6.3) to 56% (±8.1), $p<0.05$) and a reduction in the EPSP slopes from 85% (±3.6) to 36% (±3.8) ($p<0.01$) for the first EPSP and 84% (±2.7) to 51% (±4.2) ($p<0.01$) for the second. However, in comparison to the response seen in intact slices, the increase in the population spike amplitudes is neither as pronounced or prolonged in the isolated CA1 preparation.

The slope of both EPSPs are significantly reduced upon application of 1μM KA ($p<0.01$).

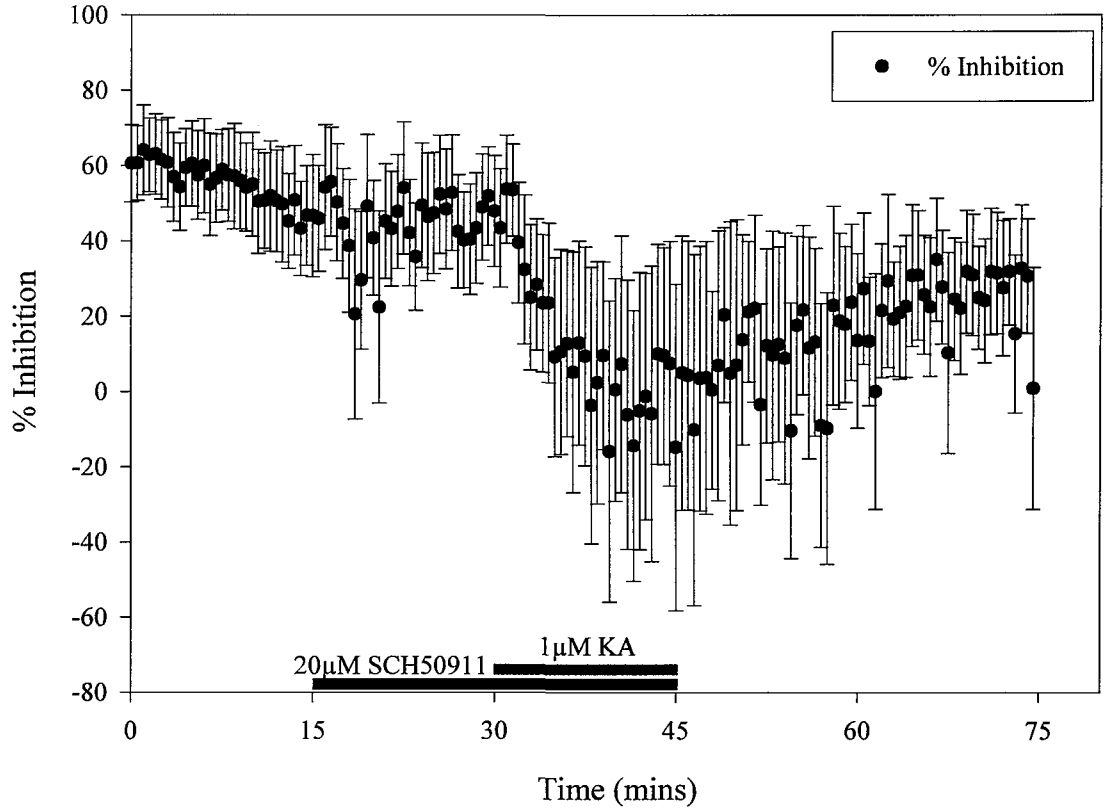

Figure 4.31 Time-course for the effects of 20μM SCH 50911 and 1μM KA on the mean percentage inhibition (± S.E.M.) recorded from *stratum pyramidale* of isolated CA1 preparations (n=5). Introducing 1μM KA to the superfusing solution in the presence of 20μM SCH 50911 causes a reduction (48% (±7.5) to 9% (±16.2), $p<0.01$) in the inhibition of the second population spike recorded using a paired-pulse protocol with a 20msec interpulse-interval. SCH50911 alone does not significantly alter the paired-pulse inhibition.

SCH50911 does not significantly alter the degree of paired-pulse inhibition in the isolated CA1 preparation (figure 4.31) and the addition of 1μM KA significantly reduces the mean percentage inhibition by the end of the application period ($p<0.01$).

4.3.6.1 Adenosine A_1 receptors and the KA response: Intact slices

It is known that levels of adenosine rise within the hippocampus during KA induced seizures in rats (Berman *et al.* 2000) following the perfusion of KA. The following series of experiments were performed therefore in order to assess the possibility of a modulatory role of adenosine on the actions of 1μM KA within the CA1 region of the hippocampus.

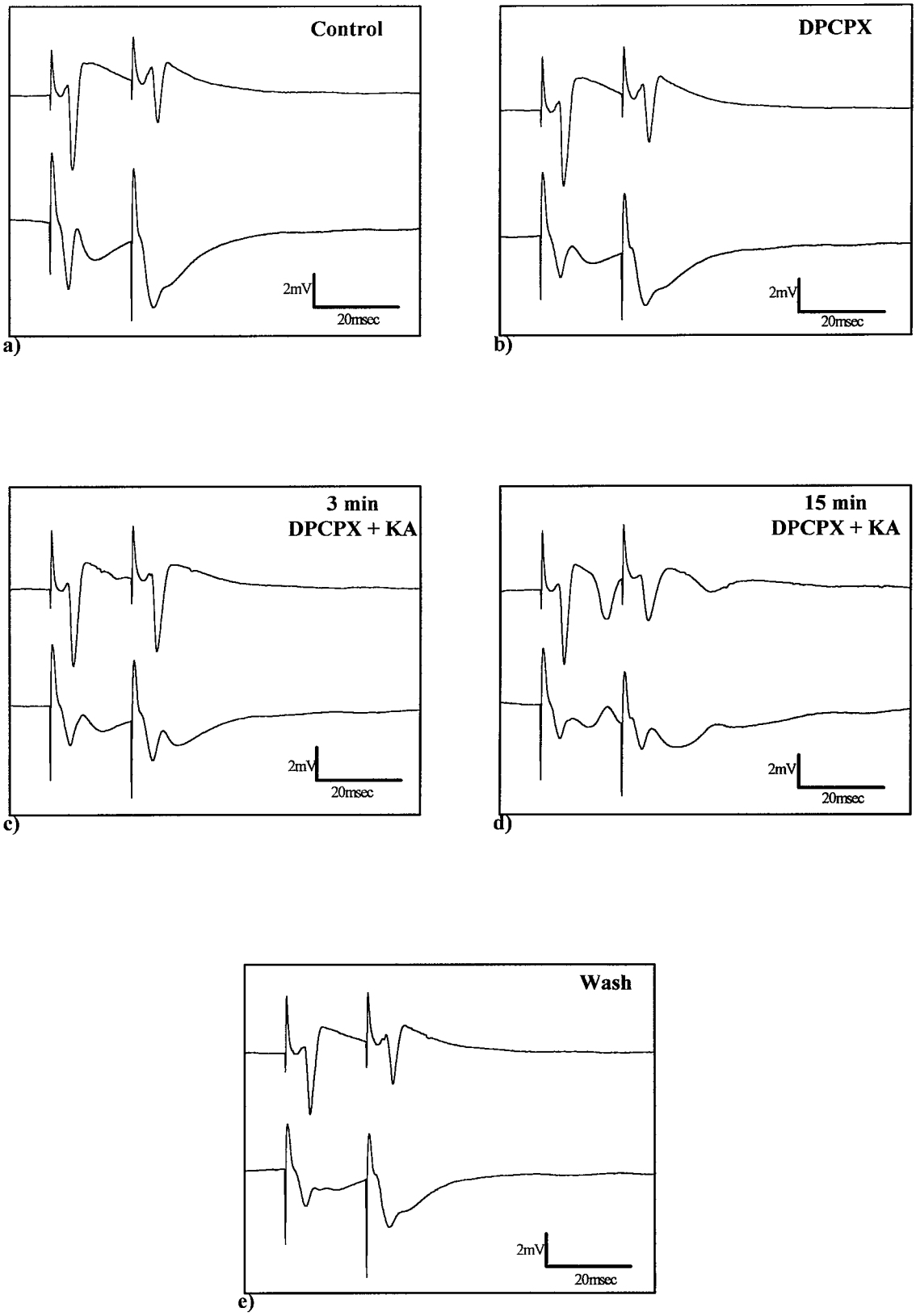

Figure 4.32 Representative traces taken from a time-course experiment to observe the effects of co-application of the adenosine A_1 antagonist DPCPX (50nM) with 1μM KA in the CA1 region of an intact hippocampal slice. Each trace is an average of three traces recorded at the following time points: a) at the end of a 15 minute control period, b) at the end of 15 minutes application of 50nM DPCPX, c) within the first three minutes of the addition of 1M KA, d) at the end of 15 minutes co-application of DPCPX and 1μM KA, e) at the end of a 30 minute wash period.

DPCPX (8-Cyclopentyl-1,3-dipropylxanthine) is an antagonist for adenosine A1 receptors. Adenosine has been shown (Burke and Nadler 1988) to reduce the K^+ evoked release of glutamate from the Schaffer collateral commissural pathway to approximately 60% of control. They proposed that this was likely to be due to the activation of adenosine A_1 receptors, possibly due to either a decreased presynaptic Ca^{2+} influx through voltage gated channels or by a downstream action which affects the functioning of these voltage gated Ca^{2+} channels. Since adenosine levels have been shown to rise during KA evoked seizures (Berman *et al.* 2000) it was of interest to investigate the possibility that adenosine receptor activation was involved in the response to KA when applied acutely. To this end, antagonists for both A_1 and A_2 receptors were applied prior to and during the application of KA in both intact and isolated CA1 slices.

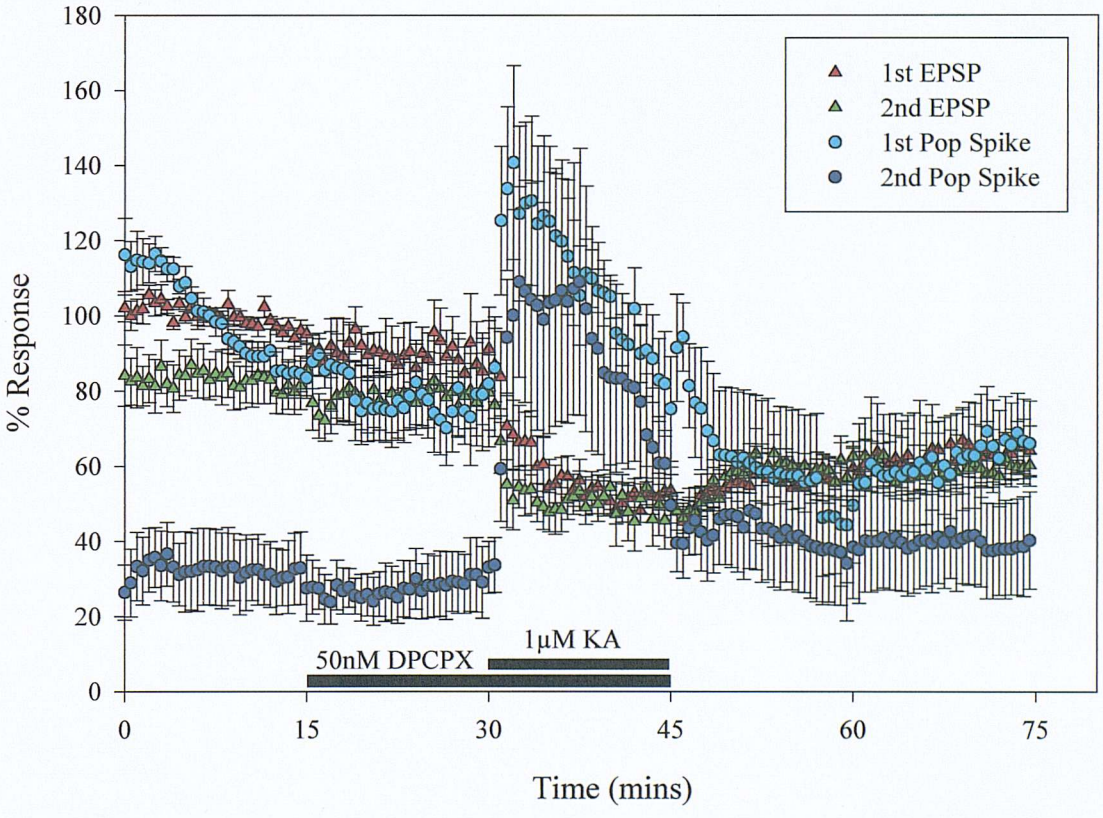

Figure 4.33 Graph showing the effects of co-application of the adenosine A_1 antagonist DPCPX and 1μM KA on the mean percentage population spike amplitude and EPSP slope (± S.E.M.) recorded from the CA1 region of intact slices (n=5). DPCPX causes no significant change in either the population spike amplitude or the EPSP slope. Application of 1μM KA again causes an increase in the amplitude of both the first and second population spikes from 77% (±7.5) to 134% (±12.7) and 30% (±5.2) to 101% (±12.7) respectively ($p<0.01$). Both the first and second EPSP slopes are reduced from 88% (±6.3) to 52% (±2.1) and 79% (±5.1) to 47% (±4.2) respectively ($p<0.01$).

Application of DPCPX alone to intact slices does not significantly affect the population spike amplitudes or the EPSP slopes (figure 4.33). Upon addition of 1μM KA, the EPSP slopes are significantly reduced ($p<0.01$). The population spikes increase in amplitude within the first three minutes of KA ($p<0.01$). This potentiation is sustained, albeit to a lesser degree until the end of the KA period (85% (±6.6) and 62% (±6.8) respectively, $p<0.01$).

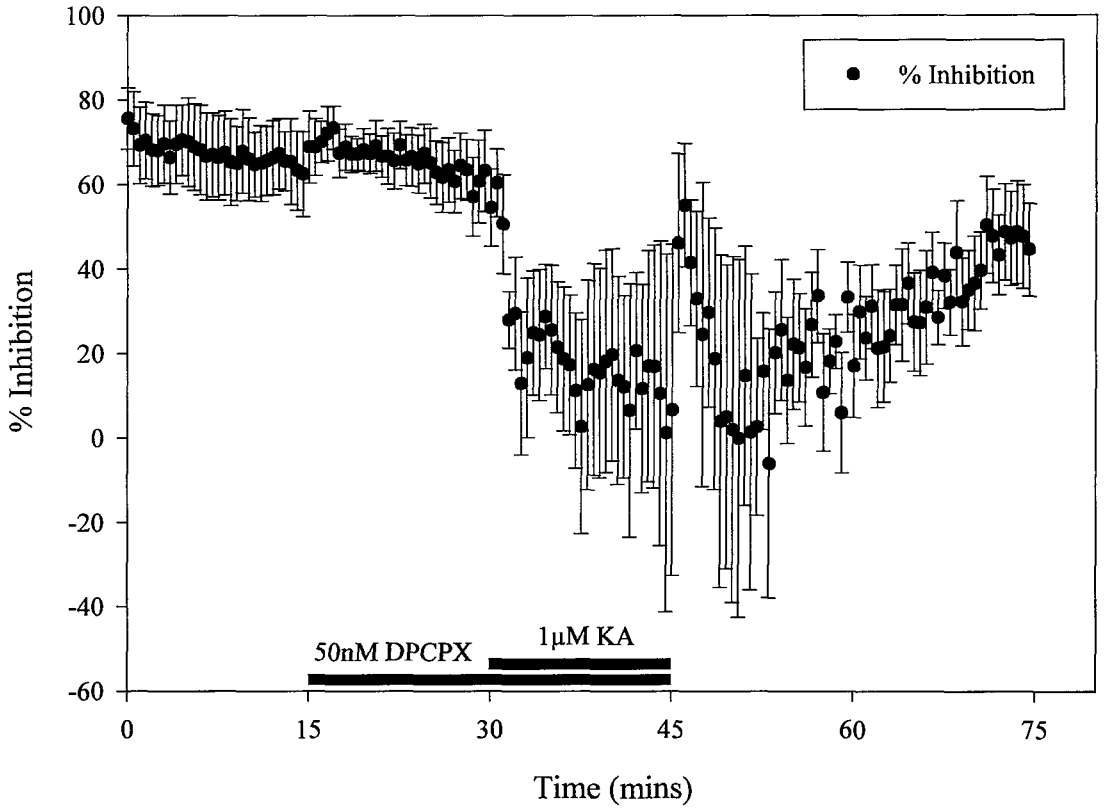

Figure 4.34 Time-course for the changes in the mean percentage inhibition (± S.E.M.) calculated from the population spike data presented in figure 3.70. Application of DPCPX causes no significant change in the paired-pulse inhibition. Addition of 1μM KA to the superfusing ACSF causes a marked reduction in the percentage inhibition from 60% (±5.2) to 10% (±19.4) by the end of 15 minutes ($p<0.05$).

There is no significant change in the percentage inhibition following the application of 50nM DPCPX (figure 4.34). On addition of 1μM KA there is a decrease in the mean percentage inhibition from 60% (±5.2) to 10% (±19.4) ($p<0.05$).

4.3.6.2 A_1 receptor modulation of the KA response in the isolated CA1

It is interesting to note that in the isolated CA1 preparation blockade of A_1 receptors with 50nM DPCPX (figure 4.36) produces a significant increase in the slope of both the first and second EPSPs ($p<0.05$). This may point to a tonic control of glutamate release from the Schaffer collateral pathway by adenosine. Although it would appear that the second population spike is reduced during the application of DPCPX, it does appear to be continuing on a downward trend that began during the control period and is therefore may not represent a drug effect. It is possible however, that an increased EPSP slope in the presence of DPCPX may indicate an increase in the excitatory drive to the CA1 interneurone population in both a feedforward and feedback manner, thus leading to a reduction in the amplitude of the second population spike.

Upon the addition of 1μM KA, both the first and second population spike amplitudes increase significantly ($p<0.01$). Again this potentiation is sustained in diminished form throughout the application of KA. The amplitude of the second spike at the end of the KA application period is not significantly different to initial values. The slopes of both the first and second EPSP decline rapidly with the introduction of 1μM KA to the recording chamber reaching 65% (±3.1) and 51% (±1.7) respectively by the end of 15 minutes ($p<0.01$).

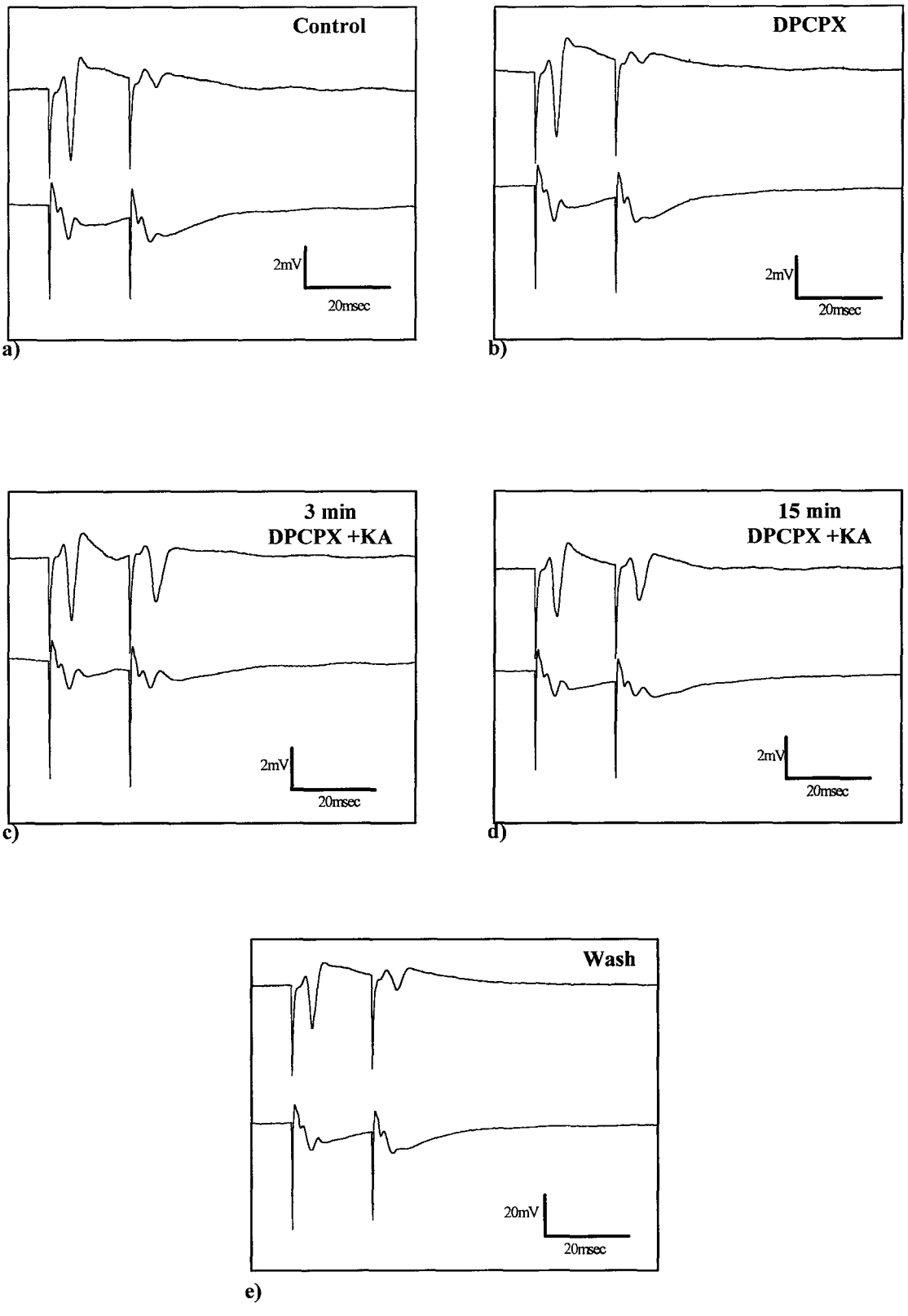

Figure 4.35 Example traces taken during a time course experiment to observe the effects of adenosine A_1 receptor antagonism on the those seen during 1M KA application. The traces seen above represent the average of three responses taken at the following time points: a) at the end of 15 minutes control stimulation, b) at the end of 15 minutes application of 50nM DPCPX, c) within the first three minutes of 1μM KA application, d) at the end of 15 minutes K application, e) at the end of a 30 minute wash period.

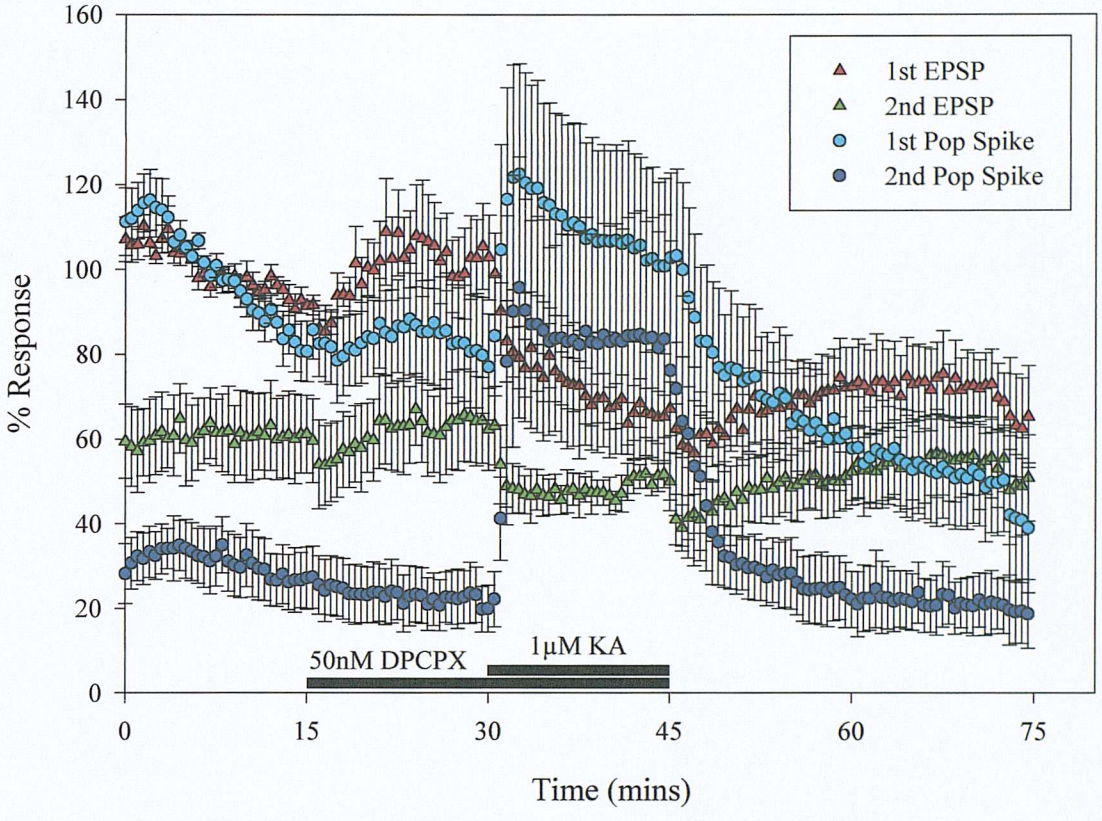

Figure 4.36 Time-course for the effects of 50nM DPCPX and 1μM KA on the mean percentage population spike amplitude and EPSP slope (± S.E.M.) recorded from isolated CA1 preparations (n=5). Application of 50nM DPCPX causes a potentiation of both the first and second EPSP percentage mean slopes from 92% (±1.9) to 104% (±5.2) and 61% (±5.4) to 65% (±5.6) respectively ($p<0.05$). DPCPX also reduces the amplitude of the second population spike from 27% (±3.7) to 22% (±3.5) ($p<0.01$) but does not significantly affect the amplitude of the first spike. Upon the addition of 1μM KA both the first and second population spike amplitudes increase from 80% (±7.2) to 120% (±14.1) for the first spike ($p<0.01$) and to 88% (±17.5) for the second ($p<0.01$). The first spike amplitude declines until the end of the KA application period (101% (±11.1), $p<0.01$) whereas the second population spike amplitude does not significantly change throughout this time. The first and second EPSP slopes both decline during the application of KA to 65% (±3.1) and 51% (±1.7) respectively ($p<0.01$).

Application of 50nM DPCPX does not significantly change the mean percentage inhibition when administered alone (figure 4.37). Addition of 1μM KA rapidly reduces the paired-pulse inhibition ($p<0.01$).

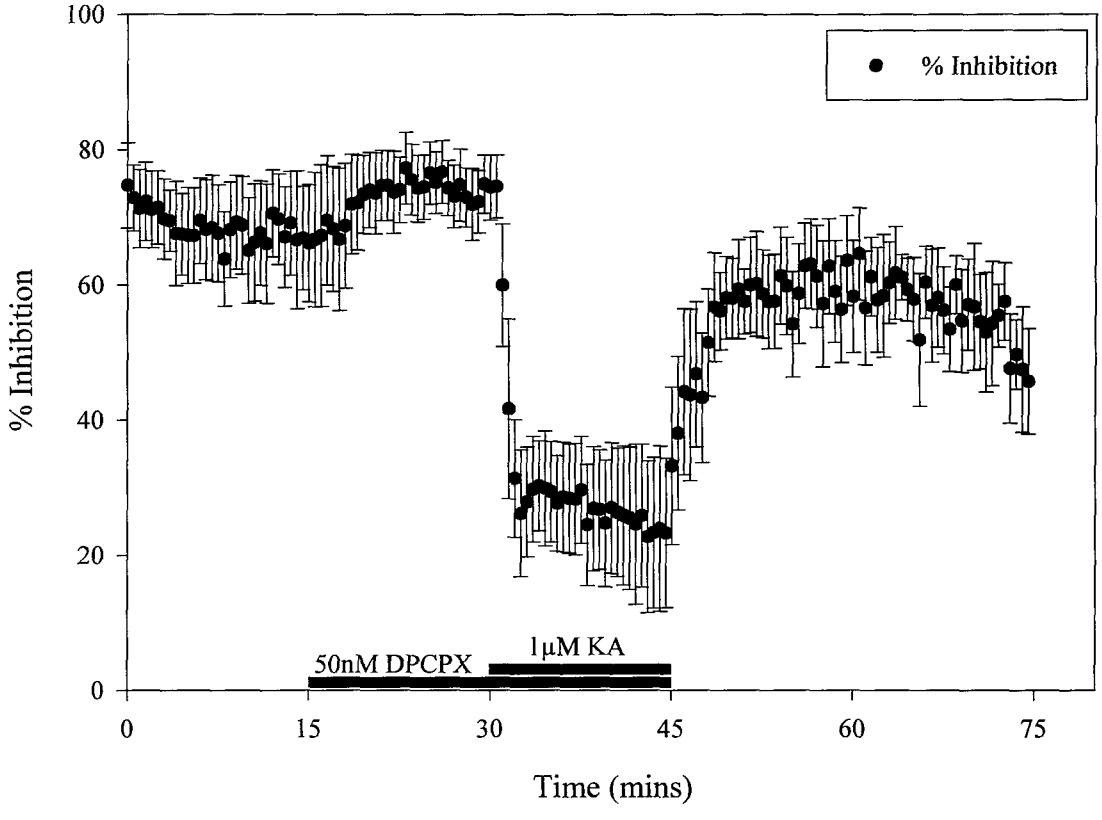

Figure 4.37 Graph of the mean percentage inhibition (± S.E.M.) of the second population spike compared to the first recorded from isolated CA1 preparations (n=5) using a 20 msec inter-pulse interval paired pulse protocol. DPCPX does not significantly alter the inhibition, whilst addition of 1μM KA caused a marked reduction in the evoked inhibition from 73% (±2.6) to 24% (±6.1) ($p<0.01$).

4.3.7.1 A_2 receptors and the KA response in the intact slice

In order to assess the any possible role of adenosine A_2 receptors in the response to KA, field recordings were made from the *stratum pyramidale* and *stratum radiatum* of the CA1 of both intact slices and isolated CA1 preparations and the A_2 antagonist DMPX (3,7-Dimethyl-1-(2-propynyl)xanthine) (10μM) and 1μM KA were co-applied. Example traces of the responses obtained from an intact slice are presented above in figure 4.38.

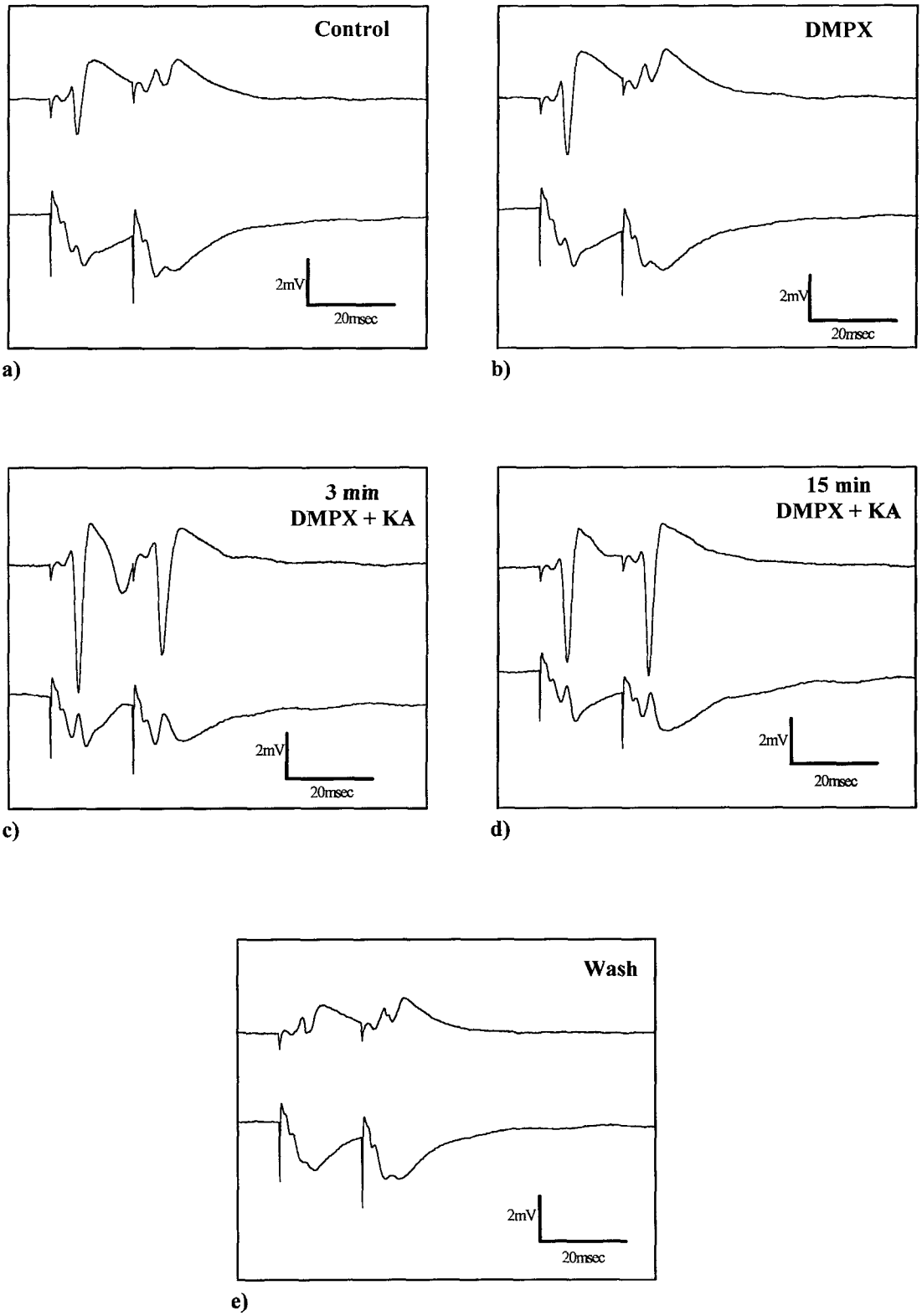

Figure 4.38 Example traces taken from a time-course experiment looking at the effect of co-application of 10μM DMPX and 1μM KA in the CA1 region of an intact hippocampal slice. Each box represents the average of three traces taken 30 seconds apart at the following time points: a) end of 15 minutes control period, b) end of 15 minutes application of 10μM DMPX, c) within three minutes of 1μM KA co-application, d) at the end of 15 minutes KA co-application, e) the end of a 30 minute wash with ACSF.

DMPX alone has no significant effect on the population spike amplitude or EPSP slope prior to the addition of KA in the intact slice preparation (figure 4.39). As KA washes into the recording chamber we can see that the amplitude of both the first and second population spikes increase significantly ($p<0.01$). This response is again sustained throughout this application period. The presence of 10μM DMPX does not prevent the KA induced reduction of the first and second EPSP slopes ($p<0.01$).

Application of 10μM DMPX does not significantly change the mean percentage inhibition calculated from the CA1 of intact slices (figure 4.40). On the addition of 1μM KA this inhibition once again undergoes a rapid ($p<0.01$) by the end of 15 minutes KA.

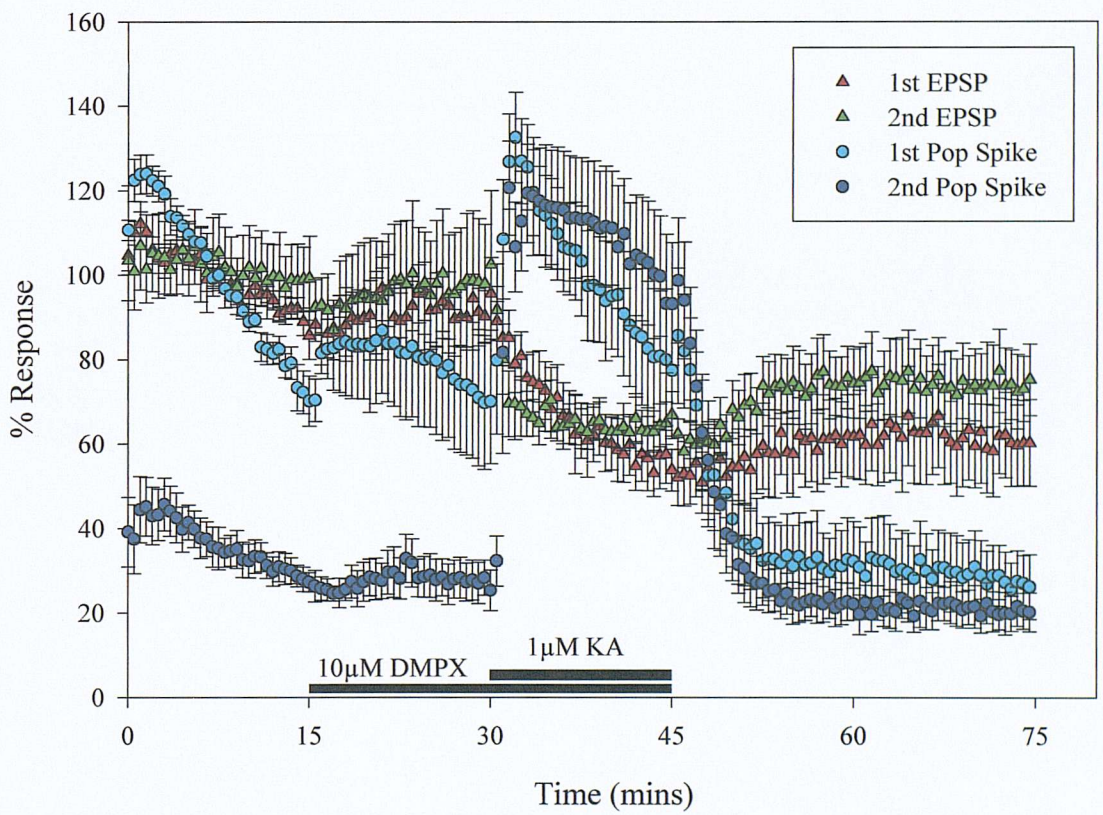

Figure 4.39 Time-course for the effects of 10μM DMPX and 1μM KA on the mean percentage population spike amplitude and EPSP slope (± S.E.M., n=5) recorded from the CA1 region of intact hippocampal slices using a paired-pulse stimulus protocol with a 20msec inter-pulse interval. Application of DMPX has no significant effect on either the slope of the EPSPs or population spike amplitudes. However on application of KA both the first and second population spikes undergo a marked potentiation from 71% (±8.6) to 129% (±5.8) and 28% (±2.5) to 113% (±6.2) respectively ($p<0.01$). This is sustained although reduced in amplitude throughout the KA application period. At the same time as this, both EPSP slopes are reduced from 92% (±3.1) to 56% (±3.7) for the first EPSP and 98% (±8.2) to 64% (±2.7) for the second ($p<0.01$).

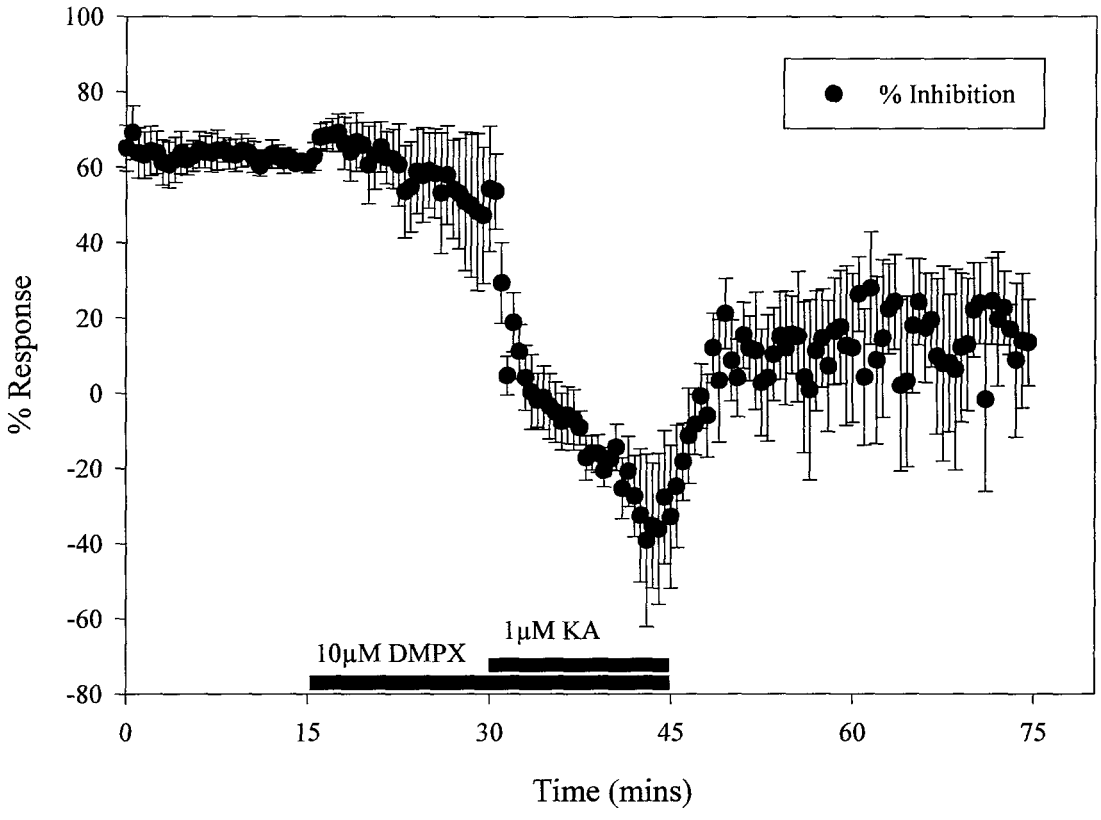

Figure 4.40 Graph of the mean percentage inhibition calculated from recordings made in the CA1 region of intact hippocampal slices (n=5) during the co-application of 10μM DMPX and 1μM KA. Introducing DMPX to the superfusing ACSF produces no significant change to the percentage inhibition, whilst the addition of 1μM KA causes a marked reduction in paired-pulse inhibition from 49% (±10.4) to 12% (±4.0) ($p<0.01$) leading to facilitation of the second population spike (-33% (±9.8), $p<0.01$).

4.3.7.2 A_2 receptors and the KA response in the isolated CA1

The same experiment was then performed in the isolated CA1 preparation in order to observe any CA1 specific effects of these drugs without any downstream effect from CA3. Figure 4.41 shows examples of the traces obtained from an isolated CA1 preparation, recording from *stratum pyramidale* and *stratum radiatum* during the application of 10μM DMPX and 1μM KA.

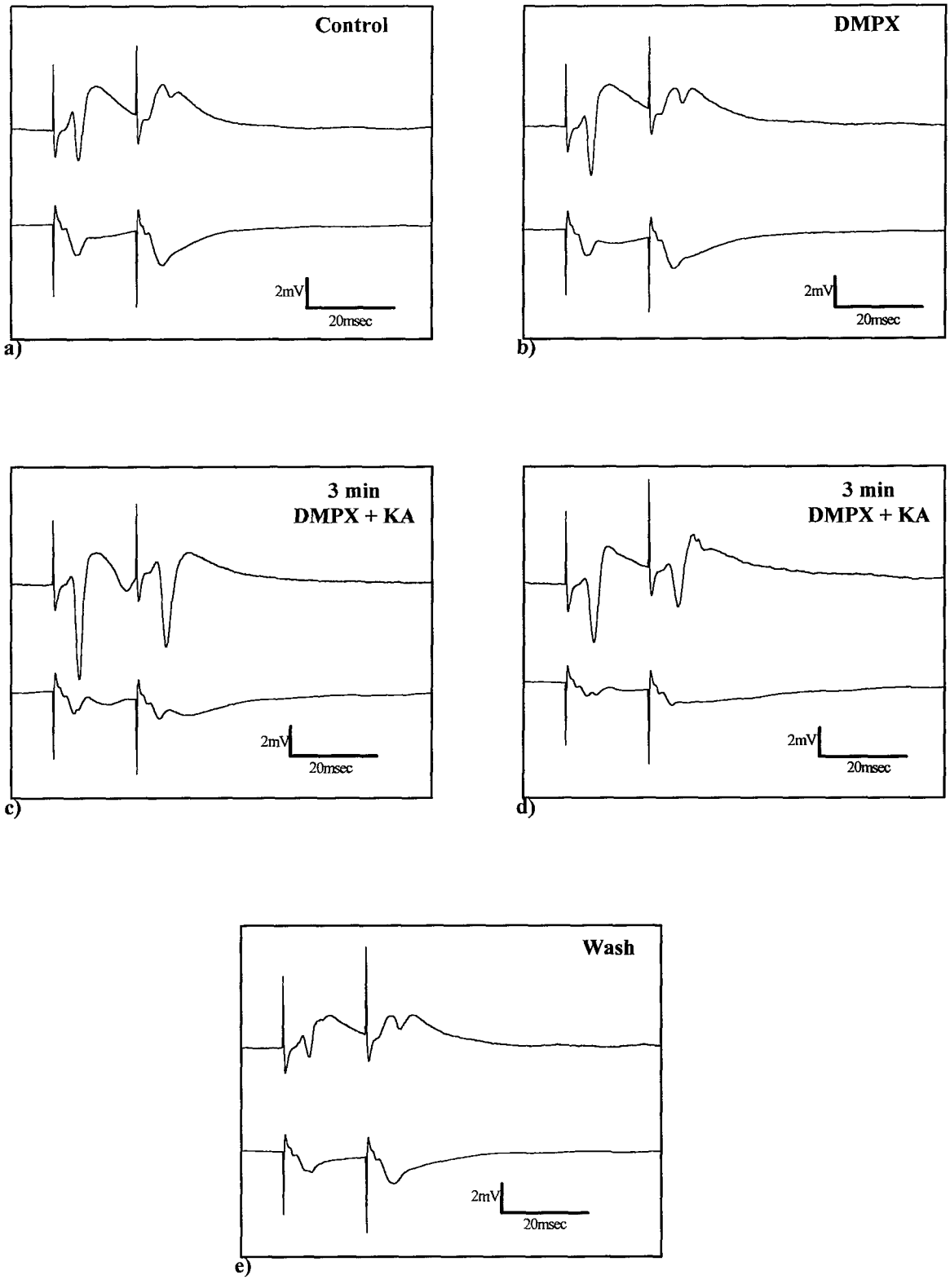

Figure 4.41 Example traces taken from a time course experiment to observe the effects of adenosine A_2 receptor blockade on the actions of 1μM KA application to an isolated CA1 preparation. Each trace is an average of three responses taken at the following time points: a) at the end of a 15 minute control period, b) at the end of 15 minutes DMPX (10μM) application, c) within the first three minutes of KA (1μM) application, d) at the end of 15 minutes KA application, e) at the end of 30 minutes wash.

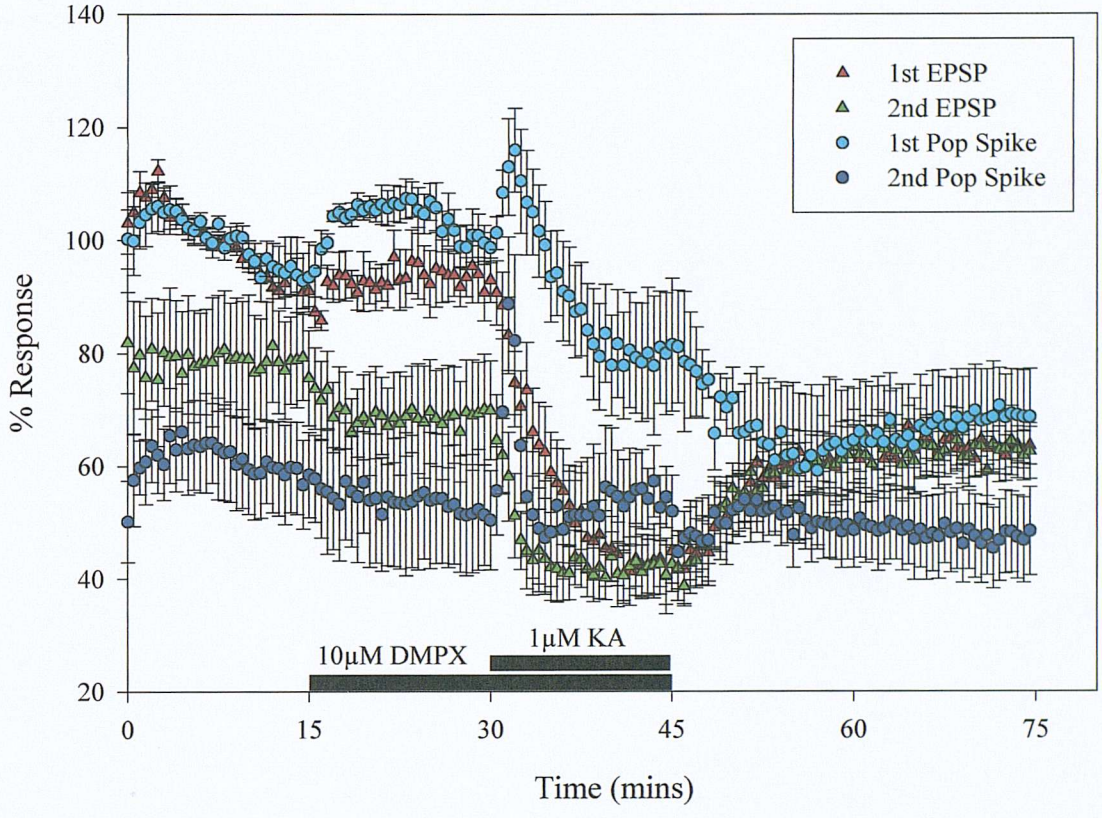

Figure 4.42 Graph showing the time-course for the effects of 10μM DMPX and 1μM KA on the mean percentage population spike amplitude and EPSP slope (± S.E.M., n=5) in isolated CA1 preparations. DMPX application causes an increase in the amplitude of the first population spike from 94% (±3.0) to 100% (±2.1) ($p<0.05$) although the second population spike is not significantly affected. The second EPSP slope undergoes a small, but significant decrease from 79% (±4.3) to 70% (±5.1) ($p<0.01$). Upon addition of 1μM KA the amplitudes of the first and second spikes increase to 113% (±4.6) in the case of the first spike and from 52% (±5.4) to 78% (±7.3) in the case of the second. Only the increase in the second spike reached significance ($p<0.05$). Both EPSP slopes undergo a marked reduction during the KA application period from 93% (±3.0) to 42% (±3.5) for the first EPSP and from 70% (±5.1) to 42% (±2.6) for the second ($p<0.01$).

DMPX (10μM) causes a significant potentiation of the first population spike in the absence of CA3 ($p<0.05$, figure 4.42). It also significantly reduces the slope of the second EPSP ($p<0.01$). Addition of 1μM KA causes a transient increase in the population spike amplitudes, however, only the increase in the second population spike reaches statistical significance ($p<0.05$). During this period, both EPSP slopes decrease significantly ($p<0.01$).

In the isolated CA1 preparation (figure 4.43), 10μM DMPX produces a significant increase in the percentage inhibition ($p<0.05$). This is reduced to 29% (±7.1) by the end of the KA application ($p<0.05$).

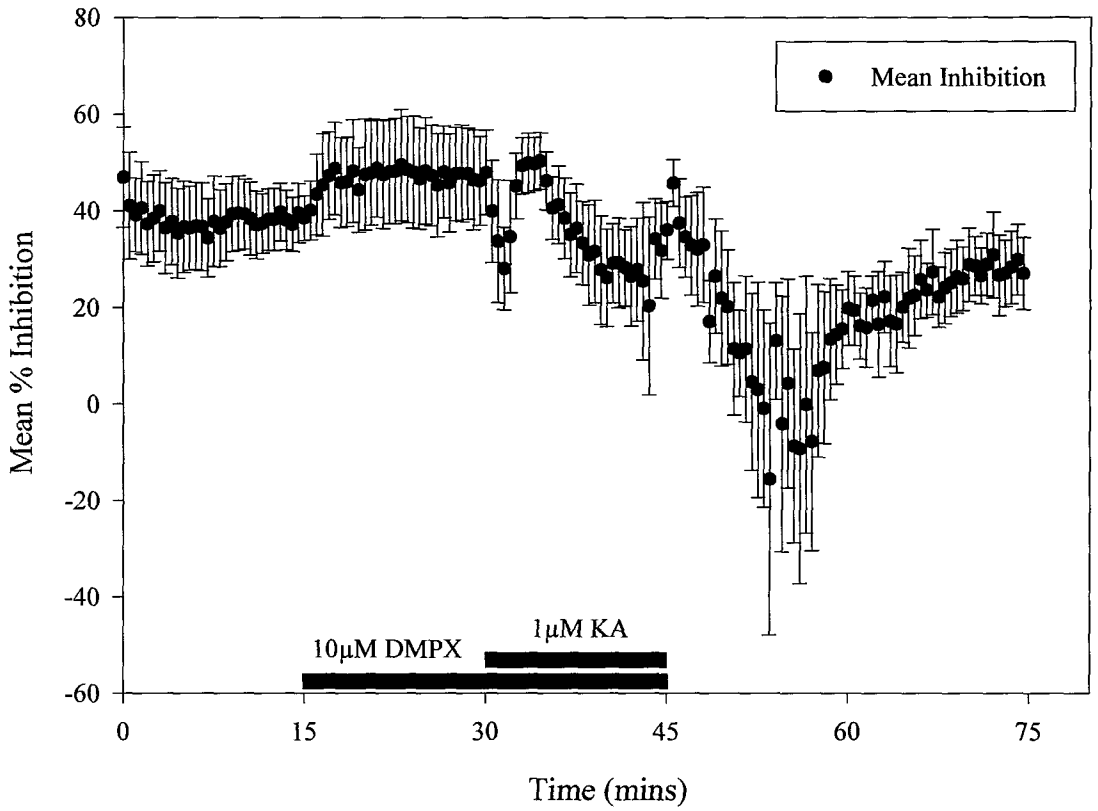

Figure 4.43 Time-course for the effects of DMPX and KA on the mean percentage inhibition (± S.E.M.) calculated from paired-pulse data recorded from *stratum pyramidale* of isolated CA1 preparations (n=5). Application of 10μM DMPX causes an increase in the percentage inhibition from 38% (±3.2) to 47% (±5.2) ($p<0.05$). On the addition of 1μM KA there is a transient decrease in inhibition to 36% (±5.3) although this is not statistically significant. By the end of this period the inhibition again decreases to 29% (±7.1).

4.3.8 Summary of results

The following series of graphs summarise the changes observed during the application of KA in the presence of antagonists for group I/II and II/III mGluRs, $GABA_B$ receptors, PKC and adenosine receptors with regards to the population spike amplitude, the EPSP slope or the percentage inhibition. In each case, responses have been normalised to the control responses obtained with 1μM KA.

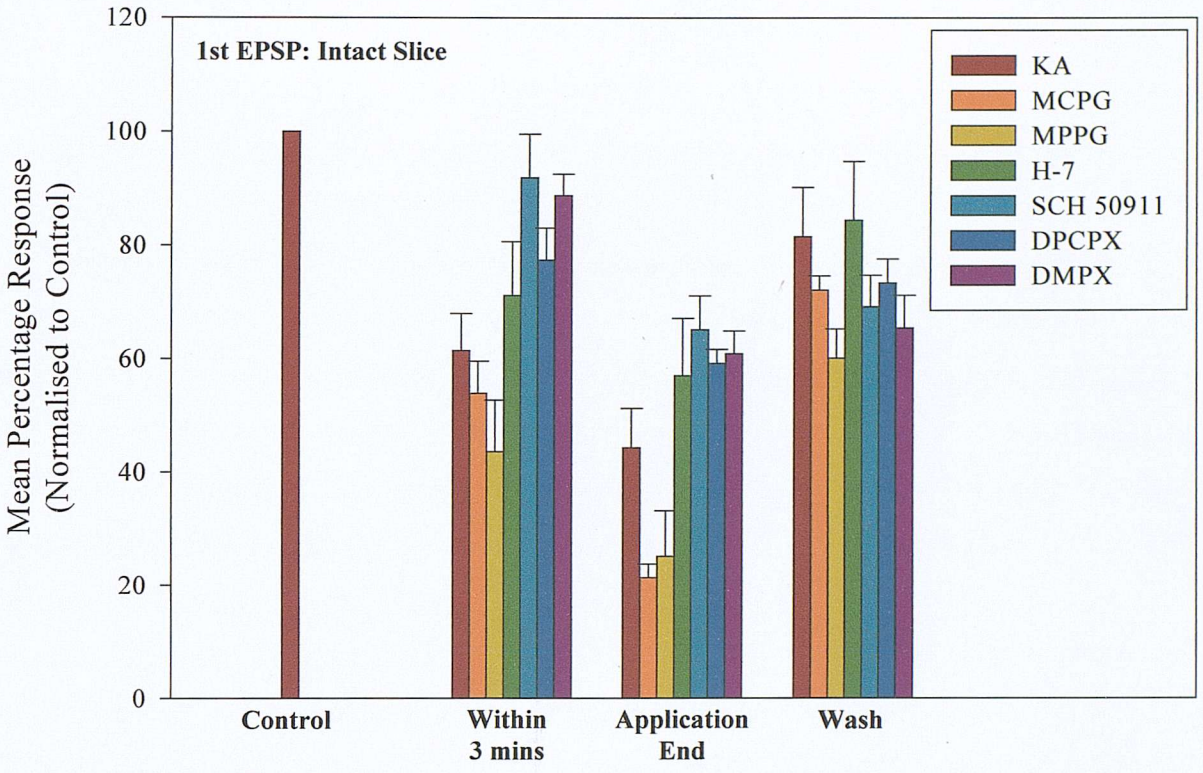

Figure 4.44 Application of 1μM KA significantly reduced the slope of the first EPSP recorded from the CA1 of intact slices. This response was significantly reduced by SCH50911 and DMPX co-application. By the end of the drug application period, co-application of DPCPX also significantly reduced the response to KA. Application of MCPG significantly enhanced the reduction in EPSP slope with KA.

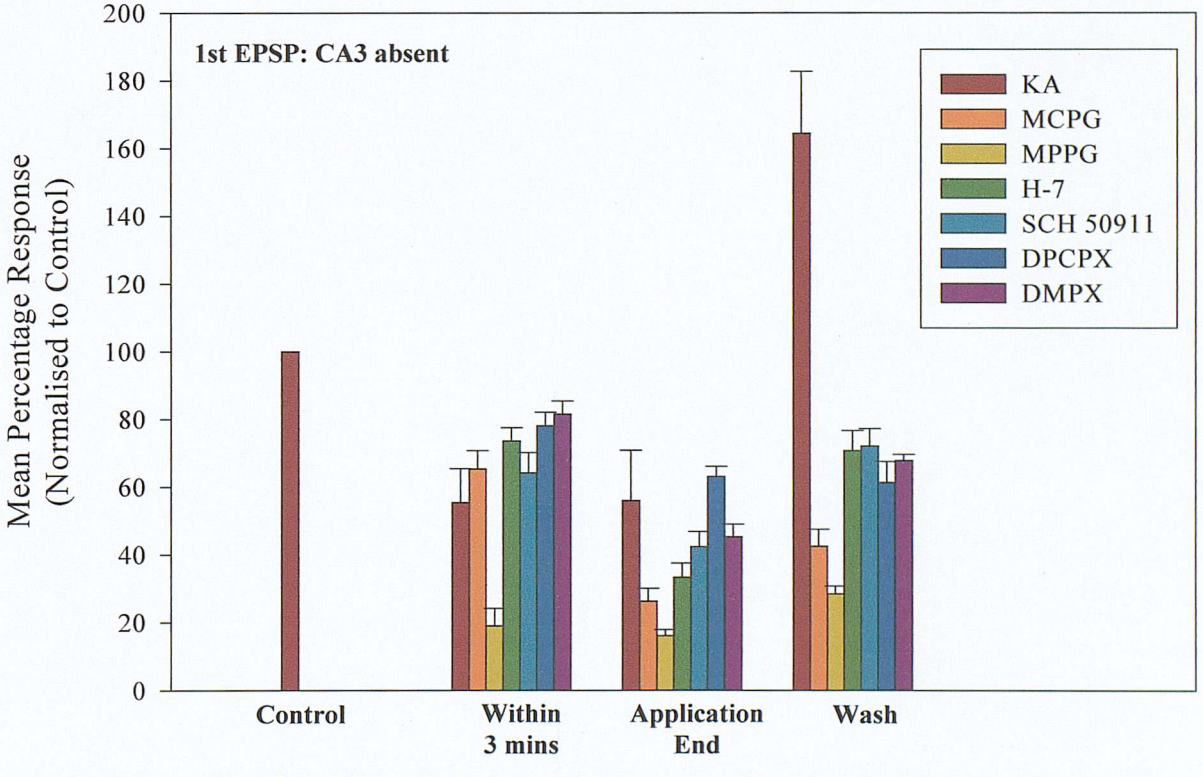

Figure 4.45 The reduction of the first EPSP slope by KA in the isolated CA1 preparation is significantly enhanced by co-application with MPPG. Application of the adenosine receptor antagonists DPCPX and DMPX both significantly reduce the initial response to KA, but are not significantly different to control by the end of the drug application period.

A comparison of the effects of antagonism of both group I/II and group II/III mGluR's on the response of the first EPSP slope in CA1 to KA in the intact slice preparation is presented in figure 4.44 on the previous page. The reduction in the normalised mean slope of the first EPSP within the first three minutes of KA application (61% (±6.6)) is significantly less in slices treated with either the $GABA_B$ receptor antagonist SCH 50911 (92% (±7.7), $p<0.01$) or the adenosine A_2 antagonist DMPX (89% (±3.8), $p<0.01$). The response in the presence of the adenosine A_1 receptor antagonist DPCPX just fails to reach significance (77% (±5.7), $p=0.08$). This effect continues until the end of the KA application period, at which point the EPSP slope in the presence of KA only has decreased to 44% (±6.9). This compares to mean normalised percentage slope values for slices in the presence of SCH 50911 of 65% (±6.0, $p<0.05$), with DPCPX of 59% (±2.4, $p<0.05$) and of 61% (±4.0, $p<0.05$) for the co-application of KA and DMPX. Co-application of slices with either the group I/II mGlur antagonist MCPG or the group II/III antagonist MPPG exhibit slope values which are greatly reduced compared to KA alone (21% (±2.4, $p<0.05$) and 25% (±8.0, $p=0.09$) respectively). The value for MPPG just fails to reach significance, which may reflect the low number of repeats in this data set.

A slightly different pattern of antagonist effectiveness against the KA response on the first EPSP slope is observed in the isolated CA1 preparation (figure 4.45). Within the first three minutes of KA application, slices which received pre-applied MPPG exhibit a markedly lower first EPSP slope (19% (±5.2)) than those which had received KA only (55% (±10.0)) ($p<0.05$), although this again may reflect the low number of repeat experiments in the MPPG group. The adenosine A_1 antagonist DPCPX significantly lowers the reduction in the EPSP slope observed with KA (78% (±4.0), $p<0.05$). This is also true for the blockade of adenosine A_2 receptors with DMPX during the first three minutes of KA application (82% (±3.9), $p<0.05$). By the end of the KA application period there is no significant difference to be found between the normalised mean first EPSP slopes of any of the treatment groups, although MPPG co-application does only just fail to reach significance ($p=0.053$). Following the was period, all groups exhibit a markedly reduced slope for the first EPSP compared with KA alone, however, this is likely to be a result of the stimulus response curve which was performed at the end of the KA application period in this data set but not at the end of any of the other groups.

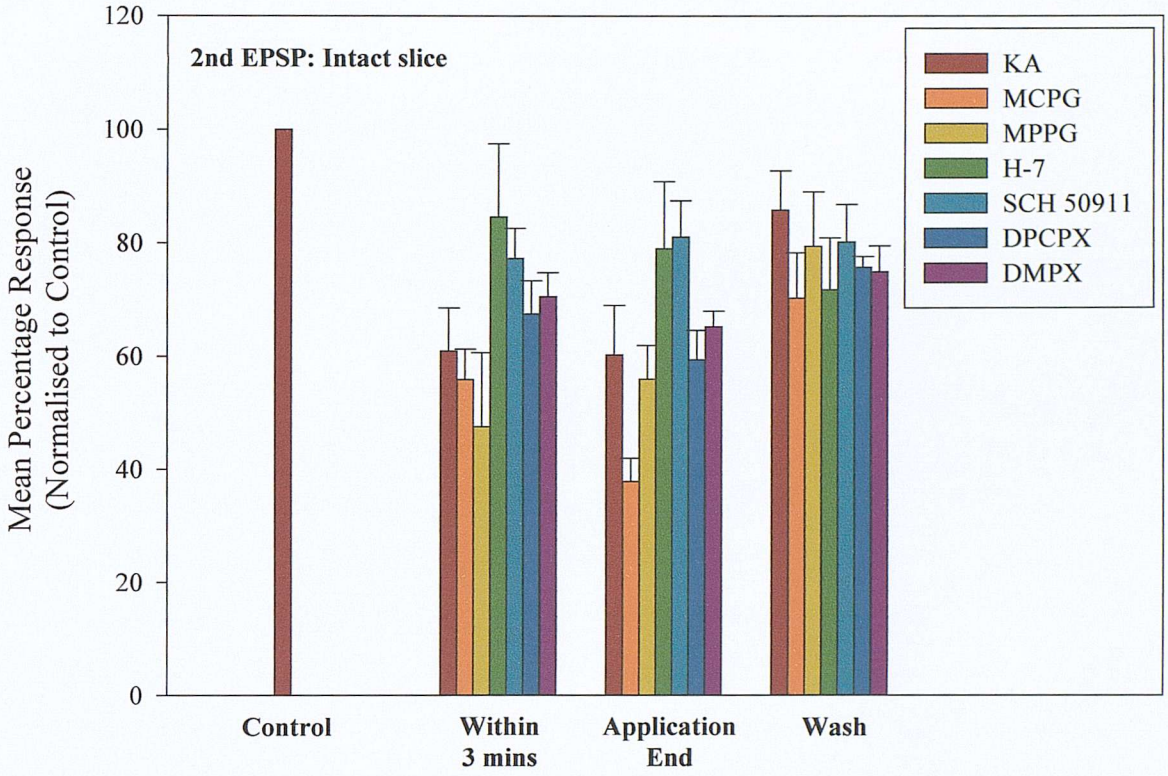

Figure 4.46 There was no significant difference observed between the action of KA alone on the second EPSP slope in the intact slice CA1 and in the presence of the various antagonists used above. However, the reduction in the response KA when co-applied with SCH50911 just failed to reach significance.

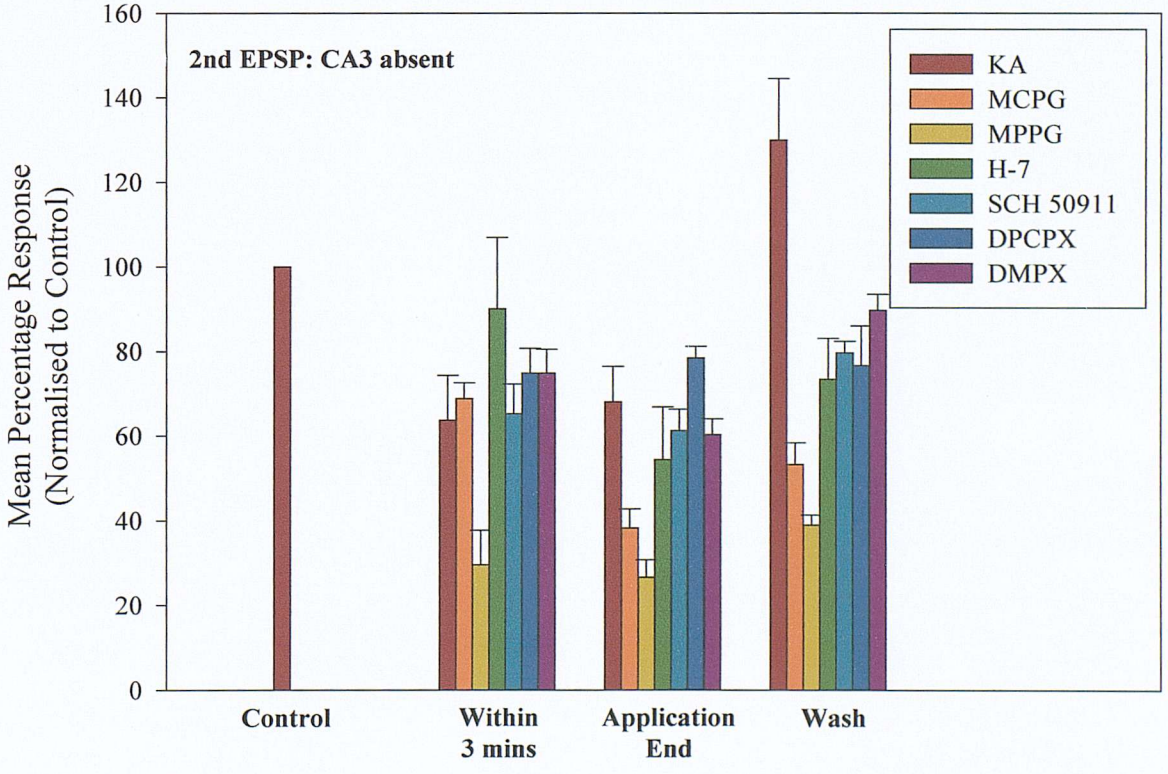

Figure 4.47 Co-application of MPPG, and latterly also MCPG significantly enhanced the reduction in the second EPSP slope that occurs with KA in the isolated CA1 preparation. No other treatments differed significantly from control.

There was no significant difference observed in mean normalised percentage slope of the second EPSP recorded during the various drug application protocols in the CA1 of intact hippocampal slice preparations (figure 4.46 on the previous page). This said, the co-application of the $GABA_B$ antagonist SCH 50911 only just failed to reach significance both within the first three minutes of KA application (77% (±5.3) compared to 61% (±7.6) for KA alone, $p=0.09$) and also at the end of 15 minutes of KA application (81% (±6.4) compared to 60% (±8.7) for KA alone, $p=0.07$).

This was not found to be the case in the isolated CA1 preparation (figure 4.47). Within the first three minutes of KA application in the absence of any antagonists, the normalised mean percentage slope of the second EPSP falls to 64% (±10.6). In the presence of the group II/III mGluR antagonist MPPG the slope is markedly reduced further to 30% (±8.2) ($p<0.05$), although once again the low number of repeats for this experiment may have produced a false positive result. By the end of the KA application period both the MPPG (27% (±4.1), $p<0.01$) and the group I/II antagonist MCPG (38% (±4.5), $p<0.05$) groups exhibit markedly reduced second EPSP slopes when compared to KA (68% (±8.4)). As with the first EPSP, all treatment groups differ significantly from the application of KA alone, probably due to short-term potentiation induced by the performance of a stimulus response curve during the end of the KA application period.

The presence of MPPG appears to block the initial increase in the first population spike amplitude caused by KA application in the CA1 of intact slices (figure 4.48) when compared to that for KA alone (92% (±10.0) and 139% (±11.3) respectively, $p<0.01$). Co-application of KA in the presence of H-7 does not result in a further increase in the first population spike amplitude within the first three minutes (101% (±3.2), $p<0.01$). In addition to this, the amplitude of the first population spike is not seen to decrease as the KA application period progresses (86% (±6.0) $p<0.01$).

In contrast to this, blockade of adenosine A_2 receptors with DMPX results in an enhanced response to KA within the first three minutes of application (181% (±8.1), $p<0.01$). In the continued presence of KA it can be seen that the presence of the group I/II mGluR antagonist MCPG leads to an exacerbation in the reduced population spike amplitude compared to KA alone (19% (±1.3) and 40% (±5.2) respectively, $p<0.05$). This reduction is attenuated by the blockade of group II/III mGluR receptors (66% (±5.4), $p<0.01$), $GABA_B$ receptors (108% (±11.1), $p<0.01$), and both adenosine A_1 (110% (±8.6), $p<0.01$) and A_2 receptors (113% (±12.1), $p<0.01$).

In the isolated CA1 preparation (figure 4.49), the initial response to the first three minutes of KA application is significantly enhanced by the blockade of group I/II mGluRs with MCPG compared to that of KA alone (344% (±26.9) compared to 117% (±3.3), $p<0.01$). Blockade of group II/III mGluRs with MPPG however results in a significant decrease in the mean normalised population spike amplitude during this period (85% (±19.6), $p<0.05$). Once again these observations are made with the stipulation that the low number of experiments in both of these groups may be responsible for the statistical significance which is observed. The presence of H-7 in the isolated slice also significantly blocks the initial increase in the first population spike amplitude following the addition of KA (107% (±3.7)) ($p<0.05$).

By the end of the KA application period both the MPPG and SCH 50911 groups exhibit an exacerbation in the reduction of the first population spike amplitude induced by KA (8% (±1.3) ($p<0.01$) and 60% (±7.9) ($p<0.05$) respectively compared to 88% (±9.9) for KA alone). Adenosine A_1 receptor antagonism appears to prevent this phenomenon (126% (±13.8), $p<0.05$).

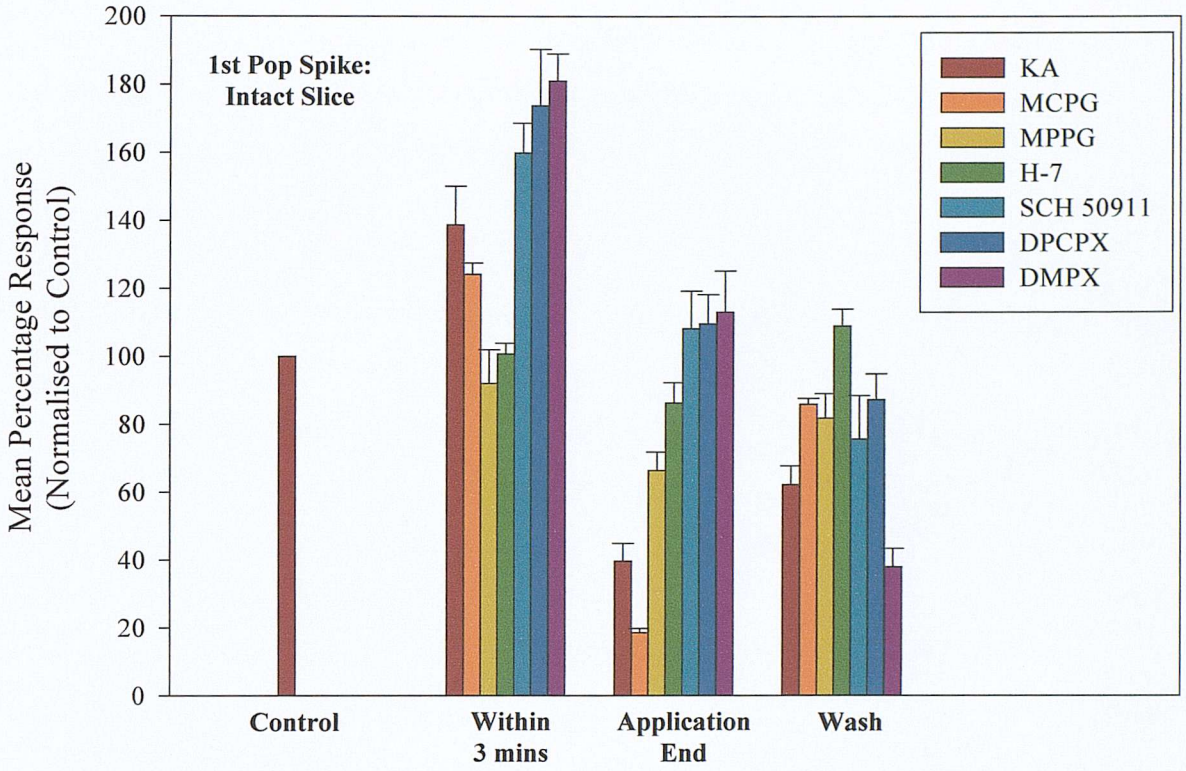

Figure 4.48 Co-application of both MPPG and H-7 block the initial increase in the first pop[ulation spike amplitude recorded from the CA1 of intact slices. Blockade of adenosine A_2 receptors with DMPX significantly enhanced the initial increase with KA. By the end of the KA application period, the presence of MCPG lead to a significantly enhanced reduction in the population spike amplitude, whilst this was significantly attenuated by SCH50911, DPCPX and DMPX.

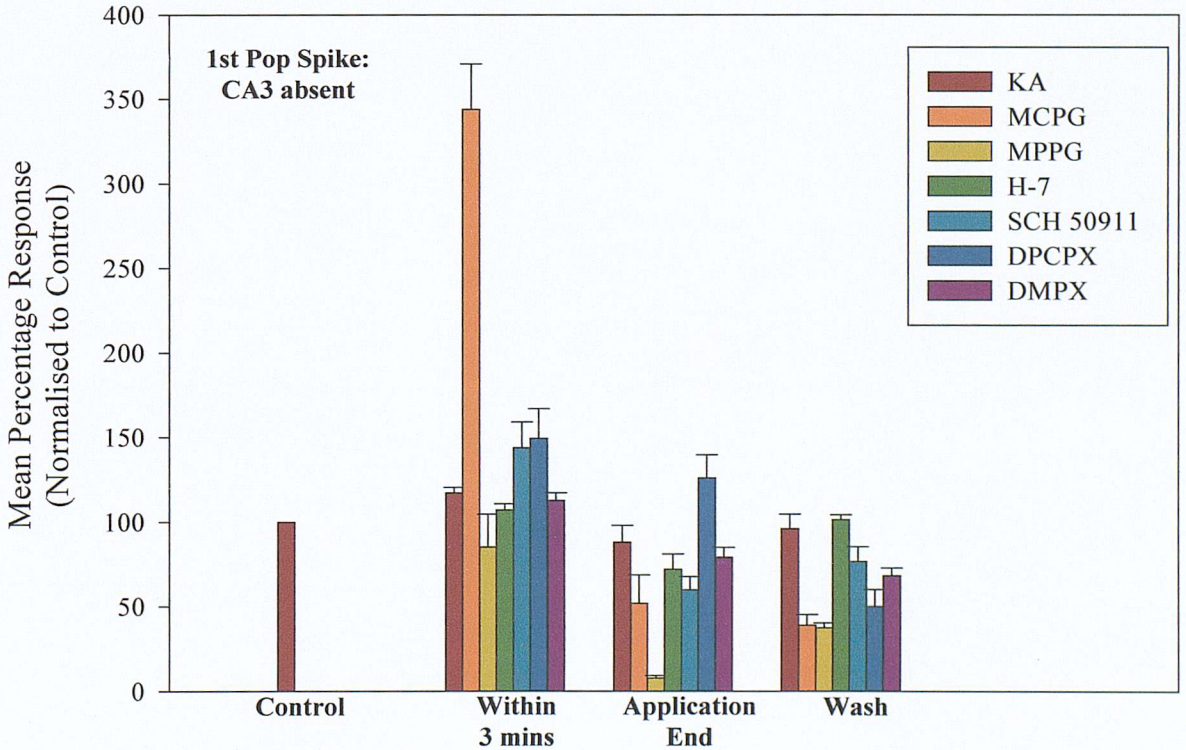

Figure 4.49 The initial response of the first population spike to KA is significantly enhanced by the presence of MCPG in the isolated CA1 preparation. In contrast, MPPG and H-7 significantly block this initial increase. By the end of the KA application period, the presence of MPPG or SCH50911 significantly enhance the reduction in population spike amplitude which occurs with KA, whilst DPCPX prevents this response.

Co-application of MPPG in the intact slice preparation (figure 4.50) appears to prevent the initial increase in the second population spike amplitude which occurs during the first three minutes of 1μM KA application (85% (±17.8) compared to 193% (±32.2) for KA only, $p<0.05$). In contrast to this blockade of $GABA_B$ receptors with SCH 50911 (399% (±32.8), $p<0.01$), adenosine A_1 receptors (333% (±41.9), $p<0.05$) and A_2 receptors (409% (±22.3), $p<0.01$) all result in an increased potentiation of the second population spike amplitude upon the application of KA.

This effect of both the $GABA_B$ and adenosine antagonists persists throughout the KA application period, apparently preventing the reduction of the second population spike as the KA application period continues. In the case of SCH 50911 application, the normalised mean percentage amplitude for the second population spike is 331% (±24.7) compared to 72% (±13.5) for KA administered alone ($p<0.01$). In the presence of DPCPX the normalised value for the second population spike is 204% (±22.5, $p<0.01$) and 353% (±29.7, $p<0.01$) for DMPX.

In the isolated CA1 preparation it can again be seen (figure 4.51) that the presence of MPPG once again prevents the increase in the second population spike amplitude that occurs during the first three minutes when KA is applied on its own (78% (±10.0) compared to 209% (±37.2) for KA alone, $p<0.05$). In the absence of an excitatory input from CA3, blockade of group I/II mGluR receptors potentiates the initial response to KA (329% (±37.3), $p<0.05$). This would also appear to be the case for the co-application of DPCPX (397% (±78.7), $p<0.05$). By the end of the KA application period, the presence of MPPG appears to result in a much greater reduction in the second population spike amplitude than is seen with KA alone (13% (±1.6) compared to 112% (±10.3), $p<0.01$). In contrast to this, the blockade of adenosine A_1 receptors with DPCPX appears to result in the continued potentiation of the second population spike amplitude until the end of the KA application period (374% (±68.3), $p<0.01$).

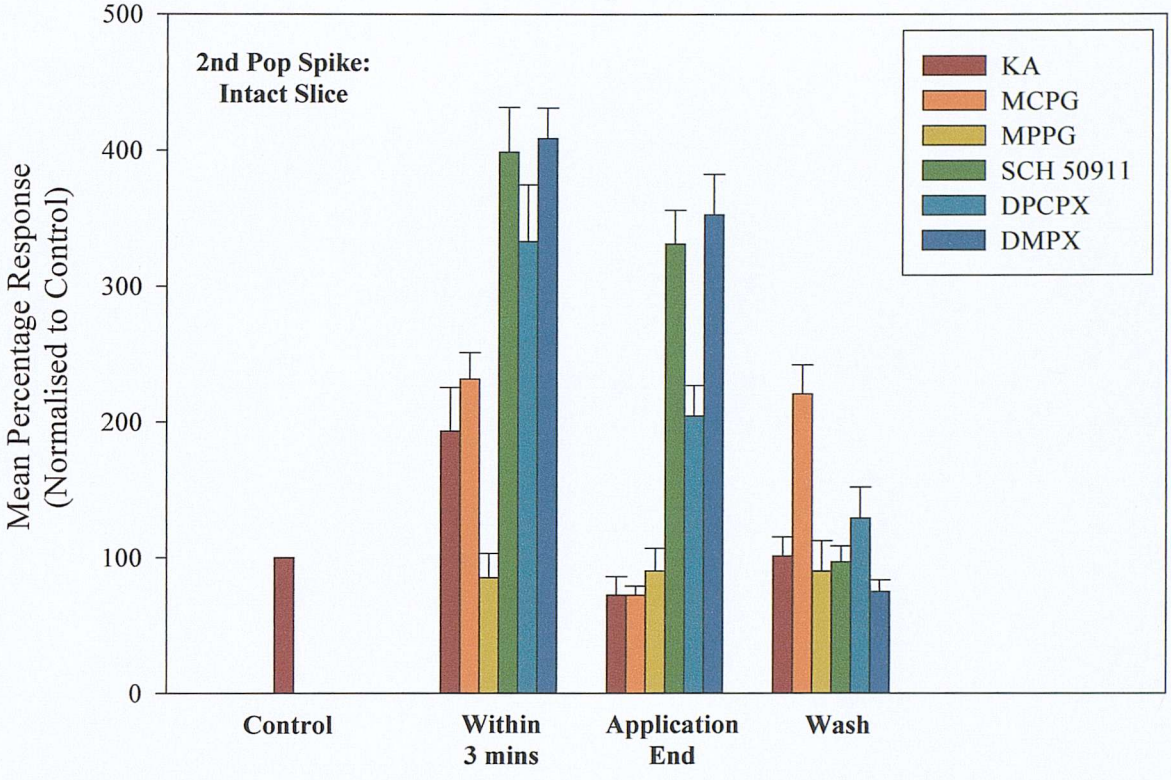

Figure 4.50 MPPG blocks the initial increase in the second population spike amplitude that occurs with 1μM KA in the intact slice CA1. This increase is significantly potentiated in the presence of SCH50911, DPCPX or DMPX. Their presence also prevents the KA induced reduction in population spike amplitude that occurs subsequently.

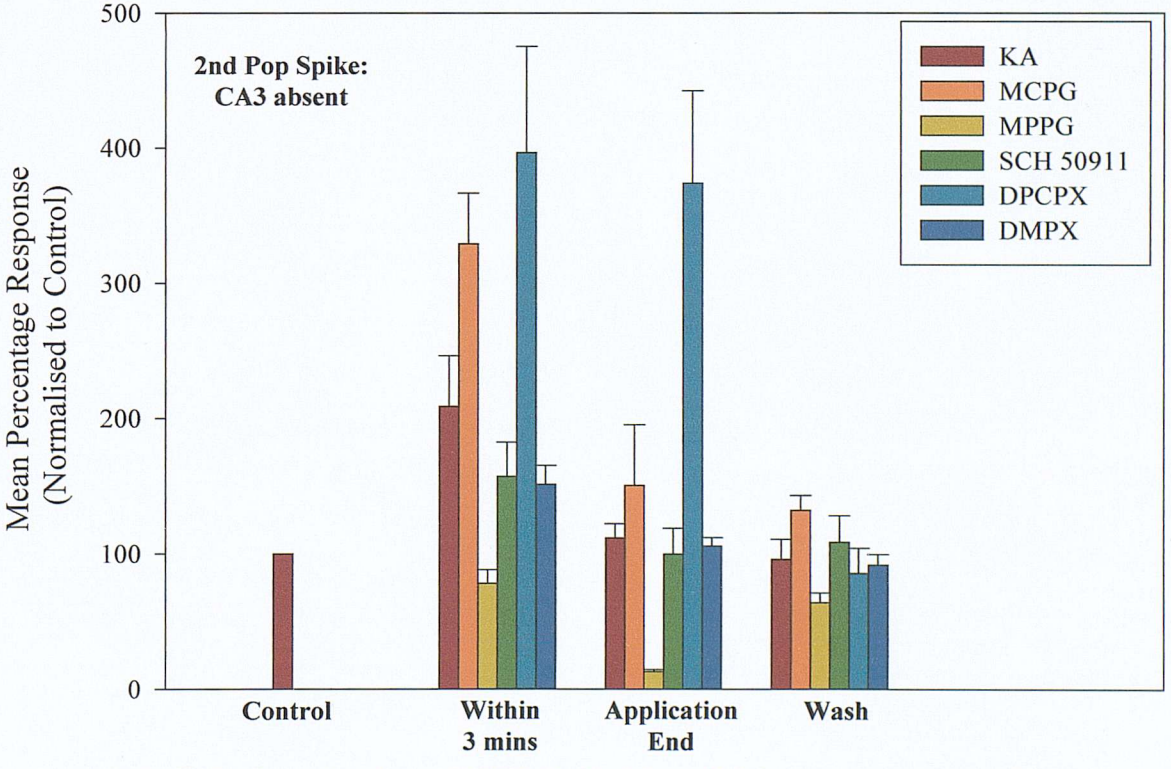

Figure 4.51 MCPG enhanced, whereas MPPG blocked the initial increase in the second population spike amplitude with KA in the isolated CA1 preparation. DPCPX co-application with KA also resulted in an enhanced initial response. By the end of the KA application period, MCPG co-application resulted in a significantly reduced population spike amplitude, whereas the DPCPX treated slices remained significantly elevated above control.

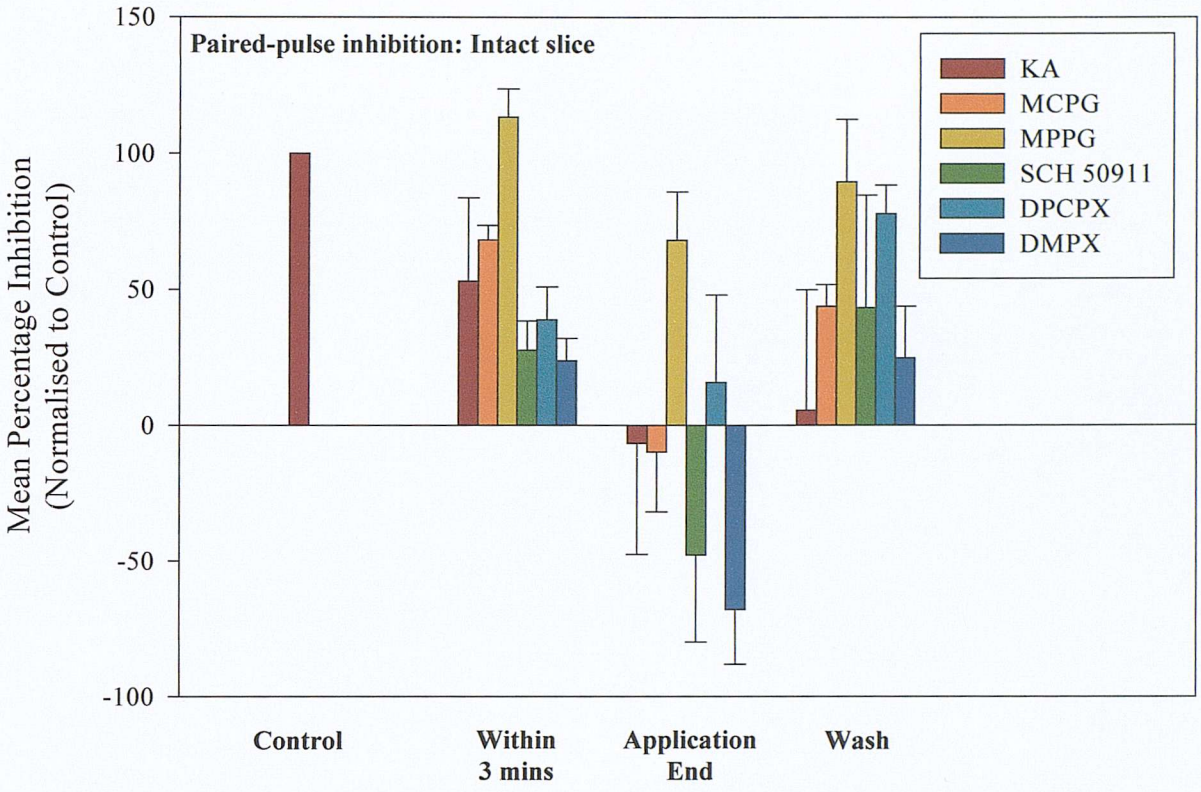

Figure 4.52 KA application reduced the paired-pulse inhibition in the CA1 of intact slices. This was not significantly blocked by any antagonist treatment.

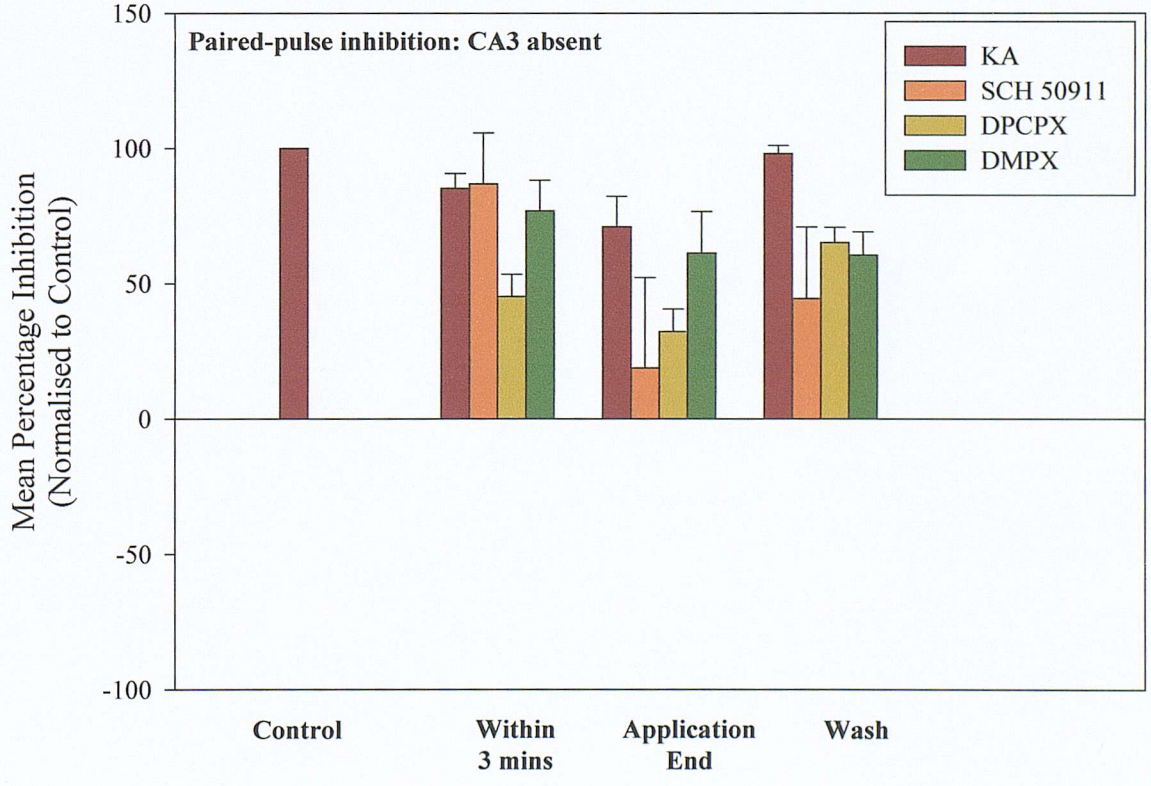

Figure 4.53 The adenosine A_1 receptor antagonist DPCPX significantly potentiated the effect of KA on paired-pulse inhibition in the isolated CA1 preparation. No other treatment group differed significantly from control.

In the intact slice preparation (figure 4.52), there is no significant difference observed between the effect of KA alone on the normalised percentage inhibition and any of the other non-ionotropic glutamate receptor drug treatments. However, this is likely to be due to the high degree of variation in the KA response in these preparations and the low number of repeat experiments for example in the MCPG (n=2) and MPPG (n=3) groups.

In the isolated slice preparation (figure 4.53) antagonism of the adenosine A_1 receptor produces a significant potentiation of the effects of KA on the inhibition both within the first three minutes of KA application (45% (±8.1) compared to 85% (±5.5) $p<0.01$) and by the end of 15 minutes KA application (32% (±8.4) compared to 71% (±11.1) for KA only, $p<0.01$). No significant difference was observed for the response to KA in the presence of either SCH50911 or DMPX in the isolated CA1 preparation.

4.4 Discussion

4.4.1 Effect of KA on the EPSP slope in CA1

As reported in the previous chapter, application of 1μM KA to both intact slices (figure 4.3) and isolated CA1 preparations (figure 4.6) results in a reduction in the slope of the EPSP recorded from *stratum radiatum*. This occurs irrespective of the presence of the CA3 and at a time when the population spike amplitude is increasing, suggesting a presynaptic response at the Schaffer collateral terminal. Whilst the data in the previous chapter is suggestive of a KA receptor mediated response, it is possible that other receptor populations may be indirectly involved. To this end, the response to KA in both intact and isolated slices was investigated in the presence of antagonists for group I/II and group II/III mGluRs, $GABA_B$ receptors and adenosine A_1 and A_2 receptors. In addition, the effect of the PKC blocker H-7 was investigated on the KA response to assess the possibility of a metabotropically coupled KA receptor as has been previously resported to be involved in the downregulation of GABA release from interneurones (Cunha *et al* 1999 and the inhibition of the I_{sAHP} recorded from CA1 pyramidal cells (Melyan *et al* 2002).

4.4.1.1 Metabotropic glutamate receptors

Metabotropic glutamate receptors (mGluRs) make up a family of at least eight 7 transmembrane domain receptors coupled to G-proteins, and can be divided into three groups related by their sequence homology (Conn and Pin 1997). Their activation results in various modulatory effects within the hippocampus.

Group I mGluRs, comprising mGluR1 and mGluR5, are able to modulate the excitability of hippocampal pyramidal cells *via* coupling to Ca^{2+}, potassium and nonselective cation channels (Shigemoto *et al.* 1997). Their activation on pyramidal cells leads to an increase in cell excitability. This is thought to be *via* a direct postsynaptic action. Both Group I and group III mGluRs (consisting of mGluR4, 6, 7and 8) modulate the release of glutamate from the Schaffer collateral terminals. It would appear that the two most likely candidates for this presynaptic modulation are mGluR5 and mGluR7 (Conn and Pin 1997). There may be some specialisation in the distribution of these receptors however, since it has been shown that mGluR7 appears to be preferentially located on presynaptic glutamatergic terminals at synapses with interneurones (Shigemoto *et al.* 1996,1997). In contrast to this, it would appear that group II and group III mGluRs

are responsible for the modulation of glutamate release from the mossy fibres synapsing onto CA3 pyramidal cells (Cao *et al.* 1995, Ishida *et al.* 1993).

The presumed sites of action of the drugs used in this chapter are presented in figure 4.54.

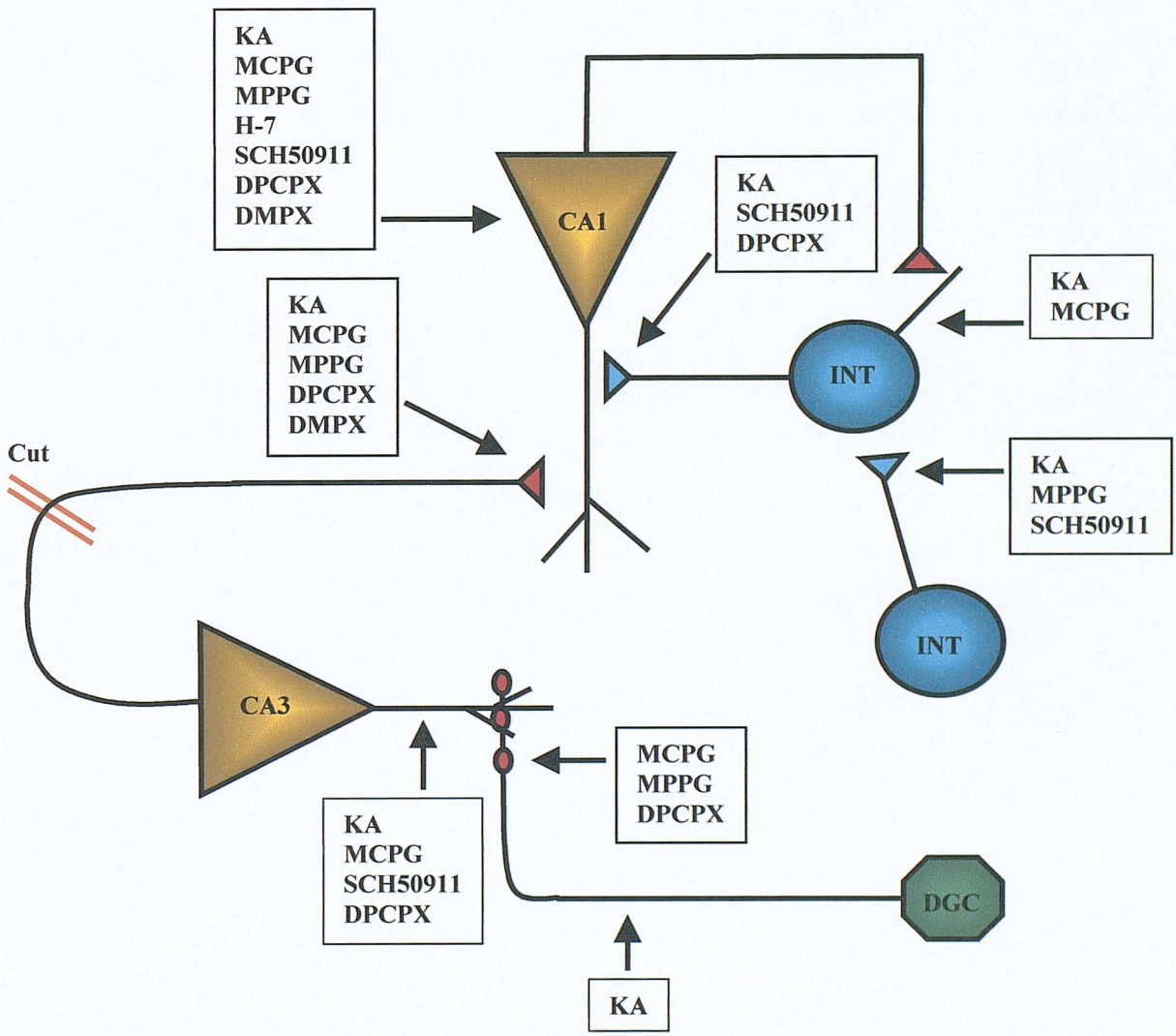

Figure 4.54 Expected sites of action within the hippocampal tri-synaptic pathway for the antagonists studied in this chapter. DGC, dentate granule cell; INT, interneurone; red triangles/ circles, glutamatergic synapse; blue triangles, GABAergic synapse

4.4.1.1.1 Group I/II mGluRs

In the isolated slice (figure 4.12) an increase in the slope of both EPSPs was also observed during the application of the group I/II mGluR antagonist MCPG. This could be explained by an increase in glutamate release from the Schaffer collateral terminals following blockade of presynaptic metabotropic receptors, which may imply that this response is somehow masked in the intact slice (figure 4.9) by a reduction in the excitability of CA3 pyramidal cells in the presence of the drug.

Upon the application of 1μM KA, the EPSP slopes decrease in both the intact and isolated preparation in a manner comparable to that observed for KA alone. This may indicate that the activation of Group I/II mGluR's plays no role in the effect of KA with respect to the release of glutamate from the Schaffer collateral terminals in either preparation. One caveat to be borne in mind is the low number of experiments in both of these data sets (n=2 for the intact slice and n=3 for the isolated CA1 preparations) which prevents any firm conclusions from being reached with regard to these data.

4.4.1.1.2 Group II/III mGluRs

The effects of the non-selective group II/III antagonist MPPG are somewhat different. In the intact slice (figure 4.15) MPPG application causes an increase in both EPSP slopes. Thus it may be that blockade of presynaptic group III metabotropic receptors on the Schaffer collateral terminals results in a facilitation of glutamate release. This in turn would be expected to increase the slope of the EPSP measured from *stratum radiatum* and at the same time to an increase in the population spike amplitude. In the isolated CA1 preparation (figure 4.18) there is no significant change seen in the population spike amplitude with MPPG, although once again the EPSP slopes are markedly increased. This would tend to point to a presynaptic site of action rather than an increased excitation of CA3 pyramidal cells.

The reduction in the first and second EPSP slopes produced by the addition of KA in the intact slice appears to be exacerbated by the presence of MPPG, although this does not reach significance.

4.4.1.2 The role of PKC

As seen previously (Corradetti *et al.* 1989), the slope of the first EPSP increased in both the intact (figure 4.21) and isolated slice (figure 4.24) in the presence of 20μM H-7. Interestingly the second EPSP exhibits a marked depression during this time, possibly due

to a reduced efficiency in the mechanisms regulating presynaptic Ca^{2+} channels on the Schaffer collateral terminals leading to a reduction in glutamate release following the second stimulus. However, it is also possible that the epileptiform activity of CA1 pyramidal cells following the first stimulus is limiting the size of the second EPSP due to a continued depolarisation following the first stimulus rendering the CA1 pyramidal cells partially refractory at the time of the second stimulus. Application of H-7 (20μM) produced no significant change in the response of the EPSP in the presence of KA however, thus suggesting that downregulation of glutamate release from the Schaffer collaterals occurs independently of PKC (or PKA) activation. This may indicate a difference the way in which KA modulates the release of neurotransmitter at excitatory and inhibitory synapses since Cunha *et al.* (1999) have demonstrated a dependence on PKC for the reduction in GABA release by KA in hippocampal synaptosomal preparations. In addition, Rodriguez-Moreno and Lerma (1998) have shown PKC inhibitors to abolish the effect of KA on evoked GABAergic inhibition.

4.4.1.3 $GABA_B$ receptor blockade

$GABA_B$ receptors are a class of inhibitory metabotropic receptors activated by GABA and coupled to inhibitory G proteins such as G_I and G_o. In the hippocampus these receptors are linked to the activation of a slow potassium conductance which leads to hyperpolarisation of the membrane. In addition to a postsynaptic locus of action, they may be located presynaptically, their activation bringing about an inhibition of transmitter release (Bowery *et al.* 1980, Lanthon and Cotman 1981). Frerking *et al* (1999) saw a reduction of approximately 50% in the KA induced inhibition of GABA mediated evoked IPSCs in the presence of the $GABA_B$ antagonist SCH50911. This may indicate a contribution of presynaptic $GABA_B$ receptor activation on interneurone terminals *via* an increase in GABA release due to activation of postsynaptic KA receptors located on the soma and dendrites of interneurones in the mechanism of KA induced downregulation of GABA release.

Since this work was carried out in hippocampal slices in which the inhibitory component had been pharmacologically isolated it was of interest to see whether a similar effect could be observed in the field response. To this end recordings were made in both intact hippocampal slices and isolated CA1 preparations during the co-application of SCH50911 and KA.

Application of 20μM SCH50911 does not significantly affect the slope of either EPSP in either the intact (figure 4.27) or isolated slice (figure 4.30) preparations. The application of 1μM KA results in a significantly reduced effect of KA on the first EPSP in intact hippocampal slices ($p<0.01$) which is not seen on the second EPSP. Neither is the effect of KA on either EPSP in the isolated CA1 (figure 4.45 and 4.47) preparation significantly different from control.

4.4.1.4 Adenosine mediated modulation of the EPSP

Adenosine plays a major role in the modulation of synaptic activity throughout the central nervous system (Kostopoulos 1988; Fredholm 1995) and is derived mainly from the hydrolysis of nucleotides by a number of endo- and ectonucleotidases (Brundege *et al.* 1997 Dunwiddie *et al.* 1997). It is known that levels of extracellular adenosine rise significantly during seizure activity (During *et al.* 1992; Berman *et al.* 2000) as well as in response to field stimulation and hypoxia (de Mendonca and Ribeiro 1997). Therefore it is possible that adenosine release may play some part in the downregulation of the release of glutamate or GABA seen with 1μM KA.

4.4.1.4.1 The A_1 receptor

The adenosine A_1 receptor appears to be particularly abundant in the hippocampus (Fastbom *et al.* 1987), and it is presumably *via* this receptor that many of adenosine's inhibitory effects on neurotransmission occur. Indeed Dunwiddie (1985) has observed adenosine to exert a tonic effect on electrophysiological activity within the hippocampus, however these effects may be temperature dependent (Masino and Dunwiddie 1999), and therefore may not be pronounced in recordings made at room temperature.

Application of the adenosine A_1 receptor antagonist DPCPX (50nM) did not significantly affect the field EPSP slopes recorded from the intact slice CA1 (figure 4.33), but interestingly potentiated the EPSP slopes in the isolated CA1 preparation ($p<0.05$) (figure 4.36). Addition of 1μM KA in the presence of DPCPX in the intact slice resulted in a reduction in both the first and second EPSP slopes. This effect was not significantly different to the response to KA alone. DPCPX significantly ($p<0.05$) reduced the response of the first (figure 4.45) but not the second (figure 4.47) EPSP to the application of KA in the isolated CA1 preparation.

4.4.1.4.2 The A_2 receptor

Application of the A_2 selective antagonist DMPX (10μM) caused no significant change to the EPSP slopes in the intact slice preparation (figure 4.39). In the isolated CA1 (figure 4.42), DMPX application resulted in a significant reduction in the slope of the second EPSP ($p<0.01$). It is possible that this phenomenon may reflect an unmasking of the inhibitory effects of A_1 receptor activation leading to a reduced presynaptic Ca^{2+} influx in both the Schaffer collaterals. This in turn would lead to a decrease in the release of glutamate and hence a reduced EPSP slope.

Since the first EPSP slope in the intact slice is significantly steeper than the KA control, it may be that A_2 blockade is somehow reducing the depressant effects of KA in the CA3, enabling an enhanced release from the Schaffer collateral terminals. It is possible that this could be occurring *via* an enhanced action of adenosine at postsynaptic A_1 receptors on CA3 pyramidal cells, preventing a depolarisation block occurring in this region following KA administration. This may in turn allow for more effective electrical coupling between CA3 and CA1.

4.4.2 Effect of KA on the first Population Spike Amplitude

4.4.2.1 Response to Kainic Acid

As described in chapter 3, application of 1μM KA caused a marked transient increase in the first population spike amplitude within the first three minutes in both the intact (figure 4.3) and isolated CA1 preparations (figure 4.6). This increase occurs at a time during which the EPSP slope has already begun to decrease, suggesting that the observed increase is not a consequence of an increase in glutamate release from the Schaffer collaterals following the stimulation of CA3 pyramidal cells by KA. In support of this, the normalised data shows that this increase in amplitude from control is only marginally greater in the intact slice CA1 (139% (±11.3)) (figure 4.48) when compared to the response of the isolated CA1 preparation (117% (±3.3)) (figure 4.49). Therefore, KA application is either directly causing an excitation of the CA1 pyramidal cell population, or indirectly resulting in an increase in the pyramidal cell output (as measured by population spike amplitude) *via* a reduction in the efficacy of GABAergic inhibitory mechanisms, or a combination of both of these.

By the end of the KA application period, the population spike amplitude is reduced from control in both preparations. This may be due to the somato-dendritic KA receptor

activation of interneurones (Cossart *et al* 1998; Frerking *et al* 1998, 1999). This would be expected to lead to an increase in GABA release and thus to a reduction in the input from the CA1 pyramidal cell population.

4.4.2.1 mGluR antagonism and KA response

4.4.2.1.1 Group I/II mGluR antagonism

In the presence of the group I/II mGluR antagonist MCPG, the amplitude of the first population spike decreased in both the intact slice (figure 4.9) and isolated CA1 preparations (figure 4.12). This may reflect a reduction in the post-synaptic response to synaptically released glutamate mediated by group I mGluRs on CA1 pyramidal cells. Thus blockade of these receptors lead to a reduction in CA1 pyramidal cell excitability and hence to a decreased population spike amplitude.

Upon the addition of 1μM KA, no significant difference was observed when compared with the increase in the normalised population spike amplitude observed during the first three minutes of KA application in the intact slice preparation (figure 4.48) in the absence of MCPG. In the isolated preparation, however, this increase was markedly potentiated compared to that for KA alone (figure 4.49). However, this marked potentiation should be treated with caution due to the low number of experiments in this treatment group.

4.4.2.1.2 Group II/III mGluR antagonism

Addition of the group II/III mGluR antagonist MPPG to the superfusing ACSF led, in the intact slice preparation (figure 4.15), to an increase in the amplitude of the population spikes recorded from CA1. There was no significant corresponding increase observed in the isolated CA1 preparation (figure 4.18). This tends to suggest that the potentiation observed in the intact slice preparation occurred as a result of the blockade of group II/III mGluRs upstream of the CA1 region.

In the intact slice (figure 4.48), the presence of MPPG causes a significant blockade of the initial increase in the population spike amplitude when compared to KA alone ($p<0.01$). This reduction in the response to KA persists throughout the KA application period. The initial effects of KA on the population spike are also significantly blocked in the isolated CA1 (figure 4.49) in the presence of MPPG ($p<0.01$). In contrast to

the intact slice, however, the reduction in the population spike amplitude following this initial phase appears to be significantly exacerbated in the isolated slice ($p<0.01$).

4.4.2.2 Protein kinase C inhibition

Introduction of the PKC inhibitor H-7 to the superfusing ACSF resulted in an increased population spike amplitude in both the intact slice (figure 4.21) and isolated CA1 preparations (figure 4.24). Corradetti *et al.* (1989) found H-7 abolished the intracellularly recorded evoked IPSPs from CA1 pyramidal cells, which lead to the onset of epileptiform activity. It is likely that this reduction in inhibitory function is responsible for the observed increase in the population spike amplitude.

Addition of KA in the presence of H-7 did not result in a further increase in population spike amplitude in either of the preparations used. Nor did it increase the number of spikes in the epileptiform burst produced by H-7. This observation may suggest agreement with those of Melyan *et al.* (2002), who found that the post-synaptic GluR6 containing receptor mediated inhibition of the I_{sAHP} in CA1 pyramidal cells was blocked by the PKC inhibitor calphostin C. Inhibition of the I_{sAHP} by KA would be expected to lead to an increase in the excitability of the pyramidal cell population in CA1. This in turn would be expected to lead to either an increased population spike amplitude or an increase in the number of spikes in the epileptiform burst. However, it is also possible that KA does not stimulate a further increase in population spike amplitude as a result of the pyramidal cell population already working at maximal output under the impaired inhibitory conditions which lead to the observed epileptiform activity.

Therefore it is possible that PKC is not involved in the KA response but its effects on inhibitory function obscure the actions of KA. Were this the case, then it would not be unreasonable to suppose that a direct excitatory effect by KA on the CA1 pyramidal cell population under conditions in which the inhibitory mechanisms were reduced could lead to an increase in the number of spikes appearing in the epileptiform burst. However, this does not occur in either intact slices (figure 4.22) or isolated CA1 preparations (figure 4.25).

Therefore, this may provide further evidence to support a metabotropic mechanism of action for KA on the CA1 pyramidal cell as opposed to an ionotropic effect.

4.4.2.3 $GABA_B$ antagonism

In both the intact (figure 4.27) and isolated slice preparations (figure 4.30), application of 20μM SCH50911 caused a significant reduction in the amplitude of both the first and second population spike, without significantly affecting the slope of either EPSP. A similar effect has been seen with the antagonist 2-hydroxy-saclofen (Caddick *et al.* 1995) which could be abolished by the co-application of phaclofen. Since the co-application of bicuculline did not alter the response to 2-hydroxy-saclofen it was deemed unlikely that blockade of $GABA_B$ receptors was causing a facilitation of tonic GABA release from interneurones and so reducing the amplitude of the population spike.

Co-application of SCH50911 with KA did not significantly affect the initial response to KA in either preparation. However, the population spike amplitude in the intact slice (figure 4.27) remains significantly elevated until the end of the KA application period. Interestingly, the converse is true for the isolated CA1 preparation (figure 4.49), the normalised population spike amplitude being significantly reduced in comparison to the normalised values for KA alone.

4.4.2.4 Adenosine Receptor Antagonism

4.4.2.4.1 The A_1 Receptor

The adenosine A_1 receptor antagonist was applied to slices both prior and during the application of KA. Application of DPCPX could result in two possible consequences. Firstly, the role of the A_1 receptor in the response to KA would be revealed. Secondly, the effect of the unopposed action of adenosine at the A_2 receptor during the KA response could emerge. The A_2 adenosine receptor has been shown to play a facilitatory role within the hippocampus. For example, activation of the A_{2A} subtype has been demonstrated by Goncalves *et al.* (1997) to facilitate synaptic activity within the CA3 region.

A_1 receptor antagonism did not significantly affect the population spike amplitudes recorded from the intact slice CA1 (figure 4.30). In the isolated slice however, it reduced the amplitude of the second population spike ($p<0.01$) (figure 4.33), which may reflect an increased excitatory drive to the interneuronal population following tonic A_2 receptor activation leading to a facilitation of glutamate release from the Schaffer collaterals. Co-administration of KA with DPCPX in the intact slice preparation resulted in a strong potentiation of the population spike which was significantly more pronounced than

observed for KA only (figure 4.48). This potentiation persisted throughout the KA application period ($p<0.01$). In addition to this the field population spike recording exhibited epileptiform activity in 2 out of the 5 slices tested by the end of the KA application period. This epileptiform activity may occur as a result of the blockade of post-synaptic A_1 receptors, which are known to exert an inhibitory influence on NMDA receptor mediated currents recorded from acutely dissociated CA1 pyramidal cells (de Mendonca *et al* 1995). In addition to this, A_1 receptor blockade prevents an adenosine mediated K^+ efflux from the postsynaptic cell. Combining these effects with the inhibitory effect of KA on the I_{sAHP} would be presumed to lead to a hyperexcitable pyramidal cell population. It is also likely that the presence of an A_1 antagonist potentiates the effects of endogenous adenosine at excitatory A_{2a} receptors (Sebastiao and Ribeiro 2000), which would be expected to lead to an increased activation of NMDA receptors, again leading to increased excitability.

A similar pattern of response is seen in the isolated CA1 preparation (figure 4.49 and 4.51) with regard to the potentiation of the first and second population spikes, which again remain elevated throughout the KA application period. Epileptiform activity was observed in 1 out of the 5 preparations tested. This would tend to indicate that an upstream effect of CA3 is not important in the maintenance of an elevated output from the pyramidal cells of CA1. This adds further weight to the hypothesis that this is a direct postsynaptic effect of CA1 pyramidal cells.

4.4.2.4.2 The A_2 Receptor

Administration of the A_2 selective antagonist DMPX caused no significant change to the population spike amplitude in the intact slice preparation (figure 4.39). However, in the isolated CA1, DMPX application resulted in a small, but significant potentiation of the first population spike ($p<0.05$) (figure 4.42). This may reflect an unopposed action of endogenously released adenosine at A_1 receptors located presynaptically on interneuronal terminals leading to a reduced presynaptic Ca^{2+} influx. This would be expected to reduce GABA release, leading to a decrease in the tonic inhibition of pyramidal cell activity and hence an increase in population spike amplitude.

In the intact slice, addition of 1μM KA in the presence of DMPX produces a potentiation of both the first and second population spikes that is significantly greater than would be expected for KA alone ($p<0.01$) (figures 4.49 and 4.51) which is sustained throughout the KA application period. This is not seen to be the case in the isolated CA1

(figures 4.50 and 4.52), in which the changes in population spike amplitude are not significantly different to control.

This prolonged duration of the increased population spike amplitude throughout the course of KA application may reflect activation of A_1 receptors on the presynaptic terminals of interneurones. Administration of KA would be expected, among it's many effects, to excite the interneurones of CA1 *via* activation of somato-dendritic KA receptors (Frerking *et al.* 1998, Cossart *et al.* 1998). This would be expected to lead to an increase in the tonic release of GABA, which would then lead to a reduction in the amplitude of the population spike. It is possible therefore that under circumstances such as the blockade of the A_2 receptor, which presumably leaves the action of tonically released adenosine at the A_1 receptor unopposed, that this release of GABA may be reduced. This may then in turn prolong the elevation of the population spike amplitude, since the post-synaptic, GluR6 mediated inhibition of the pyramidal cell I_{sAHP} has been found to be non-desensitising (Melyan *et al* 2002 and personal communication).

4.4.3 Effect of KA on paired-pulse inhibition

As previously described in chapter 3, kainate has been reported to cause an increase in stimulus evoked failures of GABAergic transmission (Frerking 1998). In addition, the frequency of miniature IPSPs recorded from CA1 pyramidal cells in the presence of tetrodotoxin was reduced by KA application (Rodriguez-Moreno *et al* 1997, Rodriguez-Moreno and Lerma 1998). This response was sensitive to both pertussis toxin and inhibitors of protein kinase C, implicating a metabotropic mechanism of action. This lead to speculation of a presynaptic, metabotropically coupled KA receptor being involved in the downregulation of GABA release from interneuronal terminals.

An alternative (or perhaps complimentary) hypothesis has been put forward for the mechanism by which KA downregulates the release of GABA from interneurones by Frerking *et al* (1998). It is known that activation of GluR5 containing KA receptors located in the somato-dendritic compartment of the interneurone leads to an increase in the number of EPSPs recorded from these interneurones. This in turn produces an increase in the frequency of interneuronal spiking and hence an increase in the release of GABA (Cossart 1998; Frerking *et al.* 1998, 1999). According to Frerking's hypothesis (1999) the release of GABA is sufficient to activate pre-synaptic $GABA_B$ receptors and thus, by an as

yet undetermined signalling cascade, reduce Ca^{2+} influx and hence the release of GABA. In Frerking's hands, antagonism of $GABA_B$ receptors did in fact reduce the effect of KA on the release of GABA by approximately 50%. However, this mechanism is contentious since Min M-Y *et al* (1999) observed no effect with $GABA_B$ antagonists on KA receptor mediated downregulation of GABA release by endogenously released glutamate following a brief burst of stimuli.

It is hoped that the data presented here may help to elucidate the possible mechanism for the effect of KA on the release of GABA from the interneurone.

4.4.3.1 Metabotropic glutamate receptor antagonism

As mentioned previously, mGluRs are involved in the regulation of glutamate and GABA release onto the principal cells of the hippocampus. In addition to this, Semyanov *et al.* (2000) have demonstrated that activation of group III mGluRs by spillover of glutamate from the synapse regulates the release of GABA from one interneurone onto its neighbours. This would presumably lead to a disinhibition of the interneuronal population, leading to a greater degree of both tonic and evoked inhibition.

It is therefore possible that blockade of mGluRs may unmask some component of the effect of KA on the inhibitory mechanisms within the slice.

4.4.3.1.1 Group I/II mGluR antagonism

Application of the group I and II antagonist MCPG to both intact (figure 4.9) and isolated hippocampal slices (figure 4.12) caused a significant depression of both the first and second population spike amplitudes. Also during this time the percentage inhibition increased (figures 4.10 and 4.113). This indicates a change in the ratio between the first and second population spikes. In the intact slice preparation (figure 4.9), this change was characterised by a greater reduction in the first spike than in the second. Conversely, in the isolated CA1 preparation, the second spike was more markedly reduced than the first (figure 4.12).

In the intact slice preparation, introduction of MCPG to the recording chamber would be expected to block the action of mGluRs at several sites. Firstly, group II receptors on the mossy fibre terminals consisting mainly of the mGluR2 subtype (Shigemoto *et al.* 1997) would be expected to exhibit a reduced if not abolished function. Activation of these receptors has been demonstrated to reduce the release of glutamate

onto CA3 pyramidal cells (Lanthorn *et al.* 1989, Yokoi *et al.* 1996). This would tend to suggest that the CA3 pyramidal cells may be in a state of greater excitation than during the control period. Secondly, activity of group I mGluR receptors on the Schaffer collateral terminals (Gereau and Conn 1995) would also be antagonised. In addition to this, MCPG would also be expected to reduce the activity of postsynaptically located group I mGluRs on the CA1 pyramidal cells (Lujan *et al* 1996). Activation of these receptors has been found to result in an excitation of CA1 pyramidal cells.

Thus the pattern of response observed in the intact slice upon the introduction of MCPG may reflect a complex series of events including a facilitation of glutamate release from the mossy fibre pathway onto the pyramidal cells of CA3. This results in a greater firing probability for these cells. This in turn could be expected to lead to an enhanced release of glutamate from the Schaffer collateral terminals. This would certainly be more likely if the metabotropic feedback control of glutamate release were compromised, as would be the case in the presence of MCPG.

From the raw data we can see that the EPSP slopes do not increase significantly in the presence of MCPG (although the second EPSP appears to rise slightly) and at the same time the population spike amplitudes fall. This could imply that blockade of postsynaptic group I mGluRs on the CA1 pyramidal cells is sufficient to prevent an increase in the excitation of the pyramidal cell population in response to an increase in glutamate release from the Schaffer collaterals. It would appear, however, that the excitatory drive to the interneurone population within the CA1 has increased. Hence the marked reduction in the second population spike.

It is possible that facilitation of glutamate release from the mossy fibres has increased the spontaneous activity of the CA3 pyramidal cell population which may have resulted in an increase in the tonic release of GABA from CA1 interneurones. This may also contribute to the reduced first population spike amplitude observed during this period.

In the isolated CA1 preparation (figure 4.12), application of MCPG results in a marked reduction in the first population spike amplitude. The second spike amplitude is also reduced, but to a much lesser degree. This would tend to suggest that the upstream effects of CA3 during the application of MCPG must have been maintaining the excitation of the CA1 pyramidal cell population. This could occur as a result of an increased excitation of CA3 pyramidal cells following a facilitation of glutamate release from the mossy fibre terminals onto CA3 pyramidal cells.

The normalised percentage inhibition calculated for co-application of MCPG with 1μM KA did not differ significantly from KA alone at any time point in the intact slice (figure 4.52).

4.4.3.1.2 Group II/III antagonism

In the intact slice MPPG application causes an increase in both the population spike amplitudes and EPSP slopes (figure 4.15) but no significant change in the percentage inhibition (figure 4.16). It could be that blockade of presynaptic group III metabotropic receptors on the Schaffer collateral terminals results in a facilitation of glutamate release. This in turn would be expected to increase the slope of the EPSP measured from *stratum radiatum* and at the same time to an increase in the population spike amplitude. In the isolated CA1 preparation (4.17) there is no significant change seen in the population spike amplitude with MPPG, although once again the EPSP slopes are markedly increased. This would tend to point to a presynaptic site of action rather than a somato-dendritic response of the CA3 pyramidal cells.

In the presence of MPPG, the response of both the first and second population spikes is altered in both preparations during the first three minutes of KA application (figures 4.48, 4.49, 4.50 and 4.51). Whereas in the presence of KA alone both the first and second population spike amplitudes increase during this time, in the presence of MPPG this response appears to be blocked. In the intact slice the blockade of the increase in the first population spike is highly significant ($p<0.01$) whilst the effect on the second spike reaches significance ($p<0.05$). In the isolated slice the inhibition of the increase in the first population spike just fails to reach significance ($p=0.052$) whilst the second spike is significantly inhibited when compared to KA alone ($p<0.05$).

This inhibition of the effect of KA on the first population spike has been dealt with in the previous section. In terms of the second population spike amplitude however, the lack of potentiation following addition of KA in the presence of MPPG would tend to suggest that that MPPG is somehow negating an effect of KA upon the interneurone population.

Semyanov *et al* (2000) observed an increase in the effects of the KA receptor mediated reduction of GABAergic transmission when in the presence of both MCPG and MSOP which they ascribed to the possible removal of feedback inhibition by glutamate acting on mGluRs on the Schaffer collateral terminals. This would have the effect of enhancing the release of glutamate and hence potentiating the spillover of glutamate onto

presynaptic KA receptors on interneuronal terminals. This in turn could contribute to an increased depression of GABA release. It is unlikely that this mechanism could be contributing to any of the effects seen here since KA presynaptically downregulates glutamate release from the Schaffer collaterals. If anything it would appear that the effect of MPPG and KA in the isolated slice, and to a lesser extent in the intact slice, are additive. This may suggest that they are working *via* separate mechanisms and that mGluRs play no direct role in the effects of KA on either glutamate or GABA release.

4.4.3.2 PKC inhibition

It has been reported (Rodriguez-Moreno *et al.* 1998, 2000; Cunha *et al.* 2000) that the reduction in GABA release by KA receptor activation can be blocked by preincubating hippocampal slices with pertussis toxin, which inhibits the functioning of G_I and G_o proteins. It was also possible to prevent this effect with inhibitors of protein kinase C (PKC) but not protein kinase A (PKA). It was hoped that paired-pulse inhibition data from these experiments might provide further evidence to either support or refute the involvement of PKC in the regulation of GABA release.

It is known that H-7 is capable of abolishing the intracellularly recorded IPSPs in pyramidal cells following stimulation of the Schaffer collateral pathway (Corradetti *et al* 1989) leading to the production of epileptiform activity recorded extracellularly from *stratum pyramidale*. This effect was likely to be due to the blockade of both tonic and evoked release of GABA from interneurone terminals.

As would be expected therefore, application of H-7 resulted in the occurrence of epileptiform activity in both the intact slice (figure 4.20) and isolated CA1 preparations (figure 4.23). This rendered paired-pulse data meaningless since inhibitory function within the slices had been abolished prior to the application of KA. Therefore, the mean number of spikes per epileptiform burst was used as an index of any improvement or exacerbation of inhibitory function during the application of H-7 and KA (figure 4.22 and 4.25).

Application of 1μM KA in the presence of 20μM H-7 does not exacerbate the epileptiform burst, which tends to imply that the reduction in GABA release caused by these drugs may occur *via* the same mechanism. However, it is also possible that the application of H-7 has so compromised GABAergic inhibition within the slice that no further change can be elicited. This may indicate that previous findings (Rodriguez-Moreno *et al.* 1998, 2000; Cunha *et al.* 2000) involving a PKC dependent pathway in the

KA receptor mediated inhibition of GABA release from interneurones should be viewed with caution.

On a purely qualitative level, the epileptiform activity appears to be less severe in the presence of KA. Although extra population spikes are still detectable, they are less pronounced and smaller in amplitude. This could be explained by the reduction in glutamate release resulting in a decreased excitation to the pyramidal cells, thus reducing the driving force for the burst.

4.4.3.3 $GABA_B$ antagonism

In the intact slice (figures 4.48 and 4.50), both the first and second population spikes potentiate to a greater degree in the presence of SCH50911 within the first three minutes of KA application. This reached significance for the second population spike ($p<0.01$). Both remain significantly larger in amplitude than control throughout the application period ($p<0.01$). Within the first three minutes of KA application the normalised mean percentage inhibition (figure 4.52) appears to be reduced further in the presence of SCH 50911. Interestingly, this change in inhibition fails to reach significance when compared to KA alone. However, this is likely to be due to the large standard error for the control group. By the end of the drug application period, the inhibition in the presence of SCH 50911 appears to be more markedly in favour of the facilitation of the second spike than in slices treated only with KA. Once again the large degree of variability meant that this difference was not found to be significant.

In the isolated CA1 preparation both population spike amplitudes are reduced from control following SCH50911 application (figure 4.30). This may imply that SCH50911 is causing a disinhibition of GABAergic interneurones *via* a reduction in the efficacy of $GABA_B$ receptor mediated autoregulation of GABA release onto neighbouring interneurones. This in turn results in an increase in both tonic and evoked inhibition, and hence a reduction in population spike amplitude.

4.4.3.4 Adenosine receptor antagonism

4.4.3.4.1 A_1 receptor antagonism

Application of the adenosine A_1 receptor antagonist DPCPX (50nM) did not significantly affect the population spike amplitudes recorded from the intact slice CA1 (figure 4.33). In the isolated slice (figure 4.36) it reduced the amplitude of the second

population spike ($p<0.01$), which may reflect an increased excitatory drive to the interneuronal population following A_1 blockade. However, this increased inhibition (figure 4.37) was not found to be significant.

Addition of 1μM KA in the presence of DPCPX in the intact slice cause a strong potentiation of both the first (figure 4.48) and second population spike amplitudes (figure 4.50) which was significantly greater than for KA only and persisted throughout the KA application period ($p<0.01$). Furthermore, the field population spike recording exhibited epileptiform activity in 2 out of the 5 slices tested by the end of the KA application period. This epileptiform activity may occur as a result of the blockade of post-synaptic A_1 receptors, which are known to exert an inhibitory influence on NMDA receptor mediated currents recorded from pyramidal cells (de Mendonca *et al* 1995). In addition to this, A_1 receptor blockade prevents an adenosine mediated K^+ efflux from the postsynaptic cell. This combination of effects may lead to a hyperexcitable pyramidal cell population under the reduced inhibitory conditions that occur in the presence of 1μM KA. It is also likely that the presence of an A_1 antagonist potentiates the effects of endogenous adenosine at excitatory A_{2a} receptors (Sebastiao and Ribeiro 2000), which would be expected to lead to an increased activation of NMDA receptors, again leading to increased excitability.

A similar pattern of response is seen in the isolated CA1 preparation with regard to the potentiation of the first (figure 4.49) and second population spikes (figure 4.51), which again remain elevated throughout the KA application period. Epileptiform activity was observed in 1 out of the 5 preparations tested. This would tend to indicate that a downstream effect of CA3 is not important in the maintenance of an elevated output from the pyramidal cells of CA1.

4.4.3.4.2 A_2 receptor antagonism

Application of the A_2 selective antagonist DMPX (10μM) caused no significant change to the population spike amplitudes in the intact slice (figure 4.39) but did result in a small, but significant potentiation of the first population spike ($p<0.05$) in the isolated CA1 preparation (figure 4.42). This phenomenon may reflect an unmasking of the inhibitory effects of A_1 receptor activation leading to a reduced presynaptic Ca^{2+} influx in both the Schaffer collateral and interneuronal terminals. This in turn would lead to a decrease in the release of transmitter from these sites. Thus if the tonic inhibition is reduced the population spike amplitude will increase and a reduction in glutamate release will lead to a decrease in the slope of the EPSP.

The increase in percentage inhibition which occurs as a result of DMPX application in the isolated CA1 preparation (figure 4.43) is due to a change in the ratio between the now potentiated first population spike and the second, which does not change.

In the intact slice, addition of 1μM KA in the presence of DMPX produces a potentiation of both the first (figure 4.48) and second (figure 4.50) population spikes that is significantly greater than would be expected for KA alone ($p<0.01$) which is sustained throughout the KA application period. This is not seen to be the case in the isolated CA1, in which the changes in population spike amplitude are not significantly different to control.

4.4.4 Summary

4.4.4.1 EPSP downregulation by KA

There appears to be no direct involvement of group I/II mGluRs in this response although it would appear that the response to KA may be potentiated in the presence of MPPG. More replications of this experiment are necessary to confirm this.

Protein kinase C does not appear to be part of the mechanism of the inhibition of glutamate release from the Schaffer collateral terminals by KA. $GABA_B$ antagonism results in a reduction in the response in the intact slice preparation but not the isolated CA1. This indicated that $GABA_B$ receptor activation is unlikely to be directly involved in the downregulation of the EPSP by KA.

Adenosine A_1, but not A_2 receptors may modulate the effects of KA on the EPSP.

Thus the evidence presented here suggests that KA reduced the field EPSP recorded from CA1 *via* an action at the presynaptic terminals of the Schaffer collateral fibres. This is likely to involve the activation of an ionotropic GluR5 containing KA receptor. It is possible that this action is modulated by both group III mGluRs and adenosine.

4.4.4.2 KA induced potentiation of the population spike

The initial potentiation of the first population spike is prevented in both the intact slice and isolated CA1 by prior application of the PKC inhibitor H-7. It would also appear to be prevented by the presence of the group II/III mGluR antagonist MPPG.

Blockade of $GABA_B$ receptors enhanced the initial effects of KA in both preparations, possibly due to a reduction in the inhibitory effects of tonically released GABA on the first population spike. Blockade of adenosine A_1 receptors also enhanced the initial effects of KA in both preparations, but A_2 receptor blockade was only effective in the intact slice.

A number of hypotheses may be put forward in order to explain this phenomenon. Firstly, activation of GluR6 (Mulle *et al* 2000, Beureau *et al.* 1999) containing KA receptors present on the pyramidal cells on CA1 may result in an excitation of these cells, leading to an increase in the amplitude of the evoked response.

However, Melyan *et al* (2001) have been unable to elicit an inward current in CA1 pyramidal cells with nanomolar concentrations of KA in animals of the same age as used in this study. Therefore this direct effect of KA on CA1 pyramidal cell excitability may occur as a result of a KA receptor mediated inhibition of a slow afterhypolarisation current (I_{sAHP}) which has been shown to be reduced in KA lesioned animals (Ashwood *et al.* 1986) rendering these cells more excitable. Melyan *et al.* (2001) have shown, using whole-cell patch clamp recordings from CA1 pyramidal cells, that application of between 100-200nM KA is capable of reducing the I_{sAHP} by some 34%. This effect of KA was observed to persist in the presence of tetrodotoxin (TTX), implying a postsynaptic locus of action. This response also continued in the presence of the AMPA specific antagonist GYKI 54266 but not the non-selective AMPA/KA antagonist CNQX. A role for the GluR5 subunit in the receptor mediating this response was eliminated since the GluR5 agonist ATPA did not cause a similar reduction in the I_{sAHP}.

Interestingly, this modulation of the I_{sAHP} may occur *via* activation of a metabotropic KA receptor since the application of KA failed to elicit an inward current and KA induced inhibition of I_{sAHP} was blocked by the PKC inhibitor calphostin C. This is supported by the data presented here for the PKC inhibitor H-7.

4.4.4.3 The effect of prolonged KA application

It is known that activation of somato-dendritic KA receptors on CA1 interneurones leads to an increase in interneuronal spiking (Cossart *et al.* 1998, Frerking *et al* 1998). This presumably leads to an increase in tonic GABAergic inhibition within the CA1. This effect is presumed to be mediated by a GluR5 containing receptor since the agonist ATPA

leads to an increase in interneuronal spiking (Cossart *et al* 1998). Indeed this could explain the reduction in the amplitude of the first population spike elicited here in both intact and isolated CA1 preparations during the addition of ATPA. This effect is most pronounced in the isolated CA1 preparation by the end of the 15 minute drug application period.

There may also be an adenosine A_1 receptor mediated component to this reduction in the population spike amplitude following prolonged KA application since DPCPX allows the population spike to remain elevated throughout the drug application period. Thus KA may stimulate release of adenosine from glial cells (Berman *et al.* 2000) resulting in a decrease in the excitability of the principal cells of CA1.

4.4.4.4 KA and the modulation of inhibitory function

The effect of KA on the inhibition was not significantly affected by blockade of group I/II mGluRs using MCPG, however group II/III antagonism with MPPG reduced the effect in the intact but not the isolated CA1 preparation.

Using the number of spikes in the epileptiform burst produced by H-7 as an index by which to assess the effect of further application of KA on inhibitory function did not result in any further exacerbation of the inhibition. This may suggest that these results agree with those of Rodriguez-Moreno *et al.* (1997, 1998) which postulated that a metabotropically linked presynaptic GluR6 receptor on interneuronal terminals was responsible for the downregulation of evoked inhibition by KA. No evidence was found to agree with Frerking *et al* (1999) that a $GABA_B$ receptor was involved in the mechanism of this response. It would appear that endogenous adenosine may also have a modulatory effect on this response, perhaps as a result of KA stimulated adenosine release from glial cells (Berman *et al* 2000).

Chapter 5

Effects of Acute and Chronic Kainic Acid Applications to Mouse Organotypic Slice Cultures

5.1 Introduction

In the previous chapters, the effects of brief (15-30 minute) KA applications to acute rat hippocampal slices were investigated. In this chapter, the effects of longer (2- 24 hour) applications of KA on hippocampal function and kainate toxicity studied in mouse organotypic slice cultures.

5.1.3 The organotypic hippocampal culture preparation

The use of organotypic hippocampal slice cultures provides an important means of carrying out long-term experiments without resorting to *in vivo* experimentation. Following a method modified from Stoppini *et al.* (1991) it is possible to maintain slice cultures on their Millipore CM membranes for several weeks, allowing experimental observations to be carried out throughout the course of the experiment. Thus the number of animals needed for an experiment may be greatly reduced and the need for their systematic culling at various stages obviated.

Organotypic hippocampal cultures are so called because they retain the typical cellular architecture of the acute slice preparation (Gähwiler 1981, Beach *et al* 1982, Stoppini *et al* 1991). Thus the trisynaptic pathway and inhibitory circuitry are functionally intact. Immunohistochemical studies have demonstrated a similar localisation for both glutamate and GABA in rat hippocampal slices to that found *in situ.* Immunostaining for glutamate was found in nerve endings within the *stratum radiatum* and *stratum oriens* (Torp *et al* 1992). GABA-like immunoreactivity in rat hippocampal cultures also displays a similar morphology and distribution to that observed *in vivo* (Streit *et al* 1989, Torp *et al* 1992), being localised predominantly to interneurones and presynaptic terminals abutting dendritic shafts and neuronal cell bodies (Torp *et al* 1992). Spontaneous and evoked IPSPs were recorded from CA3 pyramidal cells at least up to 30 DIV, indicating the presence of functional GABAergic inhibition (Streit *et al* 1989).

This said, it is still unclear as to whether they retain an "organotypic" expression pattern for the various receptors and their constituent subunits found *in vivo.* Autoradiographic binding studies (Martens and Wree 2001) have demonstrated that by 24 days *in vitro* (DIV), rat organotypic hippocampal cultures display differences in the regional distribution of [^{3}H]MK-801 and [^{3}H]AMPA binding compared to age matched controls. Their data suggests that there is a relative increase in the binding of both [^{3}H]MK-801 and [^{3}H]AMPA in the CA3 region of these cultures compared to CA1 and

the dentate gyrus. In addition, they found that the amount of [^{3}H]kainate binding was increased 3-5 times in the CA3 region of cultures when compared to age matched acute slices. Thus whilst displaying similarities to the acute slice preparation, the organotypic hippocampal slice model is not identical. This may in turn affect the functional output of the hippocampal network in this preparation.

Since this chapter deals with issues surrounding KA toxicity, the next section will deal with the proposed mechanisms underlying this phenomenon.

5.1.2 Kainic acid toxicity

The neurotoxic effects of KA have been known for a number of years (Schwob *et al* 1980, Heggli *et al* 1981, Lothman *et al* 1981), although the exact mechanisms by which KA causes cell death are unclear.

A number of mechanisms have been implicated in the neurotoxic actions of KA. For example, activation of NMDA receptors in populations of cells susceptible to excitation by KA (Berg *et al* 1993, Baran *et al* 1994) is thought to lead to an increase in oxygen-free radical production (Lafon-Cazal *et al* 1993) following an increased influx of Ca^{2+}. In support of this hypothesis, Bruce and Baudry (1995) have reported increased levels of lipid peroxidation and protein oxidation in the hippocampus of rats at 8 and 16 hours after the induction of KA seizures. In addition, they reported that KA administration increased the activity of two transcription factors (activator protein-1 and NFκB) which have previously been reported to be markers for cellular stress (Pinkus *et al* 1996, Schmitz *et al* 1995). Furthermore, KA toxicity is blocked by compounds such as EUK-134, which exhibit superoxide dismutase and catalase activity (Rong *et al* 1999).

Production of oxygen-free radicals can lead to DNA damage, giving rise to base mismatching. Indeed, hydroxyl and superoxide free radicals appear to selectively target guanine and thymidine (Belloni *et al* 1999). Intra-amygdala administration has been demonstrated to result in DNA fragmentation (Henshall *et al*, 2000), although it is likely that this phenomenon is a consequence rather than a cause of a KA-induced cell death process.

DNA fragmentation is one of the features of cell death observed during apoptosis, as is induction of the p53 tumour suppressor gene (Sakhi *et al* 1997). The transcriptional activity of p53 has been shown to be upregulated following KA-induced excitotoxicity (Liu *et al* 1999). This may lead to increased expression of the *bax* gene, the product of

which causes a release of cytochrome C from the mitochondrion into the cytoplasm (Gross *et al* 1999). When this binds to a compelx of Apaf-1 and caspase-9, it causes a subsequent activation of the pro-apoptotic caspase-3 (Liu *et al* 2001). This cleaves aspartate residues in a number of essential proteins, leading to cell death (Liu *et al* 2001).

A schematic diagram for the proposed events leading to excitotoxic cell death is presented in figure 5.1.

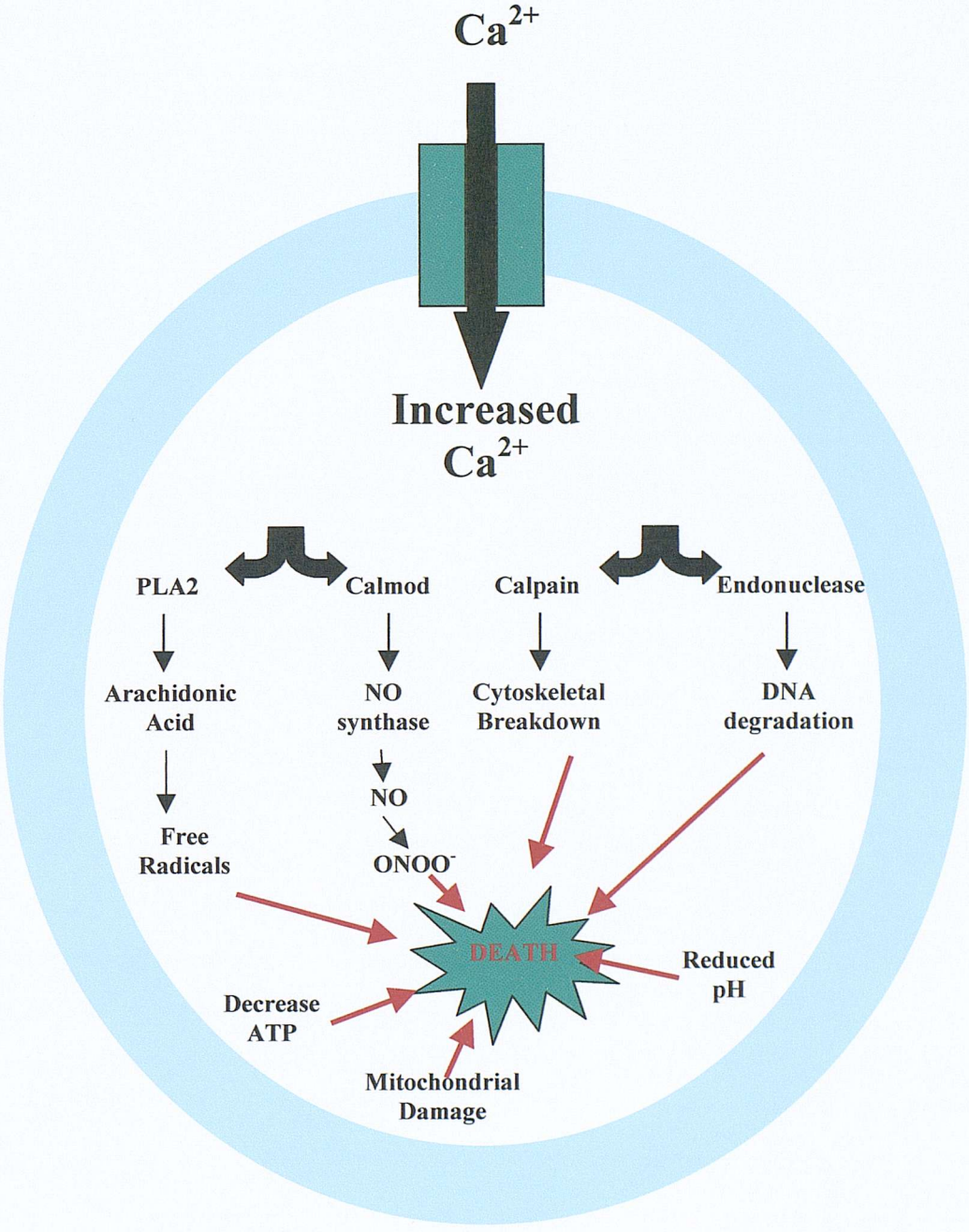

Figure 5.1 Schematic diagram of the events leading to excitotoxic cell death. Increased Ca^{2+} influx activates PLA2 and calmodulin (Calmod) leading to the production of oxygen-free radicals. In addition, calpain activation leads to cytoskeletal bdreakdown and increased endonuclease activity leads to degradation of DNA.

5.1.2 Induced tolerance to kainic acid

An adaptive mechanism has been found to occur in an organotypic model of hippocampal sclerosis, namely the kainic acid model (Best *et al.* 1996). In organotypic hippocampal slice cultures kainic acid produces a lesion identical to that seen *in vivo*. Thus there is a loss of principal cells from CA3 accompanied by a decrease in the number of parvalbumin containing neurones. It was found that by treating cultures derived from 8 day old rats at 7 days *in vitro* (DIV) with a subtoxic dose of kainic acid it was possible to reduce the extent of the lesion caused by the subsequent addition four days later of what was previously found to be a toxic dose. This was accompanied by an increase in the immunoreactivity for heat shock protein 72 (HSP 72) within CA1 (Best *et al* 1996).

This phenomenon of neuroprotection by a low dose of kainate resembles the phenomena of ischaemic tolerance (Kitagawa *et al.* 1990) and thermotolerance (Gerner and Schneider 1975). It is likely that pre-treatment with a subtoxic dose of kainate produces some form of stress response which results in the expression of the non-constitutive HSP 72. Since this expression is still maximal at 11 DIV when the toxic dose of kainate is applied it is possible that it may play some role in neuroprotection, but this is still unclear.

This phenomenon of tolerance has also been found to occur *in vivo*, it being possible to induce tolerance in the contralateral hippocampus following a previous intracerebroventricular injection of kainic acid 8 days earlier. This second injection was carried out at a time when neuropeptide Y (NPY) was known to be expressed in the contralateral hippocampus following the first injection (El Bahh *et al.* 1997).

Just as in the organotypic model, it was found that the amount of damage in stratum pyramidale of CA3 a-b was reduced in the preconditioned rats compared to an unconditioned group. They also found that the severity of seizures following contralateral kainate injection was reduced in the preconditioned group. This tolerance was seen to coincide with the expression of NPY in contralateral granule cells and mossy fibres.

NPY has previously been seen to be an important limiting factor in epileptiform activity within the hippocampus. For example it is known that 1μM NPY is capable of significantly reducing the frequency of spontaneous bursts induced in hippocampal slices by either low Mg^{2+} or 100μM picrotoxin (Klapstein and Colmers 1997). In addition to this, knock-out mouse studies have shown that in NPY deficient mice intracerebroventricular injection of kainate results in progressively worsening seizures and

death in 93% of cases. This was rarely seen in their wild-type littermates. Furthermore, if NPY deficient mice were given an intracerebroventricular infusion of NPY before the administration of kainate then death did not occur as a result of seizure activity (Baraban *et al.* 1997).

Work by two groups has indicated that hypoxia produces some form of compensatory mechanism which can protect against the onset of seizures. Bortolotto *et al.* (1991) studied the effects of bilaterally clamping the carotid arteries of rats on the induction of hippocampal kindling. The epileptogenic process of kindling represents a model of chronic focal epilepsy, and is normally induced by the daily application of repetitive stimuli to limbic structures such as the hippocampus or the amygdala, or by chemical stimulation of various brain regions.

Bilateral clamping of the carotid arteries produces a decrease in the pO_2 and temperature within vulnerable brain structures such as the hippocampus and frontal cortex during the acute phase of the clamping. It was found that, during this acute phase of this process, the mean temperature in the hippocampus decreased by 1.6°C, while the pO_2 was seen to decrease by 60%. This acute phase lasted for 24 minutes.

They found that for 14 days following clamping the GABA content of the hippocampus was significantly increased by up to 29% compared with sham operated controls. In addition the clamped group were more resistant to the kindling process, requiring more stimuli before the onset of generalised seizures. They attributed this increased resistance to a combination of increased levels of GABA, possibly indicating enhanced inhibitory mechanisms, and plastic changes in neuronal pathways responsible for the spread of seizure activity. Interestingly they also found that during the two weeks following clamping the threshold for seizure activity following the application of bicuculline increased, possibly indicating an increased functional role for GABA at postsynaptic sites.

Pohle and Rauca (1994) have shown that an 8 hour period of normobar hypoxia (9% O_2) reduces the neurotoxicity of a subcutaneous injection of 10 mg/kg kainic acid given one week later. This included both seizures and degenerative changes such as hippocampal cell death. In addition to this there was a marked reduction in the depletion of Zn^{2+} from mossy fibre terminals. It was this factor to which they attributed a possible protective role since zinc is co-released from mossy fibre terminals with glutamate, and appears to play a regulatory role in preventing excessive activation of cells by glutamate. However, if the concentration of Zn^{2+} becomes too high then it can potentiate cell death.

They proposed that if hypoxia could reduce this depletion of Zn^{2+} from mossy fibre terminals then it may also prevent the excessive release of glutamate. Another factor that may be important in this mechanism is adenosine, which is also greatly depleted during hypoxia and may regulate the release of neurotransmitters *via* a presynaptic mechanism.

This interlinking of protective effects between hypoxia and kainic acid toxicity strongly suggests that the tolerance to kainate seen by Best *et al.* (1996) may well share the same mechanism as that of the protective effects of hypoxia seen by other workers.

5.1.4 Objectives

1. To compare and contrast the field responses and paired-pulse inhibition recorded form both the CA1 and CA3 of rat or mouse acute hippocampal slices with those of mouse organotypic hippocampal cultures.
2. To compare the effects of acute application of KA in rat hippocampal slices and mouse organotypic hippocampal slice cultures.
3. To investigate the effects of chronic (24 hour) KA application on subsequent pathology.
4. To assess the effects of chronic (24 hour) KA application on CA1 and CA3 function using evoked field potential recordings from the *stratum pyramidale*.

5.2 Methods

5.2.1 Organotypic Culture

Organotypic hippocampal slice cultures were prepared according to a modified method of Stoppini *et al.* (1991), as previously described in chapter 2 from 5-7 day old MF1 mice. During the course of each experiment the hippocampi of one animal was plated out per six well tray. In order to account for possible variation between animals, prior to the commencement of drug treatments, the wells from each tray were mixed such that an even spread of cultures from different animals was achieved in each tray.

5.2.2 Electrophysiology

All electrophysiological measurements in organotypic MF1 mouse cultures following kainate application were carried out at 7-12 DIV. Recordings in acute rat slices were performed between 15-19 days old. Acute mouse slices were taken from MF1 mice

aged between 15-19 days old. Slice cultures were perfused in a modified slice recording chamber at room temperature with standard artificial cerebrospinal fluid (ACSF) with the composition (in mM): NaCl 117.8, $NaHCO_3$ 26.0, KCl 3.3, KH_2PO_4 1.3, $MgSO_4.7H_2O$ 1.0, $CaCl_2$ 2.5, glucose 21.0. This ACSF was continually bubbled with 95% O_2/5% CO_2.

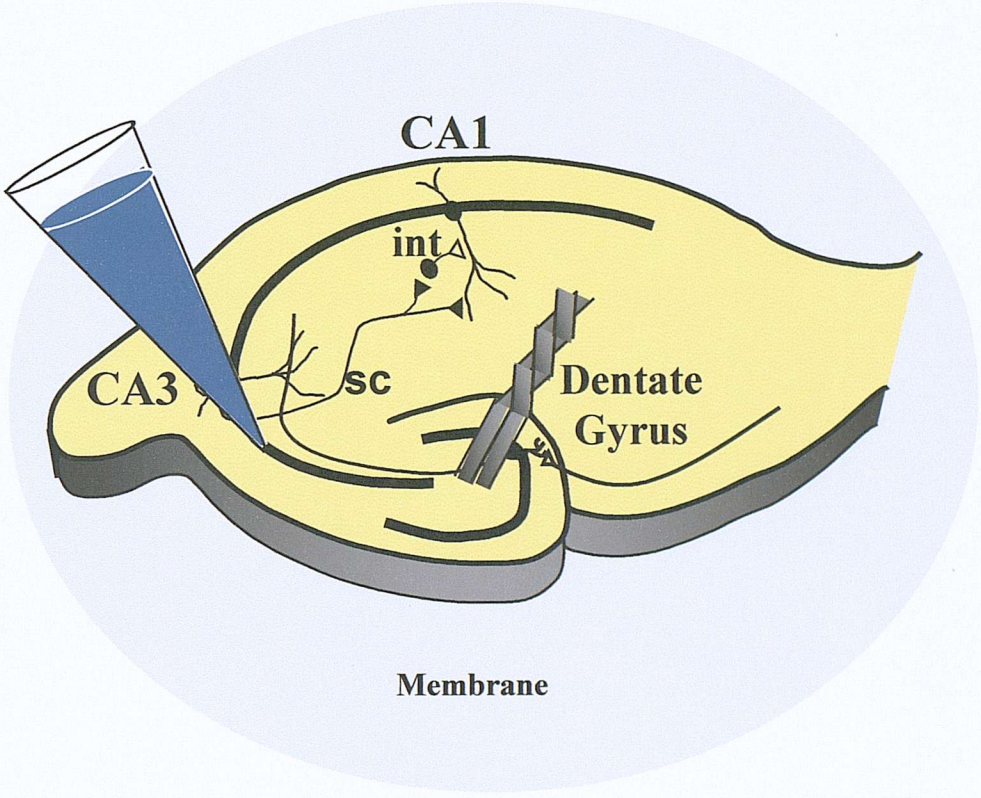

Figure 5.1A Diagram showing the positioning of the recording electrode in *stratum pyramidale* of CA3 and stimulating electrode in the hilus to stimulate mossy fibres. This allows field population spikes to be recorded from CA3 of organotypic hippocampal slice cultures. For recordings made from the CA1 region, the stimulating electrode was placed in the Schaffer collateral pathway and the recording electrode in the *stratum pyramidale* as previously shown.

Extracellular field potentials were recorded from stratum pyramidale of CA1 and CA3, following stimulation of the Schaffer collateral pathway and perforant pathway respectively. Recordings were made using glass micropipettes (4-10MΩ, 3M NaCl). Graded stimuli were applied to produce stimulus-response curves, which provided a half-maximal stimulus value. This stimulus was then used during a paired pulse protocol with stimuli 20 msec apart, thus providing information about the inhibitory systems within the hippocampus. The inhibition of the second spike was calculated as a percentage of the first

using the formula ((C-T)/C)*100, where C=conditioning (first) spike amplitude and T= test (second) spike amplitude. Kainic acid (1μM, Sigma) was applied acutely *via* the superfusing ACSF.

5.2.3 Kainic Acid Tolerance

Previous work by Best *et al.* (1996) demonstrated a long-term induction of tolerance to KA toxicity by preincubation of hippocampal slice cultures derived from Wistar rat pups with a sub-toxic dose of KA. In order to ascertain that the effects of preconditioning could also be demonstrated in mice, cultures were incubated at 7 DIV with 1μM kainic acid in the culture medium, a dose previously found to be subtoxic in rats (Best *et al.* 1996). After 24 hours this was removed by aspiration and replaced with fresh medium. Following this, at 11 DIV, slices were incubated with 5μM kainate for a further 24 hours. At 15 DIV these were stained with the fluorescent exclusion dye propidium iodide (a marker for dead cells) and visualised using a rhodamine filter set. Following this they were fixed in 4% paraformaldehyde (PFA) and subsequently stained with the Nissl stain thionin as previously described. The extent of damage to the cell layers in the cultures was compared to untreated controls and controls treated with 1μM KA at 7DIV and 5μM KA at 15 DIV. From this the percentage of each group in which the CA3 pyramidal cell layer was no longer present following incubation with 5μM KA was calculated.

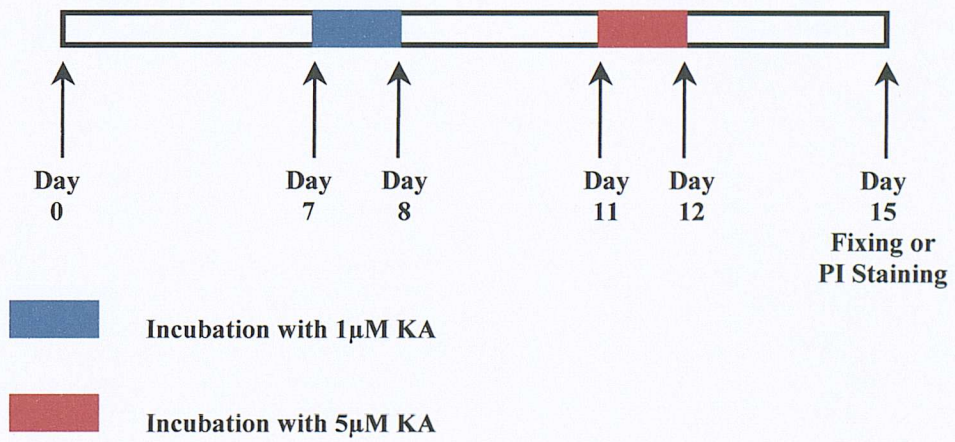

Figure 5.2 Time-line showing the protocol for a preconditioning experiment carried out in organotypic culture. Hippocampal slices from 5-7 day old MF1 mice were plated out onto Millipore CM membranes at day 0. Between day 0 and 7 the medium was changed at an interval of 3-4 days. On day 7 the medium was replaced with medium containing 1μM KA for 24 hours. This was changed for fresh, drug free medium on day 8. On day 11 the medium was again replaced this time with medium containing 5μM KA for 24 hours. This was again replaced on day 12 with drug free medium. On day 15, slices were either fixed with 4% paraformaldehyde and stained with thionin or unfixed cultures were stained with propidium iodide to assess cell viability.

5.2.3.1 Preconditioning Threshold

In order to ascertain the threshold concentration of KA required to induce neuroprotection cultures were incubated with increasing concentrations of KA at 7DIV from 250nM to 1μM KA. This was again applied in the culture medium for 24 hours, at which point it was replaced with fresh medium. In addition to this, two trays were left untreated at this time point, one being the untreated control and the other to be incubated with 5μM KA at 11 DIV. At 11 DIV the medium was again aspirated off using a pipette and all trays incubated with 5μM KA with the exception of the untreated control, which received fresh drug free medium. After a further 24 hours the medium was again replaced and the cultures kept in the incubator until 15 DIV. At this point all cultures received 6μl ml^{-1} of propidium iodide solution (Sigma) with which they were incubated for at least 30 minutes prior to visualisation. The number of slices exhibiting marked fluorescence in the CA3 region were calculated as a percentage of the total number of slices in the treatment group.

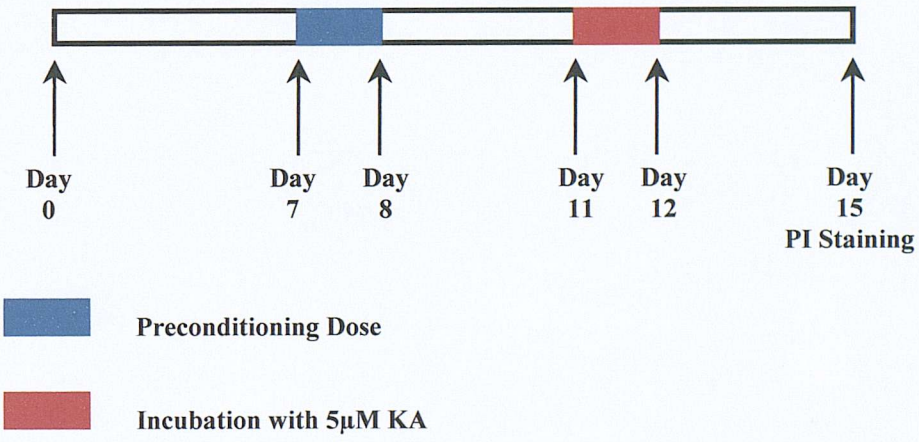

Figure 5.3 Time-line showing the events in an experiment to determine a threshold for the concentration of KA required to elicit neuroprotection to a subsequent toxic challenge with 5μM KA. Cultures were incubated at 7DIV with concentrations of KA between 250nM-1μM KA for 24 hours. At the end of this time the medium was replaced with drug free medium. At 11DIV all of the preconditioned trays and one of the two trays thus far untreated were incubated for 24 hours with medium containing 5μM KA. The medium was again replaced following this incubation. On day 15 *in vitro* cultures were stained with PI and visualised.

5.2.3.2 NMDA Receptor Blockade

To examine the possibility that the preconditioning phenomenon may result from Ca^{2+} entry *via* the NMDA receptor, cultures were incubated at 7 DIV either with 1μM KA only or with a combination of 1μM KA and 20μM MK801 and 20μM D-AP5. In addition to this, two further trays were left untreated at this time point, one being the untreated control and the other to be incubated at 11 DIV with 5μM KA as a positive control. Once again, drug incubations were 24 hours in duration, with the medium being replaced at the end of this time.

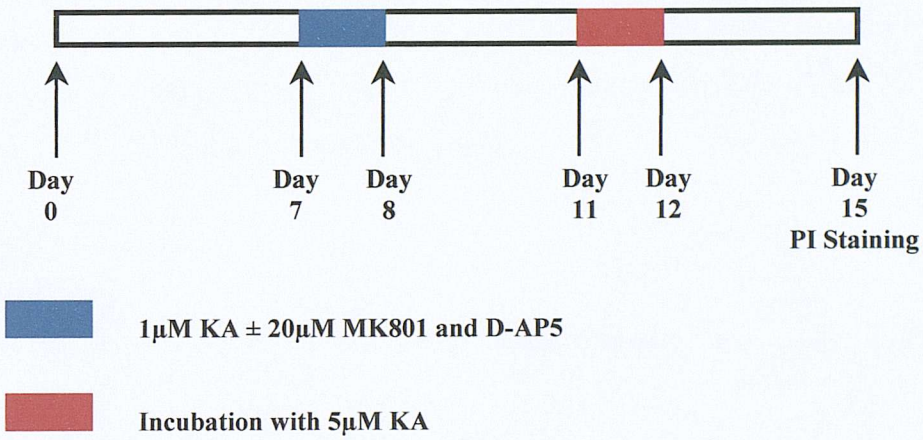

Figure 5.4 The experimental protocol for an investigation into the effect of NMDA receptor blockade in the induction of KA tolerance. The experiment is the same as previously described for the induction of tolerance with the exception that 20μM MK801 and 20μM D-AP5 was co-administered with 1μM KA at 7DIV in two trays. Otherwise, drugs were applied as before at the same time points.

5.2.4 Glutamic Acid Decarboxylase Staining

It is known that the KA lesion model of temporal lobe epilepsy (TLE) that, in addition to causing a degeneration of principal cells in the CA3 region of the hippocampus, exhibits a reduction in the number of both somatostatin immunoreactive and parvalbumin immunoreactive interneurones (Best *et al* 1993, 1994, 1996). This reduction is seen throughout CA3 and CA1. Interneurones containing calbindin D28K are similarly reduced in number following injection of KA into the dorsal hippocampus of mice (Bouilleret *et al.* 2000).

It was therefore of interest to examine the effects of this preconditioning phenomenon on the numbers of glutamic acid decarboxylase 67 (GAD67) immunoreactive cells following KA treatment. To this end hippocampal slice cultures were prepared as before and subjected to a preconditioning regimen. As before, the experiment included a group of untreated and 5μM KA treated controls. At 15 DIV these were fixed overnight with 4% PFA and immunostained for GAD67 in the manner described in chapter 2.

Slices were then counterstained with propidium iodide in order to aid identification of the anatomical regions within the slice and mounted onto slides using the aqueous mountant Crystal/Mount (Biomedia) with cover slips for light microscopy.

The number of GAD67 positive cells were counted for the dentate gyrus and hilus (taken as one unit), the CA3 and the CA1. These were then expressed as the number of positive cells per region in each treatment group.

5.3 Results

5.3.1 Electrophysiological characterisation of the mouse organotypic hippocampal slice culture

In order to ascertain to what extent the organotypic mouse hippocampal slice culture conforms to the acutely isolated hippocampal slice preparation with regards to its electrophysiological properties, the following comparisons have been made.

Population spike recordings taken from the CA1 and CA3 regions of organotypic cultures (figure 5.5) exhibit robust paired-pulse inhibition at an interpulse interval of 20msec. This is analogous to the phenomenon observed in acute slices from both rats and mice at a similar age.

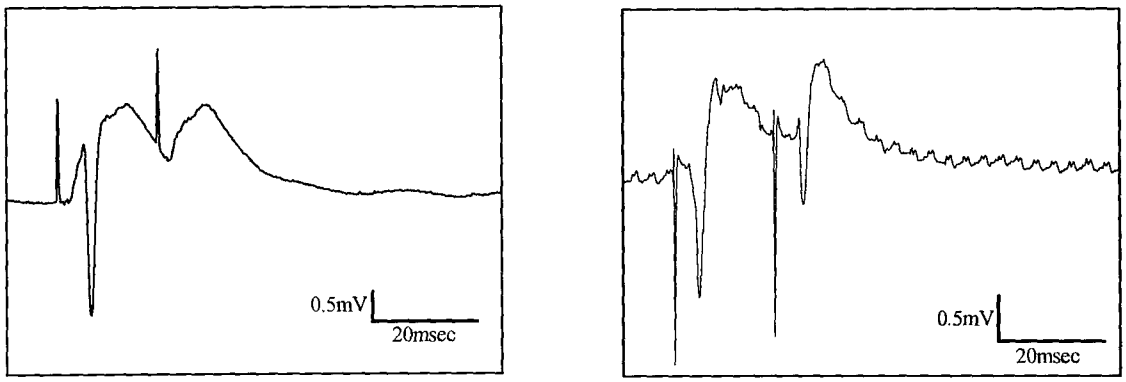

Figure 5.5 Examples of the field population spikes obtained from the CA1 (a) and CA3 (b) regions of mouse organotypic hippocampal slice cultures using a paired pulse protocol with a 20msec inter-pulse interval. Cultures were aged between 11-14 DIV.

5.3.1.2 Comparison of the electrophysiology of CA1

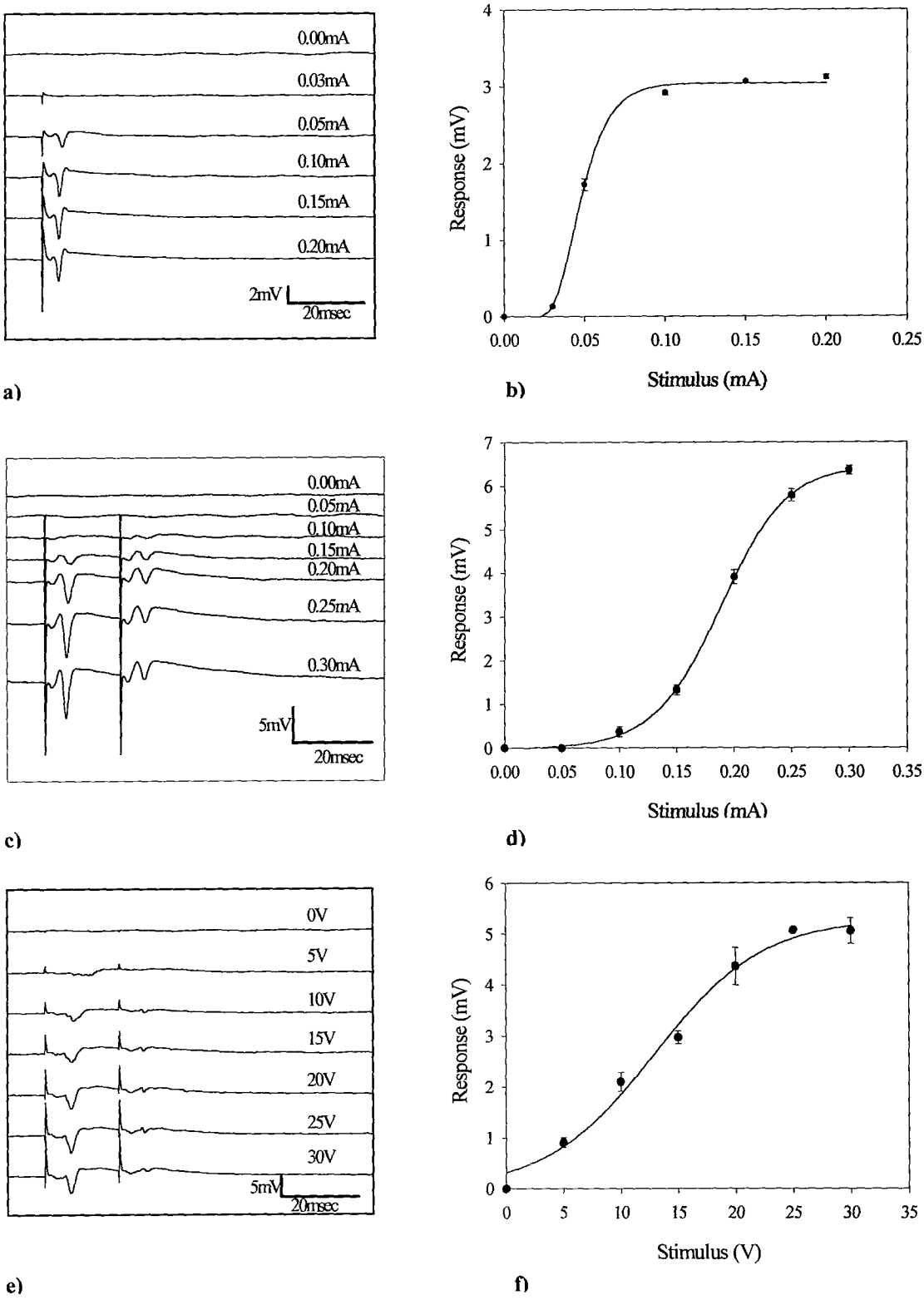

Figure 5.6 Examples of recordings made from the CA1 region of acute rat (a), acute mouse (c) and organotypic hippocampal slice preparations (e) during a stimulus- response experiment. Parts (b), (d) and (f) are the respective stimulus-response curves obtained from the first population spike data for these recordings.

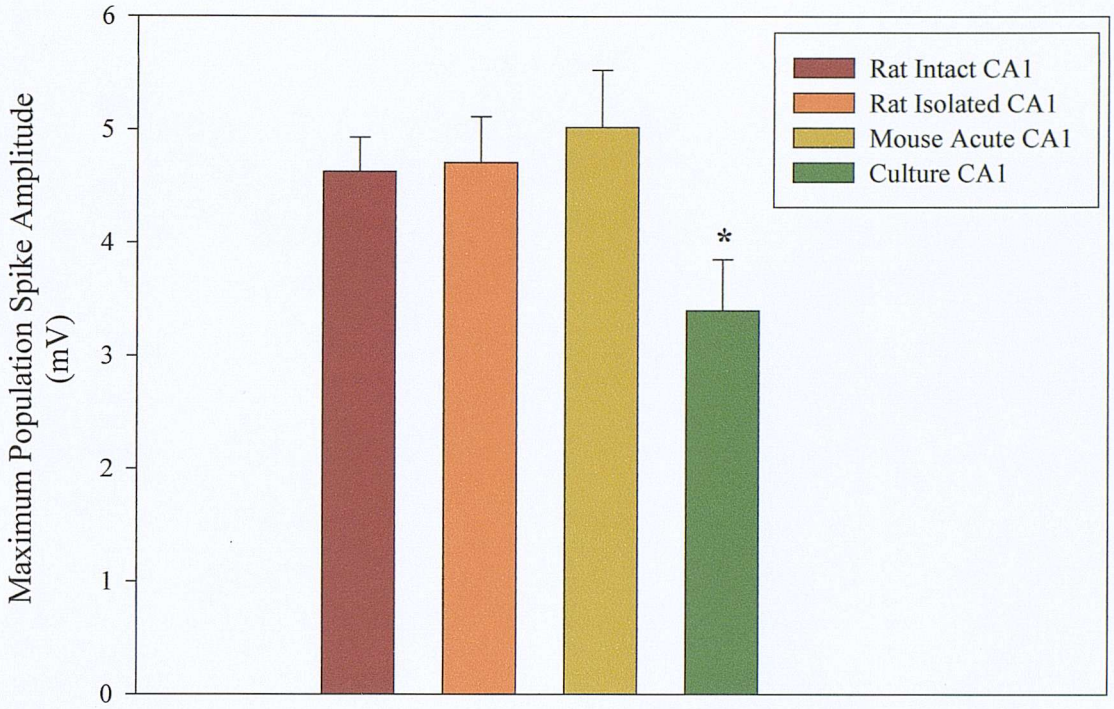

Figure 5.7 Comparison of the mean (±S.E.M.) maximal population spike elicited from the CA1 region of intact and isolated rat CA1 preparations (15-19 days old), the mouse acute slice CA1 (16-18 days old) and the CA1 of mouse organotypic hippocampal slice cultures (n=10 for all) during a stimulus-response curve. There is no significant difference between the maximal population spike elicited from the intact slice CA1 (4.6mV (±0.3)), the isolated CA1preparation (4.7mV (±0.4)) or the mouse acute slice CA1 (5.0mV (±0.5). The maximal population spike elicited from the CA1 of age matched mouse organotypic hippocampal slice cultures is significantly smaller that all other preparations tested (3.4mV (±0.5), $p<0.05$).

Examples of the population spikes elicited by incrementally increasing stimuli from the CA1 region of rat and mouse acute slices and mouse organotypic hippocampal slices, and the resulting stimulus response curves calculated from this data are presented in figure 5.6 on the previous page. The mean maximal amplitude of population spike (±S.E.M.) which it is possible to elicit from these preparations is shown graphically in figure 5.7 above. It is clear that the maximal population spike is comparable between all acute preparations, but the mouse organotypic hippocampal slice preparation's output is significantly lower ($p<0.05$). This is likely to be due to the thickness of the slice preparations used. In the acute preparation the slices are all cut at 400μm. Whilst this is also true for the slices used to prepare organotypic slices the preparation appears to reduce in thickness thereafter. By the time they are subjected to electrophysiological recording (9-12 days later) they are approximately 150μm in thickness (N. Best personal

communication). Since the population spike is a function of the firing of a population of neurones a thinner slice is likely to result in a smaller output from the slice.

A comparison of the mean (±S.E.M.) percentage inhibition calculated from CA1 over a period of 15 minutes in either cultured mouse slices or acute slices derived from both rats and mice in figure 5.8. From this we can see that the CA1 region of mouse organotypic hippocampal cultures exhibits a significantly greater degree of paried-pulse inhibition (74% (±0.7), n=5) to that calculated from either rat (60% (±0.4) n=25, $p<0.01$) or mouse CA1 (65% (±1.7) n=2, $p<0.01$). In addition, the percentage inhibiton calculated from recordings made in mouse acute slices display slightly higher percentage inhibition to that of rats ($p<0.01$).

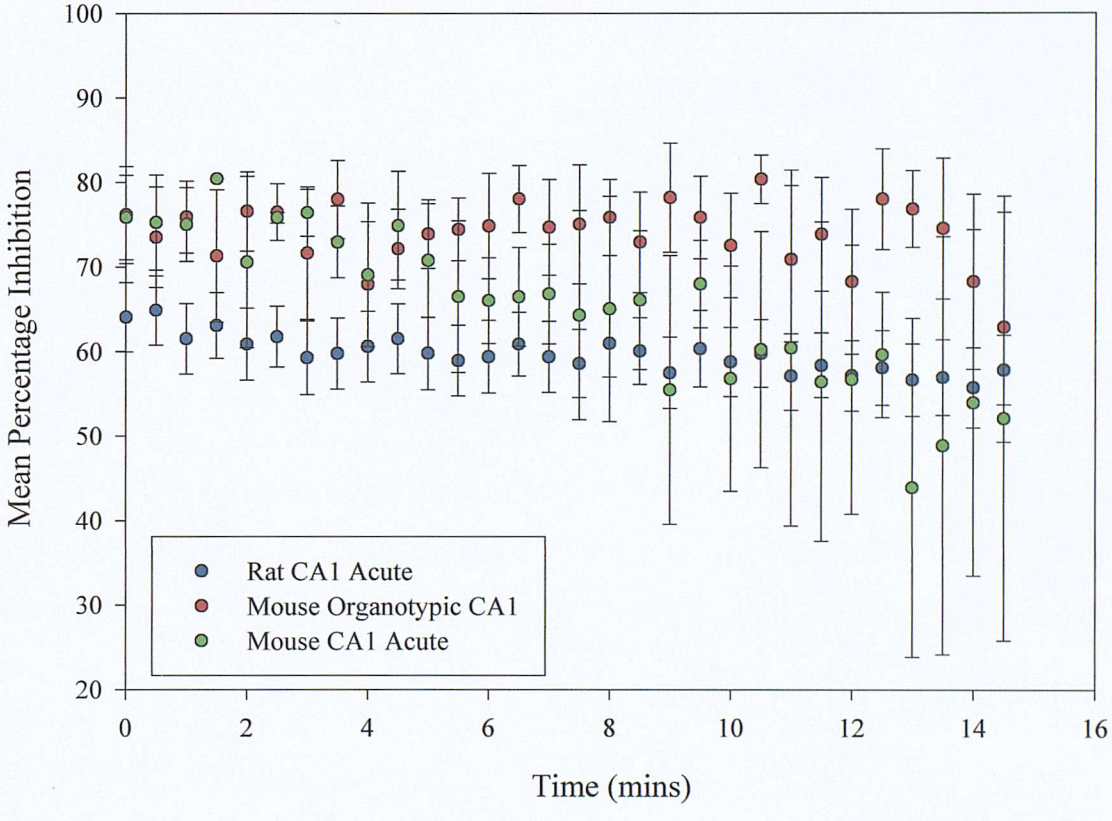

Figure 5.8 Comparison of percentage inhibition data obtained from the CA1 region of acute rat slices (15-19 days) (n=25) and organotypic mouse hippocampal slice cultures (7-11 DIV) (n=5). Organotypic mouse cultures displayed a significantly greater degree of inhibition to acute rat slices ($p<0.01$). The acute mouse CA1 displays statistically significant differences from both ($p<0.01$, n=2).

5.3.1.3 Comparison of the response to 1μM KA in CA1

The effect of 1μM KA on the population spike amplitudes recorded from the CA1 region of 7-11DIV mouse organotypic hippocampal slice cultures is presented on the following page. The mean percentage amplitude (±S.E.M.) of the first population spike is shown in figure 5.10, data for the second population spike in figure 5.11. Examples of the recordings obtained during the course of these experiments are presented in figure 5.9 below.

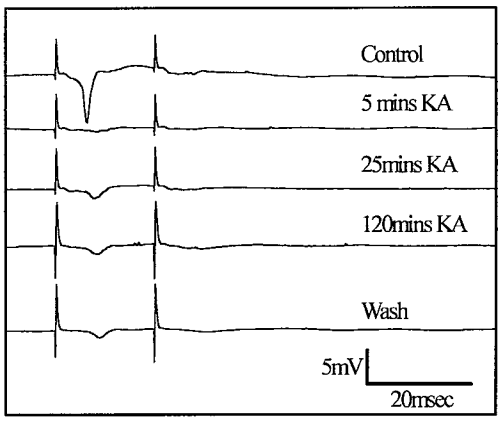

Figure 5.9 Example traces obtained from the CA1 of a mouse organotypic hippocampal slice culture during the addition of 1μM KA and wash. KA reduces the amplitude of both the first and second population spikes. This persists during the wash phase.

In the CA1 of mouse organotypic hippocampal cultures it would appear that addition of 1μM KA to the superfusing ACSF results in a rapid reduction in the mean percentage amplitudes of both the first and second population spikes. This would be consistent with a strong depolarisation of the CA1 pyramidal cell population possibly following CA3 pyramidal cell activation by KA, thus indicating a difference to the observed effect of KA in 15- 19 day rat acute slice CA1. Data for the first (figure 5.12) and second (figure 5.13) population spikes from intact rat acute slice CA1 are presented for comparison purposes on page 204. These data are repeated from figure 3.12 for ease of comparison. As previously shown in chapter 3, the application of 1μM KA to intact slices and isolated CA1 preparations results initially in an increase in the mean percentage amplitude of both the first and second population spike amplitudes. Thus there are distinct differences in the initial response to KA in cultured slices compared to rat acute slices.

Following the initial reduction in the amplitude of the first population spike in the CA1 of organotypic cultures (figure 5.10), the population spike temporarily increases in amplitude and then is further reduced. This again differs somewhat to the response of the acute rat slice, where the amplitude of the first population spike is depressed following the initial phase of the response (figure 5.12).

While it is known that KA is capable of reducing GABAergic inhibition in CA1 *via* a presynaptic action on interneuronal terminals (Frerking *et al.* 1999; Rodriguez-Moreno *et al.* 1997) this phenomenon is not seen in the data for the second population spike presented in figure 5.11. It would be expected that the second population spike amplitude would increase as the release of GABA diminished. This may be due to the presence of an intact connection between CA3 and CA1 allowing the depolarisation block in CA3 to induce a similar phenomenon in CA1 *via* a tonic release of glutamate from the Schaffer collaterals.

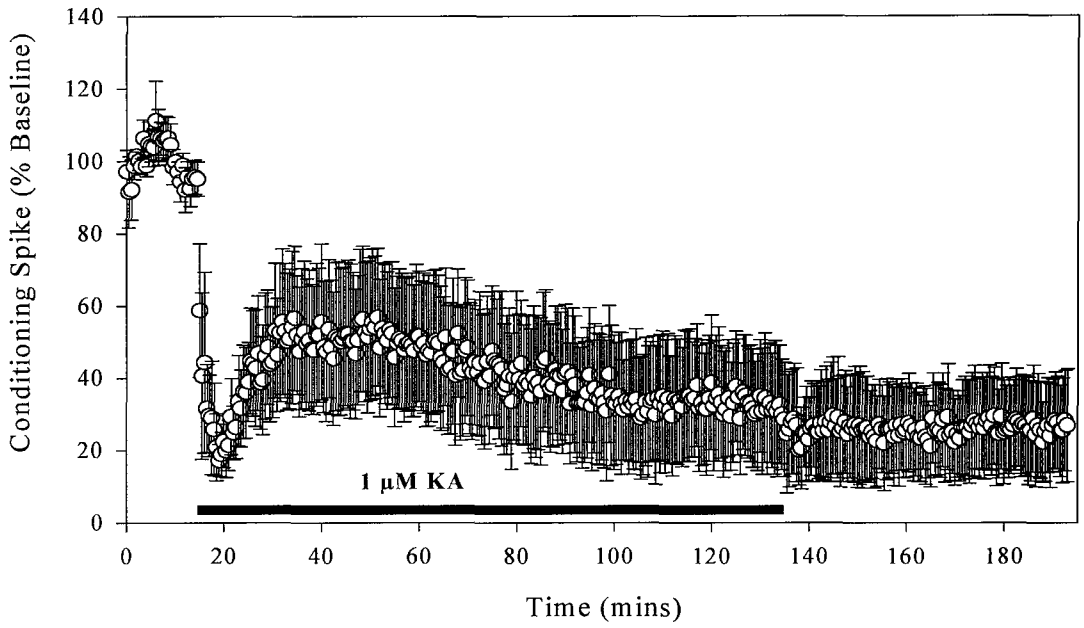

Figure 5.10 The effect of prolonged (2 hour) application on the first population spike recorded from the CA1 of mouse organotypic hippocampal cultures.The administration of 1μM KA causes an initial marked reduction in the mean percentage amplitude (±S.E.M.) of the first population spike of 11-14DIV cultures (n=5). This is folowed by a transient, partial recovery of the population spike which again declines towards the end of the experiment. As in the CA3 region, the population spike remains depressed even after 60 minutes ACSF wash.

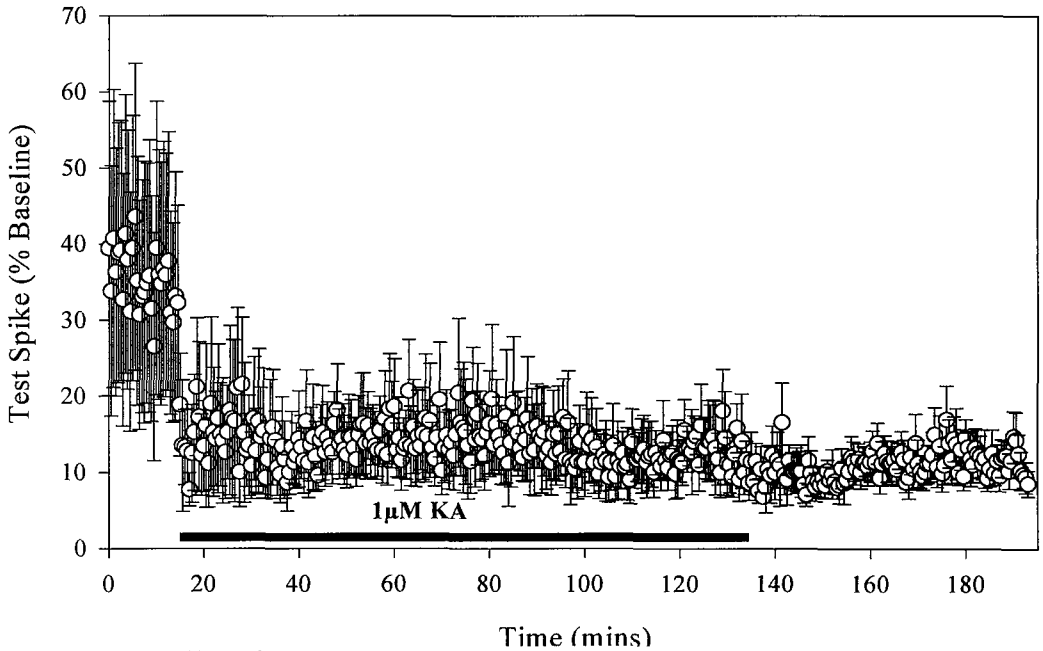

Figure 5.11 The effect of prolonged (2 hour) KA application on the second population spike recorded from the CA1 of unconditioned cultures 11-14DIV also undergoes a marked reduction in amplitude following the introduction of 1μM KA to the recording chamber. Unlike the first population spike there is no evidence of a transient increase in the mean percentage amplitude around 25 minutes into the KA application period (n=5).

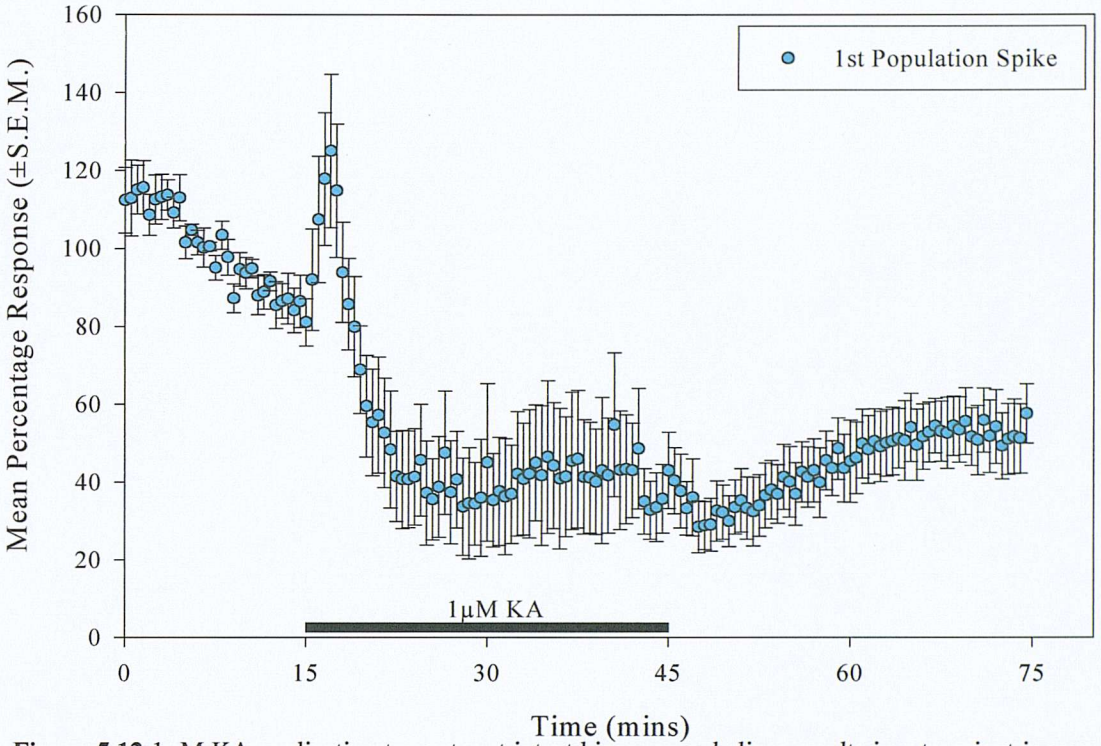

Figure 5.12 1μM KA application to acute rat intact hippocampal slices results in a transient increase in the first population spike amplitude (119% (±9.7) from control (86% (±3.4), $p<0.01$). This is followed by a reduction in the population spike amplitude to 34% (±4.5) ($p<0.01$). The first population spike data from figure 3.12 has been presented separately here for ease of comparison.

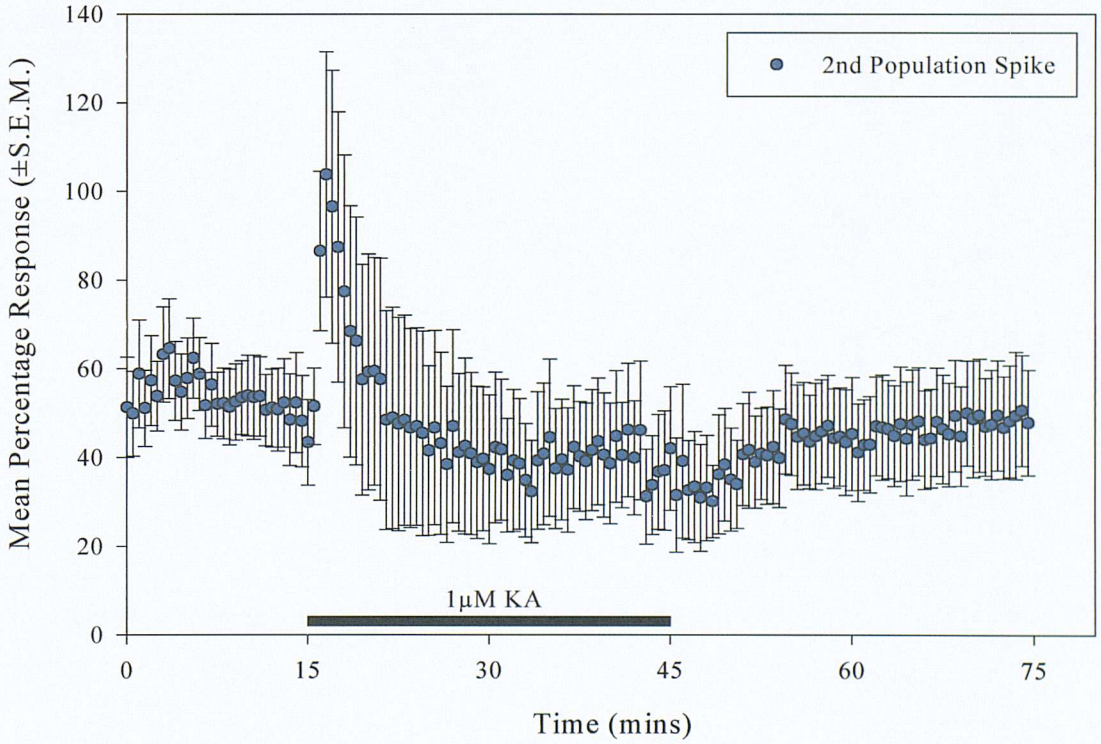

Figure 5.13 The second population spike amplitude recorded from acute intact rat hippocampal slices initially increases in the presence of 1μM KA from 50% (±5.7) to 96% (±16.0) ($p<0.01$). Following this initial phase, the amplitude of the second population spike is reduced to 36% (±6.7) ($p<0.01$). These data for the second population spike have been presented separately for ease of comparison.

5.3.2.1 Comparison of the Electrophysiology of Acute and Organotypic CA3

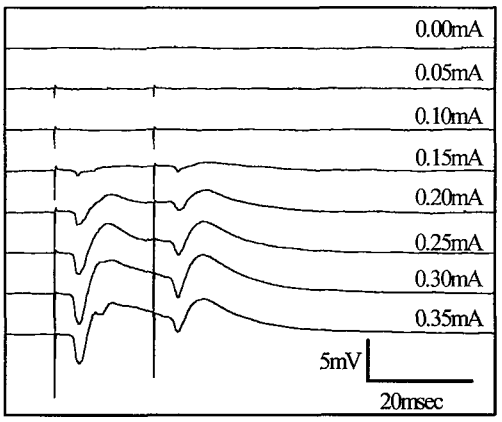

a)

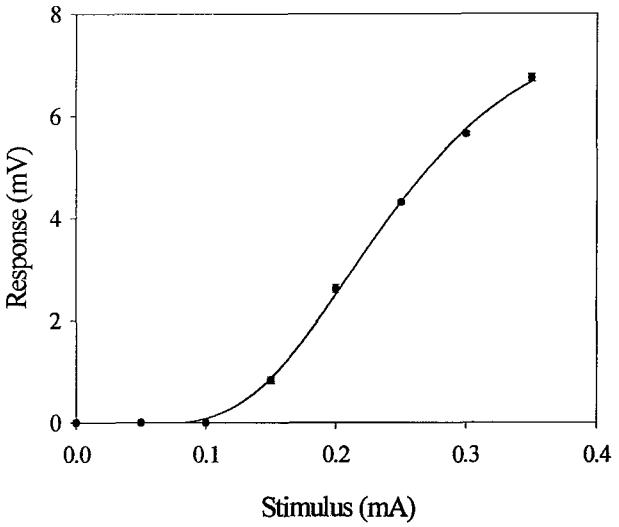

b)

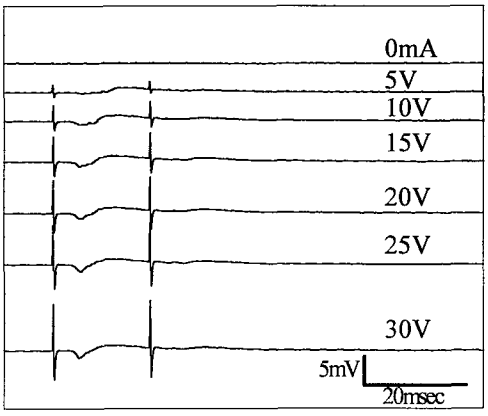

c)

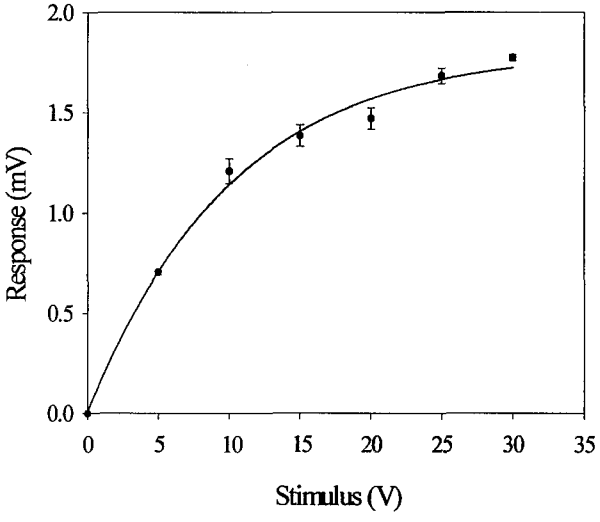

d)

Figure 5.14 Example traces of recordings taken from the CA3 region of acute mouse slices (a) and organotypic hippocampal slice cultures (c) and the stimulus response curves obtained from these data (b) and d) respectively). Note the lower maximal amplitude obtained from the organotypic slice culture.

Examples of the population spike recordings and stimulus-response curves obtained from the CA3 region of acute and organotypic mouse slices are shown in figure 5.14 on the previous page.

Figure 5.15 below shows the mean (±S.E.M.) population spike amplitude recorded during a stimulus-response experiment from these preparations. Population spikes obtained from the acute mouse CA3 are significantly larger (3.5mV (±0.5)) than those from the organotypic preparation (1.5mV (±0.1)) ($p<0.01$).

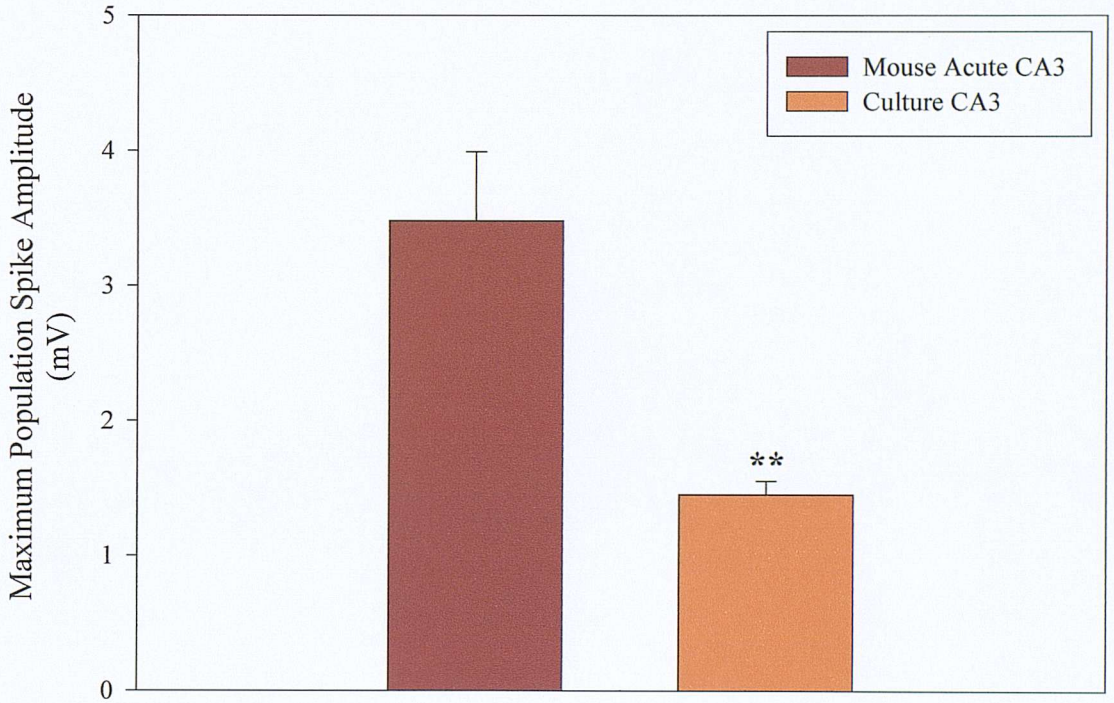

Figure 5.15 Comparison of the mean (± S.E.M.) maximal percentage population spike elicited during a stimulus-response curve from the CA3 regions of acute mouse slices (n=10) and mouse organotypic hippocampal slice cultures (n=9). The maximal response obtained from the cultured slice CA3 (1.5mV (±0.1)) was found to be significantly smaller than that for acute mouse slices (3.5mV (±0.5), $p<0.01$).

As with the CA1 region, the CA3 of organotypic slices (figure 5.16) exhibits a significantly higher degree of paired pulse inhibition (48% (±0.9)) then that observed for the acute mouse slice CA3 (24% (±0.6)) ($p<0.01$).

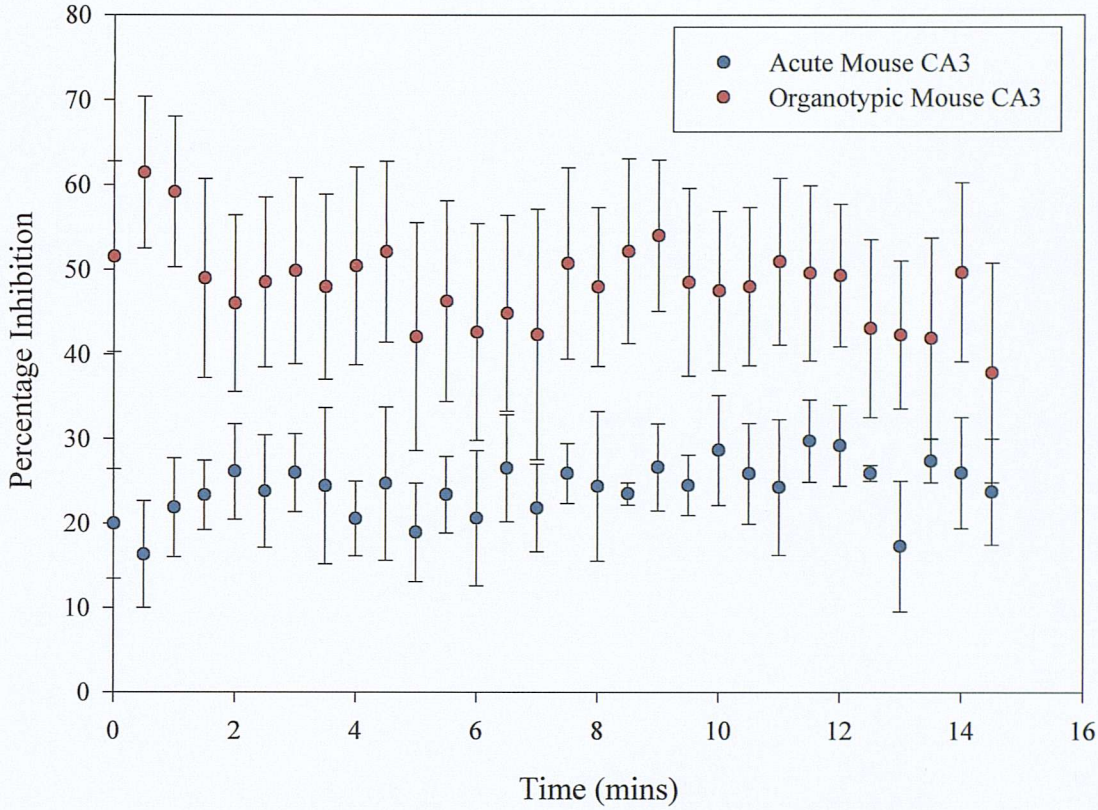

Figure 5.16 Comparison between the mean percentage inhibition (±S.E.M.) calculated from paired-pulse data recorded from the CA3 region of age matched acute mouse slices (n=4) and organotypic mouse hippocampal slice cultures (n=5). Slice cultures display a degree of inhibition (48% (±0.9) than the acute mouse preparation (24% (±0.6)). This was found to be significantly greater than that of acute slices ($p<0.01$).

5.3.2.2 Acute Kainate Application in CA3

In figure 5.18 and 5.19 we can see the effects of 1μM KA application on the conditioning and test spikes recorded from *stratum pyramidale* of the CA3 region of unconditioned organotypic hippocampal slice cultures between 11 and 14 DIV using a paired-pulse stimulus protocol. Examples of the traces obtained during the course of these experiments may be seen in figure 5.17. The application of KA causes a large reduction in the amplitude of both the first and second population spike amplitudes.

One other interesting phenomenon, which occurs in both CA3 and CA1 as a result of 120 minutes of 1μM KA application, is the apparent reduction in the output of pyramidal cells following wash. This prompted the possibility that the neuroprotective effect of 1μM KA pre-incubation may occur as a result of a decrease in the excitability of pyramidal cells in these regions. However, as shown later (figures 5.45 and 5.57), pyramidal cell responses have returned to control values by the time induced tolerance is observed.

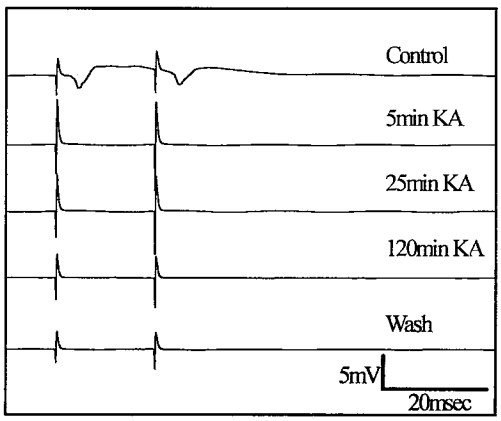

Figure 5.17 Example of the recordings obtained from the CA3 of a mouse organotypic hippocampal slice culture during the addition of 1μM KA and wash. KA rapidly abolishes both the first and second population spikes. This persists during the wash phase.

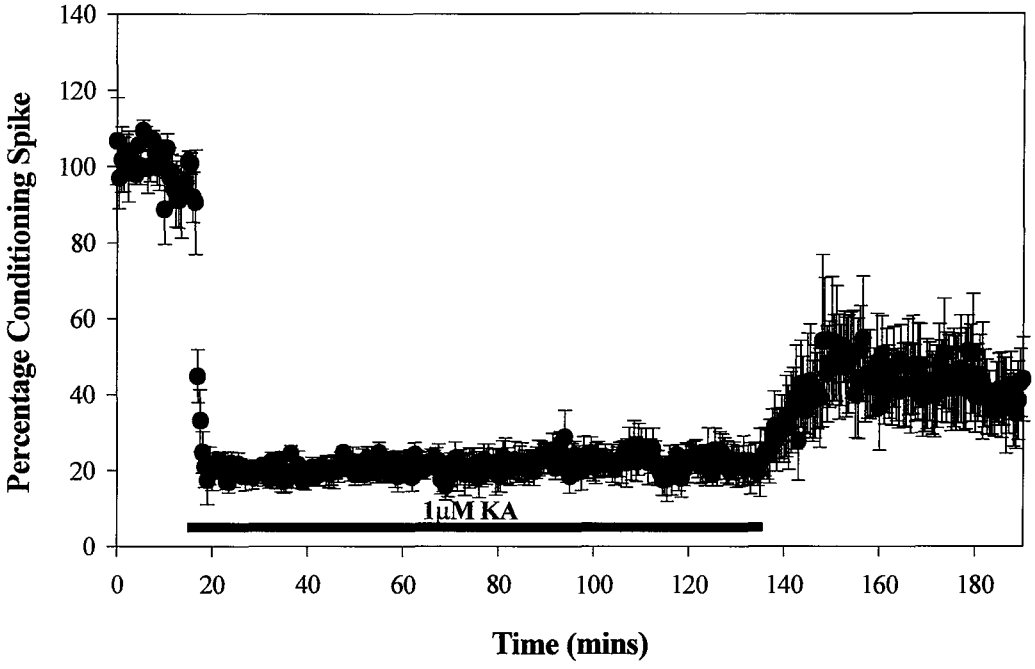

Figure 5.18 Application of 1μM KA to cultures between 11 and 14DIV caused a marked reduction in the mean amplitude (±S.E.M.) of the first population spike elicited from CA3 following paired-pulse stimulation of the mossy fibre pathway (n=5).

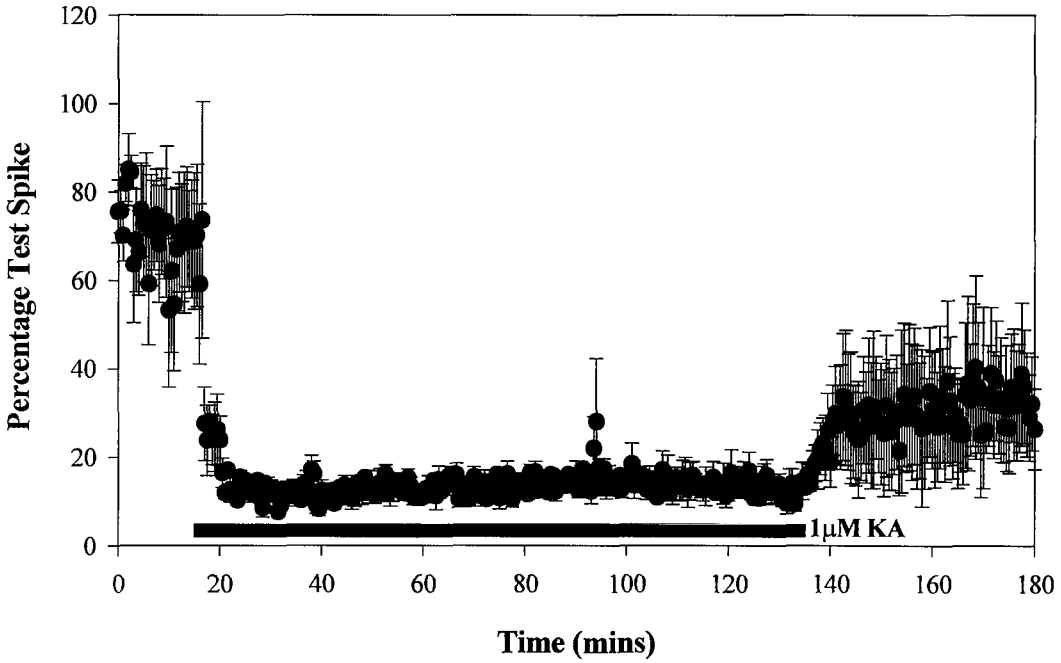

Figure 5.19 The second population spike recorded from the CA3 region of cultures of 11-14DIV also undergoes a marked reduction in mean amplitude (±S.E.M.) following the administration of 1μM KA *via* the superfusing ACSF (n=5).

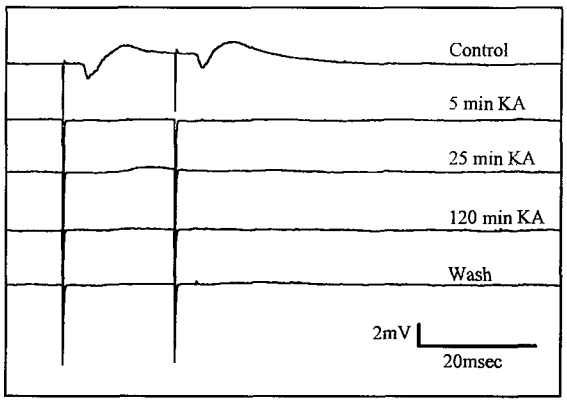

Figure 5.20 Example traces recorded from the *stratum pyramidale* of an acute hippocampal slice taken from a 12 day old MF1 mouse at the end of the control period, after 5, 25 and 120 minutes KA, and at the end of 60 minutes ACSF wash.

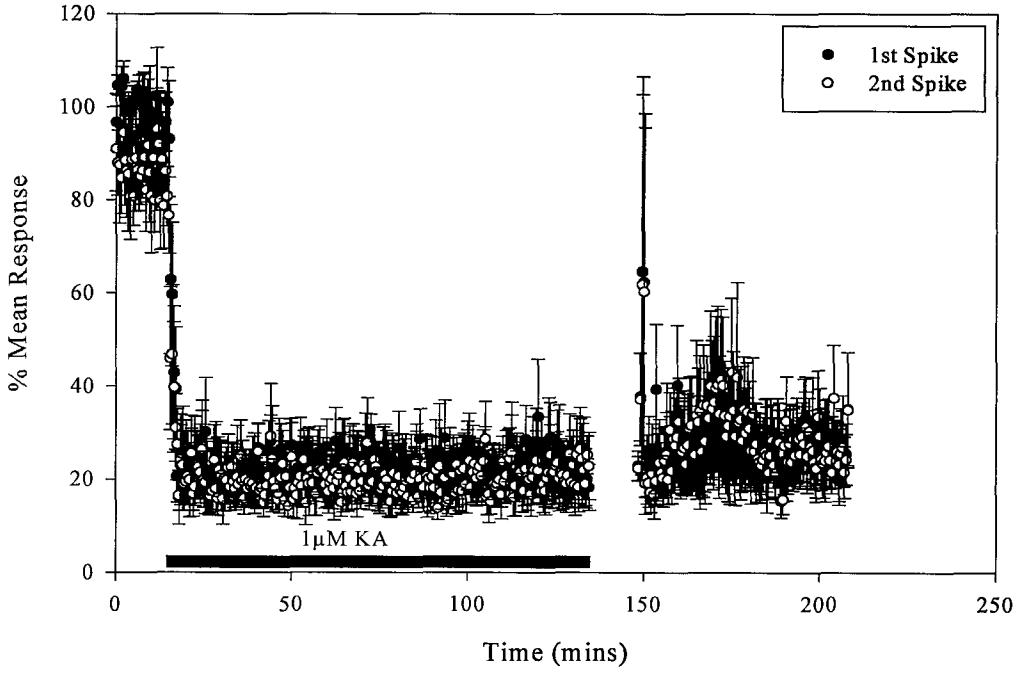

Figure 5.21 Time course for the application of 1μM KA in CA3 of acute slices. The graph shows the amplitudes of the first and second population spikes recorded from *stratum pyramidale* of CA3 during a paired-pulse protocol following stimulation of the hilus at a half-maximal stimulus amplitude. (n=5, mean ± S.E.M.)

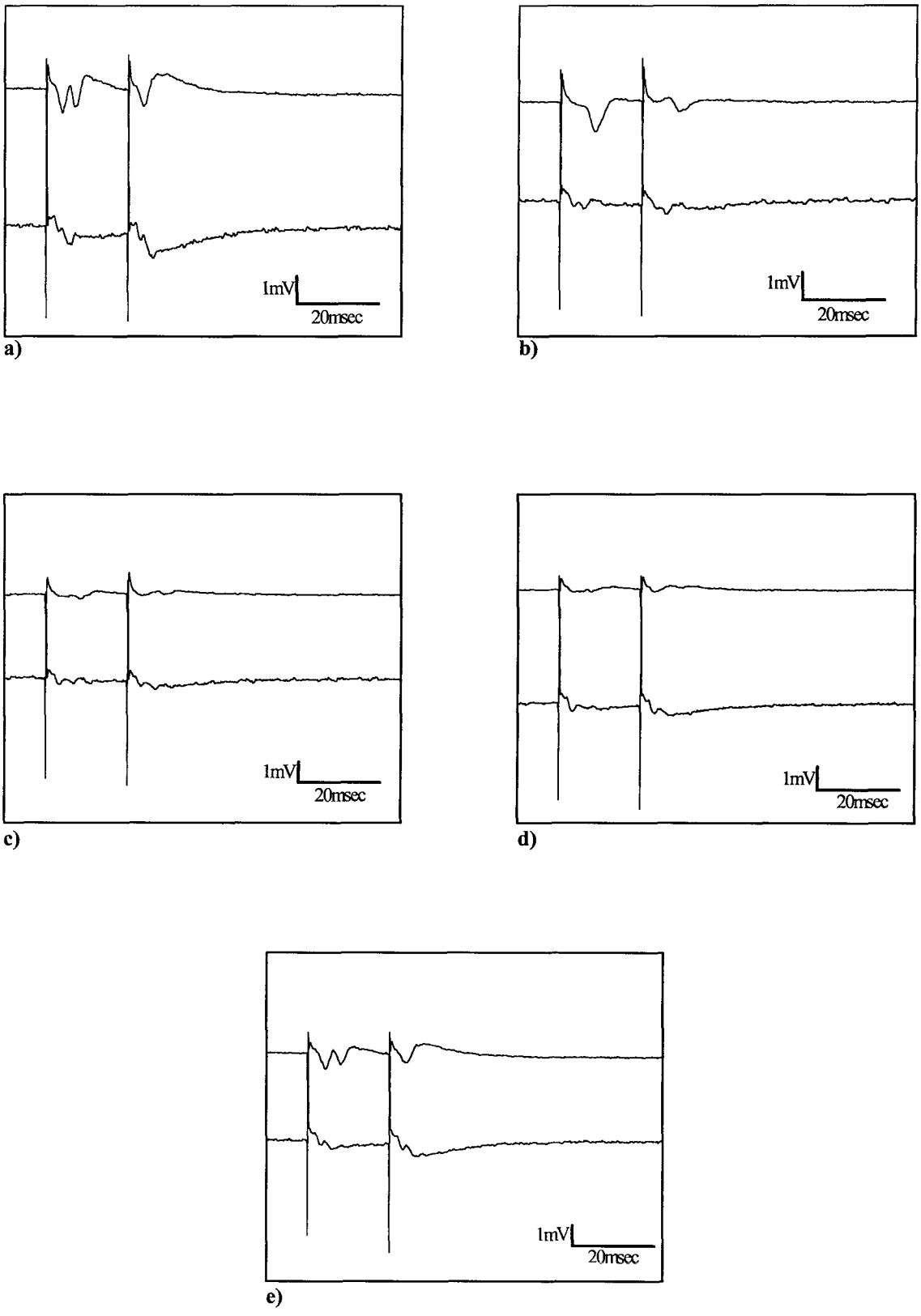

Figure 5.22 Example traces showing the effect of 1μM KA on the field population spike and EPSP recorded from the CA3 region of an acute hippocampal slice taken from a 15 day old Wistar rat. Each trace represents the average of three responses taken at the following time points: a) at the end of 15 minutes control stimulation, b) within three minutes of the start of KA administration, c) after 25 minutes KA application, d) at the end of 120 minutes KA application, e) the end of 60 minutes ACSF wash.

For the purposes of comparison, the effect of 1μM KA on the mean percentage population spike amplitude and EPSP slope (±S.E.M.) recorded using dual electrode recordings from the *stratum radiatum* and *stratum pyramidale* of the CA3 region of an acute mouse hippocampal slice are presented in figure 5.23 below. Examples of these recordings at the same time points used in chapter 3 are shown in figure 5.22 on the preceding page.

It is of note that in the CA3, the EPSP slope and population spike amplitude are both reduced with the onset of 1μM KA application.

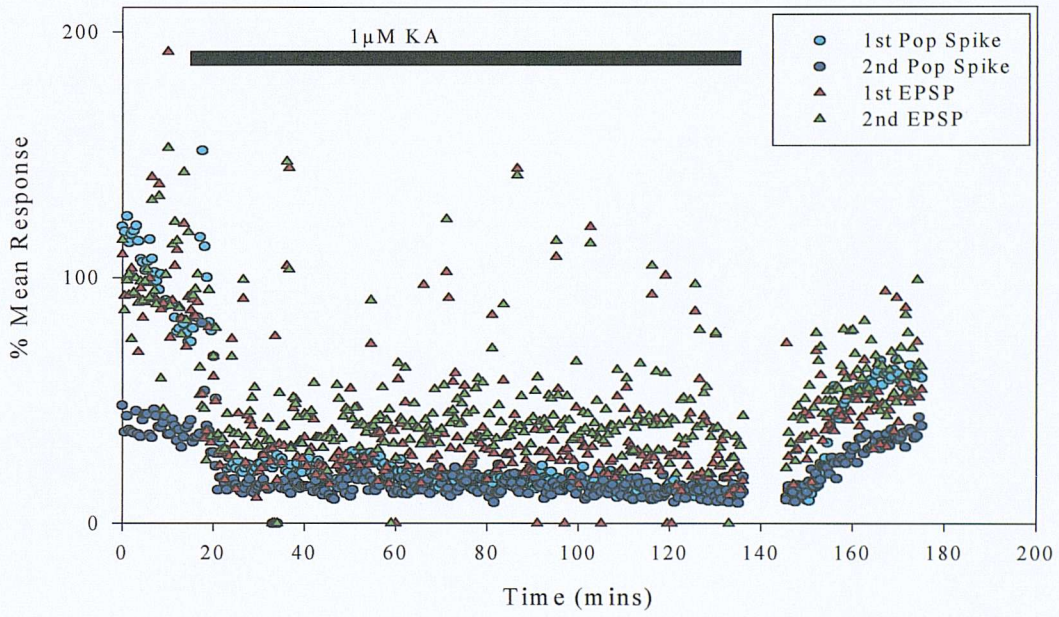

Figure 5.23 Time course for the application of 1μM KA in CA3 of acute slices using dual recordings from *stratum radiatum* and *stratum pyramidale* of a hippocampal slice taken from a 15 day old Wistar rat. Light blue and dark blue circles represent first and second population spike amplitudes and red and green triangles represent first and second EPSPs respectively. (n=1)

5.3.2 Kainic Acid Tolerance in the Organotypic Hippocampal Slice

Previous work by Best *et al* (1996) has demonstrated that it is possible to induce tolerance to KA toxicity by prior 24 hour incubation with a subtoxic concentration of KA in rat organotypic hippocampal slice cultures. The following data aims to assess whether chronic exposure to 1μM KA induces cell death and, if not, does a similar tolerance phenomenon occurs in organotypic mouse hippocampal cultures as a result of this subtoxic insult.

It can be seen (figure 5.24) that the phenomenon of kainic acid preconditioning occurs in MF1 mouse organotypic hippocampal slice cultures in much the same way as seen in Wistar rats (Best *et al.* 1996). The cultures in figure 5.24 have been treated with a 1μM KA incubation at 7 DIV (b), 5μM KA for 24 hours at 11 DIV(c), 5μM KA at 11 DIV following a 24 hour incubation with 1μM KA at 7 DIV or remained drug naive throughout the course of the experiment (a). Cultures were fixed with 4% paraformaldehyde (PFA) at 15 DIV and stained with the Nissl stain thionin. Thus the cell bodies are visible within the slice. As previously demonstrated by Best *et al.* (1996) a 24 hour incubation with 5μM KA is toxic to the pyramidal cells of CA3. This can be seen in the comparison between figure 5.24 (a) and 5.24 (c). Figure 5.24 (a) shows an untreated control culture, displaying the classic hippocampal structure, the dentate gyrus and CA3-CA1 being clearly visible. This is clearly contrasted by figure 5.24 (c), in which the CA3 region is no longer apparent, implying the death of pyramidal cells in this region. Incubation for 24 hours with 1μM KA is clearly below the toxic threshold detectable by thionin staining, as can be seen in figure 5.24 (b). The various cell body regions are all clearly seen, very much as in the control group. This is also the case for the preconditioned group which were then subsequently challenged with a 5μM KA incubation for 24 hours at 11 DIV, where again the cell layers all appear to be intact.

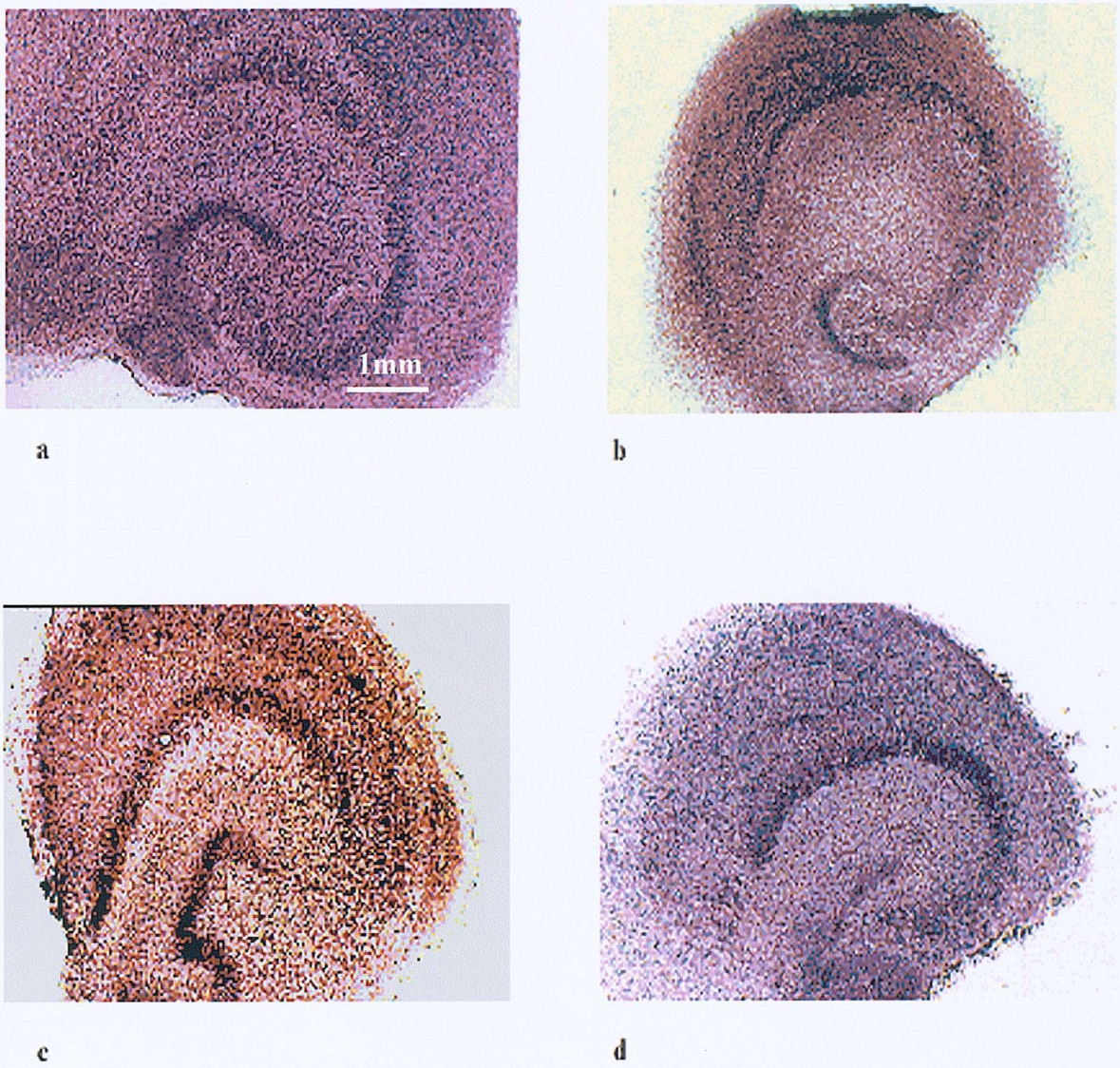

Figure 5.24 Photomicrographs showing examples of thionin stained MF1 cultures fixed at 15DIV.
a) Untreated control (n=9 slices). Note the interlocking C-shapes of the dentate gyrus and stratum pyramidale of CA3 and CA1. b) 1μM KA at 7DIV (n=28 slices), c) 5μM KA at 11DIV (n=24 slices). Stratum pyramidale of CA3 has been lesioned. d) Pre-conditioned with 1μM KA at 7DIV + 5μM KA at 11 DIV for 24 hours (n=26 slices). The hippocampal slice cultures in these treatment groups represent slices from six animals. Mag. X40

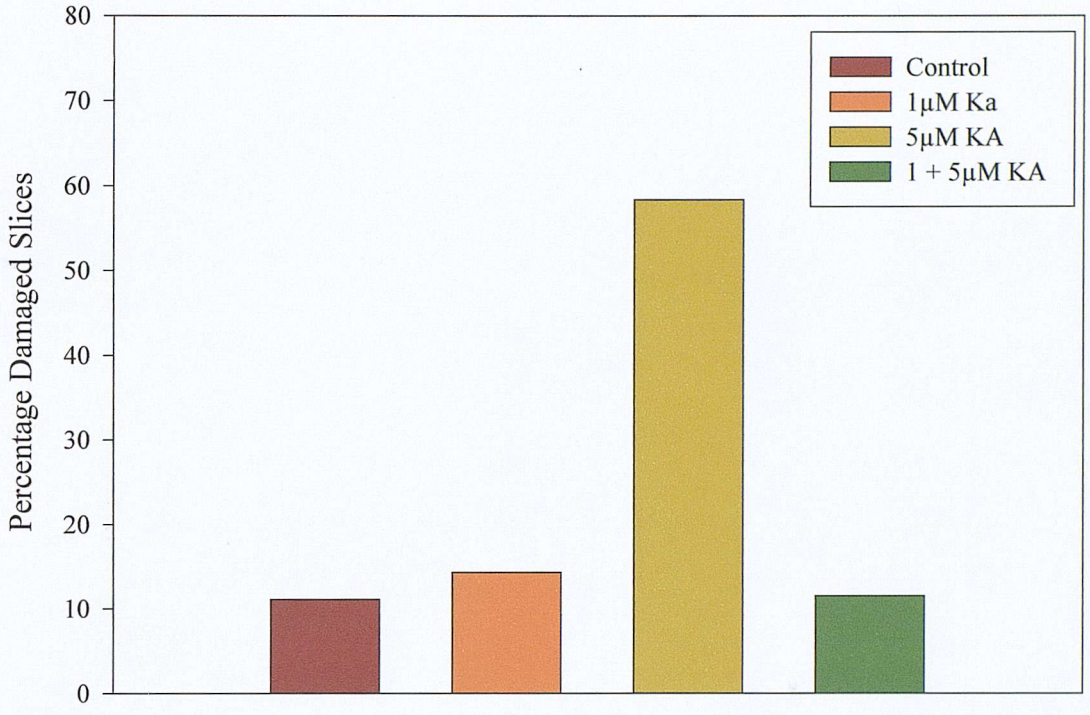

Figure 5.25 Percentage of damaged slices (i.e. slices in which CA3 is obviously lesioned) per treatment group revealed using the Nissl stain thionin. The 1μM KA incubation was carried out at 7 DIV, 5μM KA at 11 DIV. The number of slices per treatment group may be seen below in table 5.1. Each treatment group contained slice cultures derived from six separate animals.

Treatment	Percentage Damaged Slices	Total number slices
Control	11.1%	9
1μM KA (7DIV)	14.3%	28
5μM KA (11DIV)	58.3%	24
1 + 5μM KA	11.5%	26

Table 5.1 Percentage of lesioned slices visualised using the Nissl stain thionin for control, 1μM and 5μM KA incubations and 5μM KA incubation following preconditioning at 7 DIV with 1μM KA

The percentage of slices exhibiting damage to CA3 visualised using the Nissl stain thionin following various kainic acid treatments can be seen in figure 5.25. The graph shows that pre-treatment with 1μM KA for 24 hours at 7 DIV reduces the severity of the damage caused by 5μm KA within CA3. The actual percentages for this experiment are shown in table 5.1.

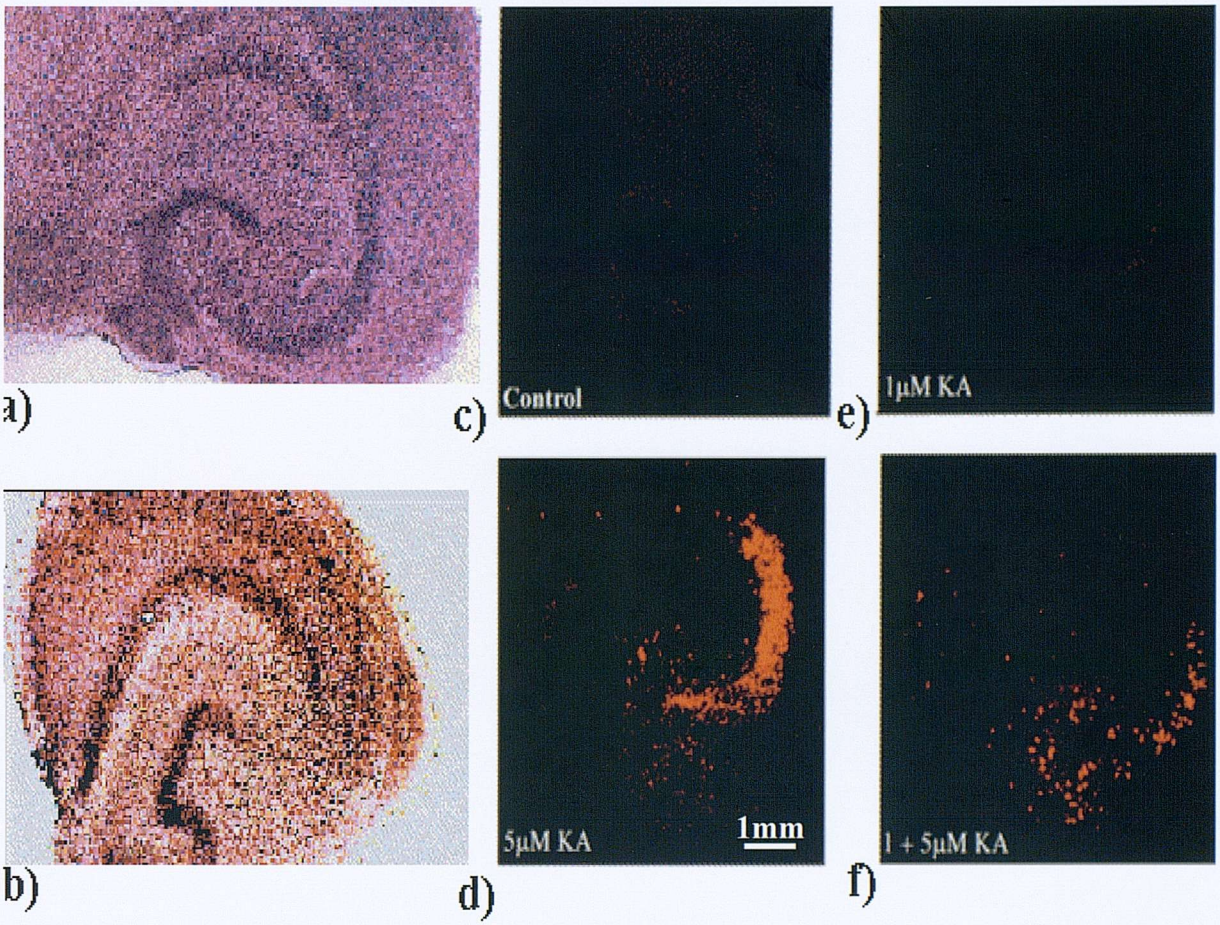

Figure 5.26 Photomicrographs of 15 DIV MF1 mouse cultures stained with thionin and the fluorescent exclusion dye propidium iodide (PI). a) thionin control, c) PI control; b) 5μM KA (11DIV) treated culture stained with thionin, d) 5μM KA (11DIV) with PI; e) 1μM KA (7DIV) with PI; f) 5μM KA following preconditioning, stained with PI. Mag. X40

Although thionin staining is a useful indicator of the presence or absence of cells, it does not provide information on the viability of those cells present. Information of this kind may be obtained by the staining of live slices with propidium iodide (PI), which is only able to fluoresce once it binds to nucleic acid. It's molecular size prevents it entering cells whose membranes are intact (*ie.* live cells), thus rendering it a useful tool to visualise dead and dying cells (Darzynkiewicz & Li 1996). Figure 5.26 shows the results of PI staining cultures at 15 DIV following a preconditioning experiment. Figure 5.26 (a) and (b) show thionin stains of an untreated control culture (a) and one subjected to 5μM KA for 24 hours at 11 DIV (b). figure 5.26 (c) and (e) exhibit little or no fluorescence, being the untreated control (c) and a culture incubated with 1μM KA for 24 hours at 7 DIV (e). This lack of fluorescence indicates little or no cell death. The classic pattern of CA3 cell

death following kainic acid is clearly visible in figure 5.26 (d). The high degree of fluorescence in this region indicates widespread pyramidal cell death following the toxic insult. This toxicity is clearly reduced as a result of preconditioning (figure 5.26 (f)). These slices were generated during a separate experiment to that presented in figure 5.25 and represent cultures derived from 6 separate animals. The actual number of slices per treatment group may be seen in table 5.2.

5.3.2.2 Preconditioning Threshold

In order to whether there is a threshold preconditioning concentration of kainate below which neuroprotection does not occur, cultures were incubated with 250nM, 500nM, 750nM and 1μM KA for 24 hours at 7 DIV. Each of these groups was subsequently challenged at 11 DIV with 5μM KA. A further unconditioned group of cultures were also treated with 5μM KA at 11 DIV. The PI data for this experiment can be seen in figure 5.27. From this and the graph in figure 5.28 we can see that although there is some small degree of neuroprotection at concentrations between 250-750nM, it is only when we reach 1μM KA that any marked difference is seen between the 5μM KA group and the preconditioned group. However, the fact that some neuroprotection is seen at sub-micromolar doses implies that it is likely to be a kainate receptor mediated phenomenon since these concentrations are unlikely to activate AMPA receptors to any significant degree. The percentages of damaged slices per group are shown in table 5.2.

5.3.2.3 NMDA Receptor Blockade During Preconditioning

Calcium entry *via* the NMDA receptor is known to activate various signalling cascades, which have downstream effects on the excitability of the cell. A preconditioning experiment was carried out in which one group of cultures were incubated with 20μM MK801 and 20μM D-AP5 at the same time as the 1μM KA preconditioning dose in order to prevent this. Figure 5.29 shows the PI data for this experiment, the results of which are shown graphically in figure 5.30. From the data it can be seen that NMDA blockade does not appear to affect the induction of kainic acid tolerance. Table 5.3 shows the percentage of CA3 damaged slices for the various treatment groups in this experiment.

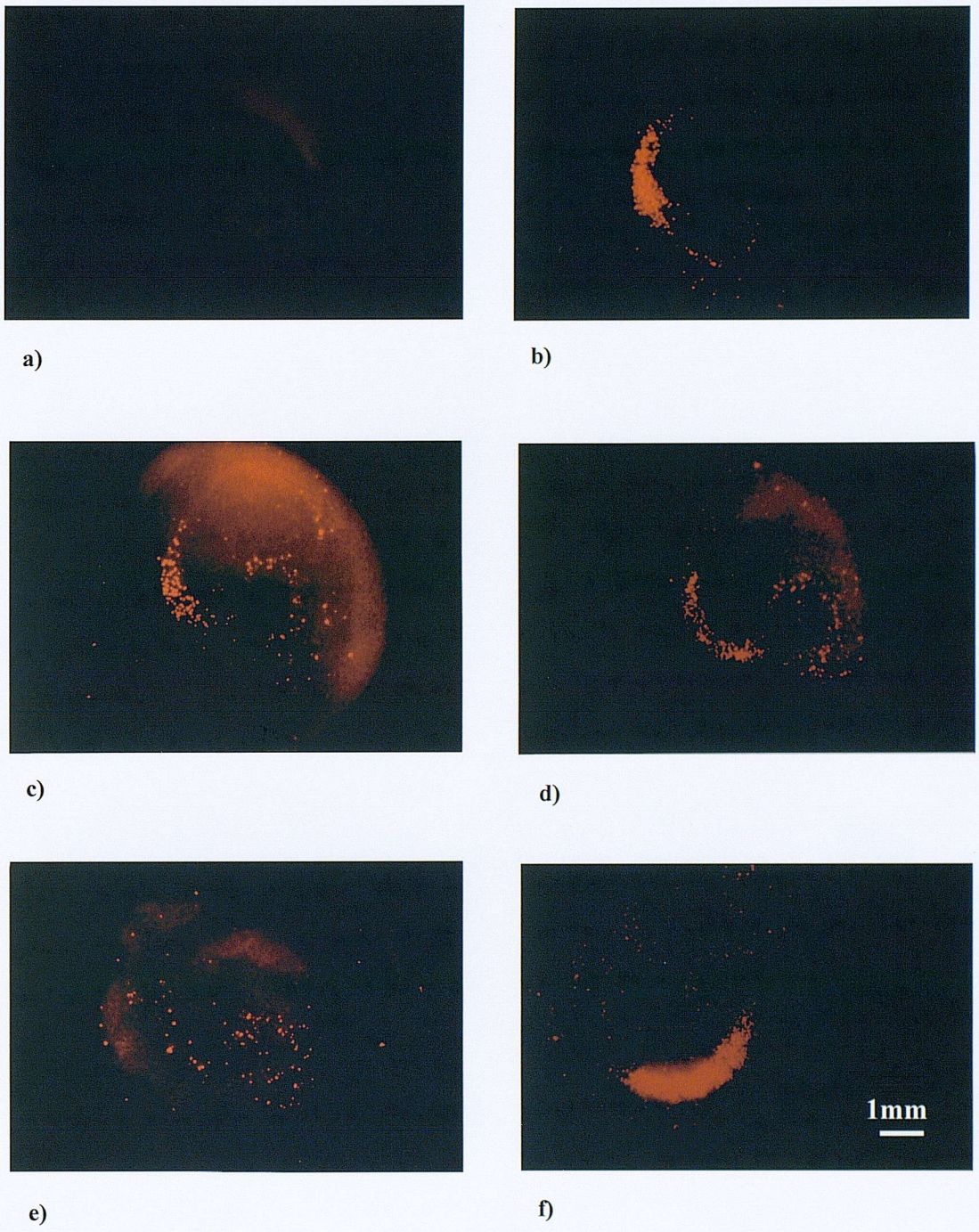

Figure 5.27 Photomicrographs of propidium iodide fluorescence elicited from 15 DIV cultures. The preconditioning dose of KA administered at 7 DIV was varied between 250nM-1μM. They were then incubated for a further 24 hours with 5μM KA at 11 DIV. a) Untreated control, b) 250nM KA preconditioning dose, c) 500nM preconditioning dose, d) 750nM dose, e) 1μM KA dose, f) 5μM KA control. The cultures in each treatment group represent slices taken from six different animals. Mag. X40

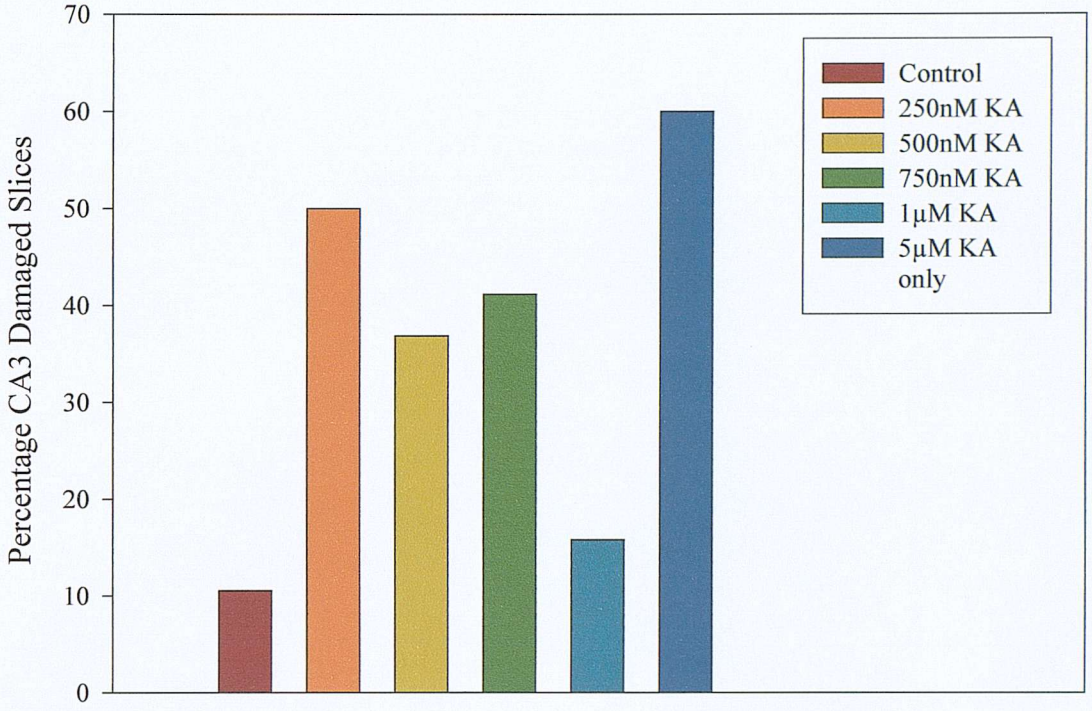

Figure 5.28 Graph showing the number of slices with extensive CA3 damage following various preconditioning doses from 250nM to 1μM KA as a percentage of the total number of slices receiving that treatment. Control slices received no treatment throughout and 5μM KA group received no preconditioning dose. All preconditioning doses were administered for 24 hours at 7DIV, followed by a 5μM KA challenge at 11DIV. All slices were stained with propidium iodide and visualised at 15 DIV.

Treatment	Percentage Damaged Slices	Number of Slices
Control	10.5 %	19
5μM KA	60%	20
250nM KA	50%	18
500nM KA	36.8%	19
750nM KA	41.2%	17
1μM KA	15.8%	19

Table 5.2 Table shows the percentage of CA3 damaged slices resulting from various preconditioning concentrations of KA administered at 7DIV followed by a toxic challenge with 5μM KA at 11 DIV. The first two rows represent the untreated and 5μM KA control groups. The last four represent cultures which were incubated with the stated concentration of KA at 7DIV for 24 hours and then challenged at 11DIV with 5μM KA for a further 24 hours.

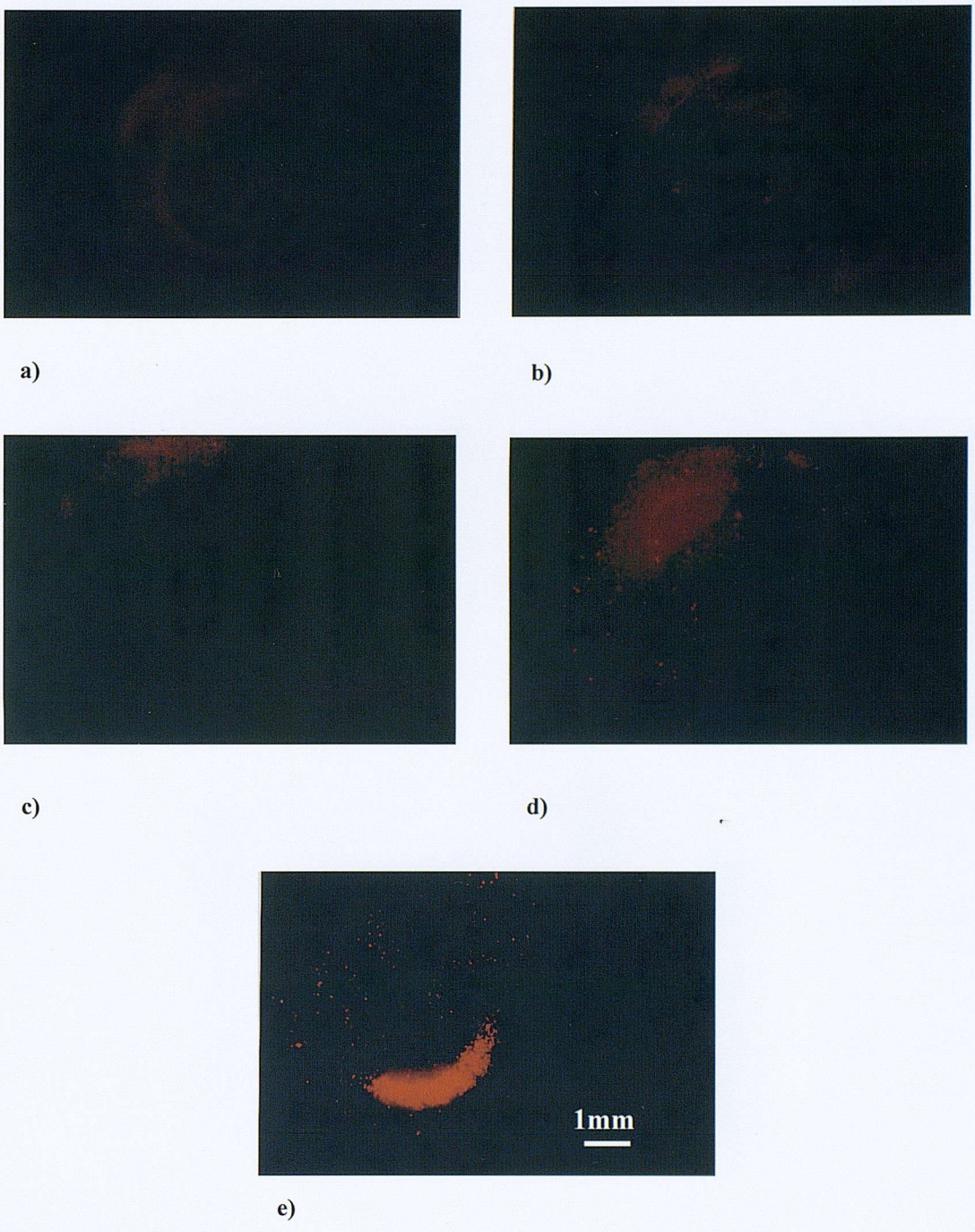

Figure 5.29 Photomicrographs of PI fluorescence elicited from 15 DIV cultures following an experiment to investigate the possible role of NMDA receptor activation as a result of KA induced depolarisation in the induction of tolerance. a) Untreated control, b) 1µm KA at 7DIV, c)1 + 5µM KA, d) 1µM KA, 20µM MK801, 20µM D-AP5 at 7DIV, 5µM KA at 11 DIV. e) 5µM KA at 11 DIV. Each treatment group consists of slices taken from six different animals. Mag. X40

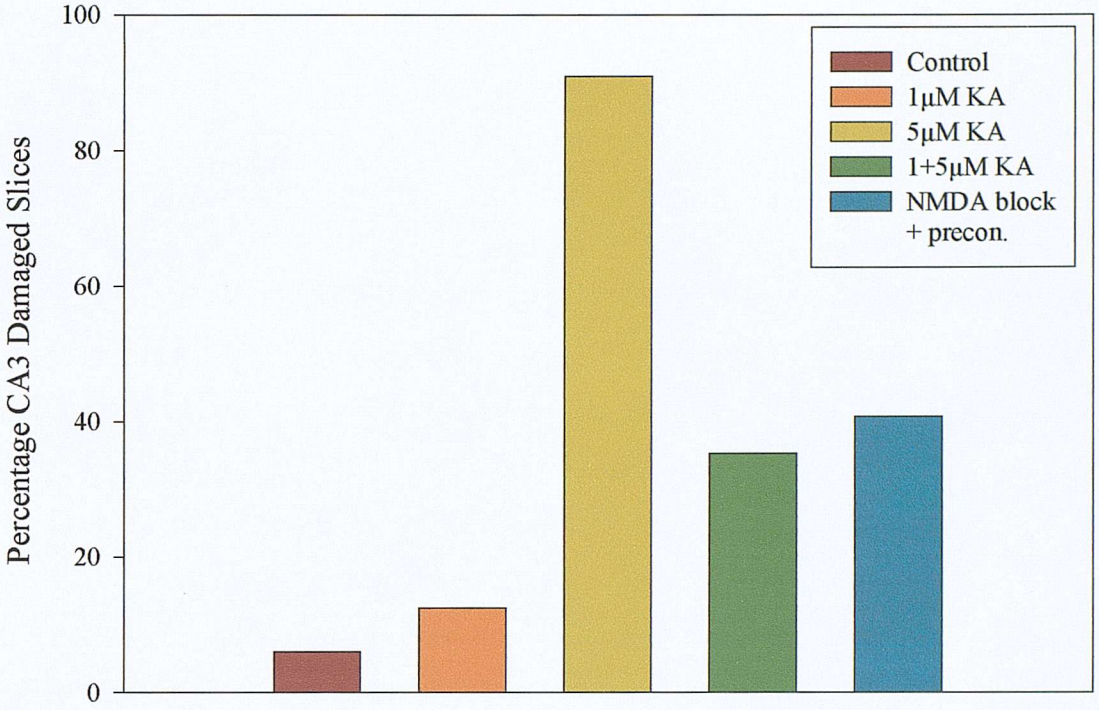

Figure 5.30 Graph showing the percentage of the total number of slices in each treatment group exhibiting severe CA3 damage indicated by propidium iodide fluorescence following pretreatment with 1μM KA or 1μM KA with 20μM MK801 and D-AP5. Bars represent number of damaged slices as a percentage of the total number of slices per group.

Treatment	Percentage Damaged Slices	Number of slices
Control	11.8%	17
1μM KA	12.5%	16
5μM KA	90.9%	11
1 + 5μM KA	35.3%	17
Precon + 20μM MK801 + D-AP5	40.7%	27

Table 5.3 Percentage of the total number of slices per treatment group exhibiting severe CA3 damage following a 24 hour incubation with 5μM KA in untreated cultures, preconditioned cultures and slices incubated with 20μM MK801and 20μM D-AP5 along with the preconditioning dose. Each group consists of slices derived from six animals.

5.3.2.4 GAD Staining

The *in vivo* kainic acid model in which kainic acid is administered intraventricularly is known to reduce the numbers of various interneuronal populations within the hippocampus (Frank, 1993, Best *et al.* 1994b). In order to assess the effect of inducing kainic acid tolerance on the susceptibility of interneurones to a subsequent kainate challenge cultures were fixed and antibody stained for GAD 67, the synthetic enzyme for GABA. Figure 5.31 shows examples of the result of GAD 67 staining in control (5.31 (a)), 1μM KA (b), 5μM KA (c) treated cultures and a preconditioned culture challenged with 5μm KA (d).

The numbers of GAD 67 positive cells in the dentate gyrus and hilus, CA3 and CA1 following various kainate treatments are shown graphically in figure 5.32. As can be seen, there are significantly fewer interneurones in the hilus and dentate gyrus, and CA3 following treatment with kainate. It is interesting to note that there is no significant difference in the number of GAD positive cells in the CA1 region. The cell counts for GAD-positive interneurones are shown in table 5.4.

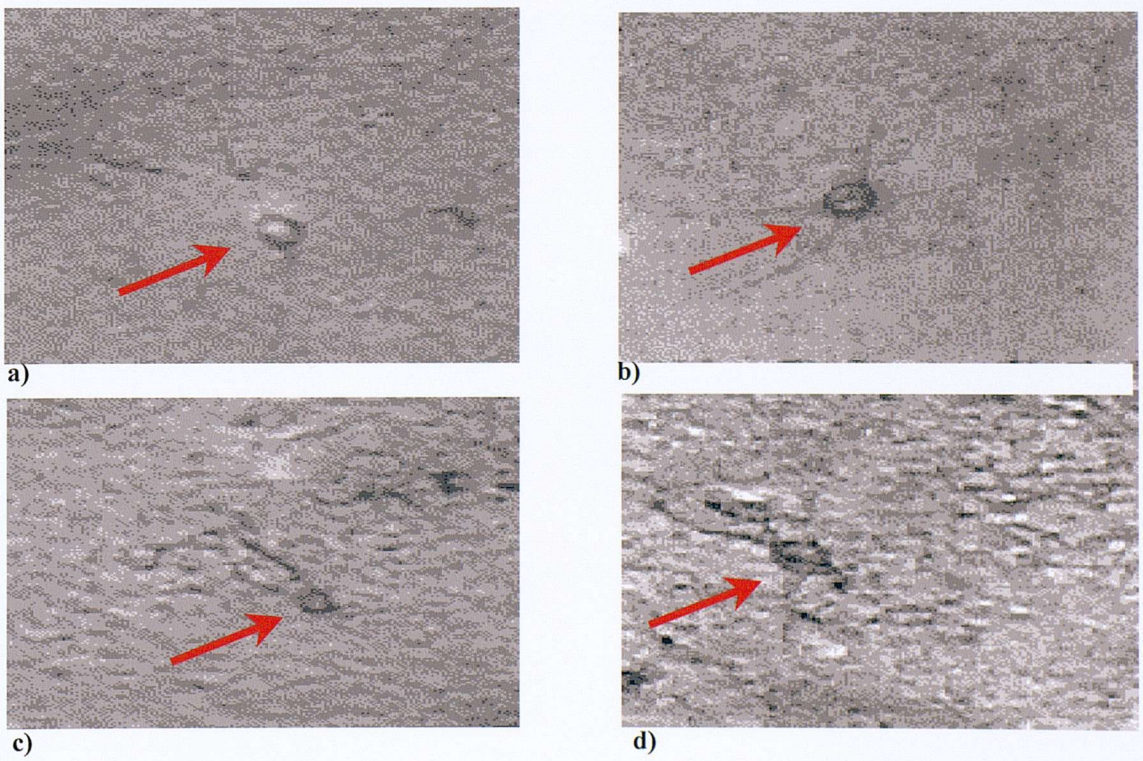

Figure 5.31 Examples of GAD stained neurones from a) control, b) culture treated with 1μM KA at 7 DIV, c) 5μM KA at 11 DIV and d) 5μM KA following preconditioning.

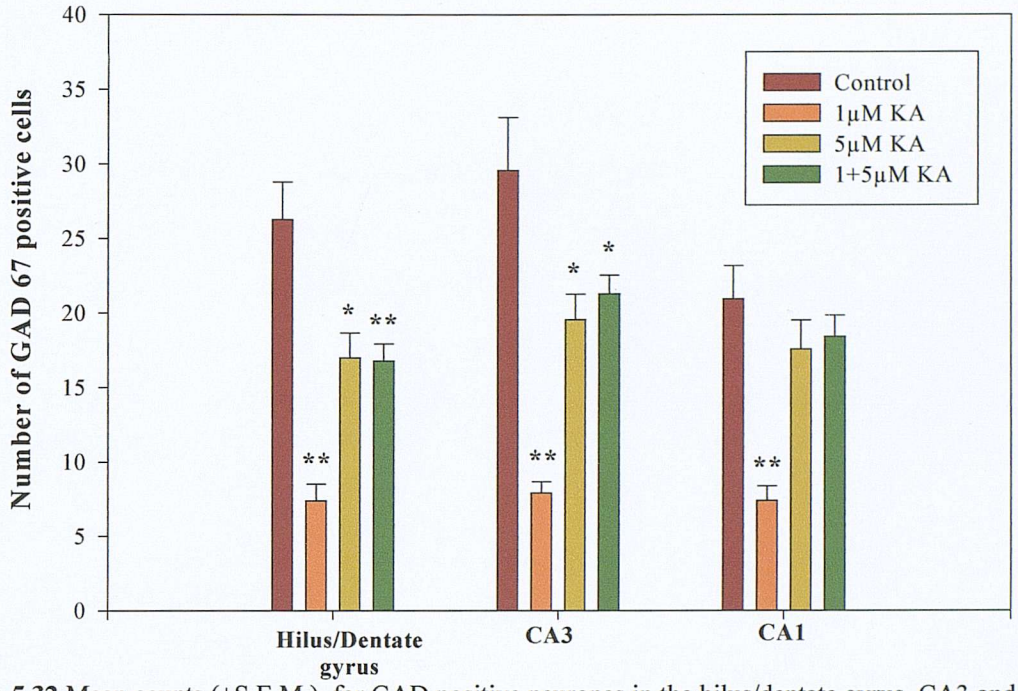

Figure 5.32 Mean counts (±S.E.M.) for GAD positive neurones in the hilus/dentate gyrus, CA3 and CA1 in cultures fixed at 15 DIV with 4% paraformaldehyde. Cultures were subjected to the following treatment protocols: 24 hour incubation with 1μM KA at 7 DIV, 24 hour incubation with 5μM KA at 11 DIV and 24 hour incubation with 5μM KA at 11 DIV following previous incubation at 7 DIV with 1μM KA for 24 hours. Each treatment group consists of slices taken from six animals. *= $p<0.05$, **=$p<0.01$, Student's Paried t-test

Treatment	Dentate/ Hilus	CA3	CA1	No. Slices
Control	25.63 (±2.29)	28.25 (±3.28)	19.75 (±2.11)	16
1μM KA	7.38 (±1.14)	7.90 (±0.75)	7.38 (±0.98)	21
5μM KA	17.00 (±1.67)	19.55 (±1.71)	17.55 (±1.96)	20
1 + 5μM KA	16.78 (±1.14)	21.28 (±1.27)	18.39 (±1.43)	18

Table 5.4 GAD-positive cell counts for a preconditioning experiment. Means cell counts (± S.E.M.) are show for untreated controls, 1μM KA at 7 DIV, 5μM at 11DIV and 1 + 5μM KA treatments. Each treatment group contains slices from six animals.

5.3.4 Preconditioning and CA3 Electrophyisiology

It was possible to record population spikes from both the CA3 and CA1 regions of organotypic cultures from 7 DIV onwards. During initial comparisons of the field population spike responses elicited from the CA3 of untreated control cultures, and those which had been preconditioned at 7DIV with a 24 hour incubation of 1μM KA, it was noticed that the inhibition of the second population spike was far greater in the control group than the preconditioned. An example of these paired pulse recordings may be seen in figure 5.33 below.

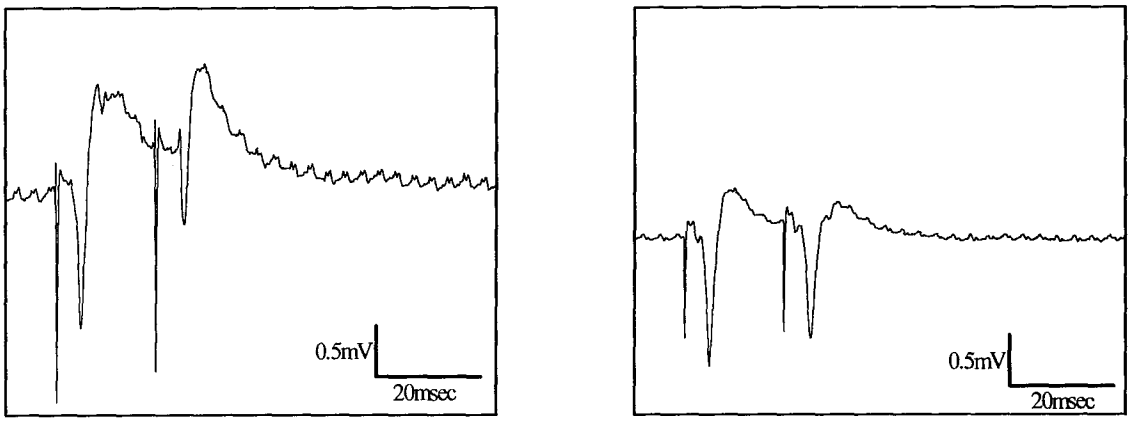

Figure 5.33 Example traces of extracellular field potentials recorded from the *stratum pyramidale* of CA3 in age matched cultures. a) represents a response to a half maximal stimulus taken from an untreated control culture, b) a response taken from a culture that was preconditioned at 7DIV for 24 hours with 1μM KA. The trace in b) exhibits a lower degree of paired pulse inhibition than that in a).

Calculating the mean (± S.E.M.) for the values obtained for the percentage inhibition in control and preconditioned cultures showed that the mean is significantly larger in control (48% (±1.9) n=6) than in preconditioned cultures (13% (±1.2) n=8) ($p<0.01$ Student's unpaired t-test). This difference may be seen graphically in figure 5.34, which shows the mean percentage inhibition calculated from both groups of cultures over a 15 minute period.

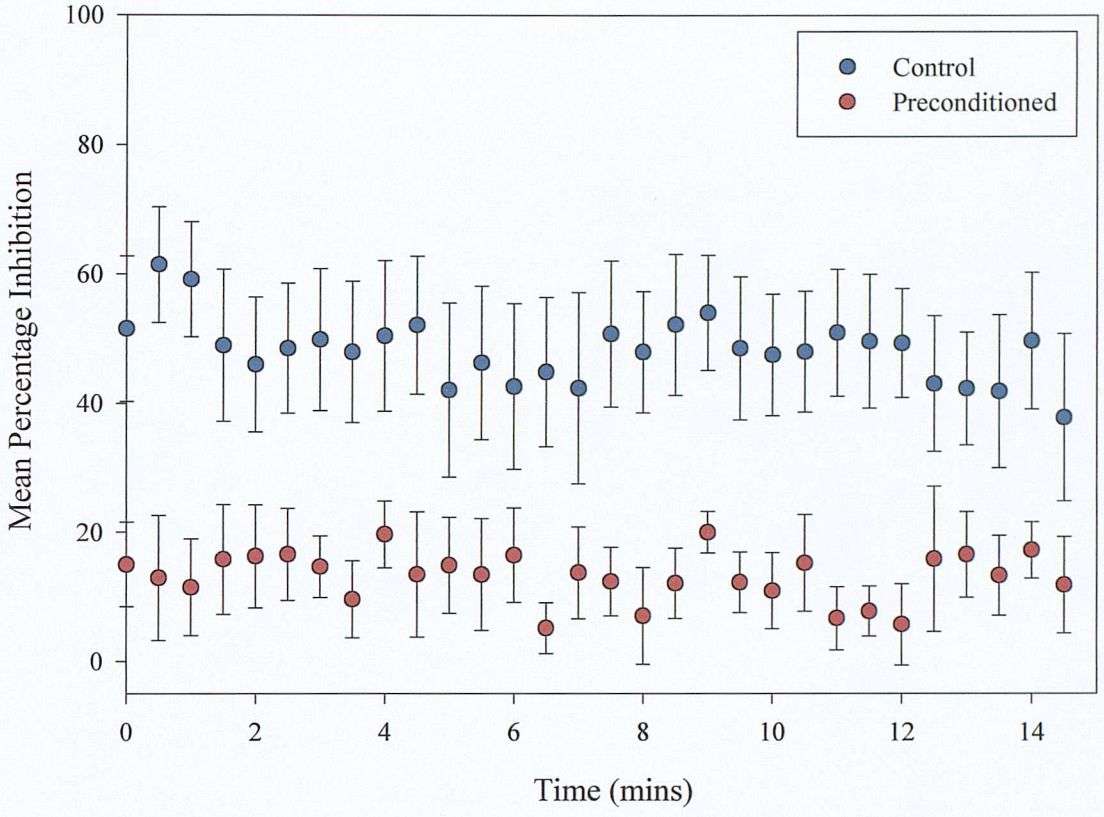

Figure 5.34 The mean percentage inhibition recorded from the CA3 region of age-matched preconditioned cultures (n=8) and untreated controls (n=6) during a 15 minute period are highly significantly different ($p<0.01$, Student's unpaired t-test). The means (±S.E.M.) calculated for the overall inhibition during this period were 48% (±1.9) for the control and 13% (±1.2) for the preconditioned groups.

Although the percentage inhibition is markedly reduced in preconditioned cultures (figure 5.34) there is in fact still some inhibition of the second population spike remaining. In order to ascertain whether this inhibition was still mediated by $GABA_A$ receptors, field recordings were made from CA3 *stratum pyramidale* during the application of various concentrations of the $GABA_A$ antagonist bicuculline methiodide (Bic) (Sigma). Bicuculline has long been known to be an antagonist at $GABA_A$ receptors (Curtis *et al.*, 1970; Olsen *et al.*, 1976), and is commonly used as an epileptogenic agent. However, more recently it has also been reported to have activity at sites other than the $GABA_A$ receptor. For example, bicuculline may possibly activate calcium release from intracellular calcium stores in cultured rat cerebellar granule cells, an effect that appears to be independent of $GABA_A$ receptors (Mestdagh and Wulfert 1999). Bicuculline, by virtue of its antagonist properties, is capable of reducing the degree of paired-pulse inhibition of the second population spike compared to the first in a dose dependant manner. Low doses of the drug (for example 1μM) reduce the inhibition whilst higher concentrations (e.g.

10μM) are capable of completely abolishing the inhibition, resulting in an epileptiform burst.

An example of the type of recording obtained from CA3 of untreated cultures during the application of 1μM Bic may be seen in figure 5.35 below. Partial blockade of $GABA_A$ receptors results in an increase in the amplitude of the second population spike as the efficacy of GABAergic inhibition is reduced. It would be expected that the amplitude of the first population spike would also increase as the effects of the tonic inhibition are presumably also being antagonised. Surprisingly, the amplitude of the first population spike actually decreases (figure 5.36), possibly due to a desynchronisation of the pyramidal cell population or perhaps due to some non-$GABA_A$ receptor mediated effect of bicuculline on pyramidal cell excitability. This effect does not appear to wash out after 30 minutes ACSF wash.

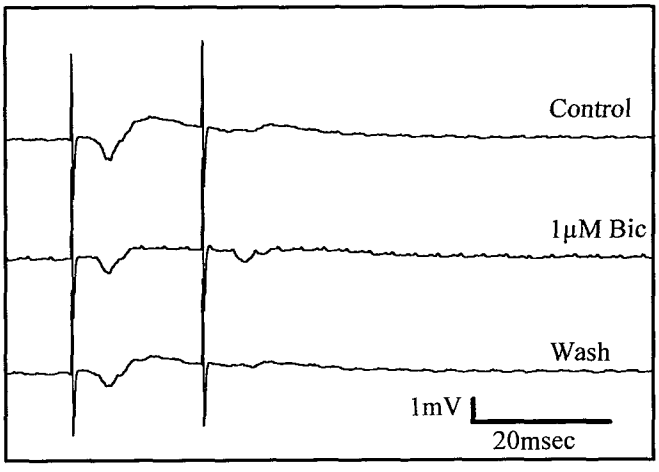

Figure 5.35 Example traces of population spike recordings from the CA3 region of an untreated control culture during the application of 1μM Bic. Note that initially there is almost complete inhibition of the second population spike, which is reduced in the presence of 1μM Bic.

The time-course for this experiment showing the mean percentage response (±S.E.M.) for the first and second population spike can be seen in figure 5.36 below.

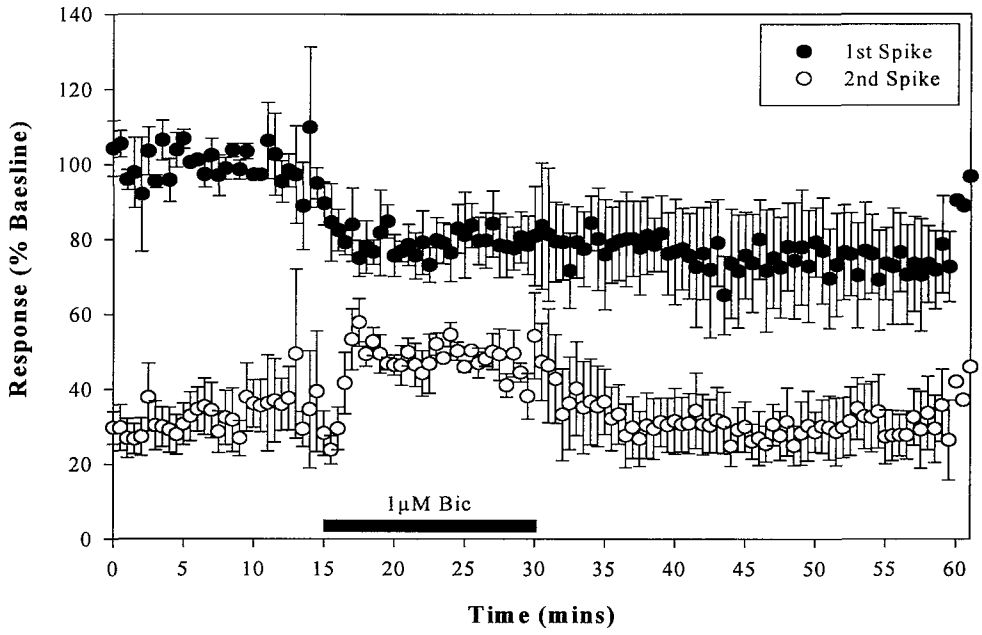

Figure 5.36 Time course for the effects of 1μM Bic in the CA3 of control cultures at 10-14 DIV. There is good initial inhibition of the second population spike during the control period. With the application of 1μM Bic the second population spike increases in amplitude from 35% (±6.8) to 44% (±3.1) by the end of 15 minutes. This implies a reduction of $GABA_A$ mediated inhibition (n=3).

The mean percentage inhibition during this experiment (figure 5.37) falls with the onset of the effects of 1μM Bic from 64% (±6.6) to 43% (±5.0). This indicates that in the untreated CA3 the inhibition of the second population spike elicited by a stimulus 20msec after the first is a $GABA_A$ receptor mediated event.

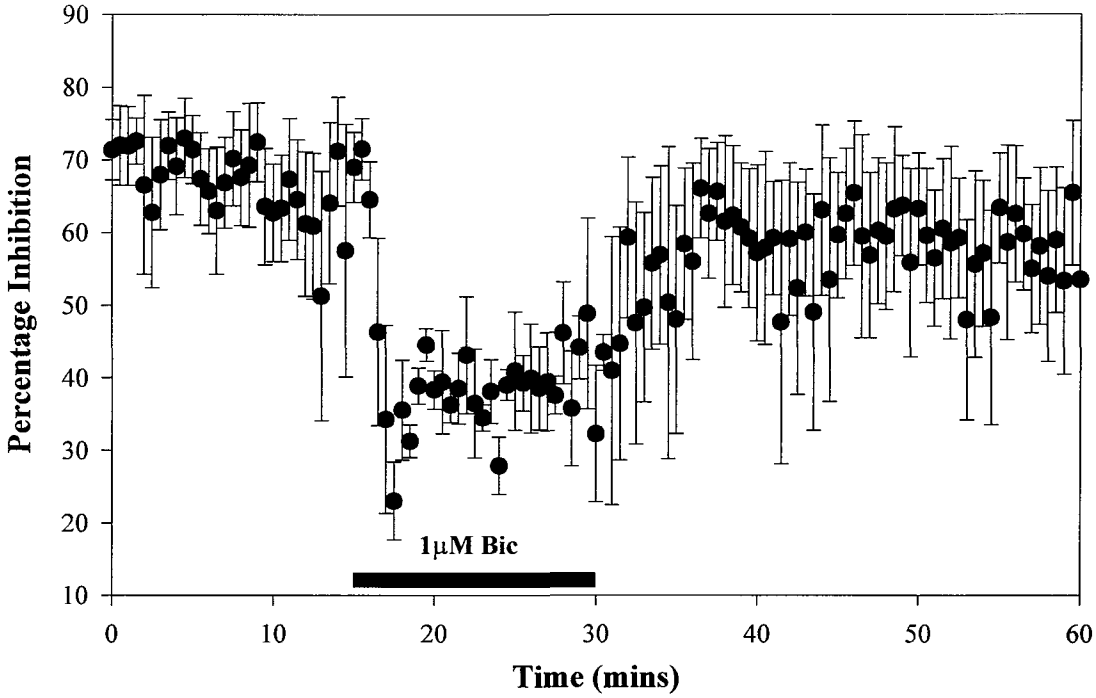

Figure 5.37 Time-course for the change in mean percentage inhibition that occurs during the application of 1μM Bic to the CA3 of untreated control cultures (n= 3). During the course of the experiment the mean percentage inhibition falls from 64% (±6.6) to 43% (±5.0) as $GABA_A$ receptors are blocked by bicuculline.

Examples of the traces obtained from preconditioned culture CA3 may be seen in figure 5.38. The time-course data for the effects of 1μM Bic application on the mean percentage amplitude of the first and second population spikes recorded from CA3 of preconditioned cultures can be seen in figure 5.39. The changes in the mean percentage inhibition (±S.E.M.) throughout this experiment are presented in figure 5.26.

Since the effect of 1μM Bic in the preconditioned CA3 showed great variability, raw data traces have been presented for all three experiments in the data set. In the first experiment (figure 5.38 a) 1μM Bic produced no change in the amplitudes of either the first or second population spike. In the second (figure 5.38 b) the multiple spiking present in the control was abolished in the presence of the drug. In the third, 1μM Bic application resulted in epileptiform activity (figure 5.38 c).

Thus the mean population spike amplitudes in figure 5.39 show no change in the first population spike and a decrease in the amplitude of the second. This in turn results in the increase observed in the mean percentage inhibition presented in figure 5.40. It would be desirable therefore for the experiment to be repeated several more times in order to gain a clearer perspective of what is actually occurring in the preconditioned CA3 during the

application of 1μM Bic. This could lead to a better idea as to whether the act of preconditioning renders the CA3 more or less prone to epileptic activity in addition to being more resistant to a number of toxic challenges.

The same is also true for the effect of 3μM Bic, which also exhibited no change in one experiment (figure 5.38 d) and epileptiform bursting in the other (figure 5.38 e). This again resulted in a mean decrease in the amplitude of the second population spike (figure 5.41) and an increase in the mean percentage inhibition (figure 5.42).

Application of 10μM Bic (figure 5.43) was sufficient to induce bursting in both cultures tested (figure 5.38 f). Therefore data for the percentage inhibition has not been presented.

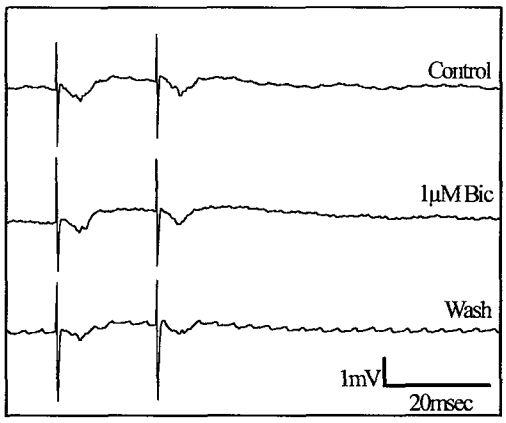

a)

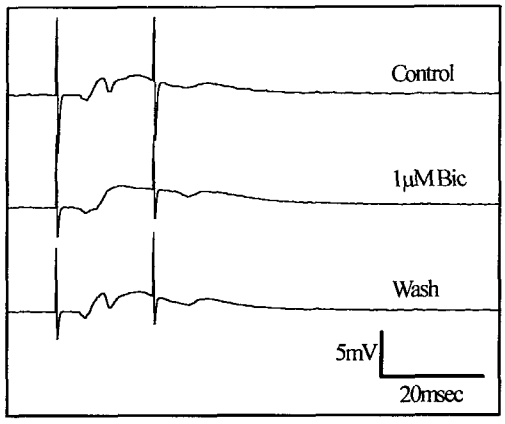

b)

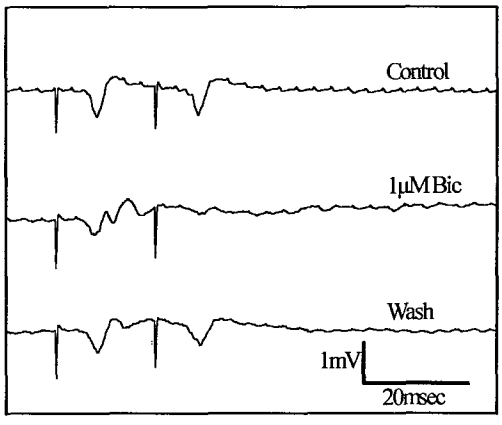

c)

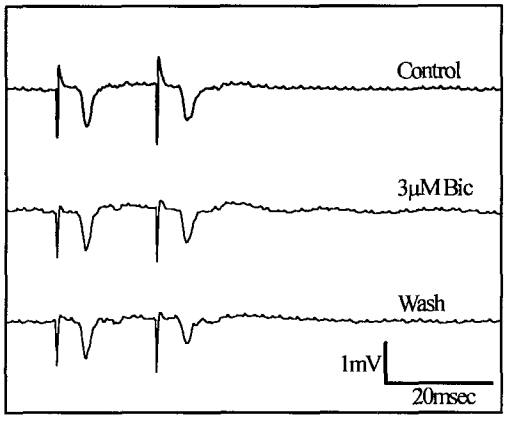

d)

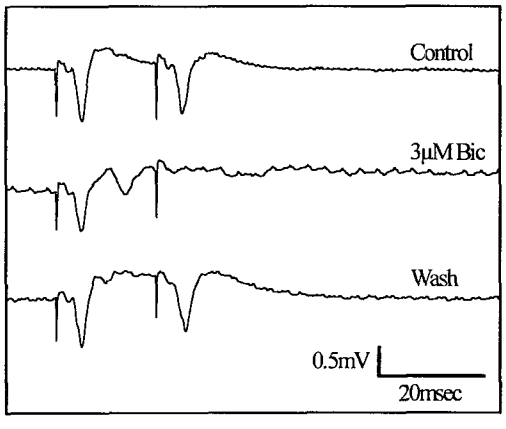

e)

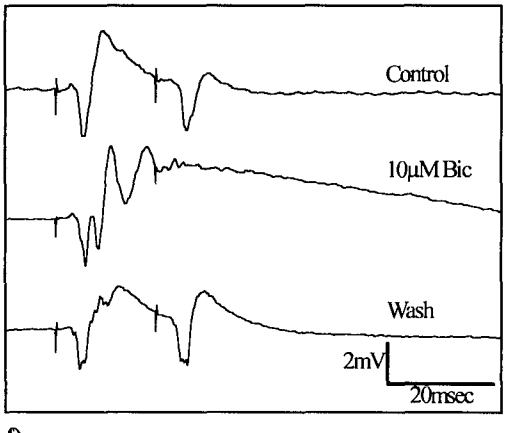

f)

Figure 5.38 Example traces showing the effect of a) 1μM Bic, b) 3μM Bic, c) 3μM Bic and d) 10μM Bic on the population spikes elicited using paired-pulse stimulation from the CA3 region of cultures preconditioned at 7DIV with 1μM KA. Note in all examples the low degree of inhibition of the second population spike in the initial control.

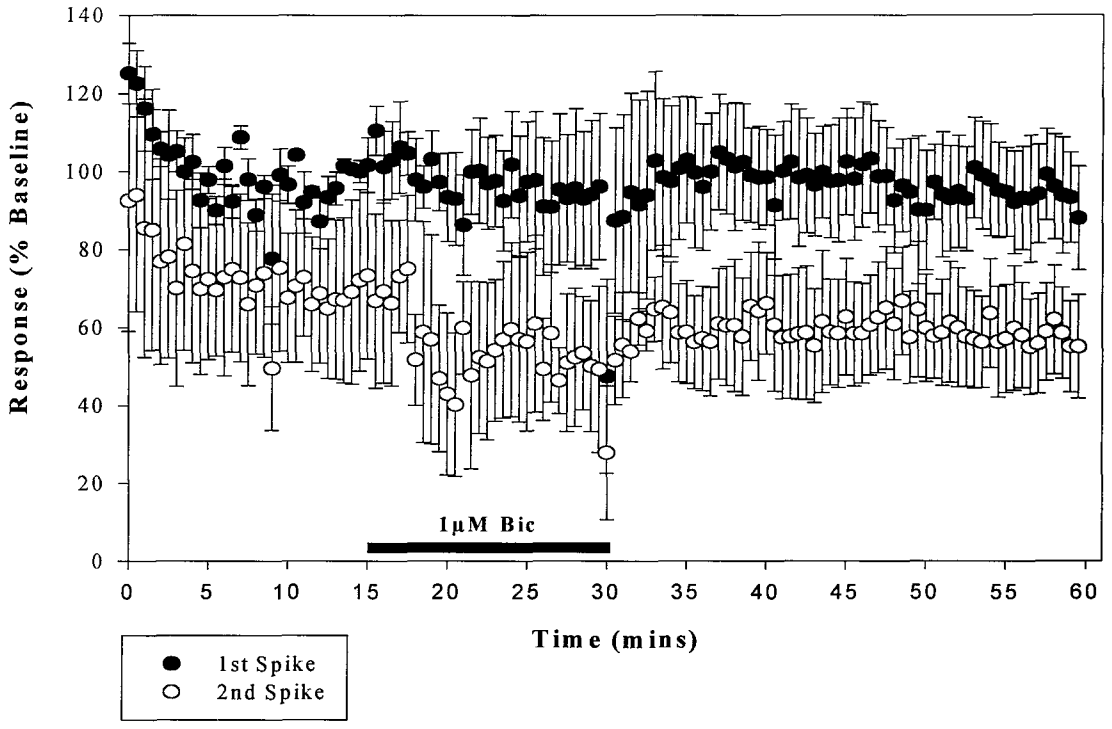

Figure 5.39 Time course for the application of 1µM Bic in preconditioned cultures. Note that the second population spike amplitude is reduced in the presence of 1µM Bic from 69% (±11.4) to 51% (±8.9) when compared to the effect seen in figure 5.22. This change, however, was not found to be significant (n=3).

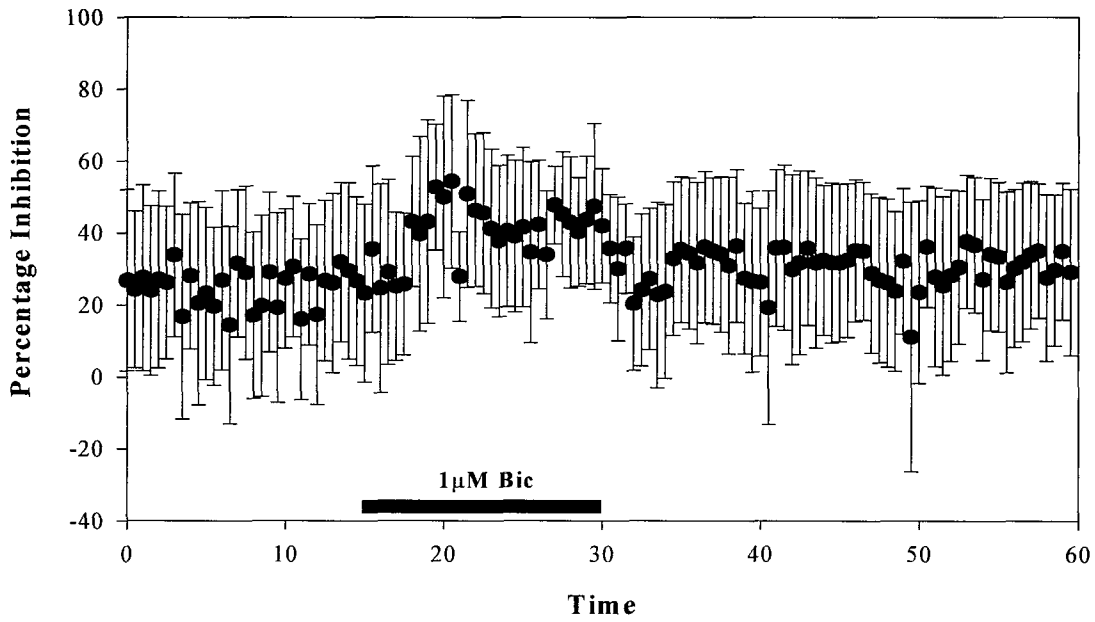

Figure 5.40 Changes in the mean percentage inhibition (±S.E.M.) calculated from paired-pulse data recorded from CA3 of preconditioned cultures during the application of 1µM Bic. As Bic washes into the recording chamber, the mean inhibition rises from 29% (±11.7) to 44% (±9.5). This change was not found to be significant (n=3).

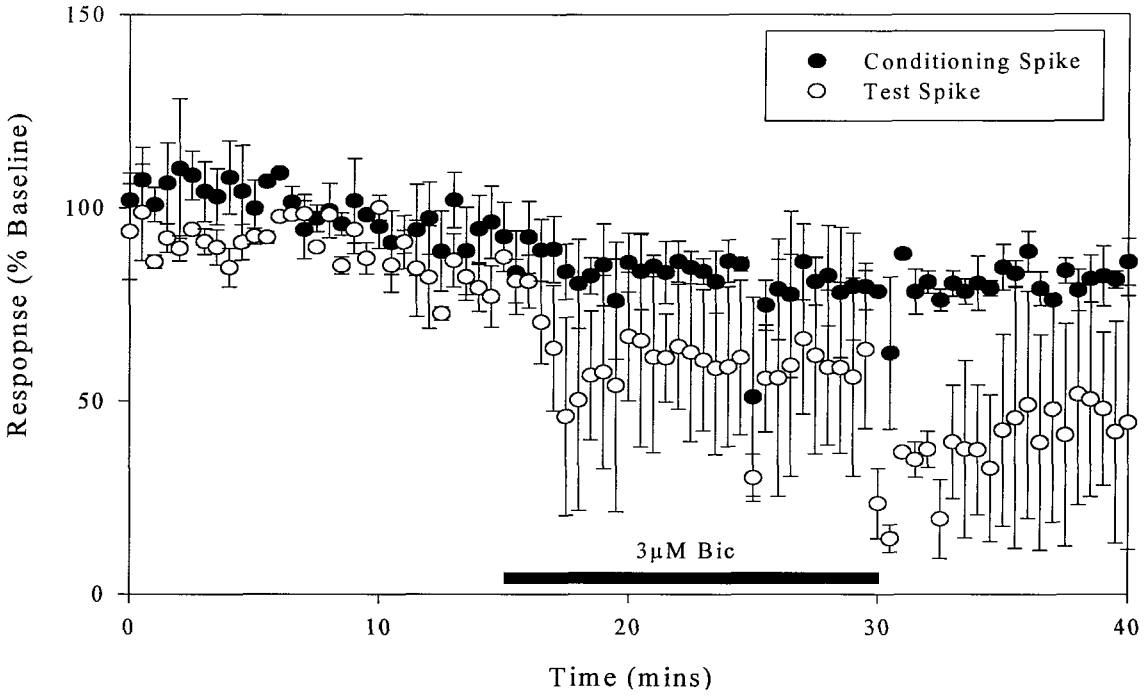

Figure 5.41 Time course for the effects of 3μM Bic in CA3 of preconditioned cultures between 11-14 DIV during a paired-pulse protocol (n=2, mean ± S.E.M.). Note the reduction in the amplitude of the second spike following Bic application from 80% (±3.1) to 60% (±10.3). This change however is likely to be due to the epileptiform activity which occurred during one of the two experiments. The example traces for this set of data can be seen in figure 5.24 b) and c).

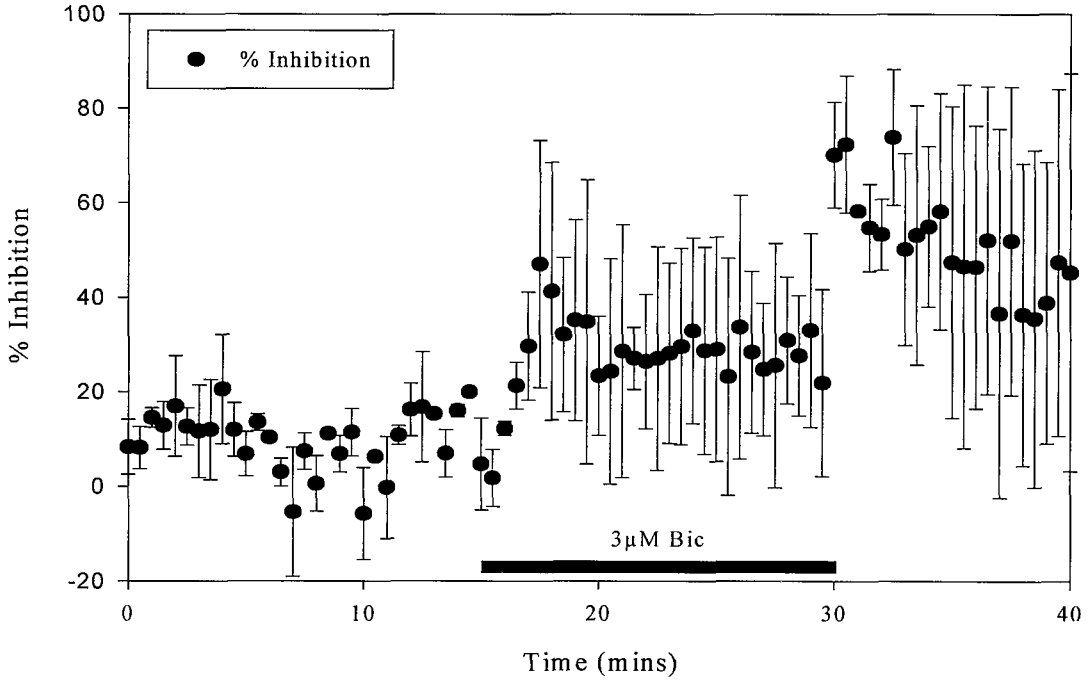

Figure 5.42 Time-course for the mean (±S.E.M) percentage inhibition if the second population spike with respect to the first recorded using paired-pulse stimulation with a 20msec inter-pulse interval in the CA3 of preconditioned cultures. Application of 3μM Bic causes a rise in the mean percentage inhibition from 14% (±2.8) to 28% (±8.3). This was not found to be significant (n=2).

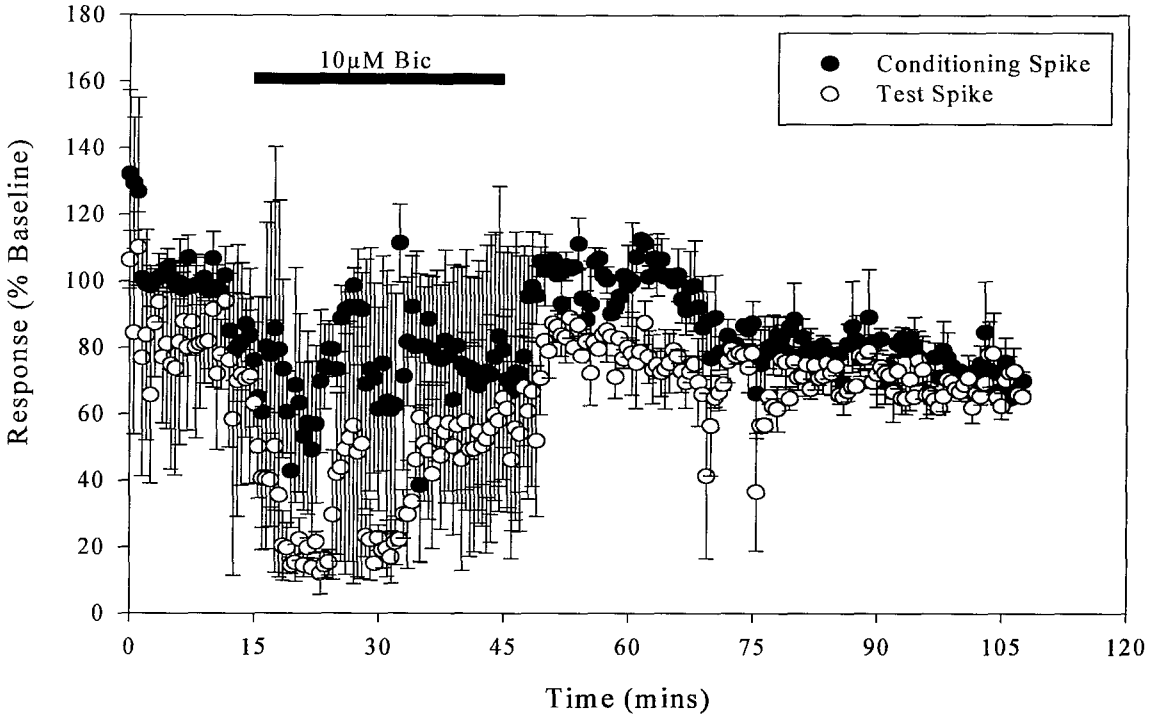

Figure 5.43 Time-course for the effect of 10μM Bic on the mean percentage amplitude (±S.E.M.) of the first and second population spikes recorded from the *stratum pyramidale* of the CA3 region of preconditioned hippocampal slice cultures (n=2). 10μM Bic application causes and epileptiform burst as can be seen in figure 5.38 d), implying that all remaining $GABA_A$ mediated inhibition has been abolished.

It is interesting to note that even though the effects of feedforward and feedback $GABA_A$ mediated inhibition in the CA3 of preconditioned cultures appears to be markedly reduced, the population spike recordings do not generally show any obvious signs of epileptiform activity in the absence of bicuculline. This is even the case under conditions of maximal stimulation which occur at the top of a stimulus response curve (figure 5.44).

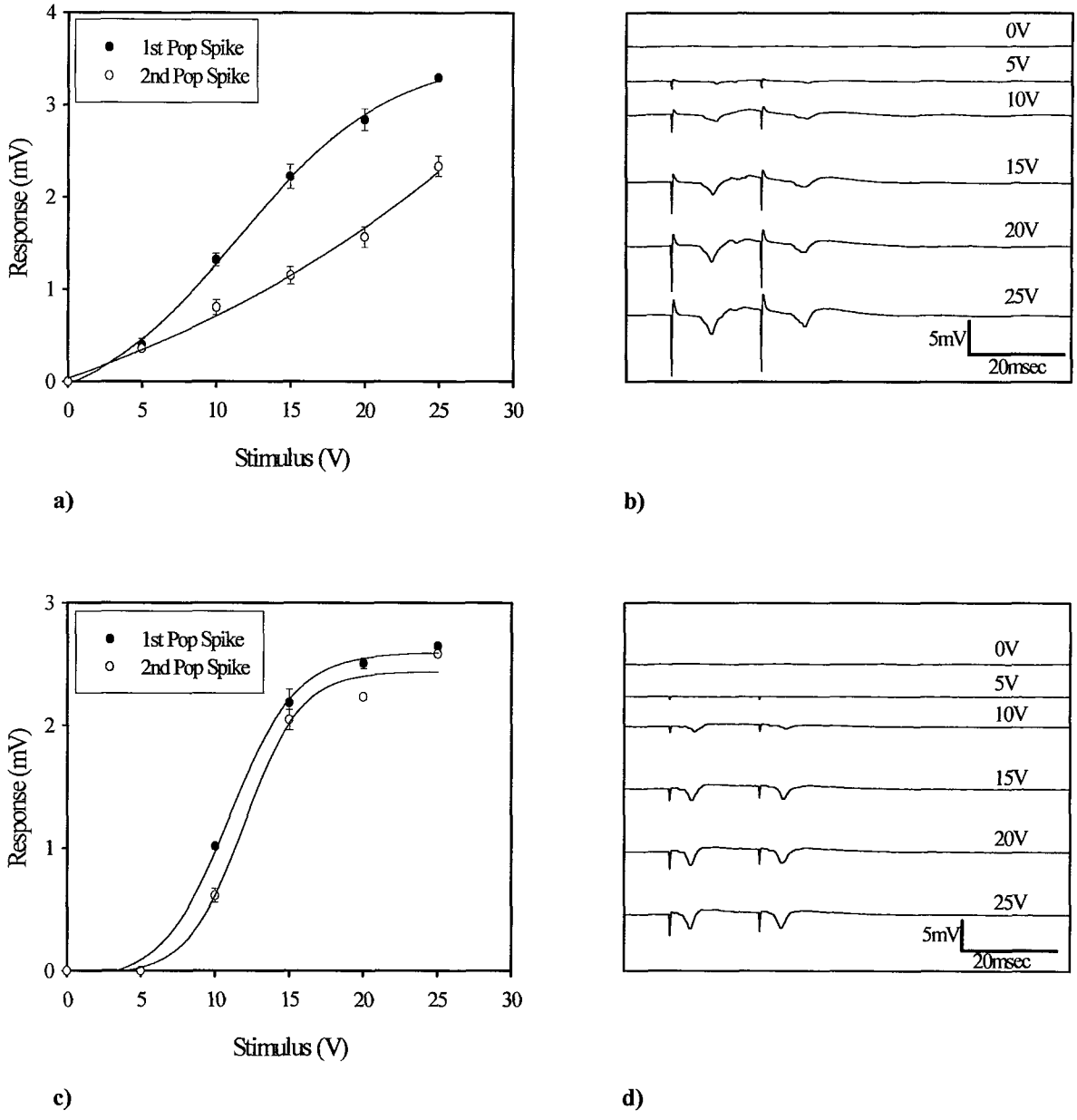

Figure 5.44 Examples of the stimulus-response curves and the raw-data traces from which they are derived for field recordings from the *stratum pyramidale* of CA3 in untreated control cultures (a) and b)) and preconditioned cultures (c) and d)). Note the close matching of the curves for the preconditioned stimulus-response (c) compared to that for the unconditioned (a), once again pointing to a reduction in the inhibitory mechanisms in CA3 following preconditioning.

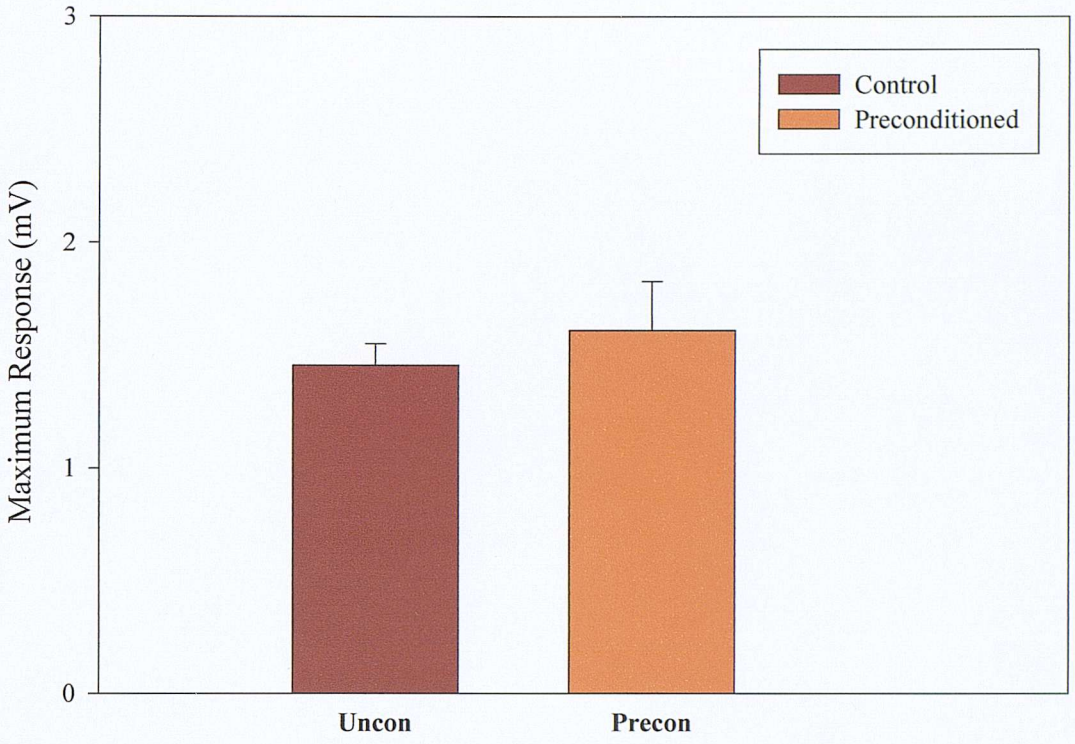

Figure 5.45 Mean (±S.E.M.) values for the maximal first population spike amplitude elicited from the CA3 of both control and preconditioned organotypic hippocampal slice cultures. The mean maximal response elicited from both groups was not found to be significantly different, being 1.5mV (±0.1) for the control and 1.6mV (±0.22) for the preconditioned group (n=9).

There is no significant difference between the maximal population spike output from the CA3 region of unconditioned cultures compared to those which have been preconditioned. This would tend to suggest that the induced tolerance phenomenon following preconditioning, which presumably indicates a state in which there is a decrease in the susceptibility of CA3 pyramidal cells to excitotoxicity, does not occur as a result of the lowering of the amplitude of the response which it is possible to elicit from this population of cells (figure 5.45). It would also suggest that there is little or no reduction in the CA3 pyramidal cell population following incubation with 1μM KA at 7DIV for 24 hours, thus adding weight to the propidium iodide data presented in figure 5.26, which showed a lack of fluorescence in the CA3 region following preconditioning. In addition to this, since the stimulus to the mossy fibre pathway required to evoke this maximal response does not change significantly either (figure 5.46), it is possible to infer two points. Namely that the mossy fibre-CA3 pyramidal cell synapse is still functional following preconditioning and that the excitability of CA3 pyramidal cells does not change in terms of the relationship between input and output from CA3.

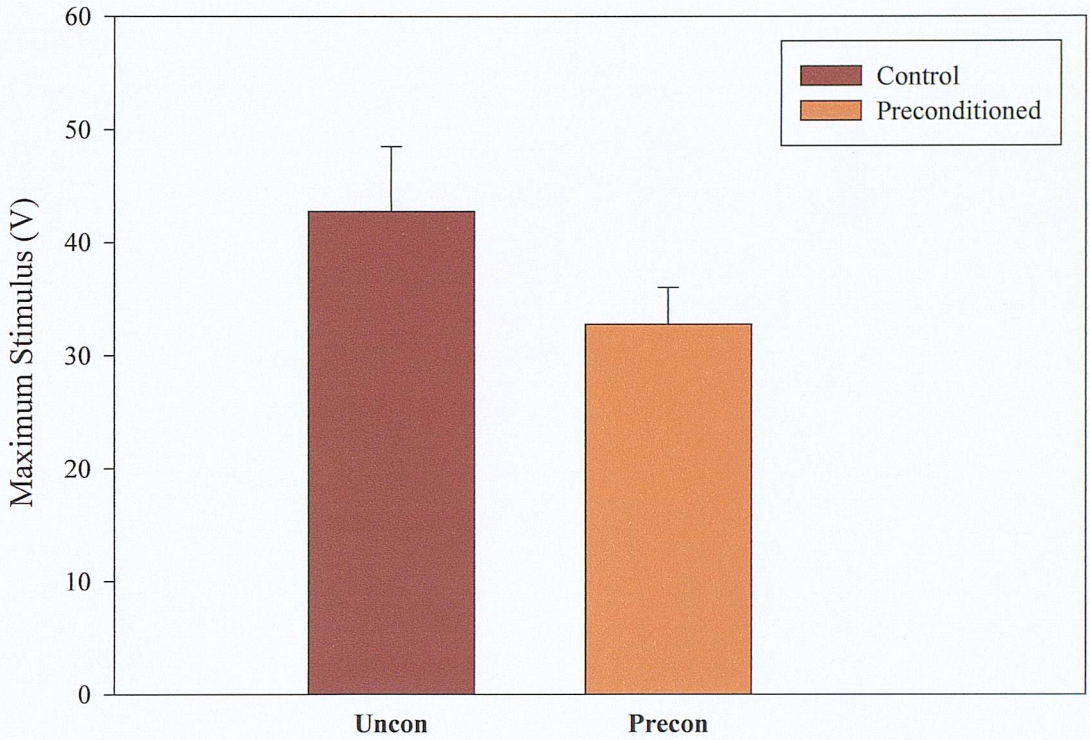

Figure 5.46 Maximal stimuli required to evoke the maximal population spike amplitude during a stimulus-response curve from the CA3 of both control and preconditioned cultures. The mean stimulus (±S.E.M.) for the control group was 43V (±5.7) whereas that for the preconditioned group of cultures was 33V (±3.2). These were not found to be significantly different (n=9).

5.3.5 Preconditioning and CA1

Comparison of the mean percentage inhibition evoked from CA1 *stratum pyramidale* revealed that although there is a far greater degree of inhibition present in the CA1 compared to the CA3 region, there is still a small but significant decrease in the percentage inhibition following preconditioning. Figure 5.47 shows examples of the population spike responses evoked by half-maximal stimuli from the CA1 using a paired-pulse protocol with a 20msec inter-pulse interval.

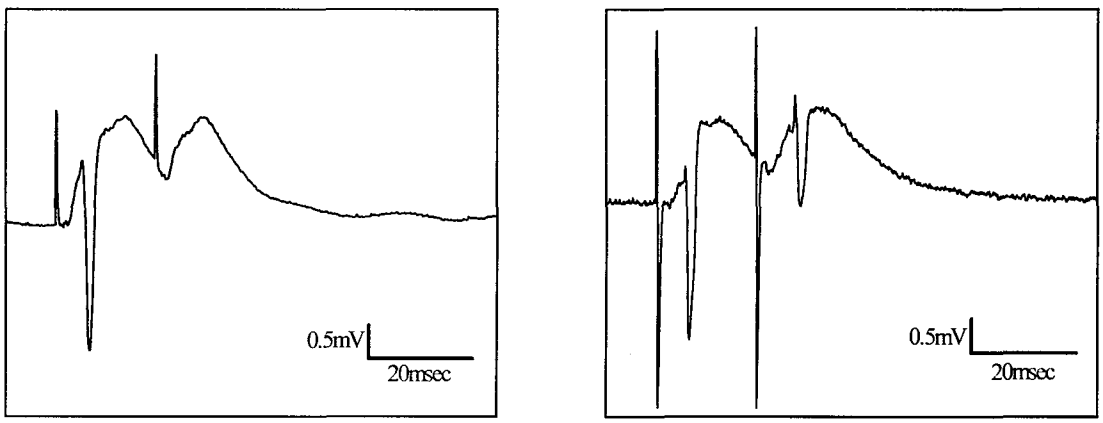

Figure 5.47 Examples of the traces obtained during extracellular recordings in the *stratum pyramidale* of the CA1 region of a) unconditioned and b) 1μM KA preconditioned cultures.

The mean percentage inhibition calculated from both unconditioned and preconditioned cultures during a fifteen minute control stimulation period can be seen in figure 5.48 below. The overall mean inhibition for this control period was calculated to be 74% (±1.1) (n=5) for unconditioned and 64% (±2.6) (n=4) for preconditioned cultures ($p<0.01$).

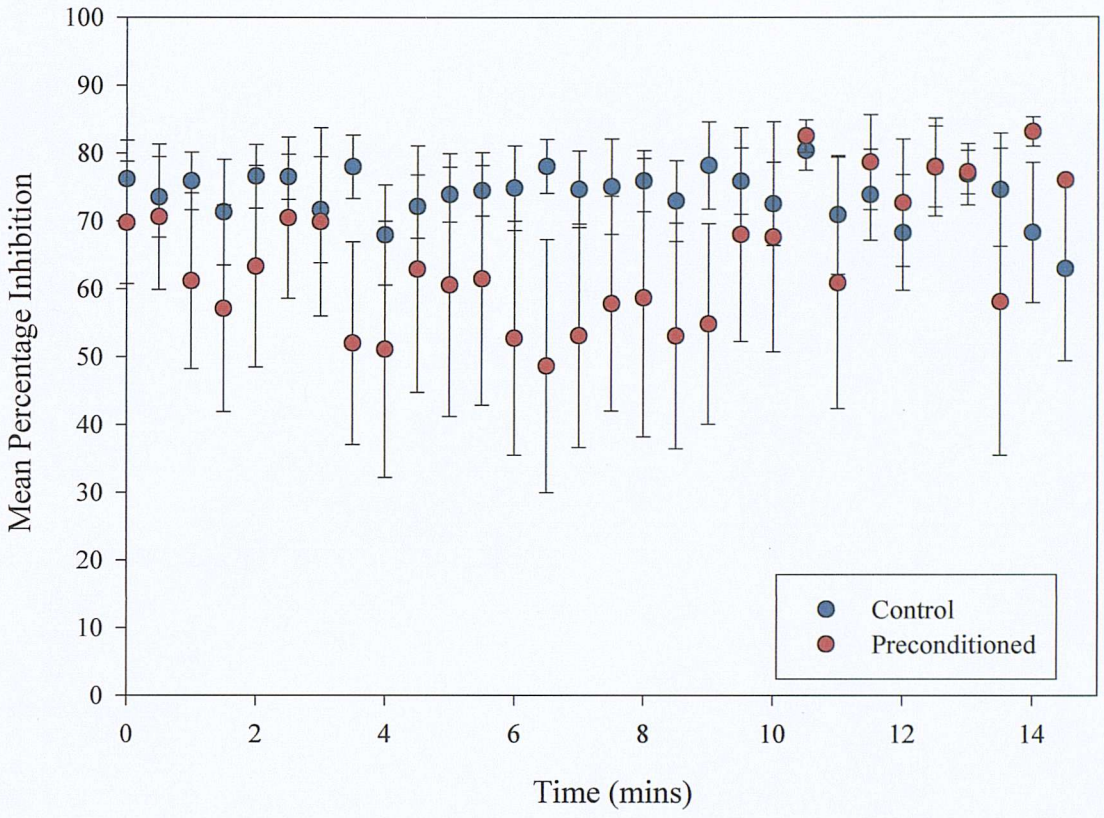

Figure 5.48 Time-course for the mean percentage inhibition (±S.E.M.) recorded from control (untreated) and preconditioned cultures over a fifteen minute period calculated from population spike data recorded from the *stratum pyramidale* of CA1. The overall mean percentage inhibition for each group calculated over this time was 74% (±1.1) (n=5) for unconditioned and 64% (±2.6) (n=4) for preconditioned cultures. Thus there is a small, but significant reduction in the paired-pulse inhibition recorded from CA1 following preconditioning with 1μM KA ($p<0.01$).

Once again, in order to examine whether this discrepancy related to a reduction in GABAergic function field recordings were made from *stratum pyramidale* of control and preconditioned cultures in order to discover whether the sensitivity to $GABA_A$ blockade had changed. Data for the effect of 10μM Bic in the CA1 of unconditioned cultures (figure 5.49) and 1μM Bic (figure 2 5.51, 5.52, 5.53) and 10μM Bic (figures 5.54, 5.55) in preconditioned cultures follow.

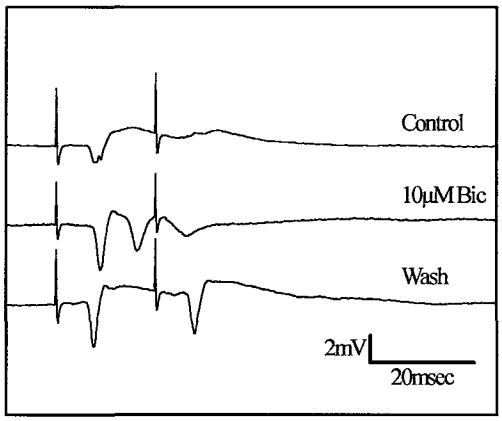

Figure 5.49 Comparison of the traces obtained from CA1 of unconditioned cultures during the application of 10μM Bic. In both groups of cultures Bic application at this concentration abolishes fast $GABA_A$ mediated inhibition, resulting in an epileptiform burst.

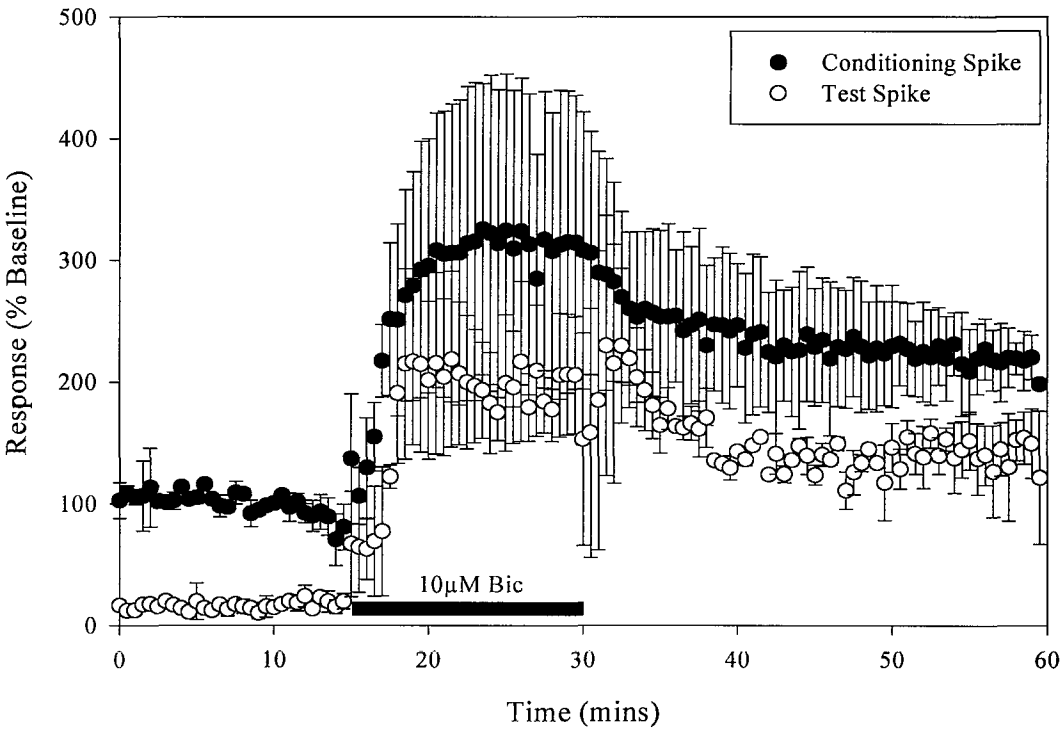

Figure 5.50 Time-course for the effect of 10μM Bic on the mean percentage amplitude (±S.E.M. n=2) of the first and second population spikes recorded from the CA1 of unconditioned control cultures using a paired-pulse protocol with a 20msec interpulse interval. As $GABA_A$ receptors are blocked it can be seen that the first and second population spike amplitudes rise as both the effects of tonic and evoked inhibition are reduced. This results in an epileptiform burst as seen in figure 5.49.

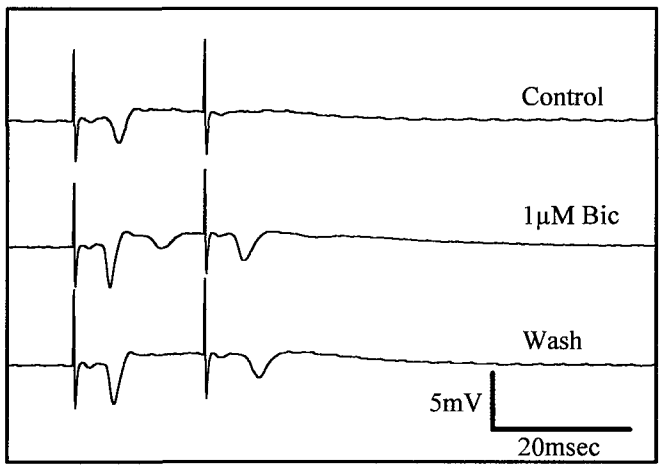

Figure 5.51 Examples of the traces obtained from the *stratum pyramidale* of the CA1 region of a preconditioned culture during the application of 1μM Bic. Blockade of $GABA_A$ receptors by Bic has been sufficient here to produce a mild epileptiform burst.

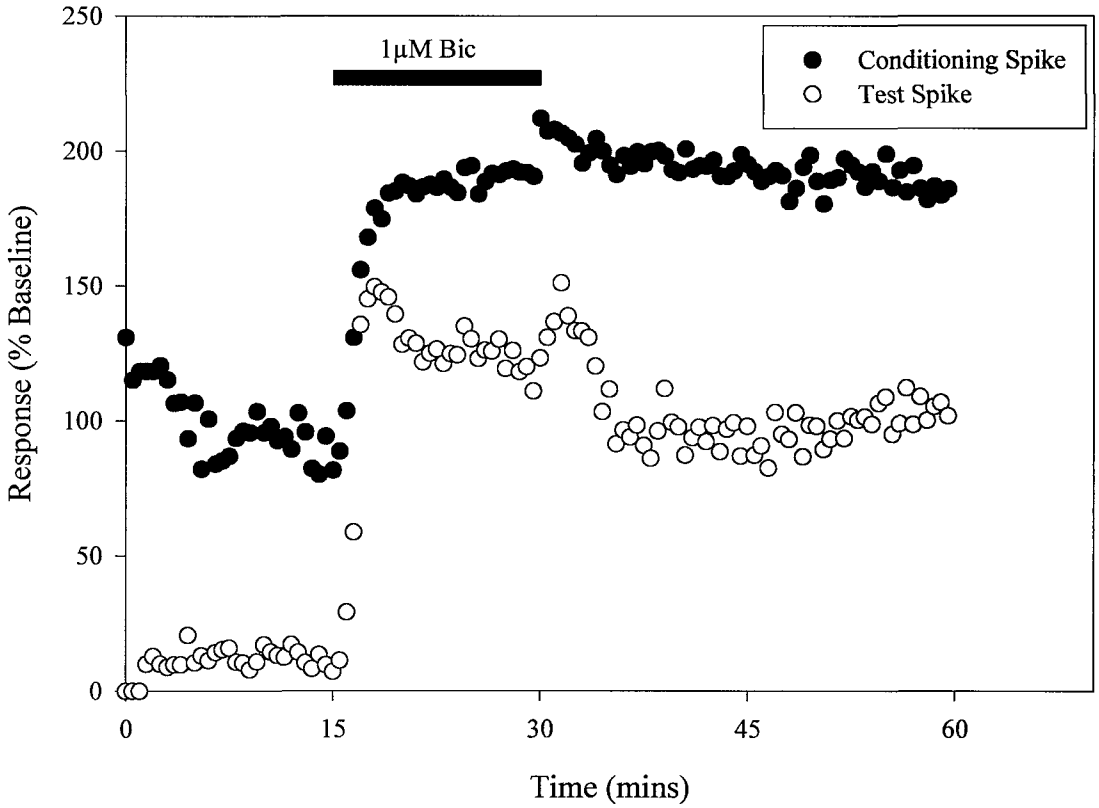

Figure 5.52 Time-course for the effect of 1μM Bic on the field population spike amplitude recorded from the CA1 region of a preconditioned culture. $GABA_A$ receptor blockade by Bic causes an increase in the first (85% (±4.4) to 198% (±7.0), $p<0.01$) and second population spike amplitude (10% (±1.8) to 118% (±3.6) $p<0.01$) as both tonic and evoked inhitition are reduced (n=1).

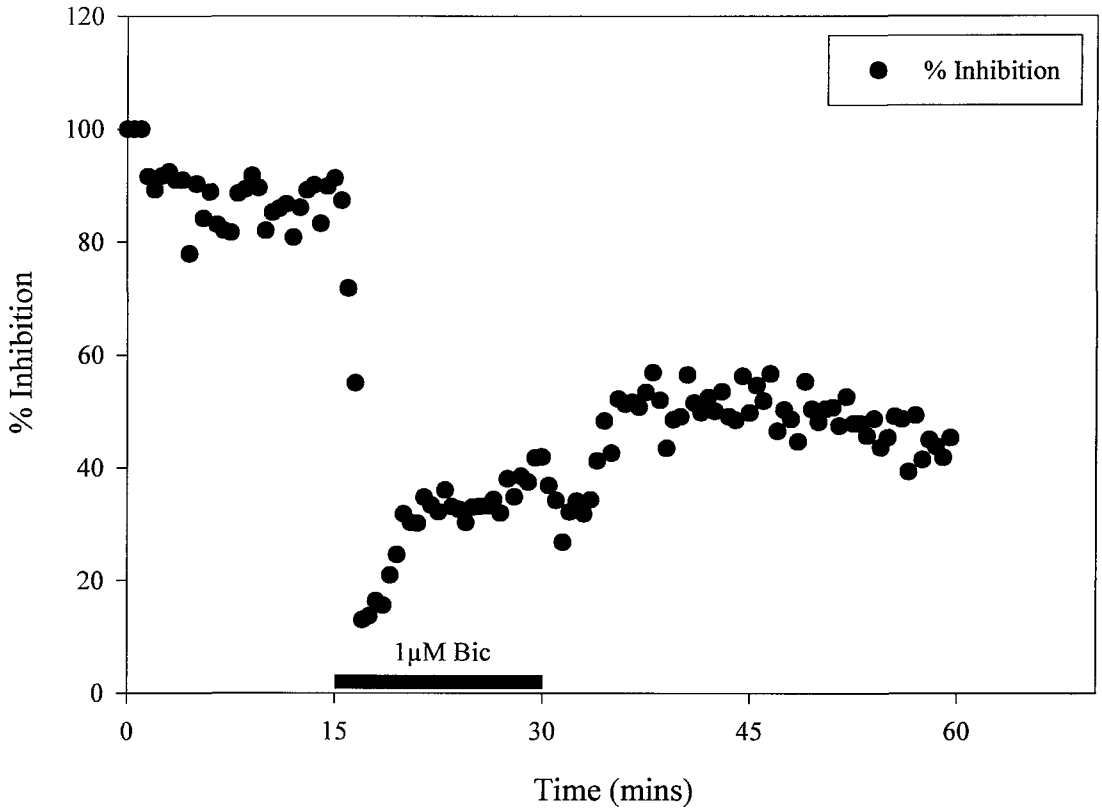

Figure 5.53 Time-course for the change in the percentage inhibition calculated from field recordings in the CA1 *stratum pyramidale* of a preconditioned culture during the application of 1μM Bic. By the end of the Bic administration period the inhibition had decreased from 88.2% (±2.5) to 40.4% (±1.4). This change was found to be highly significant ($p<0.01$, Student's paired t-test).

In figure 5.52 it is clear that administration of 1μM Bic to a preconditioned culture reduces the effects of both tonic and evoked inhibition. This results in an increase in the amplitude of both the first and second population spikes evoked by a half-maximal stimulus. This change in the population spike amplitudes results in the decrease in the percentage inhibition seen in figure 5.53.

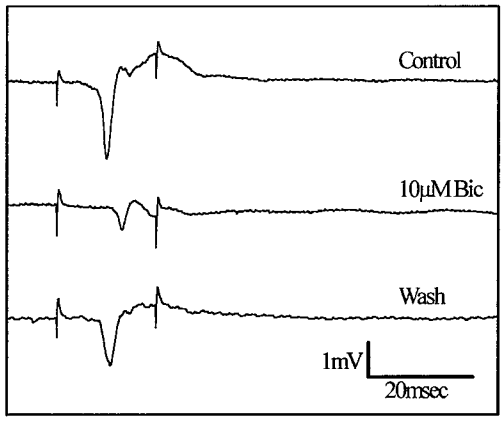

Figure 5.54 Examples of the traces obtained from the CA1 region of a preconditioned culture during the application of 10μM Bic.

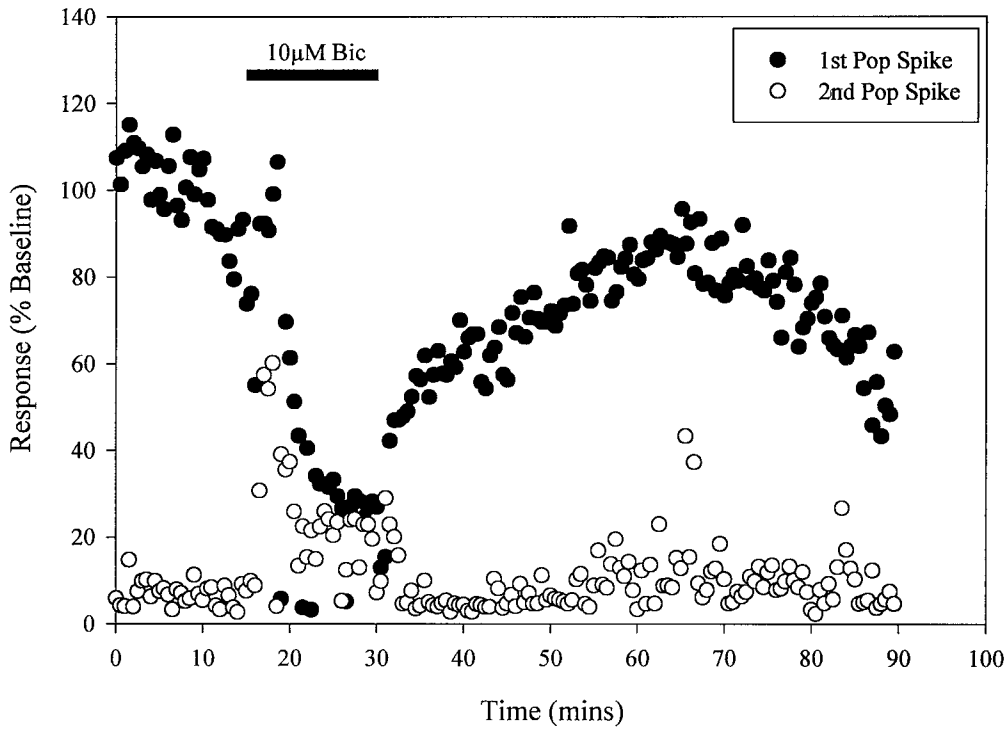

Figure 5.55 Time-course for the application of 10μM Bic to a preconditioned culture whilst recording field potentials from *stratum pyramidale* of CA1. This concentration of Bic is sufficient to abolish the effects of $GABA_A$ mediated inhibition, resulting in an epileptiform burst.

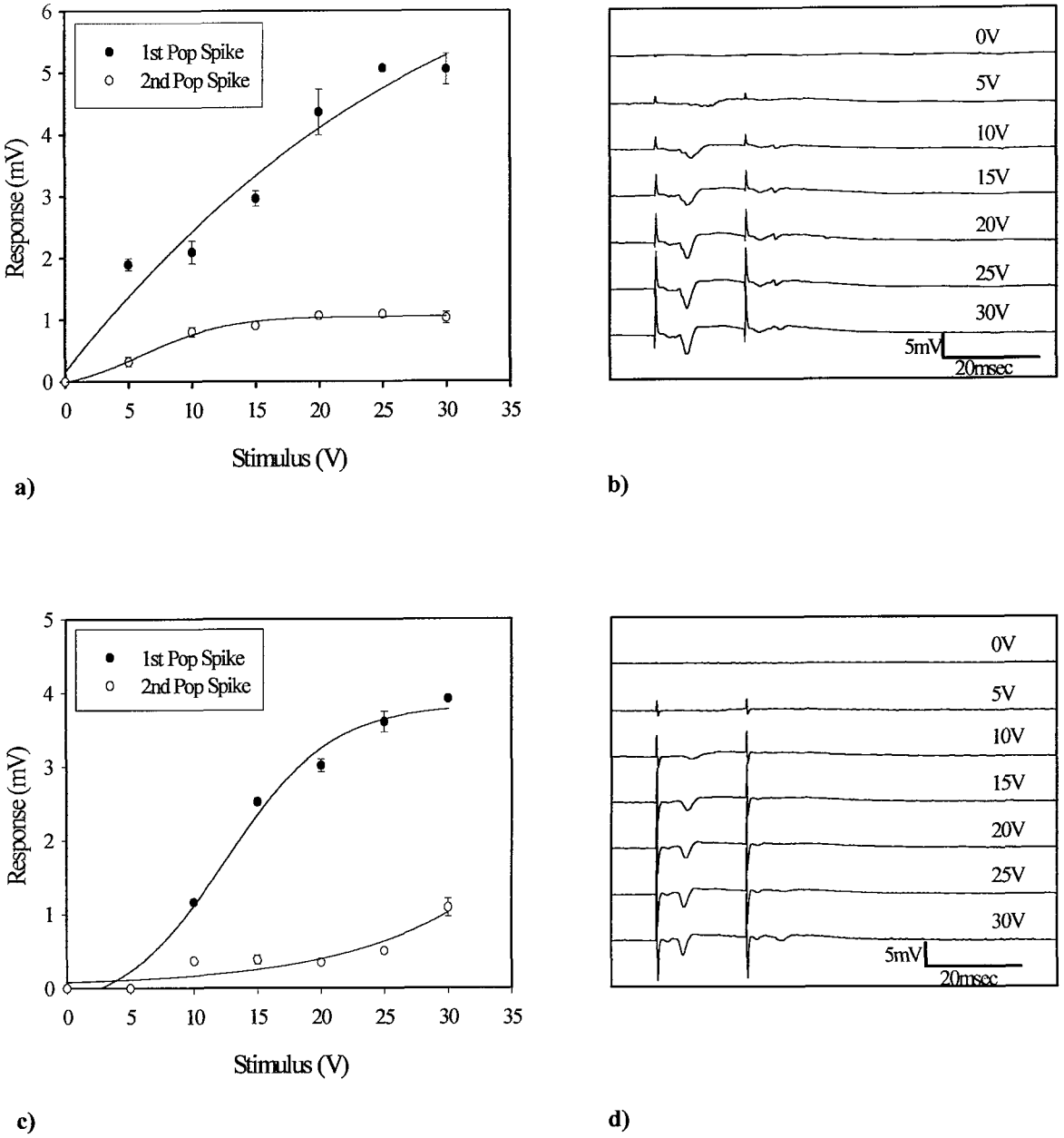

Figure 5.56 Examples of the stimulus-response curves and raw-data traces obtained from the CA1 pyramidal cell layer of unconditioned (a) and b)) and preconditioned (c) and d)) organotypic hippocampal slice cultures.

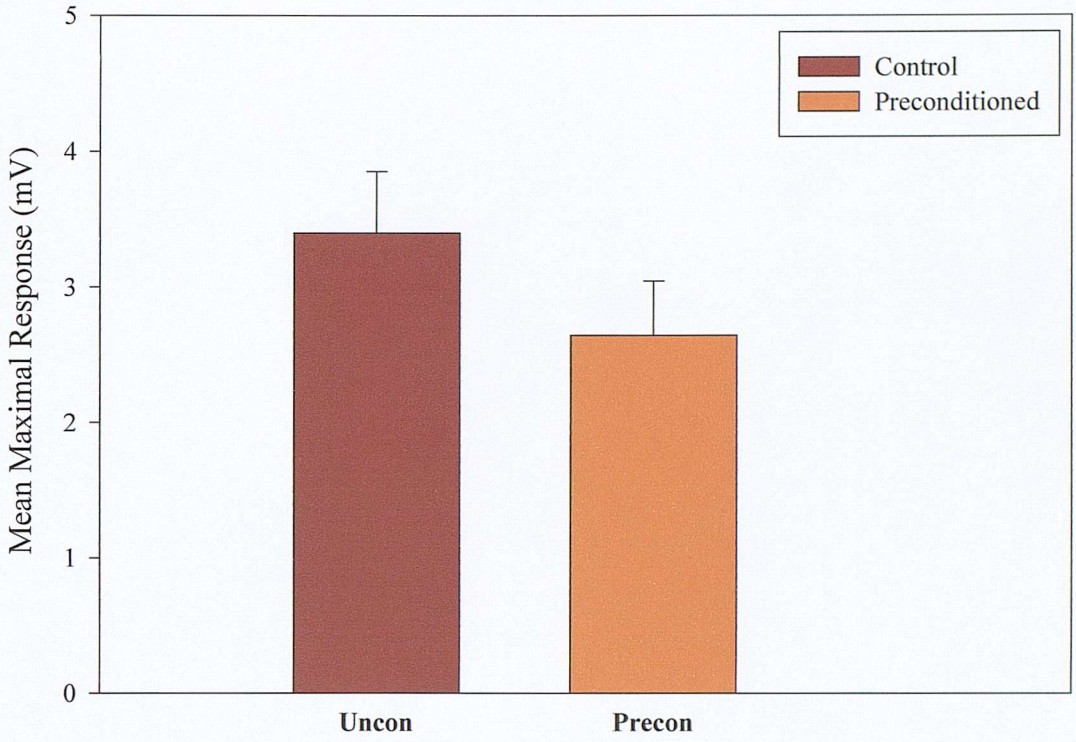

Figure 5.57 There is no significant difference in the maximal response which it is possible to elicit from the CA1of either unconditioned of preconditioned cultures. The mean response for control cultures was 3.4mV (±0.5) (n=11) compared to 2.6mV (±0.4) (n=7).

In order to assess any changes in the excitability in the CA1 region after preconditioning, the maximal population spike amplitudes (figure 5.57) and the maximal stimuli required to elicit them (figure 5.58) were compared in control and preconditioned cultures. The maximal response of the CA1 population of pyramidal cells, in much the same way as seen in CA3 is not significantly changed following preconditioning (figure 5.57). However, unlike the CA3 region, there is a significant increase in the amplitude of the stimulus required to elicit this response (figure 5.58) from 25.5V (±3.4) (n=11) in the unconditioned CA1 to 43.6V (±8.3) in the preconditioned culture group (n=7) ($p<0.05$, Student's unpaired t-test). This suggests that the excitability of the CA1 region is reduced following KA preconditioning.

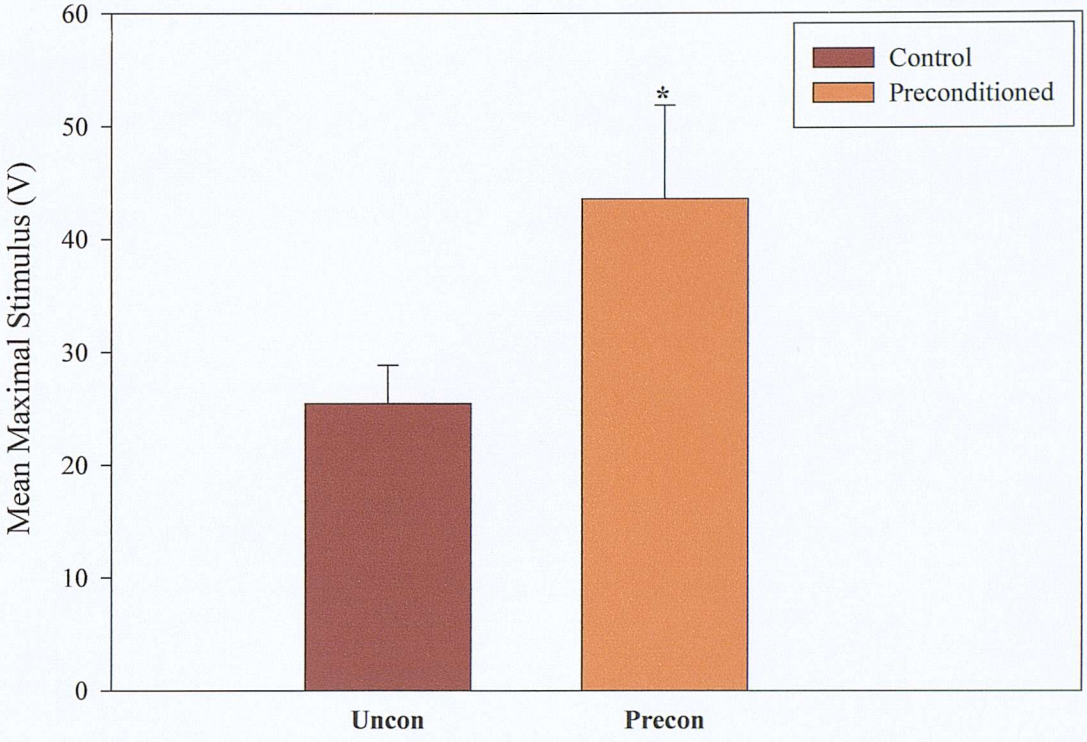

Figure 5.58 The stimulus required to elicit the maximal response from preconditioned cultures is significantly larger than that for unconditioned cultures. Preconditioned cultures required mean maximal stimulus (±S.E.M.) of 43.6V (±8.3) (n=7) compared to a stimulus of 25.5V (±3.4) (n=11) for control cultures. This was found to be statistically significant (*= $p<0.05$, Student's unpaired t-test).

5.3.6 Preconditioning and KA receptor downregulation

In order to ascertain whether the induced tolerance to KA occurred as a result of the downregulation of KA receptors in CA3, 1μM KA was administered to a 12DIV culture which had been preconditioned at 7 DIV with a 24 hour incubation with 1μM KA whilst recording field population responses from CA3. Typical traces obtained during the course of this experiment can be seen in figure 5.59.

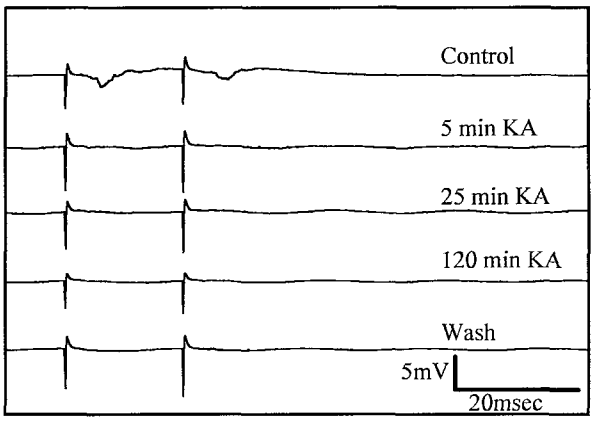

Figure 5.59 Example traces taken from an experiment to observe the effect of administering 1μM KA to a 12DIV culture preconditioned at 7DIV with 1μM KA for 24 hours. Field recordings were made in the *stratum pyramidale* of CA3. The response to KA does not appear to have been altered by the process of preconditioning, which may imply that a downregulation of KA receptors is not involved in the induction of tolerance to KA which follows preconditioning.

The response to 1μM KA in this culture bore a marked resemblance to that seen during a similar regimen carried out in cultures which were naïve to the effects of KA up to that point. This can be seen in figures 5.60 and 5.61, which show the effect of KA administration of the percentage amplitude of the first and second population spikes recorded during the course of this experiment. However, since this data set only consists of one experiment it is not possible to make any categorical statements about the possibility of KA receptor downregulation following preconditioning without further work.

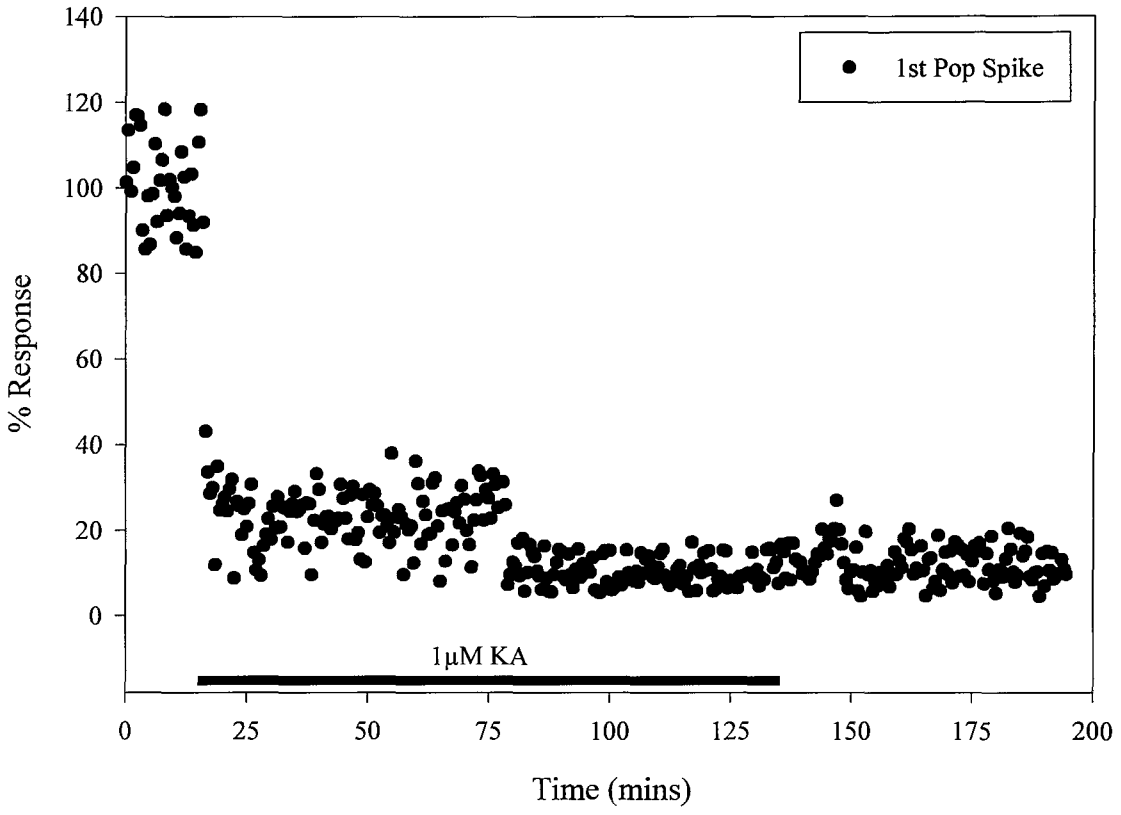

Figure 5.60 Time-course for the effect of 1μM KA on the percentage amplitude of the population spike recorded from the CA3 of a preconditioned culture at 12DIV. The onset of the KA effect causes a rapid and marked reduction in the amplitude of the first spike, probably as a result of a depolarisation block of CA3 pyramidal cells. This response does not differ significantly from that observed in the CA3 of unconditioned cultures.

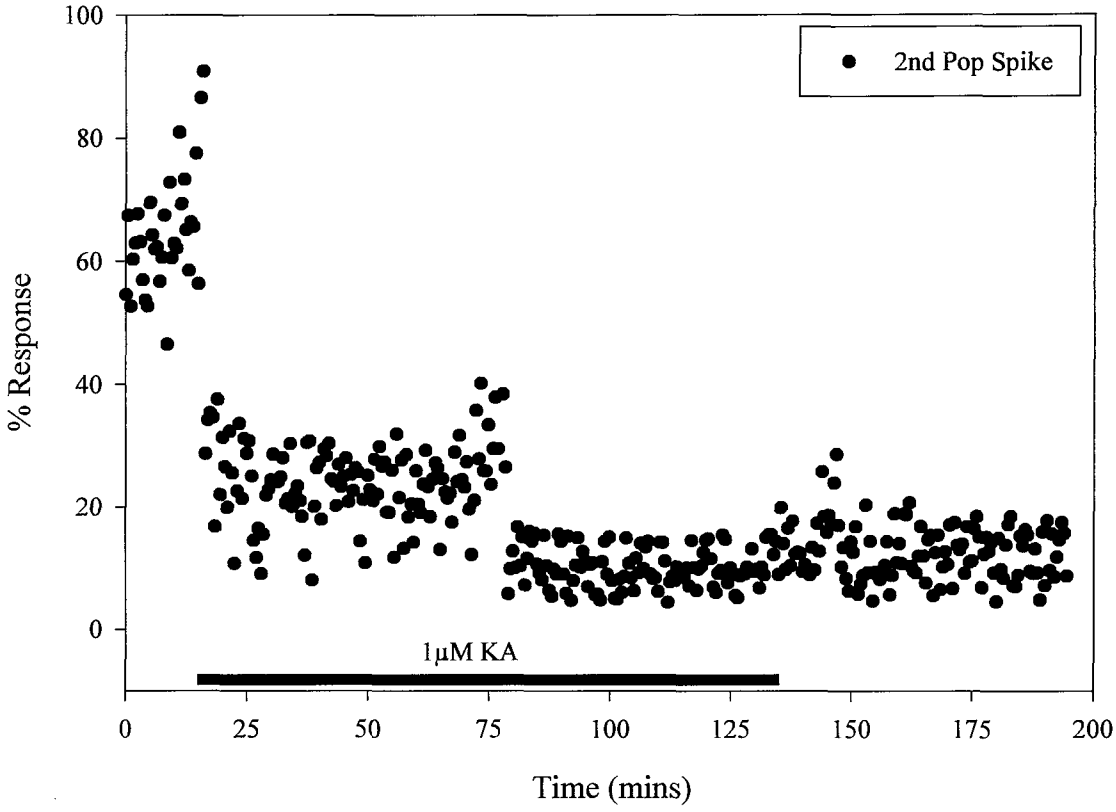

Figure 5.61 Time-course for the effect of the administration of 1μM KA on the second population spike recorded using a paired-pulse protocol in CA3 of a 12DIV preconditioned culture. Similarly to the first spike the second spike undergoes a rapid reduction in amplitude as KA washes into the recording chamber. This effect did not wash out after 60 minutes ACSF wash.

5.4 Discussion

The data presented in this chapter has been obtained in order to investigate a number of points. Firstly, it was of interest to investigate how the organotypic mouse preparation compares as a model of electrophysiological function to age matched rat and mouse acute slices. Once this system had been validated with regards to the existence of functional excitatory and inhibitory circuitry in both the CA1 and CA3, and an assessment of its comparability to acute slices had been made, the effects of acute 1μM KA application over a period of two hours were investigated.

Following this, the investigation was extended to study the effects of a chronic (24 hour) application of 1μM KA on the toxicity of subsequent KA applications, and furthermore, how this chronic application of KA affects hippocampal function.

5.4.1 Comparison of acute slices with organotypic cultures

From the data presented here, it is clear that there are both similarities and differences between the acute slice preparations obtained from both rat and mouse hippocampi and organotypic mouse hippocampal cultures.

With regards to qualitative similarities, it is possible to elicit population spikes from all preparations from both the CA1 (figure 5.6) and CA3 regions (figure 5.14). These responses exhibit paired-pulse inhibition using a 20 msec inter-pulse interval, implying the presence of a functional inhibitory circuit. Since this inhibition is abolished by the $GABA_A$ antagonist bicuculline in both the CA1 (figure 5.50) and CA3 (figure 5.37, 5.43) of organotypic hippocampal cultures it is clear that this fast inhibitory control of pyramidal cell output is mediated by $GABA_A$ receptors.

On a more quantitative level, the first population spikes elicited by a maximal stimulus are significantly greater in the acute preparations in recordings made from both CA1 and CA3. These were 4.6mV (±0.3) for the intact rat CA1 and 5.0mV (±0.5) for the mouse compared to 3.4mV (±0.5) for organotypic hippocampal cultures ($p<0.01$) and 3.5mV (±0.5) for the acute mouse CA3 compared to 1.5mV (±0.1) for the mouse organotypic CA3 ($p<0.01$).

This difference most likely occurs due to the lower cell numbers of the pyramidal cell population in the organotypic slice, since the culture thins down from the 400μm initial thickness to approximately 150μm during the 7 days in culture prior to recording (personal communication N. Best and own observation).

Interestingly, despite a lower maximal population spike amplitude in the organotypic slice, the degree of paired-pulse inhibition of the second population spike is significantly greater in this preparation than in the acute slice. This is true for both the CA1 (74% (±0.7) for the organotypic CA1 compared to 60% (±0.4) and 65% (±1.7) for the rat and mouse respectively ($p<0.01$) and the CA3 regions of the hippocampus (48% (±0.9) for the organotypic CA3 compared to 24% (±0.6) for acute mouse slices, $p<0.01$).

It is possible that the 7 days in culture allows greater recovery of the slice from the rigours of the dissection process, however this phenomenon may be a result of an increased excitatory drive to the interneurones. It is known that there is an increase in the number of recurrent excitatory collateral fibres during the development of organotypic hippocampal slice cultures (Gutierrez and Heinemann 1999,). This presumably leads to an increase in the number of excitatory synapses and hence greater interneuronal stimulation for any given stimulus than is found in the acute slice preparation.

5.4.2 Comparison of the effects of KA in acute slices and organotypic cultures

In addition to these differences, the response to 1μM KA in the CA1 region of organotypic cultures differs to that of acute rat slices. Unfortunately no recordings were made from acute mouse slices in the presence of KA, so it is unclear if this difference represents an inter-species difference or a divergence in the developmental pathways of the hippocampus *in* or *ex-vivo*. Since there is no increase in the second population spike amplitude during the application of 1μM KA to organotypic cultures (figures 5.11 and 5.19) it would tend to suggest that there is no KA receptor mediated presynaptic modulation of the release of GABA from interneurones in this preparation. Although no field EPSP recordings were made it is also possible to infer that there may be no KA receptor mediated downregulation of glutamate release from the Schaffer collateral terminals in these preparations either. This is inferred from the initial large reduction in the amplitude of the population spikes recorded from CA1 as the drug is added. This phenomenon may be more consistent with a strong depolarisation of the CA3 pyramidal cell population by the activation of postsynaptic KA receptors on these neurones (Vignes *et al* 1997) leading to an increase of glutamate release from the Schaffer collateral terminals. This, possibly coupled with a postsynaptic activation of GluR6 containing receptors on the pyramidal cells of CA1 leads to a depolarisation block of the principal cells in this region and hence a reduction in the population spike amplitude.

The transient increase in CA1 population spike amplitude may represent the induction of a depolarisation block of the pyramidal cell population of CA3 enabling stimulus driven glutamate release from the Schaffer collateral terminals to continue.

5.4.3 Induced tolerance to KA: Imaging studies

The *in vivo* intraventricular injection of kainic acid has been shown to cause a loss of the pyramidal cells in CA3 (Nadler *et al.* 1978a), and at higher concentrations to also lead to a loss of cells from CA1 and the dentate gyrus (Nadler *et al.* 1978b). Best *et al.* (1996) demonstrated this to be true also for organotypic hippocampal slice cultures derived from 8-10 day Wistar rats cultured for 11 days. In addition to the loss of CA3 pyramidal cells following intraventricular injection of KA, Best *et al.* (1993, 1994a) have also reported a loss of parvalbumin-immunoreactive interneurones within the hippocampus proper. This has also been shown to occur in organotypic culture (Best *et al.* 1996).

It is here shown that a 24-hour incubation of MF1 mouse organotypic hippocampal slice cultures with 5μM KA at 11 DIV also exhibits the same pattern of damage to CA3 as seen above (figure 5.24).

The phenomenon of induced tolerance to kainic acid induced toxicity which Best *et al.* (1996) demonstrated to occur in Wistar rat organotypic hippocampal slice cultures is shown here to also occur in MF1 mouse hippocampal cultures (figures 5.24, 5.26). Best *et al.* (1996) reported that this tolerance coincides with the peak expression of heat shock protein 72 (HSP 72), a nonconstitutive protein expressed as a response to cellular stress. Kitagawa *et al.* (1991) and Lowenstein *et al.* (1991) have also seen the expression of this protein to increase at a time that would apparently correlate with a neuroprotective response to a cellular stress of some type. In addition to an elevated level of HSP 72, *in vivo* studies have shown that this tolerance also coincides with an increase in NPY expression in granule cells of the dentate gyrus and mossy fibre terminals (El Bahh *et al.* 1997). NPY is a peptide that has been shown to reduce epileptiform activity in acute hippocampal slices (Klapstein and Colmers, 1997). NPY deficient mice have also been observed to exhibit an exacerbated response to KA induced seizures (Baraban *et al.* 1997), and may therefore also be an important factor in the neuroprotective response.

It is interesting to note that other models of neuronal damage also respond positively to a prior sub-toxic insult. For example, tolerance to an ischaemic insult has

also been demonstrated in a number of studies (Kitagawa *et al.* 1990, Simon *et al.* 1993). KA induced damage to the piriform cortex has been shown to be reduced by prior kindling (Kelly *et al.* 1994). Furthermore, Sasahira *et al* (1995) have shown that induction of epileptiform activity using the $GABA_A$ receptor antagonist bicuculline results in a reduction in the damage to CA3 observed following subsequent insults. This protection again appeared to correlate with the expression of heat-shock protein like immunoreactivity, a factor which appears to be common to both epileptic and ischaemic tolerance (Aoki *et al.* 1993, Heurteaux *et al.* 1993).

So how then does this tolerance come about? It would appear that kainate receptor activation is an important factor in this response, since tolerance occurs to a small degree at nanomolar concentrations of kainate (which are unlikely to activate AMPA receptors to any significant degree). Although it is only once the concentration reaches 1μM KA that the phenomenon is reliably seen (figure 5.27-5.28), this concentration is still unlikely to activate AMPA receptors (Kamiya and Ozawa 1998, Mulle *et al.* 2000). Also, it is around the EC_{50} value for activation of homomeric GluR6 receptors (Egebjerg *et al* 1991) which may indicate the importance of this subunit in the induction of tolerance.

In figures 5.29-5.30, it can be seen that NMDA receptor blockade by 20μM MK801 and 20μM D-AP5 does not significantly alter the induction of tolerance to KA. Therefore it is unlikely that Ca^{2+} influx *via* the NMDA receptor following CA3 pyramidal cell depolarisation by kainate (Robinson & Deadwyler 1981) is responsible for the induction of this response. However, this does not discount Ca^{2+} influx into CA3 pyramidal cells as being part of the mechanism of induction, since there are a number of voltage-gated Ca^{2+} channels present postsynaptically on pyramidal cells which are presumably activated as a result of kainate induced depolarisation.

One proposed mechanism is that KA increases extracellular adenosine levels during the application of KA (Plamondon *et al.* 1999, Blondeau *et al.* 2000, Berman *et al* 2000) resulting in the stimulation of A_1 receptors, leading to the opening of a sulphonylurea-sensitive K_{ATP} channel. This leads to a reduction of glutamate release from presynaptic terminals and postsynaptically to hyperpolarisation of the pyramidal cells of both CA3 and CA1 (Blondeau *et al.* 2000). Other contributory mechanisms are likely to include increased expression of the transcription factor c-Jun, which leads, amongst other things, to an increased synthesis of HSP72 (Kitagawa *et al.* 1991). It is likely that synaptically released Zn^{2+} also contributes to the induction of HSP72 production (Lee *et al.* 2000).

Under normal conditions, HSP72 acts to prevent abnormal protein conformations occurring during the process of translation. They also act as chaperones, regulating the binding of actin and the formation of clathrin coated vesicles (Sharp *et al* 1999). Their expression is upregulated by any cellular stress that leads to protein denaturation. This includes increases in temperature as well as the stressors previously mentioned. Upregulation of HSP72 expression may possibly occur as a result of denatured protein binding to HSP90, causing it to dissociate from a trimer formed from heat-shock factors (HSF). This trimer then becomes phosphorylated, allowing it to bind to heat-shock elements on heat-shock genes, leading to an increase in HSP expression.

Increased expression of heat shock proteins may not be the only source of protection as a result of preconditioning. Activation of c-Jun may also lead to an increased expression of manganese super-oxide dismutase (MnSOD), which catalyses the formation of H_2O_2 and O_2 from the superoxide radical (O^{2-}). Free radicals such as superoxide are thought to be generated during KA induced toxicity (Liang *et al.* 2000). This reactive oxygen species (ROS) may cause cellular damage in itself but may also lead to the production of further ROS such as the hydroxyl radical (Liang *et al* 2000) which is able to cause oxidation DNA bases, thus contributing further to cellular death. Superoxide is also capable of reaction with nitric oxide (NO) leading to the production of peroxynitrite which may cause further damage to cells by promoting lipid peroxydation and the nitration of various proteins at tyrosine residues (Beckman and Crow 1993)

One possible source of this increased production of ROS may be the influx of synaptically released Zn^{2+} from the mossy fibre terminals (Xie and Smart 1991, Henze *et al* 2000). Entry of Zn^{2+} through Ca^{2+} permeable AMPA/KA channels is sufficiently high to interfere with mitochondrial function and cause the production of ROS such as O^{2-}, thus leading to cellular damage and death (Sensi *et al* 1999).

It is known that following systemic injection of KA in rats there is an increase in the production of MnSOD, mobilised from both the mitochondria (Liang *et al* 2000) and astroglial cells (Kim *et al* 2000). Such increased production would have the effect of limiting the production of free radicals, and thus promoting cell survival during excitotoxic shock. There is evidence to suggest that such an increase in the production of MnSOD occurs during the induction of ischaemic tolerance (Ohtsuki *et al* 1992). If a similar mechanism is occurring during the induction of KA tolerance seen here, then it is not outside the realms of possibility that such an increase in MnSOD prodcution contributes to the protection that occurs.

Thus the induction of tolerance to KA may be the result of a combination of events including the increased expression of various HSPs, upregulation of NPY and MnSOD, all of which would tend to enable a cell to cope with a subsequent excitotoxic stress.

The kainate lesion has also been seen to reduce the numbers of various populations of interneurones in the hippocampus (Frank, 1993, Best *et al.* 1994b) in addition to its effects on pyramidal cells. In order to investigate whether the induction of kainate tolerance caused changes in the number of GAD expressing neurones within organotypic cultures, antibodies to GAD 67 were used to stain these cells following preconditioning. These results may be seen in figures 5.31-5.32. It was found that kainate treatment significantly reduced the number of GAD-positive neurones in the dentate gyrus and hilus and CA3 following both preconditioning and 5μM KA incubation. However there was no significant difference between the number of GAD-positive cells in these regions following 5μM KA application in unconditioned or preconditioned cultures. Thus it is unlikely that the neuroprotective effect of preconditioning extends to interneuronal populations. The interneurones of CA1 did not appear to be significantly reduced from control values following kainate. This is likely to account for the differences in paired-pulse inhibition observed between the CA3 (figure 5.34) and CA1 (figure 5.48) regions of preconditioned cultures.

5.4.4 Induction of kainic acid tolerance: electrophysiological studies

From this data we can see that preconditioning cultures with a 24 hour incubation with 1μM KA at 7 DIV results firstly in a decrease in the paired-pulse inhibition recorded from CA3 and to a lesser extent CA1. Intuitively, such a reduction in paired-pulse inhibition could be expected to lead to a pro-epileptic condition within the hippocampus. However this does not appear to be the case, since neither recordings from CA3 or CA1 generally show evidence of epileptiform activity. This appears to be true even under maximal stimulation conditions.

There is unfortunately insufficient data to know whether the threshold for epileptiform bursting in the presence of bicuculline changes following preconditioning. However, the data presented here would tend to suggest that the remainder of the paired-

pulse inhibition seen in preconditioned slices at 20msec is still mediated by $GABA_A$ receptors since it is abolished by 10μM Bic.

This data does not address any possible changes that may occur with regard to other inhibitory mechanisms, such as that mediated by $GABA_B$ receptor activation, NPY or adenosine. The latter two mechanisms have been shown to be implicated in KA preconditioning (El Bahh *et al* 1997, 2001; Blondeau *et al* 2000).

It does not appear that the reduced susceptibility of CA3 pyramidal cells to KA induced excitotoxicity occurs as a result of a decrease in the excitability of this population of neurones since neither the maximal response to simulation of the mossy fibre pathway, or the stimulus required to evoke this response changes following preconditioning. It is interesting however that the stimulus required to evoke a maximal response from CA1 pyramidal cells increases significantly following incubation with KA. This may represent a mechanism whereby seizure propagation into CA1 is reduced or even prevented.

Looking at the data for the acute application of KA to cultures between 11-14 DIV we can see that in both CA3 and CA1 both the first and second population spikes undergo a marked reduction in amplitude. In CA3 this is probably due, at least partially, to a combination of a reduction in presynaptic Ca^{2+} influx leading to a reduction in glutamate release from the mossy fibre terminals (Kamiya and Ozawa 2000). This is probably coupled with a depolarisation block of CA3 pyramidal cells *via* postsynaptic KA receptor activation (Robinson & Deadwyler 1981; Castillo *et al.* 1997, Vignes & Collingridge, 1997).

The effect of this depolarisation block in CA3 can be seen in the response of the first population spike to 1μM KA recorded from CA1. As mentioned previously there is initially a large decrease in the amplitude followed by a period of partial recovery. This phenomenon could be explained if the depolarisation of CA3 pyramidal cells was sufficiently large to overcome any presynaptic effect of KA on the Schaffer terminals (Vignes *et al.*, 1998) to decrease glutamate release. Thus an increase in glutamate release from the Schaffer collaterals would result from the sustained depolarisation in CA3, activating dendritic AMPA receptors on the CA1 pyramidal cells. As the depolarisation block continues it could be expected for the downstream effects of CA3 to be nullified, thus allowing the CA1 response to be seen more clearly.

It is also known that KA receptors are located both on the dendrites and presynaptic terminals of GABAergic interneurones (Rodriguez-Moreno *et al.*, 2000). Activation of dendritic KA receptors on interneurones has been shown to increase

interneuronal spiking (Cossart *et al.*, 1998) whilst activation of presynaptic receptors decreases GABA release (Rodriguez-Moreno *et al.*, 1997). Thus the net effect is a decrease in GABAergic inhibition.

Although this is no evidence for an effect of inhibitory mechanisms by KA here, it is likely that the depolarisation block driven by CA3 masks this effect. However, as Kamiya and Ozawa (1998) have described, 1μM KA reduces Ca^{2+} influx into Schaffer collateral terminals bringing about a decrease in the amplitude of the field EPSP. This accounts for the reduced population spike amplitude following the initial phase of the KA response in CA1.

It is also clear that the effects of a 120 minute 1μM KA application do not wash out over the period of one hour. However the fact that recordings of a similar amplitude can be made from preconditioned cultures 4 days after the removal of KA (figure 5.21) implies that this phenomenon does not represent cell death, but rather a transient decrease in pyramidal cell output. Thus it is unlikely that the reduced output directly results in the subsequent tolerance of CA3 pyramidal cells to the toxic effects of 5μM KA.

Recordings from the CA3 of a preconditioned culture during the administration of 1μM KA follow the same pattern of response as seen in control cultures. This implies that a downregulation of KA receptors due to prolonged incubation with KA is not a contributory factor in the tolerance to subsequent toxic insults. However, as stated previously, the data set needs to be increased before any definite statements can be made regarding this.

5.5 Summary

The mouse organotypic hippocampal slice preparation bears functional similarities to both mouse and rat acute slice preparations of a similar age. However, the evoked responses from both the CA1 and CA3 regions are not identical.

Population spike amplitudes from both the CA1 (figure 5.7) and the CA3 regions (figure 5.15) of organotypic mouse cultures are significantly lower than in acute slices. In addition, the degree of paired-pulse inhibition in both the CA1 (figure 5.8) and the CA3 (figure 5.16) is greater.

Applications of KA over a two hour period results in a reduction in population spike amplitude in both CA1 (figures 5.10 and 5.11) and CA3 (figures 5.18 and 5.19). The initial increase in population spike amplitudes observed in rat acute slice CA1 (figures 5.12 and 5.13) do not occur.

The data presented here for chronic (24 hour) KA application suggests that the induction of tolerance to subsequent KA toxicity occurs in mouse MF1 hippocampal slice cultures independently of NMDA receptor activation (figures 5.29-5.30) at a threshold concentration of 1μM KA (figures 5.27-5.28). This concentration is around the EC_{50} value for homomeric GluR6 receptors (Egebjerg *et al.* 1991), and may preclude the involvement of the high affinity subunits KA-1 and KA-2 in the receptor stoichiometry. Since KA toxicity is not seen at a concentration of 1μM, but is at 5μM, it is possible that this toxicity is mediated by AMPA rather than KA receptors.

The tolerance to KA toxicity does not occur as a result of an increase in inhibitory function. In fact, the opposite appears to be the case. Both the CA1 (figure 5.48) and CA3 (figure 5.34) regions of preconditioned cultures exhibit reduced paired-pulse inhibition compared to untreated, age matched control cultures. This correlates well with a reduction in GAD-67 expression in all areas of the hippocampus following preconditioning (figure 5.32).

Furthermore, since the maximal stimulus (figure 5.46) required to elicit a maximal population spike amplitude from CA3 (figure5.45) is not significantly different in control and preconditioned cultures, the excitability of the CA3 region does not appear to have changed. Therefore, the induction of tolerance to KA does not appear to result from a reduction in CA3 excitability. Interestingly, using these same indices the excitability of CA1 appears to be reduced in preconditioned cultures (figures 5.57 and 5.58). However, this may not be central to the mechanism of induced tolerance.

The lack of change in the response to acutely applied KA recorded from the CA3 of a preconditioned culture suggests that KA receptor downregulation in the CA3 may not be involved in the protection against KA toxicity. However, Zimmer *et al* (2000) have observed a reduction in mRNA for GluR6, KA-2 and possibly KA-1 in the CA3 region of rat organotypic hippocampal slice cultures exposed to 2μM KA for 3 weeks. Since there is a 3-5 fold increase in [^{3}H]KA binding in rat hippocampal slice cultures compared to acute slices, it may be that this is also the case in mouse organotypic cultures. Thus it may be that submaximal receptor occupancy may result in the responses observed here, requiring a large degree of receptor downregulation to occur before a change in response to 1μM KA is observed.

Chapter 6

Conclusions

6.1 Overview

The hippocampal slice preparation and organotypic slice culture provide a valuable model system in which to investigate both synaptic and network physiology and pharmacology. It's basic circuitry has been fully elucidated and shown to comprise of both excitatory and inhibitory synapses and it's behaviour may be modulated in a number of different ways.

The present study has investigated the effects of the potent neurotoxin kainic acid in both the short- and long-term on the network behaviour of both the CA1 and CA3 regions of the hippocampus. This has been achieved using a combination of extracellular field recordings from the *stratum radiatum* and *stratum pyramidale* of the CA1, in the case of acute rat slices, and from the *stratum pyramidale* only in the case of acute and organotypic mouse cultures.

In addition to this, propidium iodide fluorescence and glutamic acid decarboxylase (GAD) 67 immunohistochemistry has been utilised to assess the longer-term effects of a number of concentrations of KA on the various populations of principal cells and interneurones present in organotypic culture.

6.2 KA application to the acute hippocampal slice preparation

Brief (15-30 minute) applications of KA to hippocampal slices derived from 15-19 day old rats resulted in three distinct responses within the CA1 region. These effects were a reduction in the slope of the field EPSP, an initial increase in the first population spike amplitude followed by a reduction in amplitude in the intact slice preparation and a reduction in the paired-pulse inhibition. These are discussed below.

6.2.1 Modulation of glutamate release by KA

As mentioned above, KA reduced the slope of the field EPSP recorded from the *stratum radiatum* of CA1. Since this response occurred at both sub-micromolar concentrations as well as at a concentration of 1μM KA it is very likely that this effect is mediated by a KA receptor. The fact that it occurred to approximately the same degree in the presence or absence of the CA3 region and at a time at which the population spike amplitude was increasing suggests a possible presynaptic locus of action. As previously reported (Vignes *et al.* 1998) the GluR5 agonist ATPA (1μM) produced a similar response at a concentration at which it shows specificity for the GluR5 subunit. Since ATPA reduced the EPSP slope without a concurrent increase in population spike amplitude, it is

likely that KA application does not reduce EPSP slope by a direct depolarising action on the post-synaptic pyramidal cell population.

Furthermore, since the population spike amplitudes increase at the same time as the EPSP slope decreases during KA application, this would argue against the possibility that activation of $GABA_A$ receptors following GluR5 activation on interneurones is shunting excitation in the dendrites *via* increased Cl^- flux.

This reduction in the field EPSP slope recorded from CA1 appears to be accentuated in the presence of the GluR6 antagonist NS102. This may suggest that the blockade of KA receptors containing this subunit may enhance the effects of KA at receptors with different subunit compositions, such as the GluR5 subunit for example. It also indicates that the GluR6 subunit is unlikely to be involved in the mediation of this response.

Activation of AMPA receptors by fluorowillardine also resulted in a reduced EPSP slope, but the time-course for this to occur appeared to be dependent on the presence or absence of the CA3 and dentate gyrus. This is in juxtaposition to the response to 1μM KA and may indicate a difference in the mechanism of action of the two drugs. Thus it may be that AMPA receptor activation on the principal cells of CA3 results in an increase in glutamate from the Schaffer collaterals. This coupled with activation of dendritic AMPA receptors in the presence of CA1 may be sufficient to produce a partial depolarising block of the CA1 pyramidal cell population and hence reduce the EPSP amplitude *via* a decrease in trans-membrane conductance at the dendrites.

In the absence of CA3 this reduction in EPSP slope occurs after the initial three minute period during which KA has already begun to produce an effect. This provides further evidence that the downregulation of glutamate release from the Schaffer collateral pathway is not mediated directly by AMPA receptor activation. However, in order to be certain that these responses are KA receptor specific and not due to an effect of KA at AMPA receptors, it would be useful in any further experiments using field responses to apply an AMPA selective antagonist such as the non-competitive 2,3-benzodiazepine GYKI53655 (Bleakman *et al* 1996) in a 0mM Mg^{2+} ACSF solution in order to look at NMDA receptor dependent field potentials. This would circumvent the problem that field potentials are abolished by the application of AMPA receptor antagonists and would allow investigation of the effects of KA in the absence of AMPA receptor mediated events.

The EPSP in the presence of KA was not significantly affected by prior application of metabotropic receptor antagonists or inhibitors of PKC, indicating their lack of

involvement in the modulation of EPSP slope. Neither does it appear likely that spillover of GABA from inhibitory synapses following interneurone activation by KA affects excitatory synaptic transmission from the Schaffer collateral terminals since the effects of KA were not affected by $GABA_B$ receptors antagonism. However, blockade of adenosine A_2 receptors resulted in a reduction in the effects of KA on the EPSP slope. This may indicate a role for the upstream modulation of glutamate release form the Schaffer collaterals by the adenosine A_1 receptors.

In the only recording made from CA3 of acute mouse slices which monitored the EPSP during the application of 1μM KA it is clear that, in accordance with the findings of Kamiya and Ozawa (2000), the EPSP slopes are reduced in the presence of KA. This is likely to be due to a strong activation of the KA receptors which have been proposed to be located on the axons of mossy fibres, leading to what amounts to a depolarising block and hence the shut-down of the glutamate release machinery at the mossy fibre terminal.

6.2.2 The initial effect of KA on population spike amplitude

Application of 1μM KA results in what can be viewed as a biphasic response. The first population spike was observed to increase in amplitude in both the intact and isolated CA1 preparations taken from the rat hippocampus during the first three minutes of KA application. Following this initial increase there was a depression of the population spike amplitude that persisted until the drug was washed from the slice.

The initial increase is due either to a direct action of KA on the CA1 pyramidal cell population (Melyan *et al* 2002), or a reduction in the release of GABA from the presynaptic terminals of both feedforward and feedback interneurones (Rodriguez-Moreno *et al* 1997, 1998, Frerking *et al* 1998, Min *et al* 1999, Semyanov *et al* 2001). It is also possible that both these mechanisms are acting in tandem. Both of these events are likely to be mediated by GluR6 containing receptors.

Since it occurs in both intact and isolated CA1 preparations it is unlikely that excitation of the CA3 region by KA leads to an increased release of glutamate onto CA1 pyramidal cells *via* the Schaffer collaterals, thus leading to an increase in population spike amplitude.

Bureau *et al* (1999) have demonstrated a requirement for the GluR6 subunit for a functional KA current in CA1 pyramidal cells of knock-out mice, but controversy surrounds the existence of a functional KA receptor current in these neurones. Recently, Melyan *et al* (2002) have demonstrated a metabotropic KA receptor mediated inhibition of

the slow after-hyperpolarisation current in CA1 pyramidal cells from slices taken from the same age rats as used in this study. Inhibition of this current, which is thought to be mediated by a Ca^{2+} dependent K^+ channel would be expected to render the CA1 pyramidal cell population more excitable. This in turn could conceivably result in an increase in the population spike amplitude despite reduced glutamatergic transmission.

The GluR5 agonist ATPA failed to increase the first population spike in a similar manner to KA suggesting a lack of involvement of this subunit in this phase of the response. This has also been found to be the case for the KA receptor responsible for the inhibition of the I_{sAHP} (Melyan *et al* 2002). The GluR6 antagonist NS102 significantly reduced the increase in the first population spike in the intact slice CA1, but just failed to reach significance in the isolated CA1, possibly indicating a need for further replicates of this experiment. This may however reflect the poor solubility of the drug resulting in inconsistent concentrations being achieved in the tissues.

It is interesting to note that the AMPA receptor agonist produced a similar result to KA only in the intact slice preparation, possibly suggesting an excitation of CA3 pyramidal cells by fluorwillardine leading to increased excitation of CA1 pyramidal cells *via* the Schaffer collateral pathway. This again provides further evidence of a difference in the mechanism of action of the two drugs and adds further weight to the assumption that 1μM KA is acting at a KA rather than an AMPA receptor.

The initial response to KA was significantly reduced by the co-application of the group II/III mGluR antagonist MPPG but not by the group I/II antagonist MCPG.

Melyan *et al* (2002) demonstrated that the modulation of the I_{sAHP} was dependent on the activity of PKC. Therefore it would be expected that inhibitors of PKC would prevent an increase in the first population spike amplitude if a similar mechanism were in action here. Application of the PKC inhibitor H-7 resulted in an epileptiform burst in the CA1 region, rendering interpretation of co-application data more difficult. This said, it would be expected that any further increase in excitability following KA application would result in an increase in the number of spikes in the burst. Upon the addition of 1μM KA to the superfusing ACSF however, no further increase in the number of spikes occurred, possibly indicating that PKC inhibition has prevented any further increase in excitability. This may suggest that the initial increase in the population spike amplitude may occur as a result of inhibition of the I_{sAHP} current by KA.

This initial response to KA was also unaffected by antagonists for the $GABA_B$ receptor and adenosine A_1 receptors.

6.2.3 The effect of prolonged KA application on population spike amplitude

The late phase of the KA response is defined by a marked reduction in population spike amplitude. Since the inhibitory effects of KA on the I_{sAHP} have been shown to persist for at least an hour following the wash out of KA after a brief application of 15 minutes (Melyan *et al*) it would be expected that the pyramidal cell population would remain hyper-excitable throughout this time. Therefore it is unlikely that this late reduction can be explained solely by decreased glutamatergic transmission which occurs in CA1 during the application of KA. However, it is possible that the excitatory effects of KA on various interneurone populations (Cossart *et al.* 1998, Frerking *et al.* 1998, 1999) within the CA1 may account for this phenomenon.

Given that GluR5 activation on interneurones has been demonstrated to increase interneuronal spiking (Frerking *et al.*, 1998; Cossart *et al.*, 1998) and leads to an increase in the frequency of IPSCs recorded from CA1 pyramidal cells (Cossart *et al* 2001) it is possible that the continued presence of KA may lead to an increase in the concentration of GABA at synapses with pyramidal cells. This may in turn lead to an inhibition of the pyramidal cell population and hence a reduction in the population spike amplitude. In support of this hypothesis is the fact that co-application of the $GABA_B$ receptor antagonist SCH50911 results in a prolongation of the initial increase in the population spike amplitude throughout the KA application period.

6.2.4 The effect of KA on paired-pulse inhibition

During the initial phase of the application of KA to both intact and isolated CA1 preparations derived from 15-19 day old rats, the second population spike is also observed to increase in amplitude. It is likely that this occurs as a result of a reduction in the evoked inhibition *via* a KA receptor mediated mechanism such as has been reported previously by a number of groups (Cossart *et al* 1998, Frerking *et al* 1998, 1999). The mechanism for this response is still controversial, with groups reporting the involvement of presynaptic $GABA_B$ receptors (Frerking *et al* 1998, 1999) following a KA stimulated increase in the release of GABA from interneurones; presynaptic KA receptors containing a GluR6 subunit on the terminals of interneurones (Cossart *et al* 1998. Bureau *et al* 1999, Rodriguez-Moreno *et al* 1997, 1998, Min *et al* 1999); and recently the possibility that KA receptors may be found on the axons of interneurones (Semyanov *et al* 2001), excitation of which may lead to a decrease in GABA release. This latter suggestion has come from

studies on guinea pig hippocampi, and may therefore not be found to occur in the hippocampi of rats.

Cossart *et al* (1998) found application of ATPA to cause an increase in interneuronal spiking leading to an increase in the number of IPSPs recorded from CA1 pyramidal cells. The data presented in chapter 3 for the application of ATPA showed an initial increase in the mean percentage inhibition. This is consistent with GluR5 mediated excitation of interneurones resulting in an increase in the release of GABA. This data also suggests that the GluR5 subunit in not involved in the receptor responsible for the downregulation of GABA release from interneurones.

The small increase in the percentage inhibition which occurred following the application of 10μM NS102 may suggest a selective blockade of the facilitatory Glur6 homomeric receptor as reported by Mulle *et al* (2000) to be found at the presynaptic terminals of inhibitory synapses onto interneurones in $GluR5^{-/-}$ but not $GluR6^{-/-}$ mice. Antagonism at this site would be expected to result in a degree of disinhibition of these interneurones and thus lead to an increase in paired-pulse inhibition. Coapplication of NS102 with 1μM KA resulted in a small reduction in the effect of KA on the evoked inhibition, which just failed to reach significance. This however may reflect the weak antagonistic effect of NS102, and it would therefore be of interest to investigate the effect of NS102 on lower, sub-micromolar concentrations of KA. This may provide more concrete evidence for the role of the Glur6 subunit on the inhibitory network within the CA1.

The effect of fluorowillardine on the evoked inhibition was significantly greater to that observed for KA in the intact slice preparation once again suggesting mechanistic differences between the actions of KA and flurowillardine. In the intact slice, flurowillardine application initially resulted in an increase in paired-pulse inhibition. This did not occur in the isolated CA1 preparation, suggesting an upstream excitation of CA3 leading to increased excitatory drive to the CA1. This may have been sufficient to increase the excitation of both a feed forward and feedback interneurones, leading to the observed increase.

No evidence was found in this study for the involvement of $GABA_B$ receptors in the modulation of the effects of KA on the paired-pulse inhibition, since there was no significant difference in the reduction in paired pulse inhibition by KA in the presence of the $GABA_B$ antagonist SCH50911. This suggests agreement with the data of Min *et al*

(1999) rather than that of Frerking *et al* (1998, 1999) who found no role for $GABA_B$ receptors in the modulation of the evoked release of GABA from interneurones.

6.3 KA application to organotypic hippocampal slice cultures

The organotypic mouse hippocampal slice preparation bears functional similarities with acute slice preparations, in terms of an intact excitatory and inhibitory network. However, the maximal population spike amplitudes that can be evoked form both CA1 and CA3 in cultures are significantly lower than those of acute slices. This is very likely due to the lower numbers of cells in organotypic culture compared to acute slices. In addition, the degree of paired-pulse inhibition is significantly greater in both CA1 and CA3 regions of cultures.

In the CA1 of organotypic mouse hippocampal slices, the response to KA also displays some differences. Firstly, the initial increase in the population spike amplitude does not occur. In fact, the application of 1μM KA results in a rapid and large decrease in the amplitude of both population spikes. This may be indicative of a number of possibilities. It may be, for example, that the development of these cultures from 5-7 day old mice is such that the presynaptic GluR5 containing receptor on the Schaffer collateral terminals is not expressed. Thus it would be expected that excitation of the CA3 pyramidal cell population by KA would result in an increased release of glutamate from the Schaffer collaterals, which in turn could result in a depolarising block of the CA1 pyramidal cell population. A further possibility is that the concentration of KA may build up more rapidly in the organotypic culture due to the fact that the slices thin down over the course of culture. In order to investigate these possible scenarios, it would be interesting to examine the effect of KA in cultures in which the Schaffer collateral pathway had been transected. Further clarification could be obtained by the use of immunohistochemistry using antibodies raised against the GluR5 subunit, although to date adequate selective antibodies have not been developed.

Following this initial response, the amplitude of the first, but not the second population spike temporarily recovers somewhat. This may indicate the development of a depolarising block in the CA3 region, enabling stimulus driven events to occur in the CA1.

Evidence in this study that the application of 1μM KA may result in a depolarising block of the CA3 pyramidal cell population comes from the experiments carried out in both mouse acute slices and organotypic hippocampal slice cultures. Upon the application

of KA, the population spike amplitudes in the CA3 of both of these preparations undergo rapid and total reduction. Although this evidence is not as direct as, for example, intracellular recordings from individual CA3 pyramidal cells, this data is consistent with the occurrence of a prolonged depolarisation of these neurones, preventing the synchronised firing required to produce a population spike.

6.4 Chronic application of KA to mouse organotypic hippocampal slice cultures

When administered over a longer period of time, for example in the *in vivo* KA lesion model of temporal lobe epilepsy, a characteristic pattern of damage is observed to occur. For example, there is a loss of CA3 pyramidal neurones (Nadler 1978a) and at higher concentrations of KA also a loss of the principal cells of CA1 (Nadler 1978b). In addition, there is considerable loss of a number of sub-populations of interneurones, for example, those containing parvalbumin (Best *et al* 1993, 1994).

A similar loss of principal cells in the CA3 region has been observed to occur in rat organotypic hippocampal slice cultures following incubation with 5μM KA for 24 hours (Best *et al* 1996). Parvalbumin containing interneurones are also reduced in number as a result of this treatment (Best *et al.* 1996).

The data presented in chapter 5 demonstrates that MF1 mouse hippocampal slice cultures are also susceptible to damage by 5μM KA. This results in a similar pattern of cell death to the CA3 pyramidal cell population (visualised using PI fluorescence and thionin staining) as is found in the rat hippocampal slice culture. In addition data for GAD-67 immunohistochemistry indicates a reduced number of cells expressing GAD following incubation with KA.

Pre-exposure of mouse cultures to a sub-toxic concentration of KA resulted in a reduction in the toxic effects of a subsequent 5μM KA incubation four days later, much as is seen in the rat culture preparation (Best *et al* 1996). This tolerance appeared to be induced at threshold levels by 500nM and 750nM KA but was not significantly observed until a concentration of 1μM KA was achieved. In addition it was not affected by the presence of the NMDA antagonists D-AP5 and MK801 in the culture medium at the time of the preconditioning incubation. This precludes the possibility that protection of the CA3 pyramidal cell population may have occurred as a result of Ca^{2+} influx through NMDA receptors activating a signalling cascade which may have lead to this phenomenon.

It has been proposed that the preconditioning phenomenon may occur as a result of increased levels of adenosine during the induction process (Plamondon *et al* 1999, Blondeau *et al* 2000, Berman *et al* 2000). Activation of adenosine A_1 receptors then leads to a reduction in the release of glutamate presynaptically coupled with hyperpolarisation of the CA3 pyramidal cell population. However, the electrophysiological data presented here may tend to suggest that a lowering of the excitability of the CA3 pyramidal cell population following preconditioning does not occur. This is inferred from the fact that preconditioning does not significantly affect the maximal amplitude which it is possible to elicit from the CA3, nor is the stimulus required to achieve this response significantly different.

Further electrophysiological analysis of the CA3 region using field recordings from the *stratum pyramidale* revealed that preconditioned slices exhibit a significantly lower degree of paired pulse inhibition than that of control cultures. This correlates with the reduction in GAD-67 staining that occurred following preconditioning with 1μM KA.

Preliminary data suggests that this remaining inhibition may exhibit a reduced sensitivity to low concentrations of the $GABA_A$ receptor antagonist bicuculline when compared to control. However it is still abolished in the presence of 10μM bicuculline. This may suggest a change in the $GABA_A$ subunit expression following preconditioning, and it would therefore be of interest to investigate this further using subunit specific antibodies.

Paired-pulse inhibition in the CA1 region was affected in a similar manner by incubation with 1μM KA at 7 DIV. This again correlates well with the GAD-67 data, in which the expression pattern of GAD was found to be significantly reduced following preconditioning.

It is paradoxical that a scenario in which there is reduced functional inhibition should be neuroprotective. This suggests that some change has occurred either presynaptically or postsynaptically within CA3 to reduce the response to KA during the second application. Since stimulus driven events within the CA3 do not change significantly following preconditioning, it is likely that this change is occurring in the CA3 pyramidal cell population itself. However, the response of the preconditioned CA3 to further application of 1μM KA is not significantly different to that of a naieve culture. It is unlikely therefore that this protection occurs as a result of the downregulation of KA receptor numbers on the CA3 pyramidal cells.

One possible candidate for the source of this neuroprotection is HSP-72. The reduced sensitivity to KA toxicity has previously been demonstrated to occur in rats during the peak of HSP-72 expression following the initial insult (Best *et al* 1996). It would be interesting therefore to vary the time interval between the preconditioning incubation and the toxic insult in order to correlate the degree of protection with HSP-72 expression. This latter could be visualised again using immunohistochemistry. This may provide further information about the time window in which protection occurs.

Another possibility is that 1μM KA may cause activation of *c-jun* which may lead in turn to an upregulation of MnSOD production. Should this occur it would be likely that free radicals would be neutralised more rapidly thus reducing the amount of damage to the CA3 pyramidal cell population by subsequent KA incuabtions.

6.5 Summary

Kainate excites all it's targets (Ben-Ari and Cossart, 2000), therefore it is interesting that it appears that the net result of this excitation is a reduction in the output of both the CA1 and the CA3. From the data presented here, 15-30 minute applications of KA (1μM) to acute slices reduced the EPSP slope recorded from *stratum radiatum* of the CA1, probably *via* activation of GluR5 containing receptors on the presynaptic terminals of the Schaffer collateral pathway (Vignes *et al*, 1998, Kamiya and Ozawa 1998). Following a brief increase in the population spike amplitudes in CA1, KA application causes a marked reduction of the population spike amplitude in CA1 in the presence of an intact CA3-CA1 connection. This may be due to increased excitation of GluR5 receptors on interneurones (Cossart *et al* 1998, Khalilov *et al* 2002), since the $GABA_B$ antagonist SCH50911 prolonged the duration of the initial population spike increase following KA application.

This reduction in population spike amplitude is also observed in organotypic mouse slice cultures. Applications of KA (1μM for 2 hours) to these cultures resulted in a reduction in the population spike amplitudes and paired-pulse inhibition in both CA1 and CA3. This reduction persisted for up to an hour after the wash of KA from the recording chamber.

Chronic applications of KA (1μM) for 24 hours to mouse organotypic hippocampal slice cultures resulted in a reduction in the sensitivity of these cultures to subsequent applications of a toxic concentration of KA (5μM for 24 hours). Since the toxic effects of KA occur at a concentration of 5μM but not 1μM, this may suggest that

AMPA receptor activation is required for cell death to occur. The induction of tolerance required a concentration of 1μM KA and occurred even when NMDA receptors had been blocked with D-AP5 and MK-801, suggesting that Ca^{2+} entry *via* NMDA receptors is not required for this phenomenon to occur.

Investigations into the effect of chronic applications of KA to organotypic slice cultures revealed no change in the maximal population spike amplitudes capable of being evoked from either the CA1 or CA3 regions following treatment. The maximal stimulus required to elicit this population spike was significantly greater in CA1 following preconditioning, but not in CA3. This suggests that the tolerance against KA toxicity observed in the CA3 region does not occur as a result of a decrease in CA3 excitability. Interestingly, despite exhibiting resistance to the excitotoxic effects of 5μM KA, both the CA1 and CA3 regions exhibited a significant reduction in paired-pulse inhibition after chronic treatment with 1μM KA.

The mechanism by which KA induced tolerance and the receptor subunits involved in this response remains unclear. Knock-out mice for GluR5 and GluR6 (Contractor *et al* 2001) have been made, and further insight into the KA-induced tolerance to KA could be gained from their use.

References

Abele AE, Scholz KP, Scholz WK, Miller RJ. Excitotoxicity induced by enhanced excitatory neurotransmission in cultured hippocampal pyramidal neurons. Neuron. 1990;4:413-419

Agrawal SG & Evans RH The primary afferent depolarising action of kainate in the rat. Br. J. Pharmacol. 1986;87: 345-355

Andersen P., Blackstad T., Lomo T. Location and identification of excitatory synapses on hippocampal pyramidal cells. Exp. Brain Res. 1966;1: 236-248

Andersen P, Bliss TV, Skrede KK. Unit analysis of hippocampal polulation spikes. Exp Brain Res. 1971;13:208-221

Aoki M, Abe K, Kawagoe J et al. The preconditioned hippocampus accelerates HSP70 heat shock gene expression following transient ischemia in the gerbil. Neurosci Lett. 1993;155:7-10

Ashwood TJ, Lancaster B, Wheal HV. Intracellular electrophysiology of CA1 pyramidal neurones in slices of the kainic acid lesioned hippocampus of the rat. Exp Brain Res. 1986;62:189-198

Bahn S, Volk B, Wisden W. Kainate receptor gene expression in the developing rat brain. J Neurosci. 1994;14:5525-5547

Baraban S.C., Hollopeter G., Erickson J.C., Schwartzkroin P.A., Palmiter R.D. Knock-out mice reveal a critical antiepileptic role for neuropeptide Y. J. Neurosci. 1997;17: 8927-8936

Barnard E., Henley The non-NMDA receptors: types, protein structure and molecular biology. Trends in Pharmacol. Sci. 1990;11: 504-511

Baskys A, Malenka RC. Agonists at metabotropic glutamate receptors presynaptically inhibit EPSCs in neonatal rat hippocampus. J Physiol. 1991;444:687-701

Beckman JS, Crow JP. Pathological implications of nitric oxide, superoxide and peroxynitrite formation. Biochem Soc Trans. 1993;21:330-334

Ben-Ari Y, Cherubini E, Corradetti R, Gaiarsa JL. Giant synaptic potentials in immature rat CA3 hippocampal neurones. J Physiol. 1989;416:303-325

Ben-Ari Y, Cossart R. Kainate, a double agent that generates seizures: two decades of progress. Trends Neurosci. 2000;23:580-587

Berman RF, Fredholm BB, Aden U, O'Connor WT. Evidence for increased dorsal hippocampal adenosine release and metabolism during pharmacologically induced seizures in rats. Brain Res. 2000;872:44-53

Bernard A, Ferhat L, Dessi F et al. Q/R editing of the rat GluR5 and GluR6 kainate receptors in vivo and in vitro: evidence for independent developmental, pathological and cellular regulation. Eur J Neurosci. 1999;11:604-616

Bernard A, Khrestchatisky M. Assessing the extent of RNA editing in the TMII regions of GluR5 and GluR6 kainate receptors during rat brain development. J Neurochem. 1994;62:2057-2060

Best N., Mitchell J., Baimbridge K.G., and Wheal H.V. Changes in parvalbumin-immunoreactive neurons in the rat hippocampus following a kainic acid lesion. Neurosci. Lett. 1993;155: 1-6

Best N., Mitchell J., and Wheal H.V. Ultrastructure of parvalbumin-immunoreactive neurons in the CA1 area of the rat hippocampus following a kainic acid injection. Acta Neuropathol. (Berl.) 1994a;87:187-195

Best N., Mitchell J., Sundstrom L.E. and Wheal H.V. Changes in parvalbumin-immunoreactive neurons in hippocampal organotypic cultures following kainic acid. Brain Res. Assoc. Abstr. 1994b;11: 41

Best N., Sundstrom L.E., Mitchell J., Wheal H.V. Pre-exposure to subtoxic levels prevents kainic acid lesions in organotypic hippocampal slice cultures: Effects of kainic acid on parvalbumin-immunoreactive neurones and expression of heat shock protein 72 following the induction of tolerance. Eur. J. Neurosci. 1996;8: 1209-1219

Bettler B., Boulter J., Hermans-Borgmeyer I., O'Shea-Greenfield A., Deneris E.S., Moll c., Borgmeyer U., Hollmann M., Heinemann S. Cloning of a novel glutamate receptor subunit, GluR5: expression in the nervous system during development. Neuron 1990;5: 583-595

Bettler B, Egebjerg J, Sharma G et al. Cloning of a putative glutamate receptor: a low affinity kainate-binding subunit. Neuron. 1992;8:257-265

Bettler B., Mulle C., Neurotransmitter receptors II AMPA and kainate receptors. Neuropharmacol. 1995;34: 123-139

Bleakman D. Kainate receptor pharmacology and physiology. Cell Mol Life Sci. 1999;56:558-566

Bleakman D, Ogden AM, Ornstein PL, Hoo K. Pharmacological characterization of a GluR6 kainate receptor in cultured hippocampal neurons. Eur J Pharmacol. 1999;378:331-337

Bliss T.V.P., Chung S.H. and Stirling R.V. Structural and functional development of the mossy fibre system in the hippocampus of the postnatal rat. Proc. Physiol. Soc. Feb: 1974; 92-94P

Bliss T., Collingridge G. A synaptic model of memory: Long-term potentiation of the hippocampus. Nature 1983;361: 31-39

Blondeau N, Plamondon H, Richelme C et al. K(ATP) channel openers, adenosine agonists and epileptic preconditioning are stress signals inducing hippocampal neuroprotection. Neuroscience. 2000;100:465-474

Bortolotto Z., Heim C., Sieklucka M., Block F., Sontag K., Cavailhero E. Effects of bilateral clamping of carotid arteries on hippocampal kindling in rats. Physiol. Behav. 1991;49: 667-671

Bortolotto Z.A., Clarke V.R.J., Delany C.M., Parry M.C., Smolders I., Vignes M., Ho K.H., Miu P., Brinton B.T., Fantaske R. et al Kainate receptors are involved in synaptic plasticity. Nature .1999;402: 297-301

Bouilleret V, Schwaller B, Schurmans S et al. Neurodegenerative and morphogenic changes in a mouse model of temporal lobe epilepsy do not depend on the expression of the calcium-binding proteins parvalbumin, calbindin, or calretinin. Neuroscience. 2000;97:47-58

Bowe MA, Nadler JV. Developmental increase in the sensitivity to magnesium of NMDA receptors on CA1 hippocampal pyramidal cells. Brain Res Dev Brain Res. 1990;56:55-61

Bowery NG, Hill DR, Hudson AL et al. (-)Baclofen decreases neurotransmitter release in the mammalian CNS by an action at a novel GABA receptor. Nature. 1980;283:92-94

Bradley SR, Rees HD, Yi H et al. Distribution and developmental regulation of metabotropic glutamate receptor 7a in rat brain. J Neurochem. 1998;71:636-645

Brose N, Huntley GW, Stern-Bach Y et al. Differential assembly of coexpressed glutamate receptor subunits in neurons of rat cerebral cortex. J Biol Chem. 1994;269:16780-16784

Brose N, Huntley GW, Stern-Bach Y et al. Differential assembly of coexpressed glutamate receptor subunits in neurons of rat cerebral cortex. J Biol Chem. 1994;269:16780-16784

Brundege JM, Dunwiddie TV. Role of adenosine as a modulator of synaptic activity in the central nervous system. Adv Pharmacol. 1997;39:353-391

Bruno V, Copani A, Knopfel T et al. Activation of metabotropic glutamate receptors coupled to inositol phospholipid hydrolysis amplifies NMDA-induced neuronal degeneration in cultured cortical cells. Neuropharmacology. 1995;34:1089-1098

Bureau I., Bischoff S., Heinemann S.F., Mulle C. Kainate receptor mediated responses in the CA1 field of wild type and GluR6 deficient mice. J. Neurosci. 1999;19: 653-663

Burke SP, Nadler JV. Regulation of glutamate and aspartate release from slices of the hippocampal CA1 area: effects of adenosine and baclofen. J Neurochem. 1988;51:1541-1551

Caddick SJ, Stanford IM, Chad JE. 2-Hydroxy-saclofen causes a phaclofen-reversible reduction in population spike amplitude in the rat hippocampal slice. Eur J Pharmacol. 1995;274:41-46

Carswell HV, Graham DI, Stone TW. Kainate-evoked release of adenosine from the hippocampus of the anaesthetised rat: possible involvement of free radicals. J Neurochem. 1997;68:240-247

Castillo P.E., Malenka R.C., Nicholl R.A. Kainate receptors mediate a slow postsynaptic current in hippocampal CA3 neurons. Nature 1997;388: 182-186

Chittajallu R., Vignes M., Dev K.K., Barnes J.M., Collingridge G.L., Henley J.M. Regulation of glutamate release by presynaptic kainate receptors in the hippocampus. Nature 1996;379: 78-81

Chittajallu R., Braithwaite S.P., Clarke V.R.J., Henley J.M. Kainate receptors: subunits, synaptic localization and function. Trends in Pharmacol. Sci. 1999;20: 26-35

Clarke V.R.J., Ballyk B.A., Hoo K.H., Mandelzys A., Pellizari A., Bath C.P., Thomas J., Sharpe E.F., Davies C.H., Ornstein P.L. et al. A hippocampal GluR5 kainate receptor regulating inhibitory synaptic transmission. Nature 1997;389: 599-603

Conn PJ, Pin JP. Pharmacology and functions of metabotropic glutamate receptors. Annu Rev Pharmacol Toxicol. 1997;37:205-237

Contractor A, Swanson G, Heinemann SF. Kainate receptors are involved in short- and long-term plasticity at mossy fiber synapses in the hippocampus. Neuron. 2001;29:209-216

Contractor A, Swanson GT, Sailer A et al. Identification of the kainate receptor subunits underlying modulation of excitatory synaptic transmission in the CA3 region of the hippocampus. J Neurosci. 2000;20:8269-8278

Cornish SM, Wheal HV. Long-term loss of paired pulse inhibition in the kainic acid-lesioned hippocampus of the rat. Neuroscience. 1989;28:563-571

Corradetti R, Pugliese AM, Ropert N. The protein kinase C inhibitor 1-(5-isoquinolinesulphonyl)-2-methylpiperazine (H-7) disinhibits CA1 pyramidal cells in rat hippocampal slices. Br J Pharmacol. 1989;98:1376-1382

Cossart R., Esclapez M., Hirsch J.C., Bernard C., Ben-Ari Y. GluR5 kainate receptor activation in interneurones increases tonic inhibition in interneurones. Nature Neurosci. 1998;1: 470-478

Cossart R, Tyzio R, Dinocourt C et al. Presynaptic kainate receptors that enhance the release of GABA on CA1 hippocampal interneurons. Neuron. 2001;29:497-508

Costa E. From GABAA receptor diversity emerges a unified vision of GABAergic inhibition. Annu Rev Pharmacol Toxicol. 1998;38:321-350

Cui C. & Mayer M.L. Heteromeric kainate receptors formed by the coassembly of GluR5, GluR6 and GluR7. J. Neurosci. 1999;19: 8281-8291

Cunha R.A., Malva J.O., Ribeiro J.A. Kainate receptors coupled to G_i/G_o proteins in the rat hippocampus. Mol. Pharmacol. 1999;56: 429-433

Cunha RA. Adenosine as a neuromodulator and as a homeostatic regulator in the nervous system: different roles, different sources and different receptors. Neurochem Int. 2001;38:107-125

Cunha RA, Malva JO, Ribeiro JA. Pertussis toxin prevents presynaptic inhibition by kainate receptors of rat hippocampal [(3)H]GABA release. FEBS Lett. 2000;469:159-162

Curtis D.R., Duggan A.W., Felix D., Johnston G.A. GABA, bicuculline and central inhibition. Nature 1970;226: 1122-1224

Cushing A, Price-Jones MJ, Graves R et al. Measurement of calcium flux through ionotropic glutamate receptors using Cytostar-T scintillating microplates. J Neurosci Methods. 1999;90:33-36

Darzynkiewicz, Z., and Li, X. Measurements of cell death by flow cytometry, in Techniques in Apoptosis: A User's Guide Cotter, T.G. and Martin, S.J., eds., Portland Press (London, U.K.,), 1996 pp. 76-85, 89-92.

Deadwyler et al. The functional significance of LTP: In relation to sensory processing by hippocampal circuits. From Long Term Potentiation: From Biophysics to behaviour 1988 pp 499-534. Eds.: Landfield and Deadwyler. New York.

de Mendonca A, Ribeiro JA. Long-term potentiation observed upon blockade of adenosine A1 receptors in rat hippocampus is N-methyl-D-aspartate receptor-dependent. Neurosci Lett. 2000;291:81-84

de Mendonca A, Sebastiao AM, Ribeiro JA. Inhibition of NMDA receptor-mediated currents in isolated rat hippocampal neurones by adenosine A1 receptor activation. Neuroreport. 1995;6:1097-1100

Defagot MC, Villar MJ, Antonelli MC. Differential Localization of Metabotropic Glutamate Receptors during Postnatal Development. Dev Neurosci. 2002;24:272-282

De Jonge M., Racine R.J. The development and decay of kindling-induced increases in paired-pulse depression in the dentate gyrus. Brain Res. 1987;412: 318-328

Desmond NL, Colbert CM, Zhang DX, Levy WB. NMDA receptor antagonists block the induction of long-term depression in the hippocampal dentate gyrus of the anesthetized rat. Brain Res. 1991;552:93-98

Diabira D, Hennou S, Chevassus-Au-Louis N et al. Late embryonic expression of AMPA receptor function in the CA1 region of the intact hippocampus in vitro. Eur J Neurosci. 1999;11:4015-4023

Dumas TC, Foster TC. Development of metabotropic glutamate receptor-mediated synaptic inhibition. Neuroreport. 1997;8:2919-2924

Dunwiddie TV, Diao L, Proctor WR. Adenine nucleotides undergo rapid, quantitative conversion to adenosine in the extracellular space in rat hippocampus. J Neurosci. 1997;17:7673-7682

During MJ, Spencer DD. Adenosine: a potential mediator of seizure arrest and postictal refractoriness. Ann Neurol. 1992;32:618-624

Dutar P, Nicoll RA. A physiological role for GABAB receptors in the central nervous system. Nature. 1988;332:156-158

Egebjerg J, Heinemann SF. Ca2+ permeability of unedited and edited versions of the kainate selective glutamate receptor GluR6. Proc Natl Acad Sci U S A. 1993;90:755-759

Fastbom J, Pazos A, Probst A, Palacios JM. Adenosine A1 receptors in the human brain: a quantitative autoradiographic study. Neuroscience. 1987;22:827-839

Egebjerg J., Bettler B., Hermans-Borgmeyer I., Heinemann S. Cloning of the cDNA for a glutamate receptor subunit activated by kainate but not AMPA Nature 1991;351: 745-748

El Bahh B., Lurton D., Sundstrom L.E., Rougier A. Induction of tolerance and mossy fibre sprouting in the contralateral hippocampus following a unilateral intrahippocampal kainic acid injection. Neurosci. Letts. 1997;227: 135-139

Fisher R.S. & Alger B.E. Electrophysiological mechanisms of kainic acid-induced epileptiform activity in the rat hippocampal slice. J. Neurosci. 1984;4: 1312-1323

Franck JE, Schwartzkroin PA. Immature rabbit hippocampus is damaged by systemic but not intraventricular kainic acid. Brain Res. 1984;315:219-227

Frank J.E. Cell death, plasticity, and epilepsy: insights provided by experimental models of hippocampal sclerosis. In Epilepsy Models, Mechanisms, and Concepts Ed. P.A. Schwartzkroin 1993 pp281-303. Cambridge University Press.

Fredholm BB. Purinoceptors in the nervous system. Pharmacol Toxicol. 1995;76:228-239

Frerking M., Petersen C.C.H., Nicholl R.A. Mechanisms underlying kainate receptor-mediated disinhibition in the hippocampus. Proc. Nat. Acad. Sci. USA 1999;96: 12917-12922

Frerking M, Nicoll RA. Synaptic kainate receptors. Curr Opin Neurobiol. 2000;10:342-351

Fritschy JM, Meskenaite V, Weinmann O et al. GABAB-receptor splice variants GB1a and GB1b in rat brain: developmental regulation, cellular distribution and extrasynaptic localization. Eur J Neurosci. 1999;11:761-768

Garcia E.P., Mehta S., Blair L.A.C., Wells D.G., Shang J., Fukushima T., Fallon J.R., Garner C.C., Marshall J. SAP90 binds and clusters kainate receptors causing incomplete desensitisation. Neuron 1998;21: 727-739

Galvez T, Duthey B, Kniazeff J et al. Allosteric interactions between GB1 and GB2 subunits are required for optimal GABA(B) receptor function. Embo J. 2001;20:2152-2159

Gereau RWt, Conn PJ. Roles of specific metabotropic glutamate receptor subtypes in regulation of hippocampal CA1 pyramidal cell excitability. J Neurophysiol. 1995;74:122-129

Gereau RWt, Conn PJ. Multiple presynaptic metabotropic glutamate receptors modulate excitatory and inhibitory synaptic transmission in hippocampal area CA1. J Neurosci. 1995;15:6879-6889

Gerner E.W. and Schneider M.J. Induced thermal resistance in HeLa cells. Nature 1975;256: 500-502

Goncalves ML, Cunha RA, Ribeiro JA. Adenosine A2A receptors facilitate 45Ca2+ uptake through class A calcium channels in rat hippocampal CA3 but not CA1 synaptosomes. Neurosci Lett. 1997;238:73-77

Gutierrez R, Heinemann U. Synaptic reorganization in explanted cultures of rat hippocampus. Brain Res. 1999;815:304-316

Haas K.Z., Sperber E.F., Moshe S.L. and Stanton P.K. Kainic acid-induced seizures enhance dentate gyrus inhibition by downregulation of $GABA_B$ receptors. J. Neurosci. 1996;16: 4250-4260

Haglund M.M. and Schwartzkroin P.A. Role of Na, K pump, potassium regulation and IPSPs in seizures and spreading depression in immature hippocampal slices. J. Neurophysiol. 1990;63(2): 225-239

Halsay K., Buhl E., Lorinczi Z., Tamas G., Somogyi P. Synaptic target selectivity and input of GABAergic basket and bistratified interneurones in the CA1 area of rat hippocampus. Hippocampus 1996;6: 306-329

Hammond C. Cellular and molecular Neurobiology. 1996 Academic Press Inc.

Hanson A.J. Extracellular potassium concentration in juvenile and adult rat brain cortex during anoxia. Acta Physiol. Scand. 1977;99: 412-420

Henze DA, Urban NN, Barrionuevo G. The multifarious hippocampal mossy fiber pathway: a review. Neuroscience. 2000;98:407-427

Herb A, Burnashev N, Werner P et al. The KA-2 subunit of excitatory amino acid receptors shows widespread expression in brain and forms ion channels with distantly related subunits. Neuron. 1992;8:775-785

Heurteaux C, Bertaina V, Widmann C, Lazdunski M. K+ channel openers prevent global ischemia-induced expression of c-fos, c-jun, heat shock protein, and amyloid beta-protein precursor genes and neuronal death in rat hippocampus. Proc Natl Acad Sci U S A. 1993;90:9431-9435

Hill DR, Bowery NG, Hudson AL. Inhibition of GABAB receptor binding by guanyl nucleotides. J Neurochem. 1984;42:652-657

Hollmann M, O'Shea-Greenfield A, Rogers SW, Heinemann S. Cloning by functional expression of a member of the glutamate receptor family. Nature. 1989;342:643-648

Howe JR. Homomeric and heteromeric ion channels formed from the kainate-type subunits GluR6 and KA2 have very small, but different, unitary conductances. J Neurophysiol. 1996;76:510-519

Jane DE, Jones PL, Pook PC et al. Stereospecific antagonism by (+)-alpha-methyl-4-carboxyphenylglycine (MCPG) of (1S,3R)-ACPD-induced effects in neonatal rat motoneurones and rat thalamic neurones. Neuropharmacology. 1993;32:725-727

Jane DE, Pittaway K, Sunter DC et al. New phenylglycine derivatives with potent and selective antagonist activity at presynaptic glutamate receptors in neonatal rat spinal cord. Neuropharmacology. 1995;34:851-856

Janigro D, Schwartzkroin PA. Effects of GABA and baclofen on pyramidal cells in the developing rabbit hippocampus: an 'in vitro' study. Brain Res. 1988;469:171-184

Jensen F.E., Applegate C.D., Burchfield J.L., and Lomboroso C.T. Differential effects of perinatal hypoxia and anoxia on long term seizure susceptibility in the rat. Life Sci. 1991;49: 399-407

Jensen F.E., Holmes G.H., Lomboroso C.T., Blume H. and Firkusny I. Age dependent long term changes in seizure susceptibility and neurobehaviour following hypoxia in the rat. Epilepsia 1992;33: 971-980

Jensen F.E., Firkusny I. and Mower G. Differences in c-fos immunoreactivity due to age and mode of seizure induction. Mol. Brain Res. 1993;17:185-193

Jensen F.E., Tsuji M., Offut M., Firkusny I.R. and Holtzman D. Age dependent effects of hypoxia on high energy phosphate concentrations and pH in the rat brain. 1993 Dev. Brain Res.

Jensen F.E., Wang C. Hypoxia-induced hyperexcitability in vivo and in vitro in the immature hippocampus. Epilepsy Res. 1996;26: 131-140

Johnston D., Miao-Sin Wu S., Foundations of Cellular Neurophysiology 1995 pp 423-439. MIT Press

Jones KA, Borowsky B, Tamm JA et al. GABA(B) receptors function as a heteromeric assembly of the subunits GABA(B)R1 and GABA(B)R2. Nature. 1998;396:674-679

Kamiya H., Ozawa S. Kainate receptor-mediated inhibition of presynaptic Ca^{2+} influx and EPSP in area CA1 of the rat hippocampus. J. Physiol. 1998;503: 833-845

Kamiya H., Ozawa S. Kainate receptor-mediated presynaptic inhibition at the mouse hippocampal mossy fibre synapse. J. Physiol. 2000;523: 653-665

Kaupmann K, Huggel K, Heid J et al. Expression cloning of GABA(B) receptors uncovers similarity to metabotropic glutamate receptors. Nature. 1997;386:239-246

Keinanen K, Wisden W, Sommer B et al. A family of AMPA-selective glutamate receptors. Science. 1990;249:556-560

Keinanen K, Wisden W, Sommer B et al. A family of AMPA-selective glutamate receptors. Science. 1990;249:556-560

Kelly ME, McIntyre DC. Hippocampal kindling protects several structures from the neuronal damage resulting from kainic acid-induced status epilepticus. Brain Res. 1994;634:245-256

Kidd FL, Isaac JT. Kinetics and activation of postsynaptic kainate receptors at thalamocortical synapses: role of glutamate clearance. J Neurophysiol. 2001;86:1139-1148

Kim H, Bing G, Jhoo W et al. Changes of hippocampal Cu/Zn-superoxide dismutase after kainate treatment in the rat. Brain Res. 2000;853:215-226

Kirson ED, Schirra C, Konnerth A, Yaari Y. Early postnatal switch in magnesium sensitivity of NMDA receptors in rat CA1 pyramidal cells. J Physiol. 1999;521 Pt 1:99-111

Kiskin N., Krishtal O., Tsyndrenko A., Excitatory amino acid receptors in hippocampal neurones: Kainate fails to desensitise them. Neurosci. Lett. 1986;63: 225-230

Kitagawa K., Matsumoto M., Tagaya M., Hata R., Ueda H., Niinobe M., Handa N., Fukanaga R., Kimura K., Mikoshiba K., and Kamada T. "Ischaemic tolerance" phenomenon found in the brain. Brain Res. 1990;528: 21-24

Klapstein G.J. and Colmers W.F. Neuropeptide Y suppresses epileptiform activity in rat hippocampus in vitro. J. Neurophysiol. 1997;78: 1651-1661

Kleckner NW, Dingledine R. Requirement for glycine in activation of NMDA-receptors expressed in Xenopus oocytes. Science. 1988;241:835-837

Klein J, Iovino M, Vakil M et al. Ontogenetic and pharmacological studies on metabotropic glutamate receptors coupled to phospholipase D activation. Neuropharmacology. 1997;36:305-311

Knowles W., Schwartzkroin P. Local circuit synaptic interactions in hippocampal slices. J. Neurosci. 1981;1: 318

Kohler M Intrinsic connections of the retro-hippocampal region in the rat brain II The medial entorhinal area. J. Comp. Neurol. 1986;236: 504

Kohler M, Burnashev N, Sakmann B, Seeburg PH. Determinants of Ca2+ permeability in both TM1 and TM2 of high affinity kainate receptor channels: diversity by RNA editing. Neuron. 1993;10:491-500

Lanthorn TH, Cotman CW. Baclofen selectively inhibits excitatory synaptic transmission in the hippocampus. Brain Res. 1981;225:171-178

Lauri SE, Delany C, VR JC et al. Synaptic activation of a presynaptic kainate receptor facilitates AMPA receptor-mediated synaptic transmission at hippocampal mossy fibre synapses. Neuropharmacology. 2001 (a);41:907-915

Lauri SE, Bortolotto ZA, Bleakman D et al. A critical role of a facilitatory presynaptic kainate receptor in mossy fiber LTP. Neuron. 2001;32:697-709

Lerma J, Paternain AV, Naranjo JR, Mellstrom B. Functional kainate-selective glutamate receptors in cultured hippocampal neurons. Proc Natl Acad Sci U S A. 1993;90:11688-11692

Liang LP, Ho YS, Patel M. Mitochondrial superoxide production in kainate-induced hippocampal damage. Neuroscience. 2000;101:563-570

Lu J, Karadsheh M, Delpire E. Developmental regulation of the neuronal-specific isoform of K-Cl cotransporter KCC2 in postnatal rat brains. J Neurobiol. 1999;39:558-568

Liu Z., Holmes G.L., Mikati M., Lomboroso C.T., and Jensen F.E. Topographical study of electroencephalographic seizures following hypoxia in immature rats. Soc. Neurosci. Abstr. 1994;20: 396

Lowenstein D.H., Chan P.H., and Miles M.F. The stress response protein response in cultured neurons: characterisation and evidence for a protective role in excitotoxicity. Neuron 1991;7: 1053-1060

Lujan R, Nusser Z, Roberts JD et al. Perisynaptic location of metabotropic glutamate receptors mGluR1 and mGluR5 on dendrites and dendritic spines in the rat hippocampus. Eur J Neurosci. 1996;8:1488-1500

Malva JO, Ambrosio AF, Cunha RA et al. A functionally active presynaptic high-affinity kainate receptor in the rat hippocampal CA3 subregion. Neurosci Lett. 1995;185:83-86

Mano I, Teichberg VI. A tetrameric subunit stoichiometry for a glutamate receptor-channel complex. Neuroreport. 1998;9:327-331

Masino SA, Dunwiddie TV. Temperature-dependent modulation of excitatory transmission in hippocampal slices is mediated by extracellular adenosine. J Neurosci. 1999;19:1932-1939

Mayer ML, Westbrook GL, Guthrie PB. Voltage-dependent block by Mg2+ of NMDA responses in spinal cord neurones. Nature. 1984;309:261-263

Mayer M., Vyklicky L. Concanavalin A selectively reduces desensitisation of mammalian neuronal quisqualate receptors. Proc. Natl. Acad. Sci. USA 1989;86: 1411-1415

Mayer M., Partin K., Patneau D., Wong L., Vyklicky L., Benveniste M., Bowie D. Desensitisation at AMPA, kainate and NMDA receptors. In "Excitatory Amino Acids and

Synaptic Transmission" (eds H.V. Wheal and A.M. Thomson) 1991 pp 89-98 Academic Press Ltd.

McDonald J.W. and Johnston M.V. Physiological and pathophysiological roles of excitatory amino acids during central nervous system development. Brain Res. Brain Res. Rev. 1990;15: 41-70

McDonald J.W., Trescher W.H., and Johnston M.V. Susceptibility of brain to AMPA induced excitotoxicity transiently peaks during early postnatal development. Brain Res. 1992;583: 54-70

Mehta S, Wu H, Garner CC, Marshall J. Molecular mechanisms regulating the differential association of kainate receptor subunits with SAP90/PSD-95 and SAP97. J Biol Chem. 2001;276:16092-16099

Melyan Z, Wheal HV, Lancaster B. Metabotropic-mediated kainate receptor regulation of IsAHP and excitability in pyramidal cells. Neuron. 2002;34:107-114

Mestdagh N., Wulfert E. Bicuculline increases Ca^{2+} transients in rat cerebellar granule cells through non-$GABA_A$ receptor associated mechanisms. Neurosci. Lett. 1999;265 (2): 95-98

Miligram N.W., Yearwood T., Khurgel M., Ivy G.O., Racine R. Changes in inhibitory processes in the hippocampus following recurrent seizures induced by systemic administration of kainic acid. Brain Res. 1991;551: 236-246

Min M.-Y., Melyan Z., Kollmann D.M. Synaptically released glutamate reduces γ-aminobutyric acid (GABA)ergic inhibition in the hippocampus via kainate receptors. Proc. Natl. Acad. Sci. USA 1999;96: 9932-9937

Minakami R, Iida K, Hirakawa N, Sugiyama H. The expression of two splice variants of metabotropic glutamate receptor subtype 5 in the rat brain and neuronal cells during development. J Neurochem. 1995;65:1536-1542

Monyer H, Burnashev N, Laurie DJ et al. Developmental and regional expression in the rat brain and functional properties of four NMDA receptors. Neuron. 1994;12:529-540

Monyer H, Sprengel R, Schoepfer R et al. Heteromeric NMDA receptors: molecular and functional distinction of subtypes. Science. 1992;256:1217-1221

Mueller AL, Taube JS, Schwartzkroin PA. Development of hyperpolarizing inhibitory postsynaptic potentials and hyperpolarizing response to gamma-aminobutyric acid in rabbit hippocampus studied in vitro. J Neurosci. 1984;4:860-867

Mulkey RM, Malenka RC. Mechanisms underlying induction of homosynaptic long-term depression in area CA1 of the hippocampus. Neuron. 1992;9:967-975

Mulle C, Sailer A, Perez-Otano I et al. Altered synaptic physiology and reduced susceptibility to kainate-induced seizures in GluR6-deficient mice. Nature. 1998;392:601-605

Mulle C, Sailer A, Swanson GT et al. Subunit composition of kainate receptors in hippocampal interneurons. Neuron. 2000;28:475-484

Mulle C, Sailer A, Swanson GT et al. Subunit composition of kainate receptors in hippocampal interneurons. Neuron. 2000;28:475-484

Nadler J.V., Perry B.W., Cotman C.W. Intraventricular kainic acid preferentially destroys hippocampal pyramidal cells. Nature 1978a;271: 676-677

Nadler J.V., Perry B.W., Cotman C.W. Preferential vulnerability of hippocampus to intraventricular kainic acid. In Kainic Acid as Tool in Neurobiology McGeer E.G., Olney J.W. and McGeer P.L. (Eds.) 1978b pp219-237 Raven Press, New York

Nadler JV, Cuthbertson GJ. Kainic acid neurotoxicity toward hippocampal formation: dependence on specific excitatory pathways. Brain Res. 1980;195:47-56

Nadler JV, Perry BW, Gentry C, Cotman CW. Degeneration of hippocampal CA3 pyramidal cells induced by intraventricular kainic acid. J Comp Neurol. 1980;192:333-359

Nayeem N, Green TP, Martin IL, Barnard EA. Quaternary structure of the native GABAA receptor determined by electron microscopic image analysis. J Neurochem. 1994;62:815-818

Nicoll RA, Malenka RC. Contrasting properties of two forms of long-term potentiation in the hippocampus. Nature. 1995;377:115-118

Nicoll RA, Malenka RC, Kauer JA. Functional comparison of neurotransmitter receptor subtypes in mammalian central nervous system. Physiol Rev. 1990;70:513-565

Nowak L., Bregestovski P., Ascher P., Herbert A., Prochiantz A., Magnesium gates glutamate activated channels in mouse central neurons. Nature 1984;307: 462-465

Ochiishi T, Saitoh Y, Yukawa A et al. High level of adenosine A1 receptor-like immunoreactivity in the CA2/CA3a region of the adult rat hippocampus. Neuroscience. 1999;93:955-967

Ohtsuki T, Matsumoto M, Kuwabara K et al. Influence of oxidative stress on induced tolerance to ischemia in gerbil hippocampal neurons. Brain Res. 1992;599:246-252

Ohtsuki T, Matsumoto M, Kuwabara K et al. Influence of oxidative stress on induced tolerance to ischemia in gerbil hippocampal neurons. Brain Res. 1992;599:246-252

Olah ME. Identification of A2a adenosine receptor domains involved in selective coupling to Gs. Analysis of chimeric A1/A2a adenosine receptors. J Biol Chem. 1997;272:337-344

Olsen RW, Ban M, Miller T Studies on the neuropharmacological activity of bicuculline and related compounds. Brain Res. 1976;102: 283-299

Ong J, Marino V, Parker DA et al. The morpholino-acetic acid analogue Sch 50911 is a selective GABA(B) receptor antagonist in rat neocortical slices. Eur J Pharmacol. 1998;362:35-41

Ozawa S, Kamiya H, Tsuzuki K. Glutamate receptors in the mammalian central nervous system. Prog Neurobiol. 1998;54:581-618

Partin K., Patneau D., Winters C., Mayer M., Buonanno A. Selective modulation of desensitisation at AMPA versus kainate receptors by cyclothiazide and concanavalin A. Neuron 1993;11: 1069-1082

Paternain AV, Herrera MT, Nieto MA, Lerma J. GluR5 and GluR6 kainate receptor subunits coexist in hippocampal neurons and coassemble to form functional receptors. J Neurosci. 2000;20:196-205

Paternain AV, Rodriguez-Moreno A, Villarroel A, Lerma J. Activation and desensitization properties of native and recombinant kainate receptors. Neuropharmacology. 1998;37:1249-1259

Patneau DK, Mayer ML, Jane DE, Watkins JC. Activation and desensitization of AMPA/kainate receptors by novel derivatives of willardiine. J Neurosci. 1992;12:595-606

Pellegrini-Giampietro DE, Bennett MV, Zukin RS. Differential expression of three glutamate receptor genes in developing rat brain: an in situ hybridization study. Proc Natl Acad Sci U S A. 1991;88:4157-4161

Pellegrini-Giampietro D.E. Are Ca^{2+}-permeable kainate/AMPA receptors more abundant in immature brain? Neurosci. Letts. 1992;144: 65-69

Peterson C, Neal JH, Cotman CW. Development of N-methyl-D-aspartate excitotoxicity in cultured hippocampal neurons. Brain Res Dev Brain Res. 1989;48:187-195

Petralia RS, Wang YX, Wenthold RJ. Histological and ultrastructural localization of the kainate receptor subunits, KA2 and GluR6/7, in the rat nervous system using selective antipeptide antibodies. J Comp Neurol. 1994;349:85-110

Pohle W., Rauca C. Hypoxia protects against neurotoxicity of kainic acid. Brain Res. 1994;644: 297-304

Pin JP, Joly C, Heinemann SF, Bockaert J. Domains involved in the specificity of G protein activation in phospholipase C-coupled metabotropic glutamate receptors. Embo J. 1994;13:342-348

Plamondon H, Blondeau N, Heurteaux C, Lazdunski M. Mutually protective actions of kainic acid epileptic preconditioning and sublethal global ischemia on hippocampal neuronal death: involvement of adenosine A1 receptors and K(ATP) channels. J Cereb Blood Flow Metab. 1999;19:1296-1308

Plotkin MD, Snyder EY, Hebert SC, Delpire E. Expression of the Na-K-2Cl cotransporter is developmentally regulated in postnatal rat brains: a possible mechanism underlying GABA's excitatory role in immature brain. J Neurobiol. 1997;33:781-795

Psarropoulou C, Kostopoulos G, Haas HL. An electrophysiological study of the ontogenesis of adenosine receptors in the CA1 area of rat hippocampus. Brain Res Dev Brain Res. 1990;55:147-150

Rivera C, Voipio J, Payne JA et al. The K+/Cl- co-transporter KCC2 renders GABA hyperpolarizing during neuronal maturation. Nature. 1999;397:251-255

Robinson J.H., Deadwyler S.A. Kainic acid produces depolarization of CA3 pyramidal cells in the vitro hippocampal slice. Brain Res. 1981;221(1): 117-27

Rodriguez-Moreno A., Herreras O., Lerma J. Kainate receptors presynaptically downregulate GABAergic inhibition in the rat hippocampus. Neuron 1997;19: 893-901

Rodriguez-Moreno A., Lerma J. Kainate receptor modulation of GABA release involves a metabotropic function. Neuron 1998;20: 1211-1218

Rodriguez-Moreno A., Lopez-Garcia J.C., Lerma J. Two populations of kainate receptors with separate signalling mechanisms in hippocampal interneurons. Proc. Natl. Acad. Sci. USA 2000;97: 1293-1298

Rosenmund C, Stern-Bach Y, Stevens CF. The tetrameric structure of a glutamate receptor channel. Science. 1998;280:1596-1599

Sasahira M, Lowry T, Simon RP, Greenberg DA. Epileptic tolerance: prior seizures protect against seizure-induced neuronal injury. Neurosci Lett. 1995;185:95-98

Sawada S., Higashima M., Yamamoto C. Kainic acid induces long-lasting depolarizations in hippocampal neurons only when applied to stratum lucidum. Exp. Brain Res. 1988;72(1): 135-140

Scherer SE, Gallo V. Expression and regulation of kainate and AMPA receptors in the rat neural tube. J Neurosci Res. 1998;52:356-368

Schiffer HH, Swanson GT, Heinemann SF. Rat GluR7 and a carboxy-terminal splice variant, GluR7b, are functional kainate receptor subunits with a low sensitivity to glutamate. Neuron. 1997;19:1141-1146

Schoepp DD, Johnson BG, Salhoff CR et al. Selective inhibition of forskolin-stimulated cyclic AMP formation in rat hippocampus by a novel mGluR agonist, 2R,4R-4-aminopyrrolidine-2,4- dicarboxylate. Neuropharmacology. 1995;34:843-850

Schubert P, Ogata T, Marchini C et al. Protective mechanisms of adenosine in neurons and glial cells. Ann N Y Acad Sci. 1997;825:1-10

Schwartzkroin P., Scharfman H., Sloviter R. Similarities in circuitry between Ammon's horn and dentate gyrus: Local interactions and parallel processing. Prog. Brain Res. 1990;83: 269-286

Sebastiao AM, Ribeiro JA. Fine-tuning neuromodulation by adenosine. Trends Pharmacol Sci. 2000;21:341-346

Semyanov A, Kullmann DM. Modulation of GABAergic signaling among interneurons by metabotropic glutamate receptors. Neuron. 2000;25:663-672

Semyanov A, Kullmann DM. Kainate receptor-dependent axonal depolarization and action potential initiation in interneurons. Nat Neurosci. 2001;4:718-723

Sensi SL, Yin HZ, Carriedo SG et al. Preferential Zn2+ influx through Ca2+-permeable AMPA/kainate channels triggers prolonged mitochondrial superoxide production. Proc Natl Acad Sci U S A. 1999;96:2414-2419

Seress L, Frotscher M, Ribak CE. Local circuit neurons in both the dentate gyrus and Ammon's horn establish synaptic connections with principal neurons in five day old rats: a morphological basis for inhibition in early development. Exp Brain Res. 1989;78:1-9

Sharp FR, Massa SM, Swanson RA. Heat-shock protein protection. Trends Neurosci. 1999;22:97-99

Shetty AK, Turner DA. Aging impairs axonal sprouting response of dentate granule cells following target loss and partial deafferentation. J Comp Neurol. 1999;414:238-254

Shigemoto R, Kinoshita A, Wada E et al. Differential presynaptic localization of metabotropic glutamate receptor subtypes in the rat hippocampus. J Neurosci. 1997;17:7503-7522

Shimazaki K, Robinson HP, Nakajima T et al. Purification of AMPA type glutamate receptor by a spider toxin. Brain Res Mol Brain Res. 1992;13:331-337

Sieghart W. Structure and pharmacology of gamma-aminobutyric acidA receptor subtypes. Pharmacol Rev. 1995;47:181-234

Sommer B, Keinanen K, Verdoorn TA et al. Flip and flop: a cell-specific functional switch in glutamate-operated channels of the CNS. Science. 1990;249:1580-1585

Sommer B, Kohler M, Sprengel R, Seeburg PH. RNA editing in brain controls a determinant of ion flow in glutamate-gated channels. Cell. 1991;67:11-19

Sommer B., Seeburg P. Glutamate receptor channels: Novel properties and new clones. Trends in Pharmacol. Sci. 1992;13: 291-296

Sperber E.F., Haas K.Z., Stanton P.K. and Moshe S.L. Resistance of the immature hippocampus to seizure-induced synaptic reorganisation. Dev. Brain Res. 1991;60: 88-93

Stanford IM, Wheal HV, Chad JE. Bicuculline enhances the late GABAB receptor-mediated paired-pulse inhibition observed in rat hippocampal slices. Eur J Pharmacol. 1995;277:229-234

Stensbol TB, Borre L, Johansen TN et al. Resolution, absolute stereochemistry and molecular pharmacology of the enantiomers of ATPA. Eur J Pharmacol. 1999;380:153-162

Stern-Bach Y, Bettler B, Hartley M et al. Agonist selectivity of glutamate receptors is specified by two domains structurally related to bacterial amino acid-binding proteins. Neuron. 1994;13:1345-1357

Stoppini L., Buchs P.A., Muller D. A simple method for organotypic cultures of nervous tissue. J. Neurosci. Methods 1991;37: 173-182

Strecker GJ, Jackson MB, Dudek FE. Blockade of NMDA-activated channels by magnesium in the immature rat hippocampus. J Neurophysiol. 1994;72:1538-1548

Swann J.W., Brady R.J., Martin D.L., Postnatal development of GABA-mediated synaptic inhibition in rat hippocampus. Neuroscience 1989;28: 551-561

Swanson L., Sawchenko P., Cowan W. Evidence for collateral projections by neurones in Ammon's horn, the dentate gyrus, and the subiculum, a multiple retrograde labelling study in the rat. J. Neurosci. 1981;1: 548-559

Szpirer C, Molne M, Antonacci R et al. The genes encoding the glutamate receptor subunits KA1 and KA2 (GRIK4 and GRIK5) are located on separate chromosomes in human, mouse, and rat. Proc Natl Acad Sci U S A. 1994;91:11849-11853

Tancredi V, D'Antuono M, Nehlig A, Avoli M. Modulation of epileptiform activity by adenosine A1 receptor-mediated mechanisms in the juvenile rat hippocampus. J Pharmacol Exp Ther. 1998;286:1412-1419

Thompson SM. Modulation of inhibitory synaptic transmission in the hippocampus. Prog Neurobiol. 1994;42:575-609

Thompson SM, Gahwiler BH. Comparison of the actions of baclofen at pre- and postsynaptic receptors in the rat hippocampus in vitro. J Physiol. 1992;451:329-345

Trussell L., Thio L., Zorumski C., Fischbach G. Rapid desensitisation of glutamate receptors in vertebrate central neurones. Proc. Natl. Acad. Sci. USA 1988;85: 4562-4566

Turner DA, Wheal HV. Excitatory synaptic potentials in kainic acid-denervated rat CA1 pyramidal neurons. J Neurosci. 1991;11:2786-2794

Uchino S., Sakimura K., Nagahari K., Mishina M. Mutations in a putative agonist binding region of the AMPA selective glutamate receptor channel. Febs. Lett. 1992;308: 253-257

Valenzuela CF, Cardoso RA. Acute effects of ethanol on kainate receptors with different subunit compositions. J Pharmacol Exp Ther. 1999;288:1199-1206

van Hooft JA, Giuffrida R, Blatow M, Monyer H. Differential expression of group I metabotropic glutamate receptors in functionally distinct hippocampal interneurons. J Neurosci. 2000;20:3544-3551

Verdoorn TA, Johansen TH, Drejer J, Nielsen EO. Selective block of recombinant glur6 receptors by NS-102, a novel non-NMDA receptor antagonist. Eur J Pharmacol. 1994;269:43-49

Vignes M., Collingridge G.L. The synaptic activation of kainate receptors. Nature 1997;388: 179-182

Vignes M., Clarke V.R.J., Parry M.J., Bleakman D., Lodge D., Ornstein P.L., Collingridge G.L. The GluR5 subtype of kainate receptor regulates excitatory synaptic transmission in areas CA1 and CA3 of the rat hippocampus. Neuropharmacol. 1998;37: 1269-1277

Vissel B, Royle GA, Christie BR et al. The role of RNA editing of kainate receptors in synaptic plasticity and seizures. Neuron. 2001;29:217-227

Watase K, Sekiguchi M, Matsui TA et al. Dominant negative mutant of ionotropic glutamate receptor subunit GluR3: implications for the role of a cysteine residue for its channel activity and pharmacological properties. Biochem J. 1997;322 (Pt 2):385-391

Watkins J.C., Evans R.H. Cellular and synaptic basis of kainic acid-induced hippocampal epileptiform activity. Annu. Rev Pharmacol Toxicol. 1981;21: 165-204

Watkins J, Collingridge G. Phenylglycine derivatives as antagonists of metabotropic glutamate receptors. Trends Pharmacol Sci. 1994;15:333-342

Wermuth C.G., Biziere K. Pyridanzinyl-GABA derivatives – A new class of synthetic $GABA_A$ antagonists. Trends in Pharmacol. Sci. 1986;7: 421-424

Werner P, Voigt M, Keinanen K et al. Cloning of a putative high-affinity kainate receptor expressed predominantly in hippocampal CA3 cells. Nature. 1991;351:742-744

Westbrook G.L., Lothman E.W. Cellular and synaptic basis of kainic acid-induced hippocampal epileptiform activity. Brain Res. 1983;273(1): 97-109

Wilding T.J., Huettner J.E. Differential antagonism of alpha-amino-3-hydroxy-5-methyl-4-isoxazolepropionic acid preferring and kainate preferring receptors by 2,3 benzodiazepines. Mol. Pharmacol. 1995;47: 582-587

Wilding TJ, Huettner JE. Antagonist pharmacology of kainate- and alpha-amino-3-hydroxy-5-methyl-4-isoxazolepropionic acid-preferring receptors. Mol Pharmacol. 1996;49:540-546

Wilding TJ, Huettner JE. Activation and desensitization of hippocampal kainate receptors. J Neurosci. 1997;17:2713-2721

Williams S, Vachon P, Lacaille JC. Monosynaptic GABA-mediated inhibitory postsynaptic potentials in CA1 pyramidal cells of hyperexcitable hippocampal slices from kainic acid-treated rats. Neuroscience. 1993;52:541-554

Wisden W, Seeburg PH. A complex mosaic of high-affinity kainate receptors in rat brain. J Neurosci. 1993;13:3582-3598

Wojcik WJ, Neff NH. Gamma-aminobutyric acid B receptors are negatively coupled to adenylate cyclase in brain, and in the cerebellum these receptors may be associated with granule cells. Mol Pharmacol. 1984;25:24-28

Wong LA, Mayer ML, Jane DE, Watkins JC. Willardiines differentiate agonist binding sites for kainate- versus AMPA-preferring glutamate receptors in DRG and hippocampal neurons. J Neurosci. 1994;14:3881-3897

Wright RA, Schoepp DD. Differentiation of group 2 and group 3 metabotropic glutamate receptor cAMP responses in the rat hippocampus. Eur J Pharmacol. 1996;297:275-282

Wu LG, Saggau P. Adenosine inhibits evoked synaptic transmission primarily by reducing presynaptic calcium influx in area CA1 of hippocampus. Neuron. 1994;12:1139-1148

Xie XM, Smart TG. A physiological role for endogenous zinc in rat hippocampal synaptic neurotransmission. Nature. 1991;349:521-524

Yokoi M, Kobayashi K, Manabe T et al. Impairment of hippocampal mossy fiber LTD in mice lacking mGluR2. Science. 1996;273:645-647

Young D, Dragunow M. Status epilepticus may be caused by loss of adenosine anticonvulsant mechanisms. Neuroscience. 1994;58:245-261